Methods of Cancer Diagnosis, Therapy, and Prognosis

Volume 7
General Overviews, Head and Neck Cancer and Thyroid Cancer

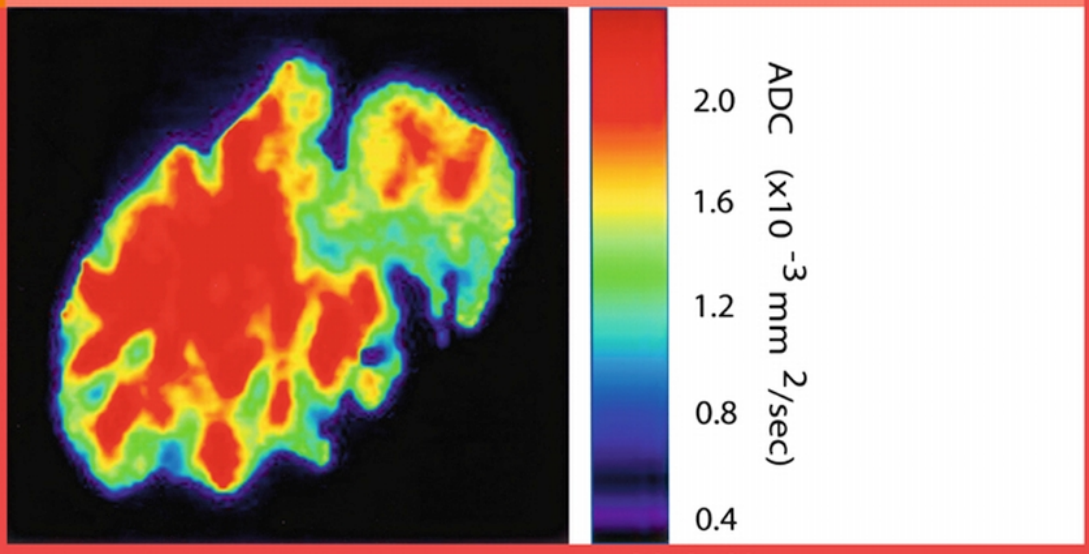

M.A. Hayat
Editor

Springer

Methods of Cancer Diagnosis, Therapy, and Prognosis

Methods of Cancer Diagnosis, Therapy, and Prognosis

Volume 7

For other titles published in this series, go to
www.springer.com/series/8172

Methods of Cancer Diagnosis, Therapy, and Prognosis

Volume 7

Methods of Cancer Diagnosis, Therapy, and Prognosis

General Overviews, Head and Neck Cancer and Thyroid Cancer

Edited by

M.A. Hayat
Department of Biological Sciences,
Kean University, Union, NJ, USA

Springer

Editor
M.A. Hayat
Department of Biological Sciences
Kean University
Union, NJ, USA

ISBN 978-90-481-3185-3 e-ISBN 978-90-481-3186-0

Library of Congress Control Number: 2009941464

Printed on acid-free paper

springer.com

New technology, for better or for worse, will be used, as that is our nature.

Lewis Thomas

You have been given the key that opens the gates of heaven; the same key opens the gates of hell.

Writing at the entrance to a Buddhist temple

Contributors

Laurent Alberti
Centre Léon Bérard, 28, Rue Laennec, 69008 Lyon, France

Juan Luis Alcázar
Department of Obstetrics and Gynecology, Clínica Universitaria de Navarra, University of Navarra, Avenida Pio XII, 36 Pamplona 31008, Spain

Damien Ambrosetti
Service d'Anatomie Pathologique, Hôpital Pasteur, 30 Avenue de la Voie Romaine, 06000 Nice, France

Yaser Atlasi
Department of Genetics, Faculty of Basic Science, Tarbiat Modares University, P.O. Box: 1411-175, Tehran, Iran

Allyson C. Baker
University of Alabama at Birmingham, NP 3537, 619 19th Street South, Birmingham, AL 35249, USA

Surinder K. Batra
Department of Biochemistry and Molecular Biology, College of Medicine, Eppley Cancer Institute 7052 Durham Research Center, University of Nebraska Medical Center, 985870 Nebraska Medical Center, Omaha, NE 68198-5870, USA

Vladimir Bilim
Department of Urology, Yamagata University Faculty of Medicine, Iida-nishi 2-2-2, Yamagata 990-9585, Japan

Michael J. Birrer
Cell and Cancer Biology, National Cancer Institute, 37 Convent Drive, Room 1068, Bethesda, MD 20892, USA

Jean-Yves Bla
INSERM U590, Centre Léon Bérard, Rue Laennec, 69008 Lyon, France

Malte Böhm
Department of Urology, Otto-von-Guericke Universität, Leipziger Str. 44, D-39120 Magdeburg, Germany

Kristin L.M. Boylan
Department of Laboratory Medicine and Pathology, The University of Minnesota Medical School, Minneapolis, MN 55455, USA

Laura Brousseau
Centre Léon Bérard, 28, rue Laennec, 69008 Lyon, France

Fanny Burel-Vandenbos
Service d'Anatomie Pathologique, Hôpital Pasteur, 30 Avenue de la Voie Romaine, 06000 Nice, France

Gabriel Caponetti
Department of Pathology, Baystate Medical Center, Tufts School of Medicine, 759 Chestnut Street, Springfield, MA 01109, USA

Nathalie Cardot-Leccia
Service d'Anatomie Pathologique, Hôpital Pasteur, 30 Avenue de la Voie Romaine, 06000 Nice, France

Philippe Cassier
Hôpital Edouard Herriot, Service d'Oncologie Médicale, Pavillon E, 5 Place d'Arsonval, 69003 Lyon, France

Tridib Chakraborty
Division of Biochemistry, Department of Pharmaceutical Technology, Jadavpur University, P.O. Box 17028, Calcutta 700032, West Bengal, India

Malay Chatterjee
Division of Biochemistry, Department of Pharmaceutical Technology, Jadavpur University, P.O. Box 17028, Calcutta 700032, West Bengal, India

David Chhieng
University of Alabama at Birmingham, 619 19th Street South, Birmingham, AL 35249, USA

William A. Cliby
Division of Gynecologic Surgery, Department of Obstetrics and Gynecology, Mayo Clinic, 200 First Street SW, Rochester, MN 55905, USA

Joseph P. Connor
University of Wisconsin-Madison, CSC H4/656, 600 Highland Avenue, Madison, WI 53792, USA

Isabelle Ray Coquard
Centre Léon Bérard, 28, Rue Laennec, 69008 Lyon, France

Dean Daya
Department of Pathology and Nuclear Medicine, Henderson General Hospital, McMaster University, 711 Concession Street, Hamilton, Ontario L8V IC3, Canada

Anne-Valérie Decouvelaere
Centre Léon Bérard, 28, Rue Laennec, 69008 Lyon, France

Bruce J. Dezube
Department of Medicine, Beth Israel Deaconess Medical Center, Harvard Medical School, Boston, MA 02215, USA

Sean C. Dowdy
Division of Gynecologic Surgery, Department of Obstetrics and Gynecology, Mayo Clinic, 200 First Street SW, Rochester, MN 55905, USA

Armelle Dufresne
Hôpital Edouard Herriot, Service d'Oncologie médicale, Pavillon E, 5 Place d'Arsonval, 69003 Lyon, France

Jérôme Fayette
Centre Léon Bérard, 28, Rue Laennec, 69008 Lyon, France

Michael Fiegl
Department of Internal Medicine/ Oncology, Academic Natters Hospital, In der Stille 20, A-6161 Natters, Austria

Olivier Gheysens
Department of Nuclear Medicine, University Hospital KU Leuven, Herestraat 49, B-3000 Leuven, Belgium

Elfriede Greimel
Department of Obstetrics and Gynecology, Medical University Graz, Auenbruggerplatz 14, A-8036 Graz, Austria

Perry W. Grigsby
Department of Radiation Oncology, Mallinckrodt Institute of Radiology, Washington University School of Medicine, Box 8224, 4921 Parkview Place, Lower Level, St. Louis, MO 63110, USA

William E. Grizzle
University of Alabama at Birmingham, 619 19th Street South, Birmingham, AL 35249, USA

Jennifer A. A. Gubbels
University of Wisconsin-Madison, CSC H4/656, 600 Highland Avenue, Madison, WI 53792, USA

Christian Hafner
Department of Dermatology, University of Regensburg, Franz-Josefstrauss-Allee 11, Regensburg 93042, Germany

Hiroshi Hashimoto
Department of Pathology and Oncology, School of Medicine, University of Occupational and Environmental Health, 1-1 Iseigaoka, Yahatanishi-ku, Kitakyushu 807-8555, Japan

Juliette Haudebourg
Service d'Anatomie Pathologique, Hôpital Pasteur, 30 Avenue de la Voie Romaine, 06000 Nice, France

Masanori Hisaoka
Department of Pathology and Oncology, School of Medicine, University of Occupational and Environmental Health, 1-1 Iseigaoka, Yahatanishi-ku, Kitakyushu 807-8555, Japan

Andrew Horvai
University of California, San Francisco, 1600 Divisadero Drive, B220, San Francisco, CA 94115, USA

Kazuhiko Ino
Department of Obstetrics and Gynecology, Nagoya University Graduate School of Medicine, 65 Tsurumai-cho, Showa-ku, Nagoya 466-8550, Japan

Toshiyuki Itoi
Department of Urology, Yamagata University Faculty of Medicine, Iida-nishi 2-2-2, Yamagata 990-9585, Japan

Seyed Mehdi Jafarnejad, Department of Genetics, Faculty of Basic Science, Tarbiat Modares University, P.O. Box: 1411-175, Tehran, Iran

Hiroaki Kajiyama
Department of Obstetrics and Gynecology, Nagoya University Graduate School of Medicine, 65 Tsurumai-cho, Showa-ku, Nagoya 466-8550, Japan

Shingo Kato
Research Central Hospital for Charged Particle Therapy, National Institute of Radiological Sciences, 4-9-1 Anagawe, Inage-ku, Chiba 263-8555, Japan

Fumitaka Kikkawa
Department of Obstetrics and Gynecology, Nagoya University Graduate School of Medicine, 65 Tsurumai-cho, Showa-ku, Nagoya 466-8550, Japan

Seung Hyup Kim
Department of Radiology, Seoul National University Bundang Hospital 300, Gumi-dong, Bundang-Gu, Songnam-si, Gyeonggi-do, 463-707, Korea

Tobias Klatte
Department of Urology, Otto-von-Guericke Universität, Leipziger Str. 44, D-39120 Magdeburg, Germany

Michael Landthaler
Department of Dermatology, Regensburg University Medical Center, Franz-Josef-Strauss-Allee 11, Regensburg 93053, Germany

Hak Jong Lee
Department of Radiology, Seoul National University Bundang Hospital 300, Gumi-dong, Bundang-Gu, Songnam-si, Gyeonggi-do, 463-707, Korea

Subodh M. Lele
Department of Biochemistry and Molecular Biology, College of Medicine, Eppley Cancer Institute, 7052 Durham Research Center, University of Nebraska Medical Center, 985870 Nebraska Medical Center, Omaha, NE 68198-5870, USA

Jonathan S. Lewin
Department of Radiology, Duke University Medical Center, Duke North-Room 1417, Erwin Road, Durham, NC 27710, USA

Lilie L. Lin
Department of Radiation Oncology, Mallinckrodt Institute of Radiology, Washington University School of Medicine, 4921 Parkview Place, Lower Level, St. Louis, MO 63110, USA

Yair Lotan
Department of Urology, The University of Texas Southwestern Medical Center, 5323 Harry Hines Boulevard, Dallas, TX 75390, USA

Ryo Maruyama
Department of Urology, Yamagata University Faculty of Medicine, Iida-nishi 2-2-2, Yamagata 990-9585, Japan

Atsuji Matsuyama
Department of Pathology and Oncology, School of Medicine, University of Occupational and Environmental Health, 1-1 Iseigaoka, Yahatanishi-ku, Kitakyushu 807-8555, Japan

Milena M. Maule
Cancer Epidemiology Unit, CeRMS and CPO-Piemonte, University of Turin, 10126 Torino, Italy

Jiri Mayer
Department of Internal Medicine/ Oncology, Academic Natters Hospital, In der Stille 20, A-6161 Natters, Austria

Pierre Méeus
Centre Léon Bérard, 28, Rue Laennec, 69008 Lyon, France

Elmar M. Merkle
Department of Radiology, Duke University Medical Center, Duke North-Room 1417, Erwin Road, Durham, NC 27710, USA

Jean-Francois Michiels
Service d'Anatomie Pathologique, Hôpital Pasteur, 30 Avenue de la Voie Romaine, 06000 Nice, France

Samuel C. Mok
Department of Gynecologiz Oncology, M.D. Anderson Cancer Center, T403908, 1515 Holcombe Boulevard, Houston, TX 77030, USA

Felix M. Mottaghy
Department of Nuclear Medicine, University Hospital KU Leuven, Herestraat 49, B-3000 Leuven, Belgium

Seyed Javad Mowla
Department of Genetics, Faculty of Basic Science, Tarbiat Modares University, P.O. Box: 1411-175, Tehran, Iran

Akihiro Nawa
Department of Obstetrics and Gynecology, Nagoya University Graduate School of Medicine, 65 Tsurumai-cho, Showa-ku, Nagoya 466-8550, Japan

Rendon C. Nelson
Department of Radiology, Duke University Medical Center, Duke North-Room 1417, Erwin Road, Durham, NC 27710, USA

Torsten O. Nielsen
PGY3 Anatomical Pathology, 1500 JPPN Vancouver General Hospital, 899 12th Avenue W, Vancouver, BC V5Z 1M9, Canada

Tatsuya Ohno
Research Central Hospital for Charged Particle Therapy, National Institute of Radiological Sciences, 4-9-1 Anagawe, Inage-ku, Chiba 263-8555, Japan

Yasemin Ozluk
Department of Pathology, Istanbul University, Faculty of Medicine, Capa, Topkapi 34390, Istanbul

Manish S. Patankar
University of Wisconsin-Madison, CSC H4/656, 600 Highland Avenue, Madison, WI 53792, USA

Liron Pantanowitz
Department of Pathology, Baystate Medical Center, Tufts School of Medicine, 759 Chestnut Street, Springfield, MA 01109, USA

Louis L. Pisters
Department of Urology, The University of Texas M.D. Anderson Cancer Center, 1515 Holcombe Boulevard, Houston, TX 77030, USA

Moorthy P. Ponnusamy
Department of Biochemistry and Molecular Biology, College of Medicine, Eppley Cancer Institute, 7052 Durham Research Center, University of Nebraska Medical Center, 985870 Nebraska Medical Center, Omaha, NE 68198-5870, USA

Francine M. Quan
Division of Hematology/Oncology, East Carolina University Brody School of Medicine, 600 Moyle Boulevard, Greenville, NC 27858, USA

Walter D.Y. Quan
Division of Hematology/Oncology, East Carolina University Brody School of Medicine, Brody 3E-127, 600 Moyle Boulevard, Greenville, NC 27858, USA

Ajay Rana
Division of Biochemistry, Department of Pharmaceutical Technology, Jadavpur University, P.O. Box 17028, Calcutta 700032, West Bengal, India

Basabi Rana
Division of Biochemistry, Department of Pharmaceutical Technology, Jadavpur University, P.O. Box 17028, Calcutta 700032, West Bengal, India

Dominique Ranchère
Centre Léon Bérard, 28, Rue Laennec, 69008 Lyon, France

Lorenzo Richiardi
Cancer Epidemiology Unit, University of Turin, Via Santena 7, 10126 Torino, Italy

Alexander Roesch
Department of Dermatology, Regensburg University Medical Center, Franz-Josef-Strauss-Allee 11, Regensburg 93053, Germany

Albert Rübben
Department of Dermatology, University Hospital RWTH Aachen, Pauwelsstrasse 30, D-52074 Aachen, Germany

Naoki Sasaki
Department of Obstetrics and Gynecology, National Defense Medical College, 3-2 Namiki, Tokorozawa, Saitama 359-8513, Japan

Kiyosumi Shibata
Department of Obstetrics and Gynecology, Nagoya University Graduate School of Medicine, 65 Tsurumai-cho, Showa-ku, Nagoya 466-8550, Japan

Ajay P. Singh
Department of Biochemistry and Molecular Biology, College of Medicine, Eppley Cancer Institute, 7052 Durham Research Center, University of Nebraska Medical Center, 985870 Nebraska Medical Center, Omaha, NE 68198-5870, USA

Amy P.N. Skubitz
Department of Laboratory Medicine and Pathology, The University of Minnesota Medical School, MMC 609, 420 Delaware Street, SE, Minneapolis, MN 55455, USA

Keith M. Skubitz
Department of Medicine, The Masonic Cancer Center, Minneapolis, MN 55455, USA

Philippe E. Spiess
Department of Urology, The University of Texas M.D. Anderson Cancer Center, 1515 Holcombe Boulevard, Houston, TX 77030, USA

Michael P. Stanley
Cell and Cancer Biology, National Cancer Institute, 37 Convent Drive, Room 1068, Bethesda, MD 20892, USA

Toru Sugiyama
Department of Obstetrics and Gynecology, National Defense Medical College, 3-2 Namiki, Tokorozawa, Saitama 359-8513, Japan

Marie-Pierre Sunyach
Centre Léon Bérard, 28, Rue Laennec, 69008 Lyon, France

Monalisa Sur
Department of Pathology and Nuclear Medicine, Henderson General Hospital, McMaster University, 711 Concession Street, Hamilton, Ontario L8V IC3, Canada

Robert S. Svatek
Department of Urology, The University of Texas Southwestern Medical Center, 5323 Harry Hines Boulevard, Dallas, TX 75390, USA

Masashi Takano
Department of Obstetrics and Gynecology, National Defense Medical College, 3-2 Namiki, Tokorozawa, Saitama 359-8513, Japan

Nizar M. Tannir
Department of Urology, The University of Texas M.D. Anderson Cancer Center, 1515 Holcombe Boulevard, Houston, TX 77030, USA

Jefferson Terry
PGY3 Anatomical Pathology, 1500 JPPN Vancouver General Hospital, 899 12th Avenue W, Vancouver, BC V5Z 1M9, Canada

Yoshihiko Tomita
Department of Urology, Yamagata University Faculty of Medicine, Iida-nishi 2-2-2, Yamagata 990-9585, Japan

Hiroshi Tsuda
Department of Obstetrics and Gynaecology, Osaka City General Hospital, 2-13-22 Miyakojimahondori, Miyakojima, Osaka 5340021, Japan

Thomas Vogt
Department of Dermatology, Regensburg University Medical Center, Franz-Josef-Strauss-Allee 11, Regensburg 93053, Germany

Eiko Yamamoto
Department of Obstetrics and Gynecology, Nagoya University Graduate School of Medicine, 65 Tsurumai-cho, Showa-ku, Nagoya 466-8550, Japan

Preface

This volume presents a detailed survey of various methodologies related to diagnosis, therapy, and prognosis of ovarian cancer, renal cancer, urinary bladder cancer, and cervical uterine cancer, while the already published Volumes 1–5 detail similar aspects of breast, lung, prostate, liver, gastrointestinal, colorectal, and biliary tract carcinomas.

It is well established that cancer is the deadliest of human diseases. The following estimated global incidence of seven types of cancers discussed in this volume indicated the seriousness of this malignancy.

Cervical uterine cancer 493,342

Urinary bladder cancer 357,000

Leukemia 300,522

Renal cancer 208,480

Ovarian cancer 204,499

Melanoma of skin 160,177

Multiple Myeloma 85,704

As in the previous five volumes of this series, each chapter is written by distinguished, practicing clinicians/surgeons/pathologists who provide methodologies for diagnosis and treatment of eight types of cancers. This volume was written by 94 oncologists representing 13 countries. Their practical experience highlights their writings, which should build and further the endeavors of the readers in this important area of disease. The text of each cancer type is divided into subheadings for the convenience of the readers. It is my hope that the current volume will join the preceding volumes of this series for assisting in the more complete understanding of globally relevant cancer syndromes. There exists a tremendous, urgent demand by the public on the scientific community to address cancer prevention, diagnosis, treatment, and hopefully cures.

I am grateful to the contributors for their promptness accepting my suggestions. I respect their dedication and diligent work in sharing their invaluable knowledge with the public through this series. Each chapter provides unique individual, practical knowledge based on the expertise and practical experience of the authors. The chapters contain the most up-to-date practical and theoretical information. I hope that these handbooks will assist the practicing readers in their clinical work.

I am thankful to Dr. Dawood Farahi and Dr. Kristie Reilly for recognizing the importance

of scholarship (research, writing, and publishing) in an institution of higher education and for providing the resources for completing this project. I appreciate receiving expert help from Myrna Ortiz and Erin McNally in preparing this volume.

M.A. Hayat
March 2009

Introduction

M.A. Hayat

The enormous burden of liver cancer on society becomes clear by considering the fact that approximately 625,000 new cases of this cancer are diagnosed globally each year. Distressingly, the number of deaths is approximately the same at 598,000 per year. Liver cancer, therefore, is the third most common cause of death from cancer. Survival rates for liver cancer are only 3–5% globally. In the United States, 19,160 new cases of liver cancer and 16,780 deaths were reported for 2007. The major risk factors for this cancer include prior infection with hepatitis B and C viruses, with the former more prevalent. Dietary exposure to fungus *Aspergillus fumigatus* (aflatoxins) also contributes to the incidence of liver cancer in many parts of the world. Tobacco use is the most serious preventable cause of cancer, as its use causes cancer of the lung, throat, mouth, liver, pancreas, urinary bladder, stomach, kidney, as well as other types. Alcohol-induced liver injury is another major risk factor for hepatocellular carcinoma (HCC).

In view of these devastating statistics, the urgency of deciphering the molecular mechanism underlying this disease, perfecting reliable diagnostic methods, understanding risk factors, developing effective targeted drugs, improving other treatments, assessing the effectiveness of therapies, and providing improved care for post-treatment patients, becomes apparent. This volume provides up-to-date information on the above-mentioned aspects of liver cancer; specifically, details of the methodologies used are included. The other seven volumes in this series provide similar information on other types of cancers.

This series of handbooks has taken the unique approach of discussing cancer diagnosis, treatment, and prognosis in the same volume. It is pointed out that this vast subject cannot be fully discussed by only one author. This is the primary reason for inviting a large number of oncologists/clinicians/surgeons to write each of the eight volumes of this series of handbooks. Another advantage of involving more than one author is to present different points of view on a specific controversial aspect of cancer. I hope these goals were accomplished in this and other published volumes of this series.

Contents of Volumes 1, 2, 3, 4, 5 and 6

Volume 1

Volume 2

Volume 3

Volume 4

Volume 5

Volume 6

Contents

Therapy

Prognosis

Therapy

Prognosis

Part I
General Methods and Overviews

Diagnosis

1
Role of RNA Interference in Understanding the Molecular Basis of Cancer

Jeffrey P. MacKeigan and L. Alex Gaither

MECHANISM OF RNA INTERFERENCE

The mechanism of RNA interference (RNAi) has been clearly established in mammalian cells since RNAi was discovered in *Caenorhabditis elegans* in 1998 (Figure. 1.1) (Fire et al. 1998). RNAi is a process of sequence specific post-transcriptional gene silencing which evolved as a host defense from viral entry and regulation of transposable genetic elements (Waterhouse et al. 2001). The double stranded RNA (dsRNA) from a transposon, virus, or plasmid is processed into short dsRNAs which initiate a series of molecular events in the cell to suppress target mRNA expression. The first event involves the binding to a ribonuclease III like protein called Dicer which cleaves the dsRNA into short interfering RNAs (siRNAs) of 19–25 base pairs long with characteristic 3′-dinucleotide overhangs. The siRNAs become incorporated into a large multiprotein complex known as the RNA-induced silencing complex (RISC) that directs the antisense siRNAs to their respective target genes and induces mRNA cleavage or translational repression. Cleavage is enabled after an ATP-helicase unwinds the RNAi duplex and the degree of complementarity between the sequences determines the efficacy of binding. A significant sequence match will result in a site-specific cleavage event, while mismatches in the sequences will prevent efficient cleavage. In some cases a weak RNAi interaction is necessary if complete loss of a protein is toxic to cells while its partial knock down is required for a particular phenotype.

Long dsRNA molecules (>500 bp) can be added directly to *C. elegans* or *Drosophila* by injection, soaking in a solution of dsRNA, or feeding them bacteria carrying dsRNA. In contrast, the direct use of siRNA in mammalian cells can only be achieved with 19–25 base pair oligonucleotides because siRNAs longer than 30 base pairs induces a significant interferon response (Elbashir et al. 2001). The siRNAs are produced by either chemical synthesis, enzymatic cleavage *in vitro*, or expression of a plasmid backbone. These siRNA molecules are Dicer products and enter the RNAi pathway at the level of the RISC complex. There are concerns that while this process does work effectively, it

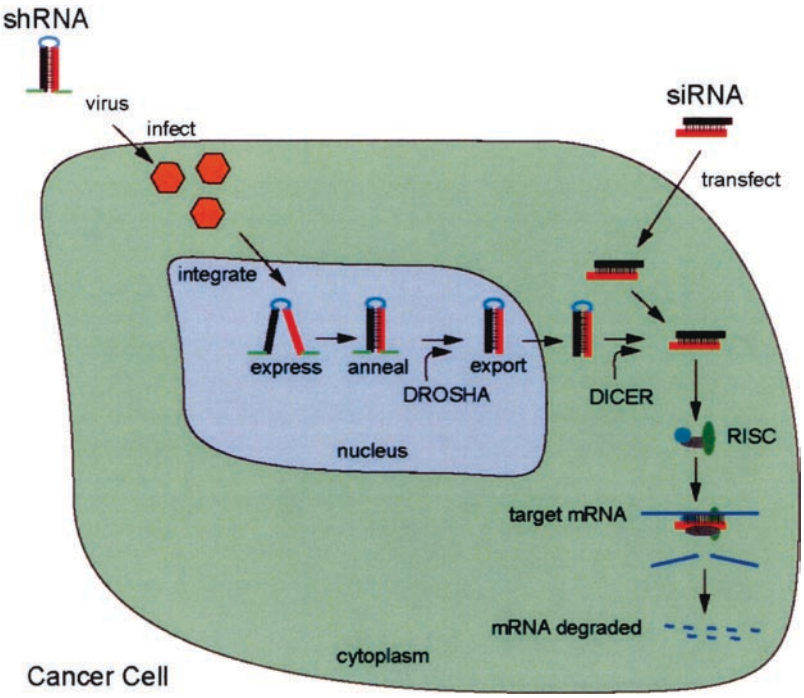

FIGURE 1.1. Mechanism of RNAi (siRNA versus shRNA). shRNAs must be packaged into a virus, infect a population of cells, integrate into the host genome, express, anneal into the hairpin structure, cleaved by Drosha, exported from the nucleus to the cytoplasm, cleaved by Dicer into the active 21mer siRNA molecule. These two processes merge with the siRNA being loaded into RISC, allowing targeted degradation of the mRNA template

is suggested to be an inefficient process to achieve knock down (Siolas et al. 2005). Because Dicer is tethered directly to the activation of the RISC complex, bypassing Dicer could result in fewer siRNAs being taken up by RISC (Miyagishi and Taira 2003). It remains to be determined if a Dicer activated RISC is better at targeting mRNA knock down than siRNAs alone, in particular for RNAi resistant transcripts.

The structure of effective siRNAs has been defined to include features of a 2-nucleotide overhang on both the 3′ ends, phosphorothiolates, and sequence specific algorithms that filter for certain bases (3′seed regions) siRNAs are introduced into mammalian cells by lipid-based formulations, electroporation, or peptide linkage. There are several reports describing the efficacy of siRNA delivery into mammalian cells including using lipid based transfection in small multiwell formats (Borawski et al. 2007). A major drawback of siRNAs is that they transiently knock down gene expression, but despite this, siRNAs have been used effectively in many different mammalian cells, primary cells, stem cells, and even *in vivo*.

Because RNAi mediated knock down in mammalian cells is transient and directly related to the proliferation rate of the cells, viral vector-based RNAi reagents were engineered to stably integrate into the genome. The initial vectors were designed with RNA polymerase III promoters that express sense and antisense strands in

tandem or in a single short hairpin RNAs (shRNA). These shRNAs are processed by Dicer to produce 21 bp siRNAs. Both tandem and single hairpin vector systems are functional in mammalian cells, but the shRNA vectors are more efficient than the tandem system at maintaining stable knock down (Mittal 2004). The shRNA expression system is a potent inducer of RNAi and can efficiently enter hard to transfect cell lines. This is likely due to the use of Dicer to process the shRNA and directly incorporate the siRNAs into RISC. Initial screens used plasmid based delivery systems, but the plasmid alone approach has been rapidly replaced with lenti-, retro-, or adenoviral based vectors. Viral mediated transduction is much more efficient than plasmid based transfection and can infect a wider variety of cell types, such as primary cells (Brummelkamp et al. 2002b).

RNAI AS A CELL BASED SCREENING TOOL

RNAi regulates gene expression at the transcriptional and translational level(s) by binding to mRNA and either inducing mRNA degradation or translation suppression by ribosomal drop off. RNAi is a sequence specific process and can selectively target mRNAs. The ability of RNAi to reduce gene expression in a selective manner makes its use in cell based assays a powerful tool for the study of genetic loss-of-function phenotypes. The algorithms for RNAi generation have dramatically improved in the past several years, so has the ability to obtain potent and specific RNAi reagents from various commercial sources. Currently, genome-wide RNAi tools have been developed and used successfully in cell based assays for novel target discovery, pathways analysis, and compound mechanism of action experiments. The ability to screen genome scale libraries in disease relevant cell based systems can lead to rapid target discovery. Loss of enzymatic activity is the primary effect of most small molecules and RNAi approaches essentially phenocopy pharmacological target inhibition. Although a compound screen can identify a phenotype, it will not always deliver the cellular target. In contrast, the target from a RNAi screen is typically known, for which a compound could then be directly synthesized. A major liability of compound screens is lack of knowledge regarding the targets the molecules interact within a cell. RNAi cell-based screens have a clear advantage over compound screens because the phenotype being measured is tethered directly to a target, and suppression of the target is a proof-of-principle that a target is validated.

The introduction of long dsRNA (>30 bp) in mammalian cells induces an interferon response which results in global changes in gene expression, and can be cytotoxic in some cell types (Elbashir et al. 2001). One way in which the interferon response can be avoided is by using siRNA as duplexes introduced into cells by transfection or of plasmids in the form of short-hairpin RNA (shRNA). shRNA is processed by Dicer to generate siRNAs in the cell, which are incorporated into the RISC complex. The antisense strand is then directed to its cognate mRNA in a sequence specific fashion. Using these RNAi approaches several proteins have been identified that directly mediate tumorigenesis. Some examples include the role of Aurora B kinase in RAS-transformed cell lines and mutant K-RAS in the pancreatic carcinomas

(Brummelkamp et al. 2002a; Kanda et al. 2005). The systematic and parallel analysis of all human genes across tumor cells or neoplastic models of cancer provides a significant opportunity to identify new targets that regulate tumor cell growth. RNAi libraries are not only valuable in cell based screens, but can also be taken *in vivo* using viral based plasmids expressing shRNAs or complex lipid formulations carrying modified siRNA duplexes.

RNAi reagents can be made synthetically, purchased from commercial sources, or obtained from academic institutions. RNAi screening libraries are available as siRNAs, either as individual duplexes or combinations of four siRNAs, and shRNA vectors as nonviral plasmids or viruses (retroviral, adenoviral, or lentiviral). siRNA reagents can be synthesized or generated from cDNAs by RNase III digestion, purchased, and/or cloned by the investigator (Yang et al. 2002). For short term acute phase assays, siRNAs are the reagent of choice given that they are easy to use across a wide range of cell lines and provide significant knock down for up to 120 h. As cells divide, siRNAs are diluted upon each successive cell division as they are not replicated, and eventually lose their activity in rapidly proliferating cells. When stable knock down is required shRNAs are used for the reason that the plasmid backbones contain selectable markers and integrate into the genomes that are copied with the cellular DNA. shRNAs are also useful to transduce hard to transfect primary cells. Because more immortalized cell lines are not likely representative of organically derived tumors, the ability to introduce shRNAs in primary tumors may reflect a phenotype more closely associated with physiologically relevant tumor cells.

Screening RNAi libraries can be done in several distinct ways. The first is by screening one reagent per well with more than one reagent targeting the same gene (gene-by-gene screens). These formats are typically set as four or more independent reagents targeting each gene and arrayed in 96 or 384 well plates (Fig. 1.2). Plasmid based shRNAs, viral expressed shRNAs, and siRNAs have all been set up using this format. There are several ways in which the RNAi reagents are screened using the multiwell approach. First, forward transfection is where the reagents are added to cells previously plated in the multiwell plates. This was the method of choice until several groups demonstrated that a "reverse" transfection procedure provides significantly higher transfection efficiencies across multiple cell types (Amarzguioui 2004; Ovcharenko et al. 2005). The reverse procedure is distinct from the forward approach in that the lipid and RNAi reagent are mixed and plated on tissue culture plates, and cells are dispensed down on top of the siRNA-lipid mixture. For viral particle transductions, lipid mediated transfection is not necessary and the forward method is used because viral uptake is a very efficient process in mammalian cells.

The second way in which RNAi screens are performed is using a pooling approach. siRNAs or shRNA viral particles, typically not plasmids, are mixed together where the multiple independent RNAi reagents are mixed in a single well. This is done for several reasons: (1) pooling reagents and gene targets dramatically reduces the number of wells that need to be screened; reducing the amount of wells screened saves both time and screen costs; (2) pooling siRNAs has been shown to improve the efficacy

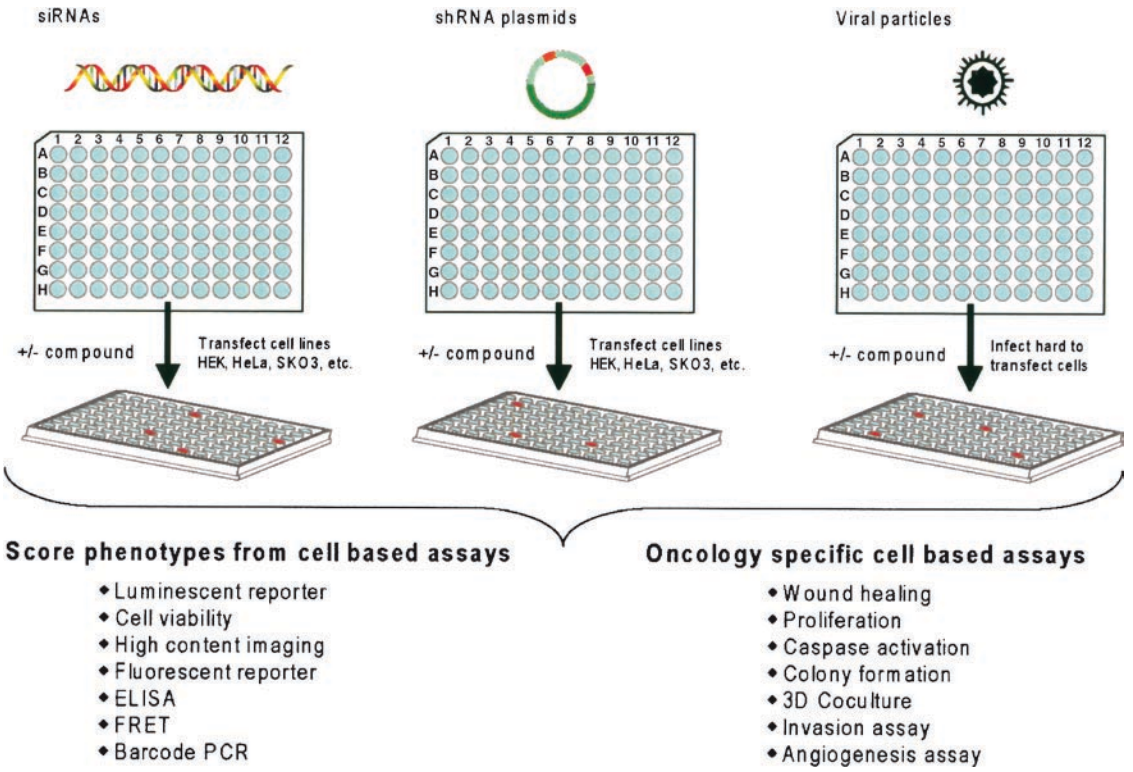

FIGURE 1.2. RNAi approaches for screening. Arrayed RNAi libraries in 96 (or 384) well format are transfected (siRNA or plasmid shRNA) or transduced (shRNA virus) into cells. After a period of time the assay is scored for observable phenotypes that score significantly above the plate (or plates) median (red wells). Lower panels display a series of assays previously reported in the literature

and reduce the off-target effects associated with using a single siRNA to knock down a gene. Pooling is not limited to mixing reagents where they all target the same gene. It has been shown that pooling can be done with entire shRNA libraries (Brummelkamp et al. 2006). The libraries are transfected into cells that can be selected for a phenotype of interest. Subsequently, the wells that score a phenotype are followed up and the unique genes targeted in the well can be further analyzed. The individual gene that contributes to the phenotype will be identified using PCR against the gene-specific shRNA. An alternative approach to pooled screens is the use of oligonucleotide microarrays and referred to as barcode screening (Paddison et al. 2004). Pooled shRNAs each carrying a unique DNA sequence, or barcode, are transfected into cells and divided into populations across many plates. The transfected cells containing different barcodes are PCR amplified, labeled with different fluorochromes, and hybridized to microarrays containing barcode specific probes. The difference in the ratios of fluorochromes predicts the shRNAs with altered frequencies and identifies genes that contribute to the phenotype understudy. Because the relative abundance of the individual shRNAs is determined, it allows for the barcode screens to be used for both positive (selected for) and negative (selected against) selection.

The utility of high throughput RNAi based screens is the flexibility of cell based assays available for this technology. From the simple cell death assays, such as ATP measurement, to complex high content screens, if a cell based assay has been effectively scaled into a 96 or 384 well format the assay can be screened using RNAi knockdown. There have been several reports of genome scale screens being run using reporter genes, ELISA, ATP quantification, and cell viability (Aza-Blanc et al. 2003; Kittler et al. 2004; Zheng et al. 2004). For complex high content assays, several microscopy based screens have also been reported (Kittler et al. 2004; Moffat et al. 2006). The complexity of the cell based assay used is only limited by the ability to miniaturize the format. For drug discovery in oncology, RNAi based screens can provide a system for target validation, target identification, compound mechanism of action (MOA), and lead optimization of compounds (Bartz et al. 2006). A constant challenge for drug development in oncology is identifying novel drug targets that are genetically relevant to the disease state. Until RNAi based screening became available, target discovery relied on exploiting changes in gene expression, chromosomal abnormalities, mutational analysis, or genetic variation of tumors. Although these approaches have historically been successful, they do not select for targets that are always amenable for drug development. By design, RNAi based screens reduce the protein levels of a specific protein, which mimics the pharmacological inhibition provided by a compound or small molecule inhibitor. It should be noted that reduction of protein levels in the cell is not the same as small molecular weight binding by a compound. A compound typically inhibits its enzymatic activity. Thus, a protein bound by a compound could remain in its native context or bind additional proteins (dominant gain of function, i.e.-cyclosporine A) which might lead to unexpected phenotypes in the cell (Liu et al. 1991).

Critical to the identification of new druggable targets in oncology is the identification of the major oncogenic events that lead to tumor progression. The challenge with this approach is finding the genes that directly drive neoplastic phenotypes without affecting the surrounding normal cells. RNAi screens can be of considerable use for identifying targets that exploit oncogene addiction, that kill cancer cells without affecting normal cells, finding synthetic lethal targets, and looking for second targets and/or pathways that can sensitize or cause resistance in response to targeted or cytotoxic therapies. Because RNAi screens can be run in an automated high-throughput fashion, many different cell lines can be screened in parallel. Thus, the causality of a gene which is toxic in a specific tumor lineage can be more easily exploited.

RNAI TO UNDERSTAND COMPOUND MECHANISM OF ACTION

One of the advantages of RNAi based screens is the ability to study pathway-based gene knockdown in the presence of a small molecular inhibitor. For example, small molecular inhibitors that target IAP (inhibitor of apoptosis) proteins combined with a siRNA based screen revealed the compounds mechanism of action (Gaither et al. 2007). The IAP proteins are

overexpressed in a wide variety of cancers and function in several ways to maintain uncontrolled cell growth. It has been shown that when a cancer cell is dependant on the overexpression of IAP proteins to suppress apoptosis, then knockdown of IAP proteins sensitized the cells to apoptotic triggers (Crnkovic-Mertens et al. 2003). Novartis has developed a peptidomimetic molecule, LBW242, which binds to XIAP and cIAP1 with nM affinities (Chauhan et al. 2007). However, as a single agent the compound only induces apoptosis in a narrow range of tumor cells. In the presence of an apoptotic trigger such as a cytotoxic, only then do the cells undergo programmed cell death. In an attempt to determine why LBW242 functions poorly as a single agent cell killer, a pathway-based siRNA screen was run to find genes that when knocked down could sensitize or reduce the activity of the compound. The goal of this approach was to identify if a gene(s) and or pathway(s) when knock downed could predict why LBW242 was not as effective as single agent therapy (Gaither et al. 2007).

To run a compound based RNAi screen, significant effort needs to be put on assay development and optimization. Parameters associated with an siRNA screen are altered by the presence of a compound, thus all transfection conditions (lipid, concentration, dilutions, etc.), growth conditions (cell density, timing, media, plate type, etc.), and assay conditions (type of assay, reagent used, etc) need to be determined on a per screen basis (Borawski et al. 2007). As each assay is distinct in its readout, time of the assay, and cell lines used, it is essential that every assay be optimized independently. Another critical parameter is determining the order of siRNA transfection and compound addition prior to running the assay. For the LBW242 siRNA screen, a dose response of LBW242 was tested over a time course in the presence of a siRNA transfection cocktail, and cytotoxicity was determined using ATP quantification. The point at which a given concentration of LBW242 could kill >90% of the cells was determined and defined as the EC90 concentration for the screen (20 μM), although it is not a true EC90 on naïve cells (1 μM) (Gaither et al. 2007). The 20 fold difference in EC90 concentration speaks to the importance of defining the screening conditions over a dose response of the molecule understudy. The reason for this effect could be the combinatorial effects of the siRNAs, the lipids, or the siRNA:lipid complex on the compounds activity.

The siRNA apoptosis repressor (or rescue) screen was run in the presence or absence of LBW242 in the SKOV3 ovarian carcinoma cell line. Notably, in the absence of IAP compound one siRNA could kill the cells on its own. This siRNA was cFLIP which is a negative regulator of caspase 8, downstream of the TNF receptor. If loss of cFLIP kills SKOV3 cells, it suggests that the TNF receptor is in a sensitized state, and the negative regulator cFLIP is preventing TNF mediated caspase 8 activation. When the repressor (cFLIP) is knocked down using RNAi, the cells are now permissible to activate extrinsic apoptosis. In contrast, in the presence of 20 μM LBW242, a population of siRNAs could confer complete resistance to LBW242 mediated killing. Interestingly, the siRNAs that caused the resistance phenotype were in the TNF pathway: TNFR, MADD, TNFα, and caspase 8. Also, another RNAi hit was the

target of the compound, XIAP itself. For XIAP to come up as a hit is surprising because the model for how LBW242 functions is to knockdown IAP proteins. It is expected that knockdown of IAP proteins would sensitize the cells to LBW242. The fact that XIAP knockdown rescues cells from LBW24 cell death reveals that the mechanism of LBW242 is more complex than simply XIAP.

As a follow up to the primary siRNA screen, shRNAs were used to generate stable SKOV3 cell lines with XIAP knocked down. Similar to the siRNA screen, the XIAP knockdown cell lines were resistant to LBW242 treatment. Because other genes in the TNF pathway were found in the screen, the logical connection is that XIAP and the TNF pathways are functionally linked to the MOA of LBW242. To test this hypothesis, the XIAP-KD cell line was treated with a dose response of LBW242 and 20 ng/mL of TNFα was spiked onto the cells. The addition of the compound and TNFα, but not TNFα alone, was sufficient to restore sensitivity to LBW242. The LBW242-TNFα treated XIAP-KD cells were not only sensitive to the compound but were also tenfold more sensitive to compound than SKOV3 wild type cells. This striking result indicates that the ability of LBW242 to kill cells directly depending on the cellular response to TNFα mediated signaling. The loss of XIAP is clearly required for LBW242 mediated killing and the XIAP-KD cells are hypersensitive to compound and TNFα, indicating the compound must have a dual role and hit more than one cellular target.

To determine the second target for LBW242, the XIAP-KD cells were transfected with siRNAs directed against cIAP1 and cIAP2 because these are closely related IAPs, and possibly a target for LBW242. A likely hypothesis is that the XIAP-KD cells have another IAP protein that compensates for the loss of XIAP and is upregulated to protect the cells from apoptosis. The XIAP-KD cells were treated with the siRNAs with or without TNFα as the sensitizing agent. If the compound is binding one or both of these IAP proteins, the siRNA transfection should phenocopy the activity of LBW242. The loss of cIAP1 in the XIAP-KD cells treated with TNFα was as toxic as LBW242 treatment under the same conditions. The knockdown of cIAP2 had no observable phenotype and a combined cIAP1-cIAP2 knock down was not anymore effective at cell killing than cIAP1 knock down alone. Western blot analysis found that LBW242 treatment could induce rapid degradation of cIAP1, consistent with the loss of cIAP1 as essential to LBW242 mediated cell death. These results solidified the second target for LBW242 as cIAP1. It should also be noted that LBW242 treatment in SKOV3 cells induced TNFα secretion in an XIAP dependent manner. Thus, in the XIAP-KD cells, LBW242 treatment is not only ineffective at cell killing, but also at inducing TNFα. Together these data demonstrated a dual mechanism of action for the peptidomimetic LBW242. First is the binding to XIAP, which is required for the induction of TNFα, second is the binding and degradation of cIAP1.

This work is a remarkable example of the power of siRNA screens to deconvolute a compound's mechanism of action, even when the target of the compound is known. LBW242 was designed and optimized for binding to XIAP and cIAP1, but the activity of the peptidomimetic compound was not as simple as binding to the target and

inhibiting its activity. The lack of a single agent activity for LBW242 was related to its ability to induce TNFα production and secretion from the cell. In most cases, when TNFα was not induced, LBW242 could not efficiently kill cells. A still unanswered question is the status of XIAP and cIAP1 in the cell lines where LBW242 has no activity. It is possible that the MOA of LBW242 is specific to the ovarian carcinoma lineage and might be the first insight into a novel biological phenomenon of SKOV3 cells. So although the original goal of the screen was achieved, several new insights regarding how to determine a compound MOA were uncovered using a siRNA screening approach.

COMPOUND SENSITIZATION, COMBINATION STRATEGIES AND SYNTHETIC LETHAL RNAI SCREENS

The first oncology combination chemotherapies led to the remission of childhood acute lymphoblastic leukemia (ALL), with the concurrent treatment of methotrexate, vincristine, mercaptopurine, and prednisone (Frei et al. 1965). The same could be said for the combinations of nitrogen mustard, vincristine, procarbazine, and prednisone for lymphoma (Moxley et al. 1967). These studies along with other examples led to a paradigm shift that combinations of conventional chemotherapuetics and molecularly targeted therapies is a rationale approach to drug discovery. The microtubule inhibitor, paclitaxel (Taxol); the platinum-based compounds (cisplatin); and the topoisomerase II inhibitors (etoposide) are each conventional chemotherapuetic agents that promote microtubule polymerization, cause DNA-damage, or inhibit DNA synthesis. A well known targeted therapy is imatinib (Gleevec), which targets the kinase responsible for chronic myeloid leukaemia (CML), known for a chromosomal translocation defect that creates an abnormal fusion protein between BCR and the kinase ABL (Druker et al. 2001; Kantarjian et al. 2002). Based on the success with imatinib it is hoped that molecular targeting of similar signaling defects in other cancers will have the same effect. Therefore, using RNAi molecules (as a molecularly targeted inhibitors) in combination with conventional chemotherapeutics is a rational approach to cancer therapy and at the very least effective in synthetic lethal target identification.

Using a cell-based assay and an ELISA specific for apoptosis, >600 known and putative kinases, along with >200 phosphatases were screened, to first assess their roles in programmed cell death (MacKeigan et al. 2005). This approach identified specific kinases and phosphatases that alone led to a dramatic increase in cell death. In subsequent siRNA screens, cells were sensitized with conventional chemotherapeutics (paclitaxel, cisplatin, etoposide) each with different mechanisms of action. This was effective in not only identifying kinases that enhance cell death, but also the thirteen phosphatases that led to drug resistance regardless of apoptotic stimuli. Although several known targets were identified, the most interesting aspect was the identification of previously unrecognized targets, such as the Akt-related kinase, SGK, or the mitochondrial kinase (PINK1/PARK6). This sensitized siRNA study illustrates a synthetic

lethal relationship between kinases and phosphatases, which can render tumor cells sensitive to chemotherapeutic agents. Similar synthetic lethality screens in mammalian cells in the coming years will no doubt uncover important second targets to known oncogenes (such as KRAS, SRC, MYC, and WNT), growth factor receptors (EGFR/ERBB2, PDGFR, and VEGFR) and molecular pathways (PI3K/AKT, mTOR/S6K, MKK/MAPK, HIF1α, BCL-2). The first tumor suppressor genes, Rb identified in retinoblastoma, or the tumor suppressor p53 each were discovered based on their dramatic effects on the cell cycle or promoting apoptosis. Likewise RNAi is a powerful approach to uncover potential tumor suppressor genes. Using this approach, groups have identified REST, PITX1, and 13 phosphatases with no known previous function and without using a high throughput RNAi screen (Kolfschoten et al. 2005; MacKeigan et al. 2005; Westbrook et al. 2005).

In 2007 three independent studies were reported where siRNA screening was used as a tool for identifying synthetic lethal interactions with chemotherapeutic compounds (Berns et al. 2007; Swanton et al. 2007; Whitehurst et al. 2007). The identification of genes that predict the efficacy of a chemotherapeutic agent is important in several ways. First, it predicts the pathway and possibly the mechanism of a compound beyond its known target. It is well established that compounds have off target effects and pharmacological inhibition of a target is known to induce distinct gene expression profiles in cells. These two effects either combined or in isolation can dramatically affect how a cell responds to compound treatment. Using siRNA screening, a common gene or pathway can be identified that would alter the activity of the compound in cells. Second, siRNA screens can identify biomarkers that predict compound efficacy and elucidate the molecular mechanism of drug resistance in patients. The two main problems associated with chemotherapy treatments are nonresponsive patients and acquired drug resistance. RNAi screens are a valuable tool to identify the genes associated with compound responsiveness through chemical synthetic lethality screens.

In contrast to the chemical lethality rescue screen is the chemical lethality sensitization screen. Whitehurst et al. (2007) reported a siRNA screen identifying the molecular mechanisms of chemoresponsivness using a lung cancer model cell line NCI-H1155. Paclitaxel is a common chemotherapy for epithelial cancers such as non-small-cell lung cancers. Although some patients show a significant response to paclitaxel, most do not. So predicting how patients respond to paclitaxel and what genes are involved in its primary resistance could not only identify markers for patient stratification but provide second targets that could be used in combination therapeutic regimens. This screen identified the proteasome as an important component of paclitaxel efficacy in lung cancer cells. This is consistent with previous reports of bortezomib showing synergy with paclitaxel in the clinic. In addition to proteasome components, the screen also identified microtubule related genes, cell adhesion molecules, genes involved in posttranslational modification, and members of the Ras family. As bortezomib-paclitaxel has been validated in the clinic, it suggests that other classes of targets could also show sensitization in the clinic. In addition, the under- or overexpression

of these genes would predict how a tumor would respond to paclitaxel *in vivo*. In addition to an expression profile analysis, a siRNA screen validates the relevance of an under expressed gene in response to a compound treatment.

Another study examined paclitaxel drug resistance in several distinct cancer lineages (colon, lung, and breast) across kinome and ceramidome siRNA libraries (Swanton et al. 2007). A set of genes targeting the spindle assembly checkpoint caused resistance to paclitaxel, while genes targeting ceramide transport sensitize to the presence of drug. In particular, a ceramide transport protein CERT, when knocked down could sensitize to several cytotoxic compounds in addition to paclitaxel. CERT is upregulated in drug-resistant cells and in refractory ovarian cancer tumors treated with paclitaxel. The identification of CERT not only implicates this gene as a target for chemotherapy-resistant tumors, but also suggests that ceramide metabolism could be a predictor for chemotherapy efficacy in the clinic. Although most tumors arise from a unique set of mutations, it is plausible that common biochemical pathways will be required for tumorigenesis in distinct tumor lineages. Whether a tumor is intrinsically resistant or develops resistance in response to drug treatment, the reversal of the resistance might be defined solely by a metabolic process such as ceramide transport. The implication of this study is that there are tools available to mechanistically determine the genetic basis of drug resistance. This provides hope that through combination therapies or genetic stratification analysis, patients can directly benefit from siRNA based screens in cell based assays.

In the third report, a genome scale shRNA retroviral screen was run in BT-474 cells (HER-2 overexpressing breast cancer cells) to examine which genes could confer resistance to trastuzumab treatment (Berns et al. 2007). Trastuzumab is thought to mediate antibody-dependent cellular cytotoxicity, but its mechanism of action in tumor cells is not entirely understood (Clynes et al. 2000). It has been shown that trastuzumab can inhibit HER-2 cleavage and inhibit PI3K signaling, resulting in a decline of proliferation (Nagata et al. 2004). In spite of this activity, greater than half of all breast cancer patients are refractory to trastuzumab therapy and do not show an improved response to combination therapy with standard of care chemotherapies (Cobleigh et al. 1999). To better understand how and why patients become resistant to trastuzumab therapy is a significant unmet medical need. In addition, identifying biomarkers that would better predict a patient's response to trastuzumab could improve treatment regimens and patient response in the clinic.

Using an shRNA barcode screening approach the authors only identified a single gene that when knocked down could confer resistance to trastuzumab, that gene was PTEN. This result suggested that loss of PTEN plays a dominant role in transtuzumab resistance because it was the only hit out of 8,000 genes analyzed. It is established that decreased PTEN expression results in hyperactivation of the PI3K pathway and can predict 25% of primary breast cancers (Saal et al. 2005). To confirm the RNAi screen, samples from HER-2 overexpression breast cancer patients receiving trastuzumab monotherapy or in combination with chemotherapy were analyzed for PTEN expression and PI3K

mutation status. It was determined that PI3K mutations and PTEN expression were able to predict trastuzumab resistance in the clinic. PTEN low tumors had a worse response to therapy and predicted resistance. Although PTEN loss and PI3K mutations were not seen in the same cells, PI3K activating mutations could also predict treatment outcome. The activating PI3K mutated tumors also showed worse progression-free survival than wild type counter parts. This study has uncovered the importance of PI3K signaling and PTEN expression status for predicting the outcome of trastuzumab therapy in breast cancer patients. RNAi based screens have now been established as a tool for identifying genes that could be used as biomarkers to determine efficacy of cancer therapies in the clinic.

For the many synthetic lethal screens run in model organisms, many new essential genes have been identified; however, these genes are not always suitable targets for drug discovery. Synthetic lethal mutants provide an important genetic tool to choose the best drug targets and with the advent of RNAi now possible in mammalian cells by simply measuring apoptosis, viability or specific signal transduction pathways. Each of these RNAi screens has identified high-priority targets, even if partial inhibition with RNAi leads to a phenotype. The difficulty arises in that further analysis of each gene target requires a return to a reductionist approach to biology and years of mechanistic analysis on each RNAi target. The next step is to functionalize and provide direct evidence of the molecular or biochemical pathway that is altered with interference or inhibition of the gene. The importance of follow-up on RNAi results cannot be overemphasized because in the absence of mechanistic studies the targets cannot be prioritized. Thus, providing the means to include genes important for mitochondrial biology or cell death and exclude genes that are rendered non-selective for normal cells.

PROBLEMS ASSOCIATED WITH RNAI BASED APPROACHES

Unintended gene silencing caused by non-specific mRNA targeting is one of the greatest concerns in the RNAi field. This unintended gene silencing is referred to as off-target effects, and though a real concern, is not considered to be insurmountable (Qiu et al. 2005). Snove and Holen (2004) investigated published siRNA sequences and found that a large percentage of published oligonucleotides had the potential to have off-target effects. This was due to the use of inappropriate programs, such as Basic Local Alignment Search Tool (BLAST), to design oligonucleotides. BLAST searching alone caused numerous examples of unintended silencing due to a homologous stretch of 6–7 base pairs being required for BLAST detection (Snove and Holen 2004). Sequences of 5–10 base pairs that could have 1 or 2 mismatches are missed by BLAST, allowing moderate but substantial hybridization to off-target sequences. Although the use of this database can detect extremely obvious sequence similarities, a significant portion of off target alignments will not be detected, rendering BLAST too insensitive.

Many sequence-associated off-target effects associated with RNAi are not caused

by homology to the coding sequences of other genes. Jackson et al. (2006) showed that seed regions, short stretches of 6–7 base pairs within the 5′ end of the guide strand, perfectly align with regions in the 3′ untranslated regions of other mRNA molecules. Therefore siRNAs that impart off-target effects do so in a manner analogous to that of endogenous microRNAs. siRNA sequences are known to non-specifically degrade mRNA, showing a bias for complementation to 3′ UTR regions within positions 2–7 of their guide strands (Jackson et al. 2006). These off-target effects were not abrogated by decreasing the concentration of siRNA and were observed with both siRNAs and shRNAs. These sequence-specific off-target effects can be overcome and current algorithms must identify and eliminate off-target effects from seed regions.

Qiu et al. (2005) estimated that ~83% of the possible 21 bp oligonucleotides within the coding sequences of the genome are unique. In contrast, this implies that 20% of siRNA sequences show homology to more than one mRNA transcript. This potential for off-target effects presents itself with a set of guidelines that researchers must follow to recapitulate phenotypes observed within an RNAi experiment. The two major validation approaches are through *repetition,* more than two potent siRNA sequences give the same phenotype, and through *rescue*, the phenotype can be restored by re-expression of the gene of interest.

While using RNAi to screen for novel modulators of a particular signal transduction pathway, it is paramount to validate the assay by demonstrating that known components of the pathway return the expected phenotype. For instance, when looking for novel negative regulators of the PI3K/AKT pathway, a crucial step would be the demonstration that knockdown of the phosphatase PTEN behaves similar to the RNAi screen hits. Although dramatic positive results will provide a rather convincing set of data, the same cannot be said for the interpretation of negative results. Negative results most commonly arise from insufficient knockdown; however, negative results could potentially arise from screening errors therefore each siRNA hit should be followed up individually.

Overall, two approaches should be utilized to follow-up any hits within a RNAi screen so as to validate that the phenotype of interest is a product of specific gene knockdown and not simply an off-target effect. First is to use multiple siRNA sequences to confirm the phenotype to the gene target. Use of at least two or three, unique RNAi sequences that give identical knockdown and identical phenotypes is strong evidence that the knockdown and phenotype correlate with each other. Second is to validate each RNAi hit using cDNA or 3′ UTR siRNA for a phenotypic rescue experiment. The latter approach entails designing siRNAs that align to the 3′ UTR of the target gene. The 3′ UTR siRNA will degrade the endogenous mRNA of the target gene, but not target exogenously expressed cDNA. The challenge with this approach is finding siRNAs targeted to the 3′ UTR that generate a significant knockdown as many 3′ UTR siRNAs are not as effective as coding sequence directed siRNAs. Validation of RNAi screen hits requires the phenotypes observed are not false-positives, false-negatives, nor off-target effects. Through validation by repetition and rescue, the RNAi screen hits from

the primary, secondary, and tertiary assays, one can be confident that the knockdown of the specific gene is on target. As RNAi-based screens are a large investment of both resources and time, follow-up of the RNAi screen hits found stands as a crucial step in the success of any large scale genome-wide screen.

In conclusion, RNAi is an excellent tool, when used skillfully, to perform compound sensitization screens to identify new combination strategies for cancer treatment. The promise of this approach is that one can easily identify novel drug targets based on the precise complementary approach of RNAi with either conventional chemotherapeutics or targeted drugs to identify the second dimensional hit, and with that, a new family of highly effective drug targets. Therefore, the combination of RNAi identified oncology targets and new tools for delivery in the next decade will combine to have a dramatic impact on new cancer therapies.

REFERENCES

Amarzguioui M (2004) Improved siRNA-mediated silencing in refractory adherent cell lines by detachment and transfection in suspension. Biotechniques 36(766–768):770

Aza-Blanc P, Cooper CL, Wagner K, Batalov S, Deveraux QL, and Cooke MP (2003) Identification of modulators of TRAIL-induced apoptosis via RNAi-based phenotypic screening. Mol Cell 12:627–637

Bartz SR, Zhang Z, Burchard J, Imakura M, Martin M, Palmieri A, Needham R, Guo J, Gordon M, Chung N, Warrener P, Jackson AL, Carleton M, Oatley M, Locco L, Santini F, Smith T, Kunapuli P, Ferrer M, Strulovici B, Friend SH, and Linsley PS (2006) Small interfering RNA screens reveal enhanced cisplatin cytotoxicity in tumor cells having both BRCA network and TP53 disruptions. Mol Cell Biol 26:9377–9386

Berns K, Horlings HM, Hennessy BT, Madiredjo M, Hijmans EM, Beelen K, Linn SC, Gonzalez-Angulo AM, Stemke-Hale K, Hauptmann M, Beijersbergen RL, Mills GB, van de Vijver MJ, and Bernards R (2007) A functional genetic approach identifies the PI3K pathway as a major determinant of trastuzumab resistance in breast cancer. Cancer Cell 12:395–402

Borawski J, Lindeman A, Buxton F, Labow M, and Gaither LA (2007) Optimization procedure for small interfering RNA transfection in a 384-well format. J Biomol Screen 12:546–559

Brummelkamp TR, Bernards R, Agami R (2002a) Stable suppression of tumorigenicity by virus-mediated RNA interference. Cancer Cell 2: 243–247

Brummelkamp TR, Bernards R, and Agami R (2002b) A system for stable expression of short interering RNAs in mammalian cells. Science 296:550–553

Brummelkamp TR, Fabius AW, Mullenders J, Madiredjo M, Velds A, Kerkhoven RM, Bernards R, and Beijersbergen RL (2006) An shRNA barcode screen provides insight into cancer cell vulnerability to MDM2 inhibitors. Nat Chem Biol 2:202–206

Chauhan D, Neri P, Velankar M, Podar K, Hideshima T, Fulciniti M, Tassone P, Raje N, Mitsiades C, Mitsiades N, Richardson P, Zawel L, Tran M, Munshi N, and Anderson KC (2007) Targeting mitochondrial factor Smac/DIABLO as therapy for multiple myeloma (MM). Blood 109:1220–1227

Clynes RA, Towers TL, Presta LG, and Ravetch JV (2000) Inhibitory Fc receptors modulate *in vivo* cytoxicity against tumor targets. Nat Med 6:443–446

Cobleigh MA, Vogel CL, Tripathy D, Robert NJ, Scholl S, Fehrenbacher L, Wolter JM, Paton V, Shak S, Lieberman G, and Slamon DJ (1999) Multinational study of the efficacy and safety of humanized anti-HER2 monoclonal antibody in women who have HER2-overexpressing metastatic breast cancer that has progressed after chemotherapy for metastatic disease. J Clin Oncol 17:2639–2648

Crnkovic-Mertens I, Hoppe-Seyler F, and Butz K (2003) Induction of apoptosis in tumor cells by

siRNA-mediated silencing of the livin/ML-IAP/KIAP gene. Oncogene 22:8330–8336

Druker BJ, Talpaz M, Resta DJ, Peng B, Buchdunger E, Ford JM, Lydon NB, Kantarjian H, Capdeville R, Ohno-Jones S, and Sawyers CL (2001) Efficacy and safety of a specific inhibitor of the BCR-ABL tyrosine kinase in chronic myeloid leukemia. N Engl J Med 344:1031–1037

Elbashir SM, Harborth J, Lendeckel W, Yalcin A, Weber K, and Tuschl T (2001) Duplexes of 21-nucleotide RNAs mediate RNA interference in cultured mammalian cells. Nature 411: 494–498

Fire A, Xu S, Montgomery MK, Kostas SA, Driver SE, and Mello CC (1998) Potent and specific genetic interference by double-stranded RNA in *Caenorhabditis elegans*. Nature 391:806–811

Frei E III, Karon M, Levin RH, Freireich EJ, Taylor RJ, Hananian J, Selawry O, Holland JF, Hoogstraten B, Wolman IJ, Abir E, Sawitsky A, Lee S, Mills SD, Burgert EO Jr, Spurr CL, Patterson RB, Ebaugh FG, James GW III, and Moon JH (1965) The effectiveness of combinations of antileukemic agents in inducing and maintaining remission in children with acute leukemia. Blood 26:642–656

Gaither LA, Porter D, Yao Y, Borawski J, Yang G, Donovan J, Sage D, Slisz J, Tran M, Straub C, Ramsey T, Iourgenko V, Huang A, Chen Y, Schlegel R, Labow M, Fawell S, Sellers WR, and Zawel L (2007) A chemical lethality rescue screen reveals roles for inhibitors of apoptosis proteins in TNFa signaling. Cancer Res 67(24):11493–11498

Jackson AL, Burchard J, Schelter J, Chau BN, Cleary M, Lim L, and Linsley PS (2006) Widespread siRNA "off-target" transcript silencing mediated by seed region sequence complementarity. RNA 12:1179–1187

Kanda A, Kawai H, Suto S, Kitajima S, Sato S, Takata T, and Tatsuka M (2005) Aurora-B/AIM-1 kinase activity is involved in Ras-mediated cell transformation. Oncogene 24:7266–7272

Kantarjian H, Sawyers C, Hochhaus A, Guilhot F, Schiffer C, Gambacorti-Passerini C, Niederwieser D, Resta D, Capdeville R, Zoellner U, Talpaz M, Druker B, Goldman J, O'Brien SG, Russell N, Fischer T, Ottmann O, Cony-Makhoul P, Facon T, Stone R, Miller C, Tallman M, Brown R, Schuster M, Loughran T, Gratwohl A, Mandelli F, Saglio G, Lazzarino M, Russo D, Baccarani M, and Morra E (2002) Hematologic and cytogenetic responses to imatinib mesylate in chronic myelogenous leukemia. N Engl J Med 346:645–652

Kittler R, Putz G, Pelletier L, Poser I, Heninger AK, Drechsel D, Fischer S, Konstantinova I, Habermann B, Grabner H, Yaspo ML, Himmelbauer H, Korn B, Neugebauer K, Pisabarro MT, and Buchholz F (2004) An endoribonuclease-prepared siRNA screen in human cells identifies genes essential for cell division. Nature 432:1036–1040

Kolfschoten IG, van Leeuwen B, Berns K, Mullenders J, Beijersbergen RL, Bernards R, Voorhoeve PM, and Agami R (2005) A genetic screen identifies PITX1 as a suppressor of RAS activity and tumorigenicity. Cell 121:849–858

Liu J, Farmer JD Jr, Lane WS, Friedman J, Weissman I, and Schreiber SL (1991) Calcineurin is a common target of cyclophilin-cyclosporin A and FKBP-FK506 complexes. Cell 66:807–815

MacKeigan JP, Murphy LO, and Blenis J (2005) Sensitized RNAi screen of human kinases and phosphatases identifies new regulators of apoptosis and chemoresistance. Nat Cell Biol 7:591–600

Mittal V (2004) Improving the efficiency of RNA interference in mammals. Nat Rev Genet 5:355–365

Miyagishi M, and Taira K (2003) Strategies for generation of an siRNA expression library directed against the human genome. Oligonucleotides 13:325–333

Moffat J, Grueneberg DA, Yang X, Kim SY, Kloepfer AM, Hinkle G, Piqani B, Eisenhaure TM, Luo B, Grenier JK, Carpenter AE, Foo SY, Stewart SA, Stockwell BR, Hacohen N, Hahn WC, Lander ES, Sabatini DM, and Root DE (2006) A lentiviral RNAi library for human and mouse genes applied to an arrayed viral high-content screen. Cell 124:1283–1298

Moxley JH 3rd, De Vita VT, Brace K, and Frei E 3rd (1967) Intensive combination chemotherapy and X-irradiation in Hodgkin's disease. Cancer Res 27:1258–1263

Nagata Y, Lan KH, Zhou X, Tan M, Esteva FJ, Sahin AA, Klos KS, Li P, Monia BP, Nguyen NT, Hortobagyi GN, Hung MC, and Yu D (2004) PTEN activation contributes to tumor inhibition by trastuzumab, and loss of PTEN predicts

trastuzumab resistance in patients. Cancer Cell 6:117–127

Ovcharenko D, Jarvis R, Hunicke-Smith S, Kelnar K, and Brown D (2005) High-throughput RNA screening *in vitro*: From cell lines to primary cells. RNA 6:985–993

Paddison PJ, Silva JM, Conklin DS, Schlabach M, Li M, Aruleba S, Balija V, O'Shaughnessy A, Gnoj L, Scobie K, Chang K, Westbrook T, Cleary M, Sachidanandam R, McCombie WR, Elledge SJ, and Hannon GJ (2004) A resource for large-scale RNA-interference-based screens in mammals. Nature 428:427–431

Qiu S, Adema CM, and Lane T (2005) A computational study of off-target effects of RNA interference. Nucleic Acids Res 33:1834–1847

Saal LH, Holm K, Maurer M, Memeo L, Su T, Wang X, Yu JS, Malmstrom PO, Mansukhani M, Enoksson J, Hibshoosh H, Borg A, and Parsons R (2005) PIK3CA mutations correlate with hormone receptors, node metastasis, and ERBB2, and are mutually exclusive with PTEN loss in human breast carcinoma. Cancer Res 65:2554–2559

Siolas D, Lerner C, Burchard J, Ge W, Linsley PS, Paddison PJ, Hannon GJ, and Cleary MA (2005) Synthetic shRNAs as potent RNAi triggers. Nat Biotechnol 23:227–231

Snove O Jr, and Holen T (2004) Many commonly used siRNAs risk off-target activity. Biochem Biophys Res Commun 319:256–263

Swanton C, Marani M, Pardo O, Warne PH, Kelly G, Sahai E, Elustondo F, Chang J, Temple J, Ahmed AA, Brenton JD, Downard J, and Nicke B (2007) Regulators of mitotic arrest and ceramide metabolism are determinants of sensitivity to paclitaxel and other chemotherapeutic drugs. Cancer Cell 11: 498–512

Waterhouse PM, Wang MB, and Lough T (2001) Gene silencing as an adaptive defence against viruses. Nature 411: 834-842

Westbrook TF, Martin ES, Schlabach MR, Leng Y, Liang AC, Feng B, Zhao JJ, Roberts TM, Mandel G, Hannon GJ, Depinho RA, Chin L, and Elledge SJ (2005) A genetic screen for candidate tumor suppressors identifies REST. Cell 121:837–848

Whitehurst AW, Bodemann BO, Cardenas J, Ferguson D, Girard L, Peyton M, Minna JD, Michnoff C, Hao W, Roth MG, Xie XJ, and White MA (2007) Synthetic lethal screen identification of chemosensitizer loci in cancer cells. Nature 446:815–819

Yang D, Buchholz F, Huang Z, Goga A, Chen CY, Brodsk FM, and Bishop JM (2002) Short RNA duplexes produced by hydrolysis with Escherichia coli RNase III mediate effective RNA interference in mammalian cells. Proc Natl Acad Sci USA 99:9942–9947

Zheng L, Liu J, Batalov S, Zhou D, Orth A, Ding S, and Schultz PG (2004) An approach to genomewide screens of expressed small interfering RNAs in mammalian cells. Proc Natl Acad Sci USA 101:135–140

2
Cancer Biomarkers (An Overview)

William C.S. Cho

INTRODUCTION

Many cancer patients are diagnosed at a stage in which the cancer is too far advanced to be cured, and most cancer treatments are effective in only a minority of patients undergoing therapy. There is thus a tremendous opportunity to improve the outcome for people with cancer by enhancing detection and treatment approaches, and biomarker is instrumental in making that transition. A biomarker is defined as any characteristic that can be objectively measured and evaluated as an indicator of normal biological processes, pathogenic processes or pharmacological response to a therapeutic intervention. A cancer biomarker is any substance that is measured biologically and associated with an increased risk of cancer. These indicators could include a broad range of biochemical entities, such as nucleic acids, proteins, carbohydrates, lipids, small metabolites, whole cells or biophysical characteristics of tissues. Because of the heterogeneity among diseases and patients, recharacterization of cancer in pathophysiological terms via biomarker is a key to the future of medicine. Detection of cancer biomarkers can be accomplished by a wide variety of methods, ranging from biochemical analysis of blood or tissue samples to biomedical imaging. There has been much interest in biomarkers of cancer risk in predicting future patterns of neoplasm, especially as cancer treatment has made such positive strides in the last few years. Successful development of cost effective tests has a profound impact on how cancer is detected, diagnosed, and treated; thus, could reduce the economic burden of cancer.

EMERGING TECHNOLOGIES FOR CANCER BIOMARKER DISCOVERY

In pace with the successful completion of the Human Genome Project, the wave of proteomics has raised the curtain on the postgenome era. The study of oncogenomics and oncoproteomics provide mankind with a better understanding of neoplasia which has the potential to revolutionize clinical practice, including cancer diagnosis and screening, individualized selection of therapeutic combinations that target the

oncogene or cancer-specific protein, real-time assessment of therapeutic efficacy and toxicity, as well as rational modulation of therapy based on changes in the cancer genetic or protein network associated with prognosis and drug resistance. Besides, oncogenomics and oncoproteomics are also applied to the discovery of new therapeutic targets and to the study of drug effects (Cho 2007a).

Recent technological advances in biomedical research, especially in oncogenomics and oncoproteomics, have made it easier to identify many new cancer biomarkers that can potentially improve cancer screening and detection, to improve the drug development process, as well as to enhance the effectiveness and safety of cancer care by allowing physicians to tailor treatment for individual patients. A brief overview of some contemporary and rapidly evolving technologies are described below (Table 2.1).

DNA Microarray

DNA microarray is a collection of microscopic DNA spots, commonly representing single genes, arrayed on a solid surface by covalent attachment to chemically suitable matrices. It is a high capacity system commonly used for monitoring the expression of many genes in parallel or for comparative genomic hybridization. Microarrays prepared by high speed robotic printing of complementary DNAs on glass are used for quantitative expression measurements of the corresponding genes. Qualitative or quantitative measurement with DNA microarray utilizes the selective nature of DNA–DNA or DNA–RNA hybridization under high stringency conditions and fluorophore-based detection. Because of the small format and high density of the arrays, microliter level of hybridization volumes can enable detection of rare transcripts in probe mixtures derived from total cellular messenger RNA.

Table 2.1. Emerging technologies for cancer biomarker discovery

Molecular type	Method of analysis
Genome	DNA microarray
	Quantitative real-time polymerase chain reaction
Transcriptome	Serial analysis of gene expression
	MicroRNA microarray
Proteome	Electrophoresis
	• Two dimensional polyacrylamide gel electrophoresis
	• Free flow electrophoresis
	• Capillary electrophoresis
	X-ray crystallography and nuclear magnetic resonance
	Surface plasmon resonance
	Mass spectrometry
	• Matrix-assisted laser desorption/ionization time-of-flight
	• Surface-enhanced laser desorption/ionization time-of-flight
	• Liquid chromatography coupled with tandem mass spectrometry
	• Linear ion trap quadrupole-Orbitrap
	Isotope-coded affinity tags
	Multiple reaction monitoring
	Absolute quantification of proteins
	Protein microarray
	Tissue array

Serial Analysis of Gene Expression

Serial analysis of gene expression (SAGE) is a technique that allows the quantitative and simultaneous analysis of a large number of transcripts. A small sequence of nucleotides from the transcript, called a tag, can effectively identify the original transcript from whence it came. Linking these tags allows for rapid sequencing analysis of multiple transcripts. By linking the tags together, only one sequencing event is required to sequence every transcript within the cell, making the task of DNA expression profiling a much less daunting one. Recently, conventional SAGE (14 bp) has been developed further to increase the tag size, such as LongSAGE (21 bp) and SuperSAGE (26 bp) (Matsumura et al. 2006).

MicroRNA Microarray

MicroRNA (miRNA) microarray is a high-throughput approach to study the expression of miRNAs in cultured cells or tissues. Unlike the traditional cDNA microarray expression profiling, RNA samples used for miRNA microarray hybridization need to be enriched for small RNAs. Usually, the first step of a miRNA microarray experiment is the isolation of total RNA and the enrichment or direct isolation of small RNA. The miRNAs are then labeled and cleaned-up, following with miRNA hybridization to arrays spotted with miRNA probes. After washes and scanning, the differential expressions of miRNAs in the samples are identified. The recent development of highly efficient labeling method and novel microarray probe design enables direct label as low as 100 ng of total RNA using Cy3 or Cy5, without fractionation or amplification, to produce precise and accurate measurements that span a linear dynamic range from 0.2 amol to 2 fmol of input miRNA. The assay is also applicable for formalin-fixed paraffin-embedded samples.

Two Dimensional Polyacrylamide Gel Electrophoresis

Two dimensional polyacrylamide gel electrophoresis (2D-PAGE) has been the mainstay of electrophoretic technology for decades and is the most widely used tool for separating proteins based on mass and charge. It can achieve the separation of thousands of different proteins in one gel. High resolution 2D-PAGE can resolve up to 10,000 protein spots per gel. However, 2D-PAGE technique is a time-consuming and labor-intensive process. It implies some inherent limitations especially concerning hydrophobic and basic proteins, and therefore they are often underrepresented in 2D-PAGE. Besides, the limitations of the technique have been low dynamic range and gel-to-gel variability. Fluorescence-based differential gel electrophoresis overcomes the problems associated with traditional 2D-PAGE and allows more accurate and sensitive quantitative proteomics studies. The 2D-PAGE with immobilized pH gradient has provided higher resolution, improved reproducibility and higher loading capacity for preparative purposes with the intent of subsequent spot identification by the high speed, automated and high-throughput mass spectrometry (MS).

Free Flow Electrophoresis

Free flow electrophoresis is a liquid-based isoelectrofocusing method working continuously in the absence of a stationary

phase or solid support material such as a gel. It separates preparatively charged particles ranging in size from molecular to cellular dimensions according to their electrophoretic mobilities or isoelectric points. Samples are injected continuously into a thin buffer film, which may be segmented or uniform, flowing through a chamber formed by two narrowly spaced glass plates. Perpendicularly to the electrolyte and sample flow, current may be applied while the fluid is flowing or while the fluid flow is transiently stopped. In any case the applied electric field leads to movement of charged sample components towards the respective counter electrode according to their electrophoretic mobilities or isoelectric points. The sample and the electrolyte used for a separation enter the separation chamber at one end and the electrolyte containing different sample components as separated bands is fractionated at the other side.

Capillary Electrophoresis

Among the variety of methods so far used for cancer screening, capillary electrophoresis (CE) represents a robust, reliable and widely used analytical tool. The visualization of CE-MS data in simplified two dimensional format allows an easy and simultaneous visual inspection of large datasets, an immediate perception of relevant differences in closely related samples, a rapid monitoring of data quality levels in different samples, as well as a fast discrimination between comigrating polypeptides and electrospray ionization-MS fragmentation ions. Around 550~1,000 fold sensitivity enhancement has been achieved recently in terms of peak intensity by online sample preconcentration technique based on dynamic pH junction in CE-MS (Imami et al. 2007).

Matrix-Assisted Laser Desorption/Ionization Time-of-Flight Mass Spectrometry

The basis of matrix-assisted laser desorption/ionization time-of-flight (MALDI-TOF) MS technology is the absorption of short pulses of laser light by a chromophoric matrix resulting in volatilization of the sample molecules dispersed in the matrix. The matrix isolates sample molecules in a chemical environment that enhances the probability of ionization without fragmentation. The ions formed are accelerated by a high voltage supply and then allowed to drift down a flight tube where they separate according to mass. Arrival at the end of the flight tube is detected and recorded by a high speed recording device. The MALDI-TOF MS has developed into a valuable tool in proteomics, it is envisioned to be most useful in conjunction with conventional biochemical techniques such as protein digests. They can be applicable to identify blocked amino termini, posttranslational modifications and mutation sites in known proteins. A significant amount of preliminary structure determination is possible on very small amounts of analyte (<10 pmol). Detailed protein characterization using the latest MALDI-TOF/TOF tandem MS (MS/MS) technology enables ultra sensitive protein identification. But for ladder sequencing and in-source fragmentation studies, it is important to minimize potential peptide impurities. Careful attention must also be given to synthetic peptide samples so as not to confuse the fragment ion signals with protonated molecular ions originating from low levels of incomplete synthesis impurities.

Surface-Enhanced Laser Desorption/ Ionization Time-of-Flight Mass Spectrometry

Surface-enhanced laser desorption/ionization (SELDI)-TOF MS is an affinity-based MS technology developed in the 1990s, which brings to the field of proteomics a user-friendly methodology. SELDI has several advantages, such as high-throughput screening because of its versatility, ease of use and speed. It is rapid, reproducible, highly sensitive (detection limit in the femtomolar range) and readily adaptable to a diagnostic format. Additionally, molecules that have been traditionally difficult to identify have been detected easily by the SELDI platform. Using addressable protein binding sites, SELDI platform provides a layer of specificity when one is probing for biomarkers along defined signaling pathways or specific posttranslationally modified protein species (Cho 2006).

Liquid Chromatography Coupled with Tandem Mass Spectrometry

The strength of the MS/MS lies in the ability to sequence information for a specific peptide in the presence of multiple peptides in the sample. Liquid chromatography (LC) is used to concentrate and separate peptides from extremely complex mixtures before sequencing by MS. Its resolving power can be dramatically enhanced by multidimensional LC separation procedures, such as multidimensional protein identification technology. LC-MS/MS has been demonstrated to enhance separation and identification of analytes in the low femtomolar range. The LC-MS/MS system integrates conventional high performance liquid chromatography pumps and columns coupled to a tandem mass spectrometer which allow efficient coupling of chromatography and ion detection. The fragmented ions allow for identification of the respective amino acids through a protein or translated nucleotide database search. A single LC-MS/MS analysis thus offers the possibility of isolating and sequencing hundreds of selected peptides from one sample. An additional advantage of this technique is the ability to identify protein targets of reactive electrophiles and map adducts to the specific amino acid.

Linear Ion Trap Quadrupole-Orbitrap

The quantitative analysis of complex biological samples has emerged as a key research area in the field of proteomics. Although quantitative proteomic experiments remain challenging, these strategies have been greatly facilitated by the development of newer high performance mass spectrometers. Mass accuracy is a key parameter of mass spectrometric performance. A new method of phase-enhanced selective ion ejection based on broadband dipolar excitation and ion ejection applicable to the Orbitrap has been developed in recent years. The method allows an isolation resolution of 28,400, which is estimated to provide a mass resolution for ion ejection of more than 100,000 (Hu et al. 2007). When a linear ion trap quadrupole (LTQ) is coupled to an Orbitrap mass analyzer, the number and quality of the peptide ratio measurements can be improved by 4- to 5-fold in compared to similar analyses done on the LTQ. The LTQ-Orbitrap can be applied for top-down proteomics (the analysis of intact proteins instead of first digesting them to peptides), in which the absolute mass accuracies for intact proteins better than 1 ppm (Makarov and Denisov 2009). There are also other mass spectrometers utilizing LTQ and

Fourier-transform ion cyclotron resonance (FT-ICR) to analyze the proteins/peptides. A substantial improvement in quantitative analysis has been reported using a LTQ-FT-ICR mass spectrometer and novel quantification software (Everley et al. 2006).

Imaging Mass Spectrometry

Cell is spatially highly organized, MS using laser to ionize the sample takes imaging MS measurements directly from tissue sections. By combining mass information with spatial resolution, imaging MS takes advantage of the molecular sensitivity of MS to analyze protein expression profiles from target tissues. It allows for direct mapping of peptides and proteins present on the surface of tissue sections and individual cells. In a typical procedure, steel plates coated with matrix solution are used to mount tissue sections. They are then dried and introduced into a mass spectrometer controlled by tailored imaging software. Molecular images are then generated from a raster over the sample surface with the aid of laser spots. Laser positions are fixed, and the sample plate is repositioned for consecutive spots. Mass spectral data are acquired for each spot from the molecules present on the irradiated area. A typical data array may contain thousands of spots, depending on the desired image resolution and a specified molecular weight range. A composite of >200 protein peaks can be detected in the mass spectrum from each spot ablated by the laser (Stoeckli et al. 2001). It is possible to generate hundreds of image maps at distinct molecular weights from a single raster. Imaging MS may help enhance biomarker discovery by shedding light on the importance of spatial localization of specific proteins during carcinogenesis and neoplasia which adds a new dimension to histopathological analysis.

Isotope-Coded Affinity Tags

Utilizing the power of MS, a high-throughput technique has been developed that facilitates direct qualitative and quantitative comparisons of complex protein mixtures, isotope-coded affinity tags analogous to the microarray approach for assessing differential gene expression between two cell states use a chemical group or label made in two different isotopic forms: heavy and light. These labels coupled to all the cysteine residues in a protein mixture. The heavy isotope is added to one sample, whereas the lighter isotope is added to the second sample. The samples are then combined, the proteins are digested, and the peptides are analyzed in a mass spectrometer. The isotopic substitutions do not affect the behavior of peptides during separations. Thus, peptides derived from the two different samples enter the spectrometer at the same time. The mass spectrometer measures the relative abundance of heavy and light peptide forms in each sample and identifies each peptide by generating and analyzing the peptide fingerprints. In this manner, a global view of protein abundance in cells or tissues in two different states can be determined. This is especially important to biomarker discovery because expression analysis of all proteins and identification of the changes that are a function of a disease process give us molecular handles to target intervention strategies.

Multiple Reaction Monitoring

The huge dynamic range of protein concentrations in body fluids exceeds 11 orders of magnitude; MS also has limitations to

identify proteins of low abundance without any prior pre-fractionation. The MS-based targeted approaches such as multiple reaction monitoring (MRM) can enable the detection of selected proteins of low abundance, but the analyzed protein/peptide mixture may not be of high complexity. On the other hand, the activity of many transcriptional regulators is significantly altered by post-translational modifications of specific sites, which can be identified by using the highly sensitive MRM experiments to trigger dependent product ion scans on a hybrid LTQ instrument. The application of MALDI triple-quadrupole MS for targeted proteomics employing an amine-specific isotopic labeling approach has an indirect benefit of the isotopic labeling technique with a significant enhancement of the a1 ion in tandem mass spectra of all peptides. The a1 ion is selected as the fragment ion for MRM to eliminate tedious method development and optimization (Melanson et al. 2006).

Absolute Quantification of Proteins

While relative quantification provides information regarding specific protein abundance changes between two conditions caused by an induced perturbation (environment-, drug- and disease-induced), the absolute quantification of proteins (AQUA) present within a complex protein mixture is valuable for the understanding of the underlying molecular biology guiding the response to an applied perturbation. The AQUA permits direct quantification of proteins and their modification states through the use of synthetic peptides which are chemically identical to their naturally occurring counterparts. The internal standard peptides, synthesized with stable isotopes, are identified by selected reaction monitoring and MS/MS, and then used to precisely quantify naturally occurring levels of the corresponding proteins and their modification states (Mayya et al. 2006).

Protein Microarray

Protein microarray is a small size planar analytical proteinchip with probes arranged in high density on which different molecules of protein are affixed at separate locations in an ordered manner to form a microscopic array. The recent development of protein microarray offers the possibility to simultaneously analyze the expression of hundreds of proteins. It is used to identify protein–protein interactions, the substrates of protein kinases or the targets of biologically active small molecules. The most common functional proteinchip is the antibody microarray, where antibodies are spotted onto the proteinchip and are used as capture molecules to detect proteins from biological samples. The innovative reverse-phase protein microarray has the potential to provide information about the state of cellular circuitry from minute samples (Wulfkuhle et al. 2006).

Tissue Array

Tissue array enables high-throughput molecular analysis of large numbers of specimens. A typical tissue array is constructed by arranging cylindrical biopsies from multiple individual tumor tissues into a tissue array block, which is then sliced into ≥200 identical slides for probing RNA or protein targets. A single immunohistochemistry or in situ hybridization experiment provides information on all specimens on the slides, whereas subsequent sections can be analyzed with other probes or antibodies.

Cancer-specific tissue arrays with various kinds of subsets can be generated (such as subsequent cancer cases, preneoplastic lesions, metastatic lesions, synchronous cancers, metachronous cancers, young patients and familial cases) for further analysis. Tissue array has expanded the scope of high-throughput molecular analysis of archival tissue specimens with multiple probes for specific genes or proteins for functional and clinical applications.

Bioinformatics

Bioinformatics is an interdisciplinary field that blends computer science and biostatistics with biological and biomedical sciences such as biochemistry, cell biology, developmental biology, genetics, genomics and physiology. Genomic and proteomic analysis generates expression information for hundreds and thousands of genes or proteins, which have to be organized, stored, analyzed and interpreted with the aid of bioinformatics. The significance of bioinformatics is increasing because the advent of high-throughput methods relies on powerful data analysis. Artificial intelligence-based systems that learn, adapt and gain experience over time are uniquely suited to genomic and proteomic data analysis because of the huge dimensionality of the genome or proteome itself. The application of these artificial intelligence systems to analyze mass spectral data derived from the genome or proteome has given rise to a new analytical paradigm.

CURRENTLY USED CANCER BIOMARKERS (TABLE 2.2)

Carcinoembryonic antigen (CEA) is a cancer biomarker that is elevated in the blood of patients with ovarian, lung, breast, pancreas, rectal and gastrointestinal tract cancers (Fleuren and Nap 1988; Molina et al. 2003;

TABLE 2.2. Currently used cancer biomarkers

Cancer type	Primary Use	Biomarker	Reference
Hepatocellular	Diagnosis	Alpha-fetoprotein	Saffroy et al. 2007
	Diagnosis	Cancer antigen 125	Lopez 2005
Colon	Treatment	Estrogen receptor	Harris et al. 2003
Rectal	Diagnosis	Carcinoembryonic antigen	Grossmann et al. 2007
Lung	Diagnosis	Neuron specific enolase	Schneider et al. 2003
	Diagnosis	Carcinoembryonic antigen	Molina et al. 2003
Gastrointestinal tract	Diagnosis	Carcinoembryonic antigen	Locker et al. 2006
Breast	Diagnosis	Carcinoembryonic antigen	Lee et al. 2004
	Treatment	Estrogen receptor	Harris et al. 2003
	Prognosis	Carbohydrate antigen 15.3	Martin et al. 2006
Prostate	Diagnosis	Prostate specific antigen	Vukotic et al. 2005
	Treatment	Estrogen receptor	Harris et al. 2003
Pancreatic	Diagnosis	Carcinoembryonic antigen	Shami et al. 2007
	Diagnosis	Carbohydrate antigen 19.9	Ni et al. 2005
Gallbladder	Diagnosis	Carbohydrate antigen 19.9	Strom et al. 1990
Ovarian	Diagnosis	Carcinoembryonic antigen	Fleuren and Nap 1988
	Treatment	Estrogen receptor	Harris et al. 2003
	Prognosis	Cancer antigen 125	Markmann et al. 2007
Nasopharyngeal	Diagnosis	Epstein-Barr virus immunoglobulins	Wong et al. 2005
Cervical	Diagnosis	Human papillomavirus E6 and E7	Yim and Park 2006
Endometrial	Treatment	Estrogen receptor	Harris et al. 2003

Lee et al. 2004; Locker et al. 2006; Grossmann et al. 2007; Shami et al. 2007; Cho 2007b). As a screening test, it can be elevated by many other factors than cancer; smoking for instance raises CEA levels. However, the level of CEA is an effective preoperative biomarker that can predict survival in postsurgery patients with colorectal cancer (Munoz Llarena et al. 2007).

For hepatocellular carcinoma (HCC), the common method of screening high risk patients by alpha-fetoprotein (AFP) and ultrasonography has been shown to result in earlier detection and consequently more easily treatable tumors and longer survival. Of the other cancer biomarkers, the newer high sensitive des-gamma-carboxy-prothrombin has been found to be useful. In addition, the AFP fractions L3, P4/5 and the +II band are highly specific for HCC (Saffroy et al. 2007).

Among routinely assayed cancer biomarkers in the laboratory, cancer antigen 125 (CA 125) is more sensitive for HCC than AFP but less specific (Lopez 2005). CA 125 can be a biomarker of ovarian cancer risk or an indicator of malignancy. Currently available screening tests for ovarian cancer include CA 125, transvaginal ultrasound, or a combination of both. But the levels of these cancer biomarkers can be high in people who have pancreatitis, kidney or liver disease, making their accuracy as cancer diagnostic tool very limited. However, CA 125 has provided a useful cancer biomarker for monitoring response to chemotherapy. It can be used to follow the progress of treatment of cancer and predict a treatment failure when levels rise despite the use of chemotherapeutic agents. A rapid fall in CA 125 during chemotherapy predicts a favorable prognosis and can be used to redistribute patients on multiarmed randomized clinical trials (Markmann et al. 2007). On the other hand, high carbohydrate antigen 19.9 in the blood can be a sign of gallbladder or pancreatic cancer (Strom et al. 1990; Ni et al. 2005).

Early diagnosis of cancer is difficult because of the lack of specific symptoms in early disease and the limited understanding of etiology and oncogenesis. There is no single biomarker sensitive enough for the early detection of breast cancer; therefore, measurement of CEA and HER-2 in abnormal nipple discharge has been approved for diagnosis of breast cancer in some countries (Kurebayashi 2004). On the other hand, it has been reported that high pre-operative carbohydrate antigen 15.3 (CA 15.3) levels correlate with large size tumors and the presence of lymph node metastases, which suggests that CA 15.3 can be used as a prognostic biomarker for breast cancer (Martin et al. 2006).

The estrogen receptor (ER) status is also one of the cancer biomarkers that are routinely used to guide treatment decisions. It is overexpressed in about 70% of breast cancer. Estrogen and the ERs have also been implicated in ovarian, colon, prostate and endometrial cancers. Advanced colon cancer is associated with a loss of ERβ, the predominant ER in colon tissue, and colon cancer is treated with ERβ specific agonists (Harris et al. 2003).

Another cancer biomarker in wide use is prostate specific antigen (PSA). It is the most important cancer biomarker in all solid tumors, indispensable in the management of prostate cancer. The higher the PSA in blood, the greater the correlation is toward the existence of prostate cancer. However, other reasons besides cancer can also cause rises in PSA, such as benign prostatic hyperplasia or prostatitis.

Nevertheless, PSA is a serum cancer biomarker currently used consistently in primary care. Although no treatment is based solely on PSA, alterations above normal can spur further diagnostic testing to catch the disease at an early stage. The degree of elevation, the rapidity of increase and the fraction of free non-bound PSA (higher in benign causes) are all factors to determine the next management procedure (Vukotic et al. 2005).

Numerous studies have supported the use of neuron specific enolase (NSE) as an aid in the diagnosis of small cell lung cancer. High serum levels of NSE (>100 μg/L) in patients with suspicion of malignancy suggest the presence of small cell lung cancer with high probability, but moderate elevations of NSE are also found in patients with benign lung diseases (Schneider et al. 2003).

Assessment of immunoglobulin A (IgA) and immunoglobulin G (IgG) antibodies responses to various Epstein-Barr virus (EBV) antigen complexes, usually involving multiple serological assays, is important for the early diagnosis of nasopharyngeal carcinoma (NPC). The use of EBV immunoglobulin assay as diagnostic biomarker for NPC is considered to be feasible and effective (Wong et al. 2005; Cho 2007c).

On the other hand, more than 98% of cervical cancer is related to human papillomavirus (HPV) infection. The identification and functional verification of host proteins associated with HPV E6 and E7 oncoproteins may provide useful information for the understanding of cervical carcinogenesis and the development of cervical cancer-specific markers (Yim and Park 2006).

BIOMARKERS FOR THE DIAGNOSIS OF CANCERS (TABLE 2.3)

Genomic-Based Biomarkers in Cancer

Pleural effusions from 59 patients with breast, lung, ovarian or colorectal cancers and 12 patients with benign diseases as a control were subjected to reverse transcription–polymerase chain reaction (RT-PCR) for detection of *MN/CA9* gene expression. The sensitivity and specificity were 89.8%

Table 2.3. Selected cancer biomarkers identified by molecular analysis

Cancer type	Primary Use	Molecular type	Biomarker	Reference
Lung	Diagnosis	Genome	*MN/CA9x*	Li et al. 2007
	Prognosis	Genome	*RASSF1A, RUNX3*	Yanagawa et al. 2007
	Prognosis	Transcriptome	*let-7*	Takamizawa et al. 2004
	Prognosis	Transcriptome	*hsa-let-7a-2, hsa-miR-155*	Yanaihara et al. 2006
	Prognosis	Proteome	Alphavbeta6	Elayadi et al. 2007
Hepatocellular	Diagnosis	Genome	*Alpha 7*	Ren et al. 2007
Colorectal	Diagnosis	Genome	*MN/CA9*	Li et al. 2007
Breast	Diagnosis	Genome	*MN/CA9*	Li et al. 2007
	Prognosis	Genome	*PAI-1*	Lei et al. 2007
	Treatment	Proteome	Cytokeratin-18	Olofsson et al. 2007
	Prognosis	Proteome	Ubiquitin, Ferritin light chain	Ricolleau et al. 2006
Head and Neck	Treatment	Genome	Epidermal growth factor receptor	Agulnik et al. 2007
	Prognosis	Genome	Krüppel-like transcription factor 6	Teixeira et al. 2007
Pancreatic	Diagnosis	Transcriptome	*miR-221, miR-301, miR-376a*	Lee et al. 2007
	Prognosis	Transcriptome	*miR-21*	Roldo et al. 2006
	Prognosis	Transcriptome	*miR-196a-2*	Bloomston et al. 2007
	Diagnosis	Proteome	Annexin II, OGFBP-2	Chen et al. 2007

(continued)

Table 2.3. (continued)

Cancer type	Primary Use	Molecular type	Biomarker	Reference
Leukemia	Treatment	Transcriptome	*miR-15, miR-16*	Cimmino et al. 2005
	Prognosis	Proteome	CD27, Interleukin-8, Interleukin-10	Kara et al. 2007
Prostate	Diagnosis	Genome	*Alpha 7*	Ren et al. 2007
	Diagnosis	Proteome	Annexin II	Yee et al. 2007
Lymphoma	Prognosis	Genome	Epstein–Barr virus DNA	Ngan et al. 2004
	Prognosis	Genome	*TP53, RB1, P16, CCND1, ATM, P27, BMI, MYC, MDM2, EZH2*	Kienle et al. 2007
	Treatment	Transcriptome	*miR-17-92*	Woods et al. 2007
Glioblastoma	Diagnosis	Genome	*Alpha 7*	Ren et al. 2007
	Treatment	Proteome	Galectin-1	Puchades et al. 2007
Neuroblastoma	Treatment	Transcriptome	*miR-34a*	Welch et al. 2007
Ovarian	Prognosis	Genome	Fibroblast growth factor 1	Birrer et al. 2007
	Diagnosis	Genome	*MN/CA9*	Li et al. 2007
	Diagnosis	Proteome	Eosinophil-derived neurotoxin, Osteopontin COOH-terminal fragments	Ye et al. 2006
Melanoma	Prognosis	Proteome	Ki-67	Pearl et al. 2007
Nasopharyngeal	Treatment	Genome	EBER-1	Ngan et al. 2001
	Treatment	Proteome	Platelet factor-4	Cho et al. 2007
	Prognosis	Proteome	Serum amyloid A, Inter-α-trypsin inhibitor	Cho et al. 2004, 2007
Leiomyosarcoma	Diagnosis	Genome	*Alpha 7*	Ren et al. 2007
Cholangio	Treatment	Transcriptome	*miR-21*	Meng et al. 2006

and 91.7% respectively, suggesting that *MN/CA9* might be a potential marker for the detection of malignant cells in effusions (Li et al. 2007).

Mutations in integrin *alpha7* were identified by sequencing genomic DNAs and cDNAs from 62 primary human tumor samples (including prostate cancer, liver cancer, glioblastoma multiforme and leiomyosarcoma), 4 cell lines and 56 matched normal tissues. A meta-analysis of integrin *alpha7* mRNA microarray data from 4 studies was performed. Kaplan-Meier analyses were used to assess survival. Integrin *alpha7* appeared to be a tumor suppressor that operated by suppressing tumor growth and retarding migration (Ren et al. 2007).

Transcriptomic-Based Biomarkers in Cancer

With the application of in situ RT-PCR, it was shown that the aberrantly expressed *miR-221*, *miR-301* and *miR-376a* were localized to pancreatic cancer cells but not to stroma or normal acini or ducts. Aberrant microRNA (miRNA) expression offered new clues to pancreatic tumorigenesis and might provide diagnostic biomarkers for pancreatic cancer (Lee et al. 2007).

Proteomic-Based Biomarkers in Cancer

Genomic changes are relatively static, whereas the proteome is dynamic, reflecting physiological and pathological changes much more acutely and accurately. Dysregulation of annexin I was associated with esophageal squamous cell carcinoma (Hu et al. 2004) and prostate cancer (Smitherman et al. 2004), while loss of annexin A1 expression was detected in head and neck cancer (Garcia Pedrero et al. 2004) and human breast cancer (Shen et al. 2005). Urine samples collected preoperatively from postmenopausal women of 128 ovarian cancer, 52 benign conditions, 44 other cancers and 188 healthy controls were

analyzed by SELDI-TOF MS and 2D-PAGE. Specific elevated posttranslationally modified urinary eosinophil-derived neurotoxin and osteopontin COOH-terminal fragments in ovarian cancer might lead to potential noninvasive screening tests for early diagnosis (Ye et al. 2006).

A semi-quantitative assessment of annexin II expression was performed in radical prostatectomy specimens from 74 patients and prostate needle core biopsy specimens from 13 patients. In high-grade prostatic intraepithelial neoplasia, annexin II staining was markedly reduced in epithelial cells but not in basal cells. Reduced annexin II expression might be a useful diagnostic biomarker to help identify small foci of moderately differentiated adenocarcinoma on needle core biopsy specimens since it was consistently expressed in benign prostatic glands (Yee et al. 2007).

The ICAT technology and MS/MS were employed to systematically study protein expression in 10 pancreatic cancers and 10 chronic pancreatitis. Annexin A2 and IGFBP-2 were overexpressed in cancer, but not in chronic pancreatitis, making them promising biomarker candidates for pancreatic cancer (Chen et al. 2007).

BIOMARKERS FOR THE TREATMENT AND PROGRESSION OF CANCERS (TABLE 2.3)

Genomic-Based Biomarkers in Cancer

Pharmacodynamic tissue studies were conducted on a phase I/II trial of erlotinib and cisplatin in 37 patients with recurrent or metastatic head and neck squamous cell carcinomas. High epidermal growth factor receptor (*EGFR*) gene copy in tumor specimens might predict which patients had an increased likelihood of response to erlotinib, and decreased phosphorylated-EGFR level in skin biopsies during therapy might represent a potential surrogate marker for improved clinical outcome (Agulnik et al. 2007).

Nasopharyngeal carcinoma is an EBV associated malignancy with a remarkable racial and geographical distribution (Cho 2007c). Profile of EBER-1 (EBV-encoded RNA) showed concordance with clinical course of either continuous remission or later progression, which suggested that EBER-1 in serum could become a useful adjunctive surrogate marker to monitor chemotherapeutic response in NPC patients with distant metastasis or advanced local recurrence (Ngan et al. 2001).

Transcriptomic-Based Biomarkers in Cancer

miRNAs are deemed to play a crucial role in the initiation and progression of human cancer. For example, *miR-15* and *miR-16* induce apoptosis by targeting *Bcl-2* in chronic lymphocytic leukemia (Cimmino et al. 2005). miRNAs from the *miR-17–92* cluster modulate tumor formation and function as oncogenes by influencing the translation of *E2F1* mRNA in lymphoma (Woods et al. 2007). *miR-21* modulates gemcitabine-induced apoptosis by phosphatase and tensin homolog deleted on chromosome 10-dependent activation of PI 3-kinase signaling in cholangiocarcinoma (Meng et al. 2006). *miR-34a* acts as a suppressor of neuroblastoma tumorigenesis by targeting the mRNA encoding E2F3 and reducing E2F3 protein levels (Welch et al. 2007). Restoration of tumor suppressor *hsa-miR-145* inhibits cancer cell growth in *EGFR* mutant lung adeno-

carcinoma (Cho et al. 2009). The chromosomal translocations associating with human tumors disrupt the repression of high mobility group A2 by *let-7* miRNA in mammalian cells (Cho 2007d).

Proteomic-Based Biomarkers in Cancer

Cytokeratin-18 levels were determined in serum from 61 breast cancer patients during docetaxel or cyclophosphamide/epirubicin/5-fluorouracil therapy. Cytokeratin-18 was found to be useful biomarker for early prediction of the response to cyclophosphamide/epirubicin/5-fluorouracil therapy in breast cancer (Olofsson et al. 2007). Galectin-1 was found to be negatively regulated by the treatment with wild-type TP53 and further downregulated by the cytotoxic chemotherapy SN38 in glioblastoma cell lines. Further examination of galectin-1 expression through microarray analysis in tumors from patients confirmed galectin-1 as a valuable biomarker and possible therapeutic target (Puchades et al. 2007).

BIOMARKERS FOR THE PROGNOSIS OF CANCERS (TABLE 2.3)

Genomic-Based Biomarkers in Cancer

Nineteen Chinese patients with lymphoepithelioma-like carcinoma of the lung were tested for EBV DNA in their serum samples by a quantitative real-time PCR technique. Patients with a pretherapy serum EBV DNA >10,000 copies/mL had significantly inferior overall survival, which suggested that circulating serum EBV DNA could be used as a tumor marker in the clinical management of patients with lymphoepithelioma-like carcinoma of the lung (Ngan et al. 2004).

In the methylation study of 10 genes in 101 non-small cell lung cancer (NSCLC) cases by methylation-specific PCR, promoter hypermethylation of *RASSF1A* and *RUNX3* genes were found to be independent biomarkers to predict the prognosis in NSCLC, particularly *RASSF1A* due to squamous cell carcinoma and *RUNX3* due to adenocarcinoma (Yanagawa et al. 2007). Eight potentially functional single nucleotide polymorphisms in 6 genes of the urokinase plasminogen activation system in 959 breast cancer patients together with 952 matched controls were genotyped and up to 15 years of follow-up. The -675 4G/5G polymorphism in the *PAI-1* gene was identified as a promising prognostic biomarker for breast cancer (Lei et al. 2007).

Oligonucleotide array comparative genomic hybridization was performed on 42 microdissected high-grade serous ovarian tumor samples. Amplification of fibroblast growth factor 1 at 5q31 in ovarian cancer tissues led to increased angiogenesis and autocrine stimulation of cancer cells, which might result in poorer overall survival in patients with high-grade advanced stage serous ovarian cancer (Birrer et al. 2007).

Quantitative expression of 20 genes in 65 mantle-cell lymphoma samples was analyzed using real-time RT-PCR. Genomic losses at the loci of *TP53*, *RB1* and *p16* were associated with reduced transcript levels of the respective genes. Several genes were correlated closely with the Ki-67 index, including the short *CCND1* variant (positive correlation), as well as *RB1*, *ATM*, *p27* and *BMI* (negative correlation). Expression levels of *Myc*, *MDM2*, *EZH2* and *CCND1* were the strongest prognostic factors independently of tumor proliferation and clinical factors (Kienle

et al. 2007). A collection of 81 well-characterized oral and oropharyngeal head and neck squamous cell carcinomas samples were analyzed against normal tissues. The Krüppel-like transcription factor 6 gene allelic loss was found to be associated with tumor recurrence and markedly decreased survival in head and neck squamous cell carcinomas (Teixeira et al. 2007).

Transcriptomic-Based Biomarkers in Cancer

The expression of *let-7* miRNA was reported to be frequently reduced in human lung cancers, and the reduced *let-7* miRNA expression was significantly associated with shorter postoperative survival. In addition, overexpression of *let-7* miRNA in A549 lung adenocarcinoma cell line inhibited lung cancer cell growth in vitro (Takamizawa et al. 2004). On the other hand, low *hsa-let-7a-2* and high *hsa-miR-155* precursor miRNA expression were found to be correlated with poor survival of lung adenocarcinomas (Yanaihara et al. 2006). The overexpression of *miR-21* in pancreatic tumors was shown to be strongly associated with both high Ki-67 proliferation index and the presence of liver metastasis. The alteration in miRNA expression was related to progression of malignancy (Roldo et al. 2006). High expression of *miR-196a-2* was found to predict poor survival in pancreatic cancer (Bloomston et al. 2007).

In 2007, the U.S. Food and Drug Administration has approved MammaPrint, a gene expression profiling service to assess the risk of recurrence in the RNA of breast cancer patients that examines 70 genes via a focused microarray (Glas et al. 2006). This approval represents a regulatory milestone as the first in vitro diagnostic multivariate index assay to acquire market clearance in the United States and is viewed as the first step toward standardizing multigene expression tests.

Proteomic-Based Biomarkers in Cancer

Expression of alphavbeta6 was assessed on 311 human lung cancer samples. Log-rank test and Cox regression analyses showed that expression of this integrin was significantly associated with poor patient outcome. Results indicated that alphavbeta6 was a prognostic biomarker for NSCLC and might serve as a receptor for targeted therapies (Elayadi et al. 2007).

A proteomic approach of SELDI-TOF MS screening was used to identify differentially cytosolic expressed proteins with a prognostic impact in 30 node-negative breast cancer patients with no relapse versus 30 patients with metastatic relapse. The protein profiling clearly showed that a high level of cytosolic ubiquitin and a low level of ferritin light chain were associated with a good prognosis in breast cancer (Ricolleau et al. 2006).

Plasma soluble CD27, interleukin (IL)-8 and IL-10 levels were assessed with enzyme-linked immunosorbent assay tests in 70 patients with B-cell chronic lymphocytic leukemia and 22 healthy donors. Soluble CD27, IL-8 and IL-10 were found to be significant prognostic factors for B-cell chronic lymphocytic leukemia (Kara et al. 2007).

Tissue arrays of 79 primary melanoma and 92 lymph node metastases were constructed from paraffin embedded tissue and Ki-67 expression examined by immunohistochemistry. High Ki-67 expression was associated with melanoma progression and multiple lymph node involvement, which might potentially form the basis of a risk analysis for patients with positive sentinel nodes (Pearl et al. 2007).

Using proteinchip profiling analysis, two isoforms of serum amyloid A (SAA) protein were identified as useful biomarkers to monitor relapse of NPC. Monitoring the patients longitudinally for SAA level by proteinchip and validated by immunoassay showed a dramatic SAA increase, which correlated with relapse and a drastic fall correlated with response to salvage chemotherapy (Cho et al. 2004). Further examination was conducted to find other serum biomarkers that were associated with active disease or chemotherapy response in NPC patients treated by two different drug combinations. Using tandem MS sequencing and immunoaffinity capture assay, two potential biomarkers were identified as a fragment of inter-α-trypsin inhibitor precursor and platelet factor-4. These disease and treatment-associated serum biomarkers might serve to diagnose and triage NPC patients for appropriate chemotherapy treatment respectively (Cho et al. 2007).

CHALLENGES AND PERSPECTIVES

Biomarker research faces several big challenges. One is the biological variability of patients' samples, which reflect the compound picture of variables stemming from differences in age, sex, exercise, diet and circadian rhythm. Although cutting-edge technologies are utilized to develop and implement cancer biomarkers for clinical use, only a handful are actually translated into fully validated diagnostic tools (Cho 2007f). Despite considerable effort and investment, most of the currently used cancer biomarkers lack high sensitivity and specificity to be useful in screening the general population, so the differentiation between some benign and malignant tumors is still a clinical challenge. Most cancer biomarkers never advance beyond the discovery phase, and the number of biomarkers validated for use in drug development or qualified for clinical applications is still very small.

While PSA is used in insurance testing to assess the risk of underlying prostate cancer, other cancer biomarkers are neither specific enough nor cost effective to use. There are also questions with PSA, as some prostate cancer may be so slow growing as to never affect eventual mortality or be unlikely to progress. Genetic testing is still not robust and accurate enough on which to forecast risk, and is not part of the testing required by insurers. On the other hand, it is recognized that many protein biomarkers may be specific protein isoforms or modified proteins, further technical developments for more effective identification and quantitation of protein isoforms and modifications would be greatly desirable.

In recent decades, knowledge about the basic biology and biochemical pathways underlying cancers has increased tremendously, but translation of that knowledge to more effective patient care and better outcomes remains a challenge. Although advances in technology have made it easier to examine many potential biomarkers in a single experiment, discovery efforts are still hampered by the limited sensitivity, specificity and capacity of current technology. There are still many obstacles to develop clinically useful cancer biomarkers, including technical challenges associated with validating potential cancer biomarkers, as well as challenges associated with developing, evaluating and incorporating the screening or diagnostic tests that make use of those cancer biomarkers into clinical practice.

Despite some notable achievements, only a few biomarkers are routinely used in oncology. Obstacles to progress could be overcome or minimized by developing different strategies to foster the work from discovery through development. Improved approaches may lead to better biomarkers for the entire spectrum of cancer health care, from chemoprevention, early detection and disease classification to drug development, treatment planning and monitoring (Cho 2007e).

The advances in oncogenomics and oncoproteomics has provided the hope of discovering novel biomarkers for use in the screening, early diagnosis and prediction of response to therapy (Cho and Cheng 2007; Cho 2009a). The current focus on cancer biomarker discovery is a result of an improved understanding of the biologic basis for carcinogenesis (Cho 2009b). Some promising strides have been made in classifying tumors at the molecular level and in selecting patients who are more likely to respond to some targeted drugs, such as trastuzumab, cetuximab, bevacizumab, gefitinib, erlotinib, imatinib, sunitinib and so on. The increasing number of potential drug targets and a plethora of diverse, new developmental agents have stimulated the search for cancer biomarkers that can reduce the time, cost and attrition rates prevalent in cancer drug development. It is hoped that the increased adoption of cancer biomarkers used in oncology will enable early proof-of-concept studies for novel therapeutic targets; accelerate the adoption of population-enrichment strategies for clinical trial recruitment; and increase the use of cancer biomarker endpoints as surrogates for clinical benefit in clinical trials.

The development of new bioinformatics tools may extract biomarker patterns with sensitivity and specificity superior to single biomarkers. However, most results needed validation by larger-scale multicentre studies. On the other hand, there is an increasing interest in complementing conventional histopathological evaluation with molecular tools that can increase the sensitivity and specificity of cancer staging for diagnostic and prognostic of locoregional or systemic recurrence. Effective use of cancer biomarkers at each stage of research and development can improve decision-making, increase clinical trial success rates and productivity, allow earlier stop/go decisions to be made and eliminating waste of resources which can otherwise be redeployed.

REFERENCES

Agulnik M, da Cunha Santos G, Hedley D, Nicklee T, Dos Reis PP, Ho J, Pond GR, Chen H, Chen S, Shyr Y, Winquist E, Soulieres D, Chen EX, Squire JA, Marrano P, Kamel-Reid S, Dancey J, Siu LL, and Tsao MS (2007) Predictive and pharmacodynamic biomarker studies in tumor and skin tissue samples of patients with recurrent or metastatic squamous cell carcinoma of the head and neck treated with erlotinib. J Clin Oncol 25:2184–2190

Birrer MJ, Johnson ME, Hao K, Wong KK, Park DC, Bell A, Welch WR, Berkowitz RS, and Mok SC (2007) Whole genome oligonucleotide-based array comparative genomic hybridization analysis identified fibroblast growth factor 1 as a prognostic marker for advanced-stage serous ovarian adenocarcinomas. J Clin Oncol 25:2281–2287

Bloomston M, Frankel WL, Petrocca F, Volinia S, Alder H, Hagan JP, Liu CG, Bhatt D, Taccioli C, and Croce CM (2007) MicroRNA expression patterns to differentiate pancreatic adenocarcinoma from normal pancreas and chronic pancreatitis. JAMA 297:1901–1908

Chen R, Brentnall TA, Pan S, Cooke K, White Moyes K, Crispin DA, Goodlett DR, Aebersold R, and Bronner MP (2007) Quantitative proteomic

analysis reveals that proteins differentially expressed in chronic pancreatitis are also frequently involved in pancreatic cancer. Mol Cell Proteomics 6:1331–1342

Cho WC (2006) Research progress in SELDI-TOF MS and its clinical applications. Chin J Biotech 22:871–876

Cho WC (2007a) Contribution of oncoproteomics to cancer biomarker discovery. Mol Cancer 6:25

Cho WC (2007b) Potentially useful biomarkers for the diagnosis, treatment and prognosis of lung cancer. Biomed Pharmacother 61:515–519

Cho WC (2007c) Nasopharyngeal carcinoma: molecular biomarker discovery and progress. Mol Cancer 6:1

Cho WC (2007d) OncomiRs: the discovery and progress of microRNAs in cancers. Mol Cancer 6:60

Cho WC (2007e) Proteomic approaches to cancer target identification. Drug Discov Today: Ther Strategies 4:245–250

Cho WC (2007f) Proteomics technologies and challenges. Genomics Proteomics Bioinformatics 5:77–85

Cho WC (2009a) An omiccs perspective on cancer research. New York, NY: Springer, Berlin

Cho WC (2009b) MicroRNAs as potential biomarkers for cancer diagnosis, prognosis and therapy. Int Biochem Cell Biol in Press

Cho WC, Cheng CH (2007) Oncoproteomics: current trends and future perspectives. Expert Rev Proteomics 4:401–410

Cho WC, Chow AS, and Au JS (2009) Restoration of tumour suppressor *hsa-miR-145* inhibits cancer cell growth in lung adenocarcinoma patients with epidermal growth factor receptor mutation. Eur J Cancer 45:2197–2206

Cho WC, Yip TT, Ngan RK, Yip TT, Podust VN, Yip C, Yiu HH, Yip V, Cheng WW, Ma VW, and Law SC (2007) Proteinchip array profiling for identification of disease- and chemotherapy-associated biomarkers of nasopharyngeal carcinoma. Clin Chem 53:241–250

Cho WC, Yip TT, Yip C, Yip V, Thulasiraman V, Ngan RK, Yip TT, Lau WH, Au JS, Law SC, Cheng WW, Ma VW, and Lim CK (2004) Identification of serum amyloid A protein as a potentially useful biomarker to monitor relapse of nasopharyngeal cancer by serum proteomic profiling. Clin Cancer Res 10:43–52

Cimmino A, Calin GA, Fabbri M, Iorio MV, Ferracin M, Shimizu M, Wojcik SE, Aqeilan RI, Zupo S, Dono M, Rassenti L, Alder H, Volinia S, Liu CG, Kipps TJ, Negrini M,and Croce CM (2005) *miR-15* and *miR-16* induce apoptosis by targeting *BCL2*. Proc Natl Acad Sci USA 102:13944–13949

Elayadi AN, Samli KN, Prudkin L, Liu YH, Bian A, Xie XJ, Wistuba II, Roth JA, McGuire MJ, and Brown KC (2007) A peptide selected by biopanning identifies the integrin alphavbeta6 as a prognostic biomarker for nonsmall cell lung cancer. Cancer Res 67:5889–5895

Everley PA, Bakalarski CE, Elias JE, Waghorne CG, Beausoleil SA, Gerber SA, Faherty BK, Zetter BR, and Gygi SP (2006) Enhanced analysis of metastatic prostate cancer using stable isotopes and high mass accuracy instrumentation. J Proteome Res 5:1224–1231

Fleuren GJ, and Nap M (1988) Carcinoembryonic antigen in primary and metastatic ovarian tumors. Gynecol Oncol 30:407–415

Garcia Pedrero JM, Fernandez MP, Morgan RO, Herrero Zapatero A, Gonzalez MV, Suarez Nieto C, and Rodrigo JP (2004) Annexin A1 down-regulation in head and neck cancer is associated with epithelial differentiation status. Am J Pathol 164:73–79

Glas AM, Floore A, Delahaye LJ, Witteveen AT, Pover RC, Bakx N, Lahti-Domenici JS, Bruinsma TJ, Warmoes MO, Bernards R, Wessels LF, and Van't Veer LJ (2006) Converting a breast cancer microarray signature into a high-throughput diagnostic test. BMC Genomics 7:278

Grossmann I, de Bock GH, Meershoek-Klein Kranenbarg WM, van de Velde CJ, and Wiggers T (2007) Carcinoembryonic antigen (CEA) measurement during follow-up for rectal carcinoma is useful even if normal levels exist before surgery. A retrospective study of CEA values in the TME trial. Eur J Surg Oncol 33:183–187

Harris HA, Albert LM, Leathurby Y, Malamas MS, Mewshaw RE, Miller CP, Kharode YP, Marzolf J, Komm BS, Winneker RC, Frail DE, Henderson RA, Zhu Y, and Keith JC Jr (2003) Evaluation of an estrogen receptor-beta agonist in animal models of human disease. Endocrinology 144:4241–4249

Hu N, Flaig MJ, Su H, Shou JZ, Roth MJ, Li WJ, Wang C, Goldstein AM, Li G, Emmert-Buck

MR, and Taylor PR (2004) Comprehensive characterization of annexin I alterations in esophageal squamous cell carcinoma. Clin Cancer Res 10:6013–6022

Hu Q, Cooks RG, and Noll RJ (2007) Phase-enhanced selective ion ejection in an Orbitrap mass spectrometer. J Am Soc Mass Spectrom 18:980–983

Imami K, Monton MR, Ishihama Y, and Terabe S (2007) Simple on-line sample preconcentration technique for peptides based on dynamic pH junction in capillary electrophoresis-mass spectrometry. J Chromatogr A 1148:250–255

Kara IO, Sahin B, and Gunesacar R (2007) Expression of soluble CD27 and interleukins-8 and -10 in B-cell chronic lymphocytic leukemia: correlation with disease stage and prognosis. Adv Ther 24:29–40

Kienle D, Katzenberger T, Ott G, Saupe D, Benner A, Kohlhammer H, Barth TF, Höller S, Kalla J, Rosenwald A, Müller-Hermelink HK, Möller P, Lichter P, Döhner H, and Stilgenbauer S (2007) Quantitative gene expression deregulation in mantle-cell lymphoma: correlation with clinical and biologic factors. J Clin Oncol 25: 2770–2777

Kurebayashi J (2004) Biomarkers in breast cancer. Gan To Kagaku Ryoho 31:1021–1026

Lee A, Kim Y, Han K, Kang CS, Jeon HM, and Shim SI (2004) Detection of tumor markers including carcinoembryonic antigen, APC, and cyclin D2 in fine-needle aspiration fluid of breast. Arch Pathol Lab Med 128:1251–1256

Lee EJ, Gusev Y, Jiang J, Nuovo GJ, Lerner MR, Frankel WL, Morgan DL, Postier RG, Brackett DJ, and Schmittgen TD (2007) Expression profiling identifies microRNA signature in pancreatic cancer. Int J Cancer 120:1046–1054

Lei H, Hemminki K, Johansson R, Altieri A, Enquist K, Henriksson R, Lenner P, and Försti A (2007) PAI-1 -675 4G/5G polymorphism as a prognostic biomarker in breast cancer. Breast Cancer Res Treat (in press)

Li G, Passebosc-Faure K, Feng G, Lambert C, Cottier M, Gentil-Perret A, Fournel P, Perol M, and Genin C (2007) *MN/CA9*: a potential gene marker for detection of malignant cells in effusions. Biomarkers 12:214–220

Locker GY, Hamilton S, Harris J, Jessup JM, Kemeny N, Macdonald JS, Somerfield MR, Hayes DF, Bast RC Jr, and ASCO (2006) ASCO 2006 update of recommendations for the use of tumor markers in gastrointestinal cancer. J Clin Oncol 24:5313–5327

Lopez JB (2005) Recent developments in the first detection of hepatocellular carcinoma. Clin Biochem Rev 26:65–79

Makarov A, Denisov E (2009) Dynamics of ions of intact proteins in the Orbitrap mass analyzer. J Am Soc Mass Spectrom 20:1486–1495

Markmann S, Gerber B, and Briese V (2007) Prognostic value of Ca 125 levels during primary therapy. Anticancer Res 27:1837–1839

Martin A, Corte MD, Alvarez AM, Rodriguez JC, Andicoechea A, Bongera M, Junquera S, Pidal D, Allende T, Muniz JL, and Vizoso F (2006) Prognostic value of pre-operative serum CA 15.3 levels in breast cancer. Anticancer Res 26:3965–3971

Matsumura H, Bin Nasir KH, Yoshida K, Ito A, Kahl G, Kruger DH, and Terauchi R (2006) SuperSAGE array: the direct use of 26-base-pair transcript tags in oligonucleotide arrays. Nat Methods 3:469–474

Mayya V, Rezual K, Wu L, Fong MB, and Han DK (2006) Absolute quantification of multisite phosphorylation by selective reaction monitoring mass spectrometry: determination of inhibitory phosphorylation status of cyclin-dependent kinases. Mol Cell Proteomics 5:1146–1157

Melanson JE, Chisholm KA, and Pinto DM (2006) Targeted comparative proteomics by liquid chromatography/matrix-assisted laser desorption/ionization triple-quadrupole mass spectrometry. Rapid Commun Mass Spectrom 20:904–910

Meng F, Henson R, Lang M, Wehbe H, Maheshwari S, Mendell JT, Jiang J, Schmittgen TD, and Patel T (2006) Involvement of human micro-RNA in growth and response to chemotherapy in human cholangiocarcinoma cell lines. Gastroenterology 130:2113–2129

Molina R, Filella X, Auge JM, Fuentes R, Bover I, Rifa J, Moreno V, Canals E, Vinolas N, Marquez A, Barreiro E, Borras J, and Viladiu P (2003) Tumor markers (CEA, CA 125, CYFRA 21–1, SCC and NSE) in patients with non-small cell lung cancer as an aid in histological diagnosis and prognosis. Comparison with the main clinical and pathological prognostic factors. Tumour Biol 24:209–218

Munoz Llarena A, Carrera Revilla S, Gil-Negrete Laborda A, Pac Ferrer J, Barcelo Galindez R,

and Lopez Vivanco G (2007) Prognostic factors associated with resectable pulmonary metastases from colorectal cancer. Arch Bronconeumol 43:309–316

Ngan RK, Lau WH, Yip TT, Cho WC, Cheng WW, Lim CK, Wan KK, Chu E, Joab I, Grunewald V, Poon YF, and Ho JH (2001) Remarkable application of serum EBV EBER-1 in monitoring response of nasopharyngeal cancer patients to salvage chemotherapy. Ann NY Acad Sci 945:73–79

Ngan RK, Yip TT, Cheng WW, Chan JK, Cho WC, Ma VW, Wan KK, Au JS, and Law CK (2004) Clinical role of circulating Epstein-Barr virus DNA as a tumor marker in lymphoepithelioma-like carcinoma of the lung. Ann NY Acad Sci 1022:1–8

Ni XG, Bai XF, Mao YL, Shao YF, Wu JX, Shan Y, Wang CF, Wang J, Tian YT, Liu Q, Xu DK, and Zhao P (2005) The clinical value of serum CEA, CA19-9, and CA242 in the diagnosis and prognosis of pancreatic cancer. Eur J Surg Oncol 31:164–169

Olofsson MH, Ueno T, Pan Y, Xu R, Cai F, van der Kuip H, Muerdter TE, Sonnenberg M, Aulitzky WE, Schwarz S, Andersson E, Shoshan MC, Havelka AM, Toi M, and Linder S (2007) Cytokeratin-18 is a useful serum biomarker for early determination of response of breast carcinomas to chemotherapy. Clin Cancer Res 13:3198–3206

Pearl RA, Pacifico MD, Richman PI, Stott DJ, Wilson GD, and Grobbelaar AO (2007) Ki-67 expression in melanoma. A potential method of risk assessment for the patient with a positive sentpenginel node. J Exp Clin Cancer Res 26:109–115

Puchades M, Nilsson CL, Emmett MR, Aldape KD, Ji Y, Lang FF, Liu TJ, and Conrad CA (2007) Proteomic investigation of glioblastoma cell lines treated with wild-type p53 and cytotoxic chemotherapy demonstrates an association between galectin-1 and p53 expression. J Proteome Res 6:869–875

Ren B, Yu YP, Tseng GC, Wu C, Chen K, Rao UN, Nelson J, Michalopoulos GK, and Luo JH (2007) Analysis of integrin *alpha7* mutations in prostate cancer, liver cancer, glioblastoma multiforme, and leiomyosarcoma. J Natl Cancer Inst 99:868–880

Ricolleau G, Charbonnel C, Lode L, Loussouarn D, Joalland MP, Bogumil R, Jourdain S, Minvielle S, Campone M, Deporte-Fety R, Campion L, and Jezequel P (2006) Surface-enhanced laser desorption/ionization time of flight mass spectrometry protein profiling identifies ubiquitin and ferritin light chain as prognostic biomarkers in node-negative breast cancer tumors. Proteomics 6:1963–1975

Roldo C, Missiaglia E, Hagan JP, Falconi M, Capelli P, Bersani S, Calin GA, Volinia S, Liu CG, Scarpa A, and Croce CM (2006) MicroRNA expression abnormalities in pancreatic endocrine and acinar tumors are associated with distinctive pathologic features and clinical behavior. J Clin Oncol 24:4677–4684

Saffroy R, Pham P, Reffas M, Takka M, Lemoine A, and Debuire B (2007) Review: new perspectives and strategy research biomarkers for hepatocellular carcinoma. Clin Chem Lab Med 45: 1169–1179

Schneider J, Philipp M, Velcovsky HG, Morr H, and Katz N (2003) Pro-gastrin-releasing peptide (ProGRP), neuron specific enolase (NSE), carcinoembryonic antigen (CEA) and cytokeratin 19-fragments (CYFRA 21-1) in patients with lung cancer in comparison to other lung diseases. Anticancer Res 23:885–893

Shami VM, Sundaram V, Stelow EB, Conaway M, Moskaluk CA, White GE, Adams RB, Yeaton P, and Kahaleh M (2007) The level of carcinoembryonic antigen and the presence of mucin as predictors of cystic pancreatic mucinous neoplasia. Pancreas 34:466–469

Shen D, Chang HR, Chen Z, He J, Lonsberry V, Elshimali Y, Chia D, Seligson D, Goodglick L, Nelson SF, and Gornbein JA (2005) Loss of annexin A1 expression in human breast cancer detected by multiple high-throughput analyses. Biochem Biophys Res Commun 326:218–227

Smitherman AB, Mohler JL, Maygarden SJ, and Ornstein DK (2004) Expression of annexin I, II and VII proteins in androgen stimulated and recurrent prostate cancer. J Urol 171:916–920

Stoeckli M, Chaurand P, Hallahan DE, and Caprioli RM (2001) Imaging mass spectrometry: a new technology for the analysis of protein expression in mammalian tissues. Nat Med 7:493–496

Strom BL, Maislin G, West SL, Atkinson B, Herlyn M, Saul S, Rodriguez-Martinez HA, Rios-Dalenz J, Iliopoulos D, and Soloway RD (1990) Serum CEA and CA 19-9: potential future diagnostic or screening tests for gallbladder cancer? Int J Cancer 45:821–824

Takamizawa J, Konishi H, Yanagisawa K, Tomida S, Osada H, Endoh H, Harano T, Yatabe Y, Nagino M, Nimura Y, Mitsudomi T, and Takahashi T (2004) Reduced expression of the *let-7* microRNAs in human lung cancers in association with shortened postoperative survival. Cancer Res 64:3753–3756

Teixeira MS, Camacho-Vanegas O, Fernandez Y, Narla G, Difeo A, Lee B, Kalir T, Friedman SL, Schlecht NF, Genden EM, Urken M, Brandwein-Gensler M, and Martignetti JA (2007) *KLF6* allelic loss is associated with tumor recurrence and markedly decreased survival in head and neck squamous cell carcinoma. Int J Cancer 121:1976–1983

Vukotic V, Cerovic S, Kozomara M, and Lazic M (2005) The predictive value of PSA in diagnosis of prostate cancer in non screened population. Acta Chir Iugosl 52:81–87

Welch C, Chen Y, and Stallings RL (2007) *MicroRNA-34a* functions as a potential tumor suppressor by inducing apoptosis in neuroblastoma cells. Oncogene 26:5017–5022

Wong MM, Lye MS, Cheng HM, and Sam CK (2005) Epstein-Barr virus serology in the diagnosis of nasopharyngeal carcinoma. Asian Pac J Allergy Immunol 23:65–67

Woods K, Thomson JM, and Hammond SM (2007) Direct regulation of an oncogenic micro-RNA cluster by E2F transcription factors. J Biol Chem 282:2130–2134

Wulfkuhle JD, Edmiston KH, Liotta LA, and Petricoin EF 3rd (2006) Technology insight: pharmacoproteomics for cancer–promises of patient-tailored medicine using protein microarrays. Nat Clin Pract Oncol 3:256–268

Yanagawa N, Tamura G, Oizumi H, Kanauchi N, Endoh M, Sadahiro M, and Motoyama T (2007) Promoter hypermethylation of *RASSF1A* and *RUNX3* genes as an independent prognostic prediction marker in surgically resected non-small cell lung cancers. Lung Cancer 58:131–138

Yanaihara N, Caplen N, Bowman E, Seike M, Kumamoto K, Yi M, Stephens RM, Okamoto A, Yokota J, Tanaka T, Calin GA, Liu CG, Croce CM, and Harris CC (2006) Unique microRNA molecular profiles in lung cancer diagnosis and prognosis. Cancer Cell 9:189–198

Ye B, Skates S, Mok SC, Horick NK, Rosenberg HF, Vitonis A, Edwards D, Sluss P, Han WK, Berkowitz RS, and Cramer DW (2006) Proteomic-based discovery and characterization of glycosylated eosinophil-derived neurotoxin and COOH-terminal osteopontin fragments for ovarian cancer in urine. Clin Cancer Res 12:432–441

Yee DS, Narula N, Ramzy I, Boker J, Ahlering TE, Skarecky DW, and Ornstein DK (2007) Reduced annexin II protein expression in high-grade prostatic intraepithelial neoplasia and prostate cancer. Arch Pathol Lab Med 131:902–908

Yim EK, and Park JS (2006) Role of proteomics in translational research in cervical cancer. Expert Rev Proteomics 3:21–36

3
Tumor Angiogenesis in Cancers: Expression of CD105 Marker

Osamu Tokunaga, Rahmawati Minhajat, and Daisuke Mori

INTRODUCTION

Angiogenesis is an important step in the process of cancer growth and wound healing (Folkman 1971). Cancer is always accompanied by angiogenesis. Angiogenesis is a complex of endothelial cell growth through an interaction of growth factors and their ligands and of sustaining matrices. Several sources of vascular endothelium are thought to participate in angiogenesis: sprouting from the preexisting blood vessel or mobilization from the bone marrow and circulation in the blood stream, and anchoring and colonization at the lesion (Asahara et al. 1999; Gunsilius et al. 2000). Whatever the source of angiogenic cells, endothelial cells express specific molecules and proliferate through an interaction with their ligands. In this chapter, the morphologic features of tumor angiogenesis, general endothelial markers of endothelium, and proliferation specific molecule CD105 are discussed.

MORPHOLOGICAL FEATURES OF TUMOR ANGIOGENESIS

The detailed structure of the newly formed blood vessel is not yet understood, although studies of the expression of marker molecules have been reported by many investigators. In normal tissue, capillaries are lined by a thin layer of tightly contiguous endothelial cells without fenestration and pores or gaps. This structure allows neither plasma leakage nor hemorrhage under physiological conditions, but they are very common in the wound healing and cancer tissue, where neoangiogenesis develops so rapidly that the structure may reflect the time lapse between vascular endothelial cell proliferation and maturation to sustain the vascular complex stability, resulting in an immature endothelial structure and vascular network (Figure. 3.1). Although the fenestration of endothelial cells is normally seen in endothelial cells of the renal glomeruli and intestinal villi, fenestration-like pores

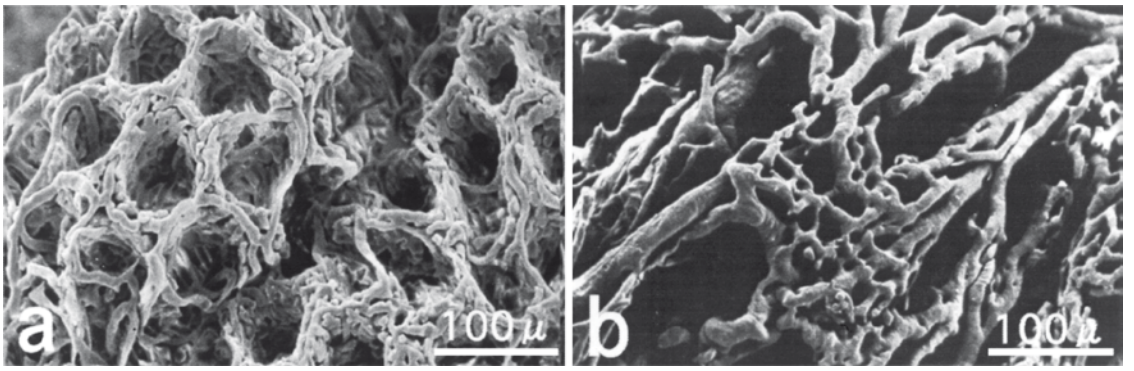

FIGURE 3.1. Normal and cancer vasculature. (**a**) Capillaries arranged orderly in the normal colon mucosa. (**b**) Disordered irregular network of the vasculature is apparent in cancer tissue. Resin cast angiography

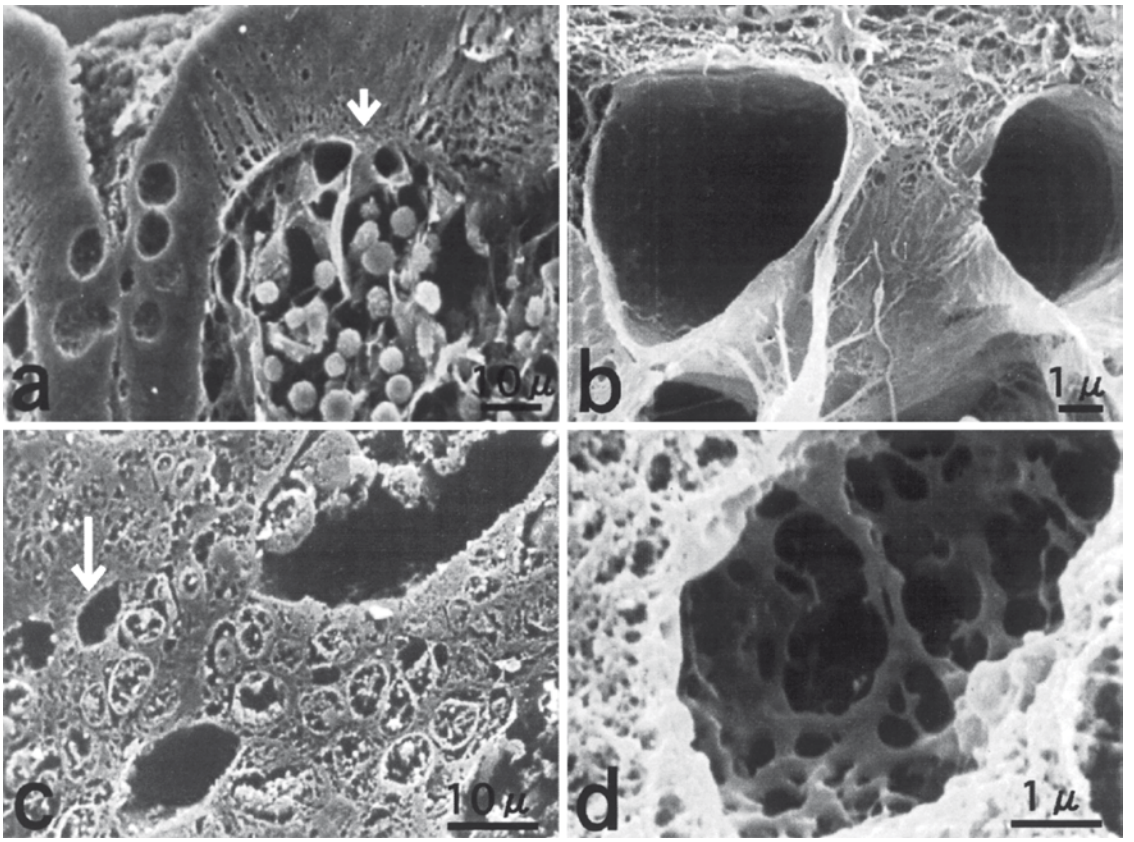

FIGURE 3.2. View of the freeze fracture in normal and cancer tissue. (**a**) Contiguous endothelial lining is smooth in normal capillaries. (**b**) Higher magnification at the short arrow. (**c**) In contrast, fenestration-like pore or gaps are common in angiogenic endothelial cells in cancer. (**d**) Higher magnification at the long arrow

and gaps or holes are common in tumor angiogenesis as seen in the discontinuous endothelium of sinusoids in normal liver and spleen. A blunt end or outpouching, and disordered vascular network are common in neoangiogenesis as observed in the freeze fracture sections of colon cancer tissue using transmission electron

microscopy (Fig. 3.2, Ogawa et al. 1999). Therefore, immature vascular structure causes easy bleeding from the cancer lesion. This disadvantage is utilized for occult blood test in stool in mass screening for colon cancer.

DETECTION OF THE ENDOTHELIUM BY IMMUNOHISTOLOGY

Antigenecity Retrieval

Conventional formalin-fixed and paraffin-embedded sections are widely used in a routine examination for immunohistological studies: immunofluorescence and immunohistochemistry in most laboratories. With formalin-fixed and paraffin-embedded sections, the antigenecity is always displaced or masked to some extent by unknown mechanisms (Shia et al. 1997). In order to obtain the best high contrast images, preliminary determination of the antibody dilution with the appropriate buffer and selection of the antigen retrieval method are essential. Several methods for performing successful antigen retrieval have been proposed. The recommended retrieval methods and antigen dilutions are shown in Table 3.1. A wide variety of antigen retrieval methods are discussed by Hayat (2002, 2004–2006).

Table 3.1. The antibodies used, antigen retrieval method, and antibody dilution

Antibody	Clone	Pretreatment	Dilution	Company
CD31	Mono	Proteinase K	20X	Dako
CD105	Mono	MW – EDTA	50X	Novocastra
CD34	Mono	AC – EDTA	50X	MBL
VEGF	Mono	AC – EDTA	100X	Santa Cruz
Flt-1	Poly	AC – EDTA	200X	Santa Cruz
Flk-1	Poly	AC – EDTA	200X	Santa Cruz
TGF-β1	Poly	AC – EDTA	100X	Santa Cruz
TGF-βRII	Poly	AC – EDTA	200X	Santa Cruz

Antigen retrieval method for immunohistochemistry. MW microwave, AC autoclave.

Immunohistology

Once the specificity of the antibody is assessed, the following quantitative immunohistological study is recommended. For immunofluorescence, 4 μm thick sections are deparaffinized and soaked in 0.01 M citrate buffer (pH 6.0) at 90°C for 40 min for antigen retrieval. The sections are treated with 10 mg/mL bovine serum albumin (BSA) to inhibit nonspecific antibody binding, and then incubated with the primary antibody for 1 h at 37°C or at 4°C overnight. After washing three times with PBS (pH 7.2), the sections are incubated with an FITC- or rhodamine (or Cy3) labeled secondary antibody raised against immunoglobulin of the primary antibody for 30 min at 37°C. If double immunofluorescence staining is desired, then a second antibody (raised in a different species) is applied and then the corresponding secondary antibody labeled with either rhodamine (or Cy3) or FITC is applied. Double FITC- and rhodamine (or Cy3) labeled samples are examined using either a fluorescence microscope or a laser microscope. To rule out a nonspecific antigen-antibody reaction, control sections are incubated with either normal murine or rabbit serum or PBS instead of the primary antibody.

For immunohistochemistry, the basic technique is the same as that of immunofluorescence. After incubation with the first primary antibody and then washing with PBS, an alkaline phosphathase labeled secondary antibody is reacted for 30 min at 37°C and visualized using BCIP/NBT substrate system that produces a blue-purple color. If double immunohistochemistry

is required, follow the same procedure as that of immunofluorescence. The second immunoreaction endproduct is visualized using the New Fuchsin Substrate Kit that produces a red color. Different substrates for other types of color development are also commercially available.

SIMULTANEOUS MASS AND COMPARATIVE STUDY: TISSUE ARRAY

To compare the level of expression simultaneously from many cases, a tissue microarray is useful and convenient (Minhajat et al. 2006a). The target area on each H and E stained slide from the representative cancer case is marked and the corresponding paraffin block is also marked. Using a tissue microarrayer (Beecher Instruments Inc., Sun Prairie, WI, USA), cylindrical cores 1.5 mm in diameter are punched out from the donor block and placed in the recipient block. As many as 250 samples can be examined simultaneously on a single microslide. The array blocks are then incubated for 30 min at 37°C to improve the adhesion between the cores and the recipient paraffin blocks. Once the microarray block is prepared, the following procedure is the same as conventional immunohistochemistry.

SPECIFIC MARKERS FOR VASCULAR ENDOTHELIUM IN TUMOR

Angiogenesis

The vascular endotheium of tumor and normal tissue is heterogeneous (Chi et al. 2003). Recent advances in immunohistological and biochemical technologies have made it possible to detect the heterogeneous endothelium. Among those markers with low specificity are lectin, vimentin, integrin, and alkaline phosphatase, which are expressed not only in endothelium but also in perivascular elements (Fox and Harris 2004).

Vascular endothelial growth factor (VEGF) is a potent mitogen in angiogenesis. It plays a central role in both normal vascular development and tumor neovascularization (Ferrara 2002). The VEGF family is composed of seven proteins with a common VEGF homology domain. The angiogenic actions of VEGF are mainly mediated through two closely related endothelium-specific receptor tyrosine kinases: Flt-1 (VEGFR-1) and Flk-1/KDR (VEGFR-2)(Faviana et al. 2002; Hicklin and Ellis 2005). Both are largely restricted to vascular endothelial cells and are overexpressed on the endothelium of tumor vasculature. All of the VEGF-A isoforms bind to both VEGFR-1 and VEGFR-2.

von Willebrand Factor (vWF) is the most familiar and reliable marker, and has been used for a long time as a conventional endothelial marker, although it is more strongly expressed in larger blood vessels than in capillary endothelial cells. vWF is also expressed in bone marrow megakaryocytes and platelets.

Other more specific reagents, CD31 and CD34 are now considered the optimal panendothelial markers (Vermeulen et al. 2002). CD34 is a single-chain transmembrane glycoprotein expressed in pluripotent stem cells and in hematopoietic stromal cells.

CD31, also called PECAM-1 (Platelet/endothelial cell adhesion molecule-1) is a single-chain type-1 membrane glycoprotein that plays a role in the adhesive interactions between adjacent endothelial cells as

well as between leukocytes and endothelial cells. CD31 is also expressed in bone marrow pluripotent hematopoietic cells and platelets. vWF, CD34, and CD31 are universally expressed and the latter two are also expressed in the proliferating active endothelial cells. Though vWF, CD34, and CD31 are used as a panendothelial markers, they react not only with newly formed blood vessels but also with normal blood vessels. Therefore, the question arises as to whether these pan-endothelial markers are ideal for the evaluation of tumor angiogenesis.

CD105/ENDOGLIN ENDOTHELIAL MARKER SPECIFIC FOR NEWLY FORMED BLOOD VESSELS

CD105/Endoglin is a receptor for transforming growth factor-β1 and -β3 (TGF-β1 and TGF-β3) and it modulates TGF-β signaling by interacting with TGF-β receptor I and/or II (TGF-βRI and/or –βRII, Duff et al. 2003). Therefore, CD105 antagonizes the inhibitory effect of TGFβ1 on endothelial cells and is essential for angiogenesis. It has been shown that CD105 is a proliferation-associated and hypoxia-inducible protein, and is preferentially expressed in the activated endothelial cells participating in neoangiogenesis (Graulich et al. 1999; Bottela et al. 2002), and is undetectable or weakly expressed in vessels of normal tissues (Minhajat et al. 2006b), with a marked tissue specificity (Burrows et al. 1995). CD105 is also weakly expressed on selected nonendothelial cells of different histotypes such as macrophages, erythroid precursors, vascular smooth muscle cells, and syncytiotrophoblasts (Fonsatti et al. 2003). Several studies have indicated CD105 to be involved in the development of blood vessels and that it represents a powerful marker of the neovascularization of various types of tumors including colon cancer (Fonsatti et al. 2000, 2003; Minhajat et al. 2006b) as seen in Fig. 3.3.

CD105 AND VASCULOGENESIS

Though the functional roles of CD105 are not fully understood, their involvement in angiogenesis, vascular development

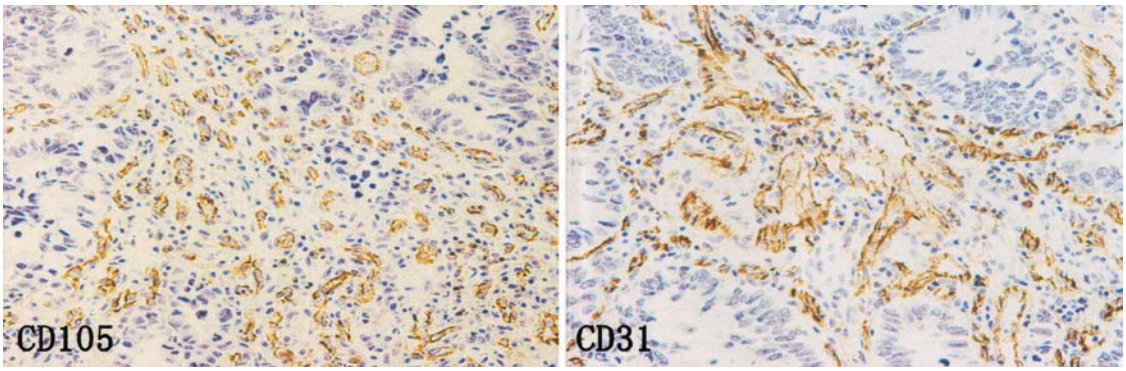

FIGURE 3.3. CD105 and CD31 immunohistochemistry on serial 4 μm thick sections of a cancer lesion. CD105 is intensely and specifically positive in small angiogenic small blood vessels, but CD31 is sparse and positive only for mature larger blood vessels: 200X

(vasculogenesis) and the maintenance of vessel wall integrity are suggested based on studies in TGF-B1- and ALK-1-null mice (Dickson et al. 1995; Urness et al. 2000). The proangiogenic role of CD105 on fetal development was demonstrated because CD105 knockout mice die in utero due to defective vascular development during early gestation (Li et al. 1999).

CD105 gene mutations are associated with hereditary type 1 hemorrhagic teleangiectasia, characterized by arteriovenous malformations and bleeding (McAllister et al. 1994). CD105 has been suggested to be a regulator of nitric oxide-dependent vascularization. The levels of CD105 expression modulate the amount of endothelial nitric oxide synthase (eNOS) in vivo and the protein levels of eNOS in vitro (Jerkic et al. 2004). Unlike other panendothelial markers such as vWF, CD31, and CD34, the superiority of anti-CD105 antibodies has been demonstrated in the evaluation of tumor angiogenesis and studied for the prediction of prognosis. Because the interruption of the blood supply to the tumor results in a reduction of the tumor size, necrosis or shrinkage of the tumor, CD105 is thus considered to be a prime vascular target of antiangiogenic cancer therapy (Fonsatti et al. 2003).

ORGAN SPECIFICITY OF CD105 POSITIVE TUMOR ANGIOGENESIS

CD31 and CD34 are expressed in vascular endothelial cells in cancer lesions as well as in those of noncancerous areas. On the other hand, CD105 expression is intense and restricted to capillary endothelial cells in cancer lesions (Figure. 3.4). In contrast, the expression of CD105 is weak and only seen in <20% of noncancerous areas in the same organs. CD105 has been demonstrated to be a more specific and sensitive marker for tumor angiogenesis than CD31 in prostatic adenocarcinoma (Wikstrom et al. 2002), and brain astrocytic tumors (Behrem et al. 2005). CD105 is also more specific than CD34 in gastric cancer (Ding et al. 2006), endometrial cancer (Saito et al. 2007), head and neck squamous cell carcinoma (Martone et al.(2005), and lung cancer (Massi et al. 2004). CD105 also has been shown to be superior for predictive survival or prognosis-related marker than other panendothelial markers (Saad et al. 2005). However, no significant difference in the CD105 expression has yet been found between cancer lesion and noncancerous areas from liver and renal cancers in vascular endothelial cells. This lack of any difference between cancer lesions and normal areas results from the characteristic structure of the cancer stroma. For example, liver cancer is composed of wide liver cancer cell sheets with sinusoidal vascular stroma where the lining endothelial cells are positive for CD105.

APPLICATION OF CD105 FOR ANTI-ANGIOGENIC CANCER THERAPY

Anti-angiogenic drugs have been developed for cancer treatment targeting VEGF, VEGF receptors, and PDGF receptors. Specifically, agents that prevent VEGF-A binding to its receptors and antibodies that directly block VEGFR-2 achieved reduction in tumor sizes and improvement in progression free survival (Marx 2007). However, side effects are also observed

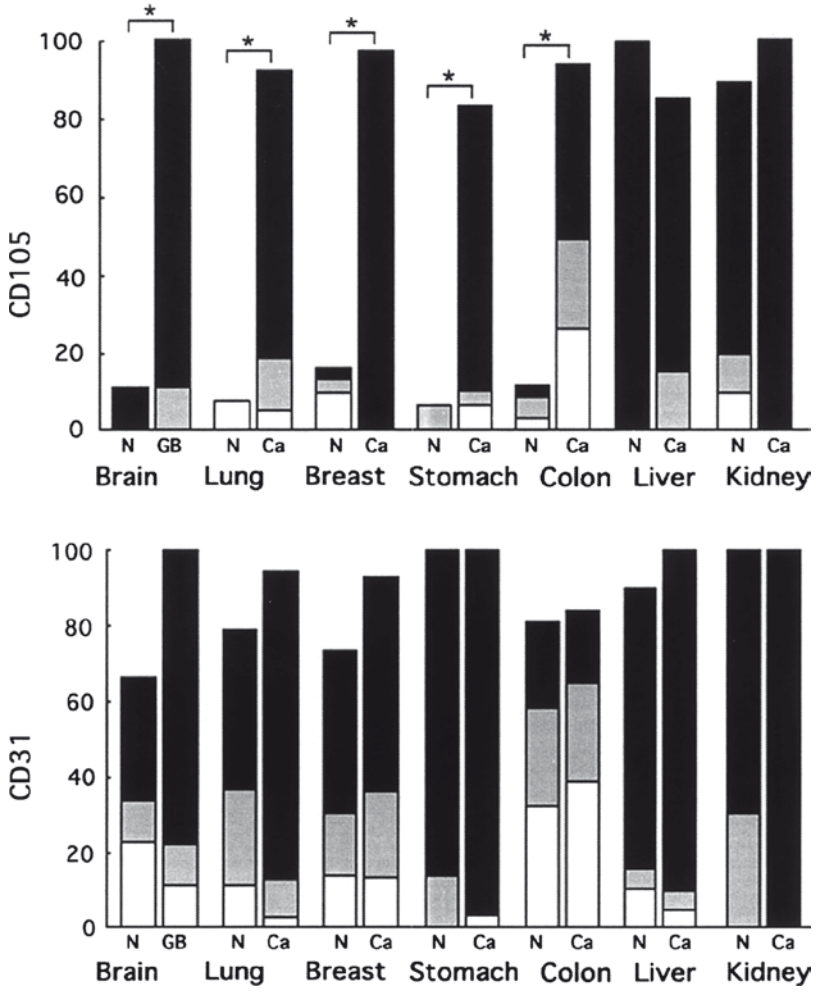

FIGURE 3.4. Organ specificity of CD105 positive blood vessels in a cancer lesion. Marked difference of CD 105 positivity is seen between angiogenic blood vessels in cancer lesions and those in non-cancerous normal tissue in the brain, lung, breast stomach, and colon, but no difference is seen in the liver and kidney. Note that CD31 is universally positive in blood vessels and no difference is seen between cancer lesions and non-cancerous normal tissue. *Statistically significant to normal tissue (N) at $P < 0.0001$, Student's *t*-test. *GB* Glioblastoma, *N* normal, *Ca* Carcinoma. Grade of Immunoreaction: (□)weak, (■)moderate, (■) strong

to occur because such molecules are universally distributed in the human vascular system.

Based on the recent advances in CD105 studies, it is most specific and sensitive molecule in activated proliferative endothelial cells within tumors. Because angiogenesis is crucial for tumor growth, CD105 is becoming a possible target for anti-angiogenesis cancer therapy (Fonsatti and Maio 2004). It has been shown that anti-CD105 antibodies specifically bind activated endothelial cells in angiogenic tissues (Dales et al. 2004; Okada et al. 2004; Taskiran et al. 2006). Anti-CD105 monoclonal antibodies (mAb) significantly inhibit the proliferation of cultured human endothelial cells (Maier et al. 1997).

DNA vaccines directed against CD105 are under trial in animal models. Oral DNA vaccines elicited a CD8+ mediated immune response against the CD105-positive target cells and suppressed dissemination of pulmonary metastasis of breast carcinoma cells (Lee et al. 2006). The targeting of CD105, as therapeutic anti-angiogenic therapy in cancer has been extensively investigated in a series of anti-CD105 mAb administration in combination with radiolabeled, immunotoxin-conjugated, or conventional chemotherapeutic regimens. Interestingly, in all these animal models the anti-tumor efficacy and anti-metastasis activities were identified, and proved the ability of anti-CD105 mAb to inhibit tumor-associated angiogenesis (Takahashi et al. 2001). Experimental anti-CD105 antibody therapy was conducted on a xenograft colon cancer model in scid mice. The cancer growth ceased and shrunk dramatically due to necrosis in the center of the tumor following intraperitoneal administration of anti-CD105 antibody every two days. Besides, such anti-CD105 antibody therapy prevented cancer metastasis to the lung when the cultured and suspended cancer cells were administered from the tail vein. Such antibody therapy prevented the secondary metastasis from the subcutaneous cancer mass originally developed in the back of the mice(unpublished data). The in vivo imaging of endothelial markers in intact tumor neovasculature can significantly help assess the efficacy of antiangiogenic agents in clinical trials. An ^{125}I-labeled monoclonal antibody has been reported to target CD105 on tumor vasculature in canine models (Fonsatti et al. 2000).

The use of anti-CD105 antibody for anti-angiogenic therapy and in vivo imaging has a great advantage of targeting the tumor and assessment for evaluation of tumor location and the efficacy of anti-CD105 cancer therapy in combination with other cancer drugs. Until now, in vivo imaging using ant-CD105 antibody has been only developed for the detection of neovascular rich tumors. If anti-CD105 antibody is combined with anticancer chemotherapeutic reagents it may, therefore, become a potent therapeutic tool for cancer in the future and also be useful in follow-up studies for the reduction or regrowth of cancer.

REFERENCES

Asahara T, Masuda H, Takahashi T, Kalka C, Pastore C, Silver M, Kearne M, Magner M, and Isner JM (1999) Bone marrow origin of endothelial progenitor cells responsible for postnatal vasculogenesis in physiological and pathological neovascularization. Circ Res 85:221–228

Behrem S, Zarkovic K, Eskinja N, and Jonjic N (2005) Endoglin is a better marker than CD31 in evaluation of angiogenesis in glioblastoma. Croat Med J 46:417–422

Bottela LM, Sanchez-Elsner T, Sanz-Rodriguez F, Kojima S, Shimada J, Guerrero-Esteo M, Cooreman MP, Ratziu V, Longo C, Vary CPH, Ramirez JR, Friedman S, and Bernabeu C (2002) Transcriptional activation of endoglin and transforming growth factor-β signaling components by cooperative interaction between Sp1 and KLF6: their potential role in the response to vascular injury. Blood 100:4001–4010

Burrows FJ, Derbyshire EJ, Tazzari PL, Amlot P, Gazdar AF, King SW, Letarte M, Vitetta ES, and Thorpe PE (1995) Up-regulation of endoglin on vascular endothelial cells in human solid tumors: implications for diagnosis and therapy. Clin Cancer Res 1:1623–1634

Chi JT, Chang HY, Haraldsen G, Jahnsen FL, Troyanskaya OG, Chang DS, Wang Z, Rockson SG, van de Rijn M, Botstein D, and Brown PO (2003) Endothelial cell diversity revealed by global expression profiling. Proc Natl Acad Sci 100:10623–10628

Dales JP, Garcia S, Andrac L, Carpentier S, Ramuz O, Lavaut MN, Allasia C, Bonnier P,

and Charpin C (2004) Prognostic significance of angiogenesis evaluated by CD105 expression compared to CD31 in 905 breast carcinomas: correlation with long-term patient outcome. Int J Oncol 24:1197–1204

Dickson MC, Martin JS, Cousins FM, Kulkarni AB, Karlsson S, and Akhurst RJ (1995) Defective haematopoiesis and vasculogenesis in transforming growth factor-beta 1 knock out mice. Development 121:1845–1854

Ding S, Li C, Lin S, Yang Y, Liu D, Han Y, Zhang Y, Li L, Zhou L, and Kumar S (2006) Comparative evaluation of microvessel density determined by CD34 or CD105 in benign and malignant gastric lesions. Hum Pathol 37:861–866

Duff SE, Li C, Garland JM, and Kumar S (2003) CD105 is important for angiogenesis: evidence and potential applications. FASEB J 17:984–992

Faviana P, Boldrini L, Spisni R, Berti P, Galleri D, Biondi R, Camacci T, Materazzi G, Pingitore R, Miccoli P, and Fontanini G (2002) Neoangiogenesis in colon cancer: correlation between vascular density, vascular endothelial growth factor (VEGF) and p53 protein expression. Oncol Rep 9:617–620

Ferrara N (2002) VEGF and the quest for tumor angiogenesis factors. Nat Rev Cancer 2:795–803

Folkman J (1971) Tumor angiogenesis: therapeutic implications. N Engl J Med 285:1182-1186

Fonsatti E, Jekunen AP, Kairemo KJA, Coral S, Snellman M, Nicotra MR, Natali PG, Altomonte M, and Maio M (2000) Endoglin is a suitable target for efficient imaging of solid tumors: in vivo evidence in a canine mammary carcinoma model. Clin Cancer Res 6:2037–2043

Fonsatti E, Altomonte M, Nicotra MR, Natali PG, and Maio M (2003) Endoglin (CD105): a powerful therapeutic target on tumor-associated angiogenetic blood vessels. Oncogene 22:6557–6563

Fonsatti E, and Maio M (2004) Highlights on endoglin (CD105): from basic findings towards clinical applications in human cancer. J Transl Med 2:18

Fox SB, Harris AL (2004) Histological quantitation of tumour angiogenesis. APMIS 112:413–430

Graulich W, Nettelbeck DM, Fischer D, Kissel T, and Muller R (1999) Cell type specificity of the human endoglin promoter. Gene 227:55–62

Gunsilius E, Duba HC, Petzer AL, Kahler CM, Grunewald K, Stockhammer G, Gabl C, Dirnhofer S, Clausen J, and Gastl G (2000) Evidence from a leukaemia model for maintenance of vascular endothelium by bone-marrow-derived endothelial cells. Lancet 355:1688–1691

Hayat MA (2002) Microscopy, immunohistochemistry, and antigen retrieval methods. Kluwer Academic/Plenum Publishers, New York

Hayat MA (ed) (2004–2006) Immunohistochemistry and in situ hybridization of human carcinomas, vols 1–4. Elsevier/Academic Press, San Diego, CA

Hicklin DJ, and Ellis LM (2005) Role of the vascular endothelial growth factor pathway in tumor growth and angiogenesis. J Clin Oncol 23:1011–1027

Jerkic M, Rivas-Elena JV, Prieto M, Carro R, Sanz-Rodriguez F, Perez-Barriocanal F, Rodriguez-Barbero A, Bernabeu C, Lopez- and Novoa JM (2004) Endoglin regulates nitric oxide-dependent vasodilatation. FASEB J 18:609–611

Lee SH, Mizutani N, Mizutani M, Luo Y, Zhou H, Kaplan C, Kim SW, Xiang R, and Reisfeld RA (2006) Endoglin (CD105) is a target for an oral DNA vaccine against breast cancer. Cancer Immunol Immunother 55:1565–1574

Li DY, Sorensen LK, Brooke BS, Urness LD, Davis EC, Taylor DG, Boak BB, and Wendel DP (1999) Defective angiogenesis in mice lacking endoglin. Science 284:1534–1537

Maier JAM, Delia D, Thorpe PE, and Gasparini G (1997) *In vitro* inhibition of endothelial cell growth by the anti-angiogenic drug AGM-1470 (TNP-460) and the anti-endoglin antibody TEC-11. Anticancer Drugs 8:238–244

Martone T, Rosso P, Albera R, Migliaretti G, Fraire F, Pignataro L, Pruneri G, Bellone G, and Cortesina G (2005) Prognostic relevance of CD105+ microvessel density in HNSCC patient outcome. Oral Oncol 41:147–155

Marx J (2007) Encouraging results for second-generation antiangiogenesis drugs. Science 308:1248–1249

Massi D, Franchi A, Paglierani M, Ketabchi S, Borgognoni L, Reali UM, and Santucci M (2004) Vasculogenic mimicry has no prognostic significance in pT3 and pT4 cutaneous melanoma. Hum Pathol 35:496–502

McAllister KA, Grogg KM, Johnson DW, Gallione CJ, Baldwin MA, Jackson CE, Helmbold EA, Markel DS, McKinnon WC, Murrell J, McCormick MK, Pericak-Vance MA, Heutink P, Oostra BA, Haitjema T, Westerman CJJ, Porteous ME, Guttmacher AE, Letarte M,

and Mar-Chuk DA (1994) Endoglin, a TGF-beta binding protein of endothelial cells, is the gene for hereditary haemorrhagic telangiectasia type 1. Nat Genet 8:345–351

Minhajat R, Mori D, Yamasaki F, Sugita Y, Satoh T, and Tokunaga O (2006a) Endoglin (CD105) expression in angiogenesis of colon cancer: analysis using tissue microarrays and comparison with other endothelial markers. Virchows Arch 448:127–134

Minhajat R, Mori D, Yamasaki F, Sugita Y, Satoh T, and Tokunaga O (2006b) Organ-specific endoglin (CD105) expression in the angiogenesis of human cancers. Pathol Int 56:717–723

Ogawa A, Miyazaki K, and Tokunaga T (1999) Distribution of newly formed vessels in human colorectal carcinomas with microangiography. Colorec Dis 1:88–100

Okada K, Satoh T, Fujimoto K, and Tokunaga O (2004) Interaction between morphology and angiogenesis in human early colorectal cancers. Pathol Int 54:490–497

Saad RS, El-Gohary Y, Memari E, Liu YL, and Silverman JF (2005) Endoglin (CD105) and vascular endothelial growth factor as prognostic markers in esophageal adenocarcinoma. Hum Pathol 36:955–961

Saito M, Sato Y, Watanabe J, Kuramoto H, Kabal S, and Fukuda T (2007) Angiogenic factors in normal endometrium and endometrial adenocarcinoma. Pathol Int 57:140–147

Shia S-R, Richard J, Cotea RJ, and Taylora CR (1997) Antigen retrieval immunohistochemistry: past, present, and future. J Histochem Cytochem 45:327–344

Takahashi N, Haba A, Matsuno F, and Seon BK (2001) Antiangiogenic therapy of established tumors in human skin/severe combined immunodeficiency mouse chimeras by anti-endoglin [CD105] monoclonal antibodies, and synergy between anti-endoglin antibody and cyclophosphamide. Cancer Res 61:7846–7854

Taskiran C, Erdem O, Onan A, Arisoy O, Acar A, Vural C, Erdem M, Ataoglu O, and Guner H (2006) The prognostic value of endoglin (CD105) expression in ovarian carcinoma. Int J Gynecol Cancer 16:1789–1793

Urness LD, Sorensen LK, and Li DY (2000) Arteriovenous malformations in mice lacking activin receptor-like kinase-1. Nat Genet 26:328–331

Vermeulen PB, Gasparini G, Fox SB, Colpaert C, Marson LP, Gion M, Belien JA, de Waal RM, Van Marck E, Magnani E, Weidner N, Harris AL, and Dirix LY (2002) Second international consensus on the methodology and criteria of evaluation of angiogenesis quantification in solid human tumours. Eur J Cancer 38:1564–1579

Wikstrom P, Lissbrant IF, Stattin P, Egevad L, and Bergh A (2002) Endoglin [CD105] is expressed on immature blood vessels and is a marker for survival in prostate cancer. Prostate 51:268–275

4
Spindle Cell Oncocytoma of the Adenohypophysis: Integrated Clinicopathologic Diagnosis by Imaging, Histology, and Immunohistochemistry

I. Vajtai and R. Sahli

INTRODUCTION

Spindle cell oncocytoma (SCO) is a non-endocrine neoplasm of uncertain histogenesis developing in and restricted to the anterior pituitary. It comprises fusiform and polygonal cells replete with mitochondria, the immunophenotype and ultrastructure of which preclude direct histogenetic identification with either adenohypophyseal secretory epithelial cells or pituicytes, as well as with any established tumor entity of local accessory tissues (e.g., meningioma; Schwannoma). In a broader context, no analogy of SCO is forthcoming with any known neoplastic condition in peripheral endocrine organs.

First characterized and reported as a distinct entity by Roncaroli et al. (2002), SCO awaits inclusion as a new item in the upcoming World Health Organization (WHO) classification of tumors of the central nervous system (provisional ICD-O code: 8290/0) (DeLellis and Lloyd 2004; Al-Shraim and Asa 2006; Roncaroli and Scheithauer 2007). It obviously is a very uncommon lesion, with a mere ten cases reported to date (Vajtai et al. 2006a; Roncaroli and Scheithauer 2007). An incidence as low as 0.4% of all sellar region tumors has been suggested by one estimate (Roncaroli et al. 2002).

CLINICAL PRESENTATION

Examples of SCO on record have been encountered in middle-aged to elderly individuals (mean age at diagnosis: 56 years; range: 26–71 years), with no apparent gender predilection. As is proper of an intrasellar mass lacking intrinsic endocrine activity, clinical signs and symptoms are those of local space occupation. In the hitherto documented occurrences, these tended to involve visual impairment (60%), partial or complete loss of adenohypophyseal function (50%), headaches (20%), as well as nausea or vomiting (20%). Secondary hyperprolactinemia due to stalk compression may be present; yet diabetes insipidus is not a feature. Furthermore, no example of tumor apoplexy has been observed.

By analogy with nonfunctioning pituitary adenomas, from which SCO ultimately is unlikely to be differentiated on clinical evidence alone, a minimal tumor size of or

exceeding 1 cm may be a prerequisite for it to become manifest.

IMAGING ASPECTS

Published references to the neuroradiology of SCO have been derived from either computed tomography (CT) or magnetic resonance imaging (MRI) studies. While specific data on maximal tumor diameter have been provided in only three cases (mean: 3.4 cm; range: 1.8–6.5 cm), all lesions were perceived as being compatible with a macroadenoma (i.e., >1 cm in diameter). On native T_1 weighted scans, SCO is solid and isointense to cerebral cortex. Moderate contrast enhancement is either diffuse or inhomogeneous; yet neither cystic change nor hemorrhage, and nor calcification have been recorded. Importantly, SCO arises in and tends to be confined to the anterior pituitary compartment, native remnants of which may have vanished completely by the time of diagnosis. There is no enlargement of the pituitary stalk. Supra- and parasellar extension are regularly seen, and the cavernous sinus may be impinged upon in some cases (Figure 4.1a and b). With one exception, that of a recurrent SCO invading the ethmoid sinus and nasopharynx, infiltration of adjacent tissues is, however, lacking (Kloub et al. 2005).

HISTOLOGY AND IMMUNOPHENOTYPE

Spindle cell oncocytoma is a moderately cellular solid and monophasic neoplasm composed of nondescript fascicles of fusiform to polygonal cells (Figure 4.1c). An unsuspectedly elaborate maze of pericellular basement membranes, including acinar-like compartments, may be appreciated on reticulin stains (Figure 4.1d). The overall eosinophilic hue of the lesion proceeds from pale to brightly pink cytoplasmic granular mitochondria that individual tumor cells tend to be replete with. While average nuclear shape may be described as "roundish to ovoid", the majority of actual nuclei more likely are felt to be slight departures from this hypothetical standard. Some nuclear pleomorphism is indeed not exceptional; yet mitotic activity tends to be largely absent. Scattered intratumoral infiltrates of reactive lymphocytes may be present, as may discrete fibrosis – especially as the tumor abuts on adjacent adenohypophyseal parenchyma. Calcification has not been described. The typical SCO will not feature either intratumoral necrosis or hemorrhage.

Although no single antigenic marker is specific for SCO, the constellation of positive and negative immunostains is distinctive enough to be considered as virtually unique.

Positive immunoreactions that are consistently found in SCO comprise S-100 protein, vimentin, and epithelial membrane antigen (EMA) (Roncaroli et al. 2002; Kloub et al. 2005; Dahiya et al. 2005; Vajtai et al. 2006b). Staining tends to be both generalized and most pronounced for S-100 protein, while EMA may react in a focal distribution and somewhat less intensely (Figure 4.1e–g). Immunostaining for mitochondrial antigens will yield a robust cytoplasmic reaction product, and is of equivalent diagnostic value as ultrastructural examination (Figure 4.1h). Expression of galectin-3 and bcl-2 respectively, has been

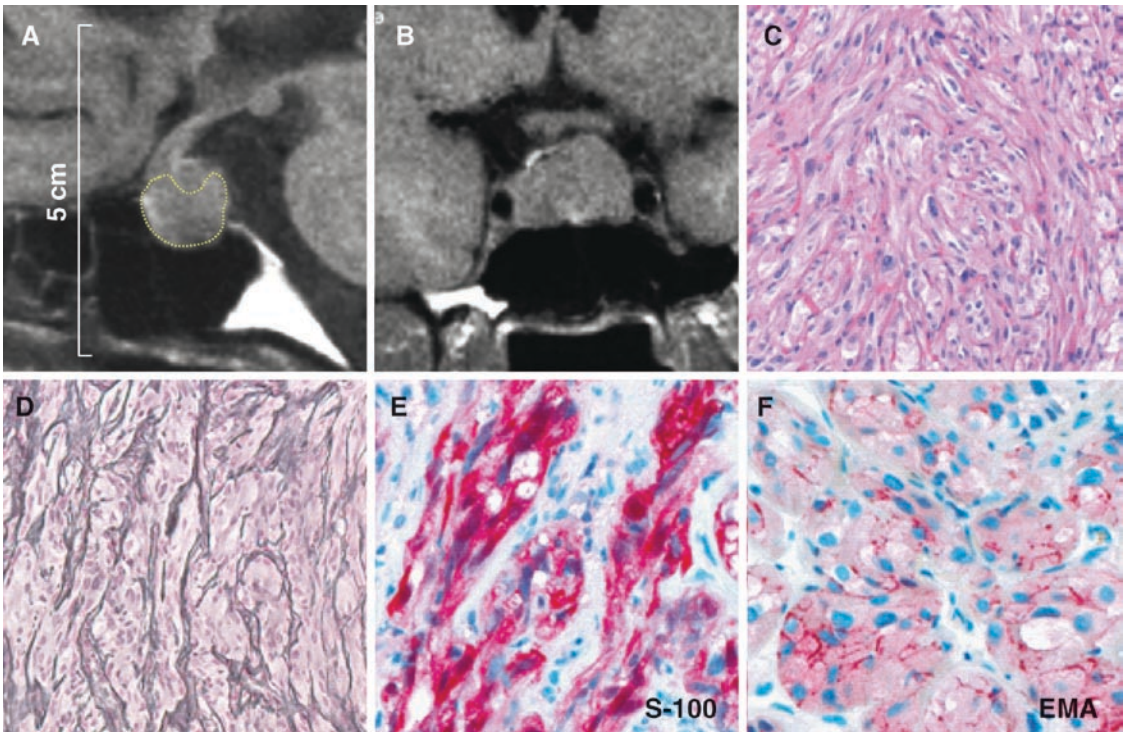

FIGURE 4.1. Sagittal (**a**) and coronal (**b**) MRI scans to show imaging aspects of SCO. Position and mass of tumor are highlighted by dotted yellow line in (**a**). At this stage of preoperative workup, SCO is unlikely to be distinguished from pituitary macroadenoma. Suprasellar extension is appreciated in (**b**); note lack of tumoral infiltration of adjacent carotid sinuses. Photomicrographs (**c** through **l**) to show salient histologic and immunophenotypic features of SCO. (**c**) Within its essentially monophasic compact texture, the tumor amalgamates slender fusiform cells and ones with epithelioid-appearing contours, both replete with intensely eosinophilic granula (hematoxylin-eosin stain; original magnification: x100). (**d**) Although quite dense, interstitial reticulin network tends to distribute haphazardly between broad fascicles rather than investing individual tumor cells (Gomori's reticulin; original magnification: x100). (**e–g**) Triple coexpression of S-100 protein, EMA, and vimentin is the most reproducible immunophenotypic trait of SCO. (**h**) Intense cytoplasmic staining with an antimitochondrial antibody corresponds to oncocytic change seen in conventional hematoxylin-eosin samples. (**i–j**) Glial differentiation in SCO is uncommon: if present, expression of astrocytic intermediate filaments will be restricted to a minority of tumor cells. (**k**) The antiapoptotic marker bcl-2 tends to produce a cytoplasmic signal. (**l**) A fair number of tumor cells in SCO may express the class II histocompatibility antigen HLA-DR, as do a subset of FSCs upon inflammatory stimuli. Immunohistochemical slides depicted in (**e**) through (**k**) were visualized using streptavidin-biotin-complex / alkaline phosphatase and new fuchsin-naphtol AS-BI as chromogen. Specimen illustrated in (**l**) was developed with horseradish peroxidase and 3,3′-diaminobenzidine; original magnification: *x*200

reported in those cases so tested (Figure 4.1k) (Roncaroli et al. 2002; Vajtai et al. 2006b). Inconstant findings include focal positivity for α-B crystallin and glial fibrillary acidic protein (GFAP) (Figure 4.1i and j), the latter being restricted to a minority of tumor cells (Vajtai et al. 2006b). We also observed significant expression of the class II histocompatibility antigen HLA-DR in some cases (Figure 4.1l; unpublished).

Negative immunostains of diagnostic relevance include in particular those markers which pituitary adenomas have been known to most consistently react positive with. Accordingly, neither generic indicators of neurosecretion (e.g., synaptophysin; chromogranins), nor individual adenohypophyseal hormones (also including the α-subunit of glycoprotein hormones) will be expressed by tumor cells of SCO. Similarly, negativity for cytokeratin(s) is a standard finding. In contradistinction from several tumor types characterized by cytoplasmic granularity, those of SCO understandably fail to express the lysosomal antigen detected by CD68. The same is true of histiocytic (lysozyme; α-1-antitrypsin), myofibroblastic (CD34), vascular endothelial (CD31; factor VIII), and smooth muscle (actin) markers.

DIFFERENTIAL DIAGNOSIS

Presently, definitive diagnosis of SCO requires microscopic study of surgically obtained tumor tissue. Pertinent radiologic assignment of the lesion to the anterior pituitary, as well as laboratory results indicating lack of intrinsic hormonal activity, nevertheless, are invaluable in appropriately preconditioning the pathologist.

We propose a practical diagnostic algorithm centered on three decision steps to be followed: i.e., (1) make sure the tumor is not an adenoma; (2) exclude other spindle cell neoplasms; (3) correctly identify cytoplasmic granula as ones of mitochondrial origin. At each decision step, there will be at least one feature whose presence or absence is mutually incompatible with either SCO or the alternative considered.

Differentiation from a pituitary adenoma will most reliably be done by showing that neither any of the major adenohypophyseal hormones nor the generic neurosecretory markers synaptophysin and chromogranin are detectable in tumor cells (Burger et al. 2002). Of note, the latter two tend to stain with remarkable intensity especially those adenoma types that often clinically present as nonfunctioning (e.g., gonadotroph cell adenomas; null cell adenomas) and/or histologically assume an oncocytic phenotype. Conscpicuously enough, such adenomas not infrequently lack significant cytokeratin immunoreactivity. Conversely, tumor cells of pituitary adenomas consistently are negative for S-100 protein, EMA, and vimentin.

Genuine spindle cell neoplasm of the sellar region that may invite misreading as SCO include pituicytoma and granular cell tumor (Burger et al. 2002). Some introductory emphasis is to be laid on "misreading" as it refers to the pathologist's alertness to details of the radiology report. To start with, both entities originate from the pituitary stalk and/or pars posterior rather than from the adenohypophysis, as does SCO. Pituicytoma is overtly astrocytic in nature; it is devoid of EMA immunoreactivity as it is of cytoplasmic granulation (Brat et al. 2000). Staining for GFAP (if often moderate) certainly is more widespread than in SCO. The rare granular cell astrocytoma is a high grade hemispheric glioma that will not be expected to visit the sellar compartment. Its granula represent phagolysosomes rather than mitochondria (Brat et al. 2002). The eponymous granula of granular cell tumor also correspond to phagolysosomes, and will henceforth be stained both with periodic acid-Schiff's reagent (PAS) and antibodies to lysosomal

antigens (Cohen-Gadol et al. 2003). While granular cell tumor, notwithstanding its purported astrocytic descent, often fails to stain for GFAP, so it also does for EMA. The astrocytic theme has recently been completed by a single case of intrasellar pleomorphic xanthoastrocytoma (Arita et al. 2002).

The spindle cell moiety of the recently described leiomyomatoid angiomatous neuroendocrine tumor (LANT) displays smooth muscle features. Moreover, this is a biphasic lesion also including a neurosecretory epithelial component akin to null cell adenoma (Vajtai et al. 2006a).

Among otherwise well-known spindle cell tumors that indeed rarely frequent the sellar compartment, meningioma and Schwannoma be mentioned (Beems et al. 1999; Burger et al. 2002; Maartens et al. 2003). Neither of these masses tends to assume an organic relationship to the anterior pituitary. The only examples of oncocytic meningoma on record developed at classic sites with conspicuous dural attachment (Roncaroli et al. 1997). While the respective immunophenotypes of meningioma and SCO will be intuited as overlapping, S-100 protein seldom actually contributes to the profile of meningiomas other than the fibrous subtype. Conversely, oncocytic change has not been known to occur in Schwannoma.

THERAPEUTIC AND PROGNOSTIC IMPLICATIONS

On the presumptive diagnosis of a nonfunctioning macroadenoma (see above), SCO will primarily be treated by microneurosurgical extirpation, as appropriate for tumor size. Particularly voluminous lesions may not be amenable to complete resection (Kloub et al. 2005; Dahiya et al. 2005). Adjuvant external beam radiotherapy has been mentioned in two such instances, in one of which this ostensibly achieved clinical benefit (Dahiya et al. 2005).

On the other hand, a postoperative outcome akin to that of a nonfunctioning macroadenoma of comparable dimensions is born out by experience with SCOs of moderate size. Specifically, while relief of visual impairment will be accomplished, functional recovery of adenohypophyseal hormone household tends to be rather poor. Panhypopituitarism (the second most frequent initial symptom) may actually ensue postoperatively, even if not present from the outset (Vajtai et al. 2006b).

Available follow-up data for patients with SCO range from 2 months to 16 years. In all but two instances, no recurrence developed during an average observation period of 6.5 years, including the longest (i.e., 16 years) postoperative interval (Roncaroli et al. 2002; Dahiya et al. 2005; Vajtai et al. 2006b).

Both recurrent tumors featured markedly increased MIB-1 labeling indices (18% and 20%, respectively); yet only one of them displayed gross invasion and regressive changes (necrosis) suggestive of malignancy (Kloub et al. 2005). However, neither of these lesions has been perceived as frankly anaplastic. Distant metastatic spread or tumor-associated death has not been mentioned.

In conclusion, and allowing for occasional departures from the rule, it is legitimate for SCOs of modest size and innocuous histology to be dealt with as primarily benign; thus, corresponding to grade I in the WHO scheme (DeLellis and Lloyd 2004; Roncaroli and Scheithauer 2007).

DISCUSSION AND PERSPECTIVES

On the understanding that tumor cells of SCO are unrelated to local meninges and Schwann cells, on the one hand, and neither neurosecretory/epithelial nor overtly glial in nature, on the other, a derivation from folliculo-stellate cells (FSC) certainly is both a tempting and plausible hypothesis (Roncaroli et al. 2002). Folliculo-stellate cells are a complement of nonendocrine sustentacular-like cells dispersed in the adenohypophyseal parenchyma. They have been known to both exert a paracrine regulatory effect on the hormone-producing population and to directly participate in their renewal cycle (Allaerts and Vankelecom 2005). The latter quality has been interpreted as one indicating a stem cell role of FSCs (Horvath and Kovacs 2002). On this background, the peculiar immunophenotype of SCO, especially as it includes simultaneous positivity for S-100 protein, EMA, vimentin, and to a lesser extent GFAP and αB-crystallin, invites reading as a recapitulation of the epithelial/glial avatars of FSCs under developmental and functional circumstances. In addition, we have recently shown that a subset of FSCs can be induced to express the class II histocompatibility epitope HLA-DR in certain inflammatory conditions of the adenohypophysis; thus, acquiring a "dendritic cell-like" antigen presenting phenotype. At present, it is unclear whether such modified HLA-DR$^+$/S100$^+$ "dendritic cell-like" FSCs are recruited from resident "classical" FSCs or derive from hematogenous monocytes. Nevertheless, the expression of HLA-DR in a substantial number of tumor cells in SCO seems to lend further support to their being interpreted as neoplastic derivatives of FSCs (Vajtai et al. 2007).

Intriguingly enough, sporadic pituitary tumors termed "folliculo-stellate cell adenoma" had been reported several years prior to the introduction of SCO (Yagishita et al. 1984). It may be expected that prospective studies of similar cases using contemporary immunohistochemical methods will eventually identify (if the above is to be holding true) what is felt to represent a "missing link" between SCO and conventional adenoma (Vajtai et al. 2007).

As a candidate for inclusion in formal classification and grading systems, SCO also needs to be characterized with respect to potential prognostic markers. Although increased nuclear MIB-1 labeling has been noted in two recurrent cases, none had shown any prospective evidence of such evolution in the primary biopsies. Henceforth, systematic studies including clinical epidemiology, radiologic presentation, and histological features in a multivariate context are warranted to address this issue.

REFERENCES

Allaerts W, and Vankelecom H (2005) History and perspectives of pituitary folliculo-stellate cell research. Eur J Endocrinol 153:1–12

Al-Shraim M, and Asa SL (2006) The 2004 World Health Organization classification of pituitary tumors: what is new? Acta Neuropathol 111:1–7

Arita K, Kurisu K, Tominaga A, Sugiyama K, Sumida M, and Hirose T (2002) Intrasellar pleomorphic xanthoastrocytoma: case report. Neurosurgery 51:1079–1082

Beems T, Grotenhuis JA, and Wesseling P (1999) Meningioma of the pituitary stalk without dural attachment: case report and review of the literature. Neurosurgery 45:1474–1477

Brat DJ, Scheithauer BW, Staugaitis SM, Holtzman RNN, Morgello S, and Burger PC (2000) Pituicytoma. A distinctive low-grade glioma

of the neurohypophysis. Am J Surg Pathol 24: 362–368

Brat DJ, Scheithauer BW, Medina-Flores R, Rosenblum MK, and Burger PC (2002) Infiltrative astrocytomas with granular cell features (granular cell astrocytomas): a study of histopathologic features, grading and outcome. Am J Surg Pathol 26:750–757

Burger PC, Scheithauer BW, and Vogel FS (eds) (2002) Region of the sella turcica. In: Surgical pathology of the nervous system and its coverings, 4th edn. Churchill Livingstone, Philadelphia, pp 437–497

Cohen-Gadol AA, Pichelmann MA, Link MJ, Scheithauer BW, Krecke KN, Young WF, Hardy J, and Giannini C (2003) Granular cell tumor of the sellar and suprasellar region: clinicopathologic study of 11 cases and literature review. Mayo Clin Proc 78:567–573

Dahiya S, Sarkar C, Hedley-White ET, Sharma MC, Zervas NT, Sridhar E, and Louis DN (2005) Spindle cell oncocytoma of the adenohypophysis: report of two cases. Acta Neuropathol 110:97–99

DeLellis RA, and Lloyd RV (eds) (2004) Pathology and genetics of tumours of endocrine organs. World Health Organization classification of tumours. IARC Press, Lyon, pp 9–47

Horvath E, Kovacs K (2002) Folliculo-stellate cells of the human pituitary: a type of adult stem cells? Ultrastruct Pathol 26:219–228

Kloub O, Perry A, Tu PH, Lipper M, and Lopes MBS (2005) Spindle cell oncocytoma of the adenohypophysis. Report of two recurrent cases. Am J Surg Pathol 29:247–253

Maartens NF, Ellegala DB, Vance ML, Lopes MBS, and Laws ER Jr (2003) Intrasellar schwannomas: report of two cases. Neurosurgery 52: 1200–1206

Roncaroli F, Riccioni L, Cerati M, Capella C, Calbucci F, Trevisan C, and Eusebi V (1997) Oncocytic meningioma. Am J Surg Pathol 21:375–382

Roncaroli F, Scheithauer BW, Cenacchi G, Horvath E, Kovacs K, Lloyd RV, Abell-Aleff P, Santi M, and Yates AJ (2002) "Spindle cell oncocytoma" of the adenohypophysis. A tumor of folliculostellate cells? Am J Surg Pathol 26:1048–1055

Roncaroli F, and Scheithauer BW (2007) Papillary tumor of the pineal region and spindle cell oncocytoma of the pituitary: new tumor entities in the 2007 WHO classification. Brain Pathol 17:314–318

Vajtai I, Sahli R, Kappeler A, Christ ER, and Seiler RW (2006a) Leiomyomatoid angiomatous neuroendocrine tumor (LANT) of the pituitary: a distinctive biphasic neoplasm with primitive secretory phenotype and smooth muscle-rich stroma. Acta Neuropathol 111:278–283

Vajtai I, Sahli R, and Kappeler A (2006b) Spindle cell oncocytoma of the adenohypophyis: report of a case with a 16-year follow-up. Pathol Res Pract 202:745–750

Vajtai I, Kappeler A, and Sahli R (2007) Folliculostellate cells of "true dendritic" type are involved in the inflammatory microenvironment of tumor immunosurveillance of pituitary adenomas. Diagn Pathol 2:20. doi:10.1186/1746-1596-2-20

Yagishita S, Itoh Y, Nakazima S, Suzuki N, Hirata K, and Yamashita T (1984) Folliculo-stellate cell adenoma of the pituitary. A light- and electron-microscopic study. Acta Neuropathol 62:340–344

5
Disseminated Carcinoma of Unknown Primary Site: Detection with F-Fluorodeoxyglucose-Positron Emission Tomography

Pascal Sève and John R. Mackey

INTRODUCTION

Carcinomas of unknown primary site (CUP) are defined by the development of an epithelial metastatic disease (epidermoid carcinomas, well or poorly differentiated adenocarcinomas, poorly differentiated or undifferentiated carcinomas) in cases where the clinical, biological, and radiological examinations fail to identify the origin at the time of the therapeutic decision (Abbruzzese et al. 1994, 1995). In a general medical oncology service, metastatic carcinomas from an unknown primary site (CUP) constitute as many as 3–5% of referred patients with solid tumors (Seve 2008; Pavlidis et al. 2003). However, this incidence varies depending on the definition of CUP, the extent of the investigations that are performed, and the details of the patient population (Seve 2008). CUPs represent clinical problems that necessitate significant interactions between pathologists, oncologists, and primary physicians. The prognosis for these forms of cancer is regarded as very poor, with <10% of survival at 5 years (Abbruzzese et al. 1994).

The absence of an identified primary tumor poses important problems in the diagnostic and therapeutic management of these patients. Indeed, conventional imaging techniques are not very effective for locating the primary site (Abbruzzese et al. 1995; Nystrom et al. 1977). In a very large series of 879 patients presenting with a CUP syndrome, the "classical" work-up leads to identification of the primary site in only 20% of cases (Abbruzzese et al. 1995). In addition, the determination of a primary and the assessment of dissemination are of crucial importance in defining the optimal treatment because the prognostic for patients affected by a CUP syndrome depends on the dissemination of the disease. Median survival is ~20 months for localized disease (lymph node involvement in only one region or a single solitary visceral metastasis) and only ~7 months for disseminated disease (Hiibner et al. 1999). The comparably good prognosis in cases of localized disease offers an option for locally curative treatment. Thus, detection of the primary tumor and accurate staging are very important in choosing an appropriate and individualized treatment plan that is adapted to the risks.

While conventional imaging methods are unable to provide identification of a primary tumor, Fluorodeoxyglucose positron emission tomography (FDG-PET) can effectively contribute to the diagnosis of CUP syndrome. Several studies reviewed the efficacy of FDG-PET in detecting unknown primary tumors in patients with cervical lymph nodes metastases from an unknown primary tumor (Fogarty et al. 2003; Nieder et al. 2001). However, FDG-PET has been less well evaluated in patients with non cervical metastases. Delgado-Bolton et al. (2003) performed a meta-analysis of the literature to evaluate the accuracy of FDG-PET in primary tumor detection in patients with CUP, but they did not distinguish patients with squamous carcinoma isolated to the head and neck from the general population of CUP patients. Several studies have explored the role of FDG-PET in small series of patients with disseminated CUP and have shown that FDG-PET is a technique that could be useful among these patients, but with very large difference between series.

The goal of this review is to systematically search the published literature for all reports of CUP and FDG-PET scanning, comprehensively review these studies to evaluate FDG-PET in the detection of primary tumors in patients presenting with carcinoma of unknown primary site, and to assess the sensitivity and specificity of FDG-PET in the detection of these tumors at various anatomic locations. Finally, we assess the resulting clinical impact of FDG-PET in CUP patients.

MATERIAL AND METHODS

A comprehensive literature search of published English-language articles, obtained using MedLine, CancerLit, and manual review of bibliographies of identified articles, revealed that between 1998 and June, 2007, 16 studies were performed that evaluated the efficacy of FDG-PET in detecting occult primaries in patients with CUP after conventional workup (Ambrosini et al. 2007; Bohuslavizki et al. 2000; Garin et al. 2007; Gutzeit et al. 2005; Kole et al. 1998; Kolesnikov-Gauthier et al. 2005; Lassen et al. 1999; Lonneux and Reffad 2000; Mantaka et al. 2003; Nanni et al. 2005; Pelosi et al. 2006; Scott et al. 2005). We excluded those studies where outcome data for the subgroup of patients with disseminated CUP were not extractable, or where only cases of isolated cervical metastases were reported. Study by Gupta et al. (1999), which focussed on cerebral metastases of unknown primary site, was excluded. Inclusion in the analysis required adequate description of the components of the workup before a diagnosis of CUP, data regarding the location of the primary tumors detected by FDG-PET, and disclosure of the numbers of accurate and inaccurate FDG-PET scans. Eligible studies required a conventional work-up including, at a minimum, the following procedures: thorough history and physical examination, chest radiographs (or chest computed tomography (CT)), abdominal and pelvic imaging with ultrasound or CT. The study by Alberini et al. (2003), where the patients voluntarily underwent FDG-PET at a very early stage (if clinical and biological examination failed to locate a primary), was excluded due to inadequate imaging. In their study of 42 patients with localised disease in CUP, Rades et al. (2001) did not separate the 21 patients with cancer not confined to the head and neck, so that we could not analyse these patients and we excluded this study.

In their study using retrospective questionnaire for referring physicians, Fencl et al. (2007), assessed the accurancy of FDG-PET in the search for the primary and the presence of a malignacy in 190 patients referred to their department because of CUP syndrome. We only included in our analysis the 82 patients with histologically proven metastases and excluded the 108 patients with suspicion of a malignancy only. Several studies (Ambrosini et al. 2007; Bohuslavizki et al. 2000; Fencl et al. 2007; Garin et al. 2007; Gutzeit et al. 2005; Kole et al. 1998; Lassen et al. 1999; Lonneux and Reffad 2000; Mantaka et al. 2003; Nanni et al. 2005; Pelosi et al. 2006) included patients with either squamous carcinoma deposits isolated to the head and neck region or non-epithelial histologies (Table 5.1) and these patients were excluded.

In aggregate, data from a total of 371 patients from 13 studies were included in the review (Ambrosini et al. 2007; Bohuslavizki et al. 2000; Fencl et al. 2007; Garin et al. 2007; Gutzeit et al. 2005; Kole et al. 1998; Kolesnikov-Gauthier et al. 2005; Lassen et al. 1999; Lonneux and Reffad 2000; Mantaka et al. 2003; Nanni et al. 2005; Pelosi et al. 2006; Scott et al. 2005). Eighty-six percent of patients had only a single organ site of metastasis. The sites of metastasis in patients with unknown primary site were as follows: nodes (46.3%), liver (12%), lung (6%), bone (11%), pleura (4%), peritoneum (4%), brain (11%), and others (10%; data not shown). Three studies did not describe the sites of metastases (Ambrosini et al., 2006; Fencl et al. 2007; Garin et al. 2007). One hundred thirty out of the one hundred seventy one patients (35%) ultimately had a primary site located either by PET, autopsy or follow-up.

Six out of the thirteen studies evaluated the potential role of combined FDG/PET/computed tomography imaging (Ambrosini et al. 2007; Fencl et al. 2007; Garin et al. 2007; Gutzeit et al. 2005; Nanni et al. 2005; Pelosi et al. 2006), and the remaining studies evaluated standard PET (Bohuslavizki et al. 2000; Kole et al. 1998; Kolesnikov-Gauthier et al. 2005; Lassen et al. 1999; Lonneux and Reffad 2000; Mantaka et al. 2003; Scott et al. 2005). FDG-PET scans were either interpreted as positive or negative by the diagnostic radiologist. To calculate sensitivity, specificity, and accuracy, true-positive was considered when FDG-PET suggested the location of the primary tumor and was subsequently confirmed, whereas false-positive was considered when this location was not confirmed (Delgado-Bolton et al. 2003). The sites suggested by FDG-PET were confirmed by histopathologic analysis of tissue obtained by biopsy or surgery, considered as the gold standard; however, imaging procedures or clinical follow-up were accepted if no histopathologic proof could be obtained. Even if other lesions were detected, when FDG-PET did not suggest the location of the primary tumor, it was considered to be true-negative if the primary tumor remained unknown in the follow-up. It was considered false-negative if the primary tumor was identified after a negative FDG-PET.

Six studies (Ambrosini et al. 2007; Garin et al. 2007; Gutzeit et al. 2005; Kolesnikov-Gauthier et al. 2005; Lassen et al. 1999; Mantaka et al. 2003) were prospective while six studies were retrospective (Bohuslavizki et al. 2000; Fencl et al. 2007; Gutzeit et al. 2005; Lonneux and Reffad 2000; Pelosi et al. 2006; Scott et al. 2005), and two not specified (Kole et al. 1998;

Table 5.1. FDG-PET detection of primary tumors and previously unrecognized metastases

Study	No. of patients (total in series)	Type	Single known site of metastases (%)	Primary tumors detected by PET (%)	PET detection of new metastases (%)
Ambrosini et al. (2007)	33 (38)	Retrospective	NS	16 (48.5)	NR
Bohuslavizki et al. (2000)	9 (53)[a]	Retrospective	9 (100)	5 (56)	1 (11)
Fencl et al. (2007)	77 (82)[a]	Prospective	NS	15 (19)	NR
Garin et al. (2007)	36 (51)	Prospective	17 (47)	8 (22)	15 (42)
Gutzeit et al. (2005)	27 (45)[b]	Retrospective	27 (100)	9 (33)	NR[c]
Kole et al. (1998)	10 (29)	NS	9 (90)	4 (40)	NR[c]
Kolesnikov-Gauthier et al. (2005)	25 (25)	Prospective	17 (68)	6 (24)	6 (24)
Lassen et al. (1999)	14 (20)	Prospective	14 (100)	8 (57)	NR[c]
Lonneux and Reffad (2000)	22 (24)	Retrospective	22 (100)	12 (55)	NR[c]
Mantaka et al. (2003)	19 (25)	Prospective	19 (100)	12 (63)	12 (63)
Nanni et al. (2005)	17 (21)	NS	17 (100)	9 (53)	3 (18)
Pelosi et al. (2006)	47 (68)	Retrospective	44 (94)	18 (38)	NR[c]
Scott et al. (2005)	31 (31)	Retrospective	NS	8 (26)	15 (48)
Total	371 (512)		190 (86)	130 (35)	52 (38)

Patients with isolated neck metastases and noncarcinoma histologies were excluded. *NR* data not reported, *NS* data not specified

[a] We also excluded patients with undifferentiated carcinoma involving cervical nodes

[b] We excluded all patients with cervical metastases since the authors did not state the histological subtypes

[c] Data reported for the overall population but not for the sub-set of patients belonging of the general population of CUP

Nanni et al. 2005). Most of the studies included patients with resected metastases or single known metastases (Table 5.1). In all studies, CUP was diagnosed only after conventional workup failed to detect a primary tumor. The definition of conventional workup varied among the 13 studies. In the studies by Kole et al. (1998) and Lassen et al. (1999), the diagnostic procedures were performed according to the primary histology of the metastases. In the study by Mantaka et al. (2003), patients with suspected lung carcinoma subsequently underwent CT or/and MRI of the thoracic region as well as bronchoscopy with final biopsy. In some studies imaging of the breast region (sonography, mammography, CT or/and magnetic resonance imaging (MRI)) were reserved to women with axillary lymphadenopathy (Mantaka et al. 2003). Due to the retrospective nature of some studies (Gutzeit et al. 2005; Fencl et al. 2007; Lonneux and Reffad, 2000; Pelosi et al. 2006; Scott et al. 2005), there were no specific requirements in terms of imaging and endoscopic procedures so that patients could enter the study population with variable prior workup.

RESULTS

Among the 371 patients with metastases from an unknown primary after conventional workup, FDG-PET detected the primary lesion in 130 (Table 5.1), for a detection rate of 35%, and the remaining scans were noninformative. Detection rates ranged from 19% (Fencl et al. 2007; Garin et al. 2007) to 63% (Mantaka et al. 2003). In those FDG-PET scans with informative results, the sensitivity, specificity, and accuracy of FDG-PET in the detection of primary tumors were 85.6%, 83.3%, and 78%, respectively (Table 5.2). Fencl's study took account of more than

TABLE 5.2. Sensitivity, specificity, and accuracy of FDG-PET in tumor detection

Study	No. of patients	TP	FP	FN	TN
Ambrosini et al. (2007)	33	16	1	0	17
Bohuslavizki et al. (2000)	9	5	0	0	4
Fencl et al. (2007)	78	15	13	14	39
Garin et al. (2007)	36	8	1	0	28
Gutzeit et al. (2005)	27	9	3	1	14
Kole et al. (1998)	10	4	0	0	6
Kolesnikov-Gauthier et al. (2005)	25	6	5	0	14
Lassen et al. (1999)	14	8	1	1	4
Lonneux and Reffad (2000)	22	12	5	0	5
Mantaka et al. (2003)	19	12	1	0	6
Nanni et al. (2005)	17	9	1	0	7
Pelosi et al. (2006)	47	18	3	4	22
Scott et al. (2005)	31	8	3	2	18
Total	371	130	37	22	184
PET sensitivity	85.6%				
PET specificity	83.3%				
PET accuracy	78%				

FDG-PET fluorodeoxyglucose positron emission tomography, *TP* true-positive, *FP* false-positive, *FN* false- negative, *FP* false-positive

half of false negatives and almost one third of false positives patients (Fencl et al. 2007). FDG-PET was compared with whole-body CT in 2 studies, comprising 52 patients (Gutzeit et al. 2005; Kolesnikov-Gauthier et al.). FDG-PET allows the detection of nine (17%) tumors that were not identified by CT. There were no tumors only detected by CT. Two studies retrospectively compared PET and CT of the chest for the diagnosis of lung cancer (Lassen et al. 1999; Lonneux and Reffad 2000). FDG-PET allowed the detection of 12 lung cancers in patients where CT of the chest was considered negative or inconclusive.

Six studies evaluated fused PET/CT in detection of the primary lesion in cancer of an unknown primary site (Ambrosini et al. 2007; Fencl et al. 2007; Garin et al. 2007; Gutzeit et al. 2005; Nanni et al. 2005; Pelosi et al. 2006). PET/CT depicted the primary tumor in 65 (27.3%) of 238 patients. Only the study by Gutzeit et al. (2005) assessed the value of FDG-PET/CT in comparison with PET and CT. In this study, PET/CT depicted the primary tumor in 15 (33%) of 45 patients, PET alone revealed the primary tumor in 11 (24%) of 45 patients while PET and CT in combination identified 13 (29%) of 45 tumors.

Of the 13 studies, 6 included data regarding FDG-PET detection of distant metastases in the group of patients without neck metastases (Table 5.1). These 6 studies included 137 patients with metastases from unknown primary tumors (Garin et al. 2007; Gutzeit et al. 2005; Kolesnikov-Gauthier et al. 2005; Mantaka et al. 2003; Nanni et al. 2005; Scott et al. 2005). In 52 of these patients (38%), additional metastases were detected by FDG-PET alone.

Data were collected on the locations of primary tumors detected by FDG-PET, as well as on the locations of false-positive and false-negative readings. There were 152 tumors in total, with each of these tumors corresponding to a true-positive or false-negative result on FDG-PET. The main site of metastases was, in order of decreasing frequency, supraclavicular or cervical nodes (13.1%), the liver (11.7%), bones (11.3%), the brain (10.8%), axillary lymph nodes (10.4%), and mediastinal lymph nodes (7.7%; data not shown).

Of the 102 primary tumors located above the diaphragm, 90 (88.2%) exhibited FDG uptake, and only 12 were not detected by PET; primary sites included the lung in 75 patients (73.5%), the breast in 18 patients (17.6%), the esophagus in 2 patients (1.9%), the thyroid in 1 patient (1%), and 6 other tumors (5.9%). Of the 50 primary

tumors located below the diaphragm, 40 (80%) exhibited FDG uptake, and only 10 were not detected by PET; primary sites included the pancreas in 12 patients (24%), the stomach in 9 patients (18%), the colon and rectum in 7 patients (14%), the ovary in 5 patients (10%), the bilary system in 4 patients (8%), the kidney and testis each in 3 patients (6%), the uterus in 2 patients (4%), and 5 other tumors (10%).

Data regarding the locations of false-positive and false-negative FDG-PET readings were collected to determine the sensitivity and specificity of PET at various locations. The specificity of FDG-PET at a given location cannot be calculated, as it is impossible to attribute true-negative results to specific sites. Therefore, the false-positive rate (i.e., false-positives as a percentage of all positive tests) is used in the analysis. Colon and rectal cancers accounted for 33.3% (7 of 21) of all false-positive FDG-PET scans but made up only 5.4% of all tumors encountered; this corresponds to a false-positive rate of 53.3% for lower gastrointestinal tumors. The false-positive rate for kidney tumors (66.6%) was higher but there was only two tumors detected by FDG-PET. False-negative FDG-PET scans were less common than false-positive scans; a factor that contributed to the observation of high overall sensitivity. FDG-PET did, however, exhibit lower sensitivity with respect to upper gastrointestinal tract, kidney, biliary system, and breast. However, there were limited numbers of tumors for each of these sites, particularly, for biliary system and kidney cancers. The sensitivity of FDG-PET at other sites than breast, upper gastrointestinal tract, biliary system and kidney was 93.9%. FDG-PET was highly accurate in the identification of lung cancers.

Seven of the ten studies (Garin et al. 2007; Kole et al. 1998; Kolesnikov-Gauthier et al. 2005; Lassen et al. 1999; Lonneux and Reffad 2000; Mantaka et al. 2003; Scott et al. 2005) provided data on changes in treatment planning in response to additional information provided by FDG-PET scans (Table 5.3). In 51 of the 157 patients in these 7 studies (32.5%), a therapeutic change was attributed to FDG-PET findings. Changes in treatment were attributable either to the detection of a primary tumor and/or to the detection of previously unknown metastases. In patients in whom an unknown primary was identified, the treatment strategy was mostly changed from CUP chemotherapy to specific therapy for the tumor site. Among these 38 patients, 26 (68%) had confirmed lung or pancreas cancers (24 and 2, respectively) whereas only 5 (13.1%) had breast, 3 had ovary (7.9%), and each 1 had esophagus, peritoneum and prostate cancers (2.6%). Six patients had surgery with curative intent including one patient with brain metastasis and a lung primary (Kolesnikov-Gauthier et al. 2005), one patient with peritoneal carcinomatosis and an ovarian primary (Kolesnikov-Gauthier et al. 2005), one patient with liver metastases and a colon primary (Lonneux and Reffad 2000), one patient with involved axillary lymph nodes and breast cancer (Lonneux and Reffad 2000), one patient with involved cervical lymph nodes and breast cancer (Mantaka et al. 2003), and one patient who presented with an isolated lung metastasis that subsequently was confirmed to be a primary bronchoalveolar carcinoma (Scott et al. 2005). Detection of unknown distant metastases led to a transition from curative to palliative intent in some patients. These data were explicit

Table 5.3. Impact of PET on treatment strategy

Studies	No. of patients	Tumors detected	Therapeutic impact (%)	Surgery	Radio therapy	Chemo therapy
Ambrosini et al. (2007)	33	16	NS	NS	NS	NS
Bohuslavizki et al. (2000)	9	5	NS	NS	NS	NS
Fencl et al. (2007)	78	15	NS	NS	NS	NS
Garin et al. (2007)	36	8	9 (25)	0[a]	2	6
Gutzeit et al. (2005)	27	9	NS	NS	NS	NS
Kole et al. (1998)	10	4	1 (10)	0	0	1
Kolesnikov-Gauthier et al. (2005)	25	6	6 (24)	2	0	4
Lassen et al. (1999)	14	8	3 (21.4)	0	0	3
Lonneux and Reffad (2000)	22	12	9 (40.9)	2	0	7
Mantaka et al. (2003)	19	12	11 (57.9)	6[b]	3	7
Nanni et al. (2005)	17	11	NS	NS	NS	NS
Pelosi et al. (2006)	47	18	NS[c]	NS	NS	NS
Scott et al. (2005)	31	8	12[d,e] (38.7)	1	NS	10
Total	371	99	51 (32.5)	6[f] (11.7)	5 (9.8)	38 (74.5)

NS data not specified

[a]In one patient, the initial anticipated treatment was surgery and chemotherapy and discovery of celiac axis nodes a led to contraindicate surgery.

[b,f]Out of these patients, five underwent surgery for diagnosis at a disseminated stage. These patients were excluded for the final analysis

[c]Data reported for the overall population but not for the sub-set of patients belonging of the general population of CUP

[d]One patient in whom a pattern of disease has been identified by PET consistent with prostate cancer was managed accordingly

[e]PET altered clinical management of respectively, eight confirmed and four unconfirmed, putative primary sites

in only the study by Garin et al. (2007). In this work, FDG-PET led to a therapeutic modification by revealing additional metastases in three cases.

Only Fencl et al. (2007) evaluated the prognostic value of the FDG-PET/CT findings. In their analysis of 82 patients with histologically proven metastasis, they found a significantly shorter survival in patients with FDG/PET findings compared with patients with negative findings. Garin et al. (2007) compared the diagnostic performances and therapeutic impact of FDG-PET between the localized and multifocal forms of CUP. They found significant differences in the detection of additional metastases in the group with multifocal forms, but no difference in the detection of the primary. The therapeutic impact seemed greater in the localized than in the multifocal forms but this difference was not statistically significant. However, these authors did not separate for this analysis the 15 patients with cervical lymphatic metastasis of epidermoid carcinoma and the 36 patients with other localizations, so that we could not generalize these data to the disseminated CUP patients.

DISCUSSION

The detection of primary tumors in patients with CUP may be important for several reasons, including finding a potentially treatable tumor and allowing therapy to be targeted as appropriately as possible. Moreover, FDG-PET allows better definition of prognosis, because prognosis depends on the stage of the disease.

Thus, detection of the primary tumor and accurate staging are very important to select appropriate risk-adapted individualized treatment. Several reports in the literature describe the efficacy of FDG-PET in detecting unknown primary tumors in patients with CUP. Most of these studies, however, are limited in size and have reported varying results. Our objective in the current review was to compile all existing literature on this topic to help guide clinical decision-making regarding the use of FDG-PET in CUP, excluding patients with squamous carcinoma deposits isolated to the head and neck region and histologies other than carcinoma. Several previous reviews of this topic have been conducted (Scott et al. 2005; Seve et al. 2007). Scott et al. (2005) reviewed, in their retrospective analysis of the use of FDG-PET in 31 patients with CUP, 6 studies involving a total of 85 patients with disseminated CUP. Their analysis revealed, in contrast with the current review, a higher primary detection rate (62% vs. 34.7% in our study) and a reduced specificity (69.2% vs. 83.3% in our study), whereas the sensitivity and the accuracy were close (83.3% and 84.9%, respectively, vs. 85.6% and 78% in our study). These discrepancies can be attributed to : (1) the inclusion of the studies by Alberini et al. (2003) and by Scott et al. (2005), in which FDG-PET was carried out early in the search for metastases, and where the database for the patients does not allow the distinction for the patients with metastases other than cervical ; (2) the report of four false-negative cases in the study by Bohuslavizki et al. (2000), although these authors reported that primary tumors were not found in these patients at clinical follow-up. Moreover, we included in our study patients with adenocarcinoma involving cervical nodes, whereas these patients were excluded in the review by Scott et al. (2005). We have published a comprehensive review of the efficacy of FDG-PET in CUP (Seve et al. 2007). This audit went beyond the review by Scott et al. (2005) by excluding inappropriate studies and including a larger data set with four further studies. Furthermore, we included unique data regarding and the sensitivity and specificity of FDG-PET at various anatomic locations and the effects of FDG-PET on patient management. In this work, we analyzed three additional recent studies including 147 supplementary patients.

Data from this review regarding primary tumor location are not fully concordant with those made in previous studies that did not necessarily use PET imaging. In their report of 879 patients referred with a diagnosis of CUP, Abbruzzese et al. (1995) found that imaging studies provided the diagnosis in 132 patients. For patients with carcinomas, the six most common diagnoses were lung (20.4%), pancreas (15.9%), and colorectal (8.3%), followed by kidney (6.8%), breast (6.1%), and stomach (6.1%). In the current study, 56.2% of all primary tumors in patients with disseminated CUP were found in the lung. Lung cancer is probably overrepresented in our review because thoracic scans were not performed for all patients, and are more sensitive than chest radiography for the detection of lung cancer (Seve 2008). In comparison to autopsy evaluations, data from the current series also suggest a lower incidence of primary tumors of the pancreas (8.5% in our study vs. 20–26% at autopsy) and a higher incidence of primary tumors of the breast (8.5% in our study

vs. 2% at autopsy) (Seve 2008). The high rate of patients with axillary, supraclavicular, brain metastases and the low rate of patients with liver metastases may explain these results.

Moreover, our findings also show a high rate of single metastasic sites in comparison to the main published series of CUP patients. In the current study, 86% of patients had only one single metastasis site while the rate, in the literature, ranges from 29% to 43% (Abbruzzese et al. 1995; Culine et al. 2002; Hess et al. 1999; Seve et al. 2006). These data indicate that patients enrolled in PET studies are selected patients and do not reflect the overall population of patients with CUP. Only Garin et al. (2007) compared the diagnostic performances and therapeutic impact of FDG-PET between the localized and multifocal forms of CUP. They found significant differences in the detection of additional metastases in the group with multifocal forms but no difference in the detection of the primary and the therapeutic impact seemed greater in the localized than in the multifocal forms. However, these authors did not separate for this analysis patients with cervical lymphatic metastasis to disseminated CUP patients.

FDG-PET imaging clearly was able to detect new metastases. Overall, the data from the current review indicated that PET imaging detected unsuspected additional sites of metastasic disease in 38% of all patients. While it is likely that this new information may have altered management in some cases, these data were only explicit in the study by Garin et al. (2007).

Six studies assessed the value of FDG-PET-CT for the diagnosis of disseminated CUP, while one study compared FDG-CT and FDG. Hybrid imaging by FDG-PET-CT eliminates the drawback of FDG-PET imaging, i.e the lack of anatomical information, and may enhance the diagnostic capacity of the method. The overall sensitivity (79.8%), specificity (85%), and accuracy (75.6%) in these six studies were not different from the other studies. However, the high rate of false-positive and false-negative in the study by Fencl et al. (2007) could underestimate the impact of FDG-PET-CT. This study using retrospective questionnaire of the referring physicians should be interpreted cautiously. By excluding this study, the overall sensitivity, specificity, and accuracy rates of FDG-PET-CT in detecting unknown primary tumors were, 91.3%, 90.7%, and 86.9%, respectively. In the comparative study by Gutzeit et al. (2005), PET/CT was able to depict more primary tumors, though not significantly, than either of the other imaging modalities. Larger comparative studies are required to definitively evaluate the relative value of PET/CT and PET for identifying a primary site tumor site.

In our audit, FDG-PET exhibited its highest accuracy for tumors of the lung and pancreas. The high sensitivity and low false-positive rates that were observed indicate that FDG-PET is a valuable supplement to conventional imaging in these locations. Conversely to our first review, we found a lower sensitivity of FDG-PET for breast cancer. As discussed before, the high rate of false-negative in the study by Fencl et al. (2007) led to these results. As there were few reports of GI, ovary, uterus, and kidney cancers, conclusions regarding the sensitivity and accuracy of FDG-PET for these settings are uncertain.

FDG-PET had a low false-positive rate for tumors located in the lungs, in the breast and in the pancreas even if, for these

two last tumors, the number of patients was limited. The low false-positive rate that was observed corresponds to a high specificity and positive predictive value for FDG-PET detection of tumors at lung and pancreas sites. At anatomic locations other than the lung, pancreas and breast, false-positive rates were higher, but the limited number of patients does not allow definitive conclusions. The lower gastrointestinal tract was the most common site of false-positive FDG uptake. False-positive FDG-PET findings subject the patient to further diagnostic endoscopies, which have associated costs and morbidities.

Therapeutic impact was evaluated in seven studies. PET-FDG examinations modified therapy in 10% to 57.9% of the patients, according to the series in question. Again, the variability of the results obtained in these studies can largely be explained by variable patient selection. By collating the results of these 7 studies, we find that FDG-PET modified the care of 51 patients out of 157 (32.5%). The majority of primary tumors diagnosed in the 42 patients were cancers of the lung and cancers of the pancreas, and the most commonly encountered modifications involve a change of the initially considered chemotherapy. Treatment for both of these cancers has undergone a significant shift during the last 5–10 years, with standard of care for patients with a good performance status now being chemotherapy. The treatment of advanced non-small-cell lung cancer (NSCLC) is based on the combination of platin and one of the following agents: taxanes, gemcitabine, vinorelbine, or irinotecan (Pfister et al. 2004). In the case of pancreatic cancer, gemcitabine has become standard of care (Burris et al. 1997). Although evidence-based medicine does not define a standard for the systemic treatment of CUP site not belonging to a specific anatomoclinical entity, chemotherapy is considered for patients with a good general health status. Standard therapy includes one of the newer cytotoxics alone or in combinations including platinum salts, taxanes, and gemcitabine (Culine et al. 2003; Greco et al. 2001). Given these regimens, it is probable that change in management plan of patients with lung and pancreatic cancer did not consistently modify the type of chemotherapy and the prognosis. However, one fourth of patients received specific therapy for breast, ovary and prostate cancers or had surgery with curative intent. Therefore, we think that the primary indications for PET in unknown primary are clinical presentations suggestive of CUP syndrome that may benefit from specific treatment, as women with axillary-lymph-node metastasis, women with peritoneal adenocarcinomatosis, and in the setting of a single metastasis when a curative treatment is planned. No study formally assessed the contribution of FDG-PET for survival in CUP patients, although Mantaka et al. (2003) reported a better survival in patients diagnosed by PET, while survival was not altered by discovery of the primary tumor in the study by Kole's et al. (1998). Only Fencl et al. (2007) evaluated the prognostic value of the FDG-PET/CT findings and found a significantly shorter survival in patients with FDG/PET findings compared with patients with negative findings. However, because of the design of their study and the short follow-up, these data require confirmation in large and prospectives studies.

While the role of routine FDG-PET early in the workup of CUP remains unproven, it may have several practical advantages.

Only Alberini et al. (2003) retrospectively assessed the value of FDG-PET prior to conventional imaging in 41 CUP patients. PET was superior to conventional diagnosis in 11 patients and prompted treatment modifications in 11 patients. Sensitivity of PET was markedly superior to CT in detecting lung cancers and abdominal primary tumours. PET scanning in the setting of CUP is likely to be beneficial for a number of reasons. Earlier diagnosis of the primary may allow more appropriate therapy at a time when the performance status is good. The majority of patients presenting with metastatic disease in the setting of CUP undergo a rapidly progressive course and if diagnosis has been delayed, for example, by multiple investigations, patients may no longer be fit enough to tolerate treatment. In addition, a reduction in the number and cost of investigations, the time requirements for the intensive investigation phase to be completed, and the number of invasive procedures with concomitant risk of complications would be advantageous for the patient and may well be cost-effective. For example, Erasmus and Patz (1999) showed that PET can replace conventional strategy and save money for the staging of NSCLC (Erasmus and Patz 1999). Further evaluation of PET with large and prospective studies, as well as cost-benefit analyses, are now warranted to confirm these hypothesis.

We acknowledge the limitations of the current review, including the possibility of publication bias, and heterogeneity among studies with regard to patient selection and diagnostic workup. Moreover, almost all patients a solitary site of metastasis and there were few patients with liver metastases. These data show that patients included in PET studies were selected and that the conclusions cannot necessarily be generalized to the overall population of patients with CUP. Despite these limitations, our findings do allow us to draw several important conclusions. In the investigations of patients with CUP, FDG-PET was found to provide information beyond that obtained by conventional workup. FDG-PET was sensitive in the detection of primary tumors and, in ~35% of cases, revealed tumors that had gone undetected by other modalities. Whole-body FDG-PET also detected previously unrecognized regional or distant metastases in ~38% of patients. FDG-PET exhibited high overall sensitivity in the detection of unknown primaries. In contrast, however, FDG-PET had low overall specificity and a high false-positive rate for lower gastrointestinal tract tumors. Overall, subsequent cancer treatment was influenced by the PET in one third of patients, particularly in those with lung and pancreatic cancer, while some patients received specific treatment for breast, ovary and prostate cancers or had surgery with curative intent. In conclusion, the review of the available evidence confirms FDG-PET to be a valuable imaging modality in the workup of patients with single site metastasis and when curative-intent therapy is planned.

REFERENCES

Abbruzzese JL, Abbruzzese MC, Hess KR, Raber MN, Lenzi R, and Frost P (1994) Unknown primary carcinoma: natural history and prognostic factors in 657 consecutive patients. J Clin Oncol 12:1272–1280

Abbruzzese JL, Abbruzzese MC, Lenzi R, Hess KR, and Raber MN (1995) Analysis of a diagnostic strategy for patients with suspected tumors of unknown origin. J Clin Oncol 13:2094–2103

Alberini JL, Belhocine T, Hustinx R, Daenen F, and Rigo P (2003) Whole-body positron emission tomography using fluorodeoxyglucose in

patients with metastases of unknown primary tumours (CUP syndrome). Nucl Med Commun 24:1081–1086

Ambrosini V, Nanni C, Rubello D, Moretti A, Battista G, Castelluci P, Farsad M, Rampin L, Fiorentini G, Franchi F, Canini R, and Fanti S (2007) 18F-FDG PET/CT in the assessment of carcinoma of unknown primary origin. Radiol Med 111:1146–1155

Bohuslavizki KH, Klutmann S, Kroger S, Sonnemann U, Buchert R, Werner JA, Mester J, and Clausen M (2000) FDG PET detection of unknown primary tumors. J Nucl Med 41:816–822

Burris HA III, Moore MJ, Andersen J, Green MR, Rothenberg ML, Modiano MR, Cripps MC, Portenoy RK, Storniolo AM, Tarassoff P, Nelson R, Dorr FA, Stephens CD, and Von Hoff DD (1997) Improvements in survival and clinical benefit with gemcitabine as first-line therapy for patients with advanced pancreas cancer: a randomized trial. J Clin Oncol 15:2403–2413

Culine S, Kramar A, Saghatchian M, Bugat R, Lesimple T, Lortholary A, Merrouche Y, Laplanche A, and Fizazi K (2002) Development and validation of a prognostic model to predict the length of survival in patients with carcinomas of an unknown primary site. J Clin Oncol 20:4679–4683

Culine S, Lortholary A, Voigt JJ, Bugat R, Theodore C, Priou F, Kaminsky MC, Lesimple T, Pivot X, Coudert B, Douillard JY, Merrouche Y, Allouache J, Goupil A, Négrier S, Viala J, Petrow P, Bouzy J, Laplanche A, and Fizazi K (2003) Cisplatin in combination with either gemcitabine or irinotecan in carcinomas of unknown primary site: results of a randomized phase II study – trial for the French Study Group on Carcinomas of Unknown Primary (GEFCAPI 01). J Clin Oncol 21:3479–3482

Delgado-Bolton RC, Fernandez-Perez C, Gonzalez-Mate A, and Carreras JL (2003) Meta-analysis of the performance of 18F-FDG PET in primary tumor detection in unknown primary tumors. J Nucl Med 44:1301–1314

Erasmus JJ, and Patz EF Jr (1999) Positron emission tomography imaging in the thorax. Clin Chest Med 20:715–724

Fencl P, Belohlavek O, Skopalova M, Jaruskova M, Kantorava I, and Simomova K (2007) Prognostic and diagnostic accuracy of FDG-PET/CT in 190 patients with carcinoma of unknown primary. Eur J Nucl Mol Imag [epub ahead of print]

Fogarty GB, Peters LJ, Stewart J, Scott C, Rischin D, and Hicks RJ (2003) The usefulness of fluorine 18-labelled deoxyglucose positron emission tomography in the investigation of patients with cervical lymphadenopathy from an unknown primary tumor. Head Neck 25:138–145

Garin E, Prigent-Lejeune F, Lesimple T, Barge ML, Rousseau C, Devillers A, Bouriel C, Mesbah H, Bernard AM, Bridji B, and Resche I (2007) Impact of PET-FDG in the diagnosis and therapeutic care of patients presenting with metastases of unknown primary. Cancer Invest 25:232–239

Greco FA, Gray J, Burris HA III, Erland JB, Morrissey LH, and Hainsworth JD (2001) Taxane-based chemotherapy for patients with carcinoma of unknown primary site. Cancer J 7:203–212

Gupta NC, Nicholson P, and Bloomfield SM (1999) FDG-PET in the staging work-up of patients with suspected intracranial metastatic tumors. Ann Surg 230:202–206

Gutzeit A, Antoch G, Kuhl H, Egelhof T, Fischer M, Hauth E, Goehde S, Bockisch A, Debatin J, and Freudenberg L (2005) Unknown primary tumors: detection with dual-modality PET/CT–initial experience. Radiology 234:227–234

Hess KR, Abbruzzese MC, Lenzi R, Raber MN, and Abbruzzese JL (1999) Classification and regression tree analysis of 1000 consecutive patients with unknown primary carcinoma. Clin Cancer Res 5:3403–3410

Hiibner G, Wildfang I, and Schmoll HJ, CUP (1999) In: Schmoll HJ (ed) Kompendium Internistische Onkologie Band 2. Berlin/Heidelberg/New York: Springer, pp 2137–2182

Kole AC, Nieweg OE, Pruim J, Hoekstra HJ, Schraffordt Koops H, Roodenburg JLN, Vaalburg W, and Vermey A (1998) Dtection of unknown occult primary tumors using positron emission tomography. Cancer 82:1160–1166

Kolesnikov-Gauthier H, Levy E, Merlet P, Kirova J, Syrota A, Carpentier P, Meignan M, and Piedbois P (2005) FDG PET in patients with cancer of an unknown primary. Nucl Med Commun 26:1059–1066

Lassen U, Daugaard G, Eigtved A, Damgaard K, and Friberg L (1999) 18F-FDG whole body positron emission tomography (PET) in patients with unknown primary tumours (UPT). Eur J Cancer 35:1076–1082

Lonneux M, and Reffad A (2000) Metastases from unknown primary tumor. PET-FDG as initial diagnostic procedure? Clin Positron Imag 3: 137–141

Mantaka P, Baum RP, Hertel A, Adams S, Niessen A, Sengupta S, and Hor G (2003) PET with 2-[F-18]-fluoro-2-deoxy-D-glucose (FDG) in patients with cancer of unknown primary (CUP): influence on patients' diagnostic and therapeutic management. Cancer Biother Radiopharm 18:47–58

Nanni C, Rubello D, Castellucci P, Farsad M, Franchi R, Toso S, Barile C, Rampin L, Nibale O, and Fanti S (2005) Role of 18F-FDG PET-CT imaging for the detection of an unknown primary tumour: preliminary results in 21 patients. Eur J Nucl Med Mol Imag 32:589–592

Nieder C, Gregoire V, and Ang KK (2001) Cervical lymph node metastases from occult squamous cell carcinoma: cut down a tree to get an apple? Int J Radiat Oncol Biol Phys 50:727–733

Nystrom JS, Weiner JM, Heffelfinger-Juttner J, Irwin LE, Bateman JR, Wolf RM (1977) Metastatic and histologic presentations in unknown primary cancer. Semin Oncol 4:53–58

Pavlidis N, Briasoulis E, Hainsworth J, and Greco FA (2003) Diagnostic and therapeutic management of cancer of an unknown primary. Eur J Cancer 39:1990–2005

Pelosi E, Pennone M, Deandreis D, Douroukas A, Mancini M, and Bisi G (2006) Role of whole body positron emission tomography/computed tomography scan with 18F-fluorodeoxyglucose in patients with biopsy proven tumor metastases from unknown primary site. Q J Nucl Med Mol Imag 50:15–22

Pfister DG, Johnson DH, Azzoli CG, Sause W, Smith TJ, Baker S Jr, Olak J, Stover D, Strawn JR, Turrisi AT, and Somerfield MR, A Society of Clinical Oncology (2004) American Society of Clinical Oncology treatment of unresectable non-small-cell lung cancer guideline: update. J Clin Oncol 22:330–353

Rades D, Kuhnel G, Wildfang I, Borner AR, Schmoll HJ, and Knapp W (2001) Localised disease in cancer of unknown primary (CUP): the value of positron emission tomography (PET) for individual therapeutic management. Ann Oncol 12:1605–1609

Scott CL, Kudaba I, Stewart JM, Hicks RJ, and Rischin D (2005) The utility of 2-deoxy-2-[F-18] fluoro-D-glucose positron emission tomography in the investigation of patients with disseminated carcinoma of unknown primary origin. Mol Imag Biol 7:236–243

Seve P, Sawyer M, Hanson J, Broussolle C, Dumontet C, and Mackey JR (2006) The influence of comorbidities, age, and performance status on the prognosis and treatment of patients with metastatic carcinomas of unknown primary site: a population-based study. Cancer 106: 2058–2066

Seve P (2008) Clinical presentations. In: Wick MR (ed) Metastatic carcinoma of unknown primary. New York: Demos, pp 1–26

Seve P, Billotey C, Broussolle C, Dumontet C, and Mackey JR (2007) The role of 2-deoxy-2-[F-18] fluoro-D-glucose positron emission tomography in disseminated carcinoma of unknown primary site. Cancer 109:292–299

6
Unknown Lymphadenopathy: Diagnosing Using an Endoscopic Ultrasound-Guided Fine-Needle Aspiration Biopsy

Ichiro. Yasuda

INTRODUCTION

The diagnosis of mediastinal and intra-abdominal lymphadenopathy is sometimes difficult, especially in patients without any other primary lesions and without any specific serological findings. This may be caused by primary lymph proliferative disorders, metastasis, sarcoidosis, tuberculosis, and so on. In cases with superficial lymph node swelling, an excisional biopsy of the superficial lymph nodes can be performed relatively easily. Otherwise, open thoracic surgery, laparotomy, or another invasive procedure such as mediastinoscopy or laparoscopy is often required, but these procedures are performed under general anesthesia, and therefore they require much time, manpower, and expense. They are also associated with higher rates of morbidity, and the tissue damage caused by the procedure may delay the start of therapy. Patients who are in serious medical conditions will also be exposed to higher anesthetic and surgical risks.

Endoscopic ultrasound-guided fine needle aspiration (EUS-FNA) is now widely used as a safe and accurate procedure for sampling intra- and extramural lesions of the gastrointestinal tract. This procedure can also be attempted for mediastinal and intra-abdominal lymphadenopathy of unknown origin. It is considered to be a useful procedure that should be attempted before performing more invasive procedures such as mediastinoscopy and open surgery.

APPLICATION

Mediastinal and intra-abdominal lymph nodes that are located at sites capable of being approached from the esophagus, stomach, or duodenum on the basis of computed tomography (CT) can be a target. A pelvic lymphadenopathy is also included if it is accessible from the rectum. Contraindications are similar to those for routine endoscopy, but patients with coagulopathy and thrombocytopenia are also generally excluded from the subject.

EQUIPMENT

Echoendoscopes and Endoscopic Ultrasound Processors

A linear (or convex array) echoendoscope is necessary for this procedure. Currently, four companies (Olympus, Pentax, Toshiba

and Fujinon) produce this type of echoendoscope, but the models from Olympus and Pentax are used most frequently. The EUS transducer is set distal to the oblique-forward- viewing lens, and it is similar in shape to those used for transabdominal studies. It has a 120° (Pentax) or 180° (Olympus) field of ultrasonic view, and is equipped with an elevator and a working channel range in size from 2.4 to 3.8 mm (Pentax; EG-363OU [2.4 mm], EG-383OUT [3.8 mm], Olympus; GF-UC240P/140P-AL5 [2.8 mm], GF-UCT240/140-AL5 [3.7 mm]; Figure. 6.1).

The echoendoscope is connected to a processor with a color Doppler function. The Pentax echoendoscope is run by a Hitachi processor (EUB-405plus, -525, -2000, -5000, -6000, or -8000), and the processor for the Olympus echoendoscope is the Aloka processor (SSD-5000, -5500, α5, or α10) or their own processor (EU-ME1). Another Olympus unit, EU-C2000/-C60 is also available for EUS-FNA. It is diminutive and very mobile, but the image quality is somewhat reduced.

Needles

Fully disposable needles ranging from 25-gauge to 19-gauge distributed by Wilson-Cook, Olympus, and GIP/Mediglobe are used for this procedure. In general, the larger needle improves the tissue yield and allows histological assessment, but increased stiffness of the needle makes its maneuverability more restrictive and difficult. A 22-gauge needle is used most frequently for conventional EUS-FNA. If the aim is to differentiate whether the lesion was benign or malignant, cytological examination is sufficient, and a 22-gauge or even 25-gauge needle can be used. However, a histological assessment is often required in the diagnosis of an unknown lymphadenopathy. Lymphoma is a frequent cause of unknown lymphadenopathy,

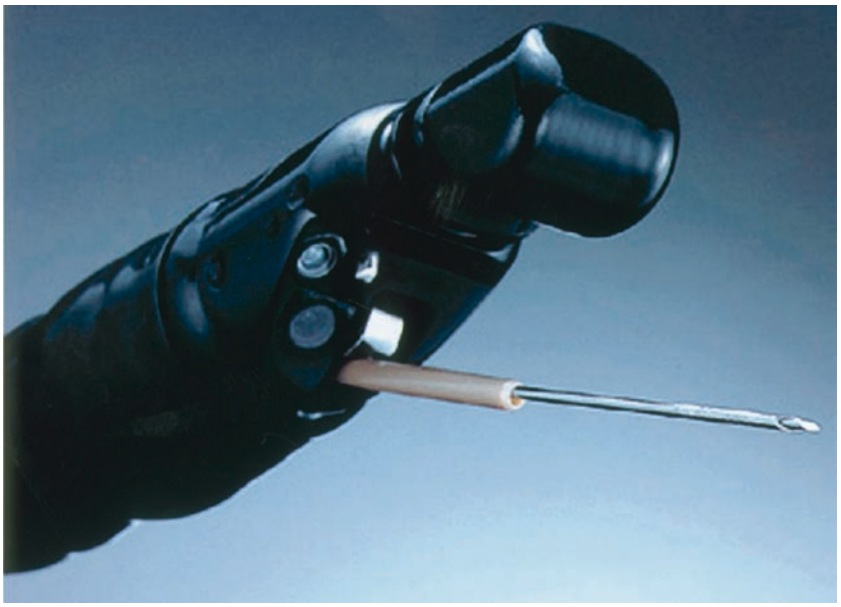

Figure 6.1. Olympus linear echoendoscope (GF-UC240P-AL5) with a 22-gauge FNA needle (EZ-shot; NA-200H-8022, Olympus)

and histopathological findings are essential for its accurate diagnosis and subclassifications of the tumor. This is because the optimal treatment strategy is determined by the subclass of lymphoma. Therefore, a larger needle such as a 19-gauge needle is preferable in that situation. A Tru-Cut needle, which has a 20 mm tissue tray with a 19-gauge outer cutting needle and a spring-loaded mechanism built into the handle that permits automated specimen procurement, may be another option to obtain core samples as Varadarajulu et al. (2004)) reported. However, its ability to puncture is compromised by the increased stiffness and the blind tip. This needle system also seems to be unsuitable for relatively small lesions (probably <2 cm) due to the automatic puncture system.

PROCEDURE

Preparations

The procedure is performed on an outpatient basis unless the patient is already hospitalized for other medical conditions. The necessary preparations are similar to those for routine endoscopy, but heavier sedation may be required because of the longer procedure time and need to minimize patient movement. Careful monitoring of blood pressure, and pulse and oxygen saturation is necessary throughout the procedure. On the other hand, routine antibiotic prophylaxis is generally considered unnecessary because the rate of bacteremia after EUS-FNA is extremely low, according to Levy et al. (2003, 2007).

Fine Needle Apiration Biopsy

The echoendoscope is advanced into the esophagus, stomach, and if necessary into the duodenum after sedation of the patient. The target lesion is observed carefully and color Doppler imaging is used to ensure that there are no major interposed vessels in the puncture path. The puncture is achieved with guidance from the real-time EUS image, after the optimal puncture site is determined (Figure. 6.2). The inner stylet is pulled back for ~1 cm to expose the sharp tip of the needle just before the puncture. After the lymph node is punctured, the stylet is pushed in again beyond the tip to prevent contamination of the gastrointestinal wall before it is completely removed. Several to-and-fro movements are made within the lymph node under continuous negative suction using a syringe. The suction is slowly released after the completion of this step. The needle is then withdrawn into the sheath followed by the withdrawal of the entire system from the biopsy channel of the echoendoscope.

Treatment of Sampled Material

The aspirated material is then expelled onto glass slides by carefully reinserting the stylet. This material is thereafter assessed macroscopically, and whitish parts of the material are removed and collected on small pieces of filter paper. The material is then put into formalin solution (3%) for pathological examination. A pathological diagnosis is made based on the findings of hematoxylin-eosin staining (Figure. 6.3) and immunopathological stains. The use of specific monoclonal antibodies is tailored to each case based on the information obtained from hematoxylin-eosin staining.

Some tissue is also smeared onto glass slides for cytological examination. The glass slides are fixed immediately in absolute

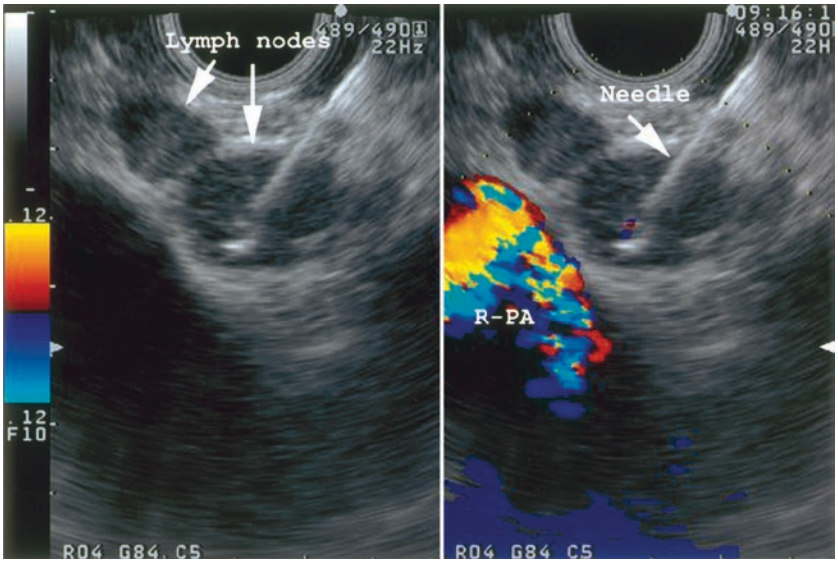

FIGURE 6.2. The left image is a fundamental ultrasound image and the right image is the simultaneous image with Color Doppler function. The needle was inserted into a mediastinal lymph node (left paratracheal lymph node) with guidance of a real-time ultrasound image to avoid interposing vessels (R-PA, right pulmonary artery)

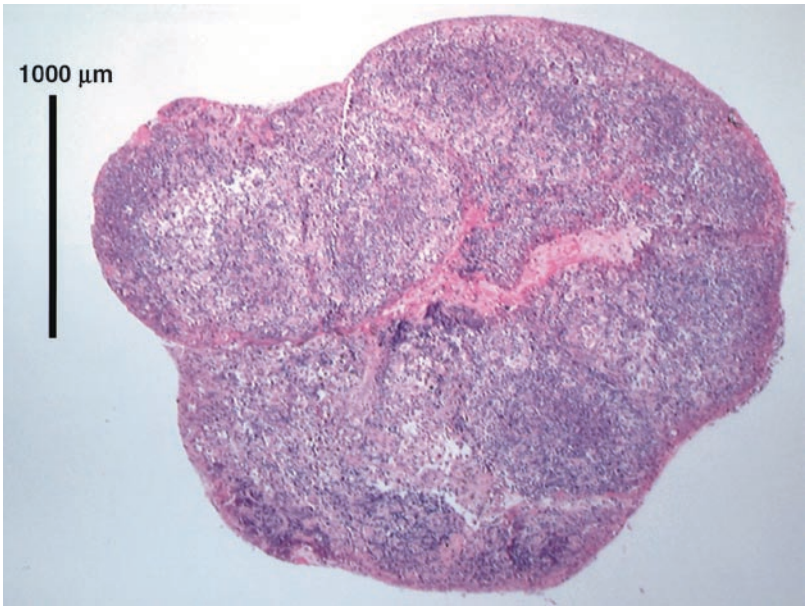

FIGURE 6.3. Low-power histological microscopic image of an entire biopsy specimen obtained by EUS-FNA biopsy (hematoxylin-eosin stain, 8×)

ethanol, and/or are left to dry in air. The choice of the fixation method depends on the preference of the institutional pathologist. Air-dried smears can be used for an immediate cytologic evaluation using Diff-Quik stain (Harleco, Gibbstown, NJ),

and also for May-Grünwald-Gimsa stain. On the other hand, alcohol-fixed smears are used for Papanicolau stain.

A microbiological examination and flow cytometry are also helpful in the diagnosis of unknown lymphadenopathy. For this purpose, additional aspirate specimens are put into saline solution and a cytological preservative solution such as RPMI and phosphate-buffered saline. Microbiological examination can differentiate bacterial infections such as tuberculosis. Itaba et al. (2007) reported that polymerase chain reaction (PCR) analysis and culture are helpful to diagnose tuberculous lymphadenitis. The efficacy of flow cytometry on the diagnosis of lymphoma by investigating cellular surface antigens has also been reported by Ribeiro et al. (2001) and Mehra et al. (2005).

The presence of an on-site cytopathologist is generally considered to be helpful to improve the diagnostic yield of EUS-FNA as Klapman et al. (2003) has reported. It may reduce the incidence of sampling error and unsatisfactory specimens. Unnecessary repeated procedures can also be prevented by an immediate evaluation of the specimens.

Management After the Procedure

The outpatients are observed for immediate complications in the recovery room at least for 2 h, and contact should be maintained after the procedure to monitor for any complications.

DIAGNOSTIC YIELD

The diagnostic ability of EUS-FNA for unknown lymphadenopathy is very high as described below. For a mediastinal lymphadenopathy of unknown etiology, Catalano et al. (2002) reported that EUS-FNA successfully established a diagnosis in 90% of 62 patients, whose final diagnoses were lung cancer (24), adenocarcinoma of unknown origin (6), lymphoma (3), breast cancer (2), ovarian cancer (1), histoplasmosis (15), sarcoidosis (6), and inflammatory/reactive (5). EUS-FNA influenced the subsequent therapy in 87% of those patients.

Devereaux et al. (2002) also assessed the clinical utility of EUS-FNA of mediastinal masses in the absence of known pulmonary malignancy. According to their data, an accurate diagnosis was made in 46 of the 49 patients (94%). Their FNA diagnosis was metastatic in 22 patients, histoplasmosis in 8 patients, sarcoidosis in 1 patient, other benign diseases in 15 patients, and nondiagnostic in 3 patients.

Yasuda et al. (2006) evaluated the diagnostic yield of EUS-FNA biopsies in 104 patients with mediastinal and intra-abdominal lymphadenopathy of unknown origin. The locations of the lymph nodes were mediastinal in 50 patients, intra-abdominal in 48 patients, and both mediastinal and intra-abdominal in 6 patients. The diagnoses made using EUS-FNA biopsy were lymphoma (48), metastasis (16), and benign/reactive (40) including 23 sarcoidosis and 2 tuberculosis. Their overall accuracy was 98%, and the histopathological results influenced the treatment strategy in 96% of the patients. The sensitivity, specificity, positive and negative predictive value for diagnosis of lymphoma was 96.0% (95% CI, 86.5–98.9), 100% (93.4–100), 100% (92.6–100), and 96.4% (87.9–99.0), respectively. Of the 50 patients with final diagnosis of lymphoma, 96% were diagnosed by EUS-FNA biopsy

alone, and it was possible to classify the lymphomas in accordance with World Health Organization (WHO) classifications in 88% of cases. Ninety-four percent of the patients were treated based on the results of the biopsy findings alone.

Complications

Possible complications related to this procedure are bleeding, infection, perforation, and needle track seeding of malignant cells. However, the incidence of these adverse events is extremely low. Indeed, in the initial two reports mentioned above, there were no complications. In addition, according to a study by Yasuda et al. (2006), the incidence of early procedural complication related to this procedure was only 1% (one patient). For example, only one patient with lymphoma had abdominal pain without bleeding and inflammation after the procedure.

REFERENCES

Catalano MF, Nayar R, Gress F, Scheiman J, Wassef W, Rosenblatt ML, and Kochman M (2002) EUS-guided fine needle aspiration in mediastinal lymphadenopathy of unknown etiology. Gastrointest Endosc 55:863–869

Devereaux BM, LeBlanc JK, Yousif E, Kesler K, Brooks J, Mathur P, Sandler A, Chappo J, Lehman GA, Sherman S, Gress F, and Ciaccia D (2002) Clinical utility of EUS-guided fine-needle aspiration of mediastinal masses in the absence of known pulmonary malignancy. Gastrointest Endosc 56:397–401

Itaba S, Yoshinaga S, Nakamura K, Mizutani T, Honda K, Takayanagi R, and Yamada K (2007) Endoscopic ultrasound-guided fine-needle aspiration for the diagnosis of peripancreatic tuberculous lymphadenitis. J Gastroenterol 42:83–86

Klapman JB, Logrono R, Dye CE, and Waxman I (2003) Clinical impact of on-site cytopathology interpretation on endoscopic ultrasound-guided fine needle aspiration. Am J Gastroenterol 98:1289–1294

Levy MJ, Norton ID, Wiersema MJ, Schwartz DA, Clain JE, Vazquez-Sequeiros E, Wilson WR, Zinsmeister AR, Jondal ML (2003) Prospective risk assessment of bacteremia and other infectious complications in patients undergoing EUS-guided FNA. Gastrointest Endosc 57:672–678

Levy MJ, Norton ID, Clain JE, Enders FB, Gleeson F, Limburg PJ, Nelson H, Rajan E, Topazian MD, Wang KK, Wiersema MJ, and Wilson WR (2007) Prospective study of bacteremia and complications with EUS-FNA of rectal and perirectal lesions. Clin Gastroenterol Hepatol 5:684–689

Mehra M, Tamhane A, and Eloubeidi MA (2005) EUS-guided FNA combined with flow cytometry in the diagnoses of suspected or recurrent intrathoracic or retroperitoneal lymphoma. Gastrointest Endosc 62:508–513

Ribeiro A, Vazquez-Sequeiros E, Wiersema LM, Wang KK, Clain JE, and Wiersema MJ (2001) EUS-guided fine-needle aspiration combined with flow cytometry and immunocytochemistry in the diagnosis of lymphoma. Gastrointest Endosc 53:485–491

Varadarajulu S, Fraig M, Schmulewitz N, Roberts S, Wildi S, Hawes RH, Hoffman BJ, and Wallace MB (2004) Comparison of EUS-guided 19-gauge Trucut needle biopsy with EUS-guided fine-needle aspiration. Endoscopy 36:397–401

Yasuda I, Tsurumi H, Omar S, Iwashita T, Kojima Y, Yamada T, Sawada M, Takami T, Moriwaki H, and Soehendra N (2006) Endoscopic ultrasound-guided fine-needle aspiration biopsy for lymphadenopathy of unknown origin. Endoscopy 38:919–924

Therapy

7
Pretargeted Radioimmunotherapy in Cancer: An Overview

Stefano Papi, Chiara Maria Grana, Mirco Bartolomei, Laura Ravasi, Marta Cremonesi, Mahila Ferrari, Luigi Martano, Lucia Garaboldi, Marco Chinol, and Giovanni Paganelli

INTRODUCTION

The concept of tumour targeting began at the turn of the twentieth century when Ehrlich (1907) postulated the idea of the "Magic Bullet" to target abnormal cells selectively on the basis of antigenic differences between normal and abnormal cells. No clinical application of this concept took place until Pressman and Keighley (1948) utilized labeled antibodies for cancer detection. Pressman et al. (1957) showed that monoclonal antibodies (MoAbs) labeled with radioactive iodine could be used in animals on a diagnostic basis. Later, Bale et al. (1960) demonstrated that tumour localizing antibodies could be used as a therapeutic agent for treating experimental neoplasms by means of the radioactivity. The modern era of targeted cancer therapy did not start until 1975, upon the publication of Kohler and Milstein's (1975) work describing the technology for the production of MoAbs, also referred to as the "hybridoma technology". This method allowed the production of a large amount of different MoAbs with high specificity towards tumour-associated antigens and opened the door to the preclinical and clinical research in the targeted radiotherapy of cancer using MoAbs, referred to as radioimmunotherapy (RIT).

Radioimmunotherapy is an area of extensive investigation at both the experimental and clinical levels (Goldenberg and Sharkey 2007). The inherent appeal of this therapy modality is its potential to specifically irradiate tumours while sparing healthy tissues. With fractionated external beam irradiation (XRT), precise focusing of the beam specifically to a tumour, especially metastatic cancers, without affecting proximal healthy organs, is impractical. On the contrary, RIT involves continuous, low-dose irradiation from tumour-targeted radionuclides. Biological effect is facilitated through energy absorption from the radionuclide's emissions. The tissue range of the nuclide's emissions, which are several millimeters when using β-particle emitters, can have a "crossfire" effect, in that even antigen negative cells in a tumour can be treated.

Radiolabeled MoAbs for therapeutic applications have two components: a tumour-targeting vector, MoAb, and the radiolabel. The science of MoAbs, including humanized and human MoAbs, radiolabeling aspects, preclinical RIT, and models for absorbed-dose calculations

have been reviewed by different groups. Most therapeutic applications of radiolabeled MoAbs have involved intact antibodies to maximize uptake and retention in the tumour. Tumour response depends on several factors that include tumour radiosensitivity, cumulative radiation dose, and dose rate.

The application of these monoclonal antibodies labeled with radionuclides has been extensively investigated for the in vivo detection and therapy of tumours. The results of experimental studies in animal models are very promising and radiolabeled monoclonal antibodies (such as ^{90}Y-Zevalin® and ^{131}I-Bexxar®) have been approved and are now commercially available as therapeutic agents of cancer. Many clinical trials of therapy with radiolabeled antibodies are in progress. Especially for very radiosensitive tumours, systemic irradiation based on ^{90}Y-immunoconjugates has proven to be very effective. Success in achieving significant remissions in patients with non-Hodgkin's lymphoma (NHL) has encouraged investigators to continue exploiting this field. In patients with NHL, complete response rates vary from 50% to 80%, particularly for high-dose studies in conjunction with myeloablation (Goldenberg and Sharkey 2006; Goldenberg et al. 2006; Sharkey et al. 2005).

Although RIT showed promising results in radiosensitive and easily accessible tumours, like NHL, in the case of radioresistant, poorly-vascolarized tumours, the limited results prompted the scientific community to develop other therapeutic strategies. Here we try to give an overview of the development of RIT by the pretargeting approach, intended to enhance its therapeutic efficacy, which is currently under investigation in different preclinical and clinical settings.

THERAPEUTIC RADIOISOTOPES

Linear energy transfer (LET) and relative biologic effectiveness (RBE) are essential radiobiologic concepts guiding the choice of the therapeutic radioisotope. In particular, LET refers to the number of ionizations caused by that radiation per unit of distance traveled. Being helium nuclei, α-particles have a high LET (~100 keV/μm), whereas β-particles (electrons) have a far lower LET (0.2 keV/μm). The different physical properties of α- and β-particles confer theoretic advantages and disadvantages to each, depending on the clinical situation (Waldmann 2003). Because the range of β-emissions extends for several millimeters, therapy with isotopes such as ^{131}I, ^{90}Y, and ^{188}Re can create a "crossfire effect," destroying tumour cells to which the radioimmunoconjugate is not directly bound. In this way β-emitters can potentially overcome resistance due to antigen-negative tumour cells. Conversely, longer-range β-emissions may also produce nonspecific cytotoxic effects by destroying surrounding normal cells. These characteristics make β-particle therapy better suited for bulky tumours or large-volume diseases. In contrast, α-particles may be better suited for the treatment of microscopic or small-volume diseases, because their short range and high energies potentially offer more efficient and specific killing of tumour cells.

Aside from the quality of radiation, such as low or high LET emission, the suitability of any specific radionuclide for RIT depends on the nuclide's radiophysical properties (such as half-life, abundances, etc.), the target tumour morphology and physiology, the MoAb's targeting kinetics,

Table 7.1. Different therapeutic radionuclides potentially useful in radioimmunotherapy

Isotope	Half-life (h)	Emission and Max Energy (keV)	Max particle range (mm)	Useful γ (keV)	Production mode
Iodine-131 (^{131}I)	193	β (610)	2.0	364	Fission product
Yttrium-90 (^{90}Y)	64	β (2280)	12.0		^{90}Sr/^{90}Y generator
Lutetium-177 (^{177}Lu)	161	β (496)	1.5	113, 208	^{176}Lu(n,γ)
Copper-67 (^{67}Cu)	62	β (577)	1.8	184	^{67}Zn(n,p)
Rhenium-186 (^{186}Re)	91	β (1080)	5.0	137	^{185}Re(n,γ)
Rhenium-188 (^{188}Re)	17	β (2120)	11.0	155	^{188}W/^{188}Re generator
Bismuth-212 (^{212}Bi)	1	α (8780)	0.09		^{224}Ra/^{212}Pb generator
Bismuth-213 (^{213}Bi)	0.77	α (>6000)	<0.1		^{225}Ac/^{213}Bi generator
Astatine-211 (^{211}At)	7.2	α (7450)	0.08		^{207}Bi(α,2n)

the fate of the nuclide after antibody metabolism in vivo, the nuclide's ready availability (preferably in a carrier-free form), and finally the development of simple and efficient clinical-scale radiolabeling methods. There are several potentially useful radionuclides, although those of practical utility comprise a short-list of a few β-particle emitters and even fewer α-particle emitters (Table 7.1). The question of whether low-energy, high-LET, Auger emitters (which require translocation of the antibody-bound radionuclide to the vicinity of the cell nucleus for cytotoxicity) can be clinically efficacious remains partially open.

^{131}I and ^{90}Y are now the two most widely used β-particle emitters. A large number of clinical RIT trials have utilized ^{131}I because of its ready availability, low cost, its imageable gamma emissions (albeit of high energy), an advantageous 8-day half-life, and a simple protein radiolabeling chemistry. However, the use of ^{131}I with internalizing MoAbs is less attractive. Lysosomal processing of internalized MoAbs and the subsequent release of the [^{131}I]-iodotyrosine catabolite from the tumour cell reduces the residence time of ^{131}I in the tumour, and thus diminishes the achievable tumour dose. One approach to overcoming the loss of radioiodine from internalizing MoAbs is labeling with radioiodinated entities which are intracellularly trapped or "residualized".

Radionuclides such as ^{111}In and ^{90}Y have been of particular interest respectively in radioimmunoscintigraphy (RIS) and RIT, respectively, due to their nuclear emissions. Among the radionuclides for therapy, ^{90}Y is of particular interest due to its superior properties, including pure β-emission and the high-dose yield per nanomole (~1.8 GBq/nmol). The maximum energy of the β particle is 2.28 MeV, which is much higher than that of ^{131}I. The 64-h physical half-life of ^{90}Y is suitable for radioimmunotherapy. Another isotope recently discovered and used often in therapy trials is ^{177}Lu. Its lower beta energy (0.5 MeV) and the combination of γ-emissions make it the ^{90}Y complementary choice, especially for dosimetric evaluations in the case of small tumours. Another potential metallic β-particle emitting radionuclide for therapy is ^{67}Cu, which has been studied clinically. Consistent production of ^{67}Cu at high specific activity has been a problem; moreover, its chemistry and radiolabel stability are not as good as those of ^{90}Y and ^{177}Lu; thus,

hampering the development of suitable candidates. Rhenium isotopes (^{186}Re and ^{188}Re) have also been used for RIT, and have sufficient γ-energies for external scintigraphy, similar to ^{131}I. Encouraging tumour responses have been achieved with antibodies labeled with either one of these radionuclides in vitro.

Recently, α-particle therapy has received renewed interest, especially with bismuth nuclides, such as ^{212}Bi and ^{213}Bi as eluates from ^{234}Ra and ^{225}Ac generators, respectively. The cyclotron-produced radiohalogen ^{211}At has also been developed for RIT. These radionuclides have energies in the several MeV range, resulting in high LET emissions (100 keV/μm) compared with the β-emission of ^{90}Y, with a 0.2 keV/μm LET_{mean}. Such high LET radiation has profound effects on DNA, causing strand breaks, if targeted selectively to the tumour because of the α-particles' short range. Hence, α-particle RIT is best used when there are micrometastases or circulating tumour cells, not bulky disease; this is the case, for example, of haematological malignancies.

It has even been suggested that combinations of radionuclides with different energies may prove more beneficial than using a single radionuclide. For example, a radionuclide with a higher energy and longer tissue range could be combined with a radionuclide of medium energy and shorter range; thus, destroying both bulky disease and micrometastases. A key requirement is a highly stable binding of the radiometal to MoAbs, because unbound radioyttrium ion accretes in bone. Because of novel chemistries developed during the last decade, chelating agents that form stable ^{90}Y complexes are now available as bifunctional reagents. The macrocyclic chelator 1,4,7,10-tetraazacyclododecane-N,N′,N′,N′′′-tetraacetic acid (DOTA) is known to form exceptionally stable metal chelates, even when one of its side-chain carboxyl groups is tied up as an amide bond, which is in contrast to the monoamide derivative for diethylenetriaminepentaacetic acid (DTPA).

Bifunctional chelating agents, such as DOTA and DTPA, complex these metal ions and are currently used in the routine practice to link the chelated radionuclide to a peptide, protein or MoAb. These conjugates act as carriers of radiometals for tumour targeting and radiotherapy. Chelates that hold radiometals with high stability under physiological conditions are essential to avoid excessive radiation damage to nontarget cells.

LIMITATIONS OF CLASSICAL RADIOIMMUNOTHERAPY IN SOLID TUMOURS

One of the problems in radio-immunotargeting relates to adverse intrinsic tumour characteristics. Tumours often display intrinsic heterogeneity in antigen density. This factor, together with the non uniformity of tumour vascularization, capillary permeability, degree of tumour necrosis and difference in interstitial pressure, account for the heterogeneous distribution of antibodies in targeted tumours (Strand et al. 1993). Hence, results of clinical RIT trials in solid tumours have been relatively disappointing. The efficacy of RIT in solid tumours using directly labeled MoAbs has been limited by a number of factors including: (1) relatively low level and heterogeneous deposition of MoAb in tumours; (2) relatively low and heterogeneous

distribution of absorbed radiation dose in tumours; and (3) radioresistance of many solid tumours, resulting in the inability to deliver sufficient tumour doses with acceptable toxicity.

One of the major problems of using radiolabeled monoclonal antibodies is a low tumour/nontumour ratio of radioactivity resulting from slow diffusion into tumours, and a prolonged period of time of 5–12 days post-injection is required before ratios rise to a sufficient level at which these can be used for specific imaging techniques. The distribution kinetics of directly labeled antibodies is less than optimal for diagnosis or specific delivery of cytotoxic radionuclides to tumour. Another problem with such procedures is the small dose of radioactivity which consequently reaches the target tumour. Accumulation of up to 20–30% of the injected dose/g of tumour has been observed in mouse tumour models; nevertheless, pharmacokinetic studies showed that only a very small dose, in the order of 0.001–0.1% injected dose/g, is more common in humans (Mann et al. 1984).

Despite the fact that MoAbs are superior to conventional polyclonal sera, these results are disappointing. A low tumour to background ratio remains the main problem of RIS and RIT today. Larger doses of injected antibodies can increase the amount delivered to the target, but this raises the potentially serious problem of intrinsic immunogenicity of the monoclonal antibodies. Unfortunately, the use of fragments displaying a faster blood clearance has not improved tumour localisation and, therefore, limited their use in RIT. Further investigations to solve the problem of high tumour/nontumour ratios led to the use of clearing agents, the so called "chasers", to lower the background radioactivity. Although the radioactivity associated with the tumour is also reduced after the use of a "chase", tumour/nontumour ratios have been improved. This approach opened the way to the development of the pretargeting practice.

PRE-TARGETING APPROACH

In an attempt to overcome the low uptake of label by a tumour and improve the tumour to blood ratio, various groups have investigated the concept of tumour pretargeting. The principle behind pretargeting was initially described by Reardon et al. (1985), who suggested that antibodies could be composed of dual binding specificity, one to a particular target and the other capable of binding a chelate. This group subsequently showed that the accumulation of an antichelate antibody in mice bearing the transplantable KHJJ tumour could be used to target a radiolabeled chelate. A "chase" step using transferrin-conjugated chelate was introduced prior to administering the radiolabeled chelate as a means of reducing the anti-chelate antibody in the blood. More recently, this same targeting model was published by Lubic et al. (2001) to show the feasibility of pretargeting ^{90}Y labeled chelate for therapy.

The essence of pretargeting involves the use of a macromolecule that is capable of binding with a high affinity to a radioactive agent of low molecular weight (usually $Mr < 10{,}000$) and can also selectively target a tumour antigen. Antibodies are modified so that the radiolabel in the following step can bind to the antibody. The modified antibody is administered first and is allowed to distribute throughout the

body to bind tumour cells expressing the antigen and to clear from the blood and normal tissues. Then, the radiolabeled agent (the "effector"), which is much smaller than antibody, is administered at a later time, ideally when the concentration of the macromolecule in the tumour is greater than in other tissues. It localizes at sites where the antibody has accumulated. If the radiolabel has higher permeation and faster clearance than the radiolabeled antibody, more rapid localization in the tumour with higher tumour-to-nontumour ratios is possible. The modified antibody or antibody-conjugate should have the same specificity and affinity for the antigen on tumour cells as the original antibody.

This sequence of events is commonly referred to as the two-step pretargeting protocol (Paganelli et al. 1992). The key for the success of the two-step method is that the macromolecule must be cleared sufficiently from the blood and normal tissues, otherwise the radioactive effector molecule will be retained wherever the macromolecule is distributed. The pharmacokinetics of the antibody-conjugate should be carefully examined to determine the optimal timing of the administration of the clearing agent or the radiolabel. To achieve the best pretargeting results, radiolabels also must have several chemical and physiological properties, such as rapid diffusion into extracellular space, rapid renal excretion, high specific activity, hydrophilicity, no protein binding in the blood, and nonimmunogenicity. Most important properties are rapid diffusion into the extracellular fluid and rapid excretion through the kidneys. To remove the residual macromolecule from the bloodstream before giving the radioactive agent at an appropriate time, administration of chasers can be important for effective tumour localization by the radiolabel. With this approach, favorable tumour to normal tissue ratios of radioactivity are achievable, because the small size of the nontargeted radioactive agent permits its rapid elimination from the body.

An alternative to the two-step protocol is the three-step protocol, in which a specific molecule recognizing the antibody-conjugate is injected after its accumulation into the tumour (Cremonesi et al. 1999). In this way it is possible to enhance the tumour/blood ratios of radioactivity and the dose deposited at the tumour site when the radiolabeled effector is injected. The most common example of three-step protocols is the avidin–biotin system, described later.

To date, the potential value of applying pretargeting strategies to cancer imaging and therapy has been demonstrated in animal models, as well as in clinical trials for many macromolecule/effector systems, with or without the chase step, using radioactive or nonradioactive effectors (Table 7.2, Fig. 7.1). Moreover, short-lived isotopes

Table 7.2. Different pretargeting methods for radionuclide delivery

Pretargeting method	Step 1	Step 2	Step 3
Avidin–biotin	MoAb-Biotin	Avidin followed by StAv	Radiolabeled biotin
StAv-biotin	MoAb-StAv	Clearing agent	Radiolabeled biotin
Bispecific antibody	bsMoAb	Radiolabeled hapten	–
Complementary oligonucleotides	MoAb-Oligo	Complementary oligo	Radiolabeled oligo

StAv streptavidin

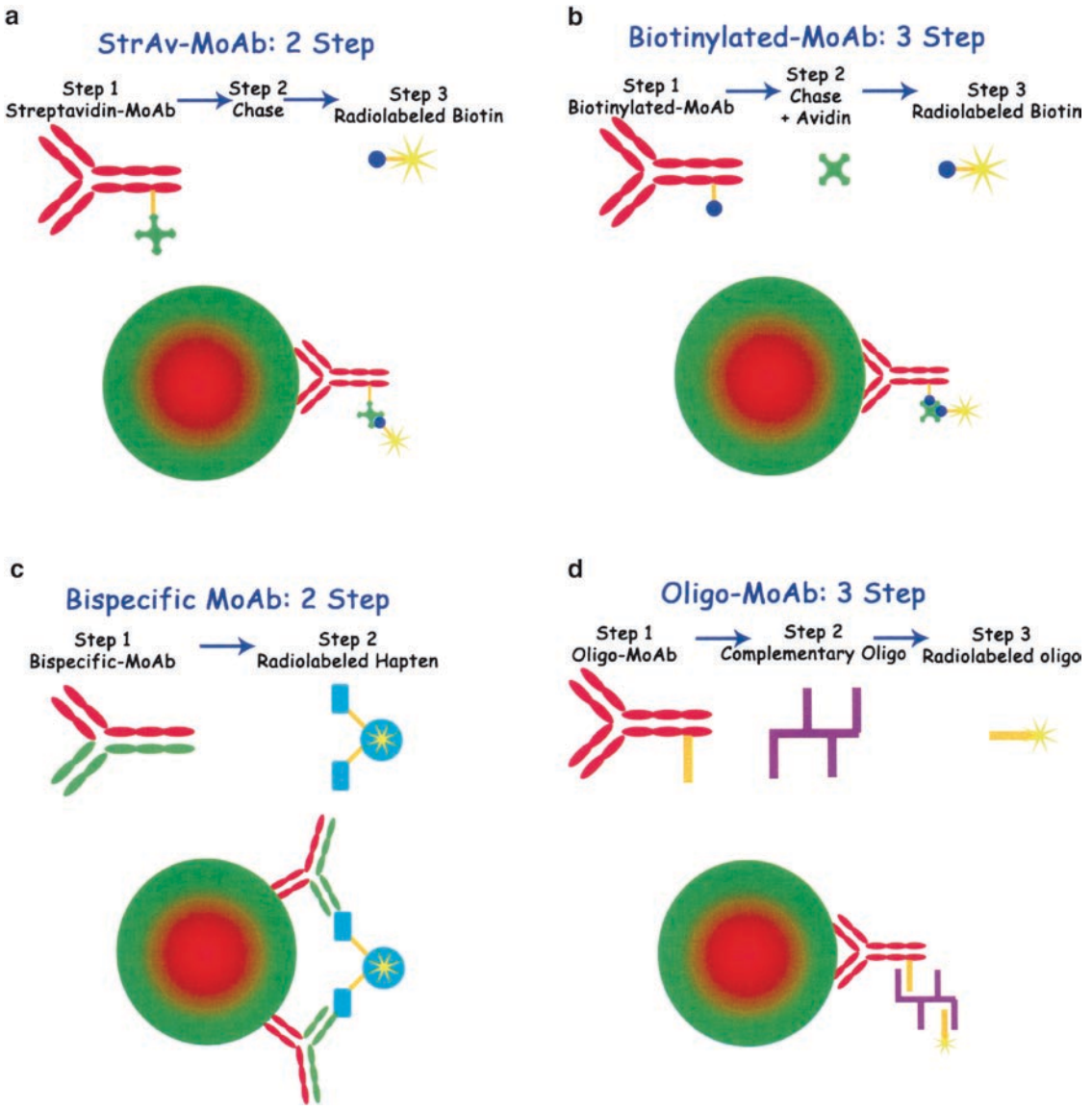

FIGURE 7.1. Mechanisms and examples of pretargeting approaches. (**a**) "Two-step" pretargeting by means of Streptavidin-IgG and radiolabeled biotin; (**b**) "three-step" pretargeting with biotinylated IgG, Avidin and radiolabeled biotin; (**c**) bi-specific MoAb pretargeting; (**d**) oligonucleotide pretargeting

can be used for imaging of tumours by recognising already localised MoAbs. Their injection time can be delayed to a time when most of the primary MoAb has been cleared from the blood and normal tissues, therefore decreasing nontumour binding and achieving, with the use of this strategy, higher tumour to nontumour ratios.

AVIDIN–BIOTIN SYSTEM

The avidin–biotin system is widely used for in vitro applications in immunohistochemistry, ELISA, and molecular biology. Avidins are a family of proteins functionally defined by their ability to bind biotin with high affinity and specificity: no

Table 7.3. Molecular properties of avidin and streptavidin

	Avidin	Streptavidin
Molecular weight	66 kDa	60 kDa
Subunits	4	4
Binding sites for biotin/mol	4	4
Isoelectric point	10.5	5–8
Carbohydrate residue	Rich	Absent
Tyrosine	6/subunit	1/subunit
Affinity for biotin	10^{-15} M	10^{-15} M

physiological compound other than biotin is recognized and bound with any strength by avidins. The molecular properties of avidins are summarized in Table 7.3. They are small oligomeric proteins, made up of four identical subunits, each bearing a single binding site for biotin. Each mole of avidin can, therefore, bind up to four moles of biotin and their binding affinity is very high. The dissociation constant of the avidin–biotin complex is of the order of 10^{-15} M. For practical purposes, the binding of biotin to avidin can be regarded as an irreversible process. Avidins include proteins produced by amphibians, reptiles and avians which are present in their eggs, currently indicated as avidins, as well as a protein produced by streptomyces avidinii, known as streptavidin. They are identical in their binding properties, but show the following differences: (1) avian avidins are glycoproteins, bearing a single-branched oligosaccharide unit of mannose and glucosamine per subunit, while streptavidin is not a glycoprotein; (2) avian avidins are very basic proteins with isoelectric points of ~10.5; being fully dissociated as cations at physiological pH, they can interact strongly with negatively charged compounds such as acidic mucopolysaccharides or nucleic acids; in contrast, streptavidin displays isoelectric points in the range 5–8.

These differences affect their pharmacokinetics and biodistribution when administered in vivo. Avidin is rapidly cleared from the circulation and accumulates in the liver. Streptavidin shows less nonspecific binding to normal tissues and remains in the blood longer than avidin. For avidin, deglycosylation or neutralization increases its circulation time. When galactose is bound to streptavidin, the blood clearance is accelerated and liver accumulation increases with the correlation to the amount of galactose bound to streptavidin. Based on the different characteristics of in vivo behaviour of avidin and streptavidin, the selection of avidin or streptavidin depends on the intended use. Avidin is usually used as a clearing agent of circulating biotinylated antibodies. On the other hand, streptavidin is used in the form of streptavidin -conjugated antibodies for pretargeting or as a radiolabeled ligand of the final step. Both avidin and streptavidin can be used in the second step of the three-step protocol involving biotinylated antibody and radiolabeled biotin (Paganelli et al. 1991).

Biotin (cis-hexahydro-2-oxo-1-H-thieno-[3,4]-imidazoline-4-valeric acid) is a 244 Da molecule commonly known as vitamin H involved in the metabolism of amino acids and carbohydrates in organisms. In the preparation of biotin labeled with radiometal, biotin is derivatized with an appropriate spacer carrying a specific chelating agent for the radiometal. Chelate stability differs for different chelating agents and for different radionuclides. For example, a significant improvement in stability for ^{90}Y was achieved by using DOTA instead of DTPA. Other biotin derivatives, carrying radioiodine bound to an aromatic ring in place of the radiometal-chelator moiety, should be examined for stability against deiodination. Biotinidase cleavage is also

critical for the stability of radiolabeled biotins. Biotinidase is the enzyme responsible for the recycling of the vitamin biotin. Human serum contains large quantities of biotinidase, with the concentration being 12 times higher than both free and bound biotin. Although most radiolabeled biotins maintain a high affinity for avidin or streptavidin and are stable in serum-free buffers, most of them are cleaved after exposure to biological fluids in vitro or administration in vivo.

The structural elements of biotin involved in binding to avidin or streptavidin are the urea moiety and nonoxidized thioether; thus, leaving the carboxylic group available for modification. For this reason, radiolabeled biotin derivatives generally have been prepared by direct functionalization of the carboxyl group of the vitamin, resulting in a CO–NH amido bond (first generation). The enzyme biotinidase specifically cleaves the CO–NH amido bond between the vitamin and the amino group of ε-lysyl residues. The most important aspect of the design of new biotin derivatives is modification such that serum biotinidase does not cleave biotin from the rest of the molecule (Wilbur et al. 2001, 2006). The new biotin derivatives could not be used for in vivo applications unless stable in the presence of biotinidase. To obtain more stable radiolabeled biotin derivatives, there have been attempts to generate steric hindrance at the level of the amido bond (second generation) or to reverse the amido bond between biotin and the labeled prosthetic group (third generation). In Figure. 7.2a these different biotin evolutions are depicted.

A novel stable biotin derivative conjugated to DOTA, devoid of the amide target site for the biotinidase, has been reported (Sabatino et al. 2003; Urbano et al. 2007) and is depicted in Figure. 7.2b. The novelty of this conjugate was that the amide carboxylic group was reduced to a methylene one, thus generating the N-aminohexyl biotinamido derivative (r-BHD) in which the amide is transformed into a secondary amine without affecting the length of the biotin side-arm involved in Av/Sav binding. The DOTA ligand in this compound was directly linked to the amino group of the reduced biotin-hexamethylenediamine derivative through one of the four N-acetic side arms. Moreover, the synthetic flexibility of r-BHD allows the synthesis of a variety of new biotin derivatives, for example, with two DOTA chelators conjugated to the side-chain of biotin, with the purpose of increasing the efficacy of targeted radionuclide therapy by delivering a higher radiation dose to the tumour. Both ^{90}Y- and ^{177}Lu-r-BHD were prepared at high SAs (5.3 and 1.3×10^2 MBq/nmol, respectively, with RCP >99%). Even though r-BHD is devoid of the primary amide target site of enzyme biotinidase, assessment of the biotinidase degradation action on ^{90}Y- and ^{177}Lu-r-BHD was evaluated in serum, showing no significant degradation. The binding affinities of ^{90}Y- and ^{177}Lu-r-BHD for Av have been evaluated by size exclusion FPLC and colorimetric HABA assay method, resulting in 85% affinity at 1:4 molar ratio.

Avidin–Biotin Pretargeting in Glioma

High grade gliomas, which constitute >40% of malignant brain tumours, remain a therapeutic challenge for which no satisfactory treatment exists. Despite surgical treatment and external-beam radiotherapy (EBRT), the prognosis is very poor. Median survival times are 6–12

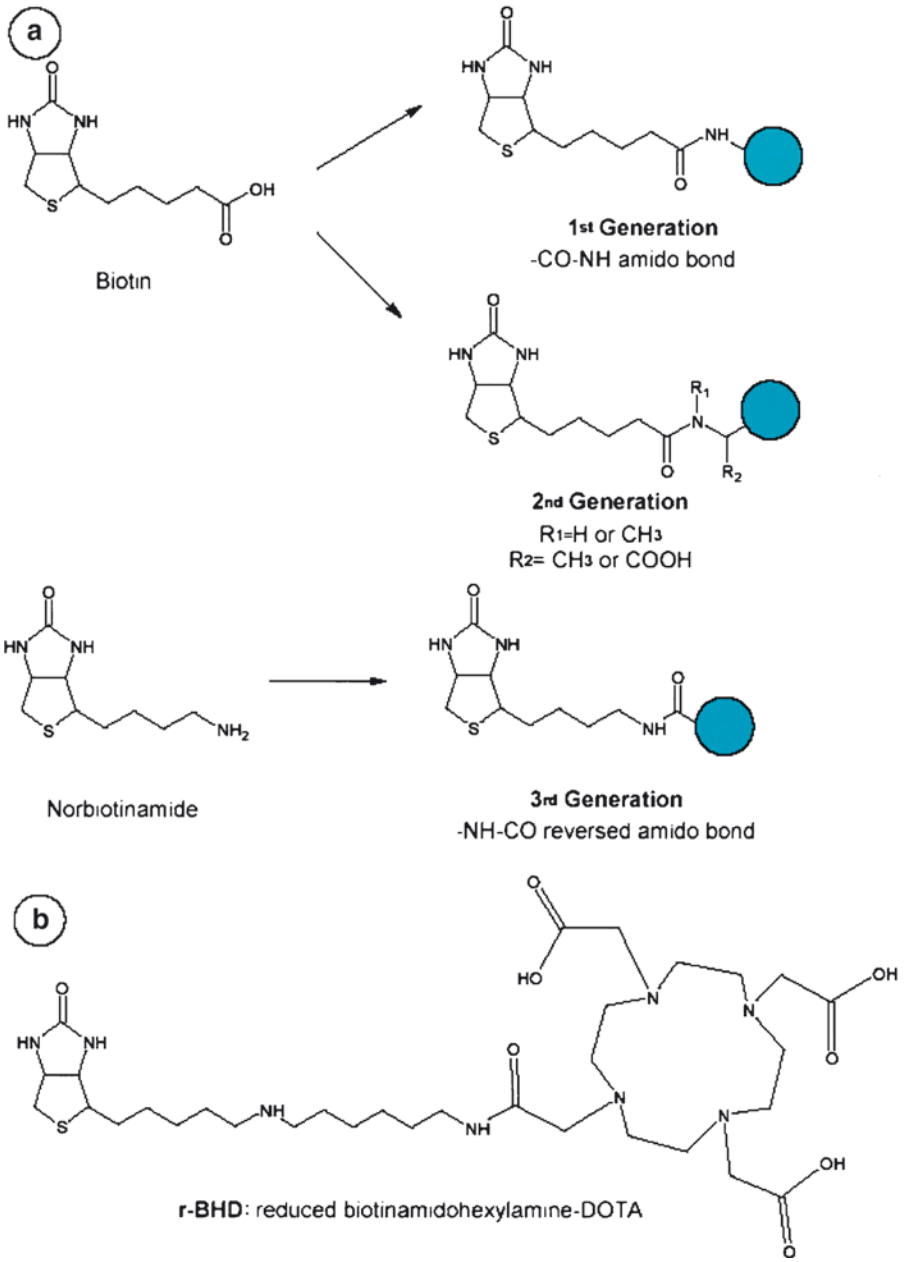

FIGURE 7.2. Different biotin-chelator generations for radiolabeling with therapeutic radionuclides

months for glioblastoma (GBM) and 15–27 months for anaplastic astrocytoma (AA). Although EBRT has been shown to prolong survival, doses >60 Gy cannot be delivered without marked neurotoxicity to the normal brain.

Tenascin-C is an extracellular matrix protein which constitutes a tumour associated antigen which is extremely abundant in high grade astrocytoma (grade III and glioblastoma), therefore, it is an appropriate antigenic target, being the

most constant feature of these tumours. It is a hexameric glycoprotein that can undergo alternative splicing resulting in large (up to 320 kDa monomer) or small (220 kDa monomer) isoforms. The large tenascin variant, which is preferentially expressed in malignant tissues, has been shown to exert anti-adhesive effects; thus, favoring tumour metastasis. Moreover, the enhanced tenascin expression in brain tumours, especially in glioblastoma multiforme, should have a critical role in microvascular cell migration and, as a consequence, in brain tumour angiogenesis. An immunosuppressive activity has also been reported for the large tenascin domain FnIIIA1A2 on activation-induced T lymphocyte proliferation and cytokine production in vitro. These features of tumour-associated tenascin make this protein a good candidate for tumour targeting. Moreover, the targeting of extracellular matrix, compared to the targeting of tumour cell surface antigens, exhibits the advantage of being unaffected by antigen modulation of tumour cells; thus, representing an ideal way for anti-tumour therapy.

Using a three-step technique our group has treated 45 eligible patients with histologically defined grade III and IV gliomas documented by CT or MRI scan prior to therapy. The first step of the protocol consisted of biotinylated antitenascin monoclonal antibodies in 100 mL of physiological saline, injected i.v., over a period of 20 min at a dose of 35 mg/m^2. Avidin and streptavidin were then administered i.v., 24–36 h after the antibody as follows: 20–30 mg of avidin as a rapid bolus (first chase) and 50 mg of streptavidin in 100 mL of saline with 2% human albumin, 30 min after the avidin. DOTA-biotin was labeled with $^{90}YCl_3$ and administered 24 h after streptavidin infusion (third step) in a dose ranging between 2.22 and 2.97 GBq/m^2 per cycle. To allow scintigraphic monitoring of radiolabel localization, the therapeutic dose was mixed with 74–111 MBq of ^{111}In-DOTA-biotin. Ten minutes before the injection of radioactive biotin, 20 mg of biotinylated human serum albumin was administered i.v., to reduce circulating levels of streptavidin (second chase). The activity of ^{111}In was used to predict the biodistribution of ^{90}Y based on the assumption that they share the same in vivo behaviour.

The clinical evaluation of all patients began 2 months after treatment. At this stage, tumour mass reduction occurred in 9/45 (20%) patients (MR + PR + CR); 55% of them had a stabilisation of the disease (SD) and 25% did not respond to therapy. Of the nine patients with reduced tumour mass at 2 months, six had grade IV glioma and three had grade III glioma The proportion of patients with a decrease of tumour mass remained stable at 2 and 6 months of follow-up (respectively, 20% and 18%), while the percentage of those in progression increased from 25% to 52%. At 12 months follow-up, all three patients with anaplastic glioma were still in good condition, while one glioblastoma patient had a minor response at 9 months and another was still in excellent condition more than 2 years after the first treatment (total of 11% MR + PR + CR). After dosimetric evaluations the absorbed doses, obtained in the group of patients with gliomas treated according to a systemic three-step protocol, were as follows: 0.7 ± 0.4 mGy/MBq in kidneys, 0.4 ± 0.3 mGy/MBq in liver and 0.2 ± 0.1 mGy/MBq in the brain, while the dose delivered to the tumour was 4.1 ± 2.4 mGy/MBq. An explanatory image is given in Figure 7.3.

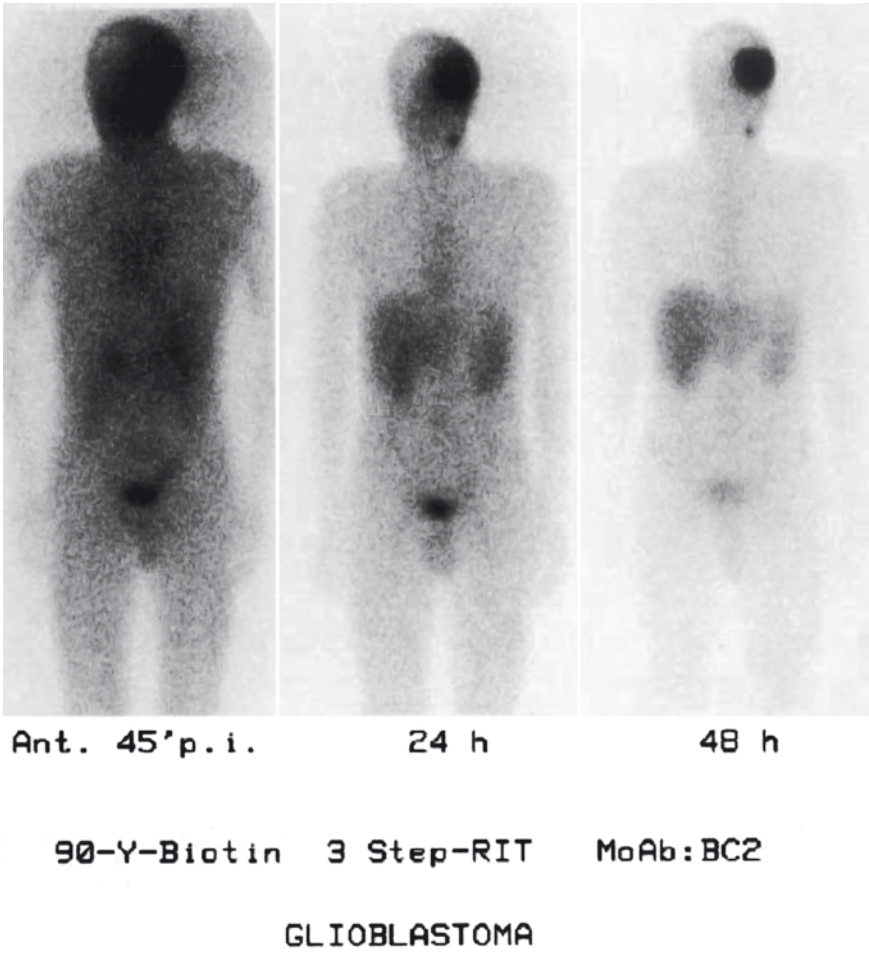

FIGURE 7.3. An example of three-step pretargeting with ^{90}Y-Biotin in a glioblastoma patient

Another pretargeting-based RIT approach has been investigated on a locoregional regimen (LR). The principal advantages of a locally delivered compound (chemotherapeutic agent or radiopharmaceutical) consist mainly in bypassing the blood-brain barrier, minimising systemic toxicity, and in achieving prolonged local drugs concentration. Several studies demonstrated that the LR infusion of ^{131}I or ^{90}Y-labeled anti-Tenascin MoAbs in glioma patients provided a safety profile and the possibility to control the growth of the tumour in the long-term. However, radiolabeled MoAbs diffuse slowly through the tumour being further hampered by poor tumour vascularity and capillary impermeability.

In a phase I–II study we investigated the safety profile and antitumour efficacy of the three-step method employing ^{90}Y-biotin in the locoregional therapy of recurrent high grade glioma (Paganelli et al. 2001). Twenty-four patients with recurrent glioma (8 anaplastic astrocytoma and 16 GBM) underwent second surgical debulking with implantation of an indwelling catheter (connected with a subcutaneous reservoir) into the surgical cavity in order to receive the radioimmunotherapeutic agents.

Biotinylated anti-tenascin MoAbs (BC2 or BC4), avidin and, finally, ^{90}Y-biotin were subsequently injected through the catheter. Each patient received two of these treatments 8–10 weeks apart and the injected activity ranged from 0.5 to 1.1 GBq. Dosage was escalated by 0.2 GBq in four consecutive groups. The treatment was well tolerated without acute side effects up to 0.7 GBq. The maximum tolerated activity was 1.1 GBq limited by neurologic toxicity. None of the patients developed haematological toxicity. In three patients infection occurred around the catheter, and was promptly treated. The average absorbed dose to the normal brain was minimal compared with that received at the surgical resection cavity interface. This study assessed that with activity ranging from 0.7 to 0.9 GBq per cycle, three-step locoregional radioimmunotherapy was safe and produced an objective response (partial and stable disease in 75% of patients).

One drawback, albeit transient, was the humoral response to streptavidin. The problem of the immunogenicity of streptavidin has also been reported by other groups. Although in the three-step approach (Paganelli et al. 1997) the HAMA response was observed in only ~10% of the patients treated, >80% of them developed severe immune responses to streptavidin (HASA). In this system, 24 h after the injection of biotinylated antitumour MoAbs, avidin is given as a chase and then streptavidin is administered instead of avidin for its longer residence time in circulation. The "avidinisation" of the tumour is indeed the critical step; once a high concentration of avidin is localized on the tumour cells, the third step, consisting in the administration of radioactive biotin or another biotinylated cytotoxic agent, will achieve the therapeutic effects. Recent studies have shown that streptavidin may be replaced by avidin conjugated with high molecular weight poly(ethylene glycol) polymer chains (PEG), which generated bioconjugates with prolonged residence in the circulation and reduced immunogenicity.

Another phase I/II study was conducted in 48 patients with histologically confirmed grade III or IV glioma to evaluate the toxicity and therapeutic efficacy of ^{90}Y-biotin using the three-step Pretargeted Antibody-Guided RadioImmunoTherapy (PAGRIT®) approach (Paganelli et al. 1999). ^{90}Y-biotin activities of 2.22–2.96 GBq/m^2 were administered and the maximum tolerated dose per cycle was determined at 2.96 GBq/m^2, which is five-fold higher than the amount of ^{90}Y injectable with radiolabeled MoAbs. The treatment was well tolerated by all patients. Seventy-five percent of them showed low haematological toxicity (grades 0–II) consisting of thrombocytopenia plus neutropenia. Two months after treatment, 12 out of 48 patients (25%) showed objective reduction of tumour mass (partial or complete response) and another 25 of them (52%) had stable disease. Even 12 months after treatment, 8 out of 48 patients (17%) still showed tumour reduction.

These results encouraged us to begin a study in which the same approach was used in an adjuvant setting soon after surgery and radiotherapy with the aim of determining the time to relapse and the overall survival in this always fatal brain tumour with an average duration of survival of 1 year (Grana et al. 2002). Thirty-seven patients with high-grade glioma were enrolled in a controlled open non-randomized study. The estimated median disease-free interval for grade III glioma

patients was more than 56 months. More remarkable were the outcomes in the treated glioblastoma patients, in whom the disease-free interval and consequently the life expectancy was much improved relative to that in the control group (*P* value of 0.01). The survival time in treated glioblastoma patients was 33.5 months, which was significantly longer than the 8 months estimated in the corresponding controls.

The versatility of the system allowed application of the avidin–biotin approach to the treatment of other solid tumours. Studies conducted in patients with ovarian carcinoma in relapse have involved the administration of a mixture of biotinylated MoAbs directly in the peritoneal cavity, followed by intracavitary or intravenous administration of the other components of the treatment (avidin/biotin). The possibility of using a wide variety of MoAbs, including in combination, in order to enhance tumour targeting is one of the main features of the three-step approach, as reported in a patient with oropharyngeal carcinoma in relapse after surgery, chemotherapy, and radiotherapy. After a cocktail of biotinylated MoAbs, avidin and streptavidin, 2.59 GBq of ^{90}Y-DOTA-biotin was injected i.v., and the MRI control showed a complete response lasting for more than 1 year (Chinol et al. 2000).

In the case of early breast cancer, breast conservative surgery followed by sentinel node biopsy (SNB) and postoperative regional radiotherapy represents the treatment of choice. External-beam radiation therapy (EBRT) accompanied with a boost to the tumour bed generally requires 6–8 weeks to be completed. This can represent a logistical problem for many patients, particularly the elderly and those who live a considerable distance from a radiation treatment facility. A radionuclide pretargeting strategy in this field is proving to be surely advantageous to deliver a radiation dose to the operated breast. This new procedure, known as Intraoperative Avidination for Radionuclide Therapy (IART® Paganelli et al. 2007) consists of two steps as follows: (1) "avidination" of the anatomical area of the tumour with native avidin, directly injected by the surgeon into and around the tumour bed; (2) targeting the anatomical area of the tumour by intravenous (IV) injection of ^{90}Y-radiolabeled biotin, 1 day later. Due to the very well known cation-exchanging properties of the inflammatory reaction, avidin is expected to be retained at the tumour bed site after surgery for several days and to act as "a new receptor" for radio-labeled biotin. A dosimetric and pharmacokinetic study with ^{111}In-DOTA-biotin has been published by Paganelli et al. (2007) showing successful preliminary results. The scintigraphic images at different time points provided evidence of a fast and stable uptake of labeled DOTA-biotin at the site of the operated breast. The radiation dose released to the tumour bed was 5.5 ± 1.1 Gy/GBq, consistent with an anticipated boost of a radionuclide targeted therapy. The fast blood clearance (<1% IA in blood 10 h p.i.) and elimination by the urine (>80%IA within 24 h) confirmed that the pharmacokinetic characteristics of ^{90}Y-DOTA-biotin are particularly favourable for radionuclide therapy and imply that total body irradiation will not be protracted. The absorbed doses to the most involved normal organs (urinary bladder, kidneys) were far from the threshold doses of tissue side effects reported in the literature (Cassady 1995; Emami et al. 1991).

In particular, for an injection of 3.7 GBq of ^{90}Y-biotin, the absorbed dose to the kidney resulted to be 4.5 ± 1.5 Gy, corresponding to a kidney BED of 4.9 ± 1.8 Gy, clearly lower than the threshold dose for kidney toxicity (Barone et al. 2005).

OTHER DEVELOPMENTS

Another pretargeting approach relies on the use of bispecific MoAb (bsMoAb). Tumour-targeting specificity has been achieved with bsMoAbs directed against tumour markers and, for the most part for the targeting of radionuclides by means of antibodies to metal chelators. Bispecific antibodies can be conveniently produced by chemically combining Fab' fragments of one antibody with specificity to a tumour antigen with another antibody specific for the effector molecule. Effector molecules initially were monovalent metal-binding chelates, but then it was shown that a divalent effector molecule greatly enhances the residence time of the effector molecule at the site. This method was called an affinity enhancement system (AES), because the bivalent effector molecule bridges two bispecific antibodies on the tumour cell surface, thereby increasing their functionally affinity. Others have subsequently verified the advantage of a divalent effector molecule over a monovalent form (Goodwin and Meares 2001; Karacay et al. 2002; Boerman et al. 2003).

The bsMoAb and avidin–biotin pretargeting approaches have their advantages and disadvantages (Goldenberg et al. 2003; Paganelli 2003). For example, the avidin–biotin system is subject to potential blockade by endogenous biotin. This is especially problematic when testing in mouse models, since mice have ~10 times more amount of biotin in their serum than that in humans. Using a biotin-deficient diet, the stores of biotin in their bodies can be minimized. Antibodies to avidin and streptavidin can develop, which could affect the subsequent use of these agents after an initial exposure. The greatest advantage of the avidin–biotin approach is the strength of the binding between avidin or streptavidin and biotin, such that once biotin is bound to avidin or streptavidin, these complexes are highly stable. In contrast, the bsMoAb approach combined with a monovalent effector molecule has a higher dissociation rate. Using a divalent effector molecule greatly enhances the cell binding but, still, antibody dissociation rates are typically several log units higher than that of the avidin–biotin complex (e.g., K_D): 10^{-15} M for biotin with streptavidin/avidin vs. 10^{-9} M most typically found for antigen-antibody complexes). In this regard it is important to emphasize that the residence time in the tumour for both bsMoAb and avidin/biotin pretargeting approaches is limited by the agent bound to the cell target, i.e. the affinity of an antibody.

The success of receptor targeting by peptides, as demonstrated by the regulatory approval of peptide imaging agents, such as ^{111}In-DTPA-pentatreotide for human neuroendocrine tumours, has prompted the adaptation of peptides for pretargeting approaches. One possible system involves the conjugation of receptor-specific peptides to long-circulating PEG, which is also derived with an avidin or streptavidin for the recognition by a radiolabeled DOTA-biotin dimer (Caliceti et al. 2002). By using PEG with branched structures, multiple peptides and other optional agents

can be attached, along with avidin or streptavidin, thereby yielding a targeting macromolecule with many of the desirable features, including multivalency for the target (through multiple peptide), multivalency for the effector (through multiple binding sites on avidin/streptavidin for biotin), reduced immunogenicity (through PEG), prolonged circulation to reach high target concentration (with PEG of suitable molecular size), and the option of rapid clearance with the use of a biotin-PEG conjugate, which should be nonimmunogenic. The trend at using smaller antibody fragments for in vivo applications has spurred the development of bispecific diabody or bispecific tetrabodies suitable for pretargeting approaches.

CONCLUSION

Pretargeted therapy has clearly shown its advantages over classical RIT, especially in the treatment of solid tumours. Among the pretargeting systems the avidin–biotin system is at a more advanced stage of development and has so far produced encouraging clinical results. Moreover, the high affinity between the two molecules has generated a variety of other therapeutic approaches, which do not involve use of radioactivity to kill the tumour cells. The system is constantly developing and high expectations are expected. For example, a new target-specific delivery system based on avidin–biotin may become a reality in the near future with the advances in gene therapy technology. It has been proposed that target tumoural tissues may be transfected with a new fusion gene containing intracellular and membrane-spanning domains of scavenger receptor ligated to avidin, which will form the extracellular domain of the fusion protein (Lehtolainen et al. 2002). At this point only the tumour target cells will express avidin on their surface, thus allowing the homing of biotinylated cytotoxic/radioactive compounds on the tumour cells. Theoretically, very low concentrations of biotinylated compounds will be necessary to achieve therapeutic effects, thus reducing their systemic side-effects dramatically.

It is emphasized that, for each pretargeting system, the optimal amount of the targeting macromolecule, the best timing of the second injection with the effector ("two-step protocol") or the chaser ("three-step protocol"), the maximum tolerated dose and the therapeutic efficacy for a certain indication need to be carefully and experimentally investigated and should serve as a basis of future trials. Using the avidin–biotin system, the goal of developing a truly targeted tumour therapy with minimal side-effects seems within reach.

REFERENCES

Bale WF, Spar IL, and Goodland RL (1960) Experi-mental radiation therapy of tumor with I-131-carrying.antibodies to fibrin. *Cancer Res 20*: 1488

Barone R, Borson-Chazot F, Valkema R, Walrand S, Chauvin F, Gogou L, Kvols LK, Krenning EP, Jamar F, and Pauwels S (2005) Patient-specific dosimetry in predicting renal toxicity with ^{90}Y-DOTATOC: relevance of kidney volume and dose rate in finding a dose–effect relationship. *J Nucl Med 46*:99S–106S

Boerman OC, van Schaijk FG, Oyen WJG, and Corstens FHM (2003) Pretargeted radioimmunotherapy of cancer: progress step by step. *J Nucl Med 44*:400–411

Caliceti P, Chinol M, Roldo M, Veronese FM, Semenzato A, Salmaso S, and Paganelli G (2002) Poly(ethylene glycol)–avidin bioconjugates: suitable candidates for tumor pretargeting. *J Control Release 83*:97–108

Cassady JR (1995) Clinical radiation nephropathy. *Int J Radiat Oncol Biol Phys 31*:1249–1256

Chinol M, Grana C, Gennari R, Cremonesi M, Geraghty JG, and Paganelli G (2000) Pretargeted radiommunotherapy of cancer. In: Abrams PG, Fritzberg, AR, Radioimmunotherapy of Cancer. Marcel Dekker, New York, pp. 223-243

Cremonesi M, Ferrari M, Chinol M, Stabin MG, Grana C, Prisco G, Robertson C, Tosi G, and Paganelli G (1999) Three-step radioimmunotherapy with yttrium-90 biotin: dosimetry and pharmacokinetics in cancer patients. *Eur J Nucl Med 26*:110–120

Ehrlich P (1907) On immunity. With special reference to the relationship between distribution and action of antigens. *J Royal Inst Publ Health 15*:321–340

Emami B, Lyman J, Brown A, Coia L, Goitein M, Munzenrider JE, Shank B, Solin LJ, and Wesson M (1991) Tolerance of normal tissue to therapeutic irradiation. *Int J Radiat Oncol Biol Phys 21*:109–122

Goldenberg DM, and Sharkey RM (2006) Advances in cancer therapy with radiolabeled monoclonal antibodies. *Q J Nucl Med Mol Imaging 50*:248–264

Goldenberg DM, and Sharkey RM (2007) Novel radiolabeled antibody conjugates. *Oncogene 26*:3734–3744

Goldenberg DM, Sharkey RM, Karacay H, McBride W, Hansen HJ, Chang CH, Rossi EA, Chatal JF, and Barbet J (2003) Radioimmunotherapy: is avidin–biotin pretargeting the preferred choice among pretargeting methods? (against). *Eur J Nucl Med Mol Imaging 30*:776–780

Goldenberg DM, Sharkey RM, Paganelli G, Barbet J, and Chatal JF (2006) Antibody pretargeting advances cancer radioimmunodetection and radioimmunotherapy. *J Clin Oncol 24*:823–834

Goodwin DA, and Meares CF (2001) Advances in pretargeting biotechnology. *Biotechnol Adv 19*:435–450

Grana C, Chinol M, Robertson C, Mazzetta C, Bartolomei M, De Cicco C, Fiorenza M, Gatti M, Caliceti P, and Paganelli G (2002) Pretargeted adjuvant radioimmunotherapy with yttrium-90-biotin in malignant glioma patients: A pilot study. *Br J Cancer* 86:207–212

Karacay H, Sharkey RM, McBride WJ, Griffiths GL, Qu Z, Chang K, Hansen HJ, Goldenberg DM (2002) Pretargeting for cancer radioimmunotherapy with bispecific antibodies: role of the bispecific antibody's valency for the tumor target antigen. *Bioconjug Chem 13*:1054–1070

Kohler G, and Milstein C (1975) Continuous cultures of fused cells secreting antibody of predefined specificity. *Nature 256*:495–497

Lehtolainen P, Taskinen A, Laukkanen J, Airenne KJ, Heino S, Lappalainen M, Ojala K, Marjomäki V, Martin JF, Kulomaa MS, and Ylä-Herttuala S (2002) Cloning and characterization of scavidin, a fusion protein for the targeted delivery of biotinylated molecules. *J Biol Chem 227*:8545–8550

Lubic SP, Goodwin DA, Meares CF, Song C, Osen M, and Hays M (2001) Biodistribution and dosimetry of pretargeted monoclonal antibody 2D12.5 and Y-Janus-DOTA in BALB/c mice with KHJJ mouse adenocarcinoma. *J Nucl Med 42*:670–678

Mann BD, Cohen MB, Saxton RE, Morton DL, Benedict WF, Korn EL, Spolter L, Graham LS, Chang CC, and Burk MW (1984) Imaging of human tumor xenografts in nude mice with radiolabeled monoclonal antibodies. Limitations of specificity due to nonspecific uptake of antibody. *Cancer 54*:1318

Paganelli G (2003) Radioimmunotherapy: is avidin–biotin pretargeting the preferred choice among pretargeting methods? (for). *Eur J Nucl Med Mol Imaging 30*:773–776

Paganelli G, Bartolomei M, Ferrari M, Cremonesi M, Broggi G, Maira G, Sturiale C, Grana C, Prisco G, Gatti M, Caliceti P, and Chinol M (2001) Pretargeted locoregional radioimmunotherapy with ^{90}Y-biotin in glioma patients: phase I study and preliminary therapeutic results. *Cancer Biother Radiopharm 16*:227–235

Paganelli G, Belloni C, Magnani P, Zito F, Pasini A, Sassi I, Meroni M, Mariani M, Vignali M, Siccardi AG, and Fazio F (1992) Two-step tumour targetting in ovarian cancer patients using biotinylated monoclonal antibodies and radioactive streptavidin. *Eur J Nucl Med 19*:322–329

Paganelli G, Chinol M, Maggiolo M, Sidoli A, Corti A, Baroni S, and Siccardi AG (1997) The three-step pretargeting approach reduces the human anti-mouse antibody response in patients submitted to radioimmunoscintigraphy and radioimmunotherapy. *Eur J Nucl Med 24*:350–351

Paganelli G, Ferrari M, Cremonesi M, De Cicco C, Galimberti V, Luini A, Veronesi P, Fiorenza M, Carminati P, Zanna C, Orecchia R, and Veronesi U (2007) IART®: intraoperative avidination for radionuclide treatment. A new way of partial breast irradiation. *Breast 16*:17–26

Paganelli G, Grana C, Chinol M, Cremonesi M, De Cicco C, De Braud F, Robertson C, Zurrida S, Casadio C, Zoboli S, Siccardi AG, and Veronesi U (1999) Antibody-guided three-step therapy for high grade glioma with yttrium-90 biotin. *Eur J Nucl Med 26*:348–357

Paganelli G, Malcovati M, and Fazio F (1991) Monoclonal antibody pretargetting techniques for tumour localization: the avidin–biotin system. International workshop on techniques for amplification of tumour targetting. *Nucl Med Commun 12*:211–34

Pressman D, and Keighley G (1948) The zone of activity of antibodies as determined by the use of radioactive tracers; the zone of activity of nephritoxic antikidney serum. *J Immunol 59*:141–146

Pressman D, Day ED, and Blau M (1957) The use of paired labelling in the determination of tumor localizing antibodies. *Cancer Res 17*:845

Reardon DT, Meares CF, Goodwin DA, McTigue M, David GS, Stone MR, Leung JP, Bartholomew RM, and Frincke JM (1985) Antibodies to metal chelates. *Nature 316*:265–268

Sabatino G, Chinol M, Paganelli G, Papi S, Chelli M, Leone G, Papini AM, De Luca A, and Ginanneschi M (2003) A new biotin derivative-DOTA conjugate as a candidate for pretargeted diagnosis and therapy of tumors. *J Med Chem 46*:3170–3173

Sharkey RM, Hajjar G, Yeldell D, Brenner A, Burton J, Rubin A, and Goldenberg DM (2005) A phase I trial combining high-dose ^{90}Y-labeled humanized anti-CEA monoclonal antibody with doxorubicin and peripheral blood stem cell rescue in advanced medullary thyroid cancer. *J Nucl Med 46*:620–633

Strand SE, Zanzonico P, and Johnson TK (1993) Pharmacokinetic modeling. *Med Phys 20*:515

Urbano N, Papi S, Ginanneschi M, De Santis R, Pace S, Lindstedt R, Ferrari L, Choi SJ, Paganelli G, and Chinol M (2007) Evaluation of a new biotin-DOTA conjugate for pretargeted antibody-guided radioimmunotherapy (PAGRIT®). *Eur J Nucl Med Mol Imaging 34*:68–77

Waldmann T (2003) ABCs of radioisotopes used for radioimmunotherapy: α- and β-emitters. *Leuk Lymphoma 44*:S107–S113

Wilbur DS, Hamlin DK, Chyan MK, Kegley BB, and Pathare PM (2001) Biotin reagents for antibody pretargeting. 5. Additional studies of biotin conjugate design to provide biotinidase stability. *Bioconjug Chem 12*:616–623

Wilbur DS, Hamlin DK, and Chyan MK (2006) Biotin reagents for antibody pretargeting. 7. Investigation of chemically inert biotinidase blocking functionalities for synthetic utility. *Bioconjug Chem 17*:1514–1522

8
Chemotherapy-Induced Neurotoxicity

Susanna B. Park and Matthew C. Kiernan

ABBREVIATIONS

CIPN	chemotherapy-induced peripheral neuropathy
CMAP	compound muscle action potential
CNS	central nervous system
DRG	dorsal root ganglia
ECOG	Eastern Cooperative Oncology Group
EMG	electromyography
EORTC	European Organization for Research and Treatment of Cancer
FACT/GOG	Functional Assessment of Cancer/Gynecologic Oncology Group
GST	glutathione *s*-transferase genes
I_h	hyperpolarization activated cation conductance
K_f^+	fast potassium channels
K_s^+	slow potassium channels
Na_p^+	persistent sodium channels
Na_t^+	transient sodium channels
NCI-CTC	National Cancer Institute – Common Toxicity Criteria
NCI-CTCAE	National Cancer Institute – Common Terminology Criteria for Adverse Events
NCS	nerve conduction studies
OSNS	Oxaliplatin Specific Neurotoxicity Scale
PNS	peripheral nervous system
QST	quantitative sensory testing
RRP	relative refractory period
SNAP	sensory nerve action potential
VPT	vibration perception threshold
WHO	World Health Organization

INTRODUCTION

Chemotherapy-induced neurotoxicity is a common and dose-limiting side effect of many cancer treatments. While other dose-limiting toxicities such as myelosuppression and hypersensitivity reactions are largely amenable to treatment, chemotherapy-induced neurotoxicity remains a significant problem, with limited treatment options and no standardized diagnostic or management criteria. Receiving a full course of chemotherapy on schedule is a critical factor that determines patient survival. Neurotoxicity may necessitate changes to dosage level, scheduling or intensity, and thereby interfere with the

ability to complete a full treatment regimen, even if therapy is proving effective.

With the majority of chemotherapies, the pathophysiological mechanisms of neurotoxicity remain unknown (Hausheer et al. 2006). Neurotoxicity may occur as a consequence of treatment with platinum agents (cisplatin, carboplatin, oxaliplatin), taxanes (paclitaxel, docetaxel) and vinca alkaloids (vincristine). Other therapies such as suramin, thalidomide, and bortezomib can also produce significant neurotoxicity (Quasthoff and Hartung 2002; Hausheer et al. 2006). Previous or coincident administration of neurotoxic chemotherapy or preexisting neuropathy may serve to accelerate the severity of symptoms (Chaudhry et al. 2003). While neuropathy may be regarded as an acceptable outcome if disease progression has been arrested, neurotoxicity becomes more problematic in the setting of adjuvant therapy.

This chapter will examine the spectrum of chemotherapy-induced neurotoxicity, with a focus on recent developments in clinical assessment and management. In addition, pathophysiological mechanisms of neurotoxicity will be explored with a focus on oxaliplatin, a novel platinum-based chemotherapy that exhibits significant dose-limiting neurotoxicity.

CLINICAL PRESENTATIONS OF NEUROTOXICITY

The most common neurotoxicity syndrome induced by chemotherapy is a predominantly sensory or mixed sensorimotor peripheral neuropathy. Symptoms include symmetrical paresthesias, dysesthesias, numbness, and pain involving the distal limbs (Quasthoff and Hartung 2002; Hausheer et al. 2006). Sensory symptoms predominate and the perception of touch, vibration and proprioception are typically impaired (Dougherty et al. 2004; Hausheer et al. 2006). Sensory loss in a 'glove-and-stocking' type distribution may be associated with a lower motor neurone pattern weakness and deep tendon areflexia (Quasthoff and Hartung 2002; Hausheer et al. 2006). Depending on the chemotherapy involved, motor and autonomic neuropathic symptoms may also develop. In some cases fasciculations, reflecting ectopic activity in motor axons, may be observed. Symptoms such as sensory ataxia, pain, and severe numbness can be disabling, in addition to interfering with normal daily functioning and quality of life.

With some therapies, neuropathic symptoms may continue to increase in severity after cessation of treatment. This 'coasting' phenomenon has been documented with cisplatin (LoMonaco et al. 1992), vincristine (Verstappen et al. 2005), and oxaliplatin (Lehky et al. 2004). Symptoms may also persist in the long term after complete cessation of treatment. A follow-up study in cisplatin-treated patients revealed mild symptoms persisting up to 17 years (Strumberg et al. 2002).

Toxicity involving the central nervous system (CNS) is relatively uncommon, as most chemotherapies do not cross the blood brain barrier. The most common CNS manifestation is sporadic encephalopathy, often following intrathecal administration (Nicolao and Giometto 2003). A variety of chemotherapies have been linked to encephalopathy, characterized by somnolescence, confusion and in some cases generalized seizures.

Ifosfamide induces severe acute encephalopathy in up to 30% of patients and may produce hallucinations, extrapyramidal symptoms, and rarely coma (Nicolao and Giometto 2003). While cisplatin has also been reported to cause encephalopathy with seizures and cortical blindness, such presentations remain extremely rare (LoMonaco et al. 1992).

INCIDENCE OF NEUROTOXICITY

The incidence of chemotherapy-induced neurotoxicity is strongly dependent on dosage and infusion duration. Neurotoxicity is typically cumulative and dose-dependent for chemotherapies such as cisplatin (LoMonaco et al. 1992; Strumberg et al. 2002), oxaliplatin (Gamelin et al. 2002), paclitaxel (Winer et al. 2004) and vincristine (Verstappen et al. 2005). However, neurotoxicity may also relate to single dose intensity, with higher single dosage and increased dose density resulting in greater toxicity (Petrioli et al. 2007).

Patient specific risk factors may also influence the incidence and severity of neurotoxic symptoms. Pre-existing neuropathy, particularly related to diabetes or excessive alcohol consumption, may increase the risk of developing chemotherapy-induced neuropathic symptoms at lower dosage levels (Chaudhry et al. 2003). Neurotoxic chemotherapy can also unmask a sub-clinical neuropathy. For instance, vincristine has been reported to reveal previously undiagnosed and asymptomatic Charcot-Marie-Tooth disease, a hereditary sensorimotor neuropathy (Naumann et al. 2001).

Previous or simultaneous administration of multiple neurotoxic chemotherapeutic agents may serve to intensify symptoms. The use of taxanes in conjunction with platinum agents to treat ovarian cancer and other cancer types exacerbates neurotoxicity (Chaudhry et al. 1994). In addition, previous treatment with neurotoxic chemotherapy may also predispose patients treated with even low doses of paclitaxel to develop severe neuropathic symptoms (Forsyth et al. 1997).

PATHOPHYSIOLOGY OF NEUROTOXICITY

The mechanisms underlying nerve damage following chemotherapy remain largely unknown. The peripheral nervous system (PNS), and especially the dorsal root ganglion (DRG), are not effectively protected by a blood barrier, and are therefore susceptible to neurotoxic damage. The similarity in symptoms induced by different chemotherapeutic agents may suggest a common mechanism of toxicity, but there is no consensus on the primary method or origin of toxicity. Clearly, a more complete understanding of the pathophysiological mechanisms involved in chemotherapy-induced peripheral neuropathy (CIPN) will assist in the development of future neuroprotective strategies.

Chemotherapy-induced neuropathy is most often described as a distal axonopathy, with retrograde or ‘dying back’ axonal degeneration (Figure 8.1). However, the initial damage may occur at the level of the neuronal cell body in the DRG, with some chemotherapies resulting in neuronopathy and subsequent anterograde axonal degeneration (Figure 8.1). The distinction between axonal and neuronal origin of toxicity may have important implications for

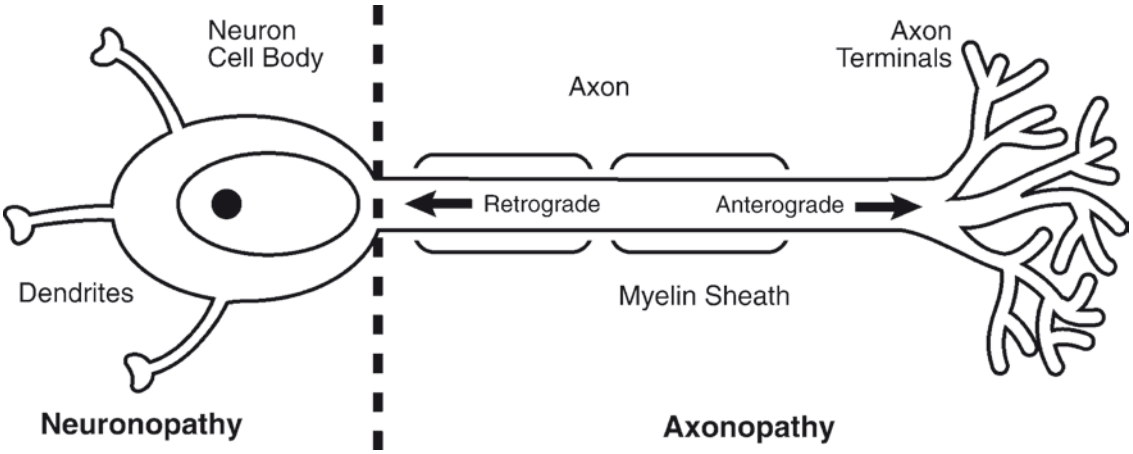

FIGURE 8.1. Pathophysiology of neurotoxicity. The pathophysiology and site of onset of chemotherapy-induced neurotoxicity may include either axonal or neuronal damage. Axonopathy results from injury to the distal axon with subsequent retrograde or 'dying back' axonal degeneration towards the neuronal cell body. Neuronopathy results from initial damage at the neuronal cell body in the dorsal root ganglion (for sensory neurons) and anterograde degeneration of the axon

the design of neuroprotective strategies, as axonal damage would theoretically seem more amenable to treatment.

Both small (unmyelinated) and large (myelinated) fiber nerve damage may be induced by chemotherapy. Nerve biopsies have revealed loss of large fibers alone with platinum analogues (Krarup-Hansen et al. 1999; Krarup-Hansen et al. 2007) or loss of both small and large fibers with taxanes (Sahenk et al. 1994). However, others have suggested that taxanes mainly affect large fibers (Dougherty et al. 2004). Differences in small and large fiber involvement may underlie the variability in symptoms between different chemotherapies, with large myelinated fiber damage causing deficits in sensation, vibration perception and proprioception, and small thinly or unmyelinated fiber damage resulting in pain (Hausheer et al. 2006).

At a molecular level, a range of potential mechanisms have been demonstrated including microtubule-associated interference with axonal transport, direct axonal toxicity involving mitochondrial dysfunction, damage to neuronal cell bodies in the DRG, and axonal ion channel dysfunction (Hausheer et al. 2006; Krarup-Hansen et al. 2007). Essentially, however, there remains no conclusive evidence to establish which mechanisms are predominant *in vivo*.

CLINICAL EVALUATION AND ASSESSMENT

Currently there is no standardized approach to the assessment of chemotherapy-induced neurotoxicity. Clinical evaluation continues to rely on subjective analysis of symptoms and their significance, typically established by means of a clinical history combined with neurological examination. A number of clinical grading scales currently in use grade the severity of symptoms using a combination of subjective and objective criteria (Postma et al. 1998). Interscale and interobserver

variability may, however, hamper the reliability and interpretation of these different scales (Postma et al. 1998).

Commonly used scales include the National Cancer Institute – Common Toxicity Criteria (NCI-CTC) Versions 1 and 2, which have recently been updated by the National Cancer Institute – Common Terminology Criteria for Adverse Events (CTCAE) Version 3 (Hausheer et al. 2006). The NCI-CTCAE uses the following grading system for sensory neuropathy: Grade 1 – loss of deep tendon reflexes or paresthesia not interfering with function; Grade 2 – sensory alteration or paresthesia interfering with function but not activities of daily living; Grade 3 – sensory alteration or paresthesia interfering with activities of daily living; Grade 4 – disabling. Other commonly used scales include the Eastern Cooperative Oncology Group (ECOG) scale, World Health Organization (WHO) criteria, and Ajani criteria (for a review see Postma et al. 1998). While most scales include objective measures of neuropathic symptoms, such as deep tendon areflexia, the primary focus remains the subjective assessment of symptom severity as graded by clinicians.

Quality of life assessments are now becoming an important tool in the assessment of chemotherapy-induced neuropathic symptoms. The European Organization for Research and Treatment of Cancer (EORTC) QLQ-CIPN20 questionnaire is a newly developed method to assess quality of life issues in CIPN (Postma et al. 1998). Using patient self-reporting of sensory, motor and autonomic symptoms, the questionnaire attempts to obtain insight into the subjective experience of CIPN. Another such tool is the Functional Assessment of Cancer/Gynecologic Oncology Group-Neurotoxicity (Fact/GOG-Ntx) questionnaire. This questionnaire has been developed and validated to evaluate the impact of CIPN on quality of life, particularly in patients with gynecological cancers where combination paclitaxel/cisplatin treatment is often used (Hausheer et al. 2006).

The development of questionnaires assessing the impact of CIPN symptoms on quality of life may aid in better understanding the significance of symptoms from a patient perspective. As patients often grade their symptoms more severely than clinicians, it is critical to include information from a patient perspective, particularly when making decisions regarding management. Ideally, the preferred method of CIPN evaluation should involve both qualitative and quantitative measurements, with both clinician and patient evaluation of symptom significance.

NEUROPHYSIOLOGICAL ASSESSMENT

The gold standard for neurophysiological assessment of CIPN remains nerve conduction studies (NCS), which measure the amplitude and conduction velocity of compound nerve action potentials to yield information regarding the number of conducting fibers and the conduction velocity of the fastest fibers (Lin et al. 2006). Measurements are typically obtained from the distal limbs, closest to the areas of greatest symptom severity in CIPN, including the median, radial and ulnar nerves in the upper limbs; and the sural and peroneal nerves in the lower limbs.

Reduction of sensory nerve action potential (SNAP) amplitude is a common finding

in CIPN induced by oxaliplatin (Lehky et al. 2004; Krishnan et al. 2005; Kiernan and Krishnan 2006; Pietrangeli et al. 2006), paclitaxel (Sahenk et al. 1994), cisplatin (LoMonaco et al. 1992), and cisplatin/paclitaxel combination therapy (Chaudhry et al. 1994). Compound muscle action potential (CMAP) amplitude is often preserved (Lehky et al. 2004; Krishnan et al. 2005), although may be reduced with some chemotherapies including paclitaxel and combination cisplatin/paclitaxel (Chaudhry et al. 1994). Although minor changes in nerve conduction velocity may occur, they are not a primary feature and often occur late in CIPN progression (Quasthoff and Hartung 2002; Krishnan et al. 2005; Pietrangeli et al. 2006; Krarup-Hansen et al. 2007).

Measurements from NCS may, however, not correlate to changes in symptom expression. Typically, changes in SNAP amplitude occur well after the onset of symptoms (Kiernan and Krishnan 2006). Measurements from NCS may also show abnormalities while clinical symptoms are not severe, or remain normal in symptomatic patients (Sahenk et al. 1994). These assessments lack sensitivity to clinical symptom expression in part because NCS measure remaining, intact nerve fibers and provide little information regarding fibers that can no longer function, or are nerve dead.

Electromyography (EMG), involving needle sampling of muscle activity, does not typically demonstrate abnormal findings in CIPN, with the exception of oxaliplatin (Quasthoff and Hartung 2002). Electromyography undertaken directly after oxaliplatin infusion has revealed marked hyperexcitability of motor neurons, with evidence of repetitive, spontaneous discharges (Wilson et al. 2002; Lehky et al. 2004). However, EMG does not generally provide additional information in the diagnosis or assessment of CIPN.

Quantitative sensory testing (QST) involves determination of the detection threshold for sensory stimuli to quantify changes in sensory perception (Forsyth et al. 1997; Hausheer et al. 2006). Such testing involves a range of testing procedures including vibration threshold detection, thermal detection, two-point touch discrimination and sharpness detection. Vibration perception threshold (VPT) measured in the large toe appears to be the most sensitive QST method for the assessment of CIPN (Chaudhry et al. 1994; Forsyth et al. 1997; Hausheer et al. 2006). The VPT is typically increased in cisplatin (Krarup-Hansen et al. 2007), paclitaxel (Forsyth et al. 1997) and cisplatin/paclitaxel neuropathy (Chaudhry et al. 1994). Although VPT is the most sensitive QST test for chemotherapy-induced neurotoxicity (Forsyth et al. 1997; Hausheer et al. 2006), it does not correlate with symptom severity or enable presymptomatic identification of early CIPN (Forsyth et al. 1997).

Increased touch, sharpness, and thermal detection thresholds have also been demonstrated in vincristine neuropathy (Dougherty et al. 2007). Thermal threshold and pin sensibility are also altered in some patients treated with paclitaxel (Forsyth et al. 1997) and cisplatin/paclitaxel (Chaudhry et al. 1994). However, these measurements are less sensitive than VPT in predicting onset and progression of symptoms.

While VPT in combination with other assessments may assist in predicting the

final severity of symptoms, QST alone cannot reliably predict or evaluate CIPN severity (Hausheer et al. 2006). In fact, QST is less sensitive than clinical examination at detecting CIPN (Forsyth et al. 1997). In addition, the sensitivity of QST in assessing long term sensory dysfunction may be limited (Strumberg et al. 2002).

It would seem that the best method to currently assess CIPN is by means of a combination of clinical and neurophysiological examination (Krishnan et al. 2005). Objective measures such as deep tendon areflexia, elevated vibration threshold, and significantly reduced sural SNAP amplitude are common features in most chemotherapy-induced neuropathic syndromes and typically correlate with the final severity of neuropathy (Chaudhry et al. 1994). Unfortunately, however, no currently available method is able to determine optimal dosing regimens to maximize therapeutic efficacy while reducing neurotoxicity. The development of better quantitative assessment techniques would seem invaluable in the future diagnosis, management and treatment of CIPN.

Nerve excitability methods have recently been adapted for clinical use (Burke et al. 2001; Kiernan et al. 2005; Lin et al. 2006). In contrast to NCS, nerve excitability studies elicit indirect information regarding axonal ion channel properties and resting membrane potential. Given that acute changes in nerve excitability may be involved in several CIPN syndromes, including oxaliplatin (Adelsberger et al. 2000; Gamelin et al. 2002; Wilson et al. 2002), nerve excitability studies may yet prove to have a unique ability to assess CIPN associated changes.

CHARACTERISTICS OF NEUROTOXIC CHEMOTHERAPIES

Taxanes

Paclitaxel (Taxol) is a taxoid class chemotherapy used to treat a variety of solid tumors, particularly ovarian, breast, non-small cell lung, and head and neck cancer (Rowinsky and Donehower 1995; Winer et al. 2004). Taxanes act to interrupt normal microtubule processing and lead to the formation of cytotoxic structures (Rowinsky and Donehower 1995). Another commonly used taxane is docetaxel (Taxotere), a semisynthetic paclitaxel analogue.

The main adverse side effects of paclitaxel are hypersensitivity reactions, neutropenia and neurotoxicity (Rowinsky and Donehower 1995). However, the use of granulocyte colony stimulating factor to prevent myelosupression and new vehicle preparations to diminish hypersensitivity reactions have reduced the impact of these adverse events (Einzig et al. 1998). Neurotoxicity remains one of the most significant paclitaxel-associated toxicities. Paclitaxel typically induces a distal sensory neuropathy with prominent paresthesias in a ‘glove-and-stocking’ pattern, numbness, distal pain, loss of deep tendon reflexes, as well as gait and fine manipulation difficulties (Sahenk et al. 1994; Rowinsky and Donehower 1995; Forsyth et al. 1997; Einzig et al. 1998; Dougherty et al. 2004). Motor and autonomic symptoms may also occur, including myalgia and orthostatic hypotension (Rowinsky and Donehower 1995; Forsyth et al. 1997) .

Neurotoxic symptoms may arise acutely after the first paclitaxel dose but typically neuropathy develops with cumulative

dosing (Sahenk et al. 1994; Rowinsky and Donehower 1995; Forsyth et al. 1997). The neuropathy is dose-dependent, with symptoms typically occurring at doses >300 mg/m^2 (Chaudhry et al. 1994; Forsyth et al. 1997; Winer et al. 2004). However, mild symptoms may occur at lower doses (200–250 mg/m^2) (Forsyth et al. 1997; Winer et al. 2004). At higher doses (350 mg/m^2), dose reductions or treatment cessation may become necessary (Einzig et al. 1998). Motor symptoms are relatively less common than sensory presentations, but may occur in up to 30% of patients at high doses (Winer et al. 2004).

The most common explanation for paclitaxel-induced neuropathy is a "dying back" distal axonopathy with subsequent damage to cell bodies in the DRG (Sahenk et al. 1994). Sural nerve biopsies in patients treated with paclitaxel have revealed a reduction in both myelinated and unmyelinated fibers (Sahenk et al. 1994). Because the antineoplastic activity of taxanes is mediated via alterations in cellular microtubule processing, it was initially anticipated that interference with efficient axonal transport could underlie neurotoxicity (Hausheer et al. 2006). However, nerve biopsies have not revealed microtubule abnormalities in paclitaxel treated axons from patient biopsies, while *in vivo* animal studies have suggested that any microtubule changes may not be functionally significant (Sahenk et al. 1994).

Cisplatin

Platinum-based agents have been used for many years to treat a variety of cancer types. Cisplatin (*cis*-diamine-dichloro-platinum) is the earliest platinum compound, in use since the 1970s to treat ovarian and testicular cancers, as well as small cell lung, urethral, gastric, and head and neck cancers (Krarup-Hansen et al. 1999). More recently, second and third generation platinum analogues have been developed to improve efficacy and reduce toxicity. Newer platinum derivatives such as carboplatin and oxaliplatin are commonly used compounds with activity against a range of cancer types. Neurotoxicity is a common consequence of all platinum based treatments, although it is rarely seen with carboplatin, as myelosuppression may limit dosing (Cassidy and Misset 2002).

Cisplatin induces a long lasting and dose-dependent cumulative sensory neuropathy (LoMonaco et al. 1992). Symptoms include distal paresthesias, reduced vibration and proprioceptive sensation, sensory ataxia, and absent deep tendon reflexes (LoMonaco et al. 1992). Ototoxicity and Lhermitte's phenomena may also occur (LoMonaco et al. 1992). While symptoms are predominately sensory, some motor involvement has been reported (LoMonaco et al. 1992). Neuropathy typically occurs at cumulative doses >250–350 mg/m^2 and is dependent on single as well as cumulative dose intensity. Neuropathy may continue to worsen after treatment cessation and recovery is often incomplete (LoMonaco et al. 1992). Mild neuropathic symptoms have been shown to persist for up to 17 years after cisplatin treatment in a minority of patients (Strumberg et al. 2002).

The underlying mechanism of cisplatin-induced peripheral neuropathy is considered to involve platinum accumulation in the DRG and subsequent cell death. Assessment of platinum levels in postmortem neural tissue of patients treated with cisplatin has revealed high concentrations in DRG and peripheral nerves, as well as loss of large neuronal cell bodies in

the DRG (Krarup-Hansen et al. 1999). Correspondingly, sural nerve biopsies have revealed loss of large fibers, while small fibers have appeared relatively spared (Krarup-Hansen et al. 1999). Nerve conduction studies of the sural, ulnar, and median nerves have shown progressive reduction in sensory response amplitudes (LoMonaco et al. 1992; Krarup-Hansen et al. 2007). However, the SNAP amplitude reduced simultaneously in both distal and proximal regions, perhaps suggesting a neuronal rather than distal axonal origin of toxicity (Krarup-Hansen et al. 2007).

Many neuroprotective strategies designed to ameliorate cisplatin associated neuropathy have been tested. Of these, trials of acetyl-L-carnitine and glutathione have shown limited success and vitamin E supplementation (300 mg/d) has been shown to reduce cisplatin neurotoxicity (Hausheer et al. 2006).

Vinca Alkaloids

Vinca alkaloids such as vincristine are used to treat hematological malignancies, particularly lymphomas and leukemias (Dougherty et al. 2007). Vincristine induces a 'glove-and-stocking' distribution sensory neuropathy with paresthesia, numbness and pain as well as difficulties in fine motor tasks (Verstappen et al. 2005; Dougherty et al. 2007). Although sensory symptoms are prominent, motor and autonomic symptoms may occur including ataxia, orthostatic hypotension, urinary retention, bowel dysfunction, and cranial nerve involvement (Verstappen et al. 2005). Symptoms may induce persistent pain and gait difficulties due to proprioceptive changes (Dougherty et al. 2007).

Neuropathic symptoms correlate strongly to dosage and typically develop at a cumulative dose of 4–8 mg (Verstappen et al. 2005). Symptoms may be long-lasting and increase in severity after cessation of treatment, with a quarter of patients reporting the most severe symptoms 4 weeks after cessation of treatment (Verstappen et al. 2005). Given that vincristine has been reported to unmask asymptomatic undiagnosed hereditary neuropathies such as Charcot-Marie-Tooth disease (Naumann et al. 2001), care should be taken to establish the presence of sub-clinical neuropathies prior to vincristine treatment, to avoid the rapid onset of severe symptoms.

Other Neurotoxic Chemotherapies

A number of other chemotherapies can induce peripheral neuropathy. Suramin, an investigational chemotherapeutic agent used in the treatment of metastatic prostate cancer, induces two types of neurotoxicity at blood plasma concentrations exceeding 350 μg/mL (Chaudhry et al. 1996). In up to 55% of patients, a distal sensorimotor axonopathy affecting both large and small fibers develops (Chaudhry et al. 1996). In 18% of patients, an inflammatory demyelinating neuropathy may develop, clinically similar to Guillain-Barré syndrome, involving weakness and sensory symptoms in lower extremities, which typically improves with plasma transfer (Chaudhry et al. 1996).

Although thalidomide has been in therapeutic use for a number of years, it has only recently been used in the treatment of multiple myeloma (Cavaletti et al. 2004). Thalidomide induces a dose-dependent sensory neuropathy with dosage >20 g inducing neuropathy in up to 72% of patients (Cavaletti et al. 2004). Symptoms include 'glove-and-stocking' distribution paresthesias, numbness and weakness,

with nerve conduction studies demonstrating reduction in both sensory and motor amplitudes (Cavaletti et al. 2004).

Bortezomib is a novel proteasome inhibitor designed to treat relapsed or refractory multiple myeloma. The most significant adverse effect of treatment is a cumulative dose-dependent sensory neuropathy (Richardson et al. 2006). Because bortezomib is used to treat relapsed or refractory multiple myeloma, patients have often been exposed to prior neurotoxic chemotherapeutic treatment. In a recent study, 80% of patients had pre-existing neuropathic symptoms which worsened with bortezomib treatment (Richardson et al. 2006). Fortunately, the majority of patients showed some reversibility of their neuropathic symptoms.

Combination taxane/platinum therapy utilizing paclitaxel and cisplatin is often used in the treatment of ovarian cancer (Chaudhry et al. 1994). As both cisplatin and paclitaxel have neurotoxic effects, neurotoxicity is dose-limiting in this regimen with rapid onset at higher doses (Chaudhry et al. 1994). Symptoms include paresthesias, numbness, gait and fine motor manipulation difficulties. Again, symptoms can continue to progress after the cessation of therapy, with some patients developing severe neuropathy three months after treatment cessation (Chaudhry et al. 1994).

Paclitaxel is also often combined with another platinum analogue, carboplatin. A combined regimen of paclitaxel and carboplatin in ovarian cancer induces neurotoxicity in the majority of patients (Pignata et al. 2006). While these patients may show recovery from symptoms within six months, use of paclitaxel/carboplatin therapy as first line therapy in ovarian cancer often results in significant long-term neuropathy, which may limit the ability to use alternative neurotoxic agents in recurrent disease (Pignata et al. 2006).

OXALIPLATIN-INDUCED NEUROTOXICITY

Oxaliplatin (*trans*-1-diaminocyclohexane oxaliplatinum) is a third generation platinum analogue developed to overcome the problem of cross resistance that occurs between other platinum analogues, such as cisplatin and carboplatin (Grothey 2003). Oxaliplatin is composed of a cyclic, rigid (1,2-diaminocyclohexane) group and is structurally distinct from other platinum analogues. Oxaliplatin acts through the formation of cytotoxic crosslinked DNA complexes, and may be more effective at inhibiting DNA synthesis than earlier platinum based agents (Grothey 2003).

Oxaliplatin is an effective treatment for metastatic colorectal cancer, and is often combined with fluorouracil and folinic acid (leucovorin) in the FOLFOX regimen (de Gramont et al. 2000). More recently, efficacy has also been demonstrated in the adjuvant setting (Petrioli et al. 2007). The major dose limiting toxicities of oxaliplatin are neurotoxicity and neutropenia. Although various methods have been trialed to reduce toxicity, neurotoxicity remains the significant adverse effect of oxaliplatin treatment (Hausheer et al. 2006).

Oxaliplatin produces two distinct neuropathic syndromes - an acute neuropathy and a cumulative dose-limiting sensory neuropathy (Grothey 2003). The risk of neurotoxicity is strongly dose related, with severe neuropathy occurring at cumulative doses over 540 mg/m^2 (Cassidy and Misset

2002). The majority of patients receiving oxaliplatin will develop neuropathic symptoms at some point during treatment, but the severity and functional significance of symptoms will vary.

Acute neuropathic symptoms occur in most (85–95%) patients receiving oxaliplatin but are not seen with other platinum agents (de Gramont et al. 2000; Grothey 2003; Hausheer et al. 2006). Symptoms are both motor and sensory, although sensory symptoms are typically more prominent (Cassidy and Misset 2002). The most common acute neuropathic symptoms include distal and perioral paresthesias and dysesthesias that are exacerbated by cold exposure (de Gramont et al. 2000; Wilson et al. 2002; Grothey 2003), oral pain with biting, and mouth numbness (Wilson et al. 2002). Motor symptoms include muscular spasm-like contractions causing stiffness and cramps in hands, feet, jaw, and legs (Gamelin et al. 2002). Tetanic jaw tightness is a less common side effect (Grothey 2003). Pharyngolaryngeal dysesthesia, a sensation of the inability to sense breathing and swallowing, is a distressing but rare side effect (Gamelin et al. 2002; Grothey 2003). Acute symptoms often develop during oxaliplatin infusion and resolve within a week, with the duration of symptoms increasing at higher cumulative dosages (Gamelin et al. 2002; Grothey 2003). Acute symptoms do not typically warrant dose reduction.

At a higher cumulative dose, oxaliplatin induces a dose-limiting sensory neuropathy (Cassidy and Misset 2002). Cumulative neurotoxicity is predominately sensory and symptoms include continuous distal paresthesias and dysesthesias which may lead to functional impairment, sensory ataxia, and disability (de Gramont et al. 2000; Gamelin et al. 2002). Unusual presentations include Lhermitte's sign and urinary retention perhaps reflecting autonomic involvement (Pietrangeli et al. 2006).

Chronic oxaliplatin-induced sensory neuropathy is dose-dependent with severe neuropathy typically occurring in 10–20% of patients at a cumulative dose of 750–850 mg/m^2 (de Gramont et al. 2000). However, severe neuropathy may develop in up to 50% of patients at higher than 850 mg/m^2 cumulative dosages (de Gramont et al. 2000). Dose reduction or cessation of treatment may become necessary if severe neurotoxic symptoms cause functional impairment or pain (Gamelin et al. 2002).

While some studies have suggested that neurotoxic symptoms are largely reversible (de Gramont et al. 2000), others have established that oxaliplatin can induce significant, long-lasting neurotoxicity (Krishnan et al. 2005; Land et al. 2007). The median recovery time for oxaliplatin-induced neuropathic symptoms is 13 weeks (de Gramont et al. 2000), although symptoms can persist for 2 years or more in up to 10% of patients (Land et al. 2007). At cumulative dosages >1,000 mg/m^2, neuropathic symptoms may persist indefinitely (Pietrangeli et al. 2006). In addition, the ‘coasting’ phenomenon has been reported with high-dose oxaliplatin treatment (130 mg/m^2) inducing the most severe neuropathic symptoms weeks after cessation of treatment (Lehky et al. 2004). Oxaliplatin-induced neuropathy is a serious concern in clinical oncology. Given the increasing application of oxaliplatin based treatment in the adjuvant setting, persistent neurotoxicity will continue to represent a significant dose-limiting adverse event.

Pathophysiological Mechanisms of Oxaliplatin Neuropathy

The etiology of oxaliplatin-induced neurotoxicity is not clearly understood. The acute neurotoxicity experienced by the majority of patients receiving oxaliplatin has been associated with significant peripheral nerve hyperexcitability (Wilson et al. 2002; Lehky et al. 2004). Electromyography has revealed spontaneous activity and repetitive motor discharges immediately following oxaliplatin treatment, even following the first dose (Wilson et al. 2002; Lehky et al. 2004). The immediate onset of symptoms may suggest a pharmacological rather than morphological basis for acute symptoms, such as a direct effect on nerve excitability caused by an axonal channelopathy.

In support of this hypothesis, several recent *in vitro* studies have suggested that oxaliplatin acts directly on voltage-gated sodium (Na^+) channel kinetics (Adelsberger et al. 2000; Gamelin et al. 2002; Wilson et al. 2002). *In vitro* experiments in rat nerve preparations have indicated that oxaliplatin markedly increases the refractory period of excitability, suggesting changes in the kinetics of voltage-gated Na^+ channels (Adelsberger et al. 2000). However, the exact mechanisms underlying Na^+ channel dysfunction remain unclear. In contrast, others have suggested that acute effects on voltage-gated potassium channels, also important in modulating axonal excitability, may be involved in oxaliplatin-induced neurotoxicity. Peripheral nerve hyperexcitability is a known feature of neuromyotonia, an acquired, autoimmune channelopathy of voltage-gated potassium channels (Kiernan et al. 2001; Hart et al. 2002).

While direct effects on axonal excitability have been implicated in the acute neurotoxicity of oxaliplatin, it is unknown if they influence the development of the more chronic neuropathy. Chronic oxaliplatin-induced neuropathy is symptomatically similar to the syndrome induced by cisplatin and other platinum agents and may be similarly associated with platinum accumulation in the DRG (Gamelin et al. 2002). The chronic neuropathy is characterized by reduced sensory compound amplitudes, with relatively preserved motor amplitudes and conduction velocities, suggestive of sensory axonal degeneration (Gamelin et al. 2002; Lehky et al. 2004; Krishnan et al. 2005).

Assessment of Oxaliplatin-Induced Neurotoxicity

The optimum evaluation of oxaliplatin-induced neurotoxicity involves the combination of clinical history, neurological examination with neurophysiological measures. As with other neurotoxic chemotherapies, several grading scales may be used to rate symptoms. Because of the unique pattern of symptoms induced by oxaliplatin, the Oxaliplatin Specific Neurotoxicity Scale (OSNS) has been developed to assess the development and progression of symptoms more accurately (de Gramont et al. 2000; Cassidy and Misset 2002; Gamelin et al. 2002). The OSNS includes three grades: Grade 1 – dysesthesia or paresthesia that completely regresses before the next cycle of therapy; Grade 2 – dysesthesia or paresthesia persisting between courses of therapy; and Grade 3 – dysesthesia or paresthesia causing functional impairment.

As indicated previously, oxaliplatin-induced neuropathy may be associated with changes on neurophysiological tests, particularly nerve conduction studies and

electromyography. Nerve conduction studies have revealed reduced amplitudes of sensory compound potentials in both upper limbs (radial nerve) and lower limbs (sural nerve) (Krishnan et al. 2005; Kiernan and Krishnan 2006). These changes in SNAP amplitude appear to correlate with grades of clinical severity using the National Cancer Institute Common Toxicity Criteria scale (Figure 8.2a and b), Oxaliplatin Specific Neurotoxicity Score (Figure 8.2c and d) and Total Neuropathy Symptom Score (Figure 8.2e and f), indicating that SNAP amplitude may be a useful measure in the assessment of severity of symptoms (Krishnan et al. 2005). Measurements from the lower limb also correlated most strongly with symptom severity, suggesting a length-dependent process (Figure 8.2). However, while sural nerve SNAP amplitude correlated more strongly to symptom severity, it was also most sensitive to amplitude reduction and complete loss, and therefore would seem

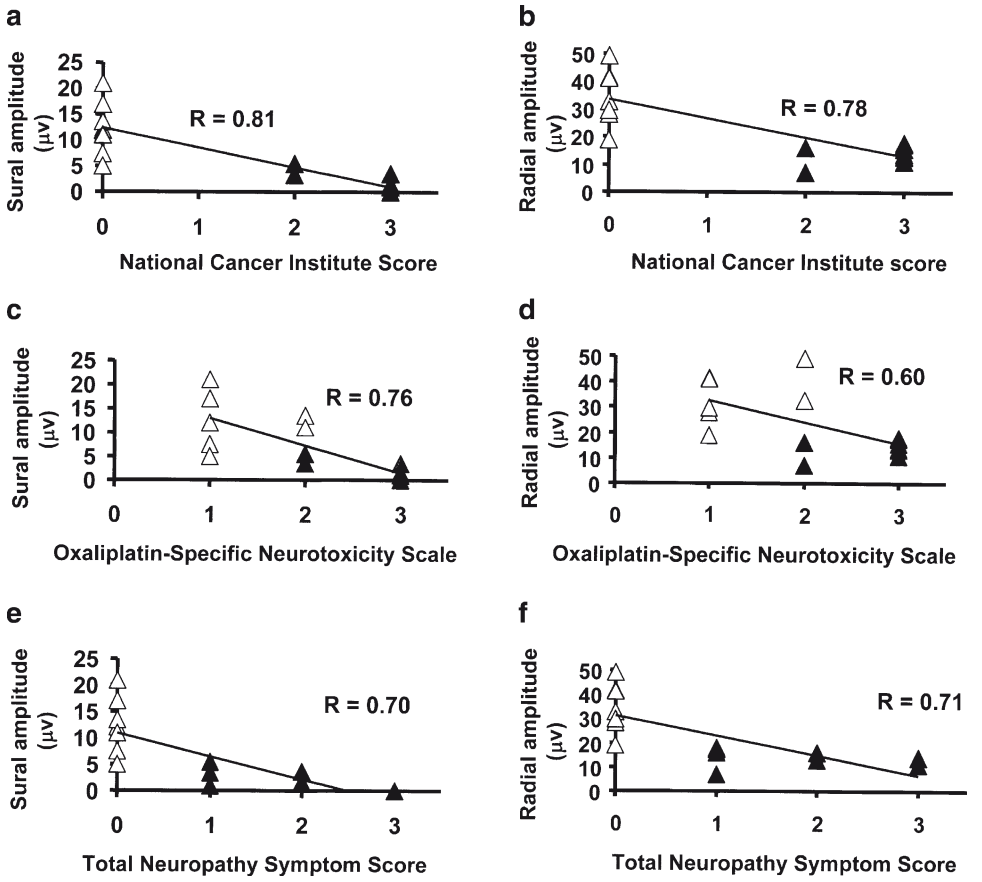

FIGURE 8.2. Correlation between clinical grading scales and electrophysiological measures in oxaliplatin-induced neuropathy. Correlation of sural (**a**, **c**, **e**) and radial (**b**, **d**, **f**) sensory nerve action potentials with commonly used rating scales: National Cancer Institute (**a**, **b**), Oxaliplatin-Specific Neurotoxicity Scale (**c**, **d**) and Total Neuropathy Symptom Score (**e**, **f**). Filled triangles represent symptomatic patients and open triangles represent patients without symptoms. All correlations were statistically significant at $p < 0.001$ (Reproduced from Krishnan et al. 2005. With permission from John Wiley & Sons, Inc.)

to be less suited to long term or prospective monitoring (Krishnan et al. 2005).

Nerve Excitability Studies in Oxaliplatin-Induced Neuropathy

Nerve excitability is determined by the activity of ion channels, pumps and exchangers activated during the conduction of nerve impulses (Burke et al. 2001; Lin et al. 2006). Nerve excitability techniques have been recently applied to investigate oxaliplatin-induced neurotoxicity (Krishnan et al. 2005; Kiernan and Krishnan 2006; Krishnan et al. 2006). Such studies may yield new insights into the pathophysiology of oxaliplatin-induced neurotoxicity, particularly as direct effects on ion channels have been proposed as a pathological mechanism (Adelsberger et al. 2000).

Briefly, assessment of nerve excitability relies on an understanding of the many ion channels involved in modulating resting membrane potential and axonal excitability (For a review, see Burke et al. 2001; Kiernan et al. 2005; Krishnan et al. 2008; Lin et al. 2006; Figure 8.3a). The major channels responsible for impulse generation are transient sodium channels (Na_t^+) that exist in high densities at the nodes of Ranvier. The Na_t^+ channels are rapidly activated by membrane depolarization to generate the upstroke of the action potential and subsequently quickly inactivate. Slow K^+ channels (K_s^+) are also highly expressed at the node but activate too slowly to be affected by a single action potential directly. The K_s channels contribute to resting membrane potential and produce accommodation to depolarization, particularly following conduction of trains of impulses as occurs with repetitive discharges. Persistent sodium channels (Na_p^+) are present at low density at the node, but affect resting membrane potential through generation of a persistent sodium current into the axon. Although not directly involved in impulse generation, the internodal region acts as a membrane capacitor to influence excitability. The initial section of the internode, the paranodal region, contains a high density of fast K^+ channels (K_f^+) which control current flow between the node and internode. Hyperpolarization activated cation conductances (I_h) and voltage-independent leak conductances (Lk) also affect axonal excitability in the internode (Figure 8.3a).

Following conduction of a single impulse, axons undergoes a series of characteristic changes in excitability, known as the recovery cycle of excitability. The recovery cycle can be assessed *in vivo* through a paired stimuli protocol delivered with varied interstimulus intervals (Figure 8.3b). After an absolute refractory period due to the inactivation of transient Na^+ channels, a relative refractory period (RRP) occurs due to gradual recovery of Na^+ channels from their inactivated state (Figure 8.3b). During the RRP, a greater than normal stimulus is required to generate an action potential. Subsequently, a period of superexcitability or greater than normal excitability occurs, followed by a late subexcitable period before the membrane potential repolarizes to baseline (Figure 8.3b). Another measure of nerve excitability, known as 'threshold electrotonus', assesses the influence of internodal conductances on axonal excitability. Threshold electrotonus measures the changes in excitability following long subthreshold conditioning pulses which alter the potential difference between the

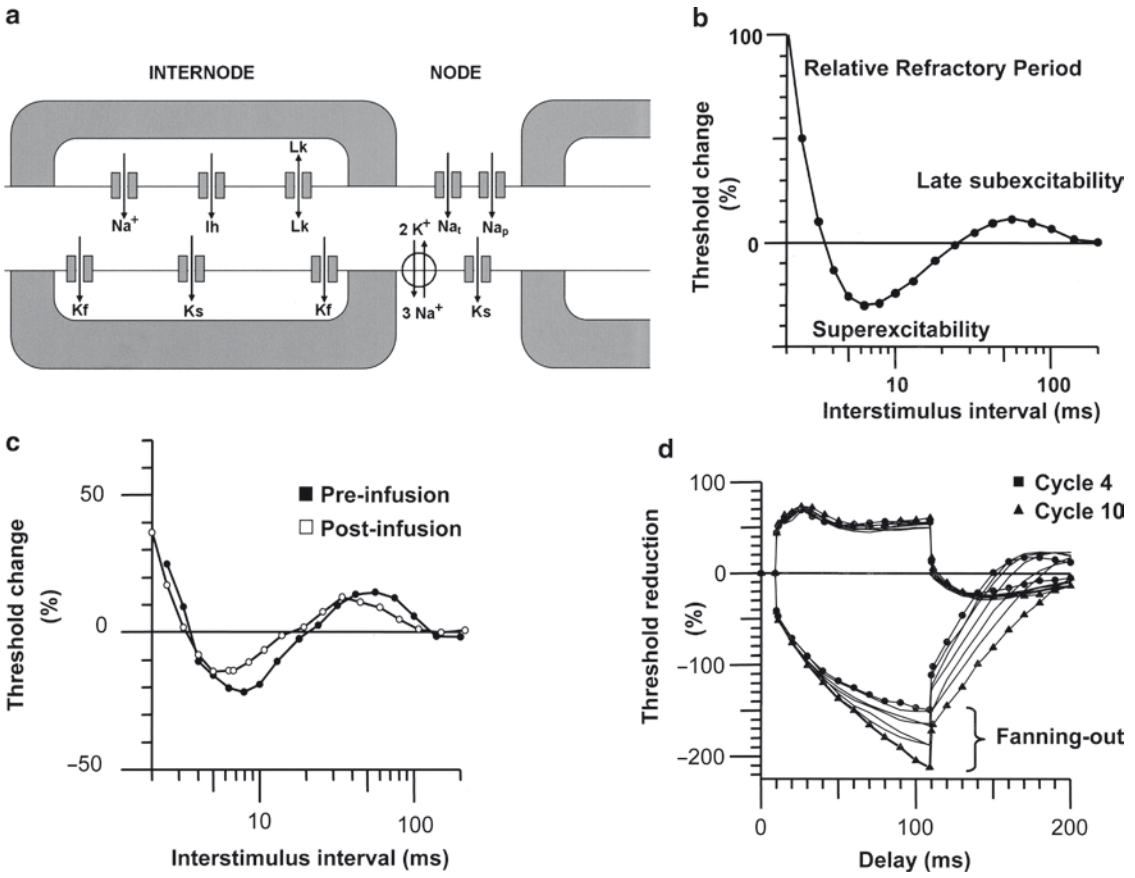

FIGURE 8.3. Changes in sensory axonal excitability induced by oxaliplatin. (**a**) Voltage-dependent conductances responsible for modulation of axonal excitability in myelinated axons. At the node, a high density of transient Na^+ channels (Na_t^+) provide the main impetus for the salutatory induction of the action potential. Persistent Na^+ channels (Na_p^+) at the node are activated at rest and affect resting membrane potential and subthreshold excitability. The internodal region under the myelin sheath acts as a capacitor to influence axonal excitability. Slow K^+ channels (K_s^+) at the node are prohibited by slow kinetics from participating in the generation and saltatory conduction of the action potential but contribute to accommodation to depolarization. Fast K^+ channels (K_f^+) are present in the paranodal region and control internodal depolarization. In the internode, the hyperpolarization activated cation conductance (I_h) may also affect excitability. The electrogenic pump (Na^+/K^+-ATPase) activates in response to impulse trains and exchanges 3 Na^+ ions for every 2 K^+ ions passed into the axon, leading to axonal hyperpolarization. Several voltage-independent 'leak' conductances (Lk) also contribute to internodal excitability. (**b**) Illustrative recovery cycle of excitability measurement, demonstrating characteristic changes in threshold with increasing interstimulus intervals and major phases: the relative refractory period (RRP), superexcitability and late subexcitability. Threshold change measures the change in current required to produce the target potential. (**c**) Characteristic changes in sensory nerve recovery cycle measurements demonstrating reduction in superexcitability after oxaliplatin infusion. Data from one patient, pre- (*black circles*) and post-infusion (*white circles*) at the fifth cycle of oxaliplatin treatment. (**d**) Threshold electrotonus measured from sensory axons in a single patient demonstrating changes with increasing cumulative oxaliplatin dosage. The threshold electrotonus measurements demonstrate marked fanning out of hyperpolarization curves with each cycle, from cycle 4 (*squares*) to cycle 10 (*triangles*)

node and internode via effects mediated by K^+ channels and inward rectification (I_h) (Figure 8.3d).

Preliminary studies of sensory nerve excitability have demonstrated marked changes immediately following infusion of oxaliplatin. Specifically, sensory nerve excitability studies conducted directly before and after oxaliplatin treatment have revealed displacement of superexcitability and a shift of the recovery cycle suggestive of alteration of Na^+ currents (Park et al. 2009a; Figure 8.3c). Additionally, distinctive cumulative changes in sensory nerve excitability have been demonstrated with progressive oxaliplatin cycles. Assessment of axonal excitability taken prior to oxaliplatin infusions from cycles 4–10 have revealed marked 'fanning out' of threshold electrotonus curves with each cycle (Figure 8.3d). These preliminary studies of sensory nerve excitability indicate that oxaliplatin induces significant changes both acutely after each infusion and with increasing cumulative dosage (Park et al. 2009b).

Studies in motor axons have also revealed significant changes in recovery cycle measurements following oxaliplatin. In particular, the pre-infusion recordings of the recovery cycle from motor axons have demonstrated a high ratio of subexcitability to superexcitability, with disappearance of superexcitability (Figure 8.4a), instead replaced by refractoriness, a property determined by transient Na^+ conductances (Burke et al. 2001; Kiernan and Krishnan 2006).

These findings were supported by post-infusion recordings in 13 patients over a series of 52 cycles of treatment demonstrating increases in the relative refractory period (RRP) from 3.4 ± 0.1 ms to 4.3 ± 0.2 ms following infusion ($P< 0.0005$), consistent with increased Na^+ channel inactivation (Kiernan and Krishnan 2006). These excitability studies suggest a selective effect of oxaliplatin on voltage-gated Na^+ channels causing prolongation of the refractory period, in agreement with the previous *in vitro* rat studies (Adelsberger et al. 2000).

Importantly, these acute alterations in axonal membrane Na^+ channel parameters appear to relate to the development of oxaliplatin-induced cumulative neuropathy. Preinfusion relative refractory period (RRP) has been found to predict chronic neuropathy development, with readings of RRP >4 ms (Figure 8.4b) in almost 90% of patients who subsequently developed chronic neuropathic symptoms (Kiernan and Krishnan 2006). The RRP value never exceeded 4 ms in any patient that remained without features of a cumulative neuropathy at the completion of oxaliplatin therapy (Figure 8.4b and c). Typically, elevated RRP recordings occurred an average of seven cycles before the development of chronic symptoms and remained elevated in subsequent cycles, while changes in patients who did not develop chronic neuropathy resolved before the next treatment cycle (Krishnan et al. 2005).

In total, these nerve excitability studies in oncology patients treated with oxaliplatin have established acute and chronic abnormalities of motor and sensory nerve excitability *in vivo*. Specifically, the changes in axonal Na^+ channel dependent-parameters, such as RRP duration, suggest that acute oxaliplatin-induced neurotoxicity may be mediated through an effect on axonal voltage-gated transient Na^+ channels. Importantly, motor excitability abnormalities preceded the onset of clinical symptoms by an average of seven cycles, which may allow sufficient time for prophylactic

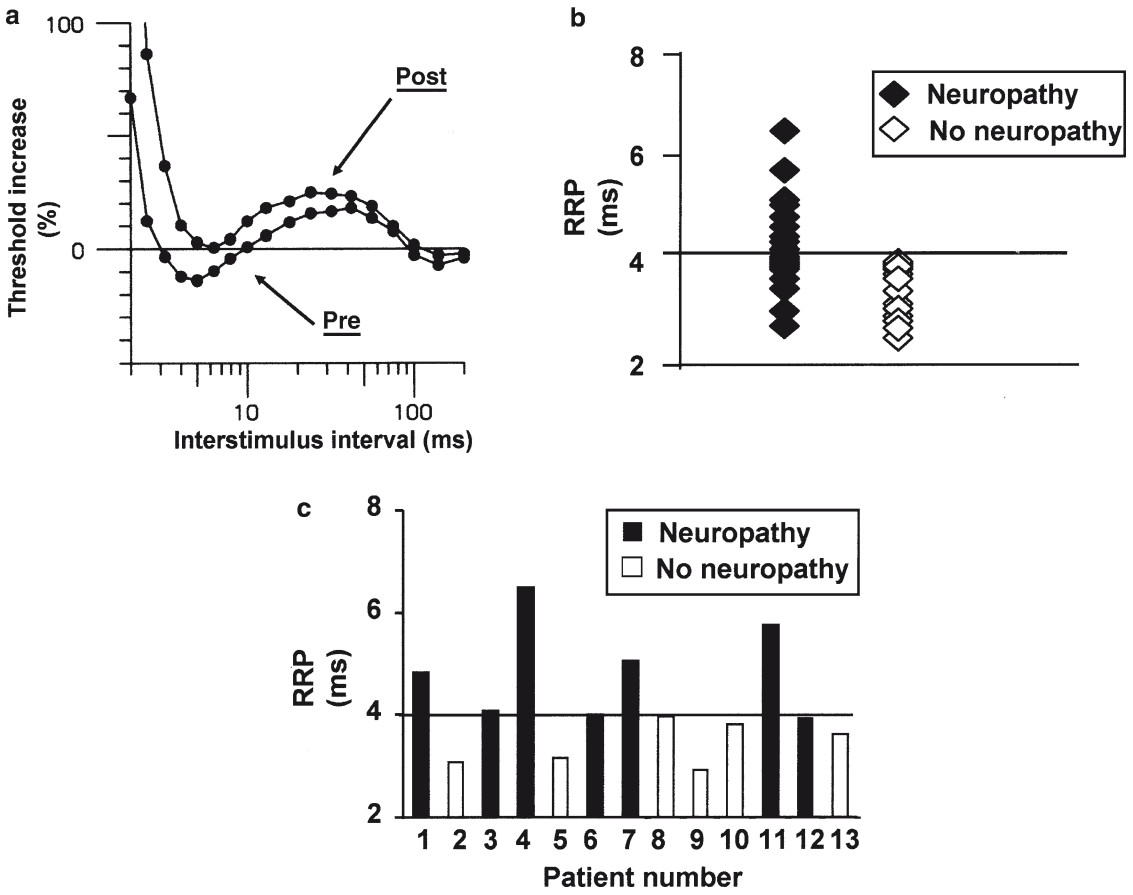

FIGURE 8.4. Changes in motor axonal excitability induced by oxaliplatin. (**a**) Recovery cycle of excitability for motor axonal measurements in a single patient before and after oxaliplatin treatment demonstrating post-infusion increases in refractoriness and decrease in superexcitability. (**b**) Scatterplot of the relative refractory period (RRP) duration both pre- and post-oxaliplatin infusion in patients who developed neuropathy (*filled diamonds*) and those who did not develop symptoms (*open diamonds*), demonstrating increased RRP duration in symptomatic patients. (**c**) Plot of pre-infusion maximal RRP in 13 patients treated with oxaliplatin illustrating the difference in RRP duration between symptomatic (*black*) and non-symptomatic (*white*) patients. No neuropathy-free patient displayed an RRP of greater than 4 ms at any cycle

therapy to be initiated. However, as oxaliplatin-induced chronic neuropathy exhibits predominately sensory symptoms, sensory nerve excitability measurements may prove to be even more sensitive in predicting the development of neuropathy. These results also lend support to an association between acute excitability changes and the subsequent development of chronic neuropathy. Specifically, acute alterations in axonal Na^+ channel function may produce axonal degeneration, leading to chronic neuropathy (Krishnan et al. 2005).

Future Directions and Neuroprotection

Several strategies have been recently trialed to lower the incidence and severity of oxaliplatin-induced neurotoxicity. Neuroprotective strategies such as xaliproden

(Susman 2006), glutamine (Wang et al. 2007), and calcium and magnesium infusions (Gamelin et al. 2004) have shown promising preliminary results, but larger scale, controlled trials are awaited. Modulations of infusion time or dose intensity may also assist in lowering the likelihood of severe neuropathy (Petrioli et al. 2007).

Confirmation of a link between the acute and chronic forms of neurotoxicity would have important implications for the development of neuroprotective strategies. Neuroprotective agents could be developed to target acute neuropathic symptoms, while also acting to reduce the development of chronic neuropathy in the long term. There is some preliminary evidence that amelioration of acute symptoms may reduce the incidence of chronic neuropathy. A study of glutamine supplementation designed to reduce the incidence of severe chronic oxaliplatin-induced neuropathy has recently been shown to be effective in reducing acute symptoms (Wang et al. 2007).

Calcium and magnesium infusions given before and after oxaliplatin have demonstrated some benefit in reducing neurotoxicity and improving the reversibility of neuropathic symptoms (Gamelin et al. 2004). Recent studies have suggested that Ca^{2+}/Mg^{2+} infusions reduce the percentage of patients that develop severe chronic neuropathic symptoms (Gamelin et al. 2004). These effects may be related to alterations in nerve excitability. Specifically, alterations in axonal Na^+ concentration may trigger reversal of the Na^+/Ca^{2+} exchanger, leading to a cascade of Ca^{2+} related processes and axonal degeneration (LoPachin and Lehning 1997; Krishnan et al. 2006). Reductions in membrane-bound Ca^{2+} may also contribute to axonal nerve hyperpolarization which commonly develops immediately following oxaliplatin infusion. However, while promising, Ca^{2+}/Mg^{2+} infusions have not been shown to completely prevent oxaliplatin-induced neurotoxicity.

Because Na^+ channel dysfunction has been implicated in oxaliplatin-induced neurotoxicity, carbamezepine, an anticonvulsant with Na^+ channel blocking properties, has been trialed as a neuroprotective agent. Although carbamazepine has shown some promising results in reducing the severity of neuropathic symptoms in oxaliplatin patients (Gamelin et al. 2002); other studies have concluded that carbamazepine does not reduce oxaliplatin-induced neurotoxicity (Wilson et al. 2002).

A number of other agents have been investigated in regards to their neuroprotective efficacy. Oral glutamine supplementation has recently been shown to reduce the incidence and severity of oxaliplatin-induced cumulative neuropathy and reduce the need for oxaliplatin dose reductions (Wang et al. 2007). Xaliproden has also been shown to reduce the risk of severe neuropathy by ~40% in oxaliplatin treated patients (Susman 2006). There are also limited positive results for gabapentin, glutathione and acetyl-L-carnitine in the treatment of oxaliplatin-induced neuropathy (Gamelin et al. 2002).

Early identification of at-risk patients will be critically important in any attempt to minimize neurotoxicity. Once early identification is possible, prophylactic treatment with neuroprotective agents may then provide the best way of preventing severe long-lasting chronic symptoms. The use of a predictive test (potentially such as measurement of nerve excitability)

may assist in identifying patients who will benefit most from intervention. Additionally, genetic factors have been identified that may confer susceptibility or resistance to oxaliplatin-induced neuropathy. Several polymorphisms in the glutathione *s*-transferase (GST) genes, which are involved in detoxification pathways, have been associated with an increased risk of developing severe oxaliplatin-induced neuropathy (Lecomte et al. 2006). Further examination of genetic predisposition to severe neuropathy may assist in targeting at-risk patients.

Modulations of infusion time may also assist in reducing the incidence of neurotoxicity. A longer 6 h infusion significantly reduced the percentage of patients with neuropathic symptoms as compared to the standard 2 h infusion time (Petrioli et al. 2007). Additionally, recent studies such as the OPTIMOX1 trial suggest that the 'stop and go' strategy of recycling the oxaliplatin regimen at regular intervals for a fixed duration may somewhat reduce severe neurotoxicity (Hausheer et al. 2006). Data from the excitability studies detailed earlier would also suggest that it may be possible to identify which patients can be safely re-exposed to an oxaliplatin-based regimen in a recycling strategy, to thereby maximize the benefit of each line of therapy.

In conclusion, chemotherapy-induced neurotoxicity remains a significant problem in clinical oncology, potentially limiting the efficacy and tolerability of the most commonly used chemotherapeutic treatments. A combination of clinical assessment, quantitative measures and quality of life evaluation will most likely yield the best current assessment of CIPN symptoms. Future research will need to focus on the development of better assessment techniques, to predict the onset of severe neuropathy prior to symptomatic expression. Such quantitative and predictive tests will also provide appropriate end points for future trials of potential neuroprotective strategies.

Acknowledgements. The support of the National Health and Medical Research Council of Australia (Project grant 400938) and the Sydney Foundation for Medical Research are gratefully acknowledged.

REFERENCES

Adelsberger H, Quasthoff S, Grosskreutz J, Lepier A, Eckel F, and Lersch C (2000) The chemotherapeutic oxaliplatin alters voltage-gated Na^+ channel kinetics on rat sensory neurons. Eur J Pharmacol 406:25–32

Burke D, Kiernan MC, and Bostock H (2001) Excitability of human axons. Clin Neurophysiol 112:1575–1585

Cassidy J, and Misset J-L (2002) Oxaliplatin-related side effects: characteristics and management. Semin Oncol 29:11–20

Cavaletti G, Beronio A, Reni L, Ghiglione E, Schenone A, Briani C, Zara G, Cocito D, Isoardo G, Ciaramitaro P, Plasmati R, Pastorelli F, Frigo M, Piatti M, and Carpo M (2004) Thalidomide sensory neurotoxicity: a clinical and neurophysiologic study. Neurology 62:2291–2293

Chaudhry V, Chaudhry M, Crawford TO, Simmons-O'Brien and E, Griffin JW (2003) Toxic neuropathy in patients with pre-existing neuropathy. Neurology 60:337–340

Chaudhry V, Eisenberger MA, Sinibaldi VJ, Sheikh K, Griffin JW, and Cornblath DR (1996) A prospective study of suramin-induced peripheral neuropathy. Brain 119:2039–2052

Chaudhry V, Rowinsky EK, Sartorius SE, Donehower RC, and Cornblath DR (1994) Peripheral neuropathy from taxol and cisplatin combination chemotherapy: Clinical and electrophysiological studies. Ann Neurol 35:304–311

de Gramont A, Figer A, Seymour M, Homerin M, Hmissi A, Cassidy J, Boni C, Cortes-Funes H, Cervantes A, Freyer G, Papamichael D, Le Bail

N, Louvet C, Hendler D, de Braud F, Wilson C, Morvan F, and Bonetti A (2000) Leucovorin and fluorouracil with or without oxaliplatin as first-line treatment in advanced colorectal cancer. J Clin Oncol 18:2938–2947

Dougherty PM, Cata JP, Burton AW, Vu K, and Weng H-R (2007) Dysfunction in multiple primary afferent fiber subtypes revealed by quantitative sensory testing in patients with chronic vincristine-induced pain. J Pain Symptom Manag 33:166–179

Dougherty PM, Cata JP, Cordella JV, Burton A, and Weng H-R (2004) Taxol-induced sensory disturbance is characterized by preferential impairment of myelinated fiber function in cancer patients. Pain 109:132–142

Einzig AI, Wiernik PH, Wadler S, Kaplan J, Benson LT, Tentoramano L, and Tan V (1998) Phase I study of paclitaxel (taxol) and granulocyte colony stimulating factor (G-CSF) in patients with unresectable malignancy. Invest New Drugs 16:29–36

Forsyth PA, Balmaceda C, Peterson K, Seidman AD, Brasher P, and DeAngelis LM (1997) Prospective study of paclitaxel-induced peripheral neuropathy with quantitative sensory testing. J Neuro-Oncol 35:47–53

Gamelin E, Gamelin L, Bossi L, and Quasthoff S (2002) Clinical aspects and molecular basis of oxaliplatin neurotoxicity: current management and development of preventive measures. Semin Oncol 29:21–33

Gamelin L, Boisdron-Celle M, Delva R, Guerin-Meyer V, Ifrah N, Morel A, and Gamelin E (2004) Prevention of oxaliplatin-related neurotoxicity by calcium and magnesium infusions: a retrospective study of 161 patients receiving oxaliplatin combined with 5-fluorouracil and leucovorin for advanced colorectal cancer. Clin Cancer Res 10:4055–4061

Grothey A (2003) Oxaliplatin-safety profile: neurotoxicity. Semin Oncol 30:5–13

Hart IK, Maddison P, Newsom-Davis J, Vincent A, and Mills KR (2002) Phenotypic variants of autoimmune peripheral nerve hyperexcitability. Brain 125:1887–1895

Hausheer FH, Schilsky RL, Bain S, Berghorn EJ, and Lieberman F (2006) Diagnosis, management, and evaluation of chemotherapy-induced peripheral neuropathy. Semin Oncol 33:15–49

Kiernan MC, Burke D, and Bostock H (2005) Nerve excitability measures: biophysical basis and use in the investigation of peripheral nerve disease. In: Dyck PJ, Thomas PK (ed) Peripheral neuropathy. Elsevier, Philadelphia

Kiernan MC, Hart IK, and Bostock H (2001) Excitability properties of motor axons in patients with spontaneous motor unit activity. J Neurol Neurosurg Psychiatry 70:56–64

Kiernan MC, and Krishnan AV (2006) The pathophysiology of oxaliplatin-induced neurotoxicity. Curr Med Chem 13:2901–2907

Krarup-Hansen A, Helweg-Larsen S, Schmalbruch H, Rorth M, and Krarup C (2007) Neuronal involvement in cisplatin neuropathy: prospective clinical and neurophysiological studies. Brain 130:1076–1088

Krarup-Hansen A, Rietz B, Krarup C, Heydorn K, Rorth M, and Schmalbruch H (1999) Histology and platinum content of sensory ganglia and sural nerves in patients treated with cisplatin and carboplatin: an autopsy study. Neuropath Appl Neuro 25:29–40

Krishnan AV, Goldstein D, Friedlander M, and Kiernan MC (2005) Oxaliplatin-induced neurotoxicity and the development of neuropathy. Muscle Nerve 32:51–60

Krishnan AV, Goldstein D, Friedlander M, and Kiernan MC (2006) Oxaliplatin and axonal Na^+ channel function in vivo. Clin Cancer Res 12:4481–4484

Krishnan AV, Lin CSY, Park SB, and Kiernan MC (2008) Assessment of nerve excitability in toxic and metabolic neuropathies. J Peripher Nerv Syst 13:7–26

Land SR, Kopec JA, Cecchini RS, Ganz PA, Wieand HS, Colangelo LH, Murphy K, Kuebler JP, Seay TE, Needles BM, Bearden JD III, Colman LK, Lanier KS, Pajon ER Jr, Cella D, Smith RE, O'Connell MJ, Costantino JP, and Wolmark N (2007) Neurotoxicity from oxaliplatin combined with weekly bolus fluorouracil and leucovorin as surgical adjuvant chemotherapy for stage II and III colon cancer: NSABP C-07. J Clin Oncol 25:2205–2211

Lecomte T, Landi B, Beaune P, Laurent-Puig P, and Loriot M-A (2006) Glutathione s-transferase p1 polymorphism (ile105val) predicts cumulative neuropathy in patients receiving oxaliplatin-based chemotherapy. Clin Cancer Res 12: 3050–3056

Lehky TJ, Leonard GD, Wilson RH, Grem JL, and Floeter MK (2004) Oxaliplatin-induced

neurotoxicity: acute hyperexcitability and chronic neuropathy. Muscle Nerve 29:387–392

Lin CSY, Kiernan MC, Burke D, and Bostock H (2006) Assessment of nerve excitability properties in peripheral nerve disease. In Kimura J (ed) Peripheral nerve diseases: Handbook of clinical neurophysiology, vol 7, pp 381–403

LoMonaco M, Milone M, Batocchi AP, Padua L, Restuccia D, and Tonali P (1992) Cisplatin neuropathy: clinical course and neurophysiological findings. J Neurol 239:199–204

LoPachin RM, Lehning EJ (1997) Mechanism of calcium entry during axon injury and degeneration. Toxicol Appl Pharmacol 143:233–244

Naumann R, Mohm J, Reuner U, Kroschinsky F, Rautenstrauss B, and Ehninger G (2001) Early recognition of hereditary motor and sensory neuropathy type 1 can avoid life-threatening vincristine neurotoxicity. Brit J Haematol 115:323–325

Nicolao P, and Giometto B (2003) Neurological toxicity of ifosfamide. Oncology 65:11–16

Park SB, Goldstein D, Lin CSY, Krishnan AV, Friedlander ML, and Kiernan MC (2009a) Acute abnormalities of sensory nerve function associated with oxaliplatin-induced neurotoxicity. J Clin Oncol 27:1243–1249

Park SB, Lin CSY, Krishnan AV, Goldstein D, Friedlander ML, and Kiernan MC (2009b) Oxaliplatin-induced neurotoxicity: Changes in axonal excitability precede development of neuropathy. Brain, in press

Petrioli R, Pascucci A, Francini E, Marsili S, Sciandivasci A, Tassi R, Civitelli S, Tanzini G, Lorenzi M, and Francini G (2007) Neurotoxicity of FOLFOX-4 as adjuvant treatment for patients with colon and gastric cancer: a randomized study of two different schedules of oxaliplatin. Cancer Chemoth Pharm, Available online April 12)

Pietrangeli A, Leandri M, Terzoli E, Jandolo B, and Garufi C (2006) Persistence of high-dose oxaliplatin-induced neuropathy at long-term follow-up. Eur Neurol 56:13–16

Pignata S, De Placido S, Biamonte R, Scambia G, Di Vagno G, Colucci G, Febbraro A, Marinaccio M, Lombardi AV, Manzione L, Carteni G, Nardi M, Danese S, Valerio MR, de Matteis A, Massidda B, Gasparini G, Di Maio M, Pisano C, and Perrone F (2006) Residual neurotoxicity in ovarian cancer patients in clinical remission after first-line chemotherapy with carboplatin and paclitaxel: The multicenter Italian trial in ovarian cancer (MITO-4) retrospective study. BMC Cancer 6:5

Postma TJ, Heimans JJ, Muller MJ, Ossenkoppele GJ, Vermorken JB, and Aaronson NK (1998) Pitfalls in grading severity of chemotherapy-induced peripheral neuropathy. Ann Oncol 9:739–744

Quasthoff S, Hartung HP (2002) Chemotherapy-induced peripheral neuropathy. J Neurol 249: 9–17

Richardson PG, Briemberg H, Jagannath S, Wen PY, Barlogie B, Berenson J, Singhal S, Siegel DS, Irwin D, Schuster M, Srkalovic G, Alexanian R, Rajkumar SV, Limentani S, Alsina M, Orlowski RZ, Najarian K, Esseltine D, Anderson KC, and Amato AA (2006) Frequency, characteristics, and reversibility of peripheral neuropathy during treatment of advanced multiple myeloma with bortezomib. J Clin Oncol 24:3113–3120

Rowinsky EK, and Donehower RC (1995) Paclitaxel (taxol). N Engl J Med 332:1004–1014

Sahenk Z, Barohn R, New P, and Mendell JR (1994) Taxol neuropathy: electrodiagnostic and sural nerve biopsy findings. Arch Neurol 51:726–729

Strumberg D, Brugge S, Korn MW, Koeppen S, Ranft J, Scheiber G, Reiners C, Mockel C, Seeber S, and Scheulen ME (2002) Evaluation of long-term toxicity in patients after cisplatin-based chemotherapy for non-seminomatous testicular cancer. Ann Oncol 13:229–236

Susman E (2006) Xaliproden lessens oxaliplatin-mediated neuropathy. Lancet Oncol. 7:288

Verstappen CCP, Koeppen S, Heimans JJ, Huijgens PC, Scheulen ME, Strumberg D, Kiburg B, and Postma TJ (2005) Dose-related vincristine-induced peripheral neuropathy with unexpected off-therapy worsening. Neurology 64:1076–1077

Wang W-S, Lin J-K, Lin T-C, Chen W-S, Jiang J-K, Wang H-S, Chiou T-J, Liu J-H, Yen C-C, and Chen P-M (2007) Oral glutamine is effective for preventing oxaliplatin-induced neuropathy in colorectal cancer patients. Oncologist 12:312–319

Wilson RH, Lehky T, Thomas RR, Quinn MG, Floeter MK, and Grem JL (2002) Acute oxaliplatin-induced peripheral nerve hyperexcitability. J Clin Oncol 20:1767–1774

Winer EP, Berry DA, Woolf S, Duggan D, Kornblith A, Harris LN, Michaelson RA, Kirshner JA, Fleming GF, Perry MC, Graham ML, Sharp SA, Keresztes R, Henderson IC, Hudis C, Muss H, and Norton L (2004) Failure of higher-dose paclitaxel to improve outcome in patients with metastatic breast cancer: cancer and Leukemia Group B trial 9342. J Clin Oncol 22:2061–2068

9
Multidrug Resistance

Ernesto Yagüe and Selina Raguz

Chemotherapy was introduced into clinical practice at the end of the Second World War when Gilman and colleagues used nitrogen mustard to treat a patient with advanced malignant lymphoma (Goodman et al. 1946). Although there are some types of cancer such as colon cancer which respond poorly, most cancers respond well to first-line chemotherapy. However, after a cancer-free period, in a percentage of cases cancer reappears and is termed relapse or progressive disease. Scientists refer to this phenomenon as acquired resistance, in contrast to the intrinsic resistance of other cancers. Another frequently used term is multidrug resistance, which refers to the phenomenon by which cells treated with a drug become cross-resistant to the cytotoxic effect of a variety of other structurally and functionally unrelated drugs, is rarely used in the clinical setting, although its use is widespread among non-clinical scientists.

INFLUENCE OF PHARMACOLOGICAL AND PHYSIOLOGICAL FACTORS

Two main types of factors contribute to the development of drug resistance. The first group include pharmacological and physiological factors such as inadequate access of the drug to the tumour, inadequate infusion rate, inadequate route of delivery, drug metabolism or drug excretion. These are extremely important issues not only in clinical practice but also fundamental in drug development and excellent recent reviews have covered those topics (Garattini 2007).

The importance of the tumour microenvironment has implications not only for the delivery of the therapeutic agent. One observation that rarely escapes the clinician is the association between metastatic invasion and chemotherapy failure and in many cellular models of drug resistance a remodelling

of the extracellular matrix has been reported (Sherman-Baust et al. 2003).

MOLECULAR MECHANISMS OF RESISTANCE TO TRADITIONAL CHEMOTHERAPY

Intracellular Drug Activation

Some drugs, such as the analogues of DNA precursors 5-fluorouracil and ara-C (cytosine arabinoside) require further biochemical modification before they are able to function (e.g. conversion to 5-fluorodeoxyuradine monophosphate in the former or to its triphosphate derivative, ara-CTP, in the latter). Resistance to 5-FU has traditionally involved inhibition of the enzyme thymidylate synthase which catalyzes the final step in the synthesis of thymidine from precursor molecules (Ooyama et al. 2007). Resistance to ara-C has often been associated with lack of deoxycytidine kinase (catalyzing the first step in its conversion to ara-CTP) expression both in vitro and in vivo (Galmarini et al. 2003).

Detoxifying Systems

The cytochromes P450 are a multi-gene family of constitutive and inducible haem-containing oxidative enzymes with an important role in the metabolism of a diverse range of xenobiotics. Although primarily expressed in the liver, they are often over-expressed in a variety of solid tumors where they can contribute to drug resistance (Fujita 2006). Another detoxifying mechanism is the glutathione (GSH) system, which includes at least two enzymes: GSH S-transferase and GSH peroxidase, has the capacity to detoxify drugs that contain very reactive chemical groups (such as alkylating agents) or to break down the active oxidizing compounds (such as hydrogen peroxide) which are produced by the action of a variety of cytotoxic agents (Townsend and Tew 2003).

DNA Repair

Many anticancer drugs (such as platinum compounds, alkylating agents, and nitrosoureas) cause direct damage to the structural integrity of the DNA, leading to the formation of covalent adducts on cellular DNA. The formation of crosslinks requires an initial reaction to form a monoadduct. For many drugs the second reaction is slow, and only a fraction of monoadducts go on to form crosslinks. It is these interstrand crosslinks that are the critical cytotoxic lesion for most bifunctional drugs. These crosslinks distort the DNA structure resulting in catastrophic consequences for a cell if unrepaired. Importantly, repair of DNA interstrand crosslinks has been demonstrated to be a mechanism of clinical resistance to melphalan (a nitrogen mustard) in multiple myeloma (Spanswick et al. 2002).

Topoisomerases are involved in maintaining the three-dimensional structure of DNA during RNA synthesis and DNA replication. A variety of drugs bind to the topoisomerase-DNA complex, stabilizing it and preventing the broken strands from being joined. These include doxorubicin and etoposide for topoisomerase II and camptothecin for topoisomerase I. Although the effect of these drugs onto the topoisomerase system is very clear in vitro, its relevance with the chemotherapy clinical outcome is less clear (Uggla et al. 2007).

Cell Death Regulation

An important aspect of carcinogenesis is resistance to cell death, in particular apoptotic cell death. Apoptosis in mammalian cells is mediated by a family of cysteine proteases, named caspases, which can be divided into two groups: initiator and effector caspases. Caspase induction can be mediated through two principal pathways. The extrinsic pathway is activated by the stimulation of death receptors on the cell surface. However, antineoplastic agents used the intrinsic pathway, which is activated in response to several extracellular and intracellular stress signals, converging in the mitochondria. This results in the permeabilization of the outer mitochondrial membrane, and the subsequent release of cytochrome c and other proapoptotic molecules, with the formation a large protein complex, the apoptosome, containing cytochrome c, apoptotic protease activating factor 1 (APAF 1) and caspase-9. Regulation of these processes occurs through the activity of antiapoptotic members of the BCL-2 family of proteins (Elmore 2007). Up-regulation of antiapoptotic proteins such as BCL-2, BCL-XL, and IAP family, inactivating mutations in pro-apoptotic proteins Bax and Bak, or p53 have been described, and the restoration of p53-mediated apoptosis in cancer cells has been sought for some time so far without a clinical application.

Membrane Proteins

Drug resistance can also result from decreased activity / expression of the uptake transporters, or alternatively, from enhanced efflux. Water-soluble drugs, such as cisplatin, nucleoside analogues and antifolates, cannot cross the plasma membrane unless they 'piggy-back' onto membrane transporters, or enter through hydrophilic channels in the membrane. An excellent review about the influence of solute carriers and channels in chemosensitivity has been published recently (Huang et al. 2004).

Hydrophobic drugs, such as doxorubicin, vinblastine, or paclitaxel, enter the cell largely by diffusion across the membrane, although this process can also be enhanced by transport proteins. Many types of drug resistant cells have increased drug efflux such that the intracellular drug concentration remains below cytotoxic levels. These cells often express one or several ATP-binding cassette (ABC) transporters. These membrane proteins, from which there are 49 different genes in the human genome, transport a variety of substrates across the membrane against a concentration gradient with the energy provided by ATP hydrolysis. Their mechanisms of action, structure, and classification has been reviewed recently (Higgins 2007). Depending of their architecture and mechanism of transport, ABC proteins are classified in seven subfamilies (A–G), although not all of them have been associated with drug resistance (Gottesman and Ling 2006). The most studied, ABCB1 (MDR1, P-glycoprotein), ABCC1 (MRP1), and ABCG2 (BCRP, breast cancer resistance protein), have been associated with the term multi-drug resistance (MDR, see above), due to the variety of compounds that these proteins can transport across the membrane.

CELLULAR MODELS TO STUDY DRUG RESISTANCE

The use of drug resistant derivatives from human and other mammalian cell lines has been of paramount importance for the

unraveling of many of the mechanisms of cancer drug resistance highlighted above. Although the use of cell lines has tremendous advantages, its use has also disadvantages. Apart from the genotypic and phenotypic drift during years of continuos culture, the most common problem encountered is their false identity. Single nucleotide polymorphisms and karyotypic analyses indicate that one of the most studied drug resistant cell lines, MCF-7/AdrR, an adriamycin resistant derivative from the breast cancer cell line MCF-7, was actually derived from ovarian adenocarcinoma OVCAR-8 cells (Liscovitch and Ravid 2007).

In the early days of the study of drug resistance, cell lines were exposed to increasing concentration of the chemotherapeutic agent in a step-wise fashion, generating drug resistant derivatives with several-hundred-fold greater resistance to the drug relative to the parental cell line. Many of the traditional drug resistant lines, such as the above described MCF-7/AdrR or KB derivatives resistant to vinblastine, colchicine and adriamycin, were generated in this way, and is a method that is still in use these days (Chauvier et al. 2002). These drug resistant lines were very important before the techniques to ectopically express foreign DNA were of routine used, since they over-expressed one or several of the molecular effectors conferring drug resistance, such as P-glycoprotein, and biochemical assays could be easily performed with them. However, such drug resistant cell lines are far from ideal when studying regulatory mechanisms controlling drug resistance since the concentration of drug used vastly exceeds that found by cancer cells.

Another protocol to generate drug resistant derivatives involves the use of single lower doses of drug than those used in the above studies. Resistance to doxorubicin and microtubule interfering agents in leukemic K562 cells (Yague et al. 2003) and to doxorubicin in experimentally transformed fibroblasts (Yague et al. 2007), for example, has been generated in such a way. The advantage of such drug resistant cells is that since the concentration of drug used to generate them resembles closely the one found in the serum of chemotherapy-treated patients, they represent a good approximation to the physiological situation.

A third, less common, approach is to treat with single, or repeated, doses of drug for a very short period (hours), mimicking the burst of drug in the serum of chemotherapy-treated patients (Agarwal and Kaye 2003), and doxorubicin resistant derivatives of breast cancer MCF-7 cells have been generated in this way (Elmore et al. 2005). However, working with leukemic K562 cells we have not seen a difference between the last two methods, since after the initial addition of drug most of the cells undergoe apoptosis, even after withdrawal of the drug and replenishment with drug-free medium (Randle et al. 2007).

It has been argued that the protocol used in the generation of resistant cells influences the mechanisms of resistance selected in such cells (Agarwal and Kaye 2003). In our experience, we have not found that to be the case. For instance, using continuous exposure to low drug doses, we have generated doxorubicin resistant derivatives from leukemic K562, experimentally transformed fibroblasts, and breast cancer MCF-7 and CAL51 cells. P-glycoprotein is responsible for the drug resistant phenotype in the former two (Yague et al. 2004; Yague et al. 2007), whereas is P-glycoprotein-independent in the last two cells (S. Raguz and E. Yagüe, unpublished observation).

Leukemic K562 Cells as a Model to Study Multi-drug Resistance

A variety of drug resistant derivatives of K562 cells can be selected by continuous exposure to low concentration of drugs (160 ng/mL doxorubicin, colchicine 20 ng/mL, or 25 μM cytosine arabinoside) (Yague et al. 2003, 2004). Drug resistant derivatives generated by step-wise selection to much higher drug concentrations have also been described (Raguz et al. 2004). Although leukemic cells generally transfect poorly, the development of nucleofection technologies (www.amaxa.com) permits transient transfection efficiencies of around 90%, expanding the possibilities for genetic manipulation. Resistance to doxorubicin and colchicine in these cells is mediated by P-glycoprotein, since stably expression of small interfering RNAs targeting *MDR1* mRNA completely reverses the multi-drug resistant phenotype to that of the drug-sensitive K562 parental cell line (Yague et al. 2004). This is important since there are published few examples where the MDR phenotype is fully knocked down, either because of a poor expression of the siRNAs or due to multifactorial drug resistance (Xu et al. 2004). Although traditional mechanisms of P-glycoprotein-mediated drug resistance involve *MDR1* gene amplification and transcriptional activation, in these cells the *MDR1* gene is neither amplified nor transcriptionally activated. The *MDR1* mRNA half-life in K562 cells is increased from 1 h in the drug sensitive to 18–24 h in the drug resistant derivatives (Yague et al. 2003). Changes in *MDR1* mRNA turnover have been previously described, although this is the first example of its association with the drug resistant phenotype. More importantly, a novel mechanism regulating P-glycoprotein expression at the level of translational initiation has been described (Randle et al. 2007). A highly folded loop structure at the 5′-end of the message renders *MDR1* transcripts difficult to translate because they compete inefficiently for the cap binding protein eIF(eukaryotic initiation factor)4E. Drug resistant cells arise from a small subpopulation of cells able to up-regulate *MDR1* mRNA levels above a critical threshold, making the transcript competitive for the translational machinery, and translating P-glycoprotein. Importantly, since the levels of available eIF4E are determined by the phosphorylation status of a family of translational repressors, the eIF4E binding proteins (4E-BP), we have speculated that compounds interfering with the PI3K-Akt-mTOR pathway (controlling the phosporylation of 4E-BP), might be used to avoid the generation of drug resistance (Randle et al. 2007).

The method for the generation of K562 drug resistant cells and methodology for detection of P-glycoprotein expression is described below:

Method for the generation of colchicine-resistant K562 cells

1. Prepare RPMI 1640 medium with 2 mM L-glutamine and 10% foetal calf serum (RPMI culture medium), and a stock of colchicine at 2 mg/mL.
2. In a 175 cm^2 culture flask seed K562 cells in 50 mL RPMI at a density of 5×10^5 cells/mL. Add colchicine to a final concentration of 20 ng/mL.
3. At day 3, add 50 mL RPMI culture medium.
4. At day 10, add again another 50 mL RPMI culture medium.

5. By this time approximately 50% of cells have died, and by day 12 some small clones (bunches of 8–16 cells) are visible after careful observation under the microscope.
6. At day 14, add another 50 mL RPMI culture medium.
7. At day 18, transfer the whole culture to 50-mL Falcon tubes and spin down the cells for 5 min at 500 × *g*. Resuspend the cell pellet in 160 mL RPMI medium with colchine (20 ng/mL final concentration).
8. This last step is the most critical. Although the few drug resistant cells that have started to grow in the last steps normally continue growing, in some instances due to insufficient resistance, all cells die.
9. Monitor the culture daily under the microscope.
10. By days 20–25 clones should be very clear and cells in culture would start to proliferate.
11. It may be necessary to change the culture medium (when the phenol red indicator becomes yellowish). In this case split the culture 1:2. Add colchicine at 20 ng/mL final concentration.
12. By day 30–35 the culture should consist mainly of colchicine-resistant K562 cells.
13. These cells express P-glycoprotein and its appearance can be easily monitored by flow cytometry (see methods below). They can be expanded by splitting the cultures 1:5 twice a week in medium containing colchicine.
14. Growth of the cells in the presence of drug is important to maintain P-glycoprotein expression in these cells. We have determined that drug-resistant K562 cells start to loose P-glycoprotein expression (see below) after a few weeks without drug and revert to the original drug sensitive phenotype after 4–5 months in the absence of drug selection.

Detection of plasma membrane P-glycoprotein by flow cytometry with monoclonal antibody UIC2

1. The assay uses 2.5–5 × 10^5 cells (a total of twice that number of cells will be needed in order to use a control).
2. Suspension cells can be counted using a hemocytometer after tryptan blue staining. For attached cells we have found that the trypsin used to release cells from the dish damages P-glycoprotein, so after washing off the medium extensively with phosphate buffer saline (PBS) detach cells with 10 mM EDTA and count them.
3. Prepare two tubes (small 5 mL tubes used in flow cytometry such as BD Falcon #352054) each with 2.5–5 × 10^5 cells and wash twice (2–3 min spin at ~100 *g*) with PBS-BSA (PBS with 0.1% bovine serum albumin).
4. Resuspend cells in a final volume of 100 μL PBS-BSA.
5. In one tube the phycoerythrin-conjugated P-glycoprotein-specific antibody UIC2 (#2370, Immunotech, Marseille, France) will be added. In the other, a phycoerythrin-conjugated mouse IgG2a isotype control (#P4810, Sigma, St. Louis, MO) to correct for unspecific binding.
6. The amounts per tube are
   a. IgG: 250 ng IgG + 0.2 μL 20 mM cyclosporin A + PBS-BSA to 100 μL
   b. UIC2: 250 ng UIC2 + 0.2 μL 20 mM cyclosporin A + PBS-BSA to 100 μL

7. It is better to do a master mix because the amount of cyclosporine (which is used to block P-glycoprotein and make it more easily recognizable by the antibody) is too low to measure. Mix and incubate at 37°C for 30 min.
8. Wash twice with PBS-BSA as above.
9. Resuspend in 300 μL PBS-BSA and protect from light.
10. Add 3 μL 1 μM TOTO3 to stain dead cells.
11. In the flow cytometer gate cells according to size (FSC), morphology (SSC), and TOTO3 exclusion (blue channel) before recording events in the red channel (phycoerythrin fluorescence). Figure 9.1 shows P-glycoprotein expression in drug resistant K562 cells.

BODIPY-taxol efflux assay

The enzymatic activity of P-glycoprotein (and other ABC transporters) can also be easily measured by flow cytometry using a fluorescent substrate such as BODIPY-taxol (BT) or rhodamine 123.

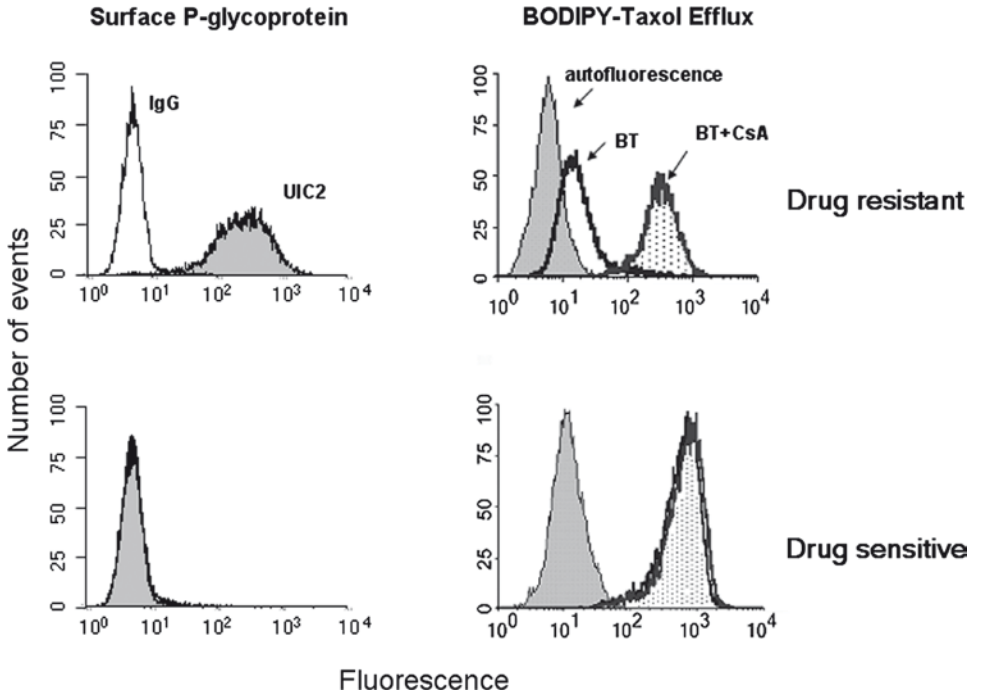

FIGURE 9.1. Detection of P-glycoprotein by flow cytometry in drug resistant K562 cells. *Left panels*: Representative flow cytometric analysis of surface P-glycoprotein expression using the UIC2-phycoerythrin-conjugated antibody (*filled* peak) and the corresponding IgG isotype control (*clear peak*). For drug sensitive cells, the IgG and UIC2 peaks overlap, showing that active P-glycoprotein is not present at the cell surface. *Right panels*: Representative flow cytometric analysis of P-glycoprotein function by efflux of the fluorescent substrate BODIPY-taxol (BT). The presence of cyclosporin A (a P-glycoprotein inhibitor) makes the fluorescent BT accumulate inside the cell (*dotted peak*). Absence of the inhibitor (*clear peak*) permits efflux and a decrease in the fluorescence of the cell. Drug sensitive cells show an overlap of the peaks with and without cyclosporin A, indicating no efflux activity. The cell autofluorescence is indicated (*grey peaks*)

1. Obtain cells as for UIC2 binding. Prepare three tubes, each with 1 x 10^6 cells.
2. Wash cells twice (spin at 100 × g for 2–3 min) with phenol-red-free DMEM containing 0.1% BSA.
3. Resuspend cells in the corresponding volume of DMEM-BSA and add the substrate and inhibitor as follows:
   a. Tube 1 (autofluorescence): 200 μL DMEM-BSA
   b. Tube 2 (BT efflux): 150 μL DMEM-BSA + 50 μL 0.05 nM BT (1 μL of 0.02 μM BT-prepared in DMSO-dissolved in 399 μL DMEM-BSA)
   c. Tube 3 (blocked efflux): 100 μL DMEM-BSA + 50 μL 0.05 nM BT (1 μL of 0.02 μM BT-prepared in DMSO-dissolved in 399 μL DMEM-BSA) + 50 μL 80 μM cyclosporin A (1 μL 20 mM cyclosporin A-prepared in ethanol-dissolved in 249 μL DMEM-BSA)
4. Incubate between 10 and 30 min at 37°C.
5. Wash twice with DMEM-BSA.
6. Resuspend in 300 μL cold DMEM-BSA or PBS-BSA and keep in the dark.
7. Add 3 μL 1 μM TOTO3 to stain dead cells.
8. Keep on ice and in the dark.
9. In the flow cytometer gate cells according to size (FSC), morphology (SSC), and TOTO3 exclusion (blue channel) before recording events in the green channel (BODIPY fluorescence). Figure 9.1 shows BODIPY-taxol efflux by P-glycoprotein in drug resistant K562 cells.

ANIMAL MODELS TO STUDY DRUG RESISTANCE

Different animal models used in experimental oncology include spontaneous, transplantable, and inducible tumours in animals, xenografts of human cancer cells, and transgenic mice.

Inducible tumours in animals adequately reflect tumorigenic processes. However, the number of compounds able to induce a defined type of tumour is limited. In addition, some carcinogens are species specific, which restricts the area of application of inducible animal neoplasias. Spontaneous tumours arise with low frequency in laboratory animals and in various age periods, which are the major disadvantages of this model. Carcinogenesis in transgenic animals is generated by over-expression of oncogenes and/or silencing to tumour suppressor genes, and the high level of expression of the transgenes argues against the physiological relevance of this model. We must not forget that human cells require more genetic changes for neoplastic transformation than do their murine counterparts. The perturbation of just two signalling pathways, involving p53 and Raf, suffices for the tumorigenic conversion of normal murine fibroblasts, while perturbation of six pathways, involving p53, pRb, PP2A, telomerase, Raf, and Ral-GEFs, is needed for human fibroblasts (Rangarajan et al. 2004). In addition, animal allografted tumours reveal some dissimilarity between this animal model and human cancers. All this makes these models of little advantage in their use to study drug resistance.

Xenografted human tumours in immunodeficient mice have two main advantages: human origin of the tumour and desired pathological type, although one of their main disadvantages is that the tumour is mainly ectopic. In addition, these models are unable to model the host-tumour interaction, due to the need for immunodeficient mice, although this limitation has been overcome with the development of three immunocompetent syngenic mouse models; for a further discussion and

references therein see Agarwal and Kaye 2003. Since the early days of drug resistance, melanoma, lung, gastric and colon carcinoma as well as T-cell leukaemia drug-resistant xenograft models were soon developed, and have played an important role in deciphering, together with cellular models, many of the molecular mechanisms involved in the drug resistant phenotype. They continue to be of particular interest for studying the physiology and pharmacokinetics of novel compounds aimed at reverting drug resistance (Chou et al. 2005). More recently, an experimental animal model of tumour progression based on naive and resistant lymphosarcoma has been developed which can be useful for testing conventional therapy alone or together with newly developed gene-targeted therapeutics (Mironova et al. 2006).

CANCER STEM CELLS AND DRUG RESISTANCE

The cancer stem cell hypothesis states that many, if not all, cancers contain a minority population of transformed self-renewing stem cells, the cancer stem cells (CSCs), which are entirely responsible for sustaining the tumour as well as giving rise to proliferating but progressively differentiating cells constituting the tumor mass. Excellent reviews have recently dealt with this topic (Burkert et al. 2006; Li and Neaves 2006). This CSCs retain the essential property of self-protection through the activity of multiple drug resistance transporters such as ABCB1 (P-glycoprotein) and / or ABCG2 (Breast Cancer Resistance Protein 1, BCRP1). The latter is responsible of the side-population (SP) phenotype early detected in both normal and acute myeologenous leukemia (AML) hematopoietic stem cells. Since *Mdr1a/1b*$^{-/-}$ (P-glycoprotein-deficient) mice are able to display a normal SP phenotype that disappears when *Abcg1* is knocked-down (Zhou et al. 2002), expression of ABCG2 and Hoechst 33342 efflux are two of the best markers of these cells. To date, the existence of CSCs has been demonstrated in AML and CML, in brain and gastrointestinal tumors, and in lung and breast cancer (de Jonge-Peeters et al. 2007).

It is chiefly because of the expression of many of the membrane transporters that a connection between CSCs and drug resistance is thought to exist. In fact the whole concept of multidrug resistance has been revised incorporating the CSC paradigm and new hypotheses for the old concepts of intrinsic and acquired drug resistance have been proposed (Dean et al. 2005). According to the acquired resistance stem-cell model, the CSCs, which express drug transporters, and are present in the original tumor mass, survive chemotherapy, whereas the committed but variably differentiated cells are killed. These cells reform the now drug resistant tumor, resulting in a heterogeneous tumor composed of CSCs and committed but variably differentiated offspring. In addition, mutation in the surviving CSCs can arise expanding the drug-resistant phenotype. Whether these hypotheses will be confirmed by further experimentation and/or will be useful in the design of therapeutic strategies, remains to be seen.

DRUG RESISTANCE IN THE CLINIC

Cell culture systems and animal models have been of pivotal in the definition of the main molecular and cellular mechanisms

responsible for the drug resistance phenotype. With them it has been relatively straight forward to demonstrate that a particular molecule (i.e. P-glycoprotein or p53) is the effector of drug resistance, due to the ease of performing knock-out or ectopic expression experiments. However, the situation in the clinic is far more complicated.

First of all, the amount of biological material, normally from a tumor biopsy, is small (leukemias are the only exception) and special care has to be taken at the operating theatre to conserve the integrity of the tissue for future analysis. This is imperative when analyzing RNA expression. Secondly, many of the techniques used routinely in the laboratory setting are not suitable for the small amount of tumour material available. For instance, one of the best methods to detect the expression of P-glycoprotein is by flow cytometry with the UIC2 monoclonal antibody. Although this technique is ideally suited for the study in leukemias, it is unsuitable when dealing with a tissue biopsy. In this case, immunohistochemical methods are routinely used in the pathology laboratory. However, and continuing with our P-glycoprotein example, the UIC2 monoclonal antibody is not suitable for such methodologies. Unfortunately, many of the other common antibodies used for P-glycoprotein detection in paraffin sections are not as good as UIC2 and show certain cross-reaction with other ABC transporters. An additional caveat in clinical studies associating a particular effector with resistance to chemotherapeutics is the lack of common methodologies in different clinical laboratories. This has already been addressed in the case of P-glycoprotein detection, where a series of recommendations have been agreed between participating centers (Huet et al. 2005).

Another important point to consider is that the association of a particular drug resistance effector in clinical samples does not necessarily correlate with an alteration in the chemotherapy response. As such, a negative correlation has been unequivocally demonstrated between P-glycoprotein expression and chemotherapy response in AML (Mahadevan and List 2004). Although similar evidence in breast cancer seems quite convincing (Clarke et al. 2005), it has not been wholly accepted in the medical community. To our knowledge, no other meta-analysis has been performed associating any of the multidrug resistance effectors with chemotherapy response.

REVERSAL OF DRUG RESISTANCE IN THE CLINICAL SETTING

Since the discovery of P-glycoprotein in the early 1980s most agents tested for the reversal of multidrug resistance in the clinic have aimed at inhibiting P-glycoprotein function. The first generation of P-glycoprotein inhibitors included verapamil, quinine and cyclosporine, which were already approved for other medical purposes. Although these compounds proved to be ineffective or toxic at the doses required to attenuate P-glycoprotein function, some clinical trials indicated that modulation of P-glycoprotein function could be achieved (Gottesman et al. 2002). This encouraged the development of a second generation of modulators, such as the cyclosporine analogue PSC-833 (Valspodar), aimed at avoiding the toxic side effects of those of the first generation. Development of second-generation inhibitors has now been discontinued, mainly due to their little success in clinical trials (PSC-833

induced pharmacological interactions that limited drug clearance and metabolism of the chemotherapeutic agent, thereby elevating plasma concentrations beyond acceptable toxicity). Third-generation inhibitors have been designed for low pharmacokinetic interaction, and inhibition of cytochrome P450 3A has been avoided with compounds such as laniquidar (R101933), oc144-093 (ONT-093), zosuquidar (LY335979), elacridar (GF-120918) and tariquidar (XR9576). A further generation of inhibitors act on a broader range of ABC transporters such as biricodar (VX-710) and GF-120918, that modulate, in addition to P-glycoprotein, MRP1 and ABCG2, respectively. Most clinical trials endpoints have not been analyzed yet; for an extended discussion of P-glycoprotein inhibitors in the clinic see Szakacs et al. 2006.

There are many different possible reasons for the failure of Phase III clinical trial targeting P-glycoprotein such as multifactorial mechanisms of resistance, toxicity of the inhibitors and unfavourable pharmacological interactions, as well as a poor clinical trial design (Szakacs et al. 2006). The latter is exemplified by the Phase III clinical trial using tariquidar as an adjunctive treatment in combination with first-line chemotherapy for patients with non-small cell lung carcinoma, where there is no strong evidence to suggests that in this type of cancer P-glycoprotein is expressed to a significant extent (Szakacs et al. 2006). Even AML patients, in which P-glycoprotein expression affects the outcome of chemotherapy, are not routinely phenotyped and current efforts to develop simple, inter-centre reproducible protocols to detect P-glycoprotein in AML blasts have been developed (Pallis et al. 2005). In such a way, trials organizers can have the choice of whether to give P-glycoprotein modulators to an unsorted cohort or to P-glycoprotein-positive patients only.

Other alternative approaches to target MDR could involve the development of agents interfering with one of several of the many regulatory steps in P-glycoprotein expression: transcription, mRNA turnover, translation, protein processing and turnover. Of these, the only one under trials (currently Phase II) is ecteinascidin 743 (ET-743), a natural product isolated from the marine organism *Ecteinascidia turbinata* (Scotto and Johnson 2001), in soft tissue sarcomas (Le Cesne et al. 2005). ET-743 is a (*tris*)-tetrahydroisoquinoline, related to members of the saframycin family of compounds that interferes with the activation of *MDR1* via the stress-responsive enhanceosome complex (Jin et al. 2000).

Acknowledgements. Research in the authors' laboratories is funded by the UK Medical Research Council.

REFERENCES

Agarwal R, and Kaye SB (2003) Ovarian cancer: strategies for overcoming resistance to chemotherapy. Nat Rev Cancer 3:502–516

Burkert J, Wright NA, and Alison MR (2006) Stem cells and cancer: an intimate relationship. J Pathol 209:287–297

Chauvier D, Morjani H, and Manfait M (2002) Homocamptothecin-Daunorubicin Association overcomes multidrug-resistance in breast cancer MCF7 cells. Breast Cancer Res Treat 73:113–125

Chou TC, Guan Y, Soenen DR, Danishefsky SJ, and Boger DL (2005) Potent reversal of multidrug resistance by ningalins and its use in drug combinations against human colon carcinoma xenograft in nude mice. Cancer Chemother Pharmacol 56:379–390

Clarke R, Leonessa F, and Trock B (2005) Multidrug resistance/P-glycoprotein and breast cancer: review and meta-analysis. Semin Oncol 32:S9–15

de Jonge-Peeters SDPWM, Kuipers F, de Vries EGE, and Vellenga E (2007) ABC transporter expression in hematopoietic stem cells and the role in AML drug resistance. Crit Rev Oncol Hemat 62:214–226

Dean M, Fojo T, and Bates S (2005) Tumour stem cells and drug resistance. Nat Rev Cancer 5:275–284

Elmore LW, Di X, Dumur C, Holt SE, and Gewirtz DA (2005) Evasion of a single-step, chemotherapy-induced senescence in breast cancer cells: implications for treatment response. Clin Cancer Res 11:2637–2643

Elmore S (2007) Apoptosis: a review of programmed cell death. Toxicol Pathol 35:495–516

Fujita K (2006) Cytochrome P450 and anticancer drugs. Curr Drug Metab 7:23–37

Galmarini CM, Thomas X, Graham K, El Jafaari A, Cros E, Jordheim L, Mackey JR, and Dumontet C (2003) Deoxycytidine kinase and cN-II nucleotidase expression in blast cells predict survival in acute myeloid leukaemia patients treated with cytarabine. Br J Haematol 122:53–60

Garattini S (2007) Pharmacokinetics in cancer chemotherapy. Eur J Cancer 43:271–282

Goodman LS, Wintrobe MM, Dameshek W, Goodman MJ, Gilman A, and McLennan MT (1946) Nitrogen mustard therapy. J Am Med Assoc 132:126–132

Gottesman MM, Fojo T, and Bates SE (2002) Multidrug resistance in cancer: role of ATP-dependent transporters. Nat Rev Cancer 2:48–58

Gottesman MM, and Ling V (2006) The molecular basis of multidrug resistance in cancer: the early years of P-glycoprotein research. FEBS Lett 580:998–1009

Higgins CF (2007) Multiple molecular mechanisms for multidrug resistance transporters. Nature 446:749–757

Huang Y, Anderle P, Bussey KJ, Barbacioru C, Shankavaram U, Dai Z, Reinhold WC, Papp A, Weinstein JN, and Sadee W (2004) Membrane transporters and channels: role of the transportome in cancer chemosensitivity and chemoresistance. Cancer Res 64:4294–4301

Huet S, Marie JP, Laurand A, and Robert J (2005) Major improvement of the reference method of the French drug resistance network for P-glycoprotein detection in human haematological malignancies. Leuk Res 29:1029–1037

Jin S, Gorfajn B, Faircloth G, and Scotto KW (2000) Ecteinascidin 743, a transcription-targeted chemotherapeutic that inhibits MDR1 activation. Proc Natl Acad Sci USA 97:6775–6779

Le Cesne A, Blay JY, Judson I, Van Oosterom A, Verweij J, Radford J, Lorigan P, Rodenhuis S, Ray-Coquard I, Bonvalot S, Collin F, Jimeno J, Di Paola E, Van Glabbeke M, and Nielsen OS (2005) Phase II study of ET-743 in advanced soft tissue sarcomas: a European Organisation for the Research and Treatment of Cancer (EORTC) soft tissue and bone sarcoma group trial. J Clin Oncol 23:576–584

Li L, and Neaves WB (2006) Normal stem cells and cancer stem cells: the niche matters. Cancer Res 66:4553–4557

Liscovitch M, and Ravid D (2007) A case study in misidentification of cancer cell lines: MCF-7/AdrR cells (re-designated NCI/ADR-RES) are derived from OVCAR-8 human ovarian carcinoma cells. Cancer Lett 245:350–352

Mahadevan D, and List AF (2004) Targeting the multidrug resistance-1 transporter in AML: molecular regulation and therapeutic strategies. Blood 104:1940–1951

Mironova N, Shklyaeva O, Andreeva E, Popova N, Kaledin V, Nikolin V, Vlassov V, and Zenkova M (2006) Animal model of drug-resistant tumor progression. Ann NY Acad Sci 1091:490–500

Ooyama A, Okayama Y, Takechi T, Sugimoto Y, Oka T, and Fukushima M (2007) Genome-wide screening of loci associated with drug resistance to 5-fluorouracil- based drugs. Cancer Sci 98:577–583

Pallis M, Fisher J, Truran L, Grundy M, Russell N, and Burnett A (2005) Reproducible measurements of AML blast p-glycoprotein function in 2 center analyses. Blood 105:1367–1368

Raguz S, Tamburo De Bella M, Tripuraneni G, Slade MJ, Higgins CF, Coombes RC, and Yague E (2004) Activation of the MDR1 upstream promoter in breast carcinoma as a surrogate for metastatic invasion. Clin Cancer Res 10:2776–2783

Randle RA, Raguz S, Higgins CF, and Yague E (2007) Role of the highly structured 5′-end region of MDR1 mRNA on P-glycoprotein expression. Biochem J 406:445–455

Rangarajan A, Hong SJ, Gifford A, and Weinberg RA (2004) Species- and cell type-specific requirements

for cellular transformation. Cancer Cell 6: 171–183

Scotto KW, and Johnson RA (2001) Transcription of the multidrug resistance gene MDR1: a therapeutic target. Mol Interv 1:117–125

Sherman-Baust CA, Weeraratna AT, Rangel LB, Pizer ES, Cho KR, Schwartz DR, Shock T, and Morin PJ (2003) Remodeling of the extracellular matrix through overexpression of collagen VI contributes to cisplatin resistance in ovarian cancer cells. Cancer Cell 3:377–386

Spanswick VJ, Craddock C, Sekhar M, Mahendra P, Shankaranarayana P, Hughes RG, Hochhauser D, and Hartley JA (2002) Repair of DNA interstrand crosslinks as a mechanism of clinical resistance to melphalan in multiple myeloma. Blood 100:224–229

Szakacs G, Paterson JK, Ludwig JA, Booth-Genthe C, and Gottesman MM (2006) Targeting multidrug resistance in cancer. Nat Rev Drug Discov 5:219–234

Townsend DM, and Tew KD (2003) The role of glutathione-S-transferase in anti-cancer drug resistance. Oncogene 22:7369–7375

Uggla B, Tina E, Nahi H, Paul C, Hoglund M, Sirsjo A, and Tidefelt U (2007) Topoisomerase IIalpha mRNA and protein expression vs. in vitro drug resistance and clinical outcome in acute leukaemia. Int J Oncol 31:153–160

Xu D, Kang H, Fisher M, and Juliano RL (2004) Strategies for inhibition of MDR1 gene expression. Mol Pharmacol 66:268–275

Yague E, Arance A, Kubitza L, O'Hare M, Jat P, Ogilvie CM, Hart IR, Higgins CF, and Raguz S (2007) Ability to acquire drug resistance arises early during the tumorigenesis process. Cancer Res 67:1130–1137

Yague E, Armesilla AL, Harrison G, Elliott J, Sardini A, Higgins CF, and Raguz S (2003) P-glycoprotein (MDR1) expression in leukemic cells is regulated at two distinct steps, mRNA stabilization and translational initiation. J Biol Chem 278:10344–10352

Yague E, Higgins CF, and Raguz S (2004) Complete reversal of multidrug resistance by stable expression of small interfering RNAs targeting MDR1. Gene Ther 11:1170–1174

Zhou S, Morris JJ, Barnes Y, Lan L, Schuetz JD, and Sorrentino BP (2002) Bcrp1 gene expression is required for normal numbers of side population stem cells in mice, and confers relative protection to mitoxantrone in hematopoietic cells in vivo. Proc Natl Acad Sci USA 99:12339–12344

10
Role of Antibodies in Cancer Treatment (An Overview)

Huguette Albrecht

INTRODUCTION

Drugs that target cancer cells more selectively than chemotherapeutics have spawned a revolution in cancer treatment (Nathan 2007). These so-called smart drugs are more effective and less toxic because they discriminate better between normal and malignant cells. A naturally occurring smart drug is an antibody that has an exquisite specificity for its target antigen. The foundations for passive immunotherapy were laid at the end of the nineteenth century, when Von Behring and Kitasato injected small doses of the diphteria toxin into animals, to produce serum that on administration to other animals provided passive immunity to diptheria. In 1908, Ehrlich grasped the potential of therapeutic antibodies when he formulated the magic bullet concept.

Therapeutic antibodies became a reality several decades later, with the advent of mouse hybridoma technology (a hybridoma is a hybrid cell produced by fusion of an antibody producing lymphocyte with a cancer cell) (Kohler and Milstein 1975). Murine monoclonal antibodies (MAbs) entered clinical studies in the early 1980s, but their inefficiency and rapid clearance due to patient's production of human anti-mouse antibodies (HAMA) quickly became apparent (Mirick et al. 2004). The combination of hybridoma and recombinant DNA technologies progressively overcame the early therapeutic setbacks of murine MAbs. Now, advances in molecular immunology and genetics enable engineering of fully human MAbs (Weiner 2006). The modular structure of an antibody facilitates the engineering of antibodies (Figure. 10.1a). Recombinant antibodies can be tailored for specific applications and linked to cytotoxic agents. The approval in 1997 by the US Federal Drug Administration (FDA) of the first therapeutic antibody for use in oncology (rituximab) boosted the development of therapeutic MAbs, which now form one of the fastest growing segments of the pharmaceutical market. This overview summarizes the current status of antibodies as they apply to passive immunotherapy for the treatment of cancer.

STRUCTURE OF AN ANTIBODY

Antibodies are immunoglobulins (Igs) produced naturally by B-lymphocytes in response to an antigenic stimulus. Among

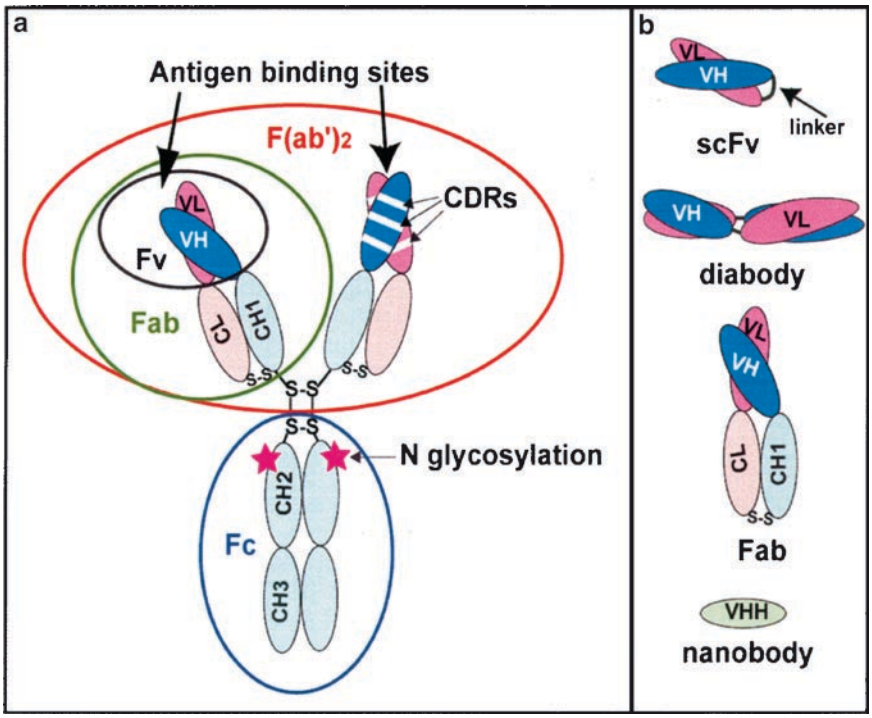

FIGURE 10.1. IgG and antibody fragments. (**a**) Structure of an IgG. Proteolytic cleavage with papain generates two monovalent Fab antibody fragments and the Fc fragment. Digestion with pepsin leads to a bivalent $F(ab')_2$ antibody fragment. (**b**) Structure of recombinant antibody fragments. Monovalent scFv (25 KD) with VH and VL domains stabilized with a linker longer than 12 amino acids (aa); bivalent diabody (50 KD) formed by non-covalent association of two scFvs with short (≤8 aa) inter-domain linkers; monovalent Fab (55 KD); and monovalent single domain antibody or nanobody (15 KD)

the five classes of Igs (M, D, E, A, and G) present in human serum, Igs of class G (IgG) are the most abundant (~75%). Therefore, for recombinant antibodies, unless otherwise defined, the term antibody refers to an IgG. The Y-shaped IgG molecule is an assembly of two light chains (23 Kilo Dalton (KD) each) with two heavy chains (50–70 KD each) held together through both, non-covalent interactions and covalent disulfide bridges (Figure. 10.1a). Variable regions (Fv), located in the upper part of the V, contain the antigen binding sites. An Fv is comprised of two variable domains (VH and VL), each of which contains three hypervariable regions or complementarity determining regions (CDRs). The CDRs form the antigen-binding pocket and constitute the unique binding properties of each antibody. The presence of two identical antigen-binding sites per molecule confers bivalency and monospecificity to an antibody. The valency determines the functional affinity (also called avidity) of an antibody. Constant regions, present in the lower V and I portions determine the IgG subclass or isotype (IgG1- IgG4). The light chain determines the IgG type (κ or λ) and subtype (λ1–λ4). The heavy chain constant region is comprised of three domains, CH1, CH2, and CH3. A proline rich hinge region, between CH1 and CH2 domains, confers flexibility to the molecule (Fig. 10.1a). The CH2 and CH3 domains

form the Fc region which upon antigen binding by the Fv region, recruits effector functions by binding to Fc receptors (FcγRs) and/or the complement. FcγRs are widely distributed on cells of the immune system and their binding to the Fc region couples the humoral with the cellular immune response. N-glycosylation, crucial for effector functions, takes place in the CH2 domain. The composition and overall structure of antibodies is conserved among mammals.

RECOMBINANT ANTIBODIES

Chimeric and Humanized Monoclonal Antibodies

Chimeric and humanized MAbs are the most common genetically engineered variants of murine MAbs. Chimeric MAbs have variable regions of mouse origin and constant regions that are human. Humanized MAbs have mouse sequences that are limited to the CDRs within the variable regions.

Human Monoclonal Antibodies

There are currently two main routes for generating fully human MAbs. One consists of either genetic assembly of human Fvs, selected from antibody fragment combinatorial libraries, with human IgG constant regions or direct selection of full length human IgGs displayed on bacteria (Mazor et al. 2007). In the other, full length human MAbs are developed through hybridoma technology, following immunization of transgenic mice, genetically engineered to express human IgGs of a given isotype (usually IgG1 and IgG2) (Weiner 2006).

Antibody Fragments

In vitro proteolytic cleavage of an IgG with papain results in three fragments: two identical fragments of binding antigen (Fab) and a crystalizable fragment (Fc). The proteolytic action of pepsin leads to one bivalent antibody fragment $F(ab')_2$ (Figure. 10.1a). The modular structure of antibodies (Figure. 10.1a) facilitates recombinant expression of the variable, antigen-binding, region independently of the constant regions. Recombinant antibody fragments may have a variety of different sizes and valencies (Holliger and Hudson 2005). The most widely used fragments include: the monovalent single-chain Fv (scFv) (25 KD); the monovalent Fab (55 KD); the bivalent diabody, a noncovalent scFv dimer (50 KD); and the monovalent single domain antibody fragment (15 KD) (Figure. 10.1b).

The first antibody fragment cloned and expressed in *E. coli* was a single chain Fv (scFv) (Skerra and Pluckthun 1988). The scFv molecule is typically stabilized by joining VH and VL domains with a 15 amino acids flexible linker ($[Gly_4Ser]_3$). ScFvs and Fabs are used as building blocks to engineer multivalent and/or multispecific antibodies (Holliger and Hudson 2005).

Antibody Fragments Combinatorial Libraries

Antibody fragment combinatorial libraries provide a way to recreate natural antibody repertoires (Hoogenboom 2005). Cloning of V genes isolated from B lymphocytes of immunized animals, by means of PCR-based technologies, led to immune combinatorial libraries with up to 10^7 different scFvs (diversity) and binding affinities in the μM range. Naïve combinatorial libraries

were subsequently developed by cloning of V genes isolated from peripheral blood lymphocytes of nonimmunized human donors.

Advances in human molecular immunology and recombinant DNA technology led initially to the construction of semi-synthetic and eventually fully synthetic antibody libraries of larger size: 10^9–10^{10}; and with binding affinities in the nM range. The direct linkage between genotype and phenotype, via display of scFv on the surface of bacteriophages, was a major breakthrough in recombinant antibody technology (McCafferty et al. 1990). Phage display is a powerful and versatile method that enables the display of large collections of antigen-binding fragments (scFv, Fab) for the selection of antigens of interest specific antibody fragments. Display technologies have been expanded to display on yeast, ribosome and bacteria and adapted to high-throughput screening of antibody fragment combinatorial libraries. Display methods, particularly ribosomal display, are also used for affinity maturation of antibodies. Antibody fragment combinatorial libraries are platforms for the discovery of new antibodies (Hoogenboom 2005). Another recent breakthrough in recombinant antibody technology is the display of full length human IgGs on bacteria (Mazor et al. 2007).

PHARMACOKINETICS OF ANTIBODIES

The structure of antibodies determines their pharmacokinetics. MAbs licensed for use in oncology are usually administered intravenously for rapid and systemic delivery into the blood circulation at high concentrations and in relatively large volumes. Oral delivery of therapeutic proteins is more challenging because of acidic pH and proteolysis encountered in the gastrointestinal tract, and the limited diffusion of large molecules through the gastrointestinal epithelium. A prerequisite for a therapeutic antibody is a prolonged (several days to weeks) circulation time in the blood. IgGs, that have a substantial longer serum half-life (23 days) than other classes of Igs, meet that condition naturally. While all Igs are large molecules (≥150 KD) and, therefore, are not eliminated through glomerular filtration in the kidneys, only IgGs can be recycled following endocytosis. The CH2 domain of the Fc region of IgGs carries the binding site for the neonatal Fc receptor (FcRn), primarily expressed on vascular endothelial cells. Following endocytosis, FcRn bound IgGs are exported into the interstitial space of tissues, while free Igs undergo degradation.

There are two major factors that influence blood clearance of IgGs: the affinity for FcRn and the nature of and the affinity for their specific target antigens. Additional factors include their immunogenicity, the degree and nature of their glycosylation and their susceptibility to proteolysis. Recombinant antibody fragments, such as scFvs (25 KD) and Fab (55 KD), that lack a FcRn binding site and have molecular weights below the glomerular filtration threshold (~70 KD), are eliminated from the blood, usually within hours. Serum half-lives of antibody fragments can be increased through PEGylation. The hydrophilic nature of polyethylene glycol (PEG) is exploited to enlarge the size of covalently attached small molecules (Chapman 2002).

The distribution of antibodies within tissues is dependent on their extravasation, which occurs primarily via convective transport and pinocytosis (Lobo et al. 2004).

The blood-tissue hydrostatic gradient drives convective transport, resulting in fluid movement from the blood to the interstitial space of tissues. Antibodies penetrate cells via pinocytosis by one of two mechanisms: binding to a receptor (FcγRs and antibody bound membrane antigen) or fluid phase endocytosis, believed to be the main route for internalization of antibodies into vascular endothelial cells.

Size, affinity, and valency are major parameters that influence the distribution of antibodies within tissues. An scFv, ~ sixfold smaller than an IgG, is more readily transported by convection. But because valency prevails over size for targeting solid tumors (Adams et al. 2006b), for therapeutic applications a large bivalent MAb is a better choice over a small monospecific antibody fragment.

TUMOR ANTIGENS

Tumor antigens are usually proteins or polysaccharides. Initially, tumor antigens were called tumor specific transplantation antigens because mice pre-exposed to irradiated cancer cells from a transplantable cell line were immune to transplanted tumor cells from that same line. Subsequently, tumor antigens were called tumor-associated antigens (TAAs) to account for the fact that they were not necessarily tumor specific but that their expression, overexpression or modification is associated with cancer. The identification of TAAs boomed following the development of the mouse hybridoma technology (Kohler and Milstein 1975). TAAs were often named after the MAbs that led to their identification, for example: CA15-3, CA19-9, DF3 and 17-1A antigens. Therefore, the same TAA has sometimes multiple names because each laboratory was using its own murine MAb. The best example for this is mucin 1 (MUC1) also known as polymorphic epithelial mucin (PEM), polymorphic urinary mucin (PUM), episialin, DF3 antigen, epithelial membrane antigen (EMA), and CA15-3.

The development of molecular biology led to the molecular characterization of TAAs and the discovery of new target antigens for MAbs present on malignant or vascular endothelial cells. Tumor antigens are now referred to as tumor specific antigens (TSA). The National Institute for Health (NIH) defines a TSA as a protein or other molecule that is unique to cancer cells, or is much more abundant in them. These molecules are usually found on the outer plasma membrane, and are thought to be potential targets for immunotherapy or other types of anticancer treatment. Examples of TSAs include glycoproteins such as MUC1, MUC16 (CA19-9), prostate membrane specific antigen (PMSA), carcinoembryonic antigen (CEA), alpha-fetoprotein (AFP), epithelial cell adhesion molecule (17-1A antigen or Ep-CAM), CD20, and receptors such as HER-2 and the epidermal growth factor receptor (EGFR). Expression of TSAs on normal cell can be specific to a developmental stage (CEA and AFP are expressed in the developing fetus) or to a certain level of cell differentiation (CDs on cells of lymphoid origin). The search for new cancer biomarkers may lead to TSAs strictly expressed on cancer cells (Shoshan and Admon 2007).

MANUFACTURING OF THERAPEUTIC MONOCLONAL ANTIBODIES

Monoclonal antibody therapies usually require high doses over a long period of time, necessitating large amounts of

purified product per patient. Therapeutic MAbs are produced in mammalian cell lines in order to best reproduce the glycosylation pattern of natural IgGs, that is critical for effector functions, and for avoiding wrong sugar motifs that could be immunogenic. Chinese hamster ovarian (CHO) and murine myeloma (NSO, SP2/0), are the most widely used cell lines. Protein production in mammalian cells has a number of drawbacks including low titer protein, long fermentation times, heterogeneous glycoproteins, viral contamination issues, and high cost. An individual MAb may cost up to US$100–1000/g to manufacture, compared to as little as US$5 for a small molecule kinase inhibitor (Tanner 2005).

Cost effective production alternatives are being explored. Potential bioreactors include milk and eggs of transgenic animals, and plants. Conservation of glycosylation patterns between birds and humans is an advantage in the use of transgenic hens. Unfavorable glycosylation patterns prevent the use of robust industrial fermentation organisms, such as yeast and filamentous fungi, even though they have the advantage of growth to high cell density in chemically defined media. This hurdle is fading with the genetic engineering of human-like glycosylation pathways into lower eukaryotes. IgG molecules with specific and homogeneous human N-linked glycans were recently produced in engineered strains of the yeast *Pichia Pastoris* (Lazar et al. 2006).

Therapeutic MAbs are purified from cell culture supernatants. The purity of each MAb product is subject to strict regulations. Purification processes are designed to remove viruses, endotoxins, aggregates, host cell proteins, and DNA from the MAb product. Typically three chromatography steps are involved in the purification process of a MAb. Viral inactivation, using low pH or detergents, is an additional step in that process. The first step usually consists of affinity chromatography on protein A. However protein A, an immunotoxin that binds to the Fc region of MAbs, tends to leach into the product and, therefore, must be removed during the downstream processing. The second step depends on the MAb and can include hydrophobic interaction, hydroxyapatite, and cation exchange chromatography. The third step is anion exchange chromatography for removal of endotoxins, DNA and retroviruses. Licensed MAbs are produced in amounts of hundreds of kilograms (Carson 2005).

MECHANISMS OF ACTION OF THERAPEUTIC MONOCLONAL ANTIBODIES (PHARMACODYNAMICS)

Unconjugated or naked MAbs promote cell death by two basic mechanisms involving different parts of their structure. Cell death can be triggered upon binding of the Fv region to a cell membrane antigen. Therapeutic MAbs can block ligand-receptor interactions that result in the disruption of a signaling cascade or trigger an intracellular signal such as apoptosis (Figure. 10.2). Alternatively, the Fc region of a MAb with a bound Ag can induce cell death by activation of other components of the immune system through antibody dependent cellular cytotoxicity (ADCC) and complement dependent cytotoxicity (CDC) (Figure. 10.2a).

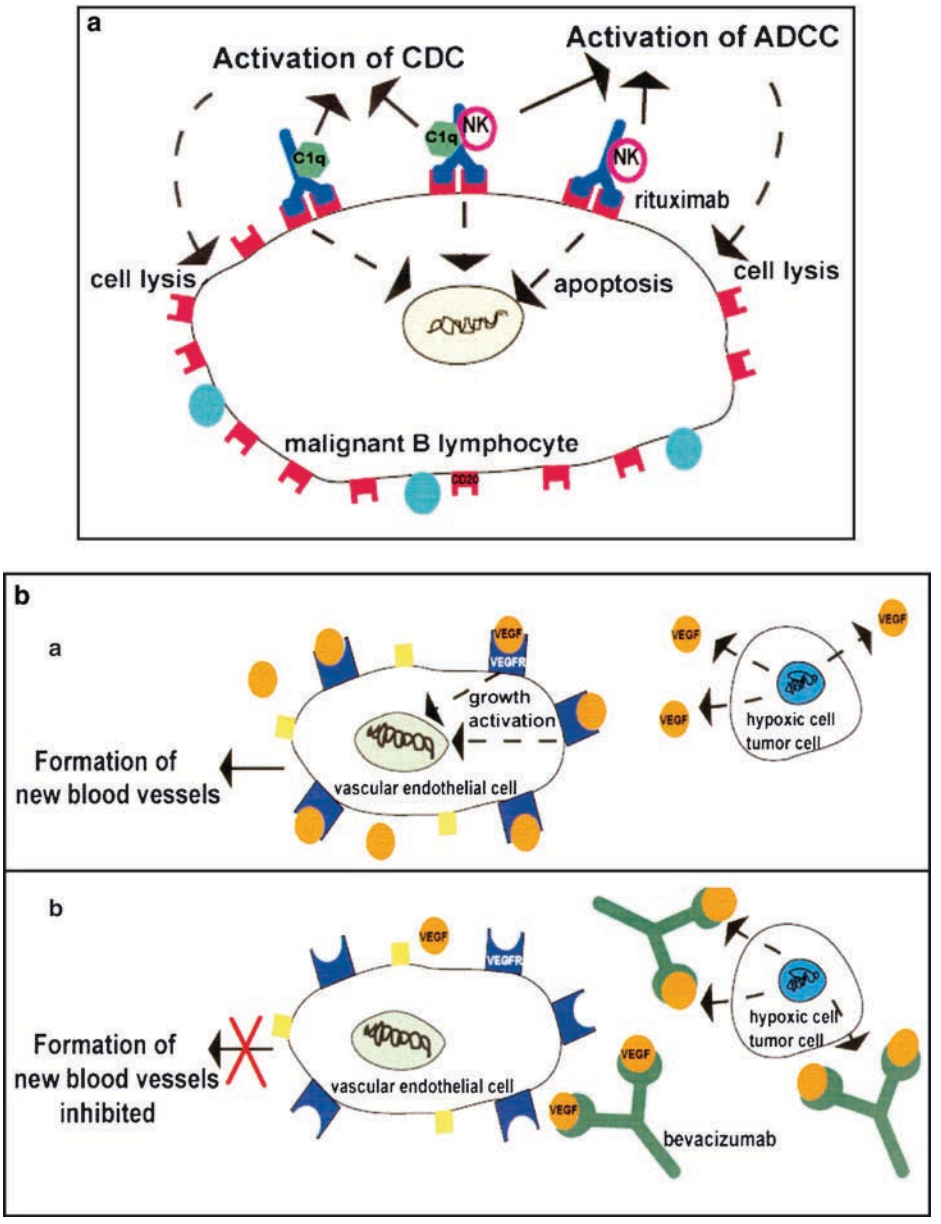

FIGURE 10.2. Mechanisms of action of therapeutic MAbs. (**a**) Rituximab. This anti-CD20 chimeric IgG1 kills cells by mediating effector functions and triggering apoptotic cell death upon binding with its Fv to multiple CD20 antigens present on the surface of B lymphocytes. Binding of natural killer (NK) cells and the C1q protein to its Fc region activate ADCC and CDC respectively. (**b**) Bevacizumab. By binding VEGF with higher affinity, this humanized IgG1 prevents the binding of VEGF, produced by hypoxic tumor cells, to VEGF receptors (VEGFRs) present on the surface of vascular endothelial cells. In the absence of bevacizumab, VEGF binds to VEGFRs and stimulates the formation of new blood vessels (**a**). In the presence of bevacizumab, the formation of new blood vessels is inhibited (**b**)

In ADCC, the antigen–antibody complex binds to Fc gamma receptors (FcγRs) present on effector cells, such as macrophages and natural killer cells, which eliminate the target cells through lysis or opsonization.

Humans have three classes of FcγRs. FcγRI (CD64), FcγRII (CD32) and FcγRIII (CD16) that differ in their affinity for IgGs. FcγRI is a high affinity receptor that preferably binds to IgG1 and IgG3, while FcγRII and FcγRIII are medium to low affinity receptors. FcγRII and FcγRIII have subtypes A and B; FcγRIIA and FcγRIIIA have two and three allotypes respectively. The different FcγRs allotypes vary in their ability to bind IgGs and to trigger ADCC. FcγRI, FcγRIIA, FcγRIIIA, and FcγRIIIB are stimulatory receptors and promote ADCC, while FcγRIIB is an inhibitory receptor and downregulates ADCC. FcγRs are expressed differentially on effector cells: natural killer cells, believed to be the main effector cells in ADCC, express only FcγRIIIA; macrophages express FcγRI, FcγRIIA, FcγRIIIA, and FcγRIIB; neutrophils express FcγRI, FcγRIIA, FcγRIIIb, and FcγRIIB (Clark 1997).

In CDC, the antigen–antibody complex activates the complement system that leads to lysis of the target cells (Fig. 10.2a). IgG isotypes 1 and 3 are the most effective in activating complement while isotype 4 is inactive. Glycosylation at the highly conserved Asn 297 within the CH2 domain of IgGs (Fig. 10.1) is critical for ADCC and CDC (Clark 1997). The IgG1 is the best choice of IgG isotype for a therapeutic MAb expected to promote cell death via ADCC and CDC in humans. Conversely, IgG2 and IgG4 are best when effector functions are unwanted. In humans, the occurrence of ADCC and CDC requires a minimum level of antigen on target cells and the presence of FcγRs with good affinity for the Fc region of the MAb. The demonstration that the engagement of FcγRs on effectors cells is a dominant component of the in vivo activity of antibodies against tumors prompted the genetic engineering of the Fc region of MAbs in order to improve their efficacy (Presta 2006).

The payload of MAbs chemically or genetically engineered into immunoconjugates with killing functions determines their mechanisms of action (Wu and Senter 2005). Radioimmunoconjugates formed by chemical attachment of radionuclides with high linear energies such as beta (^{131}I, ^{90}Y) or alpha (^{213}Bi, ^{211}At) emitters can cause DNA strand breaks and other effects resulting in cell death. Radioimmunoconjugates are attractive for their "bystander" effect that kills cells nearby targeted cells, but the systemic exposure of normal tissue to radiation is not.

Drug and toxin immunoconjugates are highly potent inhibitors of vital intracellular processes and ultimately lead to cell death. However, unlike radioimmunoconjugates, drug or toxin immunoconjugates have to deliver their lethal cargo inside tumor cells for activation of the drug or toxin through release from its carrier. Therefore, the targeting MAbs of these conjugates should be efficiently internalized into the targeted cells. Drug immunoconjugates include chemical conjugation of MAbs with inhibitors of tubulin depolymerization (maytansinoids and auristatin) and catalyst of DNA double strand breaks (calcheamicin). Toxins of plant (ricin) or bacteria (*Pseudomonas* exotoxin A), which are very potent inhibitors of protein synthesis, have been used for the production of immunotoxins as fusion proteins that have variable degrees of immunogenicity.

TOXICITIES ASSOCIATED WITH THERAPEUTIC MONOCLONAL ANTIBODIES

For FDA approval, efficacy and limited toxicity of a MAb must be demonstrated in patients during consecutive clinical trial phases (i.e., I–III and sometimes IV). Usually, phase I addresses tolerated dose and pharmacokinetics in 30–40 healthy volunteers or patients; phase II evaluates efficacy in 100–300 patients at multiple clinical sites; and phase III further evaluates efficacy and safety in 1,000–3,000 patients. Toxicity of therapeutic MAbs can have multiple causes. For unconjugated MAbs, primary causes are immunogenicity of recombinant MAbs and presence of the target antigen on normal cells and tissues. Because immune responses of patients against murine, chimeric, and humanized MAbs are more likely to occur after repeated administrations, these MAbs are usually subjected to a treatment time limit in patients who show benefit. This is no longer the case for panitumumab, the only fully human MAb currently approved for cancer treatment, on the condition that no other unacceptable toxicities arise. Toxicities associated with the presence of the target epitope on normal cells or tissues are exemplified by trastuzumab. Clinical trials showed that the major toxicity associated with this MAb is an increased risk of developing cardiac dysfunction, enhanced in patients concurrently treated with anthracycline, a known cardiotoxic drug. An understanding of the cardiac toxicity associated with trastuzumab was gained from studies in HER-2, HER-4 and neuregulin knockout mice; neuregulin activation of the HER-4/HER-2 receptor complex is a crucial step in cardiac development. Radioimmunoconjugates are subject to dose limitation imposed by the radiation toxicity to the bone marrow. Pretargeting approaches, that consist of dissociation of the targeting and toxicity delivery phases in order to reduce the toxicity to normal tissues, are under preclinical and clinical investigation (Goldenberg and Sharkey 2007).

Adverse events associated with currently approved MAbs include skin toxicity (rituximab, cetuximab, panitumumab), bleeding, thromboembolic events, proteinuria and hypertension (bevacizumab), neutropenia, thrombocytopenia and hepatic toxicity (^{90}Y-ibritumomab tiuxetan, ^{131}I-tositumomab, gemtuzumab ozogamicin) and myelosuppression (^{90}Y-ibritumomab tiuxetan, ^{131}I-tositumomab).

The development of more potent, fully human MAbs against target antigens that are well characterized molecularly and functionally should contribute to toxicity reduction. Further reduction of toxicity could be achieved through the application of personalized medicine, where the selection of a treatment is based on genotypic and/or proteomic information of each patient (Simon 2006). Currently, mandatory screenings are in place only for patients considered for radioimmunotherapy and trastuzumab therapy.

THERAPEUTIC MONOCLONAL ANTIBODIES CURRENTLY LICENSED

As of July 2007, a total of nine MAbs have FDA approval for the treatment of cancer: five of them are directed toward hemato-logic malignant neoplasms. Passive immunotherapy of solid tumor malignancies,

which represent ~90% of cancers, is more challenging because the ability of a systemically delivered MAb to reach its target antigen is influenced by its extravasation from the vasculature, tumor vascularization, lymphatic drainage, and tumor interstitial pressure. Because an estimated 0.001–0.001% of a systemically administered dose of MAb accumulates in solid tumors, higher doses of MAb, potentially leading to increased toxicity, are required for the treatment of solid tumors.

Anti-CD20 Monoclonal Antibodies

The CD20 antigen is expressed on the surface of normal B-lymphocytes and on 95% of B-cell lymphomas. **Rituximab** (Mabthera®/Rituxan®; IDEC/Genentech/Roche) is the first anticancer MAb to receive FDA approval. In 1997 rituximab, a chimeric IgG1, was approved for the treatment of patients with relapsed or refractory B-cell lymphoma, low grade or follicular, non-Hodgkin's lymphoma (NHL). This was based on a phase II trial where 166 patients who had relapsed low grade lymphoma after many previous treatments were given rituximab once a week for 4 weeks: 48% of patients responded with a median response of 12 months and 6% of them had a complete response (CR) (McLaughlin et al. 1998). In 2001, the use of rituximab was approved for retreatment of patients who have relapsed because retreatment of previous responders showed that 40% had a second response with a median response of 12 months (Davis et al. 2000). The observation that in comparison to chemotherapy alone the combination of rituximab and chemotherapy yielded higher CR rates was followed in 2006, by the approval of rituximab in combination with chemotherapy in first line treatment of diffuse large B cell NHL. In 2006, rituximab was also approved in combination with chemotherapy for first line therapy of patients with follicular NHL and for the treatment of low grade NHL in patients with stable disease who achieve a partial or complete response following first line treatment with chemotherapy.

Rituximab sensitizes cells to chemotherapy and mediates cell killing via ADCC and CDC, and apoptosis induced by crosslinking of CD20 at cell surfaces (Fig. 10.2a) (Johnson and Glennie 2003). Approximately, half of the patients treated with rituximab alone do not respond to treatment, and a subset of responsive patients acquires resistance to further treatment. An understanding of mechanisms underlying resistance to rituximab is emerging (Bonavida 2007). In the footsteps of rituximab and its therapeutic success, two other anti-CD20 MAbs were developed as radioimmunoconjugates in order to enhance the killing of tumor cells. In 2002 and 2003, **^{90}Y-ibritumomab tiuxetan** (Zevalin®; IDEC/Schering AG) and **^{131}I-tositumomab** (Bexxar®; Corixa), respectively, received FDA approval for radioimmunotherapy of NHL patients either relapsed or refractory to chemotherapy and rituximab. These are the only fully murine MAbs licensed; ^{90}Y-ibritumomab tiuxetan is an IgG1 and ^{131}I-tositumomab is an IgG2. The mandatory biodistribution and toxicity evaluations in each patient prior to treatment are performed by the administration of an imaging dose of ^{111}In-ibritumomab tiuxetan or ^{131}I-tositumomab. Phase III clinical trials showed that in comparison to rituximab or chemotherapy, the enhanced targeted cytotoxicity provided by these radioimmunoconjugates resulted in significantly

higher overall and complete responses (DeNardo 2005).

Anti-CD33 Monoclonal Antibody

The CD33 antigen is a sialoadhesin expressed on the surface of B or T lymphocytes and overexpressed in about 90% of patients with acute myeloid leukemia (AML). **Gemtuzumab ozogamicin** (Mylotarg®; Celltech/Wyeth) is an anti-CD33 humanized IgG4 chemically conjugated to calicheamicin, a potent antitumor drug. Calicheamicin becomes active once released from the internalized immunoconjugate and kills cells by cleaving double stranded DNA. A phase II study of gemtuzumab ozogamicin, in 142 patients with CD33 positive AML at first relapse, demonstrated a 29% response rate (complete response 16%; partial response 13%) (Sievers 2001). Consequently, gemtuzumab ozogamicin received FDA approval in 2000 for the treatment of AML in patients older than 60 years old. Gemtuzumab ozogamicin is the only licensed antibody-drug immunoconjugate.

Anti-CD52 Monoclonal Antibody

The CD52 antigen is a 25 KD glycoprotein highly expressed on the surface of normal and malignant B and T lymphocytes but not on hematopoietic stem cells. **Alemtuzumab** (Campath-1; ILEX) is a humanized IgG1 with efficacy in the treatment of chronic lymphocytic leukaemia (CLL). In a multicenter clinical trial, 93 patients with fludarabine resistant B cell CLL were given increasing doses of alemtuzumab three times a week for a maximum of 12 weeks. The response rates after treatment were 33% (complete response, 2%; partial response 31%), with median survival times doubling from 16 to 32 months in patients who responded to the treatment (Keating et al. 2002). Alemtuzumab received FDA approval in 2001 for the treatment of patients with chemotherapy resistant B cell CLL.

Anti-HER-2 Monoclonal Antibody

The human epidermal growth factor receptor 2 (HER-2 or ErbB2) is a member of the epidermal growth factor receptor (EGFR) or HER family of receptor tyrosine kinases. Unlike other family members, HER-2 lacks a cognate ligand and mediates lateral signaling to other HER receptors by forming heterodimers with them. Overexpression of HER-2, with subsequent constitutive kinase activation, is associated with a more aggressive malignant phenotype and occurs in ~20–30% of human breast cancers, and other cancers including non-small-cell lung cancer (NSCLC), ovarian and prostate cancers.

Trastuzumab (Herceptin™; Genentech), a humanized anti-HER-2 IgG1 (Carter et al. 2000), is the first MAb for the treatment of solid tumor malignancies, as well as the first humanized MAb to receive FDA approval. In 1998, trastuzumab was approved for use in patients with metastatic breast cancer whose tumors overexpress HER-2. Trastuzumab is indicated for treatment of patients both, in first line therapy in combination with paclitaxel and as a single agent in second and third line therapy. HER-2 overexpression for eligibility for trastuzumab is tested either by immunohistochemistry (IHC) or fluorescence in situ hybridization (FISH). In the original phase III study, patients with untreated metastatic breast cancer, screened by IHC for HER-2 overexpression, received

either trastuzumab in combination with chemotherapy (anthracycline plus phosphamide or taxane) or chemotherapy alone every 3 weeks. The combination treatment achieved a higher response (50% versus 32%), a longer median duration of response (9.1 versus 6.1 months) and a better overall median survival (25.1 versus 20.3 months) (Slamon et al. 2001).

Because cardiac dysfunction occurred in 27% of the anthracycline and cyclophosphamide plus trastuzumab treated group compared with 8% of the group given anthracycline and cyclophosphamide alone, antracycline has been replaced with doxorubicin or paclitaxel. In 2006, trastuzumab was approved in combination with chemotherapy for adjuvant treatment of patients with HER-2 overexpressing, node-positive breast cancer. In the preceding phase III trial with HER-2 positive early stage invasive breast cancer in women who had completed surgery with or without radiotherapy, at least four courses of chemotherapy, and adjuvant treatment with trastuzumab, showed an absolute benefit in terms of disease free survival at 2 years of 8.4% (Piccart-Gebhart et al. 2005).

Trastuzumab kills targeted cell in humans by a variety of mechanisms that include: increased internalization rate of trastuzumab bound HER-2, resulting in reduction or interruption of downstream signaling leading to cell cycle arrest and apoptosis; inhibition of angiogenesis by reduction of angiogenic factors such as VEGF; and possibly ADCC and CDC (Nahta and Esteva 2007). Resistance to trastuzumab has been observed in patients within a year of treatment. An understanding of the molecular mechanisms implicated in the resistance to trastuzumab is emerging and will have important implications on trastuzumab therapy strategies (Nahta and Esteva 2007).

Anti-EGFR Monoclonal Antibodies

The epidermal growth factor receptor (EGFR, also known as ErbB1 or HER1) is another member of the EGFR family of receptor tyrosine kinases. EGFR is overexpressed in numerous epithelial cancers including head and neck, breast, colon, lung, kidney, prostate, brain, bladder and pancreas (Kim et al. 2001). Overexpression of EGFR by malignant cells is associated with poor prognosis and metastatic spread. Up to 85% of patients with colorectal cancer (CRC) overexpress EGFR. Cetuximab and panitumumab are two anti-EGFR MAbs currently approved by the FDA for treatment of metastatic CRC (mCRC).

Cetuximab (Erbitux®; ImClone/Bristo-Miers Squibb) is a chimeric IgG1 that binds to the extracellular domain of EGFR with higher affinity than its natural ligands. Binding of cetuximab induces receptor internalization and reduction of the level of EGFR expressed on the cell surface, consequently blocking the EGFR signal transduction pathway (Kim et al. 2001). Cetuximab exerts its antitumor activity through inhibition of cell proliferation by inducing cell cycle arrest, apoptosis, and possibly triggering ADCC and CDC (Mendelsohn 2002). In 2004, cetuximab received FDA approval for the treatment of EGFR positive mCRC in combination with irinotecan for patients who are refractory to irinotecan, or as a single agent for patients unable to tolerate irinotecan-based chemotherapy. In the phase II trial that led to its approval, cetuximab demonstrated

activity as a single agent with an overall response rate (ORR) of 11% and in combination with irinotecan chemotherapy with an ORR of 23% in patients with irinotecan refractory advanced stage CRC (Cunningham et al. 2004). In 2006, cetuximab was approved for the treatment of locally or regionally advanced squamous cell carcinoma of head and neck (SCCHN) in combination with radiation therapy. This is based on a phase III study, which showed a median duration of overall survival of 49 months among patients who received the combined therapy as opposed to 29.3 months for patients who received radiation therapy only (Bonner et al. 2006). Cetuximab is also approved for monotherapy in patients with recurrent or metastatic SCCHN refractory to chemotherapy.

Panitumumab (Vectibix®; Abgenix/Amgen) is a fully human IgG2. This first fully human MAb, developed via Xenomouse® technology (Yang et al. 2001), has reduced antigenicity in comparison to mouse and chimeric MAbs. Panitumumab with high affinity ($K_D = 5 \times 10^{-11}$ M) and specificity for EGFR is more potent than cetuximab (50% lower inhibitory concentration). A phase III study compared the efficacy and safety of panitumumab plus best supportive care (BSC) to BSC alone in 463 patients with EGFR positive mCRC, who had progressed on standard chemotherapy. Patients treated with panitumumab had a median progression free survival of 8 weeks and an overall response rate of 10% compared to 7.3 weeks and 0%, respectively, for patients who received BSC alone (Van Cutsem et al. 2007). Panitumumab received FDA approval in 2006 for the treatment of mCRC of patients who have progressed on chemotherapy.

Anti-VEGF Monoclonal Antibody

VEGF is one of the most important angiogenic growth factors known to regulate angiogenesis. This factor is secreted by hypoxic cells, such as cells within solid tumors, to stimulate new blood vessel formation by binding to VEGF receptors on nearby endothelial cells (Ferrara 2002). **Bevacizumab** (Avastin®; Genentech) is a humanized IgG1 that prevents binding of all isoforms of VEGF-A to VEGF receptors. The inactivation of VEGF leads to normalized tumor vessels and decreased interstitial pressure, thereby enabling more efficient delivery of chemotherapy to tumor cells (Fig. 10.2b). The outcome of a phase III study led to FDA approval of bevacizumab in 2004 in first line treatment of mCRC, in combination with intravenous fluoropyrimidine chemotherapy. In this study conducted with previously untreated patients with advanced CRC, patients who received bevacizumab plus standard chemotherapy had longer progression free survival (10.6 versus 6.2 months) and survived longer (20.3 versus 15.6 months) than those who received chemotherapy alone plus placebo (Hurwitz et al. 2004). In 2006, bevacizumab received FDA approval for second line therapy of mCRC in combination with intravenous fluoropyrimidine chemotherapy**.** In 2006, the FDA also approved the use of bevacizumab in combination with chemotherapy in first line treatment of patients with unresectable, locally advanced, recurrent or metastatic non-squamous, non-small cell lung cancer (NSCLC). Genentech plans to seek FDA approval for bevacizumab in first line treatment of metastatic breast cancer and renal cell carcinoma.

THERAPEUTIC MONOCLONAL ANTIBODIES AND ANTIBODY TARGETED THERAPEUTICS UNDER INVESTIGATION

Clinical Evaluation

Studies of the process of clinical development and approval of biopharmaceuticals, including recombinant MAbs, indicate trends towards longer clinical and approval phases. The mean clinical development and approval times for new biopharmaceuticals were 68.0 and 15.9 months, respectively, between 1996 and 2000, and 83.0 and 18.5 months, respectively, between 2001 and 2005 (Reichert 2006).

Over 1,000 studies evaluate new applications of previously approved or new MAbs in the clinic (www.clinicaltrial.gov, July 2007). The efficacy of previously approved MAbs, particularly those that target signal transduction pathways, is being investigated in other therapeutic settings and tumor types. The benefit of simultaneously targeting several signaling pathways with a combination of MAbs or MAbs and small targeting drugs is under evaluation. Targeting several signaling pathways is anticipated to yield higher efficacy by overcoming intrinsic and treatment-induced resistance of cancer cells (Duesberg et al. 2007). An estimated 85 new MAbs are at various stages of clinical investigation (Reichert and Valge-Archer 2007). Five among them were chosen to illustrate trends of MAbs in development.

Variation on a Clinically Proven Target

Pertzumab (Omnitarg®; Genentech) is a humanized IgG1**,** which like trastuzumab, targets HER-2 but at a different epitope of its extracellular domain. Pertuzumab sterically disrupts HER-2 heterodimerization with other HER family members, thus preventing lateral signal transduction (Adams et al. 2006a). Pertuzumab is the first of a new class of agents known as HER dimerization inhibitors (HDIs). A phase II study is currently recruiting patients to evaluate the efficacy of combining trastuzumab with pertuzumab in the treatment of patients with unresectable, locally advanced or metastatic breast cancer that did not respond to previous treatment with trastuzumab.

Building on Characterized Murine Monoclonal Antibodies

WX-G250 (Rencarex®; WILEX) is a chimeric IgG1 that binds to carbonic anhydrase IX (G250/MN), which is present on >95% of renal cell carcinomas (RCCs) of the clear cell subtype. The cell killing mechanism of WX-G250 is ADCC. WX-G50 is being assessed for adjuvant therapy of patients with non-metastatic renal cell cancer in a phase III trial.

Human Monoclonal Antibodies Against New Targets and with Innovative Mechanisms of Action

CP675, 206 (Pfizer) is a fully human anti-CTLA4 MAb generated by using the xenomouse technology. CP-675, 206 downregulates T lymphocytes by blocking the binding between antigen 4 on cytotoxic T lymphocytes and B7 on antigen presenting cells. This is believed to help the immune system to seek out and destroy tumors. A phase III study, in patients with surgically incurable metastatic melanoma who have received no prior chemotherapy, or biochemotherapy for the treatment of metastatic disease, is comparing overall

survival for patients with advanced melanoma who receive CP-675, 206 versus patients who receive chemotherapy.

The engagement of cellular immunity for tumor elimination could also be achieved by using bispecific antibodies to physically crosslink T cells with tumor cells. To this end, bispecific T cell engager molecules (BiTEs) are thought promising for overcoming the limitations encountered in the development of bispecific antibodies during the past 20 years (Wolf et al. 2005).

Mapatumumab (HGS-ETR1, TRM1) and **lexatumumab** (HGS-ETR2) (Human Genome Science) are fully human MAbs with high affinity for the death receptors TRAIL-R1 (DR4) and TRAIL-2 (DR5), respectively. These receptors transduce apoptotic signals upon ligand binding. Preferential expression of TRAIL-R1 and TRAIL-R2 on a wide range of malignant cells makes them attractive targets. Mapatumumab and lexatumumab, are agonist MAbs: rather than blocking they initiate a signal that activates the extrinsic apoptotic pathway that leads to cell death, independently of the p53 status of the targeted cells. These agonist MAbs compete with the natural ligand, TRAIL, for binding to their cognate receptors. Phase II studies of mapatumumab in patients with relapsed or refractory NHL and relapsed or refractory NSCLC are ongoing. A phase I trial is evaluating the side effects and best dose of lexatumumab in treating young patients with solid tumors or lymphoma who have relapsed or not responded to previous treatment.

Preclinical Evaluation

In the laboratory, the fast developing field of cancer nanotechnology is the most notable. Nanoparticles are colloidal particles of submicronic size that can be manufactured from a variety of materials such as proteins, lipids, polymers, metals, and semi-conductors (Wang et al. 2007). Nanoparticles have two major attributes: versatility and passive targeting. Protein, liposomes and polymeric nanoparticles can be designed for drug and gene delivery, even across the blood brain barrier, while metallic and semi-conductor nanoparticles have imaging and hyperthermic properties that can be applied to imaging and killing of tumor cells. Nanoparticles accumulate passively in tumors due to the enhanced permeability and retention (EPR) effect, created in solid tumors by their fenestrated vasculature and poor lymphatic drainage.

Active targeting of nanoparticles, achieved by conjugating to their surfaces ligands that target tumors, can enhance their passive targeting. Antibodies are the most widely studied ligands for targeting nanoparticles. An immunonanoparticle is yet another form of immunoconjugate or antibody with a payload. The antigen-binding function provided by recombinant antibody fragments, such as scFvs, is well suited for targeting nanoparticles. In comparison to MAbs, the small size of scFvs is less likely to interfere with the distribution of the nanoparticles within tissues while their lack of Fc prevents activation of effector functions that can lead to faster clearance of the targeted nanoparticles from the body. Monovalency of scFvs is also no longer an issue in nanocarrier systems. The attachment of scFvs at high density to nanoparticles provides multivalency for improved functional affinity as well as options for multispecifity. In addition, for immunonanoparticles that deliver drugs within a cell, scFvs that become efficiently internalized can be directly selected from phage display

libraries. Anti-HER-2 and anti-EGFR scFv targeted liposomes were used successfully to target various drugs to tumors and had higher anti-tumor efficacy than non-targeted liposomes (Drummond et al. 2005).

In conclusion, clinical benefit and market potentials are the driving forces behind antibody-targeted therapies in the treatment of cancer, despite their high cost. The observation that no MAbs are used for first line monotherapy indicates that passive immunotherapy alone is useful when the tumor mass is reduced, either by other therapies or because of early diagnosis. The efficacy of therapeutic MAbs needs to be improved. This is likely to happen because three powerful factors are converging to support the emergence of therapeutic antibodies that are more potent and effective: a clinical imperative to achieve a better outcome for patients; the availability of established and emerging technologies to improve antibody performance; and the commercial drive to compete (Carter 2006). In any case, the future looks bright for antibodies in the treatment of cancer.

REFERENCES

Adams CW, Allison DE, Flagella K, Presta L, Clarke J, Dybdal N, McKeever K,and Sliwkowski MX (2006a) Humanization of a recombinant monoclonal antibody to produce a therapeutic HER dimerization inhibitor, pertuzumab. Cancer Immunol Immunother 55:717–727

Adams GP, Tai MS, McCartney JE, Marks JD, Stafford WFIII, Houston LL, Huston JS, and Weiner LM (2006b) Avidity-mediated enhancement of in vivo tumor targeting by single-chain Fv dimers. Clin Cancer Res 12:1599–1605

Bonavida B (2007) Rituximab-induced inhibition of antiapoptotic cell survival pathways: implications in chemo/immunoresistance, rituximab unresponsiveness, prognostic and novel therapeutic interventions. Oncogene 26:3629–3636

Bonner JA, Harari PM, Giralt J, Azarnia N, Shin DM, Cohen RB, Jones CU, Sur R, Raben D, Jassem J, Ove R, Kies MS, Baselga J, Youssoufian H, Amellal N, Rowinsky EK, and Ang KK (2006) Radiotherapy plus cetuximab for squamous-cell carcinoma of the head and neck. New Engl J Med 354:567–578

Carson KL (2005) Flexibility – the guiding principle for antibody manufacturing. Nat Biotechnol 23:1054–1058

Carter PJ, Fendly BM, Lewis GD, and Sliwkowski MX (2000) Development of herceptin. Breast Dis 11:103–111

Carter PJ (2006) Potent antibody therapeutics by design. Nat Rev Immunol 6:343–357

Chapman AP (2002) PEGylated antibodies and antibody fragments for improved therapy: a review. Adv Drug Deliv Rev 54:531–545

Clark MR (1997) IgG effector mechanisms. Chem Immunol 65:88–110

Cunningham D, Humblet Y, Siena S, Khayat D, Bleiberg H, Santoro A, Bets D, Mueser M, Harstrick A, Verslype C, Chau I, and Van CE (2004) Cetuximab monotherapy and cetuximab plus irinotecan in irinotecan-refractory metastatic colorectal cancer. New Engl J Med 351:337–345

Davis TA, Grillo-Lopez AJ, White CA, McLaughlin P, Czuczman MS, Link BK, Maloney DG, Weaver RL, Rosenberg J, Levy R (2000) Rituximab anti-CD20 monoclonal antibody therapy in non-Hodgkin's lymphoma: safety and efficacy of retreatment. J Clin Oncol 18:3135–3143

DeNardo GL (2005) Treatment of non-Hodgkin's lymphoma (NHL) with radiolabeled antibodies (mAbs). Semin Nucl Med 35:202–211

Drummond DC, Marx C, Guo Z, Scott G, Noble C, Wang D, Pallavicini M, Kirpotin DB, and Benz CC (2005) Enhanced pharmacodynamic and antitumor properties of a histone deacetylase inhibitor encapsulated in liposomes or ErbB2-targeted immunoliposomes. Clin Cancer Res 11:3392–3401

Duesberg P, Li R, Sachs R, Fabarius A, Upender MB, and Hehlmann R (2007) Cancer drug resistance: the central role of the karyotype. Drug Resist Updat 10:51–58

Ferrara N (2002) Role of vascular endothelial growth factor in physiologic and pathologic angiogenesis: therapeutic implications. Semin Oncol 29:10–14

Goldenberg DM, Sharkey RM (2007) Novel radiolabeled antibody conjugates. Oncogene 26:3734–3744

Holliger P, Hudson PJ (2005) Engineered antibody fragments and the rise of single domains. Nat Biotechnol 23:1126–1136

Hoogenboom HR (2005) Selecting and screening recombinant antibody libraries. Nat Biotechnol 23:1105–1116

Hurwitz H, Fehrenbacher L, Novotny W, Cartwright T, Hainsworth J, Heim W, Berlin J, Baron A, Griffing S, Holmgren E, Ferrara N, Fyfe G, Rogers B, Ross R, and Kabbinavar F (2004) Bevacizumab plus irinotecan, fluorouracil, and leucovorin for metastatic colorectal cancer. New Engl J Med 350:2335–2342

Johnson P, Glennie M (2003) The mechanisms of action of rituximab in the elimination of tumor cells. Semin Oncol 30:3–8

Keating MJ, Flinn I, Jain V, Binet JL, Hillmen P, Byrd J, Albitar M, Brettman L, Santabarbara P, Wacker B, and Rai KR (2002) Therapeutic role of alemtuzumab (Campath-1H) in patients who have failed fludarabine: results of a large international study. Blood 99:3554–3561

Kim ES, Khuri FR, and Herbst RS (2001) Epidermal growth factor receptor biology (IMC-C225). Curr Opin Oncol 13:506–513

Kohler G, Milstein C (1975) Continuous culture of fused cells secreting antibody of predefined specificity. Nature 256:495–497

Lazar GA, Dang W, Karki S, Vafa O, Peng JS, Hyun L, Chan C, Chung S, Eivazi A, Yoder SC, Vielmetter J, Carmichael DF, Hayes RJ, and Dahiyat BI (2006) Engineered antibody Fc variants with enhanced effector function. Proc Natl Acad Sci USA 103:4005–4010

Lobo ED, Hansen RJ, Balthasar JP (2004) Antibody pharmacokinetics and pharmacodynamics. J Pharm Sci 93:2645–2668

Mazor Y, Van BT, Mabry R, Iverson BL, and Georgiou G (2007) Isolation of engineered, full-length antibodies from libraries expressed in Escherichia coli. Nat Biotechnol 25:563–565

McCafferty J, Griffiths AD, Winter G, Chiswell DJ (1990) Filamentous Phage displaying antibody variable domains. Nature 348:552–554

McLaughlin P, Grillo-Lopez AJ, Link BK, Levy R, Czuczman MS, Williams ME, Heyman MR, Bence-Bruckler I, White CA, Cabanillas F, Jain V, Ho AD, Lister J, Wey K, Shen D, and Dallaire BK (1998) Rituximab chimeric anti-CD20 monoclonal antibody therapy for relapsed indolent lymphoma: half of patients respond to a four-dose treatment program. J Clin Oncol 16:2825–2833

Mendelsohn J (2002) Targeting the epidermal growth factor receptor for cancer therapy. J Clin Oncol 20:1S–13S

Mirick GR, Bradt BM, DeNardo SJ, and DeNardo GL (2004) A review of human anti-globulin antibody (HAGA, HAMA, HACA, HAHA) responses to monoclonal antibodies, not four letter words. Q J Nucl Med 48:251–257

Nahta R, Esteva FJ (2007) Trastuzumab: triumphs and tribulations. Oncogene 26:3637–3643

Nathan DG (2007) The cancer treatment revolution. Wiley, New York

Piccart-Gebhart MJ, Procter M, Leyland-Jones B, Goldhirsch A, Untch M, Smith I, Gianni L, Baselga J, Bell R, Jackisch C, Cameron D, Dowsett M, Barrios CH, Steger G, Huang CS, Andersson M, Inbar M, Lichinitser M, Lang I, Nitz U, Iwata H, Thomssen C, Lohrisch C, Suter TM, Ruschoff J, Suto T, Greatorex V, Ward C, Straehle C, McFadden E, Dolci MS, and Gelber RD (2005) Trastuzumab after adjuvant chemotherapy in HER-2-positive breast cancer. New Engl J Med 353:1659–1672

Presta LG (2006) Engineering of therapeutic antibodies to minimize immunogenicity and optimize function. Adv Drug Deliv Rev 58:640–656

Reichert JM (2006) Trends in US approvals: new biopharmaceuticals and vaccines. Trends Biotechnol 24:293–298

Reichert JM, Valge-Archer VE (2007) Development trends for monoclonal antibody cancer therapeutics. Nat Rev Drug Discov 6:349–356

Shoshan SH, Admon A (2007) Novel technologies for cancer biomarker discovery: humoral proteomics. Cancer Biomark 3:141–152

Sievers EL (2001) Efficacy and safety of gemtuzumab ozogamicin in patients with CD33-positive acute myeloid leukaemia in first relapse. Expert Opin Biol Ther 1:893–901

Simon R (2006) Validation of pharmacogenomic biomarker classifiers for treatment selection. Cancer Biomark 2:89–96

Skerra A, Pluckthun A (1988) Assembly of a functional immunoglobulin Fv fragment in Escherichia coli. Science 240:1038–1041

Slamon DJ, Leyland-Jones B, Shak S, Fuchs H, Paton V, Bajamonde A, Fleming T, Eiermann W, Wolter J, Pegram M, Baselga J, and Norton L (2001) Use of chemotherapy plus a monoclonal antibody against HER-2 for metastatic breast cancer that overexpresses HER-2. New Engl J Med 344:783–792

Tanner JE (2005) Designing antibodies for oncology. Cancer Metastasis Rev 24:585–598

Van Cutsem E, Peeters M, Siena S, Humblet Y, Hendlisz A, Neyns B, Canon JL, Van Laethem JL, Maurel J, Richardson G, Wolf M, and Amado RG (2007) Open-label phase III trial of panitumumab plus best supportive care compared with best supportive care alone in patients with chemotherapy-refractory metastatic colorectal cancer. J Clin Oncol 25:1658–1664

Wang MD, Shin DM, Simons JW, and Nie S (2007) Nanotechnology for targeted cancer therapy. Expert Rev Anticancer Ther 7:833–837

Wolf E, Hofmeister R, Kufer P, Schereth B, Band auerle PA (2005) BiTES: bispecific antibody constructs with unique anti-tumor activity. Drug Discov Today 10:1237–1244

Weiner LM (2006) Fully human therapeutic monoclonal antibodies. J Immunother 29:1–9

Wu AM, Senter PD (2005) Arming antibodies: prospects and challenges for immunoconjugates. Nat Biotechnol 23:1137–1146

Yang XD, Jia XC, Corvalan JR, Wang P, and Davis CG (2001) Development of ABX-EGF, a fully human anti-EGF receptor monoclonal antibody, for cancer therapy. Crit Rev Oncol Hematol 38:17–23

11
Incorporating Pharmacogenomics into Cancer Therapy

Wooin Lee and A. Craig Lockhart

INTRODUCTION

Heritable variations in genes associated with drug disposition and effects (i.e., drug metabolism, transport, and therapeutic target) contribute to individual heterogeneity in drug treatment response and tolerance. The terms pharmacogenetics or pharmacogenomics, which are often used interchangeably, refer to the study of how an individual's genetic inheritance affects the body's response to drugs and the use of this genetic information to predict the safety, toxicity, and/or efficacy of drugs in individual patients or groups of patients. In some cases, the term "pharmacogenetics" is used to refer to the study of differing phenotypes in association with a single gene or set of candidate genes and the term "pharmacogenomics" is used to refer to genome-wide approaches for identification or discovery of the genetic factors determining differing phenotypes. Throughout this chapter, the term "pharmacogenomics" will be used in reference to this scientific discipline. Pharmacogenomics, as it relates to cancer treatment, presents particular difficulties in comparison to other therapeutic areas, in that acquired somatic mutations in the tumors may also alter treatment outcomes and, that the narrow therapeutic window of chemotherapeutic agents makes titrations in drug dose to affect response or toxicity be a suboptimal approach. The application of pharmacogenomics into the treatment of cancer could have a considerable impact on optimizing cancer treatment for individual patients and groups of patients and also developing new chemotherapeutic agents.

Recent technological advances facilitating the efficient analysis of genetic information, the changing healthcare environment where there is an increased emphasis on evidence-based medicine, and increased demand for safer therapies all contribute to the urgency of incorporating pharmacogenomic information into treatment related decisions. This chapter review aims to provide an update on the current status of the use of pharmacogenomics in cancer treatment, current methods for genotyping, data analysis and strategies for incorporating genetic data into cancer clinical trials. Variations in tumor genetics are well recognized as an important factor in cancer treatment success; however tumor related variations are

beyond the scope of this chapter. Description of sequence variants is provided according to the recommended nomenclature (http://www.hgvs.org/mutnomen/disc.html) and NCBI SNP identification numbers (dbSNP rs#) are listed wherever applicable.

CURRENT USE OF PHARMACOGENOMICS IN CLINICAL ONCOLOGY

Despite an appreciation for the importance of genetic constitution as a factor affecting chemotherapy tolerance and efficacy, individualizing cancer treatment by incorporating genetics into treatment selection has been a protracted process. Until now two known genetic alterations have been shown to affect chemotherapy tolerance to the extent that genetic testing may be warranted prior to administration. Thiopurine methyltransferase (TPMT) metabolizes the chemotherapy agent 6-mercaptopurine (6MP) to its pharmacologically active thiopurine nucleotides. Accumulated evidence supports a causal link between *TPMT* polymorphisms and clinical effects, including toxicity. As such genetic tests are available to identify patients at risk for toxicity and to guide optimal dosing. In 2003, the Pediatric Oncology Subcommittee of the FDAs Oncologic Drugs Advisory Committee recommended revision of the 6MP label to include information on genetic testing for TPMT (Purinethol; http://www.fda.gov/cder/foi/label/2004/09053s024lbl.pdf). In a similar fashion, irinotecan toxicity has been associated with a common variation in one of the UDP-glucuronosyltransferase genes, specifically UGT1A1. Based on the available evidence, genetic information pertaining to irinotecan toxicity is now included in the revised drug labeling for irinotecan based on the recommendations of an FDA advisory committee meeting in 2004 (Camptosar; http://www.fda.gov/cder/foi/label/2005/020571s024,027,028lbl.pdf). These examples of the impact of genetic testing on cancer treatment are detailed below and other genetic variations affecting other aspects of cancer drug disposition and response that have generated sufficient data for possible incorporation into clinical use are also discussed.

Thiopurine Methyltransferase (TPMT)

Thiopurine Methyltransferase (TPMT) is a cytosolic enzyme that catalyzes the S-methylation of aromatic and heterocyclic sulphydryl compounds. Substrates of TPMT include 6-mercaptopurine (6MP), a purine antimetabolite used in the treatment of childhood acute lymphocytic leukemia (ALL). 6MP and other therapeutic antimetabolites, including 6-thioguanine and azathioprine, are methylated to their inactive metabolites by TPMT; hence, a decrease in TPMT activity could lead to decreased metabolism of these compounds and subsequent drug toxicity (McLeod et al. 2000).

As an anticancer agent, 6MP inhibits the formation of nucleotides necessary for DNA and RNA synthesis. Administered 6MP is metabolically activated to form thioinosine monophosphate (thio-IMP) in a reaction catalyzed by hypoxanthine-guanine phosphoribosyltransferase with phosphoribosyl pyrophosphate (PRPP) as a cosubstrate. Cytotoxicity primarily occurs when thio-IMP is converted to thioguanine nucleotides (TGNs) which are then incorporated into DNA and RNA.

Alternatively, thio-IMP is methylated by TPMT to methylthio-IMP, where methylthio-IMP inhibits purine synthesis which leads to cytotoxicity. As part of the catabolic pathway of 6MP, TPMT methylates 6MP to form methyl-6MP, an inactive metabolite.

The gene encoding TPMT is localized on chromosome 6 and exhibits genetic alterations which result in TPMT enzymes that undergo rapid degradation, leading to enzyme deficiency. These inherited variations can have profound effects on the bioavailability and toxicity of 6MP. The vast majority of the population (~90%) demonstrates normal TPMT enzymatic activity (McLeod et al. 2000). Most other individuals (~10%) have intermediate enzymatic activity and one out of 300 individuals has very low or undetectable TPMT activity. In cancer treatment, patients who carry genetic variants that result in profound TPMT deficiency are at risk for severe hematologic toxicities when treated with 6MP.

The molecular basis for the genetic variations associated with altered TPMT activity has been well defined. More than 20 nonsynonymous mutations have been identified in the *TPMT* gene, of which the majority has been shown to result in reduced TPMT activity. Three particular *TPMT* alleles, designated as *TPMT*2* (c.238G>C, rs1800462), *TMPT*3A* (c.[640G>A;719A>G], rs1800460), and *TPMT*3C* (c.719A>G, rs1142345), have been shown to account for ~95% of the observed cases of TPMT deficiency. The *TPMT*3A* allele is the most prevalent, with an allele frequency of 4–5%. The *TPMT*3C* variant has an allele frequency of 0.3–0.7% and the *TPMT*2* variant is less common with an observed allele frequency of 0.5% or less (McLeod et al. 2000).

In clinical practice, studies have shown that TPMT activity can have an impact on outcomes following 6MP treatment. In studies where patients who experienced dose-limiting hematological toxicity were assessed for their TPMT status, the majority of these individuals were TPMT-deficient or heterozygous for *TPMT* variants. These TPMT-deficient patients more frequently required hospitalization and platelet transfusions and were more likely to miss doses of chemotherapy. However, after adjustment of thiopurine dosages, the TPMT-deficient and heterozygous patients tolerated therapy without acute toxicity (Relling et al. 1999). Clinical outcomes in patients with ALL were improved when 6MP dose intensity was maintained without missed weeks of therapy. Appropriate 6MP dose reductions for TPMT-deficient patients have allowed for similar toxicity and survival outcomes as patients with normal TPMT levels (Relling et al. 1999). Genotyping methods have been established for the molecular diagnosis of TPMT deficiency and can assist with determining a safe starting dose for 6-MP therapy. Given the importance of *TPMT* genotype in affecting treatment outcomes, the FDA has recommended *TPMT* testing for patients with clinical evidence of severe toxicity after treatment with thiopurines.

UDP-Glucuronosyltransferase 1A1 (UGT1A1)

UDP-glucuronosyltransferases (UGT1A1) belong to a superfamily of enzymes that catalyze the glucuronidation of hydrophobic xenobiotics and endogenous substrates to their soluble forms facilitating elimination through the bile and urine. UGT1A1 is one of nine UGT1A functional proteins and it is primarily responsible for

the glucuronidation of bilirubin. There are well described heritable hyperbilirubinemic syndromes as a result of genetic variations in *UGT1A1*. Crigler–Najjar syndromes are rare genetic traits characterized by absent or very low UGT1A1 activity (Bosma et al. 1995). Gilbert's syndrome which manifests as a chronic, mild hyperbilirubinemia occurs with an incidence of ~15% in Caucasians. Gilbert's syndrome arises from genetic variations (the Gilbert's allele, also called *UGT1A1*28)* in the promoter region of the *UGT1A1* gene where seven TA repeat element is found instead of six TA repeats in the wild-type *UGT1A1* allele. Individuals homozygous for the *UGT1A1*28* allele have Gilbert's syndrome and have a reduction of UGT1A1 enzyme activity to approximate 30% of normal (Bosma et al. 1995).

The chemotherapy agent, irinotecan is a semisynthetic analog of camptothecin, originally isolated from the ornamental tree Camptotheca acuminata. Irinotecan exerts its antitumor activity by inhibiting topoisomerase I and has demonstrated antitumor activity against a variety of tumors. Irinotecan is most commonly prescribed for the treatment of tumors of the colon and other sites in the gastrointestinal tract. The dose limiting toxicities of irinotecan are diarrhea and neutropenia which occur in ~15% of treated patients and can be severe enough to necessitate hospitalization (Irinotecan Prescribing information). Wide interpatient variability in the incidence of these toxicities as well as an association between these toxicities and levels of the irinotecan metabolites, SN-38 and the glucuronidated metabolite SN-38G have been observed (Mathijssen et al. 2003). UGT1A1 is the enzyme is responsible for the glucuronidation and resulting detoxification of SN-38 to SN38G. Many clinical studies have now demonstrated that patients carrying the *UGT1A1*28* variant are at increased risk for developing irinotecan toxicity.

The potential applicability of genetic testing for *UGT1A1*28* to serve as a predictor of irinotecan toxicity, in particular neutropenia, was evaluated clinically by Innocenti et al. (2004b). In this study evaluating 69 cancer patients, genotyping for *UGT1A1*28* was predictive of irinotecan-induced Grade 4 neutropenia with a sensitivity of 50% and specificity of 95%. This study provided an impetus for testing patients for the presence of *UGT1A1*28* allele prior to treatment with an irinotecan containing regimen. In response to the observed clinical findings, the FDA recently revised the safety labeling for irinotecan, recommending that the dosing of irinotecan be altered for patients who are homozygous for the *UGT1A1*28* allele. The overall clinical applicability and cost-effectiveness of genetic testing for the *UGT1A1*28* variant remains to be fully clarified because the sensitivity and specificity of *UGT1A1*28* testing as a predictor of treatment related neutropenia has only been demonstrated in patients receiving higher doses (350 mg/m^2) of irinotecan rather than lower doses which are more frequently used. There are no specific treatment guidelines for irinotecan dose adjustments in the setting of Gilbert's Syndrome, but given the risk of toxicity in these patients, testing for *UGT1A1*28* homozygosity may be appropriate.

Other Pharmacogenomic Markers in Clinical Investigation

Drug-Metabolizing Enzymes

Dihydropyrimidine Dehydrogenase (DPD, Gene Name: DPYD)

5-Fluorouracil (5-FU) and its derivatives are commonly prescribed chemotherapy agents based on their broad antitumor activity and synergistic interactions with other chemotherapy agents when administered as combination therapy. After administration, ~5% of the administered 5-FU undergoes anabolism into cytotoxic nucleotides, whereas the other 80–95% undergoes catabolism into biologically inactive metabolites. Dihydropyrimidine dehydrogenase (DPD) encoded by the *DPYD* gene is the rate-limiting enzyme in the catabolism of pyrimidines such as uracil and thymidine. Variations in DPD activity can influence the systemic exposure to fluorodeoxyuridine monophosphate (FdUMP) and the incidence of adverse effects to 5-FU treatment. DPD activity is completely or partially deficient in 0.1% and 3–5% of individuals in the general population, respectively, and DPD deficiency has been associated with severe toxicity and fatal outcomes after 5-FU treatment (van Kuilenburg et al. 2003).

A genetic predisposition has been well established to account for many cases of DPD deficiency and multiple *DPYD* variants that result in decreased enzyme activity have been described. Unfortunately, genetic testing to predict patients at risk for 5-FU toxicity is not feasible as at least 17 variants of relatively low frequency in the *DPYD* gene have been discovered in patients with severe 5-FU toxicity (van Kuilenburg et al. 2003). *DPYD*2A* (rs3918290), a G>A variation in the invariant splice donor site resulting in a truncated protein, is the most common of the various mutations in *DPYD* with an allelic frequency of ~1.8% in European Caucasians and is estimated to be a factor in ~25% of patients who experience severe 5-FU toxicity (van Kuilenburg et al. 2003). It should be noted that a substantial number of patients who experience 5-FU toxicity do not carry functionally inactivating *DPYD* alleles. Recently, it was reported that epigenetic regulation, mainly DNA methylation, may also contribute to DPD enzyme deficiency (Ezzeldin et al. 2005). The complex genetic basis of DPD deficiency along with the low frequency of *DPYD* variants and low sensitivity and specificity of *DPYD* genotyping has hampered the application of genetic testing of DPYD into clinical practice.

Cytochrome P450 2D6 (CYP2D6)

CYP2D6 is one of the most extensively studied members of the CYP450 superfamily. The *CYP2D6* gene, located on chromosome 22 is highly polymorphic with >40 described variant alleles of varying function. Approximately 5–10% of Caucasian population is estimated carry a nonfunctional variant of *CYP2D6* where *CYP2D6*3, CYP2D6*4, CYP2D6*5* and *CYP2D6*6* with approximate allele frequencies of 2%, 20%, 4%, and 1% respectively, together account for the vast majority of the nonfunctioning phenotypes (for further information on sequence variations, refer to the website, http://www.cypalleles.ki.se).

Functional variations in CYP2D6 may be of some significance in the disposition of tamoxifen which is widely used to treat estrogen receptor-positive breast cancer. In addition to CYP3A4, CYP2D6

is responsible for converting tamoxifen into more potent anti-estrogen metabolites, 4-hydroxy-tamoxifen and endoxifen (4OH-N-desmethyltamoxifen). Therefore, a significant portion of the antitumor effect of tamoxifen is potentially dependent on the functional activity of CYP2D6. In fact, a strong association between *CYP2D6* genotype and plasma levels of endoxifen has been documented (Jin et al. 2005). To date clinical results have been inconclusive because studies assessing the association between CYP2D6 functional status and patient outcome have produced contradicting reports.

Glutathione S-Transferase P1 (GSTP1)

GSTP1 belongs to a superfamily of Phase II metabolic enzymes and appears to play a significant role in detoxification and resistance to platinum agents. An allelic variation of the *GSTP1* gene c.313A>G (p.105Ile>Val, rs947894) leads to diminished GSTP1 enzymatic activity (Watson et al. 1998). In a retrospective analysis of patients with refractory metastatic colorectal cancer treated with 5-FU and oxaliplatin, patients possessing the Val allele had superior survival (Stoehlmacher et al. 2002).

Transporter Proteins

Multidrug Resistance Protein 1 (MDR1, P-Glycoprotein, ABCB1)

P-glycoprotein (P-gp, also known as MDR1, ABCB1), the product of the *MDR1* or *ABCB1* gene, is a well characterized ATP Binding Cassette (ABC) transporter protein. The ABC transporters are ATP-dependent membrane proteins that transport a diverse array of substrates against a concentration gradient. MDR1 is most studied for its role as a mechanism of chemotherapy resistance in cancer cells. MDR1 is normally expressed in the intestine, liver, kidney, brain, and placenta, where it regulates the disposition of a variety of xenobiotics. Numerous genetic variants of differing functional status have been identified in the *ABCB1* gene, the majority of which are single nucleotide polymorphisms (SNPs) (Leschziner et al. 2007).

The most studied ABCB1 variant is the silent coding sequence variant c.3435C>T (rs1045642) reported initially by Hoffmeyer et al. (2000). The c.3435C>T allele has been associated with lower protein expression and function, measured by digoxin pharmacokinetics (Hoffmeyer et al. 2000) and recently with altered mRNA stability and substrate specificity (Kimchi-Sarfaty et al. 2007; Wang et al. 2005). However, since the initial report of this association, much of data focusing on the association between c.3435C>T and ABCB1 expression/function or clinical outcomes have produced inconsistent results (Leschziner et al. 2007). Some of clinical studies support the notion that *ABCB1* polymorphisms can affect the pharmacokinetics of anticancer drugs and response to therapy. Regarding pharmacokinetics, the c.1236C>T (rs1128503) polymorphism has been associated with higher plasma levels of irinotecan and its active metabolite SN-38 (Mathijssen et al. 2003). Similarly, *ABCB1* haplotypes have been associated with reduced renal clearance of irinotecan and its metabolites (Sai et al. 2003). In studies evaluating clinical outcomes, children with acute lymphoblastic leukemia who carried a polymorphism at the 3435 site had differing frequency of CNS relapse depending on the inherited genotype (Stanulla et al. 2005). In a similar manner homozygosity for an SNP at the

2677 locus was predictive of a shorter time to relapse and shorter overall survival in patients with acute myelogenous leukemia (Illmer et al. 2002).

Multidrug Resistance Protein 1 (MRP1, ABCC1)

MRP1 also known as ABCC1 has been most well described as a transporter conferring drug resistance in tumor cells. With the notable exception of glutathione, MRP1 has a similar substrate profile to MDR1. Given the ubiquitous expression of MRP1 in normal tissues, this transporter has been implicated in tissue defense against drugs, environmental toxins and heavy metals. Several low frequency SNPs have been identified in the *ABCC1* gene leading to decreased transporter function and in vitro alterations to chemotherapy sensitivity (Leslie et al. 2003). To date, studies linking *ABCB1* sequence variants with drug response and clinical outcome are lacking.

Multidrug Resistance Protein 2 (MRP2, cMOAT, ABCC2)

MRP2, also known as ABCC2 or canalicular multispecific organic anion transporter (cMOAT), is found to be expressed in clinical tumor samples and its expression correlated with cisplatin resistance (Hinoshita et al. 2000). MRP2 is primarily located at the apical membrane of hepatocytes, renal tubular cells and intestinal mucosa where it functions to transport organic anions and glutathione conjugated xenobiotics (Borst et al. 2006). Sequence variants in the *ABCC2* gene leading to impaired transporter function or trafficking result in the Dubin–Johnson syndrome, a rare autosomal recessive disorder characterized by conjugated hyperbilirubinemia. Heterozygosity for these variants occurs at a frequency of 0.5–1% in the population (Machida et al. 2005). Although relatively rare, alterations in *ABCC2* gene have been hypothesized to affect chemotherapy disposition and treatment outcomes. In humans, homozygosity for c.3972C>T (rs3740066) appears to affect irinotecan disposition (Innocenti et al. 2004a). To date, an important association between *ABCC2* polymorphisms and cancer treatment outcomes has not been made.

Breast Cancer Resistance Protein (BCRP, ABCP, MXR, ABCG2)

BCRP also known as ABCG2, placenta-specific ABC transporter (ABCP) or mitoxantrone resistance protein (MXR), is an ABC half transporter and putatively homodimerizes. BCRP transports a variety of chemotherapy agents including mitoxantrone, topotecan, SN-38, flavopiridol, methotrexate (Doyle and Ross 2003) conferring resistance in tumor cell lines with some overlap in its resistance profile with MDR1, MRP1, and MRP2. In normal tissues, BCRP is expressed in the placenta, heart, colon, small intestine, kidney, liver, and hematopoietic stem cells (Doyle and Ross 2003). The *ABCG2* gene encoding BCRP has multiple known polymorphisms with varying functional significance. A c.421C>A (rs2231142) variant been associated with lower BCRP protein expression and higher plasma levels of camptothecin analogs (Sparreboom et al. 2005).

Solute Carrier (SLC) Transporters

The SLC family of transporters is a large superfamily of membrane proteins that import or export a variety of endogenous substrates (neurotransmitters, nutrients, or metabolites) as well as xenobiotics. Approximately 300 SLC genes are known

to exist. SLC19A1 (RFC1) is a folate transporter with high affinity for reduced folates and MTX and common polymorphisms have been associated with variable expression of this protein. A common variant of c.80G>A (p.27Arg>His, rs1051266, allele frequency of ~50%) in the *SLC19A1* gene has been associated with differing outcomes in childhood ALL. Children with the AA genotype showed higher MTX plasma levels and had worse prognoses than those with the GG genotype (Laverdiere et al. 2002). Thus far, other studies have not confirmed these findings. Considering their wide substrate specificity, tissue distribution, and frequent genetic variations, the SLC proteins have a potential importance in cancer treatment. However, the functional significance of these proteins for cancer drug response and clinical outcome remains to be further investigated.

Drug Target, Pathway Genes

Methylenetetrahydrofolate Reductase (MTHFR)

5,10-methylenetetrahydrofolate reductase (MTHFR) regulates folate homeostasis; it catalyzes the reduction of 5,10-methylenetetrahydrofolate to 5-methyltetrahydrofolate, the predominant circulatory form of folate. MTHFR deficiency has been associated with a reduced folate pool, as well as neurological and vascular diseases (Klerk et al. 2002). A common functional variant of the *MTHFR* gene (c.665C>T, p.222Ala>Val, rs1801133) leads to reduced catalytic activity in the resulting protein. The allelic frequency of this alteration varies considerably among differing ethnic groups with a frequency of up to 45% in Europeans and East Asians, 57% in Mexicans and 11% in African Americans. The c.665C>T variant has been associated with decreased folate levels and increased toxicity in patients receiving MTX (Ulrich et al. 2001).

Thymidylate Synthase (TS, TYMS)

Thymidylate synthase (TS) is a critical enzyme in DNA synthesis and repair as it catalyzes the methylation of deoxyuridine monophosphate (dUMP) to deoxythymidine monophosphate (dTMP). TS is the primary target for 5-FU and other folate-based antimetabolites and the active metabolite of 5-FU, fluorodeoxyuridine monophosphate (FdUMP) blocks the formation of dTMP by forming a stable complex with TS. Overexpression of TS has been linked to clinical resistance to these TS-targeted agents (Marsh and McLeod 2001).

TYMS, the gene encoding TS, contains seven exons and a 5′-flanking untranslated enhancer region (TSER) containing a 28-bp tandem repeat sequence. Genetic variations involving the differing numbers of tandemly repeated sequences of TSER have been shown to be important determinants of TS expression. The two most common *TSER* alleles are the two tandem repeats (*TSER*2*, allelic frequency = 0.2–0.4) and the three tandem repeats (*TSER*3,* allelic frequency = 0.5–0.8) (Marsh and McLeod 2001). In vitro studies indicated that the *TSER*3/*3* genotype (~25% frequency in Caucasians) is associated with three to four fold higher TS protein expression than the other genotypes (Pullarkat et al. 2001). Clinical studies in colorectal cancer have demonstrated that individuals with *TSER*3/*3* genotype had a significantly lower response rate to 5-FU compared with those patients with at least one *TSER*2* allele (Pullarkat et al. 2001). Similarly in rectal cancer, patients with *TSER*3/*3* genotype had a lower probability

of tumor downstaging after receiving 5-FU chemotherapy and radiation therapy than patients who with at least one *TSER*2* allele (Villafranca et al. 2001). Other polymorphisms in *TYMS* including a G→C SNP located at the 12th nucleotide of the second tandem repeat in patients with three repeats has been associated with lower TS expression levels and better clinical outcomes (Marcuello et al. 2004). These studies suggest that *TSER* genotyping may be useful in selecting patients who are likely to respond to treatment with 5-FU or its analogs; prospective studies evaluating this relationship are in progress.

Epidermal Growth Factor Receptor (EGFR)

Epidermal growth factor receptor (EGFR) is a member of the erbB receptor family that is activated by a variety of ligands that are crucial in the formation and propagation of many tumors. EGFR is frequently dysregulated and overexpressed in a number of epithelial cancers and activation can initiate several downstream signaling pathways affecting tumorigenesis and tumor progression (Lockhart and Berlin 2005). Tageting EGFR pathway has been an attractive anticancer strategy such that monoclonal antibodies to EGFR and tyrosine kinase inhibitors (TKI) that inhibit the EGFR signaling axis have been approved for the treatment of lung and colorectal cancer. Most studies to predict response to these agents have focused on the tumoral expression of EGFR and somatic mutations in the tyrosine kinase domain of EGFR (Sharma et al. 2007). Recently however, EGFR germline polymorphisms have been evaluated in clinical studies and association was noted between improved progression free survival when lung cancer patients were treated with gefitinib (an EGFR targeted TKI) and were homozygous for fewer CA repeats in intron 1 of the *EGFR* gene (Liu et al. 2007).

DNA Repair Genes

Excision Repair Complementation Group 1 (ERCC1)

ERCC1 is an essential member of the nucleotide excision repair (NER) pathway, the primary mechanism in mammalian cells for the removal of bulky DNA adducts produced by platinum agents such as oxaliplatin (Wilson et al. 2001). In vitro, ERCC1 expression in colon cancer cell lines predicts oxaliplatin sensitivity (Arnould et al. 2003). Clinically, studies have shown an association between ERCC1 expression and response to platinum chemotherapy (Metzger et al. 1998). In other clinical studies, ERCC1 expression levels had a significant correlation with overall survival after 5-FU/oxaliplatin therapy in patients with advanced colorectal cancer whose disease had progressed through first-line chemotherapy (Shirota et al. 2001). Two common silent alterations of the *ERCC1* gene, a c.354C>T variation at codon 118 (rs11615, allelic frequency 46%) and a C→A change located in position 8092 in the 3′-UTR (rs3212986, allelic frequency 4%), have been associated with changes in clinical outcome of patients with advanced colorectal cancer treated with 5-FU/oxaliplatin (Park et al. 2003).

Xeroderma Pigmentosum Group D (XPD)/ERCC2

XPD, also known as ERCC2, is a helicase involved in the NER pathway where it plays a central role in DNA damage recognition. Several common alterations in the *XPD* gene have been reported to be associated

with differential DNA repair capacity. A common *ERCC2* variant is c.2251A>C (p.751Lys>Gln, rs13181) at codon 751. A study in patients with colorectal cancer receiving therapy with 5-FU/oxaliplatin demonstrated higher response and survival rates in individuals with the Lys/Lys genotype than individuals who had Lys/Gln or Gln/Gln genotypes (Park et al. 2001).

X-Ray Cross Complementation Group 1 (XRCC1)

XRCC1 is involved in the repair of DNA single-strand breaks as part of the base excision repair multi-enzyme complex. XRCC1 removes incorrect nucleotides that have been incorporated into DNA due to oxidative damage, and adducts formed after treatment with alkylating agents. A sequence variant of the *XRCC1* gene at codon 399 (c.1196G>A, p.399Arg>Gln, rs25487) has been associated with differing outcomes in patients with colorectal cancer treated with chemotherapy consisting of oxaliplatin and continuous infusion 5-FU, where patients carrying the Gln allele were shown to be at a higher risk of failing the 5-FU/oxaliplatin chemotherapy (Stoehlmacher et al. 2001).

METHODOLOGY

Successful incorporation of pharmacogenomics into cancer therapy would require both robust, validated genotyping methods as well as well-designed, well-executed clinical studies providing credible associations between genetic variations and drug disposition/response. General genotyping protocols and various genotyping methods are briefly discussed below. Different strategies and examples for incorporating genetic data into cancer clinical trials are also discussed in the following section.

Genotyping Assays

During the past decades, rapid technological progress has made it possible to perform large-scale, high-throughput genotyping. Different approaches and methodologies for targeted DNA sequence analyses are available with various pros and cons including factors such as cost and throughput. Careful consideration is required for the selection and analytical validation of suitable genotyping assays prior to their use in clinical studies. For more comprehensive overviews focusing specifically on the molecular principles by which various genotyping assays work, the readers are referred to available review articles (Gibson et al. 2005; Isler et al. 2007). In the following sections, we will outline general genotyping protocols and briefly compare several commonly used methods.

Typical Genotyping Protocols

Typically, genotyping protocols start with target sequence amplification primarily based on polymerase chain reaction (PCR) technology. Various detection platforms are available for allelic discrimination reactions and allele specific product identification. Depending on the mechanisms and means of allele discrimination and product detection, some or all of these steps can be performed sequentially or in parallel. The choice of a particular genotyping technology can be influenced by various factors such as the complexity of target sequences, quantitative vs qualitative results, sensitivity/accuracy, success rates, flexibility, cost and throughput.

Comparison of Different Methods

Rapid technological progress has made it possible to efficiently analyze genetic information with varying complexity. Certain genotyping methods that have been traditionally used in earlier studies (e.g., PCR-RFLP (PCR with restriction fragment length polymorphisms), allele-specific PCR (AS-PCR)) can still provide robust testing results at relatively low instrumentation cost. However, they are not amenable to multiplexing or high-throughput automation. On the other hand, the use of more recent technologies (e.g., DNA chips) allows large-scale, high-throughput genotyping at lower testing cost. A brief comparison of commonly used genotyping methods utilizing different assay platforms are provided in Table 11.1. More comprehensive coverage of various genotyping technologies is available elsewhere (Gibson et al. 2005; Isler et al. 2007).

Different Approaches in Pharmacogenomics

Studies in cancer pharmacogenomics often employ three primary strategies to identify genetic factors that associate with drug response, namely (1) candidate gene association, (2) whole-genome association, and (3) integrative in vitro/in vivo pharmacogenomic approaches.

Candidate Gene Association Strategies

Early studies of cancer pharmacogenomics have mostly utilized monogenic candidate gene association strategies, correlating variability in the efficacy and toxicity of many chemotherapeutic agents with polymorphisms in candidate genes that are likely to influence drug response. This straightforward genetic approach has yielded important findings, particularly with respect to highly penetrant and functional genetic variants. This approach examining a smaller number of starting

Table 11.1. A brief comparison of commonly used genotyping methods utilizing different assay platforms

Genotyping platform	Data format	Strength	Weakness
PCR-RFLP	Agarose gel	Simple instrumentation; low cost	Data quality subjective visual interpretation; low throughput
Pyrosequencing	Pyrogram of luciferase intensities	Providing sequency context sourround the polymorphism; real-time scoring; quantitative; good for insertions and deletions	Lengthy protocol; relatively expensive; limited throughput
TaqMan 5′ nuclease activity	Cluster plot of fluoresecent values	Simple protocol; real-time or end point scoring; easy to automate and scale up	Very high fixed cost for each SNP; limited throughput
Single base extension with mass spectrometry detection	Extend primer mass spectra	High success rate; highly accurate and sensitive; quantitative	Relatively high instrument cost/complexity; lengthy protocol; problematic multiplex PCR
Single base extension with fluorescence intensity detection	Fluorescent values	High success rate; capable of multiplexing	Relatively high instrument cost; lengthy protocol; problematic multiplex PCR
Invader assay	Agarose gel, fluorescence, mass spectrometry detection	No PCR for genotyping; simple protocol; isothermal reaction	Relatively large amount of genomic DNA required; requires optimization for each SNP

genes offers the advantage of potential cost savings and also reduces the risk of false-positive findings. However, it is possible to overlook other genes that may be important for drug response. In addition, the positive association observed could be due to linkage with other functional variant alleles or to intra-gene interaction. It is also increasingly recognized that drug response is complex, determined by the interactions of multiple genes, pathways and environmental factors. Thus, recent studies have often implemented polygenic approaches to gain a better understanding of the interplay among multiple genetic and environmental factors.

Whole-Genome Association Approaches

Another approach to studying cancer pharmacogenomics involves whole-genome association studies and/or linkage analysis, identifying portions of the genome that contain genetic variants associated with a specific phenotype. This genome-wide genetic mapping approach requires no a priori assumptions regarding genes or genomic regions associated with the drug effect under investigation. This genomic strategy has become possible with advances in genome-wide technologies such as the development of gene expression arrays, high throughput technologies, and SNP chips. This approach can potentially identify previously unidentified, functionally important candidate genes and SNPs, adding new insights into pathophysiology or pharmacology. However, this approach can also lead to the identification of SNPs or haplotypes that are not responsible for the mechanisms of altered drug response, but in linkage disequilibrium with the actual causative SNPs. Thus, further studies are required to corroborate initial associations and to assess the functional role of the associated SNPs or haplotypes. Additionally, the problem of multiple testing needs to be addressed in performing genome-wide analysis to adjust for an increased risk of false-positives.

Integrative In Vitro/In Vivo Pharmacogenomic Approaches

Another approach in cancer pharmacogenomic studies involves the integration of a diversity of genetic, functional genomic, epigenetic, and other data to elucidate the complexity of drug response. The use of multiple experimental approaches including in vitro cell-based models, in vivo studies in mice, and in vivo human trials can provide compelling and mechanistic connections between genetic variants and particular phenotypes in chemotherapy. Functional assessment of genetic alteration often involves the heterologous expression of genetic variants in in vitro cell-based model systems to facilitate functional characterization. Experimental murine models (e.g., in-bred strains, genetically engineered animals) are also increasingly used in pharmacogenomic studies as a genetic mapping resource and a tool to assess the in vivo functional impact of genetic variations in conditions where diet and environmental factors are controlled (Watters and McLeod 2002). Recently, altered epigenomic phenomena have been increasingly recognized to influence or predict drug response. For example, the methylation-associated silencing of the DNA-repair protein MGMT (O^6-methylguanine-DNA methyltransferase) was found to be predictive of clinical response of gliomas to alkylating agents (Hau et al. 2007). Data from multiple experimental approaches can be integrated to enhance our mechanistic

understanding of the complex biology between genetic variations and their impact on drug response.

IMPLEMENTATION OF PHARMACOGENOMICS IN DRUG DISCOVERY AND DEVELOPMENT

Applying pharmacogenomics to early stage cancer drug development has the potential to streamline the development processes and increase efficiency in order to bring new and improved drugs to patients. Genetic markers can be initially identified during the preclinical stages of drug discovery and early stage clinical trials and further evaluated for their predictive significance and clinical utility either retrospectively or prospectively. Application of pharmacogenomics to clinical trials may assist to target drugs to those patients who are most likely to respond, allowing for a reduction in sample size and/or trial duration. Some of the challenges encountered during the implementation of pharmacogenomics into clinical trials will be discussed including methods for incorporating genetic analysis into early and late stage drug development trials and then clinical trial designs to prospectively determine the utility of genetic markers in predicting clinical outcomes.

Early Stage Clinical Development (Phase I and II Clinical Trials)

In Phase I clinical trials, therapeutic agents are evaluated for safety, tolerability, and pharmacokinetics. A common finding in these studies is the considerable variability in the measured pharmacokinetic parameters. Genetic factors may account for some of the observed variability in toxicity and pharmacokinetics. Phase II clinical trials are designed to evaluate therapeutic agents for safety and efficacy. Several groups have demonstrated that certain genetic variants or gene expression profiles may be used to distinguish responders from non-responders. Two common pharmacogenomic approaches outlined above, candidate gene association and whole-genome association studies can be implemented into early stage clinical trials in an attempt to gain early insights into the genetic factors contributing to drug disposition, toxicity, and efficacy (Fig. 11.1). The identified candidate genes can be further evaluated in rationally designed late-stage clinical trials of larger sample size.

Candidate Gene Association Studies

Based on in vitro/in vivo preclinical results and in some cases available clinical data, the molecular processes responsible for disposition and efficacy of the therapeutic agents under testing may be known. This information can be used to select a panel of candidate genes and genetic variations to assess their association with clinical response, drug toxicity and pharmacokinetic variability. Given the small sample size and trial designs used in Phase I and II studies, the identification of associated candidate genes requires considerable allelic frequency, penetrance, and functional impact. This strategy has been successfully implemented by Sparreboom et al. (2004) in a dose-finding study with 28 patients. Ten polymorphisms in four drug disposition genes with putative relevance were assessed for their effects on tipifarnib (a farnesyltransferase inhibitor) pharmacokinetics. Even with a limited sample size,

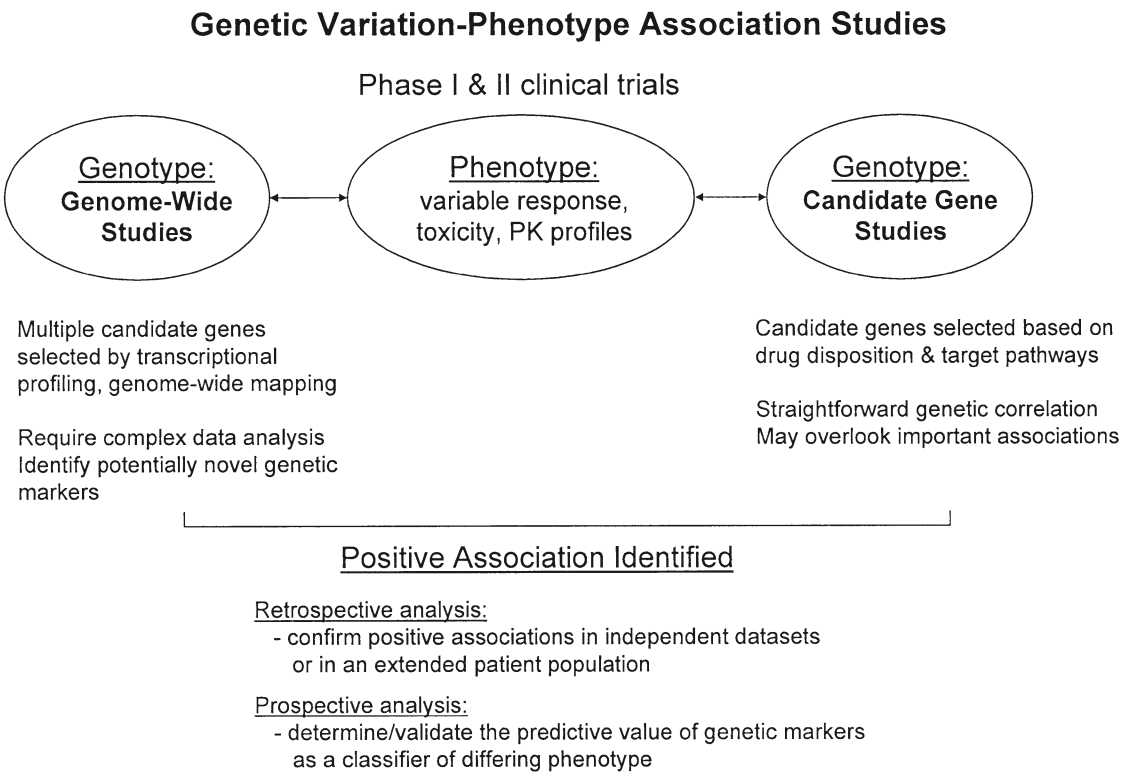

FIGURE 11.1. Common pharmacogenomic approaches to identify genotype–phenotype associations in clinical trials

a positive association between *MDR1* (*ABCB1*) genotype and tipifarnib pharmacokinetics was identified for further study, indicating the feasibility of this focused approach. A similar study by Zamboni et al. (2006) also identified an association between the *ABCG2* genotype and disposition of 9-aminocamptothecin (9AC), a metabolite of the camptothecin analog compound, 9-nitrocamptothecin (9NC). Interestingly, the association with *ABCG2* genotype was only with the disposition of 9AC, but not with that of 9NC. This finding was consistent with a previous in vitro study reporting that the wild-type forms of ABCG2 mediates the cellular efflux of 9AC, but not 9NC (Rajendra et al. 2003). These studies again indicate that the incorporation of focused pharmacogenomic approaches can yield important findings regarding the inter-individual variability of drug disposition and toxicity during early clinical trials and also provide early leads for potential correlative relationships that can be further tested in an extended patient population.

In treatment efficacy studies, candidate gene association studies are largely retrospective analyses of completed clinical trials or analysis of case series from an individual institution or group of institutions. There is one known currently accruing genotype-guided clinical cancer trial which is based on *TYMS TSER* genotype. In this study in rectal cancer patients (stage T3 and T4) being performed by McLeod et al. (2005), 'good risk' patients with the *TSER*2* allele are treated with

standard therapy (radiation and 5FU). Alternatively, patients with a 'bad risk' genotype (homozygous for *TSER*3*) receive the standard radiation and 5FU therapy along with irinotecan. Preliminary data implied an improved response rate in both treatment groups with this genetically guided approach (McLeod et al. 2005).

Whole Genome Association Studies

Microarray technology provides a powerful tool allowing in-depth analysis of gene expression profiles and detection of genetic variations. In oncology this technology has been primarily applied to obtain a gene expression pattern or a 'genetic signature' to classify different types of tumors and predict response to therapy. Phase I studies incorporating this approach are underway, but to date published reports are very limited. Gene expression profiling of tumor or surrogate tissues using microarray analysis can be used to detect genetic differences between subgroups of patients with differing toxicity and pharmacokinetic profiles. Detection of mutations/polymorphisms in a high-throughput manner can be accomplished by the use of SNP chips, but no report of the application of this technology to Phase I and II trials is available. Given the small sample size in Phase I and II trials and the high-throughput nature of microarray technology, there are a number of challenges regarding data mining and analysis, which limit the interpretation of the results from these studies.

Late-Stage Clinical Development (Phase III Clinical Trials)

Once drug development reaches Phase III clinical trials, sample sizes are generally large enough to test hypotheses generated in earlier phases of drug development. Testing of subjects may be carried out prospectively or retrospectively. Many putative genetic markers have been identified that could theoretically optimize and individualize therapy; however few tumor markers have been developed to a point that permits their reliable use in clinical practice. The reasons for infrequent testing in Phase III studies are primarily due to large sample size requirements if genetic markers are to be tested prospectively or inadequate statistical power when markers are evaluated as a correlative as part of an ongoing drug registration study.

Prospective clinical trial designs where the clinical utility of a particular genetic marker is being tested have been proposed by a number of investigators. In particular, Sargent et al. (2005) have proposed two approaches to assess the clinical utility of predictive markers in randomized clinical trials. One approach is the 'marker by treatment interaction design' where patients are initially stratified by genetic status. Within both the 'gene-positive' and 'gene-negative' groups, patients are randomly assigned to receive either the standard therapy or the experimental therapy. A second approach, 'marker-based strategy design' requires that all patients are first tested to determine their genetic status. Patients are then randomly assigned to either a gene-based or a non-gene-based treatment strategy.

A more commonly used Phase III study design incorporating pharmacogenomics would be a two-stage approach in which a study is designed as a randomized trial to compare treatments overall for all participants as part of a drug registration strategy. If the overall treatment difference does not meet a priori objectives

then a subpopulation analysis involving prespecified genotypes would be considered. This design would require that levels for declaring statistical significance, as regards genotype affecting clinical outcome, would be established to preserve the type I error rate for the overall study. In many cases when clinical pharmacogenomics studies are added as a correlative study aim to an existing clinical trial, the evidence can be of limited quality if appropriate analysis plans are not specified.

All the proposed approaches require a clear analysis plan to be in place prior to study initiation and presuppose assay validation and standardization, within the right context and with proper controls. In addition, the trial outcome, or the measurable effect due to the pharmacogenomic intervention (e.g. absolute risk, relative risk, or relative odds), must be prespecified in the study design to insure validity.

Incorporating Pharmacogenomics into Clinical Trials: Technical and Legal Issues

In most cases, searches for genetic factors that affect treatment toxicity and outcomes arise from clinical observations in patients receiving a particular treatment agent. In many of these published studies the number of patients evaluated is relatively small and the analyses are retrospective. As a consequence there may be 'ascertainment biases' where the numbers of cases and controls may be skewed towards the case phenotype making a particular clinical phenomenon appear more frequent than would be observed in the general population. To avoid 'false discovery', the 'case' phenotype, whether related to disease or outcome, should be defined prior to study initiation and sample size and power calculations should be performed in the design stage of any study. If appropriate, statistical adjustments for multiple testing must be incorporated.

With regards to cohort selection, with few exceptions, clinical trials tend to be conducted in heterogeneous populations where differences in allele frequencies between populations of different ancestry may have an impact on the genotypes detected. At the conclusion of a study in a heterogeneous population, it may be difficult to ascertain if the negative association found is due to unappreciated variations in the patient population. Alternatively given the vast numbers of SNPs in certain genes, a positive association observed could be due to linkage of the tested gene with an untyped functional variant allele or to intra-gene interaction. In many cases it is not possible to evaluate each SNP directly because of time and cost constraints. Additional variables that may confound the interpretation of genetically tailored interventions can also include poly-therapy regimens, drug compliance, and nutrition. As such, the predictive power of a genetic test may differ by dosage schedule and concurrent administered drugs.

With the exceptions of *TPMT* and *UGT1A1* genetic testing, pharmacogenomic determinants of response to chemotherapy have not been federally (FDA) regulated. Many genetic tests do not have proven analytic and clinical validity even when the testing is conducted in Clinical Laboratory Improvement Act (CLIA) certified facilities. At present most genetic testing is carried out by nonprofit organizations, requiring only Institutional Review Board approval or by biotechnology companies. If the eventual goal is federal approval of a genetic test, confidentiality

of the participants must be assured and informed consent for testing must detail the potential risks, limitations, and benefits of the proposed testing. Measures of the test's performance (sensitivity, specificity, and predictive value) must also indicate that clinical testing is warranted.

FUTURE DIRECTIONS

To date, pharmacogenomic characteristics have not been widely adapted into the care of cancer patients or into clinical trials evaluating new cancer drugs. Technological advances which allow for efficient and inexpensive genotyping and continued searches for appropriate gene candidates will enhance our understanding of the contribution of genetic factors to cancer treatment outcomes. The accessibility of these technologies should provide an opportunity to incorporate pharmacogenomics more readily into the drug development process such that these factors are considered during the stages from early clinical development to final registration rather than retrospectively after phenotypic variations are observed in treated patients.

In many of the studies discussed herein, one candidate gene was evaluated for its association with a previously identified phenotype variant. Even though significant associations have been identified in hypothesis driven trials, the predictive value of testing for a particular genotype may be relatively low, indicating that a polygenic approach may be warranted to account for the interaction of multiple genes and pathways. Haplotype analysis considers multiple polymorphisms within a candidate gene that occur in close proximity such that they are rarely separated by recombination and are in linkage equilibrium. Haplotype associations are increasingly considered such that the contributions of multiple genetic variations can be assessed simultaneously. This enables the reduction of SNP analysis from hundreds of SNPs to particular marker SNPs so fewer genotypes need to be tested for in a particular study. By reducing the number of genotypes to consider, associations between haplotypes across genes (e.g., genes that regulate metabolism and transport) so called haplotype association studies can be facilitated.

Finally, expression microarrays and proteomics are powerful platforms that generate vast amounts of data that aid in identifying alternative candidate genes for testing. These technologies should be able to complement current genotype, haplotype and phenotype approaches and provide insights into previously unrecognized involved pathways. The key component to the proper utilization of these technologies will be validated and standardized methods for data processing and statistical analysis.

REFERENCES

Arnould S, Hennebelle I, Canal P, Bugat R, and Guichard S (2003) Cellular determinants of oxaliplatin sensitivity in colon cancer cell lines. Eur J Cancer 39:112–119

Borst P, Zelcer N, van de Wetering K (2006) MRP2 and 3 in health and disease. Cancer Lett 234:51–61

Bosma PJ, Chowdhury JR, Bakker C, Gantla S, de Boer A, Oostra BA, Lindhout D, Tytgat GN, Jansen PL, Oude Elferink RP, and Chowdhury NR (1995) The genetic basis of the reduced expression of bilirubin UDP-glucuronosyltransferase 1 in Gilbert's syndrome. N Engl J Med 333: 1171–1175

Doyle LA, Ross DD (2003) Multidrug resistance mediated by the breast cancer resistance protein BCRP (ABCG2). Oncogene 22:7340–7358

Ezzeldin HH, Lee AM, Mattison LK, and Diasio RB (2005) Methylation of the DPYD promoter: an alternative mechanism for dihydropyrimidine dehydrogenase deficiency in cancer patients. Clin Cancer Res 11:8699–8705

Gibson N, Jawaid A, and March R (2005) Novel technology and the development of pharmacogenetics within the pharmaceutical industry. Pharmacogenomics 6:339–356

Hau P, Stupp R, and Hegi ME (2007) MGMT methylation status: the advent of stratified therapy in glioblastoma? Dis Markers 23:97–104

Hinoshita E, Uchiumi T, Taguchi K, Kinukawa N, Tsuneyoshi M, Maehara Y, Sugimachi K, and Kuwano M (2000) Increased expression of an ATP-binding cassette superfamily transporter, multidrug resistance protein 2, in human colorectal carcinomas. Clin Cancer Res 6:2401–2407

Hoffmeyer S, Burk O, von Richter O, Arnold HP, Brockmoller J, Johne A, Cascorbi I, Gerloff T, Roots I, Eichelbaum M, and Brinkmann U (2000) Functional polymorphisms of the human multidrug-resistance gene: multiple sequence variations and correlation of one allele with P-glycoprotein expression and activity in vivo. Proc Natl Acad Sci USA 97:3473–3478

Illmer T, Schuler US, Thiede C, Schwarz UI, Kim RB, Gotthard S, Freund D, Schakel U, Ehninger G, and Schaich M (2002) MDR1 gene polymorphisms affect therapy outcome in acute myeloid leukemia patients. Cancer Res 62:4955–4962

Innocenti F, Undevia SD, Chen PX, Das S, Ramirez J, and Dolan ME (2004a). Pharmacogenetic analysis of interindividual irinotecan (CPT-11) pharmacokinetic (PK) variability: evidence for a functional variant of ABCC2. In Proceedings of ASCO, p. 22 [abstract 2010].

Innocenti F, Undevia SD, Iyer L, Chen PX, Das S, Kocherginsky M, Karrison T, Janisch L, Ramirez J, Rudin CM, Vokes EE, and Ratain MJ (2004b) Genetic variants in the UDP-glucuronosyltransferase 1A1 gene predict the risk of severe neutropenia of irinotecan. J Clin Oncol 22:1382–1388

Isler JA, Vesterqvist OE, and Burczynski ME (2007) Analytical validation of genotyping assays in the biomarker laboratory. Pharmacogenomics 8:353–368

Jin Y, Desta Z, Stearns V, Ward B, Ho H, Lee KH, Skaar T, Storniolo AM, Li L, Araba A, Blanchard R, Nguyen A, Ullmer L, Hayden J, Lemler S, Weinshilboum RM, Rae JM, Hayes DF, and Flockhart DA (2005) CYP2D6 genotype, antidepressant use, and tamoxifen metabolism during adjuvant breast cancer treatment. J Natl Cancer Inst 97:30–39

Kimchi-Sarfaty C, Oh JM, Kim IW, Sauna ZE, Calcagno AM, Ambudkar SV, and Gottesman MM (2007) A "silent" polymorphism in the MDR1 gene changes substrate specificity. Science 315:525–528

Klerk M, Verhoef P, Clarke R, Blom HJ, Kok FJ, and Schouten EG (2002) MTHFR 677C→T polymorphism and risk of coronary heart disease: a meta-analysis. JAMA 288:2023–2031

Laverdiere C, Chiasson S, Costea I, Moghrabi A, and Krajinovic M (2002) Polymorphism G80A in the reduced folate carrier gene and its relationship to methotrexate plasma levels and outcome of childhood acute lymphoblastic leukemia. Blood 100:3832–3834

Leschziner GD, Andrew T, Leach JP, Chadwick D, Coffey AJ, Balding DJ, Bentley DR, Pirmohamed M, and Johnson MR (2007) Common ABCB1 polymorphisms are not associated with multidrug resistance in epilepsy using a gene-wide tagging approach. Pharmacogenet Genomics 17:217–220

Leslie EM, Letourneau IJ, Deeley RG, and Cole SP (2003) Functional and structural consequences of cysteine substitutions in the NH2 proximal region of the human multidrug resistance protein 1 (MRP1/ABCC1). Biochemistry 42:5214–5224

Liu G, Gurubhagavatula S, Zhou W, Wang Z, Yeap BY, Asomaning K, Su L, Heist R, Lynch TJ, and Christiani DC (2007) Epidermal growth factor receptor polymorphisms and clinical outcomes in non-small-cell lung cancer patients treated with gefitinib. Pharmacogenomics J

Lockhart AC, Berlin JD (2005) The epidermal growth factor receptor as a target for colorectal cancer therapy. Semin Oncol 32:52–60

Machida I, Wakusawa S, Sanae F, Hayashi H, Kusakabe A, Ninomiya H, Yano M, and Yoshioka K (2005) Mutational analysis of the MRP2 gene and long-term follow-up of Dubin–Johnson syndrome in Japan. J Gastroenterol 40:366–370

Marcuello E, Altes A, del Rio E, Cesar A, and Menoyo A, Baiget M (2004) Single nucleotide polymorphism in the 5′ tandem repeat sequences

of thymidylate synthase gene predicts for response to fluorouracil-based chemotherapy in advanced colorectal cancer patients. Int J Cancer 112:733–737

Marsh S, McLeod HL (2001) Thymidylate synthase pharmacogenetics in colorectal cancer. Clin Colorectal Cancer 1:175–178; discussion 179–181

Mathijssen RH, Marsh S, Karlsson MO, Xie R, Baker SD, Verweij J, Sparreboom A, and McLeod HL (2003) Irinotecan pathway genotype analysis to predict pharmacokinetics. Clin Cancer Res 9:3246–3253

McLeod HL, Krynetski EY, Relling MV, and Evans WE (2000) Genetic polymorphism of thiopurine methyltransferase and its clinical relevance for childhood acute lymphoblastic leukemia. Leukemia 14:567–572

McLeod HL, Tan B, Malyapa R, Abbey E, Picus J, Myerson R, Zehnbauer B, Mutch M, Dietz D, and Fleshman J (2005) Genotype-guided neoadjuvant therapy for rectal cancer. In: Proceedings of the American Society of Clinical Oncology [Abstract 3024]

Metzger R, Leichman CG, Danenberg KD, Danenberg PV, Lenz HJ, Hayashi K, Groshen S, Salonga D, Cohen H, Laine L, Crookes P, Silberman H, Baranda J, Konda B, and Leichman L (1998) ERCC1 mRNA levels complement thymidylate synthase mRNA levels in predicting response and survival for gastric cancer patients receiving combination cisplatin and fluorouracil chemotherapy. J Clin Oncol 16:309–316

Park DJ, Stoehlmacher J, Zhang W, Tsao-Wei DD, Groshen S, and Lenz HJ (2001) A Xeroderma pigmentosum group D gene polymorphism predicts clinical outcome to platinum-based chemotherapy in patients with advanced colorectal cancer. Cancer Res 61:8654–8658

Park DJ, Zhang W, Stoehlmacher J, Tsao-Wei D, Groshen S, Gil J, Yun J, Sones E, Mallik N, and Lenz HJ (2003) ERCC1 gene polymorphism as a predictor for clinical outcome in advanced colorectal cancer patients treated with platinum-based chemotherapy. Clin Adv Hematol Oncol 1:162–166

Pullarkat ST, Stoehlmacher J, Ghaderi V, Xiong YP, Ingles SA, Sherrod A, Warren R, and Tsao-Wei D, Groshen S, Lenz HJ (2001) Thymidylate synthase gene polymorphism determines response and toxicity of 5-FU chemotherapy. Pharmacogenomics J 1:65–70

Rajendra R, Gounder MK, Saleem A, Schellens JH, Ross DD, Bates SE, Sinko P, and Rubin EH (2003) Differential effects of the breast cancer resistance protein on the cellular accumulation and cytotoxicity of 9-aminocamptothecin and 9-nitrocamptothecin. Cancer Res 63:3228–3233

Relling MV, Hancock ML, Boyett JM, Pui CH, and Evans WE (1999) Prognostic importance of 6-mercaptopurine dose intensity in acute lymphoblastic leukemia. Blood 93:2817–2823

Sai K, Kaniwa N, Itoda M, Saito Y, Hasegawa R, Komamura K, Ueno K, Kamakura S, Kitakaze M, Shirao K, Minami H, Ohtsu A, Yoshida T, Saijo N, Kitamura Y, Kamatani N, Ozawa S, and Sawada J (2003) Haplotype analysis of ABCB1/MDR1 blocks in a Japanese population reveals genotype-dependent renal clearance of irinotecan. Pharmacogenetics 13:741–757

Sargent DJ, Conley BA, Allegra C, and Collette L (2005) Clinical trial designs for predictive marker validation in cancer treatment trials. J Clin Oncol 23:2020–2027

Sharma SV, Bell DW, Settleman J, and Haber DA (2007) Epidermal growth factor receptor mutations in lung cancer. Nat Rev Cancer 7:169–181

Shirota Y, Stoehlmacher J, Brabender J, Xiong YP, Uetake H, Danenberg KD, Groshen S, Tsao-Wei DD, Danenberg PV, and Lenz HJ (2001) ERCC1 and thymidylate synthase mRNA levels predict survival for colorectal cancer patients receiving combination oxaliplatin and fluorouracil chemotherapy. J Clin Oncol 19:4298–4304

Sparreboom A, Loos WJ, Burger H, Sissung TM, Verweij J, Figg WD, Nooter K, and Gelderblom H (2005) Effect of ABCG2 genotype on the oral bioavailability of topotecan. Cancer Biol Ther 4:650–658

Sparreboom A, Marsh S, Mathijssen RH, and Verweij J, McLeod HL (2004) Pharmacogenetics of tipifarnib (R115777) transport and metabolism in cancer patients. Invest New Drugs 22:285–289

Stanulla M, Schaffeler E, Arens S, Rathmann A, Schrauder A, Welte K, Eichelbaum M, Zanger UM, Schrappe M, and Schwab M (2005) GSTP1 and MDR1 genotypes and central nervous system relapse in childhood acute lymphoblastic leukemia. Int J Hematol 81:39–44

Stoehlmacher J, Ghaderi V, Iobal S, Groshen S, Tsao-Wei D, Park D, and Lenz HJ (2001) A polymorphism of the XRCC1 gene predicts for response to platinum based treatment in advanced colorectal cancer. Anticancer Res 21:3075–3079

Stoehlmacher J, Park DJ, Zhang W, Groshen S, Tsao-Wei DD, Yu MC, and Lenz HJ (2002) Association between glutathione S-transferase P1, T1, and M1 genetic polymorphism and survival of patients with metastatic colorectal cancer. J Natl Cancer Inst 94:936–942

Ulrich CM, Yasui Y, Storb R, Schubert MM, Wagner JL, Bigler J, Ariail KS, Keener CL, Li S, Liu H, Farin FM, and Potter JD (2001) Pharmacogenetics of methotrexate: toxicity among marrow transplantation patients varies with the methylenetetrahydrofolate reductase C677T polymorphism. Blood 98:231–234

van Kuilenburg AB, De Abreu RA, and van Gennip AH (2003) Pharmacogenetic and clinical aspects of dihydropyrimidine dehydrogenase deficiency. Ann Clin Biochem 40:41–45

Villafranca E, Okruzhnov Y, Dominguez MA, Garcia-Foncillas J, Azinovic I, Martinez E, Illarramendi JJ, Arias F, Martinez Monge R, Salgado E, Angeletti S, and Brugarolas A (2001) Polymorphisms of the repeated sequences in the enhancer region of the thymidylate synthase gene promoter may predict downstaging after preoperative chemoradiation in rectal cancer. J Clin Oncol 19:1779–1786

Wang D, Johnson AD, Papp AC, Kroetz DL, and Sadee W (2005) Multidrug resistance polypeptide 1 (MDR1, ABCB1) variant 3435C>T affects mRNA stability. Pharmacogenet Genomics 15:693–704

Watson MA, Stewart RK, Smith GB, Massey TE, and Bell DA (1998) Human glutathione S-transferase P1 polymorphisms: relationship to lung tissue enzyme activity and population frequency distribution. Carcinogenesis 19:275–280

Watters JW, McLeod HL (2002) Murine pharmacogenomics: using the mouse to understand the genetics of drug therapy. Pharmacogenomics 3:781–790

Wilson MD, Ruttan CC, Koop BF, and Glickman BW (2001) ERCC1: a comparative genomic perspective. Environ Mol Mutagen 38:209–215

Zamboni WC, Ramanathan RK, McLeod HL, Mani S, Potter DM, Strychor S, Maruca LJ, King CR, Jung LL, Parise RA, Egorin MJ, Davis TA, and Marsh S (2006) Disposition of 9-nitrocamptothecin and its 9-aminocamptothecin metabolite in relation to ABC transporter genotypes. Invest New Drugs 24:393–401

12
Cancer Stem Cells: An Overview

Eiichi Morii and Katsuyuki Aozasa

INTRODUCTION

A tumor is a proliferation of clones of a single cell that ultimately come to comprise heterogeneous cell populations as proliferation progresses and additional genetic abnormalities arise. Under these conditions, the capacity to sustain tumor formation and growth is restricted to a small population of cells with high tumorigenic ability, called cancer stem cells or tumor-initiating cells. Such cells have been identified in various malignancies, including leukemia, and brain, breast, colon, prostate, pancreas, and head and neck cancers. This chapter reviews the concept of cancer stem cells and recent advances in cancer stem cell research.

CANCER STEM CELLS: CONCEPT

Each organ is thought to contain organ- or tissue-specific stem cells. Stem cells are defined by two characteristics: their potential for self-renewal and the production of daughter or progeny cells. Stem cells undergo asymmetric division that produces an exact copy of the stem cell and a daughter cell with developmental potential. Initially, the daughter cells are similar to the parent stem cell, but sequentially they lose their self-renewing potential and differentiate to generate mature cells. The concept that cancer might arise from a rare population of cells with stem cell properties was proposed ~150 years ago (Cohnheim 1867), and tissue-specific stem cells were thought to be the origin of cancer (Pierce 1967). This concept is supported by the observation that only a small population of tumor cells can form the original tumor. When 35 patients were injected with 1 billion of their own tumor cells into the thigh or forearm, only seven of these 35 autotransplants resulted in tumor growth at the injection site (Southam and Brunschwig 1960). When cells from patients with acute myelogenic leukemia were xenotransplanted into severe combined immunodeficient (SCID) mice, only 0.1–1% of the cells had leukemia-initiating activity (Lapidot et al. 1994), indicating that as many as 10^6 tumor cells are required to form a new tumor. These findings were consistent with the results of an in vitro colony-formation assay that showed that cells with colony-forming ability are limited to quite a small

subpopulation of tumor cells (Ruben and Rafferty 1978; Reya et al. 2001). However, these observations using transplantation or colony-formation assays did not strictly demonstrate that tumors are derived from cells with stem cell properties. A major limitation of these studies was the lack of a measurement of the self-renewal potential of cancer stem cells. Recent advances in stem cell biology, including the development of new animal models to measure self-renewal ability and technology for isolating cells with surface markers for putative cancer stem cells, are described.

Many studies of the characteristics of tumor cells, including various oncogenes and tumor suppressor genes, have shown that tumors arise as genetic alterations and that tumors progress from hyperplasia to dysplasia, early cancer, and advanced cancer with metastatic potential. Because the accumulation of mutations necessary for cancer development requires a prolonged period, cancer stem cells or their immediate progenitors may be a plausible target for the initial mutation. In many tissues, including the gastrointestinal tract, blood, and skin, mature cells have a short lifespan and a limited opportunity to accumulate the multiple mutations that are a prerequisite for cancer development. Tissue stem cells with a long lifetime may undergo mutations that deregulate normal self-renewal pathways, and form cancer. Breast cancer developed in women who were exposed to atomic bomb radiation at Hiroshima and Nagasaki ~20 to 30 years after their exposure (Little and Boice 1999). In this case, women exposed to radiation as adolescents were most susceptible to developing breast cancer. This might be due to the large number of stem cells in the mammary glands of adolescents.

ISOLATION OF CANCER STEM CELLS

Recently, animal models that permit the direct assessment of stem cell properties have been developed (Figure. 12.1). The dispersed cells obtained from tumors are isolated with specific surface markers using a cell-sorting machine, and then injected into nonobese diabetic/severe combined immunodeficient (NOD/SCID) mice. Constituent cells in the resulting tumors are analyzed using surface markers, and the self-renewal ability of these cells is compared with that of the initially injected cells. Bonnet and Dick (1997) reported that a small population of leukemic cells retained the ability to transfer leukemia into NOD/SCID mice: the surface phenotype

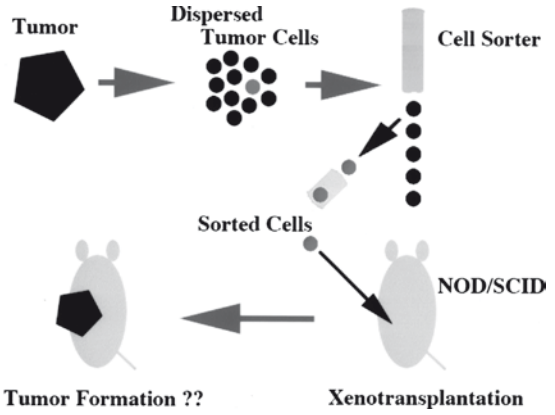

FIGURE 12.1. Scheme for isolation of cancer stem cells. Tumor is dispersed to individual cells by enzymatic or physical treatment. The dispersed tumor cells are labeled with antibodies against various surface markers, and then sorted with cell sorter. The sorted cells are xenotransplanted into NOD/SCID mice, and examined the tumorigenicity of the injected cells. When the tumor is formed by xenotransplantation, the histological and surface marker phenotypes are examined. Furthermore, the resected tumor is again dispersed, sorted, and xenotransplanted to examine the self-renewal ability

of these cells was $CD34^+$ $CD38^-$, which is similar to that of normal hematopoietic stem cells. These cells comprised <1 in 10,000 leukemia cells, and were able to transfer human leukemia into NOD/SCID mice, whereas thousands of times more cells did not possess this phenotype and were non-tumorigenic. Furthermore, the leukemia that developed recapitulated a histologic phenotype similar to that found in the original tumor. More recently, this research group showed that leukemic stem cells, as in the case of normal stem cells, are heterogeneous, with varying degrees of self-renewal potential (Wang et al. 1998). These findings suggest that leukemic stem cells, like their normal counterparts, exist in a hierarchy that is regulated developmentally. The leukemic stem cells possess the stem cell properties of self-renewal and differentiation. The self-renewal potential drives tumorigenesis, whereas differentiation contributes to heterogeneity of the tumor phenotype.

The combination of the isolation of tumor cells with surface markers and xenotransplantation of isolated cells into NOD/SCID mice is a useful method for identifying cancer stem cells in various solid tumors. This method revealed that human breast cancers contain a cancer stem cell population characterized by the surface phenotype $CD44^+$ $CD24^{low}$ (Al-Hajj et al. 2003). As few as 200 $CD44^+$ $CD24^{low}$ cells formed tumors when transplanted into NOD/SCID mice, whereas 20,000 cells that did not express $CD44^+$ $CD24^{low}$ isolated from the same tumor did not form tumors. Furthermore, consistent with the stem cell model, $CD44^+$ $CD24^{low}$ cells generated tumors that recapitulated the phenotypic heterogeneity found in the original tumor.

The existence of cancer stem cells in human brain tumors has been demonstrated (Singh et al. 2004). These cancer stem cells express the neural stem cell markers CD133 and nestin, and as few as 100 of these cells formed tumors when injected intracranially into NOD/SCID mice. By contrast, 10^5 engrafted $CD133^-$ cells did not produce a tumor. The tumors produced by the $CD133^+$ cells recapitulated the phenotypic heterogeneity found in the initial tumor.

Multiple myeloma also possesses a cancer stem cell population (Matsui et al. 2004). Multiple myeloma cells express syndecan-1 (CD138). However, a small subpopulation of cells with the phenotype of postgerminal center B cells, $CD19^+$ $CD20^+$, but $CD138^-$, formed colonies in vitro and tumors in NOD/SCID mice. In addition to these tumors, cancer stem cells have been identified in various tumors, such as prostate and head/neck cancers (Collins et al. 2005; Vescovi et al. 2006; O'Brien et al. 2007; Prince et al. 2007; Li et al. 2007). The surface markers of cancer stem cells reported in the literature are summarized in Table 12.1. These findings suggest similarity of surface markers between normal and cancer stem cells. Besides surface markers, cancer stem cells may share the self-renewing or differentiation mechanism with normal stem cells.

ORIGIN OF CANCER STEM CELLS

The following hypotheses might explain the origin of cancer stem cells (Figure. 12.2): (1) they are derived from normal stem cells with malignant transformation,

TABLE 12.1. Surface markers of normal and cancer stem cells

Organ	Species	Normal stem cell markers	Cancer stem cell markers
Hematopoietic	Human	$CD34^+$ $CD38^-$ $Thy1^-$ Lin^-	$CD34^+$ $CD38^-$ $Thy1^-$ Lin^-
	Mouse	Kit^+ $Thy1^{low}$ $Sca1^+$ Lin^-	
Breast	Mouse	$CD24^{med}$ $CD49f^{hi}$	$CD44^+$ $CD24^{low}$ ESA^+ Lin^-
Brain	Human	$CD133^+$	$CD133^+$
Lung	Mouse	$CD34^+$ $Sca1^+$ Lin^-	$CD34^+$ $Sca1^+$ Lin^-
Skin	Mouse	$CD34^+$ $CD71^{low}$ integrin-$a6^{hi}$	$CD20^+$
Prostate	Human	$CD133^+$ integrin-$a2b1^{hi}$	$CD44^+$ $CD133^+$ integrin-$a2b1^{hi}$
Head/Neck	Human	$CD44^+$ $CD105^+$ $CD166^+$	$CD44^+$

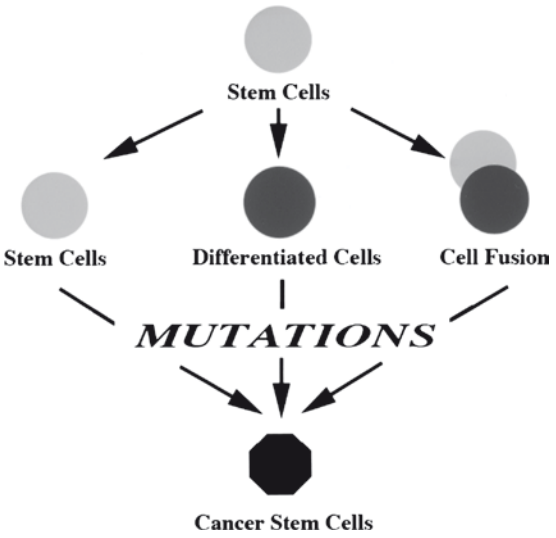

FIGURE 12.2. Scheme of the origin of cancer stem cells. Three hypotheses are presented. (1) The normal stem cells are directly mutated to become cancer stem cells. (2) The differentiated cells derived from stem cells are mutated. (3) The differentiated cells gain self-renewal ability by fusion with stem cells, and the resultant cells are mutated

(2) differentiated cells regain self-renewal ability with malignant transformation, and (3) stem cells fuse with other cells (Figure. 12.2). As described above, multiple gene mutation steps are necessary for recovery of self-renewal ability, and these steps might take a long time. It seems difficult for differentiated cells to regain self-renewal ability because of their short lifespan, and in this respect, the second hypothesis is not plausible. Stem cells are unlikely to be targets for multiple mutations because of their rarity. Therefore, the first speculation is also implausible. A combination of the first and second hypotheses, that is, transient amplifying cells derived from stem cells retain partial self-renewal ability, might explain the origin of cancer stem cells. Several reports support the notion that committed cells, not stem cells but so-called transient amplifying cells, become cancer stem cells. The coexpression of the *bcl-2* and *bcr/abl* genes in committed myeloid progenitors is sufficient to drive leukemia in mice (Jaiswal et al. 2003). The MLL-AF9 fusion protein transforms committed granulocyte-macrophage progenitor cells into leukemic stem cells (Jamieson et al. 2004). Leukemic granulocyte-macrophage progenitors gain self-renewal ability by activation of the Wnt signal cascades. The combined loss of the tumor suppressor genes $p16^{Ink4}$ and $p19^{Arf}$ and constitutive activation of the EGF receptor induce a loss of differentiation in mature brain astrocytes (Bachoo et al. 2002). These cells regain neural stem cell properties and form glioblastomas when injected into

mouse brains. Cancer stem cells can be derived from more differentiated cells that are reprogrammed to express the properties of stem cells.

Cell fusion could be one mechanism for the cellular plasticity associated with tissue stem cells (Wagers and Weissman 2004). However, it is unclear whether stem cells themselves fuse with other cell types in vivo. The fusion of stem cells and mutated cells might recover the self-renewal capacity of the mutated cells, and allow further accumulation of mutations. The fusogenic factor CD44 is one of the surface markers for cancer stem cells in breast cancer, suggesting that these cells have the capacity to fuse with other cells. The three above-mentioned hypotheses may not be mutually exclusive. In some cases, the initial mutation might occur in stem cells. In other cases, it might occur in the transient amplifying cells. Further studies are necessary to identify the origins of cancer stem cells more precisely.

EPIGENETICS AND CANCER STEM CELLS

Although almost all cells in the body possess the same genome, the phenotypes of cells show great diversity. This diversity is regulated epigenetically by activating or silencing the expression of various genes (Reik et al. 2001). Gene silencing is mainly controlled by methylation of cytosine residues in DNA at CpG dinucleotides in gene promoters, and this process is mediated by specific DNA methyltransferases and CpG island-binding proteins. Methylation prevents the binding of certain transcription factors to CpG islands. Demethylation of DNA or histone acetylation induces structural changes in chromatin that activate gene expression during differentiation.

Epigenetic changes are required for the induction of differentiation in stem cells. Embryonic stem cells deficient in either the DNA methyltransferases or the CpG island-binding proteins show severe DNA hypomethylation and complete differentiation block (Jackson et al. 2004). Cancers themselves show hypomethylation. When the DNA methylation level is reduced to 10% of that in normal cells through the introduction of mutations in DNA methyltransferase genes, cancer is more likely to develop in mice (Gaudet et al. 2003). Insulin-like growth factor 2 (IGF2) is reported to promote the growth of colorectal epithelium (Cui et al. 2003). In human colorectal cancers, 30–40% of patients show a loss of DNA methylation in the maternal *IGF2* allele (Cui et al. 1998). Loss of DNA methylation in the maternal allele of *IGF2* in peripheral blood mononuclear cells is found in ~10% of the normal human population, and this population has a five-fold greater risk for developing colorectal cancers (Cui et al. 2003). The impairment of normal methylation of genes such as *IGF2* can lead to elevated levels of IGF2, which affects growth and differentiation and promotes cancer development. Although hypomethylation of the entire genome is seen in most cancer cells, aberrant hypermethylation is often detected in the same genome. Aberrant hypermethylation is also seen in the promoter region of so-called tumor suppressor genes (Jones and Baylin 2002). Combined, typical cancer cells show both hypomethylation and hypermethylation in a mosaic manner. Regardless, epigenetic abnormalities are one of the causes of tumorigenicity.

Most of the genes expressed exclusively in normal stem cells possess CpG islands in their promoter regions. Methylation at their CpG islands appears to silence gene expression during the differentiation process. Cub-domain containing protein 1 (CDCP1) is one such protein (Ikeda et al. 2006). CDCP1 is a transmembrane protein with three extracellular CUB domains, which are important for cell–cell interactions, and intracellular tyrosine residues that are phosphorylated upon activation. CDCP1 was originally identified as an epithelial tumor antigen by comparing lung cancer cell lines and normal lung tissues. CDCP1 is expressed in leukemia, metastatic colon cancer, and breast tumors. In addition, CDCP1 is expressed in hematopoietic stem cells and mesenchymal stem/progenitor cells, but not in differentiated hematopoietic cells. Recently, we found that CDCP1 possesses CpG islands in its promoter region (Ikeda et al. 2006). Comparison of the expression of the *CDCP1* gene and the proportion of methylated CpG sequences revealed an inverse correlation between them. When demethylating reagent is added to CDCP1-negative cell lines, the level of *CDCP1* gene expression is increased dramatically. NT2 cells are derived from human embryonal carcinoma, and become mature when subjected to the action of retinoic acids. In the NT2 differentiation process, the proportion of methylated CpG sequences is increased, while the level of CDCP1 expression is reduced significantly. An inverse correlation between the expression level and methylation status is also found in clinical breast cancer specimens. These data show that epigenetic regulation is a critical mechanism for *CDCP1* gene expression. Furthermore, we found that a zinc-finger transcription factor called zfp67 binds to the promoter region of the *CDCP1* gene when few CpG islands are methylated (Kimura et al. 2006). By contrast, zfp67 does not bind to the promoter region in differentiated hematopoietic cells, such as mature T lymphocytes, monocytes, and granulocytes, in which the CpG islands of the CDCP1 promoter region are heavily methylated. Although the expression of the *CDCP1* gene in cancer stem cells has not been elucidated fully, similar epigenetic regulation in the expression of a stem cell marker gene might be in effect in cancer stem cells.

FUTURE PERSPECTIVES

The isolation of possible cancer stem cells with surface markers has been reported in various types of cancer. However, the biochemical properties of these isolated cancer stem cells have not been studied in detail due to the limited number of cancer stem cells available for research. Recently, Kondo et al. (2004) reported the heterogeneous nature of not only tumor cells but also monoclonal cell lines derived from tumors. For example, the MCF7 breast cancer cell line contains two distinct populations, which stain with Hoechst 33342 dye in different manners: one expels the dye and the other stains with the dye strongly. The former is called the side-population (SP) and the latter non-SP. SP cells give rise to both SP and non-SP cells, and SP cells are tumorigenic in NOD/SCID mice, while non-SP cells are not. After characterizing SP cells in several cell lines, Patrawala et al. (2005) reported that SP cells are more tumorigenic than non-SP cells. Because normal stem cells are SP cells

(Lin and Goodell 2006), it is reasonable to postulate that cancer stem cells are included in this population. Because many cancer stem cells have been isolated from cell lines, their biochemical properties will be elucidated in the future.

Immunohistochemistry is a useful technique for analyzing the properties of a limited number of cells. The presence of $CD44^{+}$ $CD24^{low}$ cells, which are markers of cancer stem cells, was examined in clinical samples of breast cancer, revealing that abundant $CD44^{+}$ $CD24^{low}$ cells in a tumor was a poor prognostic sign (Shipitsin et al. 2007), although another group reported contradictory results (Abraham et al. 2005). In addition, the findings reported for cancer stem cells in solid tumors vary among research groups, and await validation. Further studies are needed to clarify whether the frequency of cancer stem cells among tumor cells correlates with the patient prognosis.

During normal development, the self-renewal of stem cells is regulated by signals from the surrounding microenvironment. This microenvironment is called the stem cell niche. Stem cells residing in the niche are thought to maintain undifferentiated and self-renewal status, whereas stem cells that escape from the niche become transient amplifying cells and start to differentiate. The niche might be necessary for the self-renewal of cancer stem cells. Recently, Calabrese et al. (2007) highlighted the importance of the vascular microenvironment in brain tumor growth, that is, cotransplantation of tumor cells with endothelial cells leads to more rapid tumor formation, suggesting the importance of the vascular niche in tumor formation. Stem cells or progenitors with mutations in the vascular niche might be more likely to give rise to tumors than those outside the niche. Similarly, the finding that disruption of angiogenesis leads to a reduction of fully developed tumors suggests the critical role of the vascular niche in tumor maintenance. Once a tumor is fully-developed, cancer stem cells in the vascular niche may continue to self-renew, while those outside the niche may differentiate. Identification of the signals that regulate the self-renewal of cancer stem cells may shed light on the precise mechanism for the relationship between niche and tumorigenesis. Furthermore, additional information on specific cancer stem cell markers may allow the use of immunohistochemistry to identify the niche for cancer stem cells.

Despite the recent advances in the treatment of cancers, most therapeutic approaches to tumors fail to eradicate the entire population of tumor cells. The cancer cells that survive therapy then recur and metastasize. Stem cells expel chemicals more efficiently than their progeny (Lin and Goodell 2006), and therefore cancer stem cells are thought to be resistant to anti-cancer drugs. In fact, we recently found that the CD55-high population, which contains cancer stem cells belonging to a breast cancer cell line, is resistant to apoptotic stimuli (Xu et al. 2007). Standard anti-cancer drugs readily kill most tumor cells, but not cancer stem cells, and the remaining cancer stem cells may survive and cause recurrence. Therefore, cancer stem cells may be a novel therapeutic target in clinical oncology. To develop efficient therapy against cancer stem cells, it is necessary to identify and characterize the unique features of cancer stem cells that discriminate them from normal stem cells. Recently, loss

of the *PTEN* tumor-suppressor gene was observed in leukemia stem cells, but not in normal hematopoietic stem cells (Yilmaz et al. 2006).

REFERENCES

Abraham BK, Fritz P, McClellan M, Hauptvogel P, Athelogou M, Brauch H (2005) Prevalence of $CD44^{+}/CD24^{-/low}$ cells in breast cancer may not be associated with clinical outcome but may favor distant metastasis. Clin Cancer Res 11:1154–1159

Al-Hajj M, Wicha MS, Benito-Hernandez A, Morrison SJ, Clarke MF (2003) Prospective identification of tumorigenic breast cancer cells. Proc Natl Acad Sci USA 100:3983–3988

Bachoo RM, Maher EA, Ligon KL, Sharpless NE, Chan SS, You MJ, Tang Y, DeFrances J, Stover E, Weissleder R, Rowitch DH, Louis DN, DePinho RA (2002) Epidermal growth factor receptor and Ink4a/Arf: convergent mechanisms governing terminal differentiation and transformation along the neural stem cell to astrocyte axis. Cancer Cell 1:269–277

Bonnet D, Dick JE (1997) Human acute myeloid leukemia is organized as a hierarchy that originates from a primitive hematopoietic cell. Nat Med 3:730–737

Calabrese C, Poppleton H, Kocak M, Hogg TL, Fuller C, Hamner B, Oh EY, Gaber MW, Finklestein D, Allen M, Frank A, Bayazitov IT, Zakharenko SS, Gajjar A, Davidoff A, Gilbertson RJ (2007) A perivascular niche for brain tumor stem cells. Cancer Cell 11:69–82

Cohnheim J (1867) Ueber entzundung und eiterung. Path Anat Physiol Klin Med 40:1–79

Collins AT, Berry PA, Hyde C, Stower MJ, Maitland NJ (2005) Prospective identification of tumorigenic prostate cancer stem cells. Cancer Res 65:10946–10951

Cui H, Horon IL, Ohlsson R, Hamilton SR, Feinberg AP (1998) Loss of imprinting in normal tissue of colorectal cancer patients with microsatellite instability. Nat Med 4:1276–1280

Cui H, Cruz-Correa M, Giardiello FM, Hutcheon DF, Kafonek DR, Brandenburg S, Wu Y, He X, Powe NR, Feinberg AP (2003) Loss of IGF2 imprinting: a potential marker of colorectal cancer risk. Science 299:1753–1755

Gaudet F, Hodgson JG, Eden A, Jackson-Grusby L, Dausman J, Gray JW, Leonhardt H, Jaenisch R (2003) Induction of tumors in mice by genomic hypomethylation. Science 300:489–492

Ikeda JI, Morii E, Kimura H, Tomita Y, Takakuwa T, Hasegawa J, Kim YK, Miyoshi Y, Noguchi S, Nishida T, Aozasa K (2006) Epigenetic regulation of the expression of the novel stem cell marker CDCP1 in cancer cells. J Pathol 210:75–84

Jackson M, Krassowska A, Gilbert N, Chevassut T, Forrester L, Ansell J, Ramsahoye B (2004) Severe global DNA hypomethylation blocks differentiation and induces histone hyperacetylation in embryonic stem cells. Mol Cell Biol 24:8862–8871

Jaiswal S, Traver D, Miyamoto T, Akashi K, Lagasse E, Weissman IL (2003) Expression of BCR/ABL and BCL-2 in myeloid progenitors leads to myeloid leukemias. Proc Natl Acad Sci USA 100:10002–10007

Jamieson CH, Ailles LE, Dylla SJ, Muijtjens M, Jones C, Zehnder JL, Gotlib J, Li K, Manz MG, Keating A, Sawyers CL, Weissman IL (2004) Granulocyte-macrophage progenitors as candidate leukemic stem cells in blast-crisis CML. N Engl J Med 351:657–667

Jones PA, Baylin B (2002) The fundamental role of epigenetic events in cancer. Nat Rev 3:415–428

Kimura H, Morii E, Ikeda J, Ezoe S, Xu JX, Nakamichi N, Tomita Y, Shibayama H, Kanakura Y, Aozasa K (2006) Role of DNA methylation for expression of novel stem cell marker CDCP1 in hematopoietic cells. Leukemia 20:1551–1556

Kondo T, Setoguchi T, Taga T (2004) Persistence of a small subpopulation of cancer stem-like cells in the C6 glioma cell line. Proc Natl Acad Sci USA 101:781–786

Lapidot T, Sirard C, Vormoor J, Murdoch B, Hoang T, Caceres-Cortes J, Minden M, Paterson B, Caligiuri MA, Dick JE (1994) A cell initiating human acute myeloid leukaemia after transplantation into SCID mice. Nature 367:645–648

Li C, Heidt DG, Dalerba P, Burant CF, Zhang L, Adsay V, Wicha M, Clarke MF, Simeone DM (2007) Identification of pancreatic cancer stem cells. Cancer Res 67:1030–1037

Little MP, Boice JD Jr (1999) Comparison of breast cancer incidence in the Massachusetts tuberculosis fluoroscopy cohort and in the

Japanese atomic bomb survivors. Radiat Res 151:218–224

Lin KK, Goodell MA (2006) Purification of hematopoietic stem cells using the side population. Methods Enzymol 420:255–264

Matsui W, Huff CA, Wang Q, Malehorn MT, Barber J, Tanhehco Y, Smith BD, Civin CI, Jones RJ (2004) Characterization of clonogenic multiple myeloma cells. Blood 103:2332–2336

O'Brien CA, Pollett A, Gallinger S, Dick JE (2007) A human colon cancer cell capable of initiating tumor growth in immunodeficient mice. Nature 445:106–110

Patrawala L, Calhoun T, Schneider-Broussard R, Zhou J, Claypool K, Tang DG (2005) Side population is enriched in tumorigenic, stem-like cancer cells, whereas $ABCG2^{+}$ and $ABCG2^{-}$ cancer cells are similarly tumorigenic. Cancer Res 65:6207–6219

Pierce GB (1967) Teratocarcinoma: model for a developmental concept of cancer. Curr Top Dev Biol 2:223–246

Prince ME, Sivanandan R, Kaczorowski A, Wolf GT, Kaplan MJ, Dalerba P, Weissman IL, Clarke MF, Ailles LE (2007) Identification of a subpopulation of cells with cancer stem cell properties in head and neck squamous cell carcinoma. Proc Natl Acad Sci USA 104:973–978

Reik W, Dean W, Walter J (2001) Epigenetic reprogramming in mammalian development. Science 293:1089–1093

Reya T, Morrison SJ, Clarke MF, Weissman IL (2001) Stem cells, cancer, and cancer stem cells. Nature 414:105–111

Ruben RL, Rafferty KA (1978) Colony formation by simian virus 40-transformed human parapharyngeal cells cultured in semisolid agar. J Natl Cancer Inst 61:993–1000

Shipitsin M, Campbell LL, Argani P, Weremowicz S, Bloushtain-Qimron N, Yao J, Nikolskaya T, Serebryiskaya T, Beroukhim R, Hu M, Halushka MK, Sukumar S, Parker LM, Anderson KS, Harris LN, Garber JE, Richardson AL, Schnitt SJ, Nikolsky Y, Gelman RS, Polyak K (2007) Molecular definition of breast tumor heterogeneity. Cancer Cell 11:259–273

Singh SK, Clarke ID, Hide T, Dirks PB (2004) Cancer stem cells in nervous system tumors. Oncogene 23:7267–7273

Southam CM, Brunschwig A (1960) Quantitative studies of autotransplantation of human cancer. Cancer 14:971–978

Vescovi AL, Galli R, Reynolds BA (2006) Brain tumour stem cells. Nat Rev Cancer 6:425–436

Wagers AJ, Weissman IL (2004) Plasticity of adult stem cells. Cell 116:639–648

Wang JC, Lapidot T, Cashman JD, Doedens M, Addy L, Sutherland DR, Nayar R, Laraya P, Minden M, Keating A, Eaves AC, Eaves CJ, Dick JE (1998) High level engraftment of NOD/SCID mice by primitive normal and leukemic hematopoietic cells from patients with chronic myeloid leukemia in chronic phase. Blood 91:2406–2414

Xu JX, Morii E, Liu Y, Nakamichi N, Ikeda J, Kimura H, Aozasa K (2007) High tolerance to apoptotic stimuli induced by serum depletion and ceramide in side-population cells: high expression of CD55 as a novel character for side-population. Exp Cell Res 313:1877–1885

Yilmaz OH, Valdez R, Theisen BK, Guo W, Ferguson DO, Wu H, Morrison SJ (2006) PTEN dependence distinguishes hematopoietic stem cells from leukemia-initiating cells. Nature 441:475–482

13
Translating In Vitro Cell Lines Result into Clinical Practice

Jai Prakash Mehta, Lorraine O'Driscoll, Niall Barron, Martin Clynes, and Padraig Doolan

INTRODUCTION

Immortalized cell lines provide an easy and convenient option for analysis of biological systems compared to clinical specimens. Cell culture has gained wide popularity in the study of cancer, because of the innate continuously proliferating nature of these cell lines. Cancer cell lines are obtained by the enzymatic digestion or explant growth of tumour specimens. The main advantage of using cell lines for such research is the immortal nature of the cell lines, enabling them to be continuously cultured, distributed and studied in many labs and to act as a reliable platform for comparison of results, before advancing research to the next level. Another advantage of performing research on cell lines is ease of handling and storage. Cell lines are cultured in flasks under well-controlled nutritional and environmentalal conditions and this ensures a greater degree of reproducibility in the results. Some assays require large amount of material; with cell line models, this is generally not a constraint. Cells can be stored indefinitely in liquid nitrogen and can be used when needed. Apart from the ease in maintenance and access, cell lines offer a convenient platform for genetic manipulation of cells. Many recent studies in cancer have centered on functional aspects of gene expression changes. Cell lines offer a realistic platform to knock-down or over-express genes of interest. Due to the tremendous benefits of working on cell lines, they have dramatically contributed to basic research in cancer biology.

Recent interest has focused on extrapolating the relevance of findings from cell line models to clinical models. There are obvious differences between cell line models and clinical specimens due to the difference in environments to which they have been exposed. These differences need to be accurately defined for the results arising from the cell line studies to be clinically relevant. A detailed study on these differences will help researchers to decide on the applicability of cell line models for their particular study and will pave the way in making the results more accurate and relevant to that of clinical condition. This manuscript examines the differences between cell line models and clinical specimens, particularly focusing on breast cancer.

HOW CELL LINES ARE GENERATED

Enzymatic digestion: Tumour tissue is digested using enzymes such as collagenase, trypsin, or pronase. These enzymes break down the extracellular matrix, thereby releasing the cells which are subsequently cultured in nutrient rich medium and in a controlled environment (Doyle et al. 1998).

Explant culture: Small pieces of tissue are placed in nutrient rich medium and the cells that grow out and migrate from the primary tissue are further cultured (Doyle et al. 1998).

TYPES OF CELL CULTURE

Primary cultures: Cells obtained directly from the tissue are termed primary cultures. Primary cultures have a defined life span and undergo a process of senescence and stop dividing, while remaining viable for short time period. Studies done on primary cultures can be very useful as these cells have not been in culture for long time after procuring from the body/in vivo condition. However, primary culture has its own limitations. Since primary cultures cannot be maintained in culture for extended periods, lengthy experiments may be challenging; these cells generally cannot be distributed to other labs; and the experiments performed cannot be repeated at a later date to determine reproducibility. Many assays which require large numbers of cells cannot be performed on them.

Immortalized cell lines: These are the cells obtained from primary cultures which have attained a capability to proliferate indefinitely, due to mutations or artificial modifications. The focus of this manuscript is to compare these immortalized cell lines as models for clinical conditions.

SELECTION BIAS

The first criterion for any cell line as a useful and efficient model is unbiased representation of the corresponding clinical specimens. This would not be a problem, if cell lines could be made from any clinical specimen. This is of particular importance in breast cancer, where clinical diversity is very high, with patients being identified in various groups and sub-groups, such as basal like, ERBB2+, normal breast like, luminal subtype A, luminal subtype B and luminal subtype C (Sørlie et al. 2001). Most of the breast cancer cell lines which have been widely used in research were developed in the late 1970s. Many of these cell lines were obtained from the metastatic site rather than the primary site and were from aspirates or pleural effusions, rather than from the tumour (Burdall et al. 2003). Other common aspects to these cell lines are that most have been obtained from Estrogen- and Progesterone-receptor-negative patients with a high grade of tumour; they were aneoploid and exhibited a moderate to poorly differentiated phenotype, and they over-expressed p53 and HER-2/neu proteins (Gazdar et al. 1998). Research findings on such cell lines may be relevant to more advanced cancer, which has undergone metastasis, rather than less advanced disease, which may be still confined to tissue of origin. With the advancement in diagnosis and better awareness of the disease, most of the newly diagnosed patients are of early stage cancer and therefore research findings on metastatic cell lines may be of less relevance.

One way to overcome this problem would be to use a more diverse range of cell lines and include recently developed cell lines which have been isolated from primary sites rather than the metastasis site. For example, Gazdar et al. (1998) established a number of cell lines (HCC series) from primary tumours, together with their paired normal cell lines which may be useful for developing a better understanding of early stage breast cancer. These cell lines can be obtained from public repositories, such as ATCC (www.atcc.org).

SELECTION PRESSURE

Cell lines are typically grown in flasks and the nutrients are obtained from the medium. These cells are grown in incubators at 37°C. When there are sufficient numbers of cells, the cells are removed from the flask using trypsin and seeded to a new flask at a much lower density and allowed to grow. This process is termed "passaging" and typically the cells are identified by their name and passage number. It is quite common to find researchers working with cells with high passage number especially for very common and old cell lines, such as MCF-7. Every passage adds to a week of cell growth and selection advantage on highly proliferating cells. So, if a cell line is at passage 100, with an average time of 1 week between passages, the cells had been in culture for more than 700 days (nearly 2 years). During the process of growth, there is very likely to be a constant selection advantage on the highly proliferating cells. Thus with time, it is possible that the slowly proliferating cells are lost from the culture and replaced with highly proliferating cells. In this way, a population of highly heterogeneous cells will be reduced to a mere limited collection of highly proliferating cells, no longer representative of the primary tumour.

Several previous studies have shown that chemotherapeutic drugs are more toxic to the cell lines than to their corresponding tumours (reviewed in Szakács and Gottesman 2004). There is much more diversity in the drug sensitivity profiles of tumours compared to cell lines. These differences may be, at least in part attributed to very high rate of proliferation in cell line models compared to that of tumours (Stein et al. 2004). Another very prominent aspect in solid tumours is the cell–cell adhesion which inhibits the distribution of chemotherapeutic drugs; thereby making them less effective (Stein et al. 2004; Trédan et al. 2007). Considering these issues, drug toxicity assays optimized for highly proliferating cells may be relevant for in vitro models, but may not accurately reflect tumour sensitivity in vivo.

A partial solution to this problem lies in better management practices. The aim should be to reduce the number of times that cells are passaged and to avoid low seeding densities. Individual labs should maintain their own frozen stocks and ensure that they are not culturing the cells for long periods of time before freezing. People working in such labs should ensure that they always get their cell stock from the master stock, rather than "borrowing" from the co-workers. Day-to-day cell culturing should be kept to a minimum and researchers should revert to frozen stocks of low passage cells as frequently as possible. The aim of all these management practices should be to keep the passage number as low as possible, thereby decreasing the selection advantage to the highly proliferating cells.

Another alternative is to work on primary cell cultures. Primary cultures (as explained above) are cells which have not been immortalized and still are close in characteristics to the tumours from which they have been developed. Cells in primary cultures often cease to grow after a certain number of cycles. The results obtained from these primary cultures should be more relevant to the clinical settings as they have not been cultured for long periods of time. However, because of the limited life span and lack of access to primary tissue, this may be impractical for many types of studies.

CELL LINE PREFERENCE AND AVAILABILITY

Another aspect to consider is the availability of large numbers of cell lines. Due to the difficulty in establishing cell lines from tumours, the number of cell lines available for research is obviously more limited than the actual number of presenting tumours. The number of breast cancer cell lines identified at ATCC (www.atcc.org) using key words "Organism: Human" and "Source: Breast", reports 100 available breast cell lines as of 20th November 2007. Considering the diversity associated with the disease, the number of cell lines available may be too small to represent the wide spectrum of this disease (Lacroix and Leclercq 2004). Much of the breast cancer research reported is heavily biased towards a small number of the available cell lines. A total of 68 breast cancer cell lines were individually searched in the Pubmed for their citation frequency. The results show that most research in this field is performed on a select few of these cell lines; MCF-7 has the biggest share (58%) followed by MDA-MB-231 (15%), T47D (8%), MDA-MB-435 (3.7%) (Figure. 13.1).

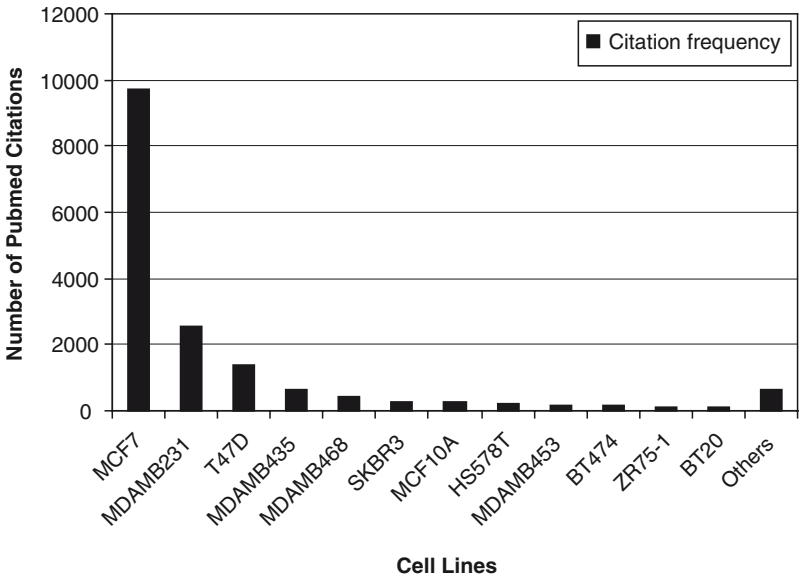

FIGURE 13.1. Pubmed citation frequency for breast cancer cell line studies (as on 12-10-2007). A total of 68 breast cancer cells were estimated for citation frequency, and only few were found to be routinely analyzed and contribute significantly to breast cancer research

One of the most common sub-groups of breast cancer tumours is the Estrogen Receptor-positive tumours. This cancer type is generally responsive to estrogen and anti-estrogens are the drugs of choice for its treatment. However, when we investigate the citation frequency of breast cancer cell lines, much of our understanding on estrogen receptor metabolism is limited to two cell lines (i.e. MCF-7 and T47D).

As every cancer is different, results derived from 1 or 2 cell lines cannot be taken as a representative result. There is an urgent need for more cell lines to be introduced into these studies. Including large numbers of cell lines in each study may be very demanding on resources of the lab, but should add to the value of the results.

In this regard, experiments designed to model clinical sub-groups such as HER-2 over-expression or BRCA1 and BRCA2 mutations suffer from a dearth of suitable cell line models. In theory, one way to overcome this problem would be to culture every patient tumour for cell line generation. The convincing point for patients would be the potential benefit if a better understanding of the tumours is developed; in terms of toxicity assays as well as genomic and/or proteomic parameters which may eventually be useful for the post-operative treatment and also will be valuable in the event of relapse. This may also generate a large amount of information from the analysis of primary cell culture, which should be more representative of the tumours (Masters 2000).

CROSS-CONTAMINATION

A significant problem identified with long-term cell culturing is the potential source of contamination by other cell lines. Contamination by foreign cell lines is considered to be rampant across most cell culture labs (Lacroix 2008). In a study by MacLeod et al. (1999), 45/252 (18%) cell lines tested were found to be contaminated by cells of foreign origin. Of the 93 cell lines from the original investigators, 27 were found to be cross-contaminated. Almost all of the contaminants (42/45) were intraspecies, mainly by the long established cell lines. HeLa cell line, which was developed in 1952, has been identified to be the most frequent contaminant in commonly used cell lines (Nelson-Rees et al. 1981). Unfortunately, once the contamination occurs, it is maintained in all further passaging. If the contaminant cell line has a higher multiplication rate, the contaminant might become the main cell type in the culture. This problem may remain un-noticed unless elaborate tests are routinely carried out to identify any such contamination. Some of the tests that can be carried out to accurately identify these contaminants are enzyme polymorphism, HLA typing, karyotyping and DNA fingerprinting. Masters et al. (2001) describes a technique termed "Short Tandem Repeat" (STR) profiling which is inexpensive and which may be used to accurately identify the authenticity of the cell lines and to identify possible contaminants.

MICROBIAL CONTAMINATION

Mycoplasma is another source of contamination, which has been estimated to contaminate some 15–35% of all cell lines (Hay et al. 1989). It normally goes unnoticed and alters the properties of the cells. It is highly infectious and in a short time can contaminate many cell populations. There are a range of screening techniques

available such as PCR based assays and indicator cell assays that can be applied to investigate the presence of *Mycoplasma*. Cell culture labs should routinely perform these tests to rule out any *Mycoplasma* contamination.

In addition to this, bacterial contamination has been found to exist at low concentrations and go unnoticed for a long time. It is of particular importance that labs which routinely use antibiotics for their cell culture are aware of this. Due to the presence of antibiotics, the resistant bacteria keep growing with the cells at a very low concentration and may alter the obtained experimental results. Antibiotics should be replaced with good management practices to rule out such problems.

Viruses are other potential contaminants which may alter the results. Unfortunately, there are no easy ways to detect viral contaminants in cell lines. However, cell line banks should carry out these tests before distributing the cells. The German Collection of Microorganism and Cell culture screens all human cell lines for some of the frequently occurring viruses (Masters 2000).

HANDLING ERRORS

Due to the long-term culturing of cell lines, there is an increased likelihood of creating variants of the original population, not only due to genetic and phenotypic drift, but also due to handling issues. The same cell lines are grown under different conditions in different labs. This leads to selection of different sub-populations from the original population, leading to inconsistency among the various labs. Osborne et al. (1987) demonstrated differences in the MCF-7 breast cancer cell lines obtained from different labs. These differences were observed in terms of proliferation, hormone receptor content, karyotype and clonogenicity. Karyotypic variation was also observed by Bahia et al. (2002) between independently-cultured strains of MCF-7 cell lines in different labs.

Labeling error is another common form of error, which may occur during long culturing periods. The obvious solution is good laboratory practices and to identify the authenticity of the cell lines using the various techniques described above.

NEW INSIGHTS: MICROARRAY GENE-EXPRESSION PROFILING OF TUMOURS AND CELL LINES

High-throughput screening methodologies such as microarrays have promised to revolutionize the profiling of cell lines and clinical samples. With microarray technology, it is now possible to quantify the gene expression levels of all possible genes in a single experiment. The ever-increasing numbers of gene expression profiles of clinical specimens and cell lines in public repositories such as Gene Expression Omnibus (GEO) www.ncbi.nlm.nih.gov/geo and Array Express www.ebi.ac.uk/arrayexpress have paved the way towards cell line and clinical specimen comparison at the transcript level a reality.

Clustering is the commonest procedure in microarray data analysis to group samples with similar expression profiles (Eisen et al. 1998). Hierarchical Clustering groups the samples based on their similarity and outputs the result as a tree structure, where the adjacent nodes are more similar than nodes

that are distant from each other. Clustering analysis on gene expression profiles of clinical samples and cell lines separate them as two different groups (Mehta et al. 2007; Ertel et al. 2006; Dairkee et al. 2004; Ross and Perou 2001). Principal component analysis (PCA) is another technique to group samples with similar expression profiles. This analysis projects the data in reduced dimensions (3-D or 2-D) where it becomes possible to draw conclusions on the similarity of samples (Raychaudhuri et al. 2000). PCA analysis was carried out by this group (Mehta et al. 2007) to demonstrate that cell lines and clinical samples are very different. In a similar analysis, Sandberg and Ernberg (2005) used Singular value decomposition (SVD) and showed that irrespective of the tumour of origin, the cell lines clustered separately. Thus, there is sufficient evidence to conclude that there is a large degree of difference in the gene expression profiles of cell lines and clinical samples.

Most of the studies comparing the gene expression profiles of cancer specimens and cell lines have identified genes related to proliferation and cell cycle to be highly up-regulated in cell lines, compared to the clinical conditions (Mehta et al. 2007; Ertel et al. 2006; Sandberg and Ernberg 2005; Dairkee et al. 2004). This seems logical, as cell lines in culture have an unlimited supply of nutrients and space to grow and the conditions are favorable to highly proliferating cells. Other important functions and pathways up-regulated in clinical conditions are ATP synthesis, one carbon pool by folate, oxidative phosphorylation, proteasome, purine metabolism, pyrimidine metabolism, ribosome, RNA polymerase (Ertel et al. 2006), as well as macromolecule processing and turnover and energy metabolism (Sandberg and Ernberg 2005).

Conversely, functions and pathways up-regulated in clinical conditions compared to cell lines include Immune response, Defence response, Complement activation classical, Complement and coagulation cascade, Matrix metalloproteinases (Mehta et al. 2007), cell communication, cell adhesion molecules (CAMs), ECM-receptor interaction (Ertel et al. 2006) and CAMs and signaling proteins (Sandberg and Ernberg 2005).

CONCLUSIONS

Despite the fact that cell lines are established from clinical tissue, the true representative nature of these cells remains a matter of debate. This review outlines the marked differences between cell lines and clinical conditions. Due to the obvious advantage and opportunity for manipulation, cell lines will continue to provide valuable information about cancer biology and the functional relevance of genes and proteins. To make findings more relevant, an awareness of the differences should be more widespread among cell culture labs. This will not only help encourage better management practices by individual labs, but it will also ensure that due consideration is given to the translational aspect of research conducted on cell lines. There is also an urgent need for a greater number of cell lines to be established, which should include those from less invasive and early stage disease and also from different groups and sub-groups of disease. Furthermore, wherever possible, the resulting immortalized cell lines should be complemented with results from primary culture and/or relevant animal models.

REFERENCES

Bahia H, Ashman JN, Cawkwell L, Lind M, Monson JR, Drew PJ, and Greenman J (2002) Karyotypic variation between independently cultured strains of the cell line MCF-7 identified by multicolour fluorescence in situ hybridization. Int J Oncol 20(3):489–494

Burdall SE, Hanby AM, Lansdown MRJ, and Speirs V (2003) Breast cancer cell lines: friend or foe? Breast Cancer Res 5:89–95

Dairkee SH, Ji Y, Ben Y, Moore DH, Meng Z, and Jeffrey SS (2004) A molecular signature of primary breast cancer cultures; patterns resembling tumour tissue. BMC Genomics . doi:10.1186/1471-2164-5-47

Doyle A, Griffiths JB, and Newell DG (1998) Basic techniques for primary cell culture and establishment of continuous culture. Cell & tissue culture laboratory procedures. Wiley, New York, pp 3A–3E

Eisen MB, Spellman PT, Brown PO, and Botstein D (1998) Cluster analysis and display of genome-wide expression patterns. Proc Natl Acad Sci U S A 95(25):14863–14868

Ertel A, Verghese A, Byers SW, Ochs M, and Tozeren A (2006) Pathways-specific differences between tumour cell lines and normal and tumour tissue cells. Mol Cancer . doi:10.1186/1476-4598-5-55

Gazdar AF, Kurvari V, Virmani A, Gollahon L, Sakaguchi M, Westerfield M, Kodagoda D, Stasny V, Cunningham HT, Wistuba II, Tomlinson G, Tonk V, Ashfaq R, Leitch AM, Minna JD, and Shay JW (1998) Characterization of paired tumour and non-tumour cell lines established from patients with breast cancer. Int J Cancer 78(6):766–774

Hay RJ, Macy ML, and Chen TR (1989) Mycoplasma infection of cultured cells. Nature 340(6232):352

Lacroix M (2008) Persistent use of false cell lines. Int J Cancer 122:1–4

Lacroix M, Leclercq G (2004) Relevance of breast cancer cell lines as models for breast tumours: an update. Breast Cancer Res Treat 83(3):249–289

MacLeod RA, Dirks WG, Matsuo Y, Kaufmann M, Milch H, and Drexler HG (1999) Widespread intraspecies cross-contamination of human tumor cell lines arising at source. Int J Cancer 83(4):555–563

Masters JR, Thomson JA, Daly-Burns B, Reid YA, Dirks WG, Packer P, Toji LH, Ohno T, Tanabe H, Arlett CF, Kelland LR, Harrison M, Virmani A, Ward TH, Ayres KL, and Debenham PG (2001) Short tandem repeat profiling provides an international reference standard for human cell lines. Proc Natl Acad Sci U S A 98(14):7656–7658

Masters JR (2000) Human cancer cell lines: fact and fantasy. Nat Rev Mol Cell Biol 1(3):233–236

Mehta JP, O'Driscoll L, Barron N, Clynes M, and Doolan P (2007) A microarray approach to translational medicine in breast cancer: how representative are cell line models of clinical conditions? Anticancer Res 27(3A):1295–1300

Nelson-Rees WA, Daniels DW, and Flandermeyer RR (1981) Cross-contamination of cells in culture. Science 212(4493):446–452

Osborne CK, Hobbs K, and Trent JM (1987) Biological differences among MCF-7 human breast cancer cell lines from different laboratories. Breast Cancer Res Treat 9(2):111–121

Raychaudhuri S, Joshua M, Stuart JM, and Altman RB (2000) Principal component analysis to summarize microarray experiments: application to sporulation time series. Pac Symp Biocomput 5:452–463

Ross DT, Perou CM (2001) A comparison of gene expression signatures from breast tumours and breast tissue derived cell lines. Dis Markers 17(2):99–109

Sandberg R, Ernberg I (2005) The molecular portrait of in vitro growth by meta-analysis of gene-expression profiles. Genome Biol 6(8):R65

Sørlie T, Perou CM, Tibshirani R, Aas T, Geisler S, Johnsen H, Hastie T, Eisen MB, van de Rijn M, Jeffrey SS, Thorsen T, Quist H, Matese JC, Brown PO, Botstein D, Eystein Lønning P, and Børresen-Dale AL (September 11, 2001) Gene expression patterns of breast carcinomas distinguish tumor subclasses with clinical implications. Proc Natl Acad Sci U S A 98(19): 10869–10874

Stein WD, Litman T, Fojo T, and Bates SE (April 15, 2004) A Serial Analysis of Gene Expression

(SAGE) database analysis of chemosensitivity: comparing solid tumors with cell lines and comparing solid tumors from different tissue origins. Cancer Res 64(8):2805–2816

Szakács G, Gottesman MM (2004) Comparing solid tumours with cell lines: implications for identifying drug resistance genes in cancer. Mol Interv 4(6):323–325

Trédan O, Galmarini CM, Patel K, and Tannock IF (October 3, 2007) Drug resistance and the solid tumor microenvironment. J Natl Cancer Inst 99(19):1441–1454

Prognosis

14
Classification of Cancer Stage Using Patient's Immune System

P. Pellegrini, I. Contasta, A.M. Berghella, T. Del Beato, and D. Adorno

INTRODUCTION

In cancer research, as Jarnicki et al. (2006) and Benzoni et al. (2007) have shown, surgery continues to be the main treatment option though irradiation and chemotherapy have become increasingly important and may, in certain cases, improve the cure rate produced by surgery. The need for accurate staging, however, prior to any treatment planning has become increasingly important in a wide variety of malignancies (Vlastos and Verkooijen 2007; Warburton et al. 2007). The detection of widespread metastatic disease in patients and the need for accurate staging before therapy has been long recognized (Skeel 1992), and there is a strong case for restaging cancer after a number of cycles of chemotherapy to determine if continued chemotherapy is required. Staging during an operative procedure is also vitally important to spare the patient the possible morbidity and mortality associated with hazardous procedures. No single staging system is universally employed for all cancers but one of the most commonly used is the pTNM classification system, devised by the American Joint Committee on Cancer et al. (1992), and based on the examination of a surgically resected specimen. This classification takes into consideration the size of the primary tumour (T), the presence and extent of regional node metastases (N), and the presence of distant metastases (M). However it is an invasive method of classification as it is based on the examination of a surgically resected specimen. Many researchers have found that tumor establishment and progression are generally allowed through a malfunction of the immune response (Jarnicki et al. 2006; Berghella et al. 2006; Contasta et al. 2006; Pellegrini et al. 2006). Hence, it is our opinion that a noninvasive method of identifying disease stage could lie with the study of immunological blood parameters.

CLASSIFICATION SYSTEM FOR CANCER STAGE

Several studies have shown that specific cytokines alter the physiological functionality of TH1, TH2, TH3, and TH17 subsets of $CD4^+$ T Helper (TH) cells in cancer (Liu et al. 2007; Jarnicki et al. 2006). Other studies underline the direct role of immunological disregulation in the

mechanisms that allow tumors to locate and expand within the host (Berghella et al. 2006; Contasta et al. 2006). These immunological alterations increase with stage progression, and therefore the network study of TH1/TH2/TH3/TH17 type cytokines (produced by the respective TH cells) is a logical step in establishing a means of classifying stage; additionally, this type of study could also provide important indications for in vivo treatment to correct the imbalance within the immune system.

TH1/TH2/TH3/TH17 CYTOKINE PHYSIOLOGICAL NETWORK IN PERIPHERAL BLOOD SAMPLES

Cytokines are the most important class of immune response mediators. The network of peripheral blood TH1/TH2/TH3/TH17 cytokines, which is believed to control the polarization of TH cells into TH1, TH2, TH3 or TH17 types, needs to be studied carefully as disturbances in this network can result in disease. It is now widely recognized that viruses and other disease carriers can endanger the homeostasis of the immune system by altering the pathways involved in the production of the above-mentioned cytokines creating an imbalance between TH1/TH2/TH3/TH17 cytokine network level relationships and functions. This, in turn, causes imbalance in the immune system determining the ongoing pathological conditions, as tumors. The study of the relationships and levels of peripheral blood TH1/TH2/TH3/TH17 cytokine networks in healthy subjects helps us understand how the normal physiological network of cytokines regulates TH-type cell polarization, and hence the type of immune response. A comparative study with groups of cancer patients, on the other hand, allows the identification of the immunological alterations within the mechanisms that regulate the different phases of the immune response in cancer development and stage progression. The goal of the comparative study is to identify markers and explain prognostic and diagnostic indices to establish an immunological method for disease prevention program and clinical stage monitoring.

TH1/TH2/TH3/HT17 Cytokine Network: Immuno System

TH1/ TH2-Type Immune Responses and the Regulating Role of the TH3-Type

For more then 35 years immunologists have classified the immune response into type 1 (TH1) which provides cell-mediated immune response, and type 2 (TH2) which supports B helper function and the humoral immune response. Cher and Mosmann (1987) reported that these responses are regulated by the TH1 and TH2 subsets of CD4+ TH cells, respectively. Although both subsets produce Interleukin (IL) 3, granulocyte monocyte colony stimulator factor (GMCSF) and tumor necrosis factor (TNF) α, only TH1 cells produce IL2, Interferon (IFN)γ, whilst TH2 cells produce other cytokines, such as IL4, IL5, IL6, and IL10 (Stevens et al. 1988). Mosmann et al. (1991) also reported that the polarization of the immune response into TH1 or TH2 cell-types is not absolute, and the ratio of these cells varies according to physiological demand and clinical conditions. During the last 30 years, research

on cytokine networks has shown that: (1) each cytokine plays a specific and crucial role in maintaining the balance within the cytokine network, which is responsible for the normal development of T cells into TH1, or TH2 cells, and hence for a normal immune response. Pathological conditions were found to arise from alterations in normal cytokine levels and relationships within the network of the cell environment; (2) the relative proportion of each TH cell-type depends on the concentration of individual cytokines present in the cell environment during resting and activation states of the immune response. The phenotypical TH-type of cells can be determined by evaluating the TH-types of cytokines that are produced by the cells. For example, IFNγ induces the proliferation of TH1 cells, while IL4 was shown to be essential for the development of TH2 cells and to inhibit the differentiation of precursors into TH1 cells. IL10 is an important physiological regulator of inflammatory and immune responses, and its in vivo production is associated with TH2-like responses. IL10 is a more powerful inhibitor of IFNγ, macrophages and TH1 functions than IL4 and so is produced when its inhibiting activities favor physiological homeostasis (Bradley et al. 1995). Furthermore, Fossa et al. (1995) reported that alterations in IL10 levels cause an imbalance in the cytokine network, which can have profound pathological consequences. Additionally, Kalinski et al. (2001) reported that IL12p40, a homodimer, also promotes TH2 immunity by acting as an IL12 antagonist, while IL12p70, a heterodimer, is a major TH1/driving cytokine promoting cell-mediated immunity. An additional CD4+ T-cell subset designated TH3, was more recently identified and functionally characterized by the production of transforming growth factor (TGF)β (Acerwenka and Swain 1999). TH3 cells have a very important regulatory role in TH1 and TH2 cell functions, and there is now increased effort being made to understand the mechanisms of TGFβ mediated TH1/TH2 immunological suppression and/or stimulation. TGFβ is thought to function as a differentiation switch, counteracting existing differentiation programs of cells as they pass from one stage of differentiation to the next.

Importance of a New Population Named TH17

The increasing immune mechanism knowledge has undermined the TH1/TH2/TH3 model hypothesis, and its hold was broken by experiments to define the role of the cytokine IL23 in experimental allergic encephalomyelite (Steinman 2007). In fact, in the light of new information it is now recognized that the TH1/TH2/TH3 model is too rigid a model to be able to explain newly identified immunological mechanisms such as autoimmune diseases. Steinman (2007) explained that IL23, although sharing the p40 subunit with the TH1 cytokine IL12, differs from IL12 because of its unique p19 subunit. IL23, unlike IL12, does not induce TH1 cells, which produce IFNy. Cua and Kastelein (2006) showed that mice, with the gene for IL23 deleted, were resistant to the induction of various animal models of autoimmunity, including EAE, collagen arthritis, and inflammatory bowel disease. IL23 drives a population of T cells that produce IL17, IL6, TNF, and named TH17. Additionally, it was reported by Bettelli et al. (2006) that TGFβ/IL6 interactions induce TH17-autoimmunity

progression, by switching cell generation from T-regulatory (T-reg) cells to TH17 cells. Consequently, T-reg and TH17 cells are generated from reciprocal developmental pathways, and IL6 and TGFβ seem to be the chief inducers of TH17 development, whereas TGFβ alone promotes the generation of T-reg cells. Furthermore, it was reported by Steinman (2007) and Colgan and Rothman (2006) that TH1 and TH2 cytokines were required to reciprocally reduce IL17. On the basis of this new finding, TH1 cells, long thought to mediate tissue damage, might only be involved in the initiation of tissue damage, without playing a decisive role. The cytokine IL17, on the other hand, is now thought to have a major role in various immune-mediated tissue injury, including organ-specific autoimmunity in the brain, heart, synovium, and intestines, allergic disorders of the lung and skin, and microbial infections of the intestines and the nervous system. In this TH1/TH2/TH3/TH17 new context, the immunological function of the TH1 cell population would be to antagonize the TH17 pathway in some manner. Without a doubt, our growing understanding of the TH17 pathway will lead to a shift in perspective concerning the functional basis of the immune system network, and give hope for improvement in the prevention and treatment of immunopathologies such as tumor disease.

METHOD TO STUDY THE TH1/TH2/TH3/HT17 CYTOKINE NETWORK

The identification of accurate markers and diagnostic indices can only be achieved through an evaluation of the immune system that takes into account physiological conditions. This entails the study of the network of relationships between TH1/TH2/TH3/TH17 cytokine levels and the behaviour of this multicomponent system; because of the complexity of biological systems, this requires the use of mathematical models that provide a framework for determining the outcome of numerous and simultaneous time-dependent and space-dependent processes (Janes and Yaffe 2006). Many advances in TH1/TH2/TH3/TH17 cytokine network research have relied on the isolation of single cytokines using in vitro experiments with individual cell types and purified cytokines, or in vivo models using mice lacking the cytokine in question through the targeted destruction of the cytokine gene. These experimental approaches have been very successful in determining the influence of individual cytokines, but they do not allow a true assessment of the relative importance of each cytokine in the physiological network where all cytokines are functioning simultaneously. There is now an increasing need to understand how the immune system functions as a whole in order to understand more fully the development of pathological conditions such as tumors, and to devise immunological indices for more effective strategies to prevent and treat these pathologies. As mentioned earlier, the only way of studying the whole integrated system would appear to be through mathematical modelling. Janes and Yaffe (2006) reported that the increasing availability of high-throughput and multiplex techniques for quantifying signalling and cellular responses makes it immediately feasible to collect large data sets on protein abundance and activity. The paradox for systems biology is that

these large data sets, by themselves, often bring more confusion than understanding. In this regard, reductionist experimental approaches seem to make more sense, simplifying the confusion. To improve understanding without adding more confusion, computational models must be indicative of a mechanism and be based on experimental data. Janes and Yaffe (2006) reported that the only way of studying biological systems would appear to be through 'data-driven models': mathematical modelling which helps users to analyze large experimental data sets by simplifying the measurements themselves.

Immune System Through Mathematical Modelling

Our immunological research on cytokine networks (Berghella et al. 2006; Contasta et al. 2006; Pellegrini et al. 2006), are examples of how data-driven modelling using statistical approaches can give important insights into the immune system. In fact, by using a data-driven modelling system approach to study the TH1/TH2/TH3/TH17 network, new insights can be gained into questions that cannot readily be answered experimentally as well as, in this specific case, an immunological method for cancer stage classification. Modelling approaches must be based on prior biological analysis of the data itself, without making assumptions concerning the underlying mechanisms. The next step is understanding the specific mechanisms involved and the selection of the most significant markers for the stage index formulation. Then marker variations within peripheral blood must be defined, and these parameter ranges evaluated in specific groups of cancer patients to establish their significance and precision as prognostic and diagnostic indices for the classification of cancer stages.

Peripheral Blood Cytokine Network

On the basis of the above information, peripheral blood levels of TH1/TH2/TH3/TH17 cytokines and other specific immunological parameters (such as soluble cytokine receptors and costimulator antigens, protein regulating cell cycle or degradation of cellular matrix) need to be studied as do their network relationships, which together are believed to control the polarization of TH cells into TH1, TH2, TH3, or TH17 types. This immunological evaluation must be carried out for each individual. To evaluate the influence of cell environment on TH polarization (which affects TH polarization), network interactions between cytokines and immunological parameters are studied in serum because serum can be considered the cell environment in peripheral blood. Cytokines produced by immunological cells are studied to establish their functional type (TH1, TH2, TH3, or TH17) and their network interactions with immunological parameters must be determined. Hence, specific TH cytokine-types are determined in whole blood culture supernatants (to study peripheral blood mononuclear cells, PBMC) and DC culture supernatants(to study antigen presenting cells), with or without stimuli (respectively activation and resting state of the immune response). The whole blood culture method is used as it reflects in vivo physiological conditions more accurately, and so is more appropriate in this study (Bloemena et al. 1989). In addition, it is a simple procedure and thus reduces the

potential for error. This method has the added advantage of not requiring the separation of cellular sub-populations which would represent an additional source of potential variation both, in an individual and among individuals. Experimental conditions with or without stimuli (as PHA and LPS), were used to evaluate the type of functional immunity in activation and resting conditions: PHA is a nonspecific T cell stimulant that provides more information on T-cell contribution (Cohen et al. 1995); while Doyle et al. (1995) reported that LPS, as a Toll-like receptor agonist, is useful in understanding and determining the influence of antigen presenting cells such as monocytes and dendritic cells.

METHODS

Serum Samples

A 5 mL sample of venous blood is collected from each subject and centrifuged within 1 h of withdrawal as physiological levels of the cytokines tend to decrease at room temperature. The serum obtained is stored and frozen in aliquots at –80°C until use.

Peripheral Blood Mononuclear Cell Separation and Generation of Dendritic Cells from Monocytes Using Dynabeads

A sample of heparinized blood (20 IU/mL blood – Liquemin-Roche) is taken from each subject and diluted 1:4 with PBS medium at room temperature. PBMCs are separated by centrifugation (160 g for 20 min at 20°C) over a Lymphoprep gradient (Nycomed Norvay). These cells are recovered from the plasma/lymphoprep interface and washed three times with medium (200 g for 10 min at 20°C). Monocytes from PBMC samples are obtained by removing T cells, B cells, NK cells, and granulocytes (if present) through the first addition of specific antibody mix to the PBMC sample and then depletion Dynabeads to capture the antibody bound cells. Dynabeads are uniform, supermagnetic, polystyrene beads coated with a Fc specific human IgG4 antibody against mouse IgG. The antibody mix contains a mixture of mouse monoclonal antibody for CD2, CD7, CD16 (specific for CD16a and CD16b), CD19, and CD56. The blocking reagent contains gamma globulins to block FcR on monocytes. These coated cells are then separated with a magnet (Dynal MPC) and discarded. PBMCs are transferred into a 15 mL tube, washed three times with PBS with centrifugation (at 225 g for 8 min at 2–8°C) and resuspended at 1×10^7 per 100–200 μL PBS. 22 μL of blocking reagent and 20 μL of antibody mix for each 1×10^7 MNC cells is added and incubated for 10 min at 2–8°C. The cells are washed (by adding 1 mL of PBS per 1 $\mu10^7\times$C and centrifugation for 8 min at 500 g) and resuspended in 0.9 mL of PBS per 1×10^7 MNC. 100 μL of Depletion Dynabeads per 1×10^7 MNC are added and incubated for 15 min at 2–8°C with gentle tilting and rotation. The total volume for cell and bead incubation should be 1 mL per 1×10^7 MNC. The rosettes are resuspended by careful pipetting 5–6 times before increasing the volume by adding 1–2 mL of PBS and placing in the Dynal Magnetic particle concentrator for 2 min. Isolated monocytes recovered should be >98% viable and free of surface bound antibody or Dynabeads. Monocytes are resuspended in RPMI 1640 (Sigma, endotoxin tested) complete medium

containing 10% of AB male human serum (heat-inactivated for 30 min at 56°C), penicillin (50 UI/mL), streptomycin (50 μg/mL), and L-glutamine (0.2 mM). The cells are incubated in 24-well plates at a concentration of 200,000 cells per mL at 37°C in a humidified atmosphere of 5% CO_2 for 8 days and stimulated with 30 ng/mL of recombinant IL4 (Preprotech-England, specific activity of $>5 \times 0^6$ U/mg), 30 ng/mL of recombinant GM-CSF (Preprotech-England, specific activity of $>1 \times 10^7$ U/mg). On day 3, IL4 and GM-CSF are added again and on day 6, immature DCs are obtained. Immature DCs are stimulated with 100 μg/mL of LPS (Sigma), 0.1 ng/mL of recombinant human IFNβ (Preprotech-England, specific activity of $>2 \times 10^7$ U/mg), 1,000 U/mL of recombinant human IFNy (Collaborative Research incorporated, biomedical products, Bedford, MA, specific activity 500,000 Units/100 μL) and DCs without stimuli are also prepared. After 2 days of culture, the supernatant is removed from each well, centrifuged at 250 g and stored frozen in aliquots at –80°C until used.

Whole Blood Cell Cultures

The whole blood culture method must be used for the network study as it reflects in vivo physiological conditions more accurately (Bloemena et al. 1989). A 15 mL sample of heparinized blood (20 IU heparin/mL blood-Liquemin-Roche) is taken from each patient, and the samples kept at room temperature are used immediately. Venous blood is diluted 1:10 with RPMI-1640 medium (Sigma, endotoxin tested) and supplemented with 0.2 mM of L-glutamine, 50 IU/mL of penicillin, 50 μg/mL streptomycin (Sigma) and 10% of human AB serum. Aliquots at 1×10^6 cells are distributed in 12 mm polypropylene tubes; 10 μg/mL of PHA (Sigma) is used for stimulation. After 3 days of culture, the supernatant is removed and cytokine levels determined. The effect of adding heparin, which prevents clotting in whole blood cultures, must also be tested.

Cytokine Detection

The solid phase sandwich enzyme linked-immuno-sorbent assay (ELISA) is used for the in vitro quantitative determination of cytokines and soluble molecules in cell culture supernatant. Briefly, a monoclonal antibody specific for cytokine detection is coated into the wells of the microtiter strips. Samples (assayed in replicate), including standards of known and unknown cytokine concentrations, are pipetted into these wells. During the first incubation, the cytokine antigens are added to the wells. After washing, a biotinylated monoclonal antibody specific for the cytokine is incubated and the enzyme streptavidin-peroxidase is added. After incubation and washing to remove all unbound enzyme, a substrate solution, which acts on the bound enzyme, is added to induce a colored reaction product. The intensity of this colored product is directly proportional to the concentration of the cytokine present in the sample. A blood sample is taken from each subject and assayed for all cytokines. Thus, all cytokines are determined in all patients. For intra-assay precision, samples of known cytokine concentration must be assayed in replicates of ten to determine precision within an assay, the coefficient of variation is &*&<10%. For inter-assay precision, samples must also be assayed 30 times in multiple assays to determine precision between assays, the coefficient of variation is <10%.

Data Analysis

Given the complexity of the analyses, software systems are essential; we use "Statgraphics full system, Statistical Graphics System by Statistical Graphics Corporation, ed. 1989, USA". The results are expressed as means ± standard deviation and the differences between groups are assessed by the Mann-Whitney U test, the two-tailed Student's t-test, the Wilcoxon rank test for paired samples, and the Chi-square test as appropriate. Network relationships between immunological parameters and stage progression are analyzed through mathematical modelling using multivariate statistical methods. As mentioned above, there is now an increasing need to understand how the immune system functions as a whole in order to understand the development of pathological conditions such as cancer, and to create immunological indices for clinical use. Currently the only way of studying the whole system would appear to be through mathematical modelling. In our studies on the TH1/TH2/TH3/TH17 cytokine network we use the mathematical modelling of multivariate statistical analyses. The next section gives a brief outline of the statistical analyses used, and we refer the reader to the references given for more detailed information (Janes and Yaffe 2006; Randerson 1993).

The multivariate statistical procedure that analyses the correlation between parameters provides us with a matrix of coefficients of correlation (that vary from –1 to +1) and significance (p), and gives the degree of correlation between parameters within the network at any one moment in time. A positive correlation indicates that the parameters vary in the same direction, while negative correlation indicates that the parameters vary in the opposite direction. Statistically independent parameters have an expected correlation of zero. The covariance analysis produces a matrix of covariance coefficients between parameters which can be positive or negative and which, in contrast to the correlation study, allows a dynamic analysis of how network components vary with respect to one another in any one moment of time. In fact, the covariance method measures the linear association between parameters. If parameters increase or decrease at the same time, the covariance is positive, whilst other changes are considered negative. The principal component analysis plots the vectors of interaction between parameters within the network. The angle between vectors is inversely proportional to the correlation between them, the same vector direction indicates a positive correlation, the opposite vector direction indicates a negative correlation. This allows for a visualization of the situation under examination. It was reported by Janes and Yaffe (2006) that principal components analysis achieves dimensionality reduction by finding new axes, called principal components, that identify the linear combinations of parameter axes most closely connected to one another. Principal components function as super-axes, which allow users to view the entire data space in just two or three dimensions that capture the most important information in each of the original parameter axes. The multiple regression and stepwise multiple regression analyses (which assume that a variable can be predicted from a set of other variables and seek the best mathematical relationship between them) are used to study the weight of each parameter in the normal balance of the parameter

network. A forward or backward selection procedure is possible in the latter method. The forward selection begins with no variables (step 0) and adds them one at a time (step 1, 2, etc.) according to the highest F-statistic values. This allows us to control the entry of variables in the model. The backward selection procedure begins with a model containing all the variables (step 0) and eliminates them one at a time (step 1, 2, etc.) according to the lowest F-statistic values. The forward selection is comparable to onset and evolution of the immune response; whilst the backward selection procedure is comparable to the physiological return to equilibrium. The simple linear regression analysis, which generates predictions and related statistics for all parameters examined, is useful for determining patient stage indices as we reported in Pellegrini et al. (1998). Patient stage indices are obtained by predicting pTNM stage values (dependent variable) from immunological parameters (independent variable) and evaluating their statistical significance (C.Corr, R- SQ, and p values). The significance is set at $p < 0.05$.

PHYSIOLOGICAL EVALUATION OF THE IMMUNE SYSTEM

The TH1/TH2/TH3/TH17 Cytokine Network in Healthy Subjects

The first step is to study the TH1/TH2/TH3/TH17 cytokine network and specific immunological parameters in healthy subjects. This type of study can illustrate how cytokines regulate, by means of induction (→) or suppression (≠), TH polarization in TH1, TH2, TH3 or TH17 cells and therefore the normal immune response. It is also a pratical and noninvasive tool for the identification of suitable peripheral blood markers, establishing ranges for use in evaluation methods for disease prevention programs. Our research in healthy subjects, shows that the normal cytokine network regulates TH polarization by means of specific relationships between TH-types of cytokines, which are different in men and women (Pellegrini et al. 2000). These relationships need to be studied experimentally to create prognostic and diagnostic clinical indices. We studied healthy men and women as hormones can influence the polarization of THs cells; none of the subjects was taking concurrent drug treatment including widely-used pharmaceuticals, such as salicylates and sex hormones (contraceptive pill, hormone replacement therapy); we ensured comparable age distribution for male and female groups, and blood samples were taken at the same time of the day to minimize effects of diurnal variation. By determining the relationships between TH-types of cytokines in serum (the cell environment network model), the influence of the cell environment on TH polarization can be evaluated. As above reported, the polarization of the immune response into TH-types of cells is not absolute, and the ratio of these cells varies with the subject's physiological and clinical conditions. In vivo and in vitro studies in mice have demonstrated that cytokines play a very important role in the development of precursor cells in TH-type cells; furthermore, the proportion of each cell type depends on the cytokines present in the cell environment during activation events. This also indicates the selective regulatory effect that TH-type cytokines reciprocally exert, as well as the importance of environmental cytokines in influencing the type of TH cell differentiation

during primary stimulation. By determining the relationships between TH-types of cytokines produced by immunological cells (the cellular network), it is possible to establish their functional cell TH-type (TH1, TH2, TH3, or TH17). Serum and cell production levels of IL12p70(→TH1, ≠TH2, →TH3 ≠TH17), IL12p40 (≠TH1, → TH2, ≠TH3, →TH17), IL2 (→TH1), IFNγ(→TH1, ≠TH2, →TH3, ≠TH17), IL4 (≠TH1, →TH2, →TH3, ≠TH17), IL6 (→ TH2, ≠TH3, →TH17) and IL10 (≠TH1, →TH2), are determined in the peripheral blood of healthy subjects: these cytokines make up the network under resting conditions. Activation conditions can be achieved by adding: (1) sIL2R and sIL6R to the basic cell environment network model because these molecules are considered activation markers; (2) production levels of cytokines by PBMCs after PHA stimulus to the basic cellular network model. The influence of antigen presenting cells can be determined by looking at serum levels of TNFα and IL1β within the cell environment network model, because these cytokines are principally produced by antigen presenting cells, and the production levels of IFNγ, IL10, and IL6, after stimulus with LPS within the cellular network model.

Cytokine Network Relationships in Men and Women

Our results reported in Pellegrini et al. (2000) show that sIL2R and sIL6R are involved in establishing equilibrium between cell TH-type polarization in the cell environment, in healthy subjects. This finding confirms our previous results on the biological role of sIL2R in the cytokine network balance in healthy controls Berghella et al. (1998). Experimental work on sIL2R and sIL6R levels in the peripheral blood could produce serum markers for the evaluation of the TH-types of cell physiological equilibrium during immune system activation for men and women. Though it was interesting to note that, in neither sex, was a significant relationship observed between IL10 and TH-types of cytokines in the environment network model. Likewise, no relationships were observed between IL10 and TH-types of cytokines in the cellular network model when using the 72 h culture. This suggests that, under normal conditions, in both sexes, the effect of IL10 on TH-types of cell polarization is short-lived. However a positive relationship between IFNγ and IL10 production was discovered in men using the 24-h culture, and a negative relationship between IL6 and IL10 in women. These relationships could be considered the expression of regulatory mechanisms responsible for restoring the initial physiological equilibrium and need to be studied experimentally. Consequently our results suggest that, in order to maintain a normal balance between TH-types of cells, the effect of IL10 on TH polarization must be short-lived, in both networks. These results concord with data demonstrating the broadly suppressive effect of IL10 on TH-type cell homeostasis; its persistence within the environmental network results in the harmful persistence of a suppressive TH2-type cell phenotype. The influence of antigen presenting cells on TH polarization appears to be exerted through both networks in both sexes. Therefore, the conclusions that we can draw are firstly: TH-types of cytokines present in the cell environment appear to be responsible for TH polarization in resting state in men; TH polarization in resting state in women, on the other hand, appears to be regulated by

cells through specific interaction between specific TH-types of cytokine production; secondly, TH-types of cytokines produced specifically by cells as well as those present in the cell environment, appear to influence TH polarization during activation and lastly, these differences need to be taken into account in.

HOW TO DEFINE IMMUNOLOGICAL PARAMETERS FOR STAGE CLASSIFICATION

After the immune network study in healthy subjects illustrating how cytokines regulate TH polarization in TH1, TH2, TH3 or TH17 cells, the second step is a comparative study with cancer patients to identify suitable peripheral blood markers for stage classification and define ranges to establish an immunological method for clinical stage monitoring.

Comparative Study with Groups of Healthy Subjects and Cancer Patients

The first step in this evaluation, is the determination of peripheral blood levels of TH1/TH2/TH3/TH17 cytokines and others specific immunological parameters in groups of cancer patients and healthy subjects (acting as a control group), followed up by the study of the relationships between parameters and disease stage progression (Berghella et al. 2006; Pellegrini et al. 2006; Contasta et al. 2006). In colon cancer, for instance, we investigated the possible prognostic significance of various cytokine serum levels and cytokine production by PBMCs, tumour-draining lymph node lymphocytes (LNLs) and tumor cells (TCs). Levels of soluble carcinoembryonic antigen (sCEA), sCD30, sIL2R and sIL6R; the PBMC expression of T, B, NK, APC cells and activation phenotypic antigens: CD3, CD4, CD8, CD19, CD16, CD56, CD57, DR, and CD25; and the proliferative responses of PBMC to IL2, IL4 and anti-CD3 monoclonal antibody were also studied. These immunological parameters were selected on the basis of their roles within the immune system providing a physiological-like model for the study. We identified levels of specific immunological parameters that varied significantly between patients and control subjects as well as parameters within the patient groups that varied between stages. It is therefore our opinion that these parameters can be used in the formulation of prognostic and diagnostic indices to classify and monitoring disease stages.

DISEASE STAGE INDICES IN COLORECTAL CANCER

Colorectal cancer is one of the most common cancers and like most cancers it is most successfully treated when diagnosed early. Unfortunately, there has been comparatively little improvement in the survival rate of colorectal cancer patients for many years and this neoplasy is generally resistant to chemotherapy. Samantas et al. (2007) pointed out that adjuvant chemotherapy improves survival for patients with stage III of the disease but it has not been shown to offer a significant benefit to patients with stage II of the disease; 20% of patients with stage II colon tumour die from disease recurrence. There is most certainly a need for non-invasive tools

that can identify patients most at risk of disease progression and, furthermore, biological diagnostic and prognostic indices for disease stage may help in the planning of more specific treatment strategies. Not surprisingly the pathogenesis of colorectal cancer is under intense investigation at molecular, organic, dietary and epidemiological levels. We reported an experimental model to investigate the prognostic and diagnostic significance of immunological parameters for the stage classification in colorectal cancer in Berghella et al. (1996). We investigated, the possible prognostic significance of serum levels of IL2, IFNγ, IL4, IL6, IL7, IL8, TNFα cytokines and sIL2R, sCD30, sICAM1 molecules; the phenotype of peripheral blood mononuclear cells (PBMCs); and PBMC proliferative response to IL2, IL4 and anti-CD3 monoclonal antibody (mCD3).

Prognostic Significance of Immunological Parameters

Our data highlight the significance of specific immunological parameters in the definition of prognostic indices for disease stage. In fact not only did we find that levels of immunological parameters varied between patients and control subjects but more importantly that parameters within the patient group varied between stages. These differences were well defined between stages I and II but not so clear cut for stages III and IV. We believe that a larger study of this type could lead to more accurate identification of patients at risk and disease stage. Additionally, as we have mentioned elsewhere, this type of evaluation could lead to a better understanding of the immunological damage that cancer causes and hence the therapy required to re-establish equilibrium. Stage I patients had higher serum levels of IL4 and IL7, and progressing from stage II to stage IV an increase of sIL2R, IL6 and a decrease of IL2 was recorded. Increases in the levels of sICAM-1 and TNF were also recorded which could be used to distinguish between stages II, III and IV, whereas IL8 levels in stage III patients were significantly different from patients with stage IV of the disease. At stage I all values of antigen expression were within the normal ranges however with progression of the disease from stages II to IV there is a significant decrease of CD4 expression and an increase of DR but in stages II and III a decrease in the CD3 expression was also found; at stage II there seems to be an increase of CD56 and at stage III the CD8 expression was higher. Only a significant decrease of proliferative response to IL-2+anti-CD3+IL-4 and to anti-CD3+IL-4 was found in the patient group when confronted with data from the control group and although the decrease of the response to the second stimulus was already evident from stage I, the decrease of response to the first stimulus started at stage II. Stage progression seems to be correlated negatively to the PBMC proliferative response to IL-2 and positively with anti-CD3 and when anti-CD3 was added to IL2.

Normal Mucosa to Adenoma and Colon Cancer

Cytokines, sIL2R and sICAM Serum Levels

As we reported in Berghella et al. (1997), the pathogenesis of cancer has been under intense investigation to identify reliable prognostic indices for the early detection of disease and this is still a current research theme. We studied a group of healthy subjects, subjects with adenomas, and colorectal cancer patients in order to identify

peripheral blood invasiveness markers in the progression from normal mucosa through adenoma to tumor. We evaluated the relationships between serum levels of interleukin IL2, sIL2R, interferon (IFN)γ, IL4, IL6, IL10 and sICAM-1 and their networks. Our results indicate that the patient's immune response changes from a cell-mediated type (typical under normal conditions) to a suppressive type (typical in tumour patients) in the progression from normal mucosa to tumour. Neither IL10 or sIL2R are implicated in the immune response of adenoma patients but both play a significant role in the immune response of cancer patients suggesting that they may be of prognostic value for the passage from adenoma to cancer. Our data indicate that sIL2R and sICAM1 are involved in the switch to invasive phases. These conclusions are drawn from the results detailed below. A significant decrease in IL2 levels was found in adenoma patients indicating a suppressive condition of the immune system. Statistically significant higher values of sIL2R and IL10 were found in colon cancer patients with respect to the adenoma group. IL10 is an important physiological regulator of inflammatory and immune responses, and its in vivo production is associated with TH2-like responses and it has found to be a more powerful and outright inhibitor of IFNγ, macrophage and TH1 functions than IL4. In healthy conditions it is only produced when its inhibiting activities favour homeostasis. Alterations in its levels or premature or persistent IL10 production causes an imbalance in the network which can have profound pathological consequences and can lead to the pathogenesis of disease. The presence of IL10 therefore suggests an increase in the suppressive activity of the immune system of colon cancer patients (in which sIL2R molecules seem to be involved) with respect to adenoma patients. Furthermore, our results indicate significant differences in sIL2R levels between adenoma patients and tumour patients at the pre-invasive phase, stage II whilst differences in IL2, IL6 and IL10 were found at the invasive phase, stages III and IV. Significant differences were already present between healthy controls and stage I patients, in IL4 and IL10 levels, and at stages II, III and IV, in sIL2R, IL2 and IL6 levels. The passage from normal mucosa to adenoma seems to be linked to a fall in IL2 while the passage from adenoma to tumour to an increase in IL10 and sIL2R. Multivariate statistical analyses were used to identify the parameters with the greatest weighting on disease progression .The covariance study showed, additionally, that the increase in sIL2R in healthy controls corresponded to an increase in IL2 and IFNγ, TH1 cell-mediated immunity cytokines; in adenoma patients an increase in TH2 IL6 and IL4 and TH1 IFNγ cytokines was recorded but not IL2, indicating IL4 suppression of TH1 cells. IL10 was not implicated; if this cytokine is produced too early it affects cytokine relationships, directing the immune system towards an inappropriate suppressive immune response and inhibiting damage repair and a return to homeostasis. In the patient group, on the other hand IL6, IFNγ, IL4, IL10 increase with sIL2R confirming the belief that IL10 is implicated in an inappropriate suppressive type response and in the passage from adenoma to tumour. Interestingly, an impairment in sICAM1 mechanisms also seems to be involved in the progression of adenoma to tumour. In fact, in

both healthy and adenoma subjects there was a parallel increase of sIL2R and sICAM1 and the latter was positively related to IL2. sICAM1 was implicated in immune cell migration to infected and damaged physiological compartments and so a positive association with IL2 indicates a relationship with cell-mediated immunity. The simple linear regression analysis confirmed these findings, as the parameter with the greatest weighting on sIL2R was IFNγ in healthy and adenoma patients but IL4 in patients. Our overall data indicate that the immune response progresses from a TH1 cell-mediated immune response type (healthy subjects) to a type with TH2 suppressive characteristics (adenoma subjects and cancer patients). However, in adenoma subjects there was no IL10 or sIL2R involvement, while these parameters were implicated in the cancer patients' immune responses. Moreover, a concurrent increase in sIL-2R and IL10 levels appears to be a prognostic factor in the passage from adenoma to cancer, whilst sIL-2R and sICAM-1 molecules appear to be involved in invasive mechanisms.

sCD30 Mechanisms Regulating TH1/TH2 Cell Functions

To gain a better understanding of the role of CD30 in the regulation of TH1/TH2 cell functions and to identify prognostic and invasiveness markers, we studied network interaction between the production of sCD30 and sBcl2 in whole blood cultures and serum levels of TH1/TH2 cytokines in healthy controls, adenoma and colorectal cancer patients, Contasta et al. (2003). Our results indicate that a decrease in CD30 expression and an abnormal increase of sBcl2 expression in the peripheral cells of adenoma and tumour patients results in a loss of equilibrium between TH1 and TH2 cells. Additionally, changes in the production of sCD30/sBcl2 and serum levels of IL2, IFNγ , IL12, IL4, IL5 and IL10 can be used as markers for the passage from normal mucosa to adenoma and from adenoma to tumor.

Accuracy of Prognostic Indices

Characterization of Disease Stage

As reported above, no single staging system is universally employed for all cancers but one of the most commonly used is the pTNM classification devised by the American Joint Committee for Cancer Staging, based on the examination of a surgically resected specimen. This classification takes into consideration the size of the primary tumour (T), the presence and extent of regional node metastases (N), and the presence of distant metastases (M). We evaluated the accuracy of our immunological parameters by comparing them with those obtained with the pTNM method, according to the system of study outlined below and reported in more detail in Pellegrini et al. (1998). The peripheral blood level determination of TH1/TH2/TH3/TH17 type cytokines and others specific immunological parameters (such as cytokine receptors, leukocyte surface markers and soluble carcinoembryonic antigen sCEA), PBMC cytokine production and PBMC proliferative response were studied in groups of cancer patients and a control group of healthy subjects. To study the networks of relationships between parameters and disease stage progression, a multivariate statistical method was adopted. As mentioned above, this type of statistic analysis is suited to the

study of biological systems because it uses the mathematical models and these analyses, by simultaneously evaluating the relationships among all variables allow the study in vitro of the in vivo immunological network response, where all cytokines are functioning simultaneously. In the multivariate statistical study we used Principal Components (PC) analysis to obtain the degree of correlation between disease stage and other parameters within the immunological network. By this method we plot the network of all parameter weights, allowing a visualization of the contribution of each parameter within the network: the length of each vector is proportional to its network contribution and the angle between any two is inversely proportional to the correlation between them. Stepwise Multiple Regression (SMR) analysis was used to study the weight of each parameter on disease stage. By this method we have effected a forward parameter selection: forward selection begins the multiple regression analysis with no variables in the model (step 0) and then adds them one at a time (steps 1, 2, etc.) according to the highest F-statistic (F-enter) values, allowing us to control the entry of variables into the model. In each step of the forward procedure, the C.Corr, the R-squared (R-SQ) and the F-enter values are re-calculated. p values lower than 0.05 were considered significant. Simple Linear Regression (SLR) analysis, which generates predictions and related statistics for all parameters examined, was used to determine prognostic index values. These were obtained by predicting patient pTNM stage values (dependent variable) from the immunological parameters (independent variable), and evaluating their statistical significance (C.Corr, R- SQ and p values). The level of significance was set at $p < 0.05$. As pointed out by the mathematical concepts, the following ranges were established for each stage: immunological index values from 0.56 to 1.55 corresponded to pTNM stage I; 1.56–2.55 to pTNM stage II; 2.56–3.55 to pTNM stage III and 3.56–4.55 to pTNM stage IV. These immunological index values were considered exact when the patient stages obtained using the pTNM method classifications were the same. The number of patients with an exact stage classification was compared to the total number of patients at that stage and the percentages obtained were used to assess the accuracy of the immunological indices in predicting disease stage. This study showed that our immunological classification is able to identify three stages: primary tumour, nodal involvement and distant metastases. Primary tumour stage corresponded to pTNM stages I and II, nodal involvement to pTNM III stage and distant metastases to pTNM IV stage. Stage II is defined more precisely by our prognostic indices. This may be due to the greater number of patients at stage II in the study or to a different progression of immunological damage with respect to histopathological parameters. If the latter is the case, an immunological stage classification could be used to define stage sub-groups and thus suitable therapy. We are currently investigating these hypotheses. By comparing our classification results with those of the pTNM method, we obtained a percentage value for each parameter indicative of the accuracy of these immunological indices in defining stage. IL4 serum level and mCD3 PBMC proliferative response emerged as the most effective parameters for establishing disease stage. The frequency expressing the

probability of an exact disease stage classification of IL4 serum level, for examples, is as follow.: an IL4 blood level value of up to 582 pg/mL is highly indicative of metastatic disease (100% probability); between 238 and 567 pg/mL nodal involvement (64% probability) and a lower probability of distant metastases (36%); lower than 223 pg/mL a primary tumor (63%), with a lower pobrability of nodal involvement (26%) and a very lost possibility of distant metastases (11%). As we hypothesized, immunological parameters can be used to predict disease stage. Further immunological studies are now required to identify other prognostic markers and their blood parameter ranges for stage classification.

Identifying Ranges for Immunological Markers

Our next aim was to investigate the possibility of identifying variation ranges for immunological markers.

Preinvasive to Invasive Colorectal Cancer

Simultaneous Measurement of sCEA and TIMP1

Matrix metalloproteinases (MMPs), zinc-dependent enzymes involved in the degradation of extracellular matrix, play an important role in physiological and pathological processes The activity of Matrix metalloproteinase 1 (MMP1), a membrane-anchored enzyme, is subject to regulation by cytokines at gene level and post-translationally by inhibitors in the extracellular space. One of these tissue inhibitors of metalloproteinases (TIMPs) is TIMP1 a member of the TIMP family. The potential diagnostic and prognostic value of serum level measurements of MMP1 and TIMP1 was evaluated by comparing them with serum levels of sCEA and p53 antibodies, since the simultaneous assessment of serum p53 antibody and sCEA appears to be effective in monitoring high risk and post-operative patients, Contasta et al. (1999). The results of our research suggest that serum levels of both TIMP1 and sCEA are useful in the monitoring of patients with colorectal cancer; sCEA as a progression marker for the transition from stage II to stage III and TIMP1 as a marker for the transition from stage III to IV. We drew these conclusions from the results of our multivariate statistical analyses on network parameter relationships and disease progression. These conclusions were supported by a statistical study of the differences in serum parameters at the various stages. Variance studies analysing the quantitative variations of these parameters through the stages allowed us to identify range values for these potential markers: the 95% confidence interval of sCEA serum levels at stage III ($18.4 \leq sCEA \leq 68.6$) and TIMP1 at stage IV ($1620 \leq TIMP1 \leq 3906$) gave statistically significant ranges (sCEA $p = 0.02$; TIMP1 $p = 0.02$) and so may be useful in patient monitoring in these phases. In fact when the serum level of sCEA is <18.4 and the level of TIMP1 <1,620, there is a 95% probability that the disease is in the pre-invasive nodal phase; when the serum level of sCEA lies between 18.4 and 68.6 ($18.4 \leq sCEA \leq 68.6$) and the level of TIMP1 is <1,620, there is a 95% probability that the disease is in the lymph nodal infiltration phase; when the level of sCEA is > 68.6 and the level of TIMP1 is ≥1620, there is a 95% probability that the disease is in the metastatic phase. In conclusion, our results indicate that the simultaneous measurement of sCEA and TIMP1 serum levels in colorectal cancer patients may have prognostic and diagnostic value for

the clinical monitoring of disease progression from pre-invasive to invasive stages.

Simultaneous Measurement of sIL2R, sIL6R, and Cytokine Serum Levels

We extended our study to other peripheral blood parameters: IFNγ, IL4, IL8, IL7, IL1β, TNFα, GMCSF, sIL2R and sIL6R (Berghella et al. 2002). Our results indicate that when serum levels of sIL2R < 522 U/mL, IL4 < 159 pg/mL and IL8 > 339 pg/mL there is a 95% probability that the disease is in stage I or II (no infiltration of lymph nodes); when serum levels of sIL2R ≥ 522 U/mL, 159 pg/mL ≤ IL4 ≤ 319 pg/mL, IL8 ≤ 339 pg/mL and IL7 < 54 pg/mL, there is a 95% probability that the disease is in stage III and the tumour has invaded the lymph nodes; when the serum levels of IL4 ≥ 431pg/mL and IL7 ≥ 54 pg/mL, there is a 95% probability that the disease is in stage IV and there is metastasis. In conclusion, the need for practical and non-invasive methods to establish disease stage in the initial screening and clinical monitoring of cancer patients is clear. As we have underlined, the difficulty in this lies in identifying non-invasive tools for establishing reliable stage diagnosis. Our experience in the field of the immunology leads us to believe that immunological blood parameters could be used to create prognostic and diagnostic indices for an immunological method of stage classification, and our subsequent research has confirmed this in colorectal cancer. Our research shows that immunological disregulation has a direct role in the mechanisms that allow the tumor to locate and expand within the host. These immunological alterations increase with stage progression therefore offering the means of identifying immunological indices for cancer stage classification. Furthermore it is important to underline that this immunological approach, evaluating patient peripheral blood, could prove to be a simpler and less invasive means of establishing cancer disease stage at an earlier phase. By using a data-driven modelling system approach to study the TH1/TH2/TH3/TH17 network, combining quantitative specific level determinations of TH1/TH2/TH3/TH17 cytokine and specific immunological parameters in correlation to the stage progression, new insights can also be gained into the immune system, insights that are not always possible adopting an experimental approach. The evaluation of cytokine networks is a unique and practical tool for assessing disease progression and we believe that our research should form the scientific rational for controlled clinical trials and further studies covering other cancer types.

REFERENCES

Acerwenka A, and Swain SL (1999) TGF-β1: immunosuppressant and viability factor for T lymphocytes. Microbes Infect 15:1291–1296

American Joint Committee on Cancer, Beahrs OM, Henson DE, Hutter RVP, and Kennedy BJ (eds) (1992) Manual for staging of cancer, 4th edn. J.B. Lippincott Company, Philadelphia, PA, ISBN 0-397-51264-3.

Benzoni E, Rossit L, Cojutti A, Bavero A, Saccomano E, Zompicchiatti A, Noce L, Bresaola F, and Intini S (2007) Analysis of survival after pancreatic resection for pathologies. Chir Ital 59:17–25

Berghella AM, Pellegrini P, Del Beato T, Maccarone D, Adorno D, and Casciani CU (1996) Prognostic Significance of immunological evaluation in colorectal cancer. Cancer Biother Radiopharm 11:355–361

Berghella AM, Pellegrini P, Del Beato T, Adorno D, and Casciani CU (1997) IL-10 and sIL2R serum levels as possible peripheral blood prognostic markers in the passage from adenoma to

colorectal cancer. Cancer Biother Radiopharm 12:265–272

Berghella AM, Pellegrini P, Del Beato T, Marini M, Tomei E, Adorno D, and Casciani CU (1998) The Significance of an increase in soluble interleukin-2 receptor level in colorectal cancer and its biological regulating role in the physiological switching of the immune response cytokine network from TH1 to TH2 and back. Cancer Immunol Immunother 45:241–249

Berghella AM, Contasta I, Pellegrini P, Del Beato T, and Adorno D (2002) Peripheral blood immunological parameters for use as markers of preinvasive to invasive colorectal cancer. Cancer Biother Radiopharm 17:43–50

Berghella AM, Contasta I, Pellegrini P, Del Beato T, and Adorno D (2006) Are immunological mechanisms involved in colon cancer and are they possible markers for biotherapy improvement? Cancer Biother Radiopharm 21:468–487

Bettelli E, Carrier Y, Gao W, Korn T, Strom TB, Oukka M, Weiner HL, and Kuchroo VK (2006) Reciprocal developmental pathways for the generation of pathogenic effector TH17 and regulatory T cells. Nature 441:235–238

Bloemena E, Roos MT, Van Heijst JL, Vossen JM, and Schellekens PT (1989) Whole-blood lymphocyte cultures. J Immunol Methods 122:161–167

Bradley LM, Yoshimoto K, and Swain SL (1995) The cytokines IL-4, IFN-gamma, and IL-12 regulate the development of subsets of memory effector helper T cells in vitro. J Immunol 155:713–724

Cher DJ, and Mosmann TR (1987) Two types of murine helper T cell clones. II. Delayed-type hypersensitivity is mediated by TH1 clones. J Immunol 138:3688–3694

Cohen SBA, Clayton J, Londei M, and Feldmann MT (1995) Cells and cytokines. In: Rickwood D, Hames BD (eds) Cytokines, 2nd edn. New York, Oxford University Press, p 179

Colgan J, and Rothman P (2006) All in the family: IL-27 suppression of TH-17 cell. Nat Immunol 7:899–901

Contasta I, Berghella AM, Pellegrini P, Del Beato T, Casciani CU, and Adorno D (1999) Relationships between the activity of MMP1/TIMP1 enzymes and the TH1/TH2 cytokine network. Cancer Biother Radiopharm 14:465–475

Contasta I, Berghella AM, Pellegrini P, and Adorno D (2003) Passage from normal mucosa to adenoma and colon cancer: alteration of normal sCD30 mechanisms regulating TH1/TH2 cell functions. Cancer Biother Radiopharm 18:549–557

Contasta I, Pellegrini P, Berghella AM, Del Beato T, and Adorno D (2006) Colon cancer and gene alterations: their immunological implications and suggestions for prognostic indices and improvements in biotherapy. Cancer Biother Radiopharm 21:488–505

Cua DJ, and Kastelein RA (2006) TGF-β a 'double agent' in the immune pathology war. Nat Immunol 7:557–655

Doyle A, Stein M, Keshav S, and Gordon S (1995) Assays for macrophage activation by cytokines. Cells and cytokines. In: Rickwood D, Hames BD (eds) Cytokines, 2nd edn. Oxford University Press, NewYork, p 269

Fossa SD, Aamdal S, Naume B, and Gallati H (1995) Serum levels of cytokines and soluble cytokines receptors in patients with metastatic renal cell carcinoma or malignant melanoma receiving IL-2- interferon-alpha combination therapy. Acta Oncol 5:599–603

Janes KA, and Yaffe MB (2006) Data-driven modelling of signal-transduction networks. Nat Rev 7:820–828

Jarnicki AG, Lysaght J, Todryk S, and Mills KHG (2006) Suppression of antitumor immunity by IL-10 and TGF-β-producing T cells infiltrating the growing tumor: influence of tumor environment on the induction of CD4+ and CD8+ regulatory T cells. J Immunol 177:896–904

Kalinski P, Vieira PL, Schuitemaker JK, De Jong EC, and Kapsenberg ML (2001) Prostaglandin E(2) is a selective inducer of interleukin-12 p40 (IL-12p40) production and an inhibitor of bioactive IL-12p70 heterodimer. Blood 97:3466–3469

Liu VC, Wong LY, Jang T, Shah AH, Park I, Yang X, Zhang Q, Lonning S, Teicher BA, and Lee C (2007) Tumor evasion of the immune system by converting CD4+CD25+ T cells into CD4+CD25+ T regulatory cells: role of tumor-derived TGF-beta. J Immunol 178:2883–2892

Mosmann TR, Schumacher JH, Street NF, Budd R, O' Garra A, Fong TA, Bond MW, Moore KW, Sher A, and Fiorentino DF (1991) Diversity of cytokine synthesis and function of mouse CD4+ T cells. Immunol Rev 123:209–229

Pellegrini P, Berghella AM, Del Beato T, Maccarone D, Casciani CU, and Adorno D (1998) Disease

stage prognostic indices in the early clinical screening of colorectal cancer patients. Cancer Biother Radiopharm 13:89–98

Pellegrini P, Contasta I, Berghella AM, Del Beato T, Casciani CU, and Adorno D (2000) The TH1 and TH2 cytokine network in healthy subjects: suggestions for experimental studies to create prognostic and diagnostic indices for biotherapeutic treatments. Cancer Biother Radiopharm 15:267–278

Pellegrini P, Berghella AM, Contasta I, Del Beato T, and Adorno D (2006) The study of patient's immune system may prove to be a useful noninvasive tool for stage classification in colon cancer. Cancer Biother Radiopharm 21:443–467

Randerson PF (1993) Ordination. In: Fry JC (ed) Biological data analysis. A practical approach. IRL Press/Oxford University Press, New York/Oxford, pp 173–208

Samantas E, Dervenis C, and Rigatos SK (2007) Adjuvant chemotherapy for colon cancer: evidence on improvement in survival. Dig Dis 25:67–75

Skeel RT (1992) Handbook of cancer chemotherapy, 3rd edn. Little Brown & Company, Boston, MA, ISBN 0-316-79574-7

Statgraphics Full system, 5.25-Version 4.0. Statistical Graphics System by Statistical Graphics Corporation 1989 STSC, Inc. ISBN 0-926683-06-3

Steinman L (2007) A brief history of TH17, the first major revision in the TH1/TH2 hypothesis of T cell–mediated tissue damage. Nat Med 13:139–144

Stevens TL, Bossie A, Sanders WM, Fernandez-Botram R, Coffman LR, Mosmann RT, and Vitetta ES (1988) Regulation of antibody isotype secretion by subsets of antigen-specific helper T cells. Nature 334:255–258

Vlastos G, and Verkooijen HM (2007) Minimally invasive approaches for diagnosis and treatment of early-stage breast cancer. Oncologist 12:1–10

Warburton G, Nikitakis NG, Roberson P, Marinos NJ, Wu T, Sauk JJ Jr, Ord RA, and Wahl SM (2007) Histopathological and lymphangiogenic parameters in relation to lymph node metastasis in early stage oral squamous cell carcinoma. J Oral Maxillofac Surg 65: 475–484

15
Late Relapse of Germ Cell Malignancies: Incidence, Management, and Prognosis

Jan Oldenburg and Sophie D. Fossa

INTRODUCTION

Half a century ago, 2 years of relapse-free survival after treatment of malignant germ cell tumors (MGCTs) were considered equivalent to cure. This view prevailed beyond the introduction of cisplatin in the 1980s until Terebelo et al. (1983) published the first series of late relapse testicular cancer patients. Nowadays, the potential of germ cell tumors to recur many years after apparently successful state-of-the-art treatment is increasingly recognized, and is regarded as one of the most important challenges regarding the long-term cure of these neoplasms in today's clinical oncology.

This chapter focuses on three issues of late relapsing MGCTs:

1. Incidence and impact of initial treatment on the risk of late relapse
2. Detection and differential diagnosis, including pathology
3. Treatment and prognosis

INCIDENCE

A recent review by Oldenburg et al. (2006), hereafter referred to as "our review" or "our pooled analysis", revealed that only 1–6% of all MGCT patients experience a late relapse. Due to their rarity, systematic analyses of late relapses have been restricted to large centers, which often serve as referral centers. Calculation of the incidence, however, requires the number of primarily treated patients. This information is often lacking in series from referral centers.

Furthermore, inclusion criteria for late relapsing patients differ: some series included patients with prior early relapses, that is, within 2 years after treatment. Gerl et al. (1997) showed that early relapse was associated with subsequent late relapses. Inclusion of patients with extragonadal germ cell tumors (EGGCTs), who according to Oldenburg et al. (2006) are more prone to develop late relapses than those with testicular cancer, may also increase the late relapse incidence.

Our pooled analysis of reports on late relapses comprising 3,700 non-seminoma- and 2,200 seminoma patients revealed 119 and 31 late relapses, respectively. The mean cumulative incidence was 3.2% in non-seminoma patients and is significantly higher than the corresponding figure of 1.4% in patients with seminoma.

Late recurrences were in 284 out of 557 cases (55%) localized in the retroperitoneal space, (Table 15.1). The chest (either lungs or mediastinal lymph nodes) comprised the relapse localization in 26% of both histological types; with seminoma patients having their relapse mostly in mediastinal lymph nodes (27%) whereas non-seminoma patients rather experience recurrences in the lungs/pleura (17%). However, abdominal radiotherapy and retroperitoneal lymph node dissection (RPLND) considerably reduce the risk of a retroperitoneal relapses in the respective patient groups. Risk estimation of late relapses has to be based on multiple factors, especially histology, initial stage, and prior treatment.

SEMINOMA CLINICAL STAGE I

Approximately 80% of seminoma patients present without detectable metastases, that is clinical stage I disease. Disease-specific survival rate is 99% independent of which of the following three management strategies are applied: radiotherapy, surveillance or carboplatin. Our data indicate a crude relapse-rate of 1.4–6.9% after radiotherapy; 15.2–19.3% after surveillance, and 0–8.6% after one or two cycles of carboplatin. Martin et al. (2007) calculated the risk of relapse to be highest within the first 2 years, regardless of the management strategy (>5% annual hazard rate for surveillance, and >1% for radiotherapy or carboplatin). Recurrences thereafter are very rare with an annual hazard rate between 0.25–1% from the fourth to the sixth year after treatment, with isolated late relapses occurring beyond 6 years. Nevertheless, in our pooled analysis, 27% of late relapsing seminoma patients had initially clinical stage I. This figure is considerably lower than the corresponding proportion of clinical stage I of 80% among unselected

Table 15.1. Localization of late recurrences

Primary histology	Study	Retroperitoneum (incl. retrocrural)	Mediastinum	Lung/Pleura	Neck/Supracl.	Pelvis	Others	All*
Non-seminoma	Borge et al. 1988	7	2	2	3			14
	Baniel et al. 1995	43	10	19	0	6	5	83
	Gerl et al. 1997	21	7	8	5			41
	George et al. 2003	51	8	21	7	12	21	120
	Dieckmann et al. 2005	49	6	8	6		3	72
	Oldenburg et al. 2006	8	1	4	1	2		16
	Sharp et al. 2006	57	9	15	8		24	113
	Geldart et al. 2006	14	2	6	4		6	32
	Total	250	45	83	34	20	59	491
		50.9%	9.2%	16.9%	6.9%	4.1%	12.0%	100.0%
Seminoma	Borge et al. 1988		4	1	2			7
	Dieckmann et al. 2005	32	8	0	4		3	47
	Oldenburg et al. 2006	2	5	1	3	1		12
	Total	34	17	2	9	1	3	66
		54.8%	27.4%	3.2%	14.5%	1.6%	4.8%	100.0%
	Both histologies	284	62	85	43	21	62	557
		51.0%	11.1%	15.3%	7.7%	3.8%	11.1%	100.0%

*Multiple sites of relapse have been detected in some patients, therefore the number of sites exceeds exceed the number of patients.

seminoma patients, indicating that these patients are less prone to develop late relapses than those with higher stages.

Adjuvant radiotherapy to the para-aortic and ipsilateral pelvic lymph nodes has been standard treatment of stage I seminoma during the last 50–60 years. However, applying radiotherapy to all patients with seminoma clinical stage I implies unnecessary treatment to 80% of patients who do not harbor retroperitoneal micro-metastases. It has been shown that small retroperitoneal metastases in these patients could be treated subsequently by radiotherapy or chemotherapy, when relapses are verified by CT scans. This is the rationale for surveillance. Principally, frequent follow-up visits are necessary during the first 2–3 years with decreasing frequency later on. Rete testis invasion and size of the primary tumor (>4 cm) were identified as significant risk factors for relapse. Of 638 stage I seminoma patients, Warde et al. (2002) reported 38 out of a total of 121 relapses to occur after 2 years, including six patients who relapsed after 6 years, with the latest relapse detected after 12 years.

Carboplatin as adjuvant treatment of clinical stage I seminoma in the 1980s was investigated by Oliver et al. (2005) who initiated a large randomized trial between single dose of carboplatin and radiotherapy. The 3 year relapse-free survival showed no significant difference (95.9% and 94.8%, respectively). Mirroring the surveillance series, retroperitoneal relapses dominated in the carboplatin-treated cohort. In this group the latest relapse was at 50 months; however, the median follow-up of 4 years is too short to conclude regarding the true risk of late relapse or long term efficacy of salvage multi-agent chemotherapy.

Aparicio et al. (2003) from the Spanish Collaborative Group applied a risk-adapted strategy: Patients without rete testis invasion and tumors <4 cm are followed by surveillance whereas those with one or both of these risk factors are treated with two cycles of carboplatin (400 mg/m^2 usually 3–4 weeks apart). The relapse-rate after carboplatin varied between 0% and 3.3% without any reported relapses after 28 months of treatment. However, median follow-up is still relatively short with a maximum of 52 months.

SEMINOMA CLINICAL STAGE >I

Presence of infra-diaphragmatic metastases only, that is CS II, usually prompts radiotherapy and/or chemotherapy. Preliminary data suggest the use of both treatment strategies as promising, in particular in patients with stage IIb, but confirmation by randomized trials is needed. In patients with infra-diaphragmal metastases <5 cm, relapses later than 3 years after radiotherapy are exceedingly rare. Bulky (>5 cm) metastases, however, might recur after radiotherapy. Three to four cycles of cisplatin-based chemotherapy (with or without bleomycin) thus has become the treatment of choice in patients with advanced seminoma CS II and CS III. After chemotherapy, residual masses <3 cm are usually not removed since they rarely comprise viable tumor. For larger persistent masses however, RPLND should be considered, although surgery is often complicated by extensive fibrosis. De Santis et al. (2004) suggested that positron emission tomography (PET) might guide the clinician whether or not viable tumor is present.

NONSEMINOMA CLINICAL STAGE I

Approximately, one third of late relapses in non-seminoma patients occur in initial CS I. Patients with clinical stage I are managed by surveillance, primary retroperitoneal lymph node dissection (RPLND), or adjuvant chemotherapy and survival approaches 100%. Prediction of occult metastases by vascular invasion and other risk factors like percentage >70% of tumor cells positive for MIB-1 proliferation staining, and >50% embryonal carcinoma usually prompts adjuvant treatment. The impact of these factors with respect to late relapses remains therefore uncertain.

Surveillance is often restricted to patients without any high-risk factors. Compliance is of utmost importance for this strategy, and most of the cancer-related deaths within these patients are due to nonadherence to the follow-up protocol. Shahidi et al. (2002) from the Royal Marsden Hospital reported 12 late relapses among 372 patients (3.2%). Also very late relapses, that is, 5 years after orchiectomy, may occur during surveillance.

Retroperitoneal metastases are identified in the RPLND specimen in 10–33% of unselected clinical stage I patients, and in 50% of patients with presence of vascular invasion. After primary RPLND by an expert surgeon <1% of patients will experience a late relapse, most of which do not arise from the retroperitoneal space. The extent of post-chemotherapy RPLND has an impact on the risk of subsequent relapses, (Figure 15.1); modified template RPLND excludes retroperitoneal residual masses less reliably than complete bilateral nerve-sparing template dissections as demonstrated by Carver et al. (2007) from the Memorial Sloan Kettering cancer Center. Teratoma is of particular importance in this setting because these slow-growing tumors are usually resistant to chemotherapy and radiotherapy. Although the risk of retroperitoneal teratoma increases by the proportion of these cells in the primary testicular tumor, absence of such cells does not preclude retroperitoneal teratoma. A primary RPLND is probably the most effective means to avoid late recurrences in the retroperitoneum, but variable inclusion criteria and short follow-up times hamper the comparability of late relapse risks according to different treatment modalities.

Laparoscopic RPLND in stage I non-seminoma appears promising with respect to short hospitalization time and few acute complications. However, exploration of the retroperitoneal space by this technique is not as safe as by an open approach. Unless proven to be noninferior with respect to late-relapses by randomized controlled trials against open RPLND, we caution against its routine use.

Adjuvant chemotherapy is usually reserved for high-risk non-seminoma CS I patients. Late relapses are rarely reported after this treatment. However, follow-up time is seldom sufficiently long to conclude on these late events. Potential drawbacks of this treatment comprise left-behind teratoma and selection of cisplatin resistant residual viable non-teratomatous MGCT cells. Shahidi et al. (2002) identified the presence of teratoma in excised tissues as the only factor predictive of late relapses in a multivariate logistic regression of data from 1,263 men with testicular cancer. Patients with pure teratoma or a high percentage of teratomatous elements in the orchiectomy specimen thus may benefit from a complete RPLND.

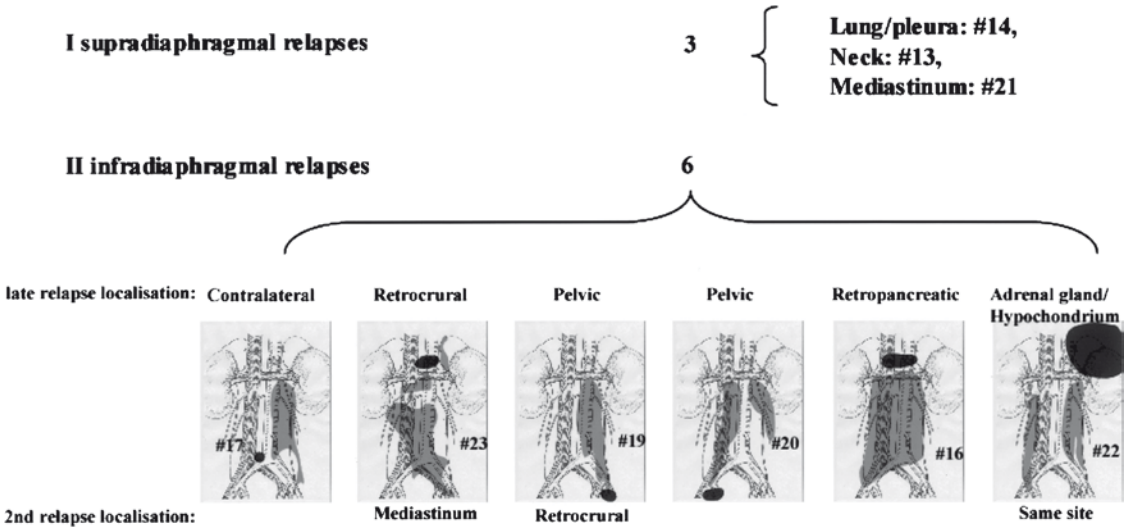

FIGURE 15.1. Late relapse sites of 9 non-seminoma TC patients after post-chemotherapy RPLND. Sketches show operation-fields/templates in *light grey* and site of first relapse in *dark grey*

In conclusion, the data presented here are not mature enough for a final recommendation of how late relapses are best avoided in CS I non-seminoma patients. Reliance on primary RPLND and adjuvant chemotherapy by cancer centers in the United States of America and Western European countries, respectively, inhibits large international studies comparing efficacy of both approaches with respect to late relapses.

NONSEMINOMA CLINICAL STAGE >I

Treatment in metastatic patients usually consists of cisplatin-based chemotherapy with or without surgery, although low stage II may be managed by RPLND only. Adjuvant chemotherapy after RPLND in pathological stage II may not confer any benefit as demonstrated by Fizazi et al. (2001). Elevated tumor markers or stage CS IIb should initiate chemotherapy and resection of residual masses rather than primary RPLND. Residual post-chemotherapy masses comprise complete necrosis, teratoma, or vital MGCT in 50–60%, 30–40%, and 5–20%, respectively.

Control of the retroperitoneal space, the most frequent site of late relapse, is important with respect to prevention of subsequent late relapses in metastatic non-seminoma patients. Post-chemotherapy nerve-sparing RPLND is technically more challenging than primary RPLND and should be performed by an experienced surgeon to ensure resection of all residual masses. Patients with no or very small (<2 cm) residual retroperitoneal metastases might not profit from post-chemotherapy RPLND, because the relapse rate is considered low. However, in a Norwegian series of 87 operated patients with residual retroperitoneal masses ≤2 cm, 33% had teratoma (27%) or vital MGCT

(6%) (five of six patients with vital MGCT had lesions ≤1 cm).

Again, extent of the resection is important, as selective removal of post-chemotherapy residual masses only, and not whole templates, might leave behind teratomatous elements with the potential of late recurrence. Timely removal of post-chemotherapy residual masses from extra-retroperitoneal sites is therapeutic in patients with teratoma and a subset of those with vital tumor and prevents subsequent relapses.

DETECTION AND DIFFERENTIAL DIAGNOSIS

Pain in the back or an abdominal tumor represent frequent symptoms in relapsing testicular cancer patients. In order to shorten the patient's -and doctor's delay, both the testicular cancer survivor himself and his general physician should be informed that late relapses may occur even many years after successful treatment.

Routine follow-up examinations may reveal late relapses incidentally. Elevated tumor markers, radiological findings or palpable masses are often the first steps towards the diagnosis of a late relapse. Our pooled analysis of 426 late relapsing patients showed elevated AFP and/or HCG in 207 (49%) 100 (24%) patients, respectively. In other words, at the time of late relapse every second and every fourth patient has elevated AFP and/or HCG.

No broad international consensus has been reached as to evidence-based follow-up recommendations of TC patients. The European Germ Cell Cancer Consensus Group found the literature not comprehensive enough to give such guidelines. Comprehensive and regularly updated information is found at the EAU website: http://www.uroweb.org or at the website of the American National Comprehensive Cancer Network (NCCN): http://www.nccn.org

Both expert groups agree on the following issues: Non-seminoma CSI patients under surveillance should be followed beyond 5 years by annual physical examinations, tumor marker control, and chest X-ray. However, concerning the length of follow-up, the recommendations are disparate: The EAU assumes 10 years of follow-up in CSI testicular cancer sufficient and recommends annual abdominal CT scans after 5 years only when regarded indicated. The NCCN encourages annual controls for the years 6+ including annual abdomino-pelvic CT scans in CS I non-semimoma.

Repeated CT scans of the abdomen can be omitted in the routine follow-up of non-seminoma patients who have undergone a RPLND. The same holds true for seminoma patients after dog-leg radiotherapy. However, pelvic recurrences in patients after the paraaortic strip technique occur, and follow-up of these patients should include pelvic CT scans. Ongoing abdomino-pelvic CTs should be taken during surveillance and after single agent carboplatin. The value of these CT images is considerably increased when previous pictures are available for comparison.

Imaging of malignant tissues by PET is based on an increased uptake of substances such as fluorodeoxyglucose (FDG). Germ cell tumors are usually fast-growing and characterized by a high FDG uptake, and PET differentiates reliably between necrotic and viable non-teratomatous malignant tumor. Late relapsing germ cell tumors are, as an exception from the rule, often slow-growing and PET might be less

suitable in this setting, especially because mature teratoma is not detected. In seminoma >3cm, De Santis et al. (2004) demonstrated PET to predict viable malignant tumor after chemotherapy more reliably than CT. PET should be suitable to detect late seminoma relapses. However, after eventual transition to non-seminoma/teratoma, or in case of small lesions, negative PET scans might not be reliable.

Non-seminoma patients harbor teratomatous residual post-chemotherapy masses in 25–44%. PET scans are, therefore, only of limited value for the decision whether or not residual lesions should be resected. However, in "marker-only" relapses, PET may localize their source and thereby guide planning of surgery.

Duration and frequency of follow-up in MGCT patients in order to detect late relapses is debated. The first systematic report by Terebelo et al. (1983) on patients with late relapsing MGCTs concluded that follow-up should be extended from the usual 2–5 years before cure can be stated. Subsequently, late relapses have been reported to occur even decades after primary treatment, and lifelong follow-up in all MGCT patients has been advocated by several authorities (Baniel et al. 1995; Gerl et al. 1997; George et al. 2003). One rationale behind a prolonged follow-up is to detect subclinical relapses before they advance further with subsequent diminished chances of cure. Patients with symptoms at late relapse had a three to four times lower chance of survival compared to those without symptoms (George et al. 2003). However, in a German report by Dieckmann et al. (2005) and a Norwegian series by Oldenburg et al. (2003, 2006) symptomatic patients did not fare worse than asymptomatic ones.

The rationale that earlier detected relapses represent a less advanced disease with a better prognosis is conceivable, although the data are not yet conclusive. Lifelong follow-up in all MGCT patients, however, will exceed the out-patient capacity of many cancer centers.

Until achievement of evidence-based recommendations, we assume follow-up of all patients for at least 10 years as reasonable. The following patients should be considered for lifelong follow-up: those with previous relapse after chemotherapy, those with high amounts of teratoma in the primary tumor, those with advanced disease, and those with primary EGGCT. Also, in patients in whom persisting residual tumor cannot be removed, which may be due to inoperability of patient or tumor, lifelong follow-up should be pursued.

Differential diagnoses in case of suspected late relapsing MGCT comprise: metastases from a new contralateral testicular cancer, a new primary EGGCT, somatic transformation of teratoma or a new non-germ cell malignancy. Differentiation between transformed teratoma and a new non-MGCT primary requires expert pathologists who should base their diagnosis on a representative presalvage biopsy and comparison with the primary specimen. Achievement of a representative presalvage biopsy is of great importance as the choice of appropriate treatment, and survival depends on it, as illustrated by Figure 15.2.

Teratoma is the most often encountered histological element in late relapsing MGCT patients. On CT, mature teratoma might appear as areas of soft tissue density sometimes combined with complex cysts, corresponding to sometimes observable slight AFP and/or HCG elevation by leakage of cystic fluid into the serum.

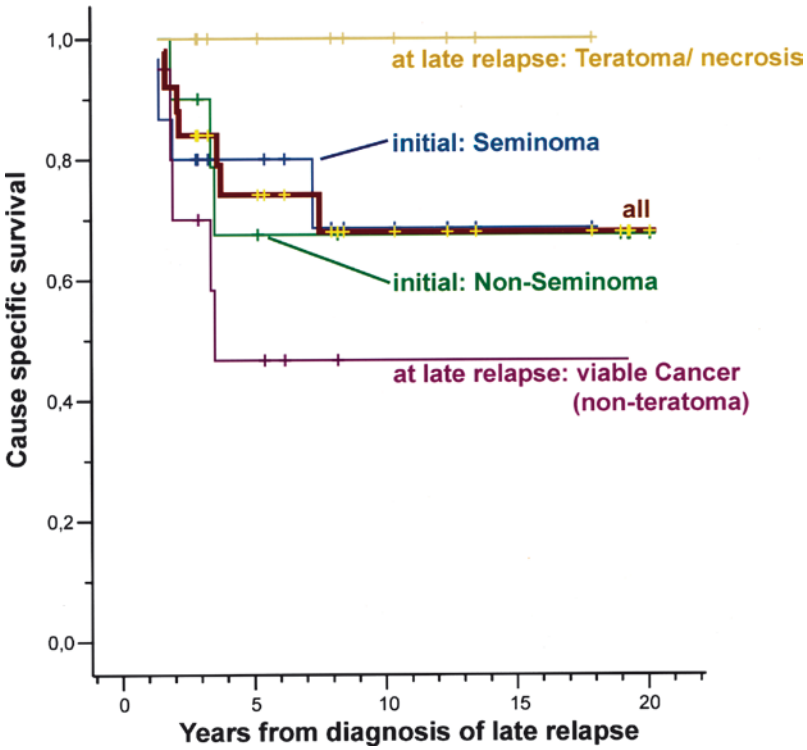

FIGURE 15.2. Cancer-specific survival after diagnosis of late relapse according to initial- and late relapse histology

Calcification and other more seldom radiographic findings are reviewed pictorially by Rutherford et al. (2006).

The histological diagnosis of teratoma is usually straightforward but can be complicated by somatic differentiation which is found in 3–9% of late relapsing patients after prior platinum-based chemotherapy. These non-MGCTs occur usually later than 2 years after treatment, and Michael et al. (2000) reported these histological types to be present in 23% of 91 late relapsing MGCT patients. Various sarcoma-subtypes, undifferentiated cancer, and adenocarcinoma are the most common types. Presence of isochromosome 12p reflects germ cell tumor clonality and might be used in case of uncertainty, because it is also found in late relapses. Yolk sac tumor might be found as often as in each second late relapsing MGCT. Its atypical appearances with glandular-, parietal-, clear cell-, or hepatoid pattern, however, may lead to underreporting in some cases (Figure 15.3). Virtually all other histological types which are encountered at initial diagnose may also be found at late relapse, including shift from seminoma to non-seminoma and, more seldom, vice versa.

TREATMENT AND SURVIVAL

Optimal treatment for the individual patient requires careful evaluation and planning by

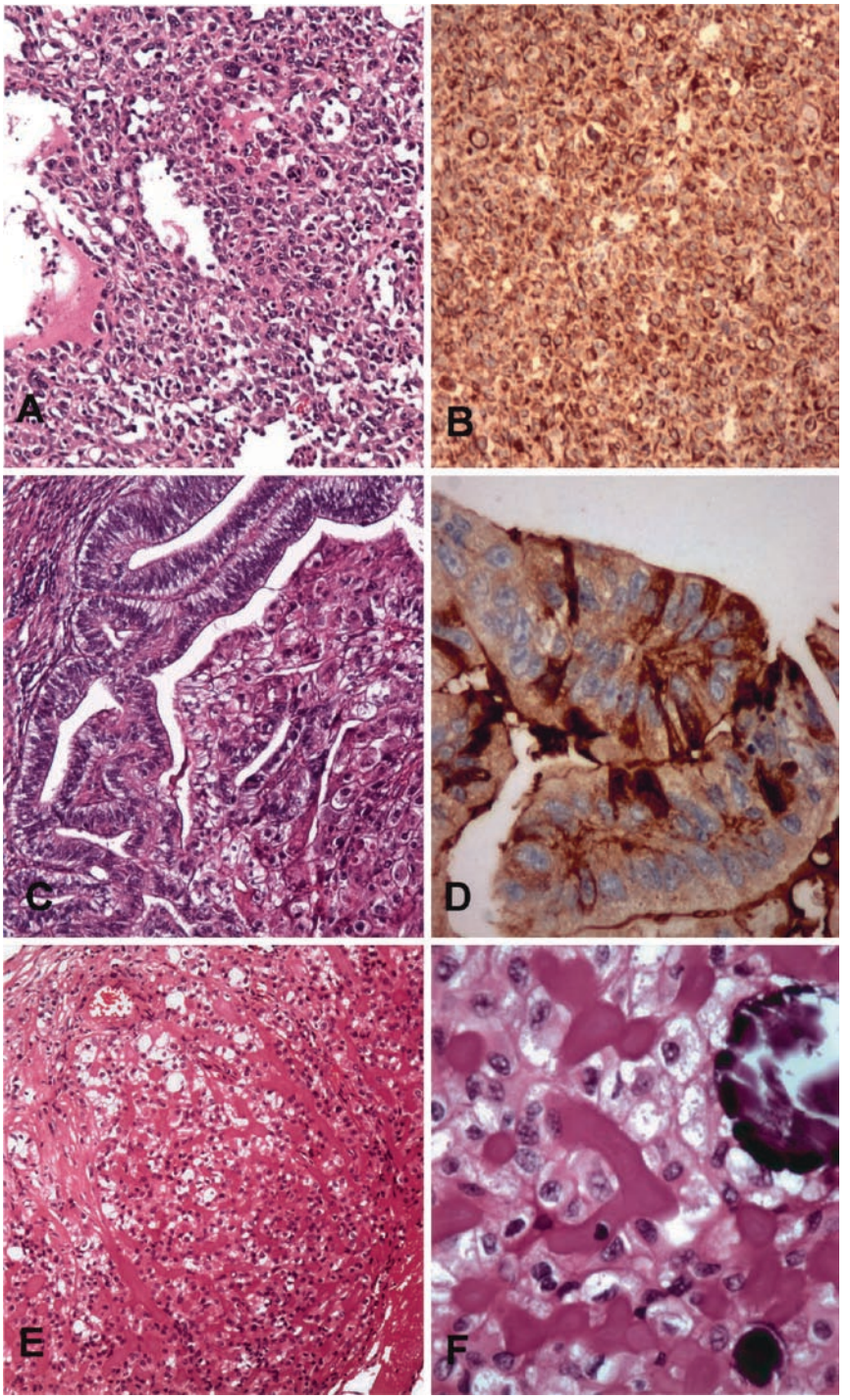

FIGURE 15.3. Histology of recurrent germinal cell tumors. (**a**) and (**b**) Undifferentiated carcinoma. (**a**) Hematoxylin and Eosin (HE); (**b**) Cytokeratin (AE1/AE3). (**c**) and (**d**) Yolk sac tumor with glandular pattern; (**c**) HE; (**d**) Alpha fetoprotein (AFP). (**e**) and (**f**) Yolk sac tumor with parietal pattern; HE (Photos by G.C. Alfsen, MD.PhD)

an experienced inter-disciplinary team of urological surgeons, oncologists, pathologists and radiologists and possibly also vascular, thoracic, orthopedic, and neurosurgeons. It has been shown that survival of poor prognosis patients is increased by treatment in high-volume centers. We are convinced that this rationale also applies to late relapsing patients.

Patients with late relapsing MGCT should be treated according to a representative pre-salvage biopsy. Teratoma may be found in both initial seminoma and non-seminoma and a cure is only achieved by a complete resection in these patients. In particular in patients with somatic differentiated teratoma a complete resection is the treatment of choice as salvage chemotherapy has only limited effect.

Seminoma

Late relapsing seminoma patients under surveillance are cured by radiotherapy, cisplatin-based chemotherapy or, more rarely, surgery. After radiation in seminoma CS I relapses occur nearly exclusively outside the prior radiation field and are usually cured by cisplatin-based chemotherapy. However, in case of inguinal localized relapse further radiation or pelvic lymph node dissection may be sufficient. Relapses following single agent carboplatin are mostly salvaged by cisplatin-based chemotherapy or by radiotherapy. Relapse after cisplatin-based chemotherapy in advanced seminoma is very rare. Approximately 50% of these patients are cured by alternative salvage chemotherapy. Salvage surgery should always be considered though it seems to be less often applied than in non-seminoma.

Non-seminoma

Surgery is considered the most important part of treatment in late relapsing previously chemotherapy treated non-seminoma patients and increases the chances of cure. Even patients with chemo-refractory germ cell tumors have a definitive chance to be cured by salvage surgery. Incomplete resection of viable residual tumor portends a poor prognosis. Repeated operations, due to incomplete resection of viable tumor, are technically very challenging and should probably best be avoided by ensuring that only surgeons with special expertise operate on relapsing patients. Chemotherapy-naïve patients appear to have the best chances to be cured, whereas the response to salvage chemotherapy in previously chemotherapy treated patients is usually low.

If chemotherapy is required a second time, alternative cytotoxic-agents should preferentially be used. The combination of paclitaxel, ifosfamide, and cisplatin (TIP) had been demonstrated to yield durable complete responses in 63–73% in patients with relapsed testicular cancer. Kondagunta et al. (2005) reported progression-free survival rates of 50% and 78% in late and early relapsing patients after four cycles of TIP and removal of resectable residual masses, respectively.

The enhanced experience in treatment of late relapsing MGCT patients combined with increased vigilance towards detection might have contributed to improving cure rates during the recent years (Baniel et al. 1995, 26%; Gerl et al. 1997, 36%; Shahidi et al. 2002, 69%; George et al. 2003, 47%; Dieckmann et al. 2005, 63%; Oldenburg et al. 2006, 68%; Sharp et al. 2006, 60%; Geldart et al. 2006, 75%).

In conclusion, MGCT patients suspected to have a late relapse should be referred to an experienced hospital for diagnosis and treatment. Such policy does not only provide the best chances of cure but enables also gathering of urgently required information regarding these rare tumors. Complete removal of post-chemotherapy residual retroperitoneal masses is an essential part of initial treatment. All MGCT patients should be followed-up for at least 10 years. Lifelong follow-up for the detection of late relapses is a controversial issue and may, in our view, be indicated in the following patients: those with previous relapse after chemotherapy, those with high amounts of teratoma and primary metastases, and in those with primary EGGCT.

These conclusions are based on 500 cases reported in several rather heterogeneous series during the last 20 years.

REFERENCES

Aparicio J, Garcia del Muro X, Maroto P, Paz-Ares L, Alba E, Saenz A, Terrasa J, Barnadas A, Almenar D, Arranz JA, Sanchez M, Fernandez A, Sastre J, Carles J, Dorca J, Guma J, Yuste AL, and Germa JR (2003) Multicenter study evaluating a dual policy of postorchiectomy surveillance and selective adjuvant single-agent carboplatin for patients with clinical stage I seminoma. Ann Oncol 14:867–872

Baniel J, Foster RS, Gonin R, Messemer JE, Donohue JP, and Einhorn LH (1995) Late relapse of testicular cancer. J Clin Oncol 13:1170–1176

Borge N, Fosså SD, Ous S, Stenwig AE, Lien HH (1988) Late recurrence of testicular cancer. J Clin Oncol 6:1248–1253

Carver BS, Shayegan B, Eggener S, Stasi J, Motzer RJ, Bosl GJ, and Sheinfeld J (2007) Incidence of metastatic nonseminomatous germ cell tumor outside the boundaries of a modified postchemotherapy retroperitoneal lymph node dissection. J Clin Oncol 25:4365–4369

De Santis M, Becherer A, Bokemeyer C, Stoiber F, Oechsle K, Sellner F, Lang A, Kletter K, Dohmen BM, Dittrich C, and Pont J (2004) 2–18fluoro-deoxy-D-glucose positron emission tomography is a reliable predictor for viable tumor in postchemotherapy seminoma: an update of the prospective multicentric SEMPET trial. J Clin Oncol 22:1034–1039

Dieckmann KP, Albers P, Classen J, De Wit M, Pichlmeier U, Rick O, Mullerleile U, and Kuczyk M (2005) Late relapse of testicular germ cell neoplasms: a descriptive analysis of 122 cases. J Urol 173:824–829

Fizazi K, Tjulandin S, Salvioni R, Germà-Lluch JR, Bouzy J, Ragan D, Bokemeyer C, Gerl A, Fléchon A, de Bono JS, Stenning S, Horwich A, Pont J, Albers P, De Giorgi U, Bower M, Bulanov A, Pizzocaro G, Aparicio J, Nichols CR, Théodore C, Hartmann JT, Schmoll HJ, Kaye SB, Culine S, Droz JP, and Mahé C (2001) Viable malignant cells after primary chemotherapy for disseminated nonseminomatous germ cell tumors: prognostic factors and role of post-surgery chemotherapy—results from an international study group. J Clin Oncol 19:2647–2657

Geldart TR, Gale J, McKendrick J, Kirby J, and Mead G (2006) Late relapse of metastatic testicular nonseminomatous germ cell cancer: surgery is needed for cure. BJU Int 98:353–358

George DW, Foster RS, Hromas RA, Robertson KA, Vance GH, Ulbright TM, Gobbett TA, Heiber DJ, Heerema NA, Ramsey HC, Thurston VC, Jung SH, Shen JZ, Finch DE, Kelley MP, and Einhorn LH (2003) Update on late relapse of germ cell tumor: a clinical and molecular analysis. J Clin Oncol 21:113–122

Gerl A, Clemm C, Schmeller N, Hentrich M, Lamerz R, and Wilmanns W (1997) Late relapse of germ cell tumors after cisplatin-based chemotherapy. Ann Oncol 8:41–47

Kondagunta GV, Bacik J, Donadio A, Bajorin D, Marion S, Sheinfeld J, Bosl GJ, and Motzer RJ (2005) Combination of paclitaxel, ifosfamide, and cisplatin is an effective second-line therapy for patients with relapsed testicular germ cell tumors. J Clin Oncol 23:6549–6555

Martin JM, Panzarella T, Zwahlen DR, and Chung P, Warde P (2007) Evidence-based guidelines for following stage 1 seminoma. Cancer 109: 2248–2256

Michael H, Lucia J, Foster RS, and Ulbright TM (2000) The pathology of late recurrence of testicular germ cell tumors. Am J Surg Pathol 24:257–273

Oldenburg J, Alfsen GC, Lien HH, Aass N, Waehre H, and Fossa SD (2003) Postchemotherapy retroperitoneal surgery remains necessary in patients with nonseminomatous testicular cancer and minimal residual tumor masses. J Clin Oncol 21:3310–3317

Oldenburg J, Alfsen GC, Waehre H, amd Fossa SD (2006) Late recurrences of germ cell malignancies: a population-based experience over three decades. Br J Cancer 94:820–827

Oliver RTD, Mason MD, Mead GM, von der Maase H, Rustin GJS, Joffe JK, de Wit R, Aass N, Graham JD, Coleman R, Kirk SJ, and Stenning SP (2005) Radiotherapy versus single-dose carboplatin in adjuvant treatment of stage I seminoma: a randomised trial. Lancet 366:293–300

Rutherford E, Ferguson J, Geldart T, Mead G, Smart J, and Tung K (2006) Late relapse of metastatic non-seminomatous testicular germ cell tumours. Clin Radiol 61:907–915

Shahidi M, Norman AR, Dearnaley DP, Nicholls J, Horwich A, and Huddart RA (2002) Late recurrence in 1263 men with testicular germ cell tumors. Multivariate analysis of risk factors and implications for management. Cancer 95:520–530

Sharp DS, Carver BS, Eggener SE, Kondagunta GV, Motzer RJ, Bosl GJ, and Sheinfeld J (2006) Clinical outcome of patients managed for late relapse of germ cell tumor. J Clin Oncol 24:4550

Terebelo HR, Taylor HG, Brown A, Martin N, Stutz FH, Blom J, and Geier L (1983) Late relapse of testicular cancer. J Clin Oncol 1:566–571

Warde P, Specht L, Horwich A, Oliver T, Panzarella T, Gospodarowicz M, and von der Masse H (2002) Prognostic factors for relapse in stage I seminoma managed by surveillance: a pooled analysis. J Clin Oncol 20:4448–4452

Part II
Head and Neck Cancer

16
Head and Neck Squamous Cell Carcinoma: Therapy with Fusaric Acid/Paclitaxel

Brendan C. Stack Jr., Brett Clarke, Joshua McElderry, Yeumeng Dai, and Jian-Hui Ye

INTRODUCTION

Head and neck squamous cell cancer (HNSCC) accounts for 3% of new cancer cases and 2% of cancer mortality annually in the United States (Jemal et al. 2007). Globally, HNSCC affects >500,000 patients each year, making it the 6th in incidence and the 7th in mortality in the world (Parkin et al. 2001, 2005). The chance of recurrence of advanced stage HNSCC within 2 years of treatment is > 50%. The risk of death from a second primary cancer in patients with early-stage HNSCC is higher than the risk of dying of the original primary tumor (Carew and Shah 1998). The risk of developing a second primary increases 3% per year of survival following diagnosis and treatment of the first head and neck cancer.

Across races, head and neck cancer has demonstrated slight decreased incidence except among American Indian males for laryngeal cancer and Asian/Pacific Islander males for oropharyngeal cancer (Edwards et al. 2005). Current treatment options for most head and neck cancers continue to be surgical excision with or without radiation, radiation alone, or chemotherapy with radiation depending on location, stage of disease, and patient preference. While advances have been made in the delivery of treatment, especially in the field of radiation oncology and chemotherapy, little change has been seen in the overall survival of head and neck cancer patients for decades (Jemal et al. 2007). Currently, no effective single agent chemotherapy treatment regimen is available for head and neck cancer. Additionally, oral chemotherapy is currently limited in its use, usually as second or third line therapy or in a clinical trial.

A NEW CLASS OF AGENTS FOR HEAD AND NECK CANCER?

Mycotoxins are highly toxic compounds produced by fungi usually for the purposes of self-defense or to dissolve cell membranes as part of their fungal pathogenicity. Fusaric acid (FA), a physiologic metabolite of tryptophan and picolinic acid, is produced by Fusarium species as a mycotoxin. The fungal source of FA most commonly results from infection of cereals crops or other agricultural commodities as they spoil in moist conditions.

Also known as 5-butlypicolinic acid, FA has been reported to have many effects within the human host (Wang and Ng 1999). Fusaric acid raises serum melatonin, 5-hydroxytryptamine, tyrosine, and dopamine. These increases are thought to be from FA inhibition of tyrosine hydroxylase and dopamine beta-hydroxylase. Fusaric acid has been shown to have an anti-hypertensive effect from a reduction of peripheral vascular resistance through peripheral arteriolar vasodilation.

Fusaric acid reduces catecholamine synthesis in lymphocytes, which may affect their cytotoxic activity on solid tumors, and it also has been shown to induce DNA damage in vitro in cultured larynx cancer cells. It is cytostatic to human fibroblasts and cytotoxic to colon and mammary adenocarcinomas and epidermoid carcinoma. Picolinic acid (PA), a precursor carboxylic acid of FA, has been shown to be cytotoxic to many malignancies as well (Fernandez-Pol et al. 1993). However, FA consumption may also be a risk factor for esophageal cancer (Voss et al. 1999).

A NEW TARGET IN THE HEAD AND NECK CANCER CELL?

DNA binding by zinc finger proteins (ZFPs), their possible intranuclear functions and their modulation of the cell cycle has led us to pursue investigation of metallopanstimulin (MPS) as a possible ZFP involved in control of HNSCC. Metallopanstimulin, detected in tissue and sera of HNSCC patients, is a promising marker of this disease (Stack et al. 2000; Wadsworth et al. 2004). This worker has been studied in thousands of patients by radioimmuno assay, antibody indicator tests, and mass spectroscopy and has consistently been elevated in HNSCC patients when compared to controls. Not only is MPS a putative marker of HNSCC, but also it is felt to be a possible effector molecule in the neoplasia.

Metallopanstimulin-1 (MPS-1) was identified, cloned and characterized from a cDNA library constructed from a human mammary carcinoma cell line (MDA-468) that was stimulated by the growth factors TGF-B1 and EGF in the presence of cyclohexamide (Fernandez-Pol et al. 1994). It is a multifunctional gene product that is homologous to the rat S27 (Fernandez-Pol 1996). Metallopanstimulin-1 is a 10 kD ribosomal subunit ZFP that is present in all tissues and expressed in increased quantities in a wide spectrum of proliferating tissues and oncogenic processes (Ganger et al. 2001).

Observation of elevations MPS in HNSCC samples and its structure/function as a ZFP have led some to the hypothesis that compounds that interact with ZFP's such as MPS might prove to be potential new chemotherapeutic agents for HNSCC and other malignancies. A class of carboxylic acids derived from nicotinic acid (PA and FA) that are physiologically present can chelate divalent cations. Chelation of divalent cations (Zn, Ca, Cu, Se, etc.) rob metalloproteins of their catalytic core, changing their three dimensional structure, and theoretically impairing or disabling their functional activity.

Because many metalloproteins (e.g., MPS) are involved in DNA repair and promotion of ongoing cell growth and proliferation (Kalenik et al. 1997; Medici et al. 1999; Yuan et al. 2001), and are known to be elevated in HNSCC, chelation may be an alternative means of inducing

cellular arrest, if not apoptosis. This might be accomplished by administration of supra-physiologic amounts of one of these carboxylic acids.

EVIDENCE FOR FURAIC ACID AS A NEW HEAD AND NECK CANCER THERAPY

Fusaric acid has demonstrated antitumorigenic activity in non-epidermoid carcinomas such as adenocarcinoma and hepatocellular carcinoma (Fernandez-Pol et al. 1993; Ogata et al. 2001). Our data demonstrate a suppressive effect of FA upon two HNSCC lines (Hep-2 and UMSCC-1) as measured by two modalities in vitro (Stack et al. 2004a, b). We have also demonstrated that fusaric acid reduces cell populations and increases apoptosis when compared to controls. These findings have now been observed in six head and neck cancer cell lines. Additionally, in a docetaxel resistant head and neck cancer cell line, FA demonstrates a concentration driven suppression of cell growth. Fusaric acid changes cell cycle dynamics resulting in cell cycle arrest or cell death when compared to control (Figure. 16.1). Flow cytometry observations from FA treatment in vitro include: G1 arrest, decreased mitosis, a shortened G2 phase, and an increased G0 peak.

Follow up studies with FA in an in vivo model support the initial in vitro observations cited above. Intralesional injection of HNSCC tumor xenografts into balb-c nude mice treated with FA demonstrate decreased tumor size (by weight) and increased latency time to appearance (Figure. 16.2). These findings were also observed when FA was administered enterally in the same mouse model orally administered FA when combined with parenteral taxol (Figure. 16.3) or carboplatin also

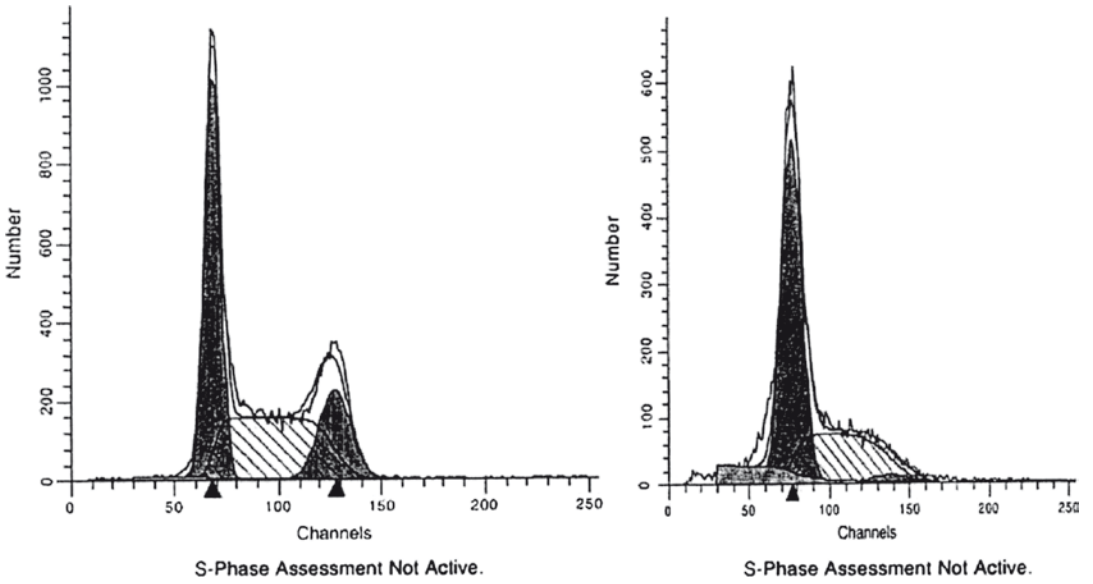

FIGURE 16.1. Changes in flow cytometry profiles between control and FA treated UMSCC-1 head and neck cancer cell line at 72 h

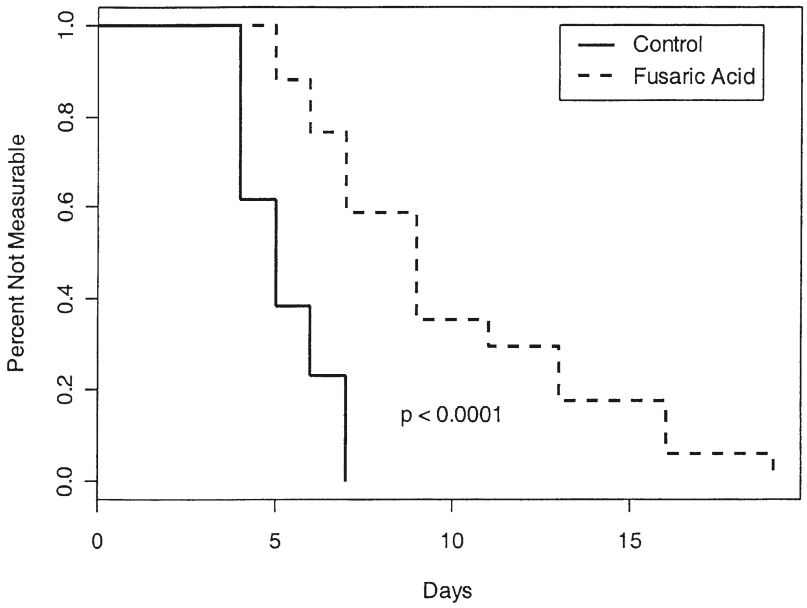

FIGURE 16.2. Kaplan–Meier plots of day of first measurable tumor (5 mm^3), control vs. FA intralesional injection treatment

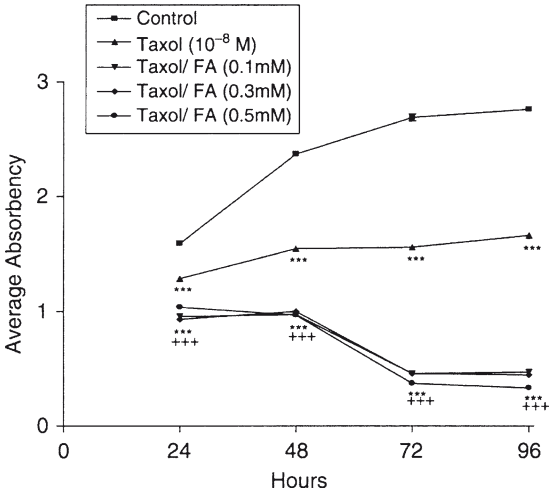

FIGURE 16.3. Growth of SCC-1 cells, as determined by the MTS assay subjected to paclitaxel (10^{-8} M) (taxol) and/or fusaric acid (0.1, 0.3, 0.5 mM) (FA) over a 96 h period. Drugs or an equivalent volume of sterile water (control) were added 24 h after seeding 1000 cells/well into 96-well micro test plates; media and drugs were replace daily. Values represent mean absorbencies + SE for 6 wells/treatment at each time point. Significantly different from controls at $P<0.001$ (***). Significantly different from taxol treated cultures at $P < 0.001$ (+ + +).

show a greater tumor suppression than either parenteral agent administered alone.

These initial experiments demonstrate a promising new area of research upon a novel class of agents with activity against an aggressive form of carcinoma. Although its exact mechanism is still unknown, FA is thought to be active by increasing damage to DNA and preventing its synthesis and repair (Fernandez-Pol et al. 1993). This may be in part from chelation of divalent cations from catalytic metalloproteins. Chelation as a mechanism has been observed as the effect of other compounds upon cancer (Cox et al. 2003). They reported tetrathiomolybdate chelates copper from proangiogenic molecules thereby causing a reversible growth arrest in squamous cell carcinoma (SCC) in vitro. This is felt to be a result of a decreased vascular proliferation within the tumor bed. Conversely, chelation has also been shown to activate proangiogenic genes including vascular endothelial growth factor (VEGF)

in other models (Rapella et al. 2002). We have also observed many cytokine changes induced by FA which may also explain its cytostatic or cytocidal effects.

Fusaric acid has been previously shown to induce cell cycle arrest and even apoptosis in some cell lines (Ogata et al. 2001; Stack et al. 2004a). We also observed significant apoptosis in HEP-2 cells which was time period and concentration dependent. Interestingly, UMSCC-1 tumor cells did not demonstrated apoptotic activity on terminal nick end label (TUNEL) assay. Portier et al. (2006) compared the use of flow cytometry to TUNEL and other methods of evaluating for apoptosis in brain tissue. They suggested that flow cytometry had greater sensitivity and specificity than enzyme-linked immunoassays, electrophoresis, or TUNEL. They noted that TUNEL has produced false- positive staining. None of the methods for identifying apoptosis were considered equivalent. It is possible in our study that improved ability of flow cytometry to identify apoptotic cells accounted for the significant levels observed in vitro. Unexpectedly, in vitro exposure to fusaric acid promotes apoptosis and proangiogenic VEGF production. This in vitro response did not, however, translate into increased angiogenesis in vivo as seen by CD 34 histochemical staining. Shang et al. (2007) recently reported positive correlation of VEGF expression to increased microvascular density, tumor metastatic activity, and stage in oral SCC (Li et al. 2005). Shieh et al. (2004) observed that tumor cells can actually function as endothelial cells, providing vascular access to the tumor.

Tarceva has well documented anticancer activity in EGFR positive cancers (Cohen et al. 2005). It has been shown effective against HNSCC in combination with radiation or as a single agent second line therapy. We saw a strong antitumorigenic activity in vivo from TA and combination FA + TA. No significant differences was appreciated between FA, TA, or FA + TA groups making it difficult to account for or discount FA involvement in this antitumor response. Additionally, power analysis from prior data suggests a larger sample size is needed for a power of 80% or greater. A larger number of FA and FA + TA treated mice may have demonstrated significant difference in tumor weights from control.

In summary, fusaric acid appears to be tumoristatic and tumoricidal in vitro and in vivo models of HNSCC, respectively. Its novel mechanism provides an alternative to present therapies. Fusaric acid has an effect as a single agent when injected or ingested. It has synergy with conventional parenteral agent's taxol and carboplatin. It has shown effect in resistant cell lines which may offer the possibility of its use in the setting of treatment failure. Study of oral FA in combination with another oral agent with EGF inhibition has failed to show synergism thus far. Further investigations including FA mechanism and toxicity are being conducted in anticipation of phase I/II research with this novel compound.

REFERENCES

Carew JF, Shah JP (1998) Advances in multimodality therapy for laryngeal cancer. CA Cancer J Clin 48:211–228

Cohen MH, Johnson JR, Chen YF, Sridharo R, and Pazdur R (2005) FDA drug approval summary: Erlotinib (Tarceva) tablets. Oncologist 10:461–466

Cox C, Merajver SD, Yoo S, Dick RD, Brewer GJ, Lee JS-L, and Teknos TN (2003) Inhibition of the growth of squamous cell carcinoma by tetrathiomolybdate-induced copper suppression in a murine model. Arch Otolaryngol 129:781–785

Edwards BK, Brown ML, Wingo PA, Howe HL, Ward E, Ries LAG, Schrag D, Jamison PM,

Jemal A, Wu XC, Friedman C, Harlan L, Warren J, Anderson RN, and Pickle LW (2005) Annual report to the nation on the status of cancer, 1975–2002, featuring population-based trends in cancer treatment. J Natl Cancer Inst 97:1407–1427

Fernandez-Pol JA, Klos DJ, and Hamilton PD (1993) Cytotoxic activity of fusaric acid on human adenocarcinoma cells in tissue culture. Anticancer Res 13:57–64

Fernandez-Pol JA, Klos DJ, and Hamilton PD (1994) Metallopanstimulin gene product produced in a baculovirus expression system is a nuclear phosphoprotein that binds to DNA. Cell Growth Differ 5:811–825

Fernandez-Pol JA (1996) Metallopanstimulin as a novel tumor marker in sera of patients with various types of common cancers: implications for prevention and therapy. Anticancer Res 16:2177–2185

Ganger DR, Hamilton PD, Klos DJ, Jakate S, McChesney L, and Fernandez-Pol JA (2001) Differential expression of metallopanstimulin/S27 ribosomal protein in hepatic regeneration and neoplasia. Cancer Detect Prev 25:231–236

Jemal A, Siegel R, Ward E, Murray T, Xu J, Thun MJ (2007) Cancer statistics. CA Cancer J Clin 53:5–26

Kalenik JL, Chen D, Bradley ME, Chen SJ, and Lee TC (1997) Yeast two-hybrid cloning of a novel zinc finger protein that interacts with the multifunctional transcription factor YY1. Nucleic Acids Res 25:843–849

Li C, Shintani S, Terakado N, Klosek SK, Ishilawa T, Nakashio K, and Hamakawa H (2005) Microvessel density and expression of vascular endothelial growth factor, basic fibroblast growth factor, and platelet-derived endothelial growth factor in oral squamous cell carcinomas. Int J Oral Maxillofac Surg 34:559–565

Medici N, Abbondanza C, Nigro V, Rossi V, Piluso G, Belsito A, Gallo L, Roscigno A, Bontempo P, Puca AA, Molinari AM, Moncharmont B, and Puca GA (1999) Identification of a DNA binding protein cooperating with estrogen receptor as RIZ (retinoblastoma interacting zinc finger protein). Biochem Biophys Res Commun 264:983–989

Ogata S, Inuoe K, Iwata K, Koumura K, and Tagichi H (2001) Apoptosis induced by picolinic acid related compounds in HL-60 cells. Biosci Biotechnol Biochem 65:2337–2339

Parkin DM, Bray F, Ferlay J, and Pisani P (2001) Estimating the world cancer burden: Globocan 2000. Int J Cancer 94:153–156

Parkin DM, Bray F, Ferlay J, and Pisani P (2005) Global cancer statistics, 2002. CA Cancer J Clin 55:74–108

Portier BP, Ferrari DC, and Taglialatela G (2006) Rapid assay for quantitative measurement of apoptosis in cultured cells and brain tissue. J Neurosci Methods 155:134–142

Rapella A, Negrioli A, Melillo G, Pastprino S, Varesio L, and Bosco MC (2002) Flavopiridol inhibits vascular endothelia growth factor production induced by hypoxia or picolinic acid in human neuroblastoma. Int J Cancer 99:658–664

Shang ZJ, Li JR, and Li ZB (2007) Upregulation of serum and tissue vascular endothelial growth factor correlates with angiogenesis and prognosis of oral squamous cell carcinoma. J Oral Maxillofac Surg 65:17–21

Shieh YS, Lee HS, Shiah SG, Chu YW, Wu CW, and Chang LW (2004) Role of angiogenic and non-angiogenic mechanisms in oral squamous cell carcinoma: correlation with histologic differentiation and tumor progression. J Oral Pathol Med 33:601–606

Stack BC Jr, Dalsaso TA, Lee C Jr, Lowe VJ, Hamilton PD, Fletcher JW, and Fernandez-Pol JA (2000) Overexpression of MPS antigens by squamous cell carcinomas of the head and neck: Immunohistochemical and serological correlation with FDG positron emission tomography. Anticancer Res 19:5503–5510

Stack BC Jr, Hansen JP, Ruda JM, Jaglowski J, Shvidler J, and Hollenbeak CS (2004a) Fusaric acid: a novel agent and mechanism to treat HNSCC. Otolaryngol Head Neck Surg 131:54–60

Stack BC Jr, Hollenbeak CS, Lee CM, Dunphy FR, Lowe VJ, and Hamilton PD (2004b) Metallopanstimulin as a marker for head and neck cancer. World J Surg Oncol 2:45

Voss KA, Porter JK, Bacon CW, Meredith FI, and Norred WP (1999) Fusaric acid and modification of the subchronic toxicity to rats of fumonisins in F. moniliforme culture material. Food Chem Toxicol 37:853–861

Wadsworth JT, Somers KD, Cazares LH, Adam B-L, Malik G, Stack BC Jr, Semmes OJ, and Wright GL Jr (2004) Identification of head

and neck cancer patients using serum protein profiles. Arch Otolaryngol Head Neck Surg 130:98–104

Wang H, Ng TB (1999) Pharmacological activities of fusaric acid (5-butylpicolinic acid). Life Sci 65(9):849–856

Yuan Z, Huang X, Zhang W, Zhang M, Wan T, and Cao X (2001) Cloning and characterization of a novel zinc finger protein (MDZF) that is associated with monocytic differentiation of acute promyelocytic leukemia cells. J Cancer Res Clin Oncol 127:659–667

17
Early Stage Oral Squamous Cell Carcinoma: Use of Signal Transducer and Activator of Transcription 3 as a Risk Factor for Poor Diagnosis

N.G. Shah and T.I. Trivedi

INTRODUCTION

Head and neck cancer accounts for 5–10% of all tumors, and cancer of the oral cavity accounts for 30% of all head and neck cancers. Currently, nodal status is the single most important clinical prognostic indicator for survival. While the 5 year survival of patients with T1 and T2 disease in the absence of nodal disease can be as high as 70–80%, and 50–60% in patients with T3 and T4 disease in the absence of nodal disease, the 5 year survival drops by half in the presence of nodal disease to 25–30%. Thus, new diagnostic attempts are aimed to establish parameters leading to improved survival of patients with oral cancer that is predominantly squamous cell type in nature.

Oral squamous cell carcinoma (OSCC) is a molecular disease involving accumulation of genetic alterations. Even the normal appearing mucosa may have accumulated premalignant genetic changes that 'condemn' it to the formation of cancer. Hence, identification of these early genetic alterations in the tissue would enhance our understanding of the biology of oral carcinogenesis, facilitating diagnosis of early stage OSCC and thereby design therapies that specifically target oral tumor cells. Recently, it was reported by Darnell (2002) that a wide array of oncogenic alterations may exert their effect by stimulating a relatively limited number of transforming factors, overactivity of which represents the point of convergence of multiple cancer related molecular and signaling alterations. In this context, it was reported by Song and Grandis (2000) that constitutive activation of family of transcription factors known as Signal Transducers and Activators of Transcription (STATs) directly contribute to the progression of head and neck squamous cell carcinoma (HNSCC) and hold great promise for the development of more rational and effective treatment. The focus of the current chapter is STAT3 in OSCC, as a risk factor for poor diagnosis with special emphasis on the methodological approaches employed for studying STAT3 expression, although not in use clinically, but nevertheless plays a crucial role in the development of oral carcinogenesis.

SIGNAL TRANSDUCERS AND ACTIVATORS OF TRANSCRIPTION

It was reported by Clavin (2002) that Darnell's team first identified STAT genes in 1992. They code for a set of proteins often referred to as latent cytoplasmic transcription factors. It was reported by Darnell (1997) that STATs were named by virtue of their novel and unique dual functions: as cytoplasmic signaling proteins that transmit a signal from the cell surface to the nucleus and as nuclear transcription factors that directly participate in gene regulation by activating a diverse set of genes. It was reported by Calo et al. (2003) that the STAT family in human consists of seven different members (STAT1, STAT2, STAT3, STAT4, STAT5a, STAT5b, and STAT6) identified in three chromosomal clusters: STAT1 and STAT4 map on chromosome 2, STAT2 and STAT6 on chromosome 12, and STAT3 and STAT5a and 5b on chromosome 17. Despite functional differences of individual STAT proteins, according to crystallographic studies and protein sequence, STAT proteins are made up of ~850 amino acids except for STAT2 and STAT6 that have amino acids between 750 and 800 and range in size from 90 to 115 kDa. Further, it was reported by Nikitakis et al. (2004) that STAT proteins share distinct structural domains and the sequence of STAT domains from the amino (NH2) to the carboxyl (COOH) end of the molecule are as follows: NH2-terminal, coiled coil, DNA binding, linker, Src-homology 2 (SH2) and carboxyl-terminal transactivation domains, each of which is important for specific physiological functions of these proteins.

NH2-Terminal Domain This region is highly conserved, provides protein–protein interaction sites and is required for the dimer–dimer interactions to form tetramers or oligomers of STAT molecules. It was reported by John et al. (1999) that the tetramerization of STAT contributes to stabilize the STAT-DNA binding by means of the interaction with tandemly arranged low-affinity binding sites; thus, increasing transcriptional activity. Furthermore, it was reported by Strehlow and Schindler (1998) that the NH2-terminal domain may regulate nuclear translocation and STAT deactivation further controlling transcriptional activity of activated STAT molecules.

Coiled Coil Domain It is a four-stranded helical structure located in the region of STATs between residues 130 and 315. It was reported by Nikitakis et al. (2004) that this domain interacts with potentially important regulatory proteins and other transcriptional factors.

DNA Binding Domain It is located in the region of STATs between amino acids 320 and 475 and is structurally very similar to the immunoglobulin-like DNA binding domain. It was reported by Darnell (1997) that this domain enables STATs interaction with specific response elements within the promoter sequence of target genes.

Linker Domain It was reported by Chen et al. (1998) that this α-helical linker with yet unknown function spans conserved residues 488 to 576 between the DNA binding and SH2 domains. However, it was reported by Nikitakis et al. (2004) that this domain might be implicated in DNA binding stability and transcriptosome assembly.

SH2 Domain It is located in the region of STATs, between the amino acid residues

600 and 700. It was reported by Shuai (1999) that this domain is required for the recruitment of STATs to phosphorylated receptors and for the reciprocal SH2-phosphotyrosine interactions between monomeric STATs to form dimers. The binding of STATs to the receptor occurs through the interaction of the STAT SH2 domain with the phosphorylated tyrosine present in the receptor docking site. Furthermore, it was reported by Becker et al. (1998) that the differences in the STAT SH2 domain bring about selectivity of the STAT proteins binding to the different cytokine receptors.

Transactivation Domain It is located at the C-terminal region of STAT, between residues 661 and 851, and is involved in communication with transcriptional complexes. It is reported by Calo et al. (2003) that a conserved serine in this STAT domain (except for STAT2 and STAT6, which have no such serine) is a phosphorylation site and may enhance the DNA binding affinity and transcriptional activity of certain STATs.

ACTIVATION OF SIGNAL TRANSDUCERS AND ACTIVATORS OF TRANSCRIPTION SIGNALING

In the non-stimulated cells, STAT proteins exist in the cytoplasm as monomers or NH2-terminal head to head dimers. Moreover, all members of the STAT family are not activated simultaneously but rather in varying combinations depending on the activating ligand and the physiological requirements. It was reported by Darnell (1997), and Bromberg and Darnell (2000) that the STAT activation process occurs typically in response to extracellular signaling proteins including growth factors, cytokines, hormones, and peptides acting through cytokine receptors or intrinsic receptor tyrosine kinases, and involves the transformation of a latent cytoplasmic protein to an active molecule capable of translocating to the nucleus and inducing transcription of specific target genes. The first step in this series of cellular events is initiated by interaction between extracellular signaling protein and its cognate receptor causing receptor dimerization or oligomerization. Ligand induced receptor stimulation results in kinase induced phosphorylation of tyrosine residues within the cytoplasmic tail of the receptor, thereby creating docking sites for recruitment of molecules recognizing phosphotyrosine via their phosphotyrosine binding domain or SH2 domain. It was reported by Chen et al. (1998) that STAT proteins become activated by phosphorylation on a single tyrosine, near residue 700. This event causes dissociation of STATs and formation of immediate homo- or hetero- dimers via reciprocal interaction between the SH2 domain of one monomer and the phosphorylated tyrosine domain of the other. These activated dimers translocate in the nucleus, recognize specific DNA response elements in the promoters of target genes, bind to them, and activate transcription. It was reported by Haspel et al. (1996) that STAT proteins are subsequently inactivated by tyrosine dephosphorylation and return to the cytoplasm.

It was reported by Bromberg et al. (1999) that the ligand dependent activation of STATs is often associated with differentiation and/or growth regulation, while constitutive activation of STATs (i.e., activation without known requirements for

extracellular polypeptides) is associated with growth deregulation. Depending on their specific functions, STATs can be divided into two groups. One group comprises of STAT2, STAT4, and STAT6, which are activated by a small number of cytokines and play a distinct role in the development of T-cells and in interferon-γ signaling. The other group includes STAT1, STAT3, and STAT5, activated in different tissues by means of a series of ligands, and involved in interferon signaling, development of mammary gland and response to growth hormone, and embryogenesis, respectively. It was reported by Bromberg (2002) that this latter group of STATs plays an important role in controlling cell-cycle progression and apoptosis, and thus contributes to oncogenesis. In addition, it was reported by Garcia and Jove (1998) that tumor cell lines as well as tissues from human cancers contain constitutively activated STAT proteins, very frequently STAT3. Hence, STAT3 might be considered as molecular marker for early detection of certain types of cancers, and also as a prognostic indicator for determining tumor aggressiveness and response to various treatments.

SIGNAL TRANSDUCER AND ACTIVATOR OF TRANSCRIPTION 3

It was reported by Wegenka et al. (1994) that originally STAT3 was termed acute-phase response factor (APRF) because it was first identified as a DNA binding activity within interleukin-6 stimulated hepatocytes that was capable of selectively interacting with an enhancer element in the promoter of the acute-phase response genes. It is located on human chromosome 17q21.2. Structurally, STAT3 is similar to other STAT proteins, having conserved NH2-terminal domain, DNA binding domain, SH2 domain, and a C-terminal domain. It is activated by tyrosine phosphorylation at a single site close to the C-terminus (Tyr705), as well as by serine phosphorylation at a site within the transactivation domain (Ser727). It was reported by Caldenhoven et al. (1996) that STAT3 contains a splice variant, STAT3β. Compared to wild-type STAT3, STAT3β has seven new amino acids and lacks an internal domain of 50 base pairs from the C-terminal of STAT3. This splice product is a naturally occurring isoform of STAT3 and encodes a 80 kDa protein which also lacks the Ser727 phosphorylation site.

PHYSIOLOGICAL ROLE OF SIGNAL TRANSDUCER AND ACTIVATOR OF TRANSCRIPTION 3

The exact function of STAT3 is difficult to define because it was reported by Takeda et al. (1997) that in knockout mice the embryos die early during embryogenesis before reaching the gastrulation stage. Nevertheless, it was reported by Akira (2000) that STAT3 might be essential for early embryonic development, possibly involved in gastrulation or visceral endoderm function. From in vitro studies, it was reported by Sano et al. (1999) that STAT3 plays an important role in migration of skin epidermic cells, and is essential for skin remodeling (e.g., during the hair cycle and wound-healing processes). In addition, it was reported by Chapman et al. (1999) that STAT3 is involved in the involution of the post-lactating mammary gland, an apoptotic process involving the epithelial

cells and resulting from an increased level of the insulin-like growth factor binding protein-5. Subsequently, it was reported by Akira (2000) that STAT3 plays a crucial role in a variety of biological functions, including cell growth, suppression and induction of apoptosis, and cell motility.

SIGNAL TRANSDUCER AND ACTIVATOR OF TRANSCRIPTION 3 IN ONCOGENESIS

It was first reported by Yu et al. (1995) that constitutive activation of STAT3 was linked to Src oncoprotein, a non-receptor phosphotyrosine kinase. In subsequent studies, it was reported by Catlett-Falcone et al. (1999), and Song and Grandis (2000) that v-Abl and v-Src transformed cell lines and tumors show constitutive activation of STAT3. These studies suggested that deregulation of STAT3 signaling due to aberrant activation of protein tyrosine kinases by specific classes of oncoproteins contributes to oncogenesis by eliciting permanent alterations in cells' genetic programs such as cell differentiation, proliferation, and apoptosis. However, it was reported by Bromberg et al. (1999) that STAT3 assumes the role of a true protooncogene, providing the first genetic evidence, through experiments with a constitutively active mutant of STAT3 (STAT3C) capable of inducing malignant transformation in fibroblasts. It was reported by Buettner et al. (2002) that STAT3 participates in oncogenesis through upregulation of genes encoding apoptosis inhibitors (Bcl-xl, Mcl-1, and survivin), cycle regulators (cyclin D1 and c-Myc) and inducers of angiogenesis (vascular endothelial growth factor). Moreover, a potentially important consequence of the anti-apoptotic activity of STAT3 is that it may be able to confer resistance to chemotherapy and radiation therapy, both of which rely on apoptotic mechanism to kill tumor cells. Thus, constitutive STAT3 signaling represents a key molecular event in the multistep process of tumorigenesis, and provides the basis to investigate the clinical significance of constitutive STAT3 activation in tumors where it is detected to establish the therapeutic potential of inhibition of aberrant STAT3 activity.

SIGNAL TRANSDUCER AND ACTIVATOR OF TRANSCRIPTION 3 IN ORAL SQUAMOUS CELL CARCINOMA

It was reported by Grandis et al. (2000), and Song and Grandis (2000) from initial investigations in HNSCC that constitutive STAT3 activation was most likely secondary to aberrant transforming growth factor-α/epidermal growth factor receptor signaling. These findings suggested a role of STAT3 in carcinogenesis. Subsequent studies investigated the clinical relevance of STAT3 in OSCC. The different approaches used for studying STAT3 and its mRNA expression include electrophoretic mobility shift assay (EMSA), in situ hybridization, immunoblotting, immunohistochemical localization, and reverse transcription–polymerase chain reaction (RT-PCR).

Electrophoretic Mobility Shift Assay

Electrophoretic Mobility Shift Assay (EMSA) also known as Gel Shift or Band Shift Assay is a simple, rapid, very sensitive technique for studying gene regulation

and determining protein-DNA interactions. The assay uses non-denaturing polyacrylamide gel electrophoresis for detecting sequence-specific DNA binding proteins. It is based on the observation that complexes of protein and DNA migrate through a non-denaturing polyacrylamide gel more slowly than free DNA fragments or double-stranded oligonucleotides. The EMSA is carried out by first incubating a protein(s) such as nuclear or cell extract with a ^{32}P end-labeled DNA fragment containing the putative protein binding site. The reaction products are then analyzed on a non-denaturing polyacrylamide gel. The specificity of the DNA binding protein for the putative binding site is established by competition experiments, using DNA fragments or oligonucleotides containing a binding site for the protein of interest or other unrelated DNA sequences.

Competition Mobility Shift Assay

Competition binding assay is used to assess the sequence specificity of protein-DNA interactions. This is necessary because the protein preparations will contain both specific and nonspecific DNA binding proteins. For a specific competitor, the same DNA fragment (unlabeled) as the probe can be used. The nonspecific competitor can be essentially any fragment with an unlabeled sequence.

Super Shift Assay

Super shift assay is a variation of the mobility shift DNA binding assay, in which antibodies are used to identify proteins present in the protein-DNA complex. Addition of a specific antibody to the binding reaction can have one of several effects. If the protein recognized by the antibody is not involved in complex formation, addition of the antibody will have no effect. If protein that forms the complex is recognized by the antibody, the antibody will either block complex formation or it will form an antibody-protein-DNA ternary complex, and thereby specifically result in a further reduction in the mobility of the protein-DNA complex (supershift). Results may be different depending upon whether the antibody is added before or after the protein binds DNA (particularly if there are epitopes on the DNA binding surface of the protein). The mobility shift assay or super shift assay includes the following steps: (1) preparation of a radioactively labeled DNA probe containing particular DNA binding site; (2) preparation of 4% non-denaturing polyacrylamide gel; (3) in mobility shift assay, the binding reaction consists of a protein mixture bound to the 5,000 to 20,000 cpm radiolabeled DNA probe (≥ 10 femtomoles). In case of super shift assay, the binding mixture contains protein extract, DNA probe and antibody specific for DNA binding protein. To another binding mix, an equivalent amount of nonspecific control antibody is added; (4) electrophoresis of protein-DNA complexes through the gel.

Method

For performing EMSA, whole cell extracts, nuclear or cytoplasmic extracts were prepared at 0°C to 4°C, preferably in a cold room with all equipments and buffers precooled. For preparation of nuclear extracts, tissue or tissue culture cells were collected, washed, and suspended in hypotonic buffer. The swollen cells were homogenized and nuclei were pelleted. The cytoplasmic fraction was removed and nuclei were resuspended in a low-salt buffer. Gentle dropwise

addition of a high-salt buffer then released soluble proteins from the nuclei without lysing the nuclei. Following extraction, the nuclei were removed by centrifugation, the nuclear extract (supernatant) was dialyzed into a moderate salt solution, and any precipitated protein was removed by centrifugation. The optimum extraction conditions for specific cells and applications were determined with higher or lower potassium chloride concentration. It was reported by Wong et al. (1994) that in order to avoid dialysis, 0.1% Triton-X 100 was included in all buffers, and extracts were diluted in buffer D (storage buffer) to reduce salt concentration. The cytoplasmic extract was obtained by adding cytoplasmic extract buffer to the cytoplasmic fraction, which was mixed thoroughly and centrifuged. The cytoplasmic fraction was dialyzed into dialysis buffer and any precipitated material removed by centrifugation.

It was reported by Grandis et al. (1998) that STAT3 activation by EMSA was evaluated using binding reactions containing 20 μg extracted protein and radiolabeled high-affinity serum inducible element (hSIE) duplex oligonucleotide. Furthermore, it was reported by Wong et al. (1994) that radiolabeling was done with ^{32}P dGTP (6000 Ci/mmol) and using Klenow fragment of DNA polymerase I. Binding reaction mixtures (25 μl) contained the indicated 20 μg whole cell extract, 5 femtomoles (~10^5 cpm) of radiolabeled DNA fragment and 2 μg of denatured salmon sperm DNA in binding buffer. Reaction mixtures were incubated for 20 min at room temperature, then 5 μl of 0.1% bromophenol blue in binding buffer was added, and the mixture was immediately added on a 4% polyacrylamide gel. Electrophoresis was performed in 0.25X Tris borate buffer (TBE buffer in 89 mM Tris base, 89 mM boric acid and 2 mM EDTA, pH 8.0) at 175 V with buffer recirculation. Quantitation of the STAT3 signal was performed by scanning sis-inducible factor-A (SIF-A) band using Molecular Dynamics Personal Densitometer SI and IMAGE QUANT software. Normalization between blots was accomplished by running U937 cell lysates (5 μg) that demonstrate activation of STAT3 on each gel. Activation of STAT3 was assessed by determining the presence of DNA binding activity, as manifested by SIF activity. This was resolved into 3 different protein-DNA complexes termed SIF-A (representing STAT3 homodimer), SIF-B (representing STAT3/STAT1 heterodimer) and SIF-C (representing STAT1 homodimer). The SIF-A and SIF-B complex were verified with super shift assay and DNA binding purification studies. For supershift assays, extracts were incubated with STAT3 polyclonal antibody (C-20, Santa Cruz Biotechnology).

DNA Binding Affinity Purification

It was reported by Grandis et al. (1998) that for DNA binding affinity purification, whole cell extracts were prepared using high salt buffer. Extracts were mixed with salmon sperm DNA (500 μg/ml) and incubated at 4°C for 10 min. This mixture was incubated at 4°C for 40 min more with streptavidin-conjugated paramagnetic beads (Dynabead M280 strepavidin; Dynal Inc., Lake Success, NY), to which biotinylated tandem hSIE duplex oligonucleotides had previously been bound. After this incubation, the beads were washed 5 times with high salt buffer containing 0.05% Nonidet-P 40 and 200 μg/ml salmon sperm DNA. Proteins were eluted in high salt buffer containing 1.2 mol/L NaCl. The

STAT3 antibody used was directed against the NH2-terminal portion of the protein (amino acids 1–175; Transduction Labs).

Results

In Vitro Studies

It was reported by Grandis et al. (1998) that compared with normal mucosal epithelial cells, all 7 HNSCC cell lines examined revealed varying degrees of constitutive activation of a hSIE binding activity specific for STAT3. The predominant complex formed was SIF-A (STAT3 homodimer) and SIF-B (STAT3/STAT1 heterodimer). Furthermore, super shift assays and DNA binding affinity purification studies also revealed constitutive activation of STAT3 in HNSCC cell lines.

In Vivo Studies

It was reported by Grandis et al. (2000) that even in HNSCC tumor tissues, STAT3 was constitutively activated. For this, samples of HNSCC (oral cavity, oropharynx, hypopharynx, and larynx) and normal mucosa distant from the tumor were obtained from 19 patients undergoing primary surgical resection for head and neck cancer. Controls included seven age and gender matched oropharyngeal mucosa. Analysis of EMSA for STAT3 DNA binding activity revealed 8- to 10-fold increased levels of constitutively activated STAT3, in both the tumor and in the histologically normal mucosa from HNSCC compared with levels in the normal mucosa from controls without cancer. As in the cell lines, SIF-A (STAT3 homodimer) and SIF-B (STAT3/STAT1 heterodimer) were the predominant complexes formed, and supershift assays confirmed that SIF-A and SIF-B contained STAT3. This was also confirmed with in situ hybridization.

In Situ Hybridization

In situ hybridization is a method of localizing, either mRNA within the cytoplasm or DNA within the chromosomes of the nucleus, by hybridizing the sequence of interest to a complimentary strand of a nucleotide probe. The basic technique utilizes the fact that DNA and RNA will undergo hydrogen bonding to complimentary sequences of DNA or RNA. By labeling sequences of DNA or RNA of sufficient length (~50–300 base pairs), selective probes can be made to detect particular sequences of DNA or RNA. The application of these probes to tissue sections allows DNA or RNA to be localized within tissue regions and cell types. The sensitivity of the technique is such that threshold levels of detection are in the region of 10–20 copies of mRNA or DNA per cell. Normal hybridization requires the isolation of DNA or RNA, separating it on a gel, blotting it onto nitrocellulose membrane, and probing it with a complimentary sequence.

Method

It was reported by Grandis et al. (2000) that for standard light microscopy of cryostat sections, the tissues were lightly fixed in 2% paraformaldehyde, were infused with 30% sucrose overnight, and were frozen in liquid nitrogen-cooled isopentane. Five-micrometer sections were cut on a Microm cryostat, were mounted on polylysine-coated or Superfrost (Fisher) slides and were labeled. The samples were prepared for hybridization by 3×5 min washes in 1X phosphate buffered saline (PBS), followed by incubation in a solution of 1X PBS containing 0.1 mg/ml of DNase Rq1. Thereafter, the samples were postfixed in a 1X PBS solution containing

2% paraformaldehyde for 30 min at room temperature followed by 3 × 5 min 1X PBS washes. ^{35}S-labeled hSIE duplex oligonucleotide (via end-labeling) was then applied to the samples by placing ~100 µl of probe onto 25×25 mm coverslips and rolling the slides onto the coverslips. The slides were placed into a microscope box containing a moist paper towel and were allowed to incubate for 60 min at 30°C. After hybridization, the samples were washed three times in 1X PBS and were subjected to an ethanol dehydration series. After complete drying, the slides were dipped into Kodak NTB-2 (Eastman Kodak) autoradiography emulsion. The dipped slides were air dried for 4 h, placed in a light-tight container, and were stored in a 4°C refrigerator for 7 days. At the end of 7 days, the samples were developed using D-19 developer for 4 min and Rapid Fix photographic fixer for 4.5 min. The samples were counterstained with toluidine blue and then were coverslipped by using cytoseal mounting media.

Results

In Vivo Studies

Using the above method, it was reported by Grandis et al. (2000) that activated STAT3 was derived from the epithelial cells. High powered microscopy demonstrated increased activated STAT3 at the tumor stromal interface, and that the cells containing activated STAT3 were epithelial cells and not tumor infiltrating lymphocytes. This increase in constitutive STAT3 activation in tissue specimens from patients with HNSCC was also associated with increase in STAT3 protein expression and STAT3 tyrosine phosphorylation when compared to mucosal specimens from controls in immunoblotting studies

Immunoblotting

Immunoblotting or Western Blotting allows investigators to determine with a specific primary antibody the relative amounts of the protein present in different samples. Briefly, samples are prepared from tissues or cells that are homogenized in a buffer that protects the protein of interest from degradation. The sample is separated using sodium dodecyl sulphate polyacrylamide gel electrophoresis (SDS-PAGE) and then transferred to a membrane for detection. The membrane is incubated with a generic protein (such as milk proteins) to bind to any remaining sticky places on the membrane. A primary antibody is then added to the solution, which is able to bind to its specific protein. A secondary antibody-enzyme conjugate, which recognizes the primary antibody, is added to find locations where the primary antibody is bound.

Method

It was reported by Grandis et al. (1998) that for immunoblotting studies, whole cell extracts were mixed with 2X SDS sample buffer (125 mmol/L Tris-HCl, pH 6.8; 4% SDS; 20% glycerol; 10% 2-mercaptoethanol) at 1:1 ratio and were heated for 5 min at 100°C. Proteins (50 µg/lane) were separated by 12.5% SDS-PAGE and transferred onto a nitrocellulose membrane (MSI; Westboro, MA). Prestained molecular weight markers (GIBCO BRL; Gaithersburg, MD) were included in each gel. Membranes were blocked for 30 min in Tris-buffered saline (TBS: 10 mmol/L Tris-HCl, pH 7.5 and 150 mmol/L NaCl) with 0.5% Tween-20 (TBST) and 5% bovine serum albumin (BSA). After blocking, membranes were incubated with a primary antibody; mouse anti-human STAT3 monoclonal (Transduction Labs, Lexington,

KY), a rabbit polyclonal anti-HA-probe (Y-11) (Santa Cruz Biotechgnology) or a phosphospecific anti-STAT3 pTyr(705) rabbit polyclonal (Quality Controlled Biochemicals; Hopkington, MA) in TBST and 1% BSA. After washing the membranes three times with TBST (5 min each), they were incubated with horseradish peroxidase-conjugated secondary antibody in TBST and 1% BSA for 30 min. Subsequently, membranes were washed three times with TBST and developed using the enhanced chemiluminescence (ECL) detection system (Amersham Life Science, Inc; Arlington Heights, IL).

Results

In Vitro Studies

Using immunoblotting studies, it was reported by Grandis et al. (1998) that in HNSCC cell lines increased STAT3 protein expression levels were observed compared with normal mucosal epithelial cells. Similarly, phosphotyrosine STAT3 immunoblotting demonstrated elevated STAT3 tyrosine phosphorylation in HNSCC cell lines compared to the levels detected in normal mucosal epithelial cells. This clearly showed that increase in STAT3 activation was associated with increased STAT3 tyrosine phosphorylation.

In Vivo Studies

Using immunoblotting studies, it was reported by Grandis et al. (2000) that tissues from patients with HNSCC were also associated with increase in STAT3 protein expression and STAT3 tyrosine phosphorylation when compared to mucosal specimens from controls. A 2.12-fold increase in STAT3 protein expression was seen in HNSCC tumors compared to normal mucosa from non cancer patients ($P=0.021$) and a 2.32-fold increase in tumors compared to normal mucosa from HNSCC patients ($P=0.006$). Moreover, similar studies using phosphospecific anti-STAT3 pTyr(705) antibody demonstrated increased phosphorylated STAT3 in both tumors ($P=0.002$) and normal mucosa samples from HNSCC patients ($P = 0.001$) compared to normal mucosa from control patients. In a similar study using phosphospecific anti-STAT3 pTyr(705) antibody, it was reported by Nagpal et al. (2002) that high STAT3 accumulation was seen in all stages of OSCC in contrast with normal oral samples in which phospho STAT3 was totally absent.

Immunohistochemical Localization

Immunohistochemical localization is a method of detecting the presence of specific proteins in cells or tissues and consists of the following steps: (1) primary antibody binds to specific antigen; (2) antibody-antigen complex is bound by a secondary, enzyme-conjugated, antibody; (3) in the presence of substrate and chromogen, the enzyme forms a coloured deposit at the sites of antibody–antigen binding.

Method

It was reported by Shah et al. (2006) that for the detection of STAT3 expression, the avidin-biotin-complex (ABComplex) technique was used. For this, tumors were fixed in 10% neutral buffered formalin (pH 7.4) at 4°C for 72 h and then embedded in paraffin. Tissue sections (4 μm thick) were mounted on 3-aminopropyltriethoxy silane-coated slides. The sections were deparaffinized and rehydrated by passing through xylene I and II for 20 min each, xylene:absolute alcohol (1:1) for 30 min

and absolute alcohol, 90%, and 70% alcohol for 15 min each. The slides were then immersed in methanol with 3% H_2O_2 for 30 min, followed by two washes of TBS for 5 min each to block endogenous peroxidase activity. The cell membrane was permeabilized by 0.2% Triton X-100 in distilled water for 20 min, and then the slides were rinsed twice in distilled water and washed for 5 min in TBS. To retrieve antigenicity, the sections were heated in 10 mM citrate buffer (pH 6.0) for 20 min in a pressure cooker and then allowed to cool at room temperature. Nonspecific conjugation was blocked with normal rabbit serum (DAKO, Denmark), diluted 1:10 in TBS and applied to the sections for a minimum of 20 min at room temperature. The excess blocking serum was removed from the sections and mouse monoclonal anti-human STAT3 antibody (F-2; Santa Cruz Biotechnology, Santa Cruz, CA) at a dilution 1:100 in TBS was added to the sections. Sections were incubated at 4°C overnight in a moist chamber. Next day, the slides were washed twice in TBS for 10 min each and the sections were allowed to react with secondary biotinylated anti-mouse rabbit immunoglobulin antibody (Dako, Denmark) diluted 1:50 in TBS and incubated for 40 min at room temperature. The slides were washed thrice in TBS for 10 min each. Tertiary antibody was prepared 30 min prior to addition to the sections, using mixture of Reagent A-streptavidin and Reagent B-biotinylated horseradish peroxidase in 0.05 M Tris-HCl (pH 7.5). ABComplex was added and incubated for 40 min at room temperature. The slides were then washed three times in TBS for 5 min each. After three washes, the specific immune reaction was identified using hydrogen peroxide (H_2O_2) as a substrate and 3, 3′–diaminobenzidinetetra-hydrochloride (DAB) as a chromogen. Freshly prepared DAB solution in 50 mM Tris-HCl (pH 7.5) and containing 0.005% H_2O_2 was added to each section for 5 min, and all incubations were carried out at room temperature. To remove extra DAB from the slides, each slide was rinsed twice in distilled water for 10 min each. Sections were lightly counterstained with Mayer's haematoxylin. To destain the unwanted haematoxylin, each section was given just a single dip in acid–alcohol and immediately the sections were rinsed in distilled water twice for 10 min each. In the final step, sections were dehydrated and cleared by passing through graded alcohol of 70%, 90%, and 100%, xylene: alcohol (1:1) and xylene for 15 min each. These were mounted in dibutyl phthalate xylene and observed under a light microscope. As positive controls, formalin-fixed paraffin-embedded tissue sections with intense staining for STAT3 were included with each staining procedure. For negative control, the primary antibody was replaced with normal serum. All the sections were scored independently by two individual observers, familiar with immunohistopathology but unaware of the clinical outcome of the patients. Sections were examined for evidence of cytoplasmic or nuclear staining and scoring was done by semi-quantitative method ranging from negative (no staining or ≤10% of cells) to 3+ (1+ staining in 11–30% of cells: weak, 2+ staining in 31–50% of cells: moderate and 3+ staining in >50% of cells: intense) was used. The other investigators have used a similar technique with modifications.

Results

In Vivo Studies

Using immunohistochemical localization, it was reported by Grandis et al. (2000)

that the epithelial cells of OSCC tissues were the primary source of STAT3 protein expression. Moreover, tissue staining with anti-STAT3 pTyr(705) antibody in normal mucosa from controls without HNSCC demonstrated phosphorylated STAT3 only in the basal epithelial layer. In contrast, in histologically normal mucosa from patients with tumor, phosphorylated STAT3 was detected throughout the entire epithelium. This finding of increased STAT3 activation and phosphorylated STAT3 levels in the histologically normal surrounding mucosa implicated a role of STAT3 in early carcinogenesis.

This was followed by the analysis of STAT3 in relation to clinicopathological parameters in a large sample series of OSCC patients. It was reported by Nagpal et al. (2002) that for assessing STAT3 immunoreactivity, tissue samples from 90 patients of tobacco chewing-mediated OSCC representing different stages, sites (buccal mucosa, tongue, and angle of mouth-mandible and maxilla) and differentiation states were examined. Together with these were also examined normal oral samples ($N=8$) and premalignant lesions ($N=8$) obtained from patients without cancer undergoing non oncologic surgical procedures. Both cytoplasmic and nuclear localization of STAT3 was detected in the primary OSCC tumors. Overall 58.9% of OSCC tumors showed very high STAT3 protein accumulation and 23.3% showed intermediate accumulation, whereas 17.8% of OSCC tumors were negative for STAT3. No STAT3 was detected in normal samples and only one out of eight premalignant lesions showed intermediate STAT3 accumulation. Further, significant correlation was not observed with various clinicopathological parameters except for tumor size. Of the OSCC patients representing early classification (T1 + T2) of carcinogenesis, 74.4% showed high STAT3 staining, whereas only 47.1% of OSCC representing late classification (T3 + T4) of carcinogenesis showed moderate STAT3 staining ($P=0.033$). Thus, STAT3 activation is an early event in oral carcinogenesis and is subsequently degraded as the disease advanced.

In a related study examining both, phosphorylated and inactive form of STAT3 in normal oral epithelium ($N=10$), epithelium adjacent to the tumor and the tumor itself ($N=84$), it was reported by Klosek et al. (2004) that the inactive cytoplasmic form of STAT3 was present in normal, non-cancer tissues and OSCC. On the other hand, the phosphorylated form of STAT3 was seen in the nuclei of 74% of OSCC tissues but not in the normal oral mucosa. Further, the phosphorylated form of STAT3 was present in the epithelium adjacent to the cancer suggesting that STAT3 is an early event in oral carcinogenesis. Also, the phosphorylated form of STAT3 significantly correlated with tumor stage ($P=0.011$) but not gender, site of cancer, lymph node status, differentiation or stage or pattern of invasion. In another study, it was reported by Arany et al. (2003) that STAT3 expression was inversely correlated with respect to tumor differentiation in HNSCC: STAT3 levels were higher in poorly differentiated tumors. However, none of the above investigators reported its prognostic value. The prognostic value of STAT3 was reported by Masuda et al. (2002) and Shah et al. (2006).

From a study of primary SCC of the posterior tongue ($N=51$), stained with phosphospecific STAT3 antibody that is, activated form of STAT3, it was reported by Masuda et al. (2002) that 37% (19/51) of the tumors positive for STAT3 displayed

strong staining in 50% of the tumor cells. In the other tumors scored negative, 19 were negative, 10 exhibited weak and 3 exhibited moderate staining for phosphospecific STAT3. Furthermore, increased levels of phosphospecific STAT3 significantly correlated with nodal metastasis, clinical stage, and lower survival rates, suggesting that STAT3 activation in OSCC may provide a novel prognostic factor.

In another study evaluating STAT3 expression in normal oral tissues ($N=12$), oral premalignant lesions ($N=60$), and OSCC of the buccal mucosa and tongue ($N=135$), it was reported by Shah et al. (2006, 2007) that only cytoplasmic staining was seen in one out of eight normal oral tissues, whereas in premalignant and malignant lesions, cytoplasmic staining was observed in 10% and 18% patients, respectively. On the other hand, in premalignant and malignant lesions, nuclear reactivity was observed in 35% and 44% patients, respectively (Figure 17.1). Dysplasia displayed higher STAT3 positivity (60%) compared to hyperplasia (17%). Similarly, STAT3 positivity was higher in advanced stage carcinomas (79%) compared to early stage carcinomas (45%). However, the noteworthy observation was that in advanced stage carcinomas only 18% of the STAT3 positive patients showed intense staining compared to 52% of the STAT3 positive early stage patients. The presence of intense staining in a portion of advanced stage patients indicated active involvement of STAT3 in a subset of late stage tumors, and suggested a dual role of STAT3 in OSCC – as anti-apoptotic during tumor initiation and as a critical regulatory switch governing cell cycle progression during tumor progression. Alternately, in malignant tumors, STAT3 might be functioning as an antidote to apoptosis until other genes take over the function of cell viability. Furthermore, in multivariate logistic regression analysis for defining potential risk predictors in oral carcinogenesis, it was observed that STAT3 was significantly involved in progression of hyperplasia to dysplasia (Odds Ratio=17.16, $P=0.0001$) and of early stage disease to advanced stage disease (Odds Ratio=4.49, $P=0.0001$) at step 2, after EGFR. Thus, it was concluded that STAT3 activation is an early event in oral carcinogenesis.

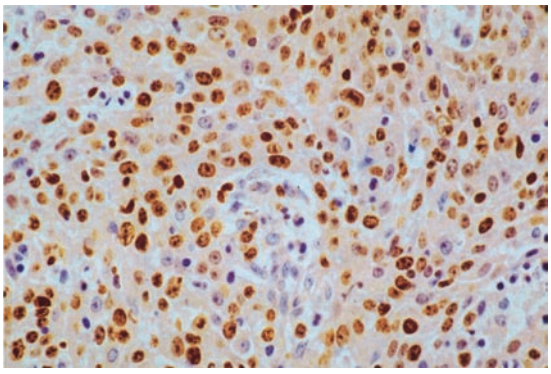

FIGURE 17.1. Nuclear staining for STAT3, clearly depicted in a well differentiated oral squamous cell carcinoma of the buccal mucosa

Compared to clinicopathological parameters in OSCC, it was reported by Shah et al. (2006) that STAT3 protein expression showed significant positive correlation with disease stage ($P=0.001$), nodal status ($P=0.033$) and tumor size ($P=0.001$). Regarding survival, multivariate survival analysis using Cox proportional hazard regression model showed that in early stage OSCC patients, nuclear STAT3 was a significant risk factor for both, recurrence of disease and poor overall survival with a relative harazd ratio of 3.23 and 4.20, respectively. Multivariate survival analysis even with the addition of markers such as EGFR, c-myc, H-ras, p53, cyclin D1, p16, Rb, Ki-67, and Bcl2, indicated that early stage patient whose tumor showed

nuclear STAT3 immunoreactivity was 3.23 times more likely to develop recurrence compared to an early stage patient with absence of STAT3 immunoreactivity. Similarly, Shah et al. (2009) reported that nuclear STAT3 emerged as a significant predictor of worse overall survival in early stage patients. Thus, it was concluded that the superiority of STAT3 over other molecular markers may underlie the fact that prognosis is directly related to tumor biology manifested by its multiple aspect. The other markers may predict one or the other aspect of cancer biology and not the overall biological behaviour, whereas STAT3 might most likely do so, because it is an important transcription factor for many genes that may regulate all aspects of cancer biology. Thus, STAT3 may represent a significant molecular marker for poor prognosis in early stage OSCC.

Reverse Transcription–Polymerase Chain Reaction

It is a sensitive method for the detection of mRNA expression levels. Traditionally, RT-PCR involves two steps: the RT reaction and PCR amplification. RNA is first reverse transcribed into cDNA using a reverse transcriptase, and the resulting cDNA is used as templates for subsequent PCR amplification using primers specific for one or more genes. RT-PCR can also be carried out as one-step RT-PCR in which all reaction components are mixed in one tube prior to starting the reactions.

Method

For total RNA extraction from OSCC tissues, the single-step acid guanidinium thiocyanate phenol chloroform extraction method reported by Chomczynski and Sacchi (1987) was used. Alternately, commercially available total RNA extraction kits can also be used. The purity of the recovered RNA was measured spectrophotometrically at 260 and 280 nm wavelength. The quality of the isolated RNA was confirmed by agarose gel electrophoresis. For STAT3 mRNA expression, it was reported by Trivedi et al. (2009). that 1 μg of total cellular RNA was reverse transcribed to cDNA, and RT-PCR performed using the one step GeneAmp EZ r*Tth* RNA PCR kit (Perkin Elmer, USA) and following the kit's protocol. The STAT3 primer sequences used were: the 5′ primer (5′- TCT CCT ACT TCT GCT ATC TTT GAG -3′) and the 3′ primer (5′- ATG GGT CTC AGA GAA CAC ATC -3′). The reaction was performed as follows: reverse transcription at 60°C for 30 min, an initial denaturation at 94°C for 1 min, followed by 35 cycles of PCR (94°C for 45 s, 59°C for 45 s, and 72°C for 1 min) and a final extension at 72°C for 10 min. The amplified products along with the 50 base pair ladder were electrophoresed on 1.8% agarose gel, stained with ethidium bromide and visualized under UV transilluminator. The band size noted was 116 base pair (Figure 17.2). Furthermore, the intensity of PCR products was measured and integrated on Gel Documentation System (Bio-Rad) using the Molecular Analyst Software, in units of counts/mm^2. As positive control for STAT3 mRNA amplification, OSCC tissue displaying strong amplification was used. Negative control reaction was run without addition of the template.

Results

In Vivo Studies

From additional experiments with RT-PCR to study STAT3 mRNA expression, it was reported by Nagpal et al. (2002) that STAT3

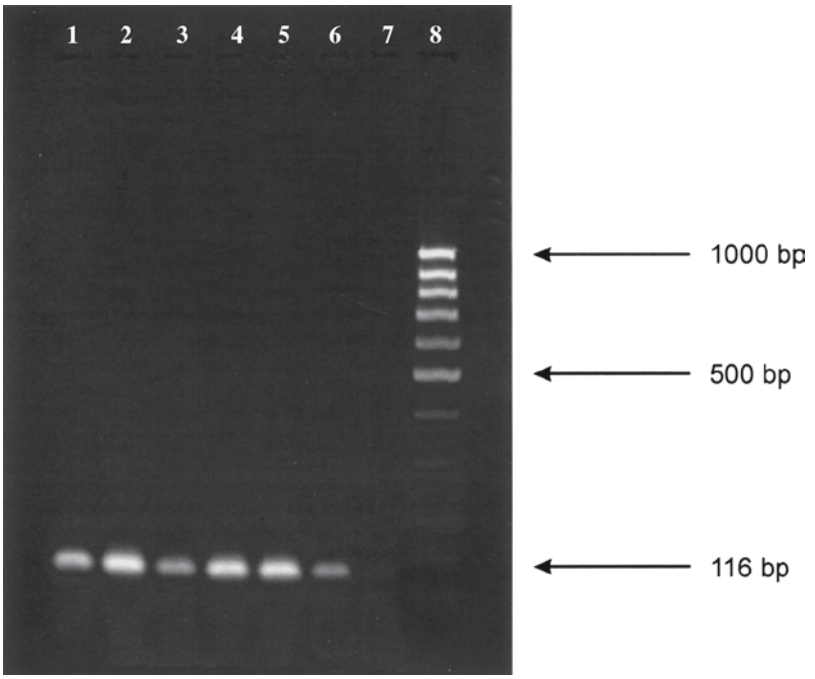

FIGURE 17.2. Representative STAT3 mRNA (116 bp) expression in oral cancer patients. Lanes 1–6: oral squamous cell carcinoma; lane 7: negative control; lane 8: 50 bp ladder

mRNA expression was high in T1 and T2 classification (early stages), moderate in T3 and T4 (late stages) and no expression in normal oral tissues. This suggested that STAT3 activation is an early event in oral carcinogenesis. Apart from Nagpal et al. (2002), STAT3 mRNA expression was reported by Trivedi et al. (2009).

It was reported by Trivedi et al. (2009) that STAT3 mRNA expression in oral premalignant lesions ($N=35$), histologically normal mucosa adjacent to tumor ($N=70$) and in OSCC ($N=70$) in terms of mean ± standard error was 1405 ± 224.82, 2088.23 ± 190.63, and 2457.84 ± 184.72, respectively, and in terms of median, it was 1203, 1852, and 2246, respectively. A progressive increase in STAT3 mRNA expression from premalignant lesions, to histologically normal mucosa adjacent to tumors to malignant tumors was noted, suggesting upregulation of STAT3 mRNA expression in oral carcinogenesis. Also STAT3 mRNA expression in premalignant lesions suggested it to be an early event in oral carcinogenesis. Furthermore, the expression of STAT3 mRNA in histologically normal mucosa adjacent to the tumor reinforced the "field cancerization" hypothesis. Alternately, the presence of STAT3 mRNA expression in histologically normal mucosa adjacent to tumors may be the result of a paracrine effect of STAT3 expression due to factors released by the tumors. Concerning clinicopathological parameters and clinical outcome, STAT3 mRNA expression in tumors showed significant correlation with tumor size ($P=0.048$). However, the STAT3 mRNA expression in histologically normal mucosa adjacent to tumors showed significant correlation with lymphatic permeation ($P=0.025$), and in total patients was a significant predictor of relapse free survival at step 1 and overall survival at step 2 after tumor stage with a relative hazard ratio of 4.81 and 4.78,

respectively. Even in early stage patients, using Kaplan-Meier survival estimations STAT3 mRNA expression in histologically normal mucosa adjacent to tumors was a significant prognostic factor for relapse free survival ($P=0.047$). Thus, STAT3 mRNA expression may be regarded as a marker of early undetectable carcinogenesis and an important tool with regard to prognostic evaluation.

Collectively, these findings point to the crucial role of STAT3 in OSCC. Constitutive STAT3 activation is an early event in oral carcinogenesis and is associated with indicators of poor prognosis, and hence represents a potential risk factor for poor diagnosis in early stage OSCC. In combination with established prognosticators, STAT3 expression might therefore allow a more precise identification of patients with aggressive phenotype likely to benefit from potential anti-STAT3 inhibitors as therapeutics.

REFERENCES

Akira S (2000) Roles of STAT3 defined by tissue-specific gene targeting. Oncogene 19:2607–2611

Arany I, Chen SH, Megyesi JK, Adler-Strothz K, Chen Z, Rajaraman S, Ember IA, Tyring SK, Brysk MM (2003) Differentiation-dependent expression of signal transducers and activators of transcription (STATs) might modify responses to growth factors in the cancers of the head and neck. Cancer Lett 199:83–89

Becker S, Groner B, Muller CW (1998) Three-dimensional structure of the STAT3b homodimer bound to DNA. Nature (Lond) 394:145–151

Bromberg J, Darnell JE Jr (2000) The role of STATs in transcriptional control and their impact on cellular function. Oncogene 19:2468–2473

Bromberg JF (2002) Stat proteins and oncogenesis (review). J Clin Invest 109:1139–1142

Bromberg JF, Wrzeszczynska MH, Devgan G, Zhao Y, Pestell RG, Albanese C, Darnell JE Jr (1999) Stat3 as an oncogene. Cell 98:295–303

Buettner R, Mora LB, Jove R (2002) Activated Stat signaling in human tumors provides novel molecular targets for therapeutic intervention. Clin Cancer Res 8:945–954

Caldenhoven E, van Dijk TB, Solari R, Armstrong J, Raaijmakers JA, Lammers JW, Koenderman L, de Groot RP (1996) STAT3beta, a splice variant of transcription factor STAT3, is a dominant negative regulator of transcription. J Biol Chem 271:13221–13227

Calo V, Migliavacca M, Bazan V, Macaluso M, Buscemi M, Gebbia N, Russo A (2003) STAT proteins: from normal control of cellular events to tumorigenesis. J Cell Physiol 197:157–168

Catlett-Falcone R, Landowski TH, Oshiro MM, Turkson J, Levitzki A, Savino R, Ciliberto G, Moscinciski L, Fernandez-Luna JL, Nunez G, Dalton WS, Jove R (1999) Constitutive activation of Stat3 signaling confers resistance to apoptosis in human U266 myeloma cells. Immunity 10:105–115

Chapman RS, Lourenco PC, Tonner E, Flint DJ, Selbert S, Takeda K, Akira S, Clarke AR, Watson CJ (1999) Suppression of epithelial apoptosis and delayed mammary gland involution in mice with a conditional knockout of Stat3. Genes Dev 13:2604–2616

Chen X, Vinkemeier U, Zhao Y, Jeruzalmu D, Darnell JE Jr, Kuriyan J (1998) Crystal structure of a tyrosine phosphorylated Stat-1 dimer bound to DNA. Cell 93:827–839

Chomczynski P, Sacchi N (1987) Single-step method of RNA isolation by acid guanidinium thiocyanate-phenol-chloroform extraction. Anal Biochem 162:156–159

Clavin W (2002) One gene, two important proteins. www.eurekalert.org/pub_releases/2002-09/ru-ogt091202.php (14 Sept 2002)

Darnell JE Jr (1997) STATs and gene regulation. Science 277:1630–1635

Darnell JE Jr (2002) Transcription factor as target for cancer therapy. Nat Rev Cancer 2:740–749

Garcia R, Jove R (1998) Activation of STAT transcription factors in oncogenic tyrosine kinase signaling. J Biomed Sci 5:79–85

Grandis JR, Drenning SD, Chakraborty A, Zhou MY, Zeng Q, Pitt AS, Tweardy DJ (1998) Requirement of Stat3 but not Stat1 activation for epidermal growth factor receptor-mediated cell growth in vitro. J Clin Invest 102:1385–1392

Grandis JR, Drenning SD, Zeng Q, Watkins SC, Melhem MF, Endo S, Johnson DE, Huang L, He Y, Kim JD (2000) Constitutive activation of Stat3 signaling abrogates apoptosis in squamous cell carcinogenesis in vivo. Proc Natl Acad Sci USA 97:4227–4232

Haspel RL, Salditt-Georgieff M, Darnell JE Jr (1996) The rapid inactivation of nuclear tyrosine phosphorylated Stat1 depends on a protein tyrosine phosphatase. EMBO J 15:6262–6268

John S, VinKemeier U, Soldaini E, Darnell JE Jr, Leonard WJ (1999) The significance of tetrameization in promoter recruitment by STAT5. Mol Cell Biol 19:1910–1918

Klosek SK, Nakashiro KI, Hara S, Li C, Shintani S, Hamakava H (2004) Constitutive activation of Stat3 correlates with increased expression of the c-Met/ HGF receptor in oral squamous cell carcinoma. Oncol Reports 12:293–296

Masuda M, Suzui M, Yasumatu R, Nakashima T, Kuratomi Y, Azuma K, Tomita K, Komiyama S, Weinstein IB (2002) Constitutive activation of signal transducers and activators of transcription 3 correlates with cyclin D1 overexpression and may provide a novel prognostic marker in head and neck squamous cell carcinoma. Cancer Res 62:3351–3355

Nagpal JK, Mishra R, Das BR (2002) Activation of Stat-3 as one of the early events in tobacco chewing-mediated oral carcinogenesis. Cancer 94:2393–2400

Nikitakis NG, Siavash H, Sauk JJ (2004) Targeting the STAT pathway in head and neck cancer: recent advances and future prospects. Curr Cancer Drug Targets 4:637–651

Sano S, Itami S, Takeda K, Tarutani M, Yamaguchi Y, Miura H, Yoshikawa K, Akira S, Takeda J (1999) Keratinocyte-specific ablation of Stat3 exhibits impaired skin remodeling, but does not affect skin morphognesis. EMBO J 18:4657–4668

Shah NG, Trivedi TI, Tankshali RA, Goswami JV, Jetly DH, Kobawala TP, Shukla SN, Shah PM, Verma RJ (2006) Stat3 expression in oral squamous cell carcinoma: association with clinicopathological parameters and survival. Int J Biol Markers 21:175–183

Shah NG, Trivedi TI, Tankshali RA, Goswami JV, Shah JS, Jetly DH, Kobawala TP, Patel KC, Shukla SN, Shah PM, Verma RJ (2007) Molecular alterations in oral carcinogenesis: Significant risk predictors in malignant transformation and tumor progression. Int J Biol Markers 22:132–143

Shah NG, Trivedi TI, Tankshali RA, Goswami JV, Jetly DH, Shukla SN, Shah PM, Verma RJ (2009) Prognostic significance of molecular markets in oral squamous cell carcinoma. A multivariate analysis. Head Neck (In Press)

Shuai K (1999) The STAT family of proteins in cytokine signaling. Prog Biophys Mol Biol 71:405–422

Song JI, Grandis JR (2000) STAT signaling in head and neck cancer. Oncogene 19:2489–2495

Strehlow I, Schindler C (1998) Amino-terminal signal transducer and activator of transcription (STAT) domains regulate nuclear translocation and STAT deactivation. J Biol Chem 273: 28049–28056

Takeda K, Noguchi K, Shi W, Tanaka T, Matsumoto M, Yoshida N, Kishimoto T, Akira S (1997) Targeted disruption of the mouse Stat3 gene leads to early embryonic lethality. Proc Natl Acad Sci USA 94:2607–2611

Trivedi TI, Shah NG, Tankshali RA, Goswami JV, Shah JS, Shukla SN, Shah PM (2009) Stat3: A potential risk factor in oral squamous cell carcinoma. Oral Oncology Supplement 3:223, P3.67

Wegenka UM, Lutticken C, Buschmann J, Yuan J, Lottspeich F, Müller-Esterl W, Schindler C, Roeb E, Heinrich PC, Horn F (1994) The interleukin-6-activated acute-phase response factor is antigenically and functionally related to members of the signal transducer and activator of transcription (STAT) family. Mol Cell Biol 14:3186–3196

Wong P, Severns CW, Guyer NB, Wrights TM (1994) A unique palindromic element mediates *g*-interferon induction of mig gene expression. Mol Cell Biol 14:914–922

Yu CL, Meyer DJ, Campbell GS, Larner AC, Carter-Su C, Schwartz J, Jove R (1995) Enhanced DNA-binding activity of a Stat3-related protein in cells transformed by the Src oncoprotein. Science 269:81–83

18
Salivary Gland Tumors: Preoperative Tissue Characterization with Apparent Diffusion Coefficient Mapping

Takashi Nakamura, Misa Sumi, and MarcVan Cauteren

INTRODUCTION

Diffusion-weighted imaging is a magnetic resonance (MR) imaging technology used to measure the Brownian motion of water molecules in tissues. The technique, therefore, is expected to contribute to the evaluation of diseased states of the organs and tissues. However, due to its inherent susceptibility to motion artifacts, the clinical application of the imaging has been limited to the brain (Thoeny and De Keyzer 2007). Due to several technical innovations (particularly faster imaging techniques), diffusion-weighted imaging can now be applied to extracranial organs for imaging diagnosis (Takahara et al. 2004). Here, we describe tissue characterization of salivary gland tumors by using diffusion-weighted imaging with a surface coil. Using this technique, clinicians can know the 2-dimensional (2D) distribution of various tissues in salivary gland tumors before surgery; this information may help predict tumor characteristics, including its benign or malignant state.

DIFFUSION-WEIGHTED IMAGING

Diffusion occurs due to the non-ending movement of every single molecule in the universe. This motion is called the thermal motion, and would only stop when molecules are cooled down to the absolute zero, i.e., −273°C. In liquids, molecules constantly bump into each other, and also bump into other molecules. The resulting motion is random, neither the speed nor the direction can be predicted. The process can best be visualized by dropping a droplet of ink into water. The small ink bubbles will be forced to spread in the water due to the collisions with the water molecules. If one could ignore gravitation (which results in the downward force on the ink), the ink would stay around the original position but individual droplets would spread over the complete water container. This phenomenon was first observed by Brown (1828), although Ingenhousz may claim he was the first in 1785. Brown (1828) observed minute particles inside the vacuoles of pollen

moving around in a jittery way; several good simulations of this motion can be found on the internet: (http://geocities.com/piratord/browni/Difus.html).

Einstein (1905) gave this phenomenon a sound mathematical description and a physical interpretation. He also defined the diffusion factor D, and used the theory to derive the size of the particles undergoing the Brownian motion. Perrin (http://nobelprize.org/nobel_prizes/physics/laureates/1926/perrin-lecture.html) used Einstein's theory to give the first proof (albeit indirect) of the discontinuous structure of matter or, in other words, that molecules exist.

Following Einstein, let us consider a free diffusion process, where the molecules only undergo the collisions with other similar molecules in a homogeneous container without boundaries. The probability of finding a specific molecule that was at the position identified as the origin (i.e., r = 0) is then determined by two laws: $<r>=0$ and $<r^2>= 6Dt$ (<> is defined as the average) (Einstein 1905).

The first law means that the molecules will spread around the original position but will not move as a whole. (We are ignoring gravitation here.) The second law describes the way the individual particles will spread so that the probability of finding them away from the original site becomes more common with time. The speed at which this spread occurs is characterized by D, the diffusion factor. The diffusion factor will be a function of the size of the diffusing molecules (mostly we look at water), the viscosity of the medium (this determines the speed of travelling in between collisions), and the temperature (as the underlying cause of diffusion is thermal motion) (Einstein 1905).

This completely free diffusion process is more a mathematical concept than a physical reality, especially if we look at diffusion inside a human body. The environment of water molecules, wherever they are in the body, can hardly be called homogeneous; there are membranes, macromolecules, fibers, and other structures that seriously hamper the diffusion process. It should be noted, however, that looking at very short times, when the water molecules did not have enough time to travel around significantly, the diffusion can be considered free.

This environment will result in a diffusion which is not entirely free. The resulting speed of particles in this microenvironment will thus become a function of time and the geometry of the environment, and will no longer obey the Einstein laws. In this way we can no longer talk about a free diffusion coefficient, and we therefore need to introduce the apparent diffusion coefficient (ADC), to describe the process in vivo. Also, the ADC measure will depend on the way it is measured, and more specifically the timing of the sequence (Le Bihan et al. 1986).

However, because the diffusion process is dominated by its environment and the obstacles it encounters, diffusion imaging becomes a unique technique allowing us to probe structures well below the spatial resolution of the images. As an extension, diffusion can also be used to estimate the size of cells or other motion-hampering structures, e.g., using a technique called q-space imaging (Callaghan et al. 1990).

Measurement of Diffusion-Weighted Imaging

Measuring diffusion or picking up its influence to create diffusion weighted images is quite a feat. We are indeed monitoring motions over a distance of a few micrometers, while the spatial resolution

of MR images is typically in the order of millimeters. This feat can be achieved because we are using techniques to see the intravoxel incoherent motion (IVIM) (Le Bihan et al. 1986). In general, MR image formation is based upon the refocusing of many spins within one voxel to create a strong signal. If, however, the refocusing is disturbed for one reason or another, the signal will be weaker.

To render MR imaging sensitive to the diffusion of water molecules, a spin-echo pulse sequence is usually used. The sequence basically comprised first (90°) and second (180°) radiofrequency (RF) pulses and two rectangular gradient pulses of equal size, which are generated before and after the second 180° RF pulse. These two gradients differently affect the static and moving water molecules. For a static water molecule, the cumulative phase shift in the presence of a magnetic field gradient is proportional to the strength of the field, duration of the gradient, and the (fixed) special location of the molecule. After the first 90° RF pulse, the static water molecule starts to accrue phase. The rotation gets faster with increasing field strength along the direction of the gradient, and thus depends on the position. The subsequent 180° radiofrequency pulse then rotates the vectors around the vertical axis. In the case of a static molecule, which does not move significantly between the first and second gradients, the extra rotation elicited by the second gradient is identical to the first one, and thus the molecule will be in phase at the end of the second gradient (initial phase shift is reversed by the 180° RF pulse). On the other hand, for a moving water molecule, the rotation changes between the first and second RF pulse. A net phase shift is the result. The dispersion of the phase shifts depends on the variance of the displacements. This dispersion results in the attenuation of signal amplitude, which depends on the diffusion coefficient, gradient intensity, and time of diffusion measurement (Le Bihan et al. 1986).

The echo planar imaging (EPI) sequence has a very narrow bandwidth per pixel along the phase-encoding direction (Farzaneh et al. 1990). Therefore, the EPI sequence is inherently susceptible to the air–tissue boundaries and field inhomogeneity (Thoeny and De Keyzer 2007). Diffusion-weighted single-shot EPI can be combined with parallel imaging technique such as sensitivity encoding (SENSE) in order to reduce the artifacts caused by the low bandwidth per pixel (Pruessmann et al. 1999; Kurihara et al. 2002). In the single-shot EPI sequence coupled with the SENSE technique, the train of gradient echoes in the EPI readout is greatly reduced, and k-space traverses per unit become much faster. Therefore, the sensitivity of EPI to the artifacts can be markedly diminished, thereby improving the image quality.

As described earlier, the signal attenuation in a diffusion-weighted sequence depends upon the diffusion sensitizing gradients. When we now acquire images with different strengths of these gradients, then we will acquire images with different diffusion weighting. We can then use the pixel intensities of these two images to calculate a diffusion coefficient. The attenuation of the signal depends on three parameters: the amplitude of the gradient, the duration of the gradient, and the interval between the two gradient lobes. All these parameters are combined in one convenient parameter, called the b-value (Le Bihan et al. 1986). The convenience

of the value stems from the fact that the pixel intensity attenuation will vary exponentially with b and D:

$$S(b) = S(0)\exp(-b * D) \qquad (18.1)$$

There are, however, two issues to be considered with this approach. First, apart from the diffusion motion there is other incoherent motion within a voxel that can lead to a change in the signal. This is particularly true for perfusion. Especially for lower diffusion gradients the water molecules in blood perfusing the tissue through the capillary bed will be seen as being in a pseudo-random motion in the tortuous capillaries. One must thus be aware of the influence of perfusion when measuring the diffusion coefficient. In particular, if one wants to calculate diffusion coefficients the source data should not include images acquired with diffusion weighting gradients corresponding to a b-value less than ~300 s/mm^2. In the context of this chapter one must also be aware of the influence of salivary flow in the glands.

Second, for a typical diffusion weighted sequence the timing is such that the probability of the water molecules (especially those inside cells) hitting an obstacle is fairly high. Indeed, the root mean square displacement will be of the order of tens of micrometer. We can, therefore, no longer speak of a real diffusion process, as explained above, and we thus can only calculate an (ADC).

The calculation of the ADC is based on the formula introduced above, showing that the diffusion weighted signal decays in intensity in an exponential way with respect to the b-factor of the sequence. Typical b values for clinical diffusion weighted imaging are from 600 to 2,000 s/mm^2, depending on the anatomy of interest. For organs with an intrinsically high ADC (e.g., prostate) higher b-values are needed to give a good contrast with lesions. Most parts of the body can be scanned with a b-value of 800–1,000 s/mm^2. In general, one wants to keep the b-value as low as possible since there is an signal-to-noise ratio (SNR) penalty when going to higher b-values. Also, for higher b-values the SNR becomes so low that one must be careful when using these data for ADC calculation as the signal may have dropped close to or below the noise level, potentially leading to a gross miscalculation of the ADC.

Clinical Use of Diffusion Weighted Imaging

The clinical usefulness of diffusion weighted imaging was first shown for stroke imaging (Moseley et al. 1990; van Gelderen et al. 1994). It was shown that diffusion weighted imaging showed the lesion at a much earlier stage than T2 weighted imaging. Also, in combination with perfusion imaging, it is thought to show the viable brain regions. For a very long time, diffusion weighted imaging remained limited to the brain, mainly because of the sensitiveness of the imaging technique to motion and susceptibility artifacts. Recently, however, mainly due to the advent of parallel imaging allowing single-shot techniques with decent spatial resolution, we could overcome this limitation. Indeed, DWIBS (diffusion weighted whole body imaging with background signal suppression) shows great potential for oncology (Takahara et al. 2004). The contrast-to-noise ratio for lesions is very high, leading to a very high sensitivity of the technique.

The clinical usefulness of DWI is based on the basic mechanism for diffusion contrast.

Diffusion seems to be influenced by many parameters; first, there are the "physical" parameters like temperature, pressure, and viscosity (these are most important in free diffusion regime). Second, there are physiological parameters. These are the most important when there is extracellular matrices and fluids, as is mostly the case in the clinical context. These physiological parameters include cellularity, the amount and ratio of intracellular and extracellular water, nucleus/cytoplasm ratio and (if we are not careful) vascularity. A change in any of these will result in a change in the pixel intensity of a diffusion weighted sequence.

We can simplify the image by noting that the ratio between intracellular and extracellular water seems to be the main defining factor. Indeed, the pixel intensity measured would be the result of a weighted averaging of signals coming from extracellular water, intracellular water, and water in the vascular space. The diffusion-weighted signal will vary with b in a complicated way, also depending on the exchange between the three components (van Gelderen et al. 1994). If we use b-values large enough to eliminate signal from the vascular space, then the signal originates solely from intracellular and extracellular water.

In clinical practice only a few images with different b-values are acquired, so a mathematically proper analysis cannot be performed, both because of the limited number of b-values and because of the low SNR of high b-value clinical images. Instead a hugely simplified equation, typically based on two measurements, is frequently used:

$$\mathrm{ADC} = \ln[S(b1)/S(b2)]/(b2\text{-}b1) \quad (18.2)$$

We repeat ourselves when noting that this equation would be valid only for free single-exponential diffusion. In reality, situation is more complicated.

Early experiments have also shown that the diffusion coefficient of intracellular water is approximately one order of magnitude lower than that of extracellular water (van Gelderen et al. 1994). Relatively more intracellular water in a voxel will thus result in a lower averaged ADC, and hence higher signal in a diffusion weighted image. In case there is no organized extracellular matrix (e.g. in bile, in mucus, or inside an abscess or in the urethra and bladder), the viscosity will determine the diffusion properties. One must be conscious of this as the higher signal in more viscous fluids may look like T2-shinethrough to the unsuspecting eye.

Note also that there are a few tissues that show high diffusion weighted signal even in the normal state. These organs are: prostate gland, testes, endometrium, ovary, spleen, tonsil, lymph nodes, bone marrow, and peripheral nerves. Nerves show low diffusion coefficient values for diffusion sensitizing gradients perpendicular to the nerve bundles but high coefficients parallel to the bundles. They show diffusion anisotropy, just like white matter fiber bundles in the brain. We will not discuss anisotropy in this chapter.

Diffusion weighed imaging offers an image contrast unique to MR. More importantly it shows good contrast between normal tissue and diseased tissue. We can understand why because we know that the diffusion contrast is determined by the intracellular water/extracellular water ratio.

The first diffusion weighted images in patients were images taken from stroke patients. These patients' cells swell under the ischemic conditions. This swelling changes the intracellular water/extracellular water ratio such that the proportional influence

of intracellular water increases, and therefore we see a decrease of the overall diffusion coefficient. Cancer lesions also tend to be associated with high cell density than in normal tissues, leading to a lower ADC than normal tissue. This leads to the application of diffusion weighted imaging outside the brain, notably in the DWIBS technique (Takahara et al. 2004).

Body diffusion weighted imaging was rarely used in the past, but the preliminary results suggest that DWIBS could be used as an excellent screening tool as it shows a very high sensitivity for lesions. Interestingly, we can also follow apoptosis resulting from therapy. Clearly where apoptosis occurs the cellular superstructure will disappear, so that the ADC will be that of the extracellular water. This will result in an increase of the ADC. This could give us a powerful tool for follow-up studies.

In this chapter we also introduce the potential clinical usefulness of studying the spatial distribution of ADCs within an organ, instead of merely looking at an average value over a certain region of interest (ROI). Recently, the spatial resolution of diffusion-weighted imaging has become sufficiently high also in small organs such as the salivary glands, through the use of dedicated coils and sequences. Early results are very encouraging (Eida et al. 2007).

SALIVARY GLAND TUMORS

Salivary gland tumors represent 3–5% of all head and neck tumors, with the parotid glands being the most frequent (between 64% and 80%) sites (Barnes et al. 2005). Benign tumors represent 54–79% of these tumors. The majority (70–85%) of parotid gland tumors are benign. Tumors of the submandibular and sublingual glands are more likely to be malignant; ~40% of submandibular tumors and 70–90% of sublingual tumors are malignant. Salivary gland tumors also occur in minor salivary glands of the palate, buccal mucosa, lips, tongue, retromolar pad, and glossopharyngeal area. Approximately half of all minor salivary gland tumors are malignant.

Pleomorphic adenomas are the most common (~50%) benign epithelial tumors of the salivary glands. Pleomorphic adenomas tend to form well-defined ovoid tumors. They are often encapsulated but may exhibit a pedunculated outgrowth, for example, from the superficial to the deep lobes of the parotid gland. Glandular, ductal, or solid structures of epithelial elements are major components of this tumor. The lesion also comprises mesenchymal tissues, which may be frequently associated with cartilaginous or fibromyxomatous tissues. The lesion may be associated with cysts, hemorrhage, necrosis, or calcification.

Warthin's tumor is the second commonest tumor of the salivary glands. The tumor exclusively occurs in the parotid gland, typically in the tail. It may occur as multiple masses within one or both parotid glands. The tumor is composed of glandular and cystic structures, which sometimes exhibit a papillary cystic arrangement, lined by a double layer of epithelium, comprising inner columnar eosinophilic or oncocytic cells surrounded by smaller basal cells. The stroma contains varying amounts of lymphoid tissues with germinal centers.

Cystadenoma is a benign epithelial tumor characterized by multiple small cystic spaces or a single large cyst surrounded by lobules of salivary glands or by connective tissues.

Mucoepidermoid carcinoma represents ~30% of the malignant tumors of the

salivary glands and arises most commonly (~50%) in the parotid gland, followed by the minor salivary glands (~45%). The tumor is characterized by mucous, intermediate, or epidermoid cells. Low-grade tumors are well circumscribed; they usually contain large cystic areas with mucinous components and abundant mucous cells that are lined by epidermoid components. The mucous cells are large with pale cytoplasm and peripherally displaced nuclei. High-grade tumors are poorly circumscribed, infiltrative, and exhibit dominant proliferation of epidermoid components; mucous cells are rarely observed.

Adenoid cystic carcinoma represents ~10% of all epithelial salivary gland tumors and most frequently involves the parotid, submandibular, and minor salivary glands. The tumor is well-circumscribed, but only partially encapsulated and invariably infiltrative. The tumor is rarely associated with cyst formation and hemorrhage. Histopathologically, adenoid cystic carcinoma is classified into tubular, cribriform, or solid type. The tubular type comprises tubules lined by inner epithelial and outer myoepithelial cells. The cribriform pattern is the most frequent and is characterized by nests of cells with microcystic spaces. These spaces are filled with hyaline or basophilic mucoid material. The solid type contains sheets of uniform basaloid cells lacking tubule or microcyst formation. These three types may appear as a dominant feature of the tumor or as a part of the tumor. This tumor has a tendency to spread via nerves. Perineural invasion is the hallmark of this tumor; tumors may extend along nerves for a considerable distance from the boundary of primary lesions.

Acinic cell carcinoma represents ~9% of all malignant tumors of the parotid gland. The parotid gland is the most common site (~80%) of origin of this tumor, and bilateral involvement is observed in 3% of the patients. Metastasis to the regional lymph nodes is not uncommon, followed by frequent metastasis to more distant sites, most commonly the lung. The tumort is either a solid mass or partially cystic. Histologically, the acinic cell carcinoma recapitulates serous cells with bubbly basophilic cytoplasm containing zymogen granules.

Salivary duct carcinoma is a very aggressive tumor; histologically, it displays squamoid appearance, reminiscent of mucoepidermoid carcinoma or squamous cell carcinoma. Perineural spread is also common in this malignant neoplasm, and lymph node metastasis is not uncommon.

Cystadenocarcinoma is characterized by predominantly cystic growth that is often associated with intraluminal papillary growth. Approximately 65% tumors occur in the major salivary glands. Compared to the other benign and malignant salivary gland tumors, this tumor involves the sublingual gland more frequently.

2D ADC Color Mapping of Salivary Gland Tumors

Salivary gland tumors comprise distinctive tissues, including proliferating tumor cells, myxomatous tissues, lymphoid tissues, necrosis, and cysts (Barnes et al. 2005) (Figure 18.1). Analyzing a large ROI in a histologically heterogeneous tumor may, therefore, result in spurious results with regard to tumor histology. To avoid this potential error, 2D analysis using high-resolution MR imaging is mandatory for precise tissue characterization of salivary gland tumors.

We obtain ADC maps by using 2 b factors (500 and 1,000 s/mm^2). Isotropic diffusion

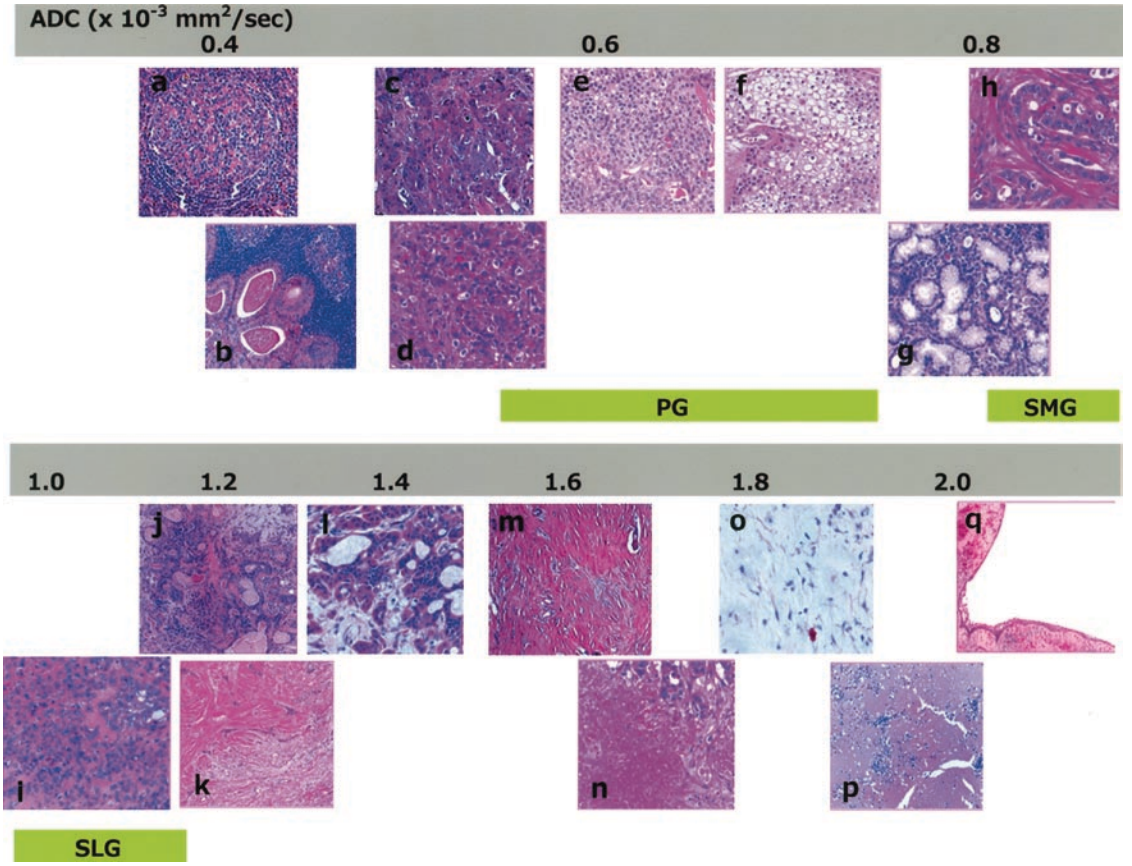

FIGURE 18.1. ADCs of various tissues in salivary gland tumors and of healthy major salivary glands. (**a**) Lymphoma lesion with germinal center; (**b**) lymphoid tissues in Warthin's tumor; (**c**) densely packed, poorly differentiated cancer cells in adenocarcinoma; (**d**) densely packed cancer cells in salivary duct carcinoma; (**e**) epidermoid cancer cells in mucoepidermoid carcinoma; (**f**) polygonal, clear cancer cells in mucoepidermoid carcinoma; (**g**) abundant mucous cells lined by epidermoid cells in mucoepidermoid carcinoma; (**h**) cancer cell nests in fibrous connective tissues of salivary duct carcinoma; (**i**) plasmacytoid proliferation in pleomorphic adenoma; (**j**) proliferating tumor cells associated with multiple small cystic areas in pleomorphic adenoma; (**k**) myxoid area with significant hyalinization; (**l**) mixed area of ductal and solid epithelial components and mesenchymal tissues associated with cartilaginous and fibromyxoid materials; (**m**) necrotic area in adenocarcinoma; (**n**), necrotic area in salivary duct carcinoma; (**o**) homogeneous myxomatous tissues in pleomorphic adenoma; (**p**) large necrotic area in Warthin's tumor; (**q**) large cystic area in pleomorphic adenoma. *PG* parotid gland, *SMG* submandibular gland, *SLG* sublingual gland

images are obtained, by applying both the b factors along the three orthogonal directions. This procedure requires additional time to perform. To prevent susceptibility artifacts, we use the SENSE technique (SENSE factor = 2) that reduces echo train length during the diffusion-weighted imaging. The total image acquisition time can be 1 min 32 s/20 slices using SENSE technique. This rapid imaging allows us to obtain ADC maps without significant motion artefacts.

To obtain 2D ADC maps from salivary gland tumors, a ROI is placed manually

on a fat-suppressed T2-weighted image so that the ROI encompasses the whole tumor area on that image. Then, the ROI is automatically copied and pasted onto the corresponding ADC map. The ADC of each tumor can be represented as an average of three mid-sections of the lesion or of whole sections of the tumor.

Gray-scale ADC map images obtained from the tumors are saved in the TIF format and then converted to color ADC map images (Figs. 18.2 and 18.3). Consequently, tumor areas having high ADCs are displayed as color areas of shorter wavelengths such as red and tumor areas having low ADCs, as color areas of longer wavelengths such as blue. These procedures can be performed on a personal computer by using OsiriX software (http://www.osirix-viewer.com).

ADC characterization of salivary gland tumors can be performed by determining the area having an extremely low ADC ($<0.6 \times 10^{-3}$ mm^2/s), low ADC (0.6×10^{-3} mm^2/s to $<1.2 \times 10^{-3}$ mm^2/s), intermediate ADC (1.2×10^{-3} mm^2/s to $<1.8 \times 10^{-3}$ mm^2/s), or high ADC ($\geq 1.8 \times 10^{-3}$ mm^2/s), relative to the total maximum tumor area on the ADC maps. Imaging software, such as ImageJ (Wayne Rasband; http://rsb.info.nih.gov/ij/), may be useful. The obtained results can be expressed as percentage areas.

Diffusion-weighted imaging has been advocated as functional imaging of the parotid glands. Any changes in the water content of the cells and interstitial tissues are considered to affect the ADC levels of the glands. The ADC was decreased in the salivary glands with impaired function (Sumi et al. 2002), and stimulation of the salivary gland function increased the ADC levels of the glands (Thoeny et al. 2005). Therefore, different cellular and tissue components in salivary gland tumors would significantly affect the ADC levels of the tumors. In general, growing cancer lesions are considered to have relatively rich water content; this nature of tumor cells, particularly of malignant tumor cells, significantly decreases the ADC levels of a tumor. Further, water that is confined in the cell significantly limits the water movement (Sumi et al. 2003). However, salivary gland tumors are known to display a wide spectrum of histological features. Therefore, tumor contrast on diffusion-weighted images may be significantly affected by variations in the proportions of tumor tissue components, i.e., the stages of tumor cell differentiation, presence or absence of necrotic tissues and cyst formation, density of the tumor cells, and degenerative changes of the interstitial tissues, such as myxomatous changes.

ADCs of Healthy Major Salivary Glands

The relative contents of the secretory acinus and the relative amounts of the intralobular and extralobular adipose tissues differ among the three major salivary glands (Barnes et al. 2005). The parotid gland is almost purely serous and contains abundant intralobular and extralobular adipose tissue. The adipose tissue increases in relative volume with age. The submandibular gland is a mixed-type gland; it is predominantly serous (~90%) with some mucous element. On the other hand, the sublingual gland is predominantly mucous.

Considering these differences in the parenchymal components, it can be expected that the imaging features of the three major salivary glands would be somewhat different. Indeed, the parotid gland exhibits low atten-

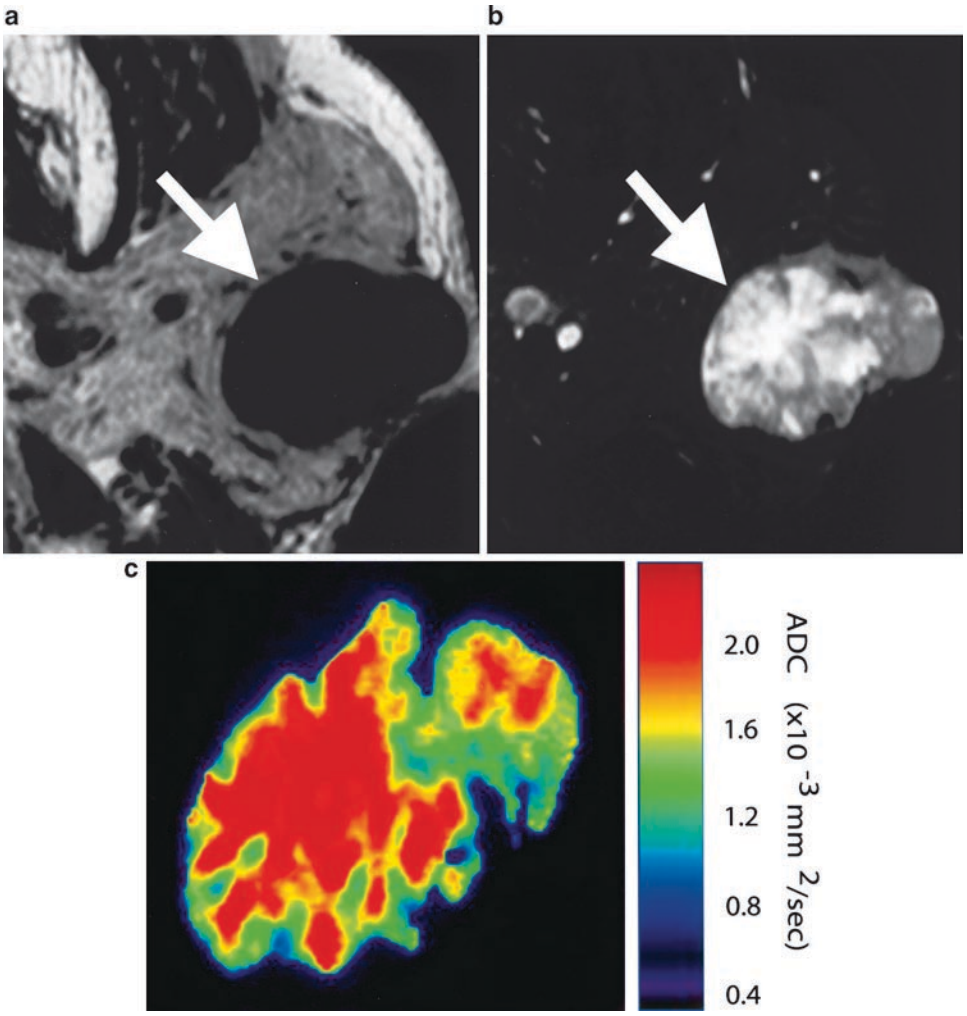

FIGURE 18.2. Fifty-nine-year-old woman with pleomorphic adenoma of parotid gland. (**a**) Axial T1-weighted (TR/TE = 500 ms/15 ms) image using 47-mm microscopy coil shows tumor (*arrow*) with homogeneous architecture and hypointense signals relative to gland. (**b**) Axial fat-suppressed T2-weighted (TR/TE = 4677 ms/80 ms) image using 47-mm microscopy coil shows tumor (*arrow*) with heterogeneous signals. (**c**) Axial ADC map shows that tumor contains high ADC area and peripheral intermediate ADC area

uation on CT due to its rich adipose tissue content. On ultrasound, the healthy parotid gland exhibits numerous echogenicity in the gland parenchyma originating from the adipose tissue in the gland. Consistent with this, the parotid glands are most hyperintense among the three major salivary glands on T1-weighted MR images. Interestingly, the sublingual glands are more hyperintense on T1-weighted images than the submandibular glands (Thoeny 2007; Sumi et al. 1999). Because the submandibular and sublingual glands do not contain significant amounts of fat tissue, the observed differences in signal intensity between these glands might be due to differences in the structures of the acinus-duct system or differences in the proportion of the serous and mucous components in the duct, acinus, or both (Sumi et al. 1999). In this

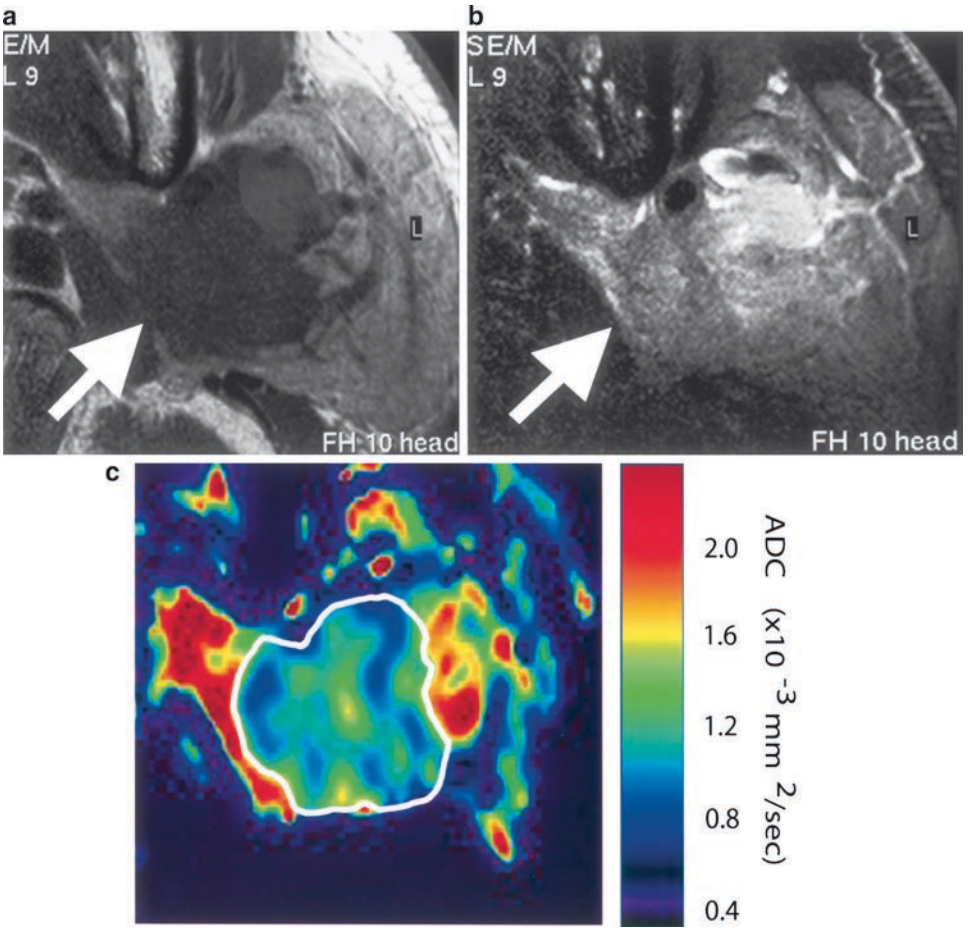

FIGURE 18.3. Eighty-one-year-old man with salivary duct carcinoma of parotid gland. (**a**) Axial T1-weighted (TR/TE = 500 ms/15 ms) image using 47-mm microscopy coil shows tumor (*arrow*) with homogeneous architecture and hypointense signals relative to gland. (**b**) Axial fat-suppressed T2-weighted (TR/TE = 4677 ms/80 ms) image using 47-mm microscopy coil shows tumor (*arrow*) with heterogeneous signals. (**c**) Axial ADC map shows that tumor (indicated by *white contour*) contains intermediate and low ADC areas

regard, greater amounts of proteinaceous content in the sublingual and, to a lesser degree, in the submandibular glands might increase the intensity levels of the glands on T1-weighted images.

Recently, we found that the ADC levels were significantly different among the major salivary glands (Sumi et al. 2002; Eida et al. 2007) (Figure 18.1). The ADCs of the parotid glands were lowest ($0.63 \pm 0.11 \times 10^{-3}$ mm^2/s) among the major salivary glands, followed by those of the submandibular glands ($0.87 \pm 0.05 \times 10^{-3}$ mm^2/s). The sublingual glands showed the highest ADCs ($0.97 \pm 0.09 \times 10^{-3}$ mm^2/s). At present, we do not have any definite explanation for the observed differences in the ADC levels among the major salivary glands. ADCs are considered to be greatly affected by cell density, cell size, nuclear-to-cytoplasmic ratio, the viscosity of the intra- and extracellular fluids, and the

serous and mucous contents. The major salivary glands may have distinct tissue profiles of these cellular and extracellular features.

It should be noted that considerable differences among the ADC values of healthy salivary glands are found in published reports (Eida et al. 2007; Thoeny et al. 2004; Zhang et al. 2001). It is plausible that these differences may result from the use of different b values in these studies. Alternatively, the spread in ADC values of the salivary glands can possibly be correlated to the production of saliva at the time of measurement (Thoeny et al. 2005). Therefore, different studies should be carefully interpreted.

ADCs of Benign Salivary Gland Tumors

As mentioned earlier, benign salivary gland tumors comprise distinctive tissues, including proliferating tumor cells, myxomatous tissues, lymphoid tissues, necrosis, and cysts. In our recent study, we compared the 2D ADC maps and histological features of excised tumor specimen (Eida et al. 2007). Pleomorphic adenomas are generally homogeneous on T1-weighted images and heterogeneous on fat-suppressed T2-weighted images (Motoori et al. 2004; Eida et al. 2007) (Figure 18.2a, b). The 2D ADC maps show that that the areas of proliferating tumor cells are associated with intermediate ADC levels. The tumor areas that contain large cystic areas or myxomatous lesions exhibit high ADCs (Figure 18.2c).

Warthin's tumors are relatively homogeneous on T1- and T2-weighted images (Ikeda et al. 2004; Eida et al. 2007). In contrast, the ADC distributions are often heterogeneous, being composed of areas with extremely low ADC indicating lymphoid tissues and areas with high ADCs indicating cyst formation among the lymphoid tissues.

ADCs of Malignant Salivary Gland Tumors

Mucoepidermoid carcinomas are homogeneous in architecture on T1-weighted images and are slightly heterogeneous on T2-weighted images. Low to intermediate signal intensity can be observed on T1- and T2-weighted images (Thoeny 2007). Homogeneous tumor areas with low ADCs correspond to areas with polygonal or round cell proliferation.

Adenocarcinoma and adenoid cystic carcinoma exhibit relatively homogeneous signals on T1- and T2-weighted images. The tumors exhibit low intensity on T1-weighted images and high intensity on T2-weighted images (Eida et al. 2007). ADC maps may display speckled patterns of low to high ADCs. These heterogenous patterns of ADC maps are attributable to small necrotic or cystic areas distributed in the tumors.

Salivary duct carcinomas are homogeneous with low intensity on T1-weighted images and heterogeneous with intermediate to high signal intensity on T2-weighted images (Motoori et al. 2005) (Figure 18.3a, b). ADC mapping may demonstrate a mixed pattern of low and intermediate ADCs, consistent with the aggressive proliferation of cancer cells with squamoid appearance (Figure 18.3c).

Malignant lymphomas in the salivary glands are homogeneous on T1- and T2-weighted images. On ADC maps, the tumors are almost exceptionally homogeneous with extremely low ADCs ($<0.5 \times 10^{-3}$ mm^2/s) throughout the lesions; this may reflect the homogeneous growth pattern of lymphoma cells.

TISSUE CHARACTERIZATION WITH APPARENT DIFFUSION COEFFICIENT MAPPING

Figure 18.1 summarizes the ADCs of various tissues of salivary gland tumors and those of healthy parotid, submandibular, and sublingual glands. Lymphoid tissues are categorized into the salivary gland tumor tissue group having the lowest ADCs ($<0.5 \times 10^{-3}$ mm^2/s). The ADCs of epidermoid tumor cell areas are low, but higher than those of lymphoid cells. The ADCs of the areas containing mucus-secreting cancer cells are also low, but slightly higher than those of areas containing epidermoid cancer cells. Increases in the amounts of fibrous connective tissue between cancer cell nests decrease the ADC levels of the tumor. The presence of mucins and myxomatous materials in the extracellular matrix increases the ADCs. Thus, mixtures of cellular and connective tissue components result in intermediate ADCs. Cystic areas reveal the highest ADCs.

The ADCs of necrotic tissues were higher than those of viable tissues (Lyng et al. 2000). In patients with head and neck squamous cell carcinomas, necrotic areas are frequently observed in metastatic nodes (Nakamura and Sumi 2007). Therefore, metastatic nodes exhibited significantly higher ADCs than the benign reactive nodes in the necks of these patients. In contrast, nodal lymphomas, which are rarely associated with necrosis, had the ADCs significantly lower than those in benign reactive nodes. These observations could be successfully explained by the notion that the ADC is dominated here by the intracellular water component. However, in necrotic tissues, where the cell membranes are lost, larger diffusion distance is allowed. Furthermore, there are two types of necrosis; liquefaction and coagulation necroses. The resulting viscosity will be different. It is plausible, but not proven yet, that the ADCs are different between liquefaction and coagulation necroses (Nakamura and Sumi 2007).

The recent study has demonstrated that myxomatous tissues have high ADCs (~1.8 $\times 10^{-3}$ mm^2/s) (Eida et al. 2007). In addition, benign tumors frequently contain cystic components, which also contribute to the high ADC levels seen in benign tumors. In contrast, areas with high ADCs are rare or very limited in the case of malignant salivary gland tumors. Thus, the presence of tumor areas with high ADCs could be an important criterion in differentiating benign salivary gland tumors from malignant ones. In malignant salivary gland tumors, areas with extremely low or low ADCs were found to occupy major parts of the tumor, consistent with hypercellularity and thus high intracellular water-to-extracellular water ratio of malignant tumors. However, Warthin's tumors also contain significant areas with extremely low or low ADCs. Therefore, the use of the low or extremely low ADC criterion did not yield a good result in differentiating between benign and malignant tumors (Eida et al. 2007).

APPLICATIONS OF APPARENT DIFFUSION COEFFICIENT MAPPING TO THE DIAGNOSIS OF MALIGNANT LESIONS

One of the major targets for the use of many imaging techniques is differentiating between benign and malignant lesions in various organs. As mentioned earlier, the

diffusion-weighted imaging technique is very sensitive to molecular displacements. This characteristic might be useful for differentiating between benign and malignant lesions. Diffusion-weighted imaging was able to differentiate between benign and malignant lesions in the liver, breast, metastatic nodes in the neck, and pharyngeal carcinomas (Taouli et al. 2003; Sinha et al. 2002; Sumi et al. 2003, 2007). Interestingly, the gradings of some malignant tumor types can be predicted by using the ADC values (Sumi et al. 2003, 2007).

HIGH-RESOLUTION IMAGING OF MALIGNANT LESIONS

We can use different types of surface coils (for example, 47-mm microscopy coil and 110-mm S coil) so that obtained 2D ADC maps could successfully correlate with the corresponding histology. The use of a surface coil greatly improved the resolution of diffusion-weighted imaging. However, the resolution of the obtained images was still insufficient for the effective correlation between MR images and histology, particularly in cases wherein the use of a smaller coil (microscopy coil) was limited due to the anatomical locations of the tumors. This is because the SENSE technique cannot be applied using the 47-mm surface coil. This coil is also associated with the shortcomings in the diagnosis of tumors located in the deep parts of the neck. Therefore, the 110-mm surface coil is more convenient for routine examinations despite its lower resolution than the 47-mm coil. Further technological innovations for high-resolution MR imaging are required for continuing improvement in diffusion-weighted image quality.

In conclusion, ADC mapping allows tissue characterization of salivary gland tumors. The obtained 2D distribution patterns of various tumor tissues are very characteristic of some tumor types, and these patterns may be distinct between benign and malignant salivary gland tumors. This technique would also be useful in differentiating between benign and malignant tumors in other organs and for the evaluation of treatment efficacy in malignant lesions.

REFERENCES

Barnes L, Everson JW, Reichar P, Sidransky D (2005) Pathology and genetics of head and neck tumors; World Health Organization Classification of Tumours. IARC Press, Lyon

Brown R (1828) A brief account of microscopipcal observations made in the months of June, July, and August, 1827, on the particles contained in the pollen of plants; and on the general existence of active molecules in organic and inorganic bodies. Philos Mag 4:161–173

Callaghan PT, Macgowan D, Packer KJ, Zelaya FO (1990) High resolution q-space imaging in porous structures. J Magn Reson 90:177–182

Eida S, Sumi M, Sakihama N, Takahashi H, Nakamura T (2007) Apparent diffusion coefficient mapping of salivary gland tumors: prediction of the benignancy and malignancy. AJNR Am J Neuroradiol 28:116–121

Einstein A (1905) Über die von der molekularkinetischen Theorie der Wärme geforderte Bewegung von in ruhenden Flüssigkeiten suspendierten Teilchen. Ann Phys (Leipzig) 17:549–560

Farzaneh F, Riederer SJ, Pelc NJ (1990) Analysis of T2 limitations and off-resonance effects on spatial resolution and artifacts in echo-planar imaging. Magn Reson Med 14:123–139

Ikeda M, Motoori K, Hanazawa T, Nagai Y, Yamamoto S, Ueda T, Funatsu H, Ito H (2004) Warthin tumor of the parotid gland: diagnostic value of MR imaging with histopathologic correlation. AJNR Am J Neuroradiol 25:1256–1262

Le Bihan D, Breton E, Lallemand D, Grenier P, Cabanis E, Laval-Jeantet M (1986) MR imaging of intravoxel incoherent motions: application to

diffusion and perfusion in neurologic disorders. Radiology 161:401–407

Kurihara Y, Yakushiji YK, Tani I, Nakajima Y, Van Cauteren M (2002) Coil sensitivity encoding in MR imaging: advantages and disadvantages in clinical practice. AJR Am J Roentgenol 178:1087–1091

Lyng H, Haraldseth O, Rofstad EK (2000) Measurement of cell density and necrotic fraction in human melanoma xenografts by diffusion weighted magnetic resonance imaging. Magn Reson Med 43:828–836

Moseley ME, Cohen Y, Mintorovitch J, Kurcharczyk J, Chileuitt L, Shimizu H, Kurcharczyk J, Wendland MF, Weintein PR (1990) Early detection of regional cerebral ischemia in cats: comparison of diffusion- and T2-weighted MRI and spectroscopy. Magn Reson Med 14:330–346

Motoori K, Iida Y, Nagai Y, Yamamoto S, Ueda T, Funatsu H, Ito H, Okamoto Y (2005) MR imaging of salivary duct carcinoma. AJNR Am J Neuroradiol 26:1201–1206

Motoori K, Yamamoto S, Ueda T, Nakano K, Muto T, Nagai Y, Ikeda M, Funatsu H, Ito H (2004) Inter- and intratumoral variability in magnetic resonance imaging of pleomorphic adenoma. J Compt Assist Tomogr 28:233–246

Nakamura T, Sumi M (2007) Nodal imaging in the neck: recent advances in US, CT and MR imaging of metastatic nodes. Eur Radiol 17:1235–1241

Pruessmann KP, Weiger M, Scheidegger MB, Boesiger P (1999) SENSE: sensitivity encoding for fast MRI. Magn Reson Med 42:952–962

Sinha S, Lucas-Quesada FA, Sinha U, DeBruhl N, Bassett LW (2002) In vivo diffusion-weighted MRI of the breast: potential for lesion characterization. J Magn Reson Imaging 15:693–704

Sumi M, Ichikawa Y, Nakamura T (2007) Diagnostic ability of apparent diffusion coefficients for lymphomas and carcinomas in the pharynx. Eur Radiol 17:2631–2637

Sumi M, Izumi M, Yonetsu K, Nakamura T (1999) Sublingual gland: MR features of normal and diseased states. AJR Am J Roentgenol 172:717–722

Sumi M, Sakihama N, Sumi T, Morikawa M, Uetani M, Kabasawa H, Shigeno K, Hayashi K, Takahashi H, Nakamura T (2003) Discrimination of metastatic cervical lymph nodes with diffusion-weighted MR imaging in patients with head and neck cancer. AJNR Am J Neuroradiol 24:1627–1634

Sumi M, Takagi Y, Uetani M, Morikawa M, Hayashi K, Kabasawa H, Aikawa K, Nakamura T (2002) Diffusion-weighted echoplanar MR imaging of the salivary glands. AJR Am J Roentgenol 178:959–965

Takahara T, Imai Y, Yamashita T, Yasuda S, Nasu S, Van Cauteren M (2004) Diffusion weighted whole body imaging with background body signal suppressed (DWIBS): technical improvement using free breathing, STIR and high resolution 3D display. Radiat Med 22:275–282

Taouli B, Vilgrain V, Dumont E, Daire JL, Fan B, Menu Y (2003) Evaluation of liver diffusion isotropy and characterization of focal hepatic lesions with two single-shot echo-planar MR imaging sequences: prospective study in 66 patients. Radiology 226:71–78

Thoeny HC (2007) Imaging of salivary gland tumours. Cancer Imaging 7:52–62

Thoeny HC, De Keyzer F (2007) Extracranial applications of diffusion-weighted magnetic resonance imaging. Eur Radiol 17:1385–1393

Thoeny HC, De Keyzer F, Boesch C, Hermans R (2004) Diffusion-weighted imaging of the parotid gland: influence of the choice of *b*-values on the apparent diffusion coefficient value. J Magn Reson Imaging 20:786–790

Thoeny HC, De Keyzer F, Claus FG, Sunaert S, Hermans R (2005) Gustatory stimulation changes the apparent diffusion coefficient of salivary glands: initial experience. Radiology 235:629–634

van Gelderen P, de Vleeschouwer MHM, DesPres D, Pekar J, van Zijl PCM, Moonen CTW (1994) Water diffusion and acute stroke. Magn Res Med 31:154–163

Zhang L, Murata Y, Ishida R, Ohashi I, Yoshimura R, Shibuya H (2001) Functional evaluation with intravoxel incoherent motion echo-planar MRI in irradiated salivary glands: a correlative study with salivary gland scintigraphy. J Magn Reson Imaging 14:223–229

19
Role of Human Papillomavirus in Tonsillar Cancer

Eva Munck-Wikland, Lalle Hammarstedt, and Hanna Dahlstrand

INTRODUCTION

Tonsillar cancer is the most common of the oropharyngeal malignancies and belongs to the group of head and neck cancer that originate in the Waldeyer's ring. Smoking and alcohol are regarded as the main etiological factors for head and neck squamous cell carcinoma (HNSCC), but these tumors also occur in some 15–20% of patients without these risk factors. Accumulating data indicate that high risk human papillomavirus (HPV) is associated with a subgroup of HNSCC mainly oropharyngeal cancer (Gillison and Shah 2001; Mellin et al. 2000), and studies indicate that a history of smoking and high-risk HPV seropositivity, together, increase the risk for HNSCC suggesting that there is either an additive or synergistic relationship between these two risk factors.

TONSILLAR CANCER

Tonsillar cancer is occasionally diagnosed at an early stage but more commonly when regional metastases are present. Quite frequently the patients have seeked their general practitioners due to "a sore throat" and been treated with antibiotics prior cancer diagnosis. Patients may present with a lump in the neck as the sole symptom and later, after examination, the primary tumor of the tonsil is found. One sided ear pain or swallowing difficulty is another common first symptom.

Treatment for tonsillar cancer varies considerably worldwide. There are still centers where surgery is the initial treatment, but gradually tonsillar cancer is regarded as an "oncologic" disease where oncologic treatment e.g., radiation, possibly in concert with chemotherapy, is the first line treatment and surgery is reserved for salvage. However, in the case of (extensive) regional metastasis at diagnosis, neck dissection is frequently planned to be included in the primary treatment after the oncologic session.

There have been improvements in the treatment of HNSCC during the last years, leading to a decreased morbidity and increased quality of life, but 5-year survival rates are still low.

HUMAN PAPILLOMAVIRUS (HPV)

There are more than 100 HPV types divided into high-risk HPV (16, 18, 31, and 33) found to be associated with human

cancer, of which cervical carcinoma is the most studied, and low-risk HPV associated with benign hyperplastic lesions, i.e., common warts, chondylomas, and papillomas. The genome of HPVs consists of double-stranded circular DNA, enclosed in a 52–55 nm viral capsid. The genome is divided into a noncoding region and the early and late coding regions. The early region encodes for the early proteins E1–E2 and E4–7, which are important for pathogenesis and transformation, while the late region encodes for L1 and L2 the two capsid proteins.

When zur Hausen in 1976 proposed that cervical cancer might be caused by human papillomavirus (HPV), the scientific community accepted that HPV could potentially be involved in the development of *some* but definitely *not all* cervical cancers. Today it is fully accepted that different types of HPVs are present and instrumental in the induction of almost all cervical cancers as well as some other types of human cancers (zur Hausen 2002).

In 1983 HPV was suggested to have a role in the pathogenesis of head and neck cancer due to morphologic features (Syrjanen et al. 1983). Since then, substantial molecular evidence to support this finding has been revealed (Gillison and Shah 2001). HPV-16 is today encountered in a substantial proportion of oropharyngeal cancer (Mellin et al. 2000; D'Souza et al. 2007; Dahlgren et al. 2003; Hammarstedt et al. 2006) and has been identified in 90% of HPV-positive HNSCC. HPV 18, 31, and 33 has been found in the remaining cases. The viruses exert their carcinogenic power by producing two oncoproteins encoded by the viral E6 and E7 genes. E6 binds to the cellular protein p53 and degrades it, while E7 binds to pRb and abrogates its function. When normal p53 and pRb intracellular levels are reduced, cell cycle control is hampered, cell cycle entrance and DNA synthesis are promoted, and apoptosis is blocked (zur Hausen et al. 2002) Furthermore, there is upregulation of other cell cycle factors such as p16 ^{INK4A} (Hanahan and Weinberg 2000).

Also of interest is that the L1, the major capsid protein, can self assemble and form virus like particles, which are useful for vaccination against HPV infections (Rose et al. 1993).

EPIDEMIOLOGY

The incidence of head and neck cancer shows large variability worldwide with high incidence rates in parts of India, South East Asia and some parts of Europe. Regarding tonsillar cancer specifically, incidence rates are high in the Western world, especially in some parts of the US and Australia. In Europe, incidence rates vary with the highest rates seen in France. The Eastern countries like China generally present low incidence rates (http://www-dep.iarc.fr/GLOBOCAN, accessed October 2006). Interestingly, Hong Kong, with a strong Western influence, has higher incidence rates (Li et al. 2007).

Historically, the incidence of tonsillar cancer has shown a dramatic increase in Europe as well as in the US, without an increase in traditional risk factors, i.e smoking and alcohol (Figure 19.1) (Hammarstedt et al. 2007). Parallel to this, there has been a similar increase in the proportion of HPV positive tonsillar cancer. In Sweden, this increase has been from 23% HPV positive

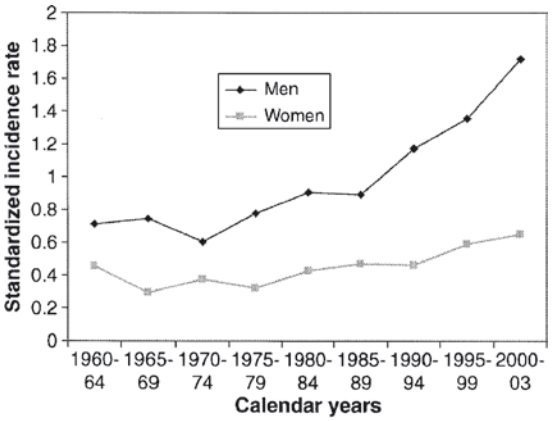

FIGURE 19.1. The incidence of tonsillar cancer in Sweden since 1960 (Reproduced from Hammarstedt et al. 2007. With permission from www.informaworld.com.)

tumors in the 1970s to 68% in 2000–2002 (Table 19.1). The vast majority of the tumors harbour HPV-16 (Hammarstedt et al. 2006). Patients with HPV positive tumors are younger at diagnosis and more often non-smokers (D'Souza et al. 2007; Gillison an Shah 2001; Li et al. 2003; Mellin et al. 2000).

EVIDENCE OF HPV ROLE IN CARCINOGENESIS

HPV DNA is now present in about 70% of tonsillar cancer diagnosed in the Stockholm area (Hammarstedt et al. 2006). But, HPV-DNA presence in tumor tissue does not necessarily imply viral involvement in the carcinogenesis but may reflect a transient infection. Importantly, when using DNA as well as RNA in situ hybridization, the viral genome and its transcription products (performed on HPV-16) have been located in cancer cells, both at primary site and in the metastasis, but not in the surrounding stroma (Strome et al. 2002).

HPV-16 E6 and E7 mRNA expression is known to be essential for transformation in cervical cancer. The expression of these oncogenes have earlier been detected in tonsillar cancer; however, in studies only including a few oropharyngeal or tonsillar cancer cases. But, recently we found that E6 and/or E7mRNA were expressed in almost all accessible HPV-16 positive cases, strongly supporting an oncogenic role of HPV-16 in tonsillar cancer (Lindquist et al. 2007). We examined the diagnostic tonsillar cancer specimen from 192 patients. Extraction of RNA and expression of mRNA, monitored by presence of the housekeeping gene RNase P, were successfully determined in 53/54 of the 86 HPV-16 positive samples. In the remaining 32 samples either the paraffin blocks were not available or there was insufficient material. Expression of

TABLE 19.1. Presence of HPV DNA in pretreatment tonsillar squamous cell carcinoma biopsies obtained between 1970 and 2002

Calender years	Number of cases	Numbers of pre-treatment biopsies	Excluded	Presence of HPV DNA	P-value
1970–1979	84	39	9	7/30 (23%)	
1980–1989	133	55	13	12/42 (28%)	0.79
1990–1999	168	95	11	48/84 (57%)	0.0025
2000–2002	92	48	1	32/47 (68%)	<0.001
Total	477	237	34	99/203 (49%)	

Source: Reproduced from Hammarstedt et al. (2006). With permission from Wiley.

HPV-16 E6 mRNA (estimated as 0.06–9.94 copies/1,000 copies RNAsP) and /or E7 mRNA (0.6–68.4 copies/1,000 copies RNAsP) were detected in 50/53 (94%) of the samples, i.e., 42 samples expressed both E6 and E7, and 8 samples expressed only E7 (Table 19.2).

Mork et al. (2001) performed a nested case-control study investigating HPV infection as a risk factor for head and neck cancer. This seroepidemiological study investigated serum samples from 292 persons who later developed HNSCC, on average 9.4 years prior to diagnosis, and 1,568 matched controls. The prevalence of seropositivity for HPV-16 was twice as high in the patient group compared to that of the control group, and was found to be a significant risk factor for head and neck cancer 2.2 (95% CI, 1.4–3.4). When investigating the risk to develop cancer according to tumor location, the highest risk was found for oropharyngeal cancer (odds ratio 10.2) and cancer of the base of the tongue (odds ratio 20.7). Cancer of the base of the tongue belongs to the oropharyngeal cancer group. Fifty percent of oropharyngeal cancer and 14% of tongue cancers contained HPV-16 DNA and corresponded with prediagnostic seropositivity of HPV-16.

D'Souza et al. (2007) recently published another case-control study including 100 patients with oropharyngeal cancer and 200 controls in order to evaluate the association between HPV infection and oropharyngeal cancer. They found that oropharyngeal cancer was significantly associated with oral HPV-16 infection and seropositivity for the HPV-16 L1 capsid protein. HPV-16 DNA was detected in 72% of the oropharyngeal cancer specimen and 64% of the cancer patients were seropositive for E6, E7, or both. Four percent of the controls had an oral HPV infection, 7% were HPV-16 L1 seropositive , and 4% were seropositive for E6 and E7.

HPV-16 has also been demonstrated in metastases of HNSCC by in situ hybridization (Begum et al. 2007). HPV-16 was detected in 10/19 metastases from the oropharynx but in none of 46 metastases from other head and neck sites. HPV was *not* detected in two branchial cleft cysts misdiagnosed as metastatic squamous cell carcinoma, but HPV was detected in three out of ten metastases from occult primary tumors. Thus, when HPV-16 is found in neck nodes with unknown primary tumor the origin is most likely within the oropharynx.

Smeets et al. (2007) demonstrated HPV-DNA by PCR in 24/143 oral and oropharyngeal tumors, but could confirm viral involvement by E6/E7 expression analysis only in 12/24 samples. Thus, the presence of HPV-DNA did not per se mean that the virus was biologically active. It was shown that the tumors with transcriptionally active HPV lacked p53 mutations and exhibited a limited number of genetic imbalances, whereas their counterparts without transcriptionally active HPV showed p53 mutations in 75% and many genomic imbalances. (Braakhuis et al. 2004; Smeets et al. 2006). By considering detection of HPV E6 expression in frozen biopsies as gold standard for valid HPV infection, Smeets et al. (2007) found p16 immunostaining followed by GP5+/6+ PCR on the p16-positive cases to harvest a 100% sensitivity and specificity for assumed clinically relevant HPV infection.

SEXUAL BEHAVIOUR AND OROPHARYNGEAL CANCER

Sexually transmitted HPV is believed to cause virtually all cervical cancers (zur Hausen 2002) and the relation between sexual risk behaviour, HPV infection and oropharyngeal cancer has been a subject of interest for quite some time. D'Souza et al.(2007) found, in a case-control study, that a high life-time number of vaginal, and/or oral sex partners, engagement in casual sex, early age at first intercourse and infrequent use of condoms are each associated with HPV-16 positive oropharyngeal cancer. These data support that oral HPV infection is sexually acquired, but it cannot be ruled out that transmission of HPV could be possible through direct mouth to mouth contact or other means.

It is important to keep in mind that HPV is found in a substantial proportion of tonsillar and base of tongue cancer but not as frequently in other oral cavity subsites. Thus, studies dealing with the relation between sexual habits and oral/oropharyngeal cancer may not find increased risk between sexual risk behaviour and cancer because the HPV positive ones only constitute a proportion of the whole group.

Kreimer et al. (2004) performed a study to determine the prevalence and distribution of genital-mucosal type HPV infections in the oral region and tonsillar epithelium. High-risk HPV-16 infection was found in 1% of tonsils from healthy subjects while HIV patients showed an HPV prevalence of 7.5%. Tonsillar HPV infection was found to be strongly associated with HIV infection, immunosuppression, and certain sexual behavior in univariate analysis. The difference in prevalence between HIV-negative and HIV-positive subjects could not be explained by differences in sexual behaviour but could possibly be attributed to immunosuppression in the HIV group.

HPV AND PROGNOSIS IN TONSILLAR CANCER

All studies conducted by our group show a clear benefit from having HPV in the tumor (Dahlgren et al. 2004). This, in spite of the fact that patients with HPV positive tumors more often present with regional metastasis at diagnosis (Lindquist et al. 2007), a feature which is known to decrease survival significantly in all other HNSCC. In fact, HPV proved to be the strongest prognostic factor independent of age, sex, and tumor stage (Mellin et al. 2000; Lindquist et al. 2007).

Ragin and Taioli (2007) reviewed all published articles and conducted a meta-analysis on the overall relationship between HPV infection and overall survival and disease-free survival in HNSCC. Patients with HPV-positive HNSCC had a lower risk of dying, and a lower risk of recurrence than HPV-negative HNSCC patients. Site-specific analyses show that patients with HPV-positive oropharyngeal tumours had a 28% reduced risk of death in comparison to patients with HPV-negative oropharyngeal tumours. There was no difference in overall survival between HPV-positive and negative non-oropharyngeal patients.

Weinberger et al. (2006) found that patients harbouring HPV 16 positive oropharyngeal cancer with high p16 expression by microarray showed a 79% over all survival while patients with HPV negative cancers and/or low p16 expression had a 18–20% survival.

The reason why HPV-positive oropharyngeal cancers benefit from a better survival is not yet understood. It may depend on epidemiological reasons, such as reduced exposure to tobacco and alcohol that implies an overall better health. It could also relate to p53. If the carcinogenesis is carried out through E6 inactivation but not mutation of p53, the p53 function is not entirely lost and p53 can still help induce apoptosis and cell death by radiation therapy.

We know from our own studies and others that HPV-positive and -negative tonsillar cancer show different genomic imbalances (Dahlgren et al. 2003). By comparative genomic hybridization analysis we found a significant difference in the distribution of DNA gains and losses between the HPV-positive and –negative tonsillar cancer specimen. Gain on chromosome 3q24qter was more commonly seen in HPV-positive cancer, while gain on chromosome 7q11.2-q22 was found only in HPV negative cancer. Gains of 3q and 8q were in accordance with earlier reports from HNSCC. But, loss of chromosome 3p, which is frequently found in HNSCC, was found in only 16% of the tonsillar cancers. Again, this supports the view of tonsillar cancer being an exclusive entity in the family of HNSCC.

IMPACT OF VIRAL LOAD ON PROGNOSIS

Earlier studies (Kim et al. 2007; Mellin et al. 2002) indicated that a high viral load correlated with better survival. These studies included only a limited amount of patients. However, in a larger study of 150 patients with tonsillar cancer where 86 were HPV-16 positive, we could not confirm that viral load was of significant prognostic value (Lindquist et al. 2007).

$P16^{INK4A}$ – A SURROGATE MARKER FOR HPV 16

Progression through the cell cycle from G1 into S phase is a critical checkpoint controlled by cyclins and associated cyclin-dependent kinases (CDKs), such as cyclin D and CDK4. A main function of the tumor suppressor retinoblastoma (pRb) protein is to repress transcription of essential DNA synthesis genes, thus inhibiting transition into the S-phase. PRb represses these genes by binding to its cofactor E2F. Accumulation of cyclin D-dependent kinases triggers phosphorylation of pRb, releasing E2F from pRb, and thereby cancelling pRb repression. The cyclin D-dependent kinases are inhibited by CDK inhibitors, one of these being the tumor suppressor protein $p16^{INK4a.}$ (zur Hausen et al. 2002; Hanahan and Weinberg 2000). Through the binding of p16 and other CDK inhibitors to cyclin D-dependent kinases, pRb remains hypophosphorylated, and cell cycle progression into the S-phase is prevented. In high-risk HPV, the E7 oncoprotein binds to pRb leading to its degradation, releasing E2F and resulting in cell cycle progression into the S-phase. High-levels of $p16^{INK4a}$ have been found to correlate with inactive pRb and $p16^{INK4a}$ overexpression has been shown to reflect a loss of negative feedback by pRb on $p16^{INK4a}$ gene transcription (Li et al. 1994; Parry et al. 1995). Thus, in high-risk HPV-positive and pRb dysfunctional cervical cancer overexpression of p16 ^{INK4a} is observed, while no

$p16^{INK4a}$ is seen in HPV-negative lesions. Therefore, $p16^{INK4a}$ overexpression may be seen as a surrogate biomarker for the presence of high-risk HPV. Li et al. (2003) have shown that the presence of HPV correlated with overexpression of $p16^{INK4a}$, as well as reduced expression of cyclin-D and pRb in tonsillar carcinoma.

We found that $p16^{INK4a}$ analysis using immunohistochemistry with the primary monoclonal mouse anti-human $p16^{INK4a}$ antibody (clone E6H4, DakoCytomation A/S, Carpinteria, CA, US) showed a sensitivity of 80% and specificity of 73% as compared with HPV PCR results (Mellin Dahlstrand et al. 2005). Specificity was also correlated to the grading of the $p16^{INK4a}$ staining: the higher the grading the better the specificity. Interestingly, all but one of the patients with a high grade of $p16^{INK4a}$ staining, i.e., >50% of the cells were stained, were disease-free one month after radiotherapy. Furthermore, where 3–10 year follow up data were available 92% (12/13) of the patients with high grade staining remained tumor free. High grade of $p16^{INK4a}$ staining was even better than HPV PCR analysis in predicting radioresponse and may prove to be a useful tool when designing treatment strategies for patients with tonsillar cancer.

HPV IN OTHER OROPHARYNGEAL CANCER

We examined a patient material from 1970 to 2002 where 40% of base of tongue cancer showed HPV positivity while only 2.3% of the mobile tongue cancer specimen harboured HPV. For patients with base of tongue cancer the presence of HPV was similar to tonsillar cancer, a strong favourable prognostic factor (Dahlgren et al. 2004).

FUTURE PERSPECTIVES

The development of HPV L1 virus-like particles (VLP) vaccines is a potentially major advance in prevention of cervical cancer. These vaccines are based on the self-assembly of recombinant L1 protein into non-infectious capsids that contain no genetic material (Rose et al. 1993). Two VLP vaccines have been developed for primary HPV vaccination. Both vaccines target HPV 16 and HPV 18, one of the vaccines includes a standard alum adjuvant and targets also HPV6 and HPV 11. Both vaccines have shown nearly perfect efficacy against HPV infection and related cytological and histological endpoints for up to 5 years (Paavonen et al. 2007). The vaccines do not treat existing infections or lesions and cross-protection against other HPV types is partial or non-existent. Therefore, the current HPV vaccines are most certain to yield the greatest public health benefit in girls at an age before most have begun sexual activity.

The use of efficient prophylactic vaccines for high-risk HPVs will eventually have impact on the incidence of HPV-positive HNSCC. However it will take time until this effect will be evident since vaccination has not been shown to be effective in already infected individuals. Moreover, the effect on tonsillar cancer incidence will depend on whether or not only girls or also boys will be vaccinated.

Focus of interest for future research should be to identify the reason(s) for the better survival and better response to radiation therapy in order to possibly

reduce the aggressiveness in treatment for the HPV-positive patients and thereby reduce the lifelong side-effects. At this point, when chemotherapy and targeted therapy is evolving, a combined therapy where radiation is reduced could also be feasible.

METHODS OF HPV DETECTION AND GENOTYPING

All current HPV detection methods are based on detection of the viral nuclei acids since HPV cannot be cultured.

Polymerase Chain Reaction (PCR)

A common and the most sensitive technique for the detection of HPV is based on amplification of selected viral DNA sequences by PCR. Screening for multiple types of HPV by PCR is performed by using HPV consensus/general primers (e.g. GP5+/6+, My09/11, CPI/IIG) (de Roda Husman et al. 1995; Tieben et al. 1993). The sensitivity of PCR is high, detecting 1–10 copies of viral genome.

In detail, a broad spectrum PCR for detection of at least 27 HPV types is performed using the primers GP5+/ GP6+ (de Roda Husman et al. 1995). The final volume of 50 μL contain a solution of 50 mM potassium chloride, 10 mM Tris-chloride (pH 8.3), 200 μM of each deoxynucleotide, 2 mM magnesium chloride and contained 20 pmol of each primer and 1 U of Taq polymerase. A volume of 5μL, containing 50–150 ng of DNA extracted from the biopsy of is added. Amplification of 40 cycles consisted of one initial denaturation for 5 min at 95°C, a primer annealing cycle for 30 s at 45°C and a primer extension cycle for 1 min at 72°C, followed by 38 identical cycles except for the denaturation time of 30 s. The last cycle differed only with regard to the primer extension time, which was 5 min. If additional HPV types are of interest or if one need to exclude false negatives as a result of disrupted L1, another type of consensus primer as the CpI/IIG (complementary to E1) can be used (Tieben et al. 1993). The CpI/IIG PCR is run under the same conditions with the exception of that 3 mM $MgCl_2$, 0.05% BSA, 17 pmol of CpI and 26 pmol of CpIIG, and 2.5 U of Taq DNA polymerase is used, and that the PCR program consisted of 5 min at 94°C, 35 cycles of 95°C for 60 s, 55°C for 60 s, 72°C for 120 s and then 72°C for 10 min.

Hybrid Capture

Hybrid Capture 2 (HC2) is a method designed for detection of selected mixture of five low-risk and 13 high-risk HPV types (Digene Corporation, Gaithburg, Maryland), (Hesselink et al. 2004). The HC 2 test is the only FDA approved HPV detection test available. The assay uses the fact that HPV DNA hybridizes with synthetic RNA probes complementary to DNA sequences to specific HPV types. The sensitivity for the test is lower than to PCR, equivalent to 1 pg HPV DNA (5,000 copies of HPV genome) although a sensitivity down to 500 copies of HPV genome has been reported (Hesselink et al. 2004).

DNA In Situ Hybridization (ISH)

DNA in situ hybridization (ISH) does not only detect the viral DNA, but can also localize the virus within in the natural morphology of the tissue. Tissue sections are put on slides and the tissue sections are

hybridized with labeled DNA or RNA probes after denaturation. One commercial DNA ISH kit to detect high-risk HPV types as well as low- risk HPV types, using two separate fluorescent-labeled probe cocktails is from Ventana Medical Systems. These are INFORM HPV Tissue High Risk Probe, containing a mix of probes hybridizing with HPV-16, -18, -31, -33, -35, -45, -51, -52, -56, -58, -59, -68 and -70 and INFORM HPV Tissue Low Risk Probe, containing probes hybridizing with HPV-6, -11, -42, -43, and -44. Five µm sections is processed in the automated system BenchMark® XT (Ventana Medical Systems) as described by the manufacturer. Sections are deparaffinized briefly by proteolytic digestion (ISH-protease 2, Ventana Medical Systems) for 2 min, followed by denaturation of DNA. Thereafter the probe mixture is added and after hybridization with the probe mix for 2 h, visualization is performed. The sensitivity differs between different ISH methods but is generally lower to both PCR and HC2 and not suitable for screening (Hesselink et al. 2004).

HPV Genotyping

After the consensus/general PCR screening, the PCR product can be HPV typed by a reverse hybridization technique called reverse line blot (RLB) or line probe assay depending on which consensus/general primers that was used for the initial HPV detection (van den Brule et al. 2002).

Alternatively, HPV typing may be performed by a type-specific PCR (Hagmar et al. 1992). The HPV type-specific primers bind to a sequence found in a single HPV type (often in E6 or E7) and do not cross-bind to other HPV types. For example the specific typing PCR is run as above described for the GP+ PCR with the difference that the annealing temperature used is 55°C and the magnesium chloride concentration in the PCR mixture is 1.5 mM.

A third alternative is using restriction fragment length polymorphism (RFLP), done by digesting the consensus PCR product, yielding a HPV type specific pattern (Lungu et al. 1992)

HPV typing can also be performed by sequencing the consensus/general PCR product (Mellin et al. 2002). HPV direct cycle sequencing can be done after purifying the general/consensus PCR products (using for instance High Pure PCR Purification Product Kit, Roche Diagnostics) using the Big Dye Terminator Cycle Sequencing Kit(Applied Biosystems). For accuracy both DNA strands should be sequenced and can be aligned e.g., to those available at NCBI BLAST GenBank (http://www.ncbi.nlm.nih.gov/BLAST/).

Sequencing and RFLP is not suitable for detection of multiple HPV. The type specific PCR may detect multiple HPV types (one at a time) but is restricted to amount of DNA and number of type specific primer available.

HPV mRNA Amplification and Detection

The detection of mRNA of E6/E7 is of stronger predictive value for an active carcinogenesis than detection of viral DNA. Detection of viral mRNA can be done by reverse transcriptase (RT) PCR or by nuclei acid sequence based amplification NASBA (Sotlar et al. 2004; Smits et al. 1995). RNA can for example be extracted using Roche High Pure RNA kit (Roche Diagnostics, Stockholm, Sweden). Before cDNA synthesis, one can run a regular HPV-16 type specific PCR (as decribed above) on the samples to eliminate the

possibility of contaminating viral DNA. cDNA is then synthesized from extracted RNA e.g., by using SuperScript® III First-Strand Synthesis SuperMix for qRT-PCR kit (Invitrogen, Copenhagen, Denmark). A quantitative real-time PCR with a SybrGreen protocol in an iCycler iQ (iCycler iQ Real-time PCR Detection System; BioRad, Sundbyberg, Sweden) can be used to estimate cDNA viral load as a measurement of mRNA quantity in the samples. The seduence for E6 primers is 5′-GAGCGACCCAGAAAGTTACCA-3′ and 5′-AAATCCGCAAAAGCAAAGTCA-3′ and for E7 5′-ACCGGACAGAGCCCATTACAA-3′ and 5′-GTGCCCATTAACAGGTCTTCC-3′. The 25 μL PCR mix, consisted of 12.5 μL iQ SYBR Green Supermix (Bio-Rad, Sundbyberg, Sweden) and 1.25 μL (10 pmol μL^{-1}) each of the HPV-16 primers. The program consists of 50°C for 2 min and 95°C for 10 min, followed by 40 cycles of denaturation at 95°C for 15 s, and annealing and elongation at 60°C for 1 min. Finally, a melting curve, starting at 40°C and increasing by 0.5°C every 10 s until 120°C is reached, is run to verify the specificity of the obtained amplicons.. The RNase P kit above can be used to estimate expression of the human gene RNase P internal control.

HPV Serology

The detection of genotype-specific HPV capsid antibody in serum suggests a past or current infection (Pagliusi et al. 2006). However, approximately 50% of the patients with HPV DNA positive lesion develop a systemic neutralizing antibody response (Carter et al. 2001). HPV capsid antibody serology analysis is widely used in epidemiological studies and the antibody level correlates strongly to protection against the infection (Pagliusi et al. 2006).

HPV DNA Load

The amount of HPV DNA copies per human genome equivalent, the viral load, can be of interest. The viral load of subclinical infections has been show to correlate to the potential risk of future malignancy (Gravitt et al. 2007). For example to estimate the amount of HPV-16 copies a quantitative real-time PCR method (TaqMan), based on the 5′–3′ exonuclease activity of Taq DNA polymerase can be used. A dilution series of the pGEM-T plasmid with HPV-16 E6 insert can be used in each real time assay as a standard to calculate the number of viral copies. The real-time PCR is carried out with the same HPV-16 specific primers as in Hagmar et al. (1992) with the addition of a fluorogenic probe (16E6TQP) located in HPV-16 E6 designed with the following sequence 6-FAM-CCGGTCCACCGACCCCTTATATTATGGAATCTT-TAMRA-3′-phosphate. The PCR volume of 25 μL consists of 2.5 μL TaqMan PCR Buffer (Applied Biosystems), 200 μM of each dNTP, 1.5 mM of $MgCl_2$, 10 pmol of each primer, 5 pmol of the probe, 0.5 U Taq Gold DNA polymerase (Applied Biosystems), and 10 μL of template. The PCR was carried out in a PE Applied Biosystems 7700 Sequence Detector with an initial step of 50°C for 2 min, 95°C for 10 min, followed by 40 cycles of 15 s at 95°C and 1 min at 60°C. As an estimation of the human genome content, a commercial kit an be used, e.g. an assay measuring the expression of the human RNase P gene (TaqMan® RNase P Detection Reagents Kit, Applied Biosystems, Stockholm, Sweden). Calculation of viral load can be preformed as described in Lindquist et al. (2007).

REFERENCES

Begum S, Gillison ML, Nicol TL, Westra WH (2007) Detection of human papillomavirus-16 in fine-needle aspirates to determine tumor origin in patients with metastatic squamous cell carcinoma of the head and neck. Clin Cancer Res 13:1186–1191

Braakhuis BJ, Snijders PJ, Keune WJ, Meijer CJ, Ruijter-Schippers HJ, Leemans CR, Brakenhoff RH (2004) Genetic patterns in head and neck cancers that contain or lack transcriptionally active human papillomavirus. J Natl Cancer Inst 96:998–1006

van den Brule AJ, Pol R, Fransen-Daalmeijer N, Schouls LM, Meijer CJ, Snijders PJ (2002) GP5+/6+ PCR followed by reverse line blot analysis enables rapid and high-throughput identification of human papillomavirus genotypes. J Clin Microbiol 40:779–787

Carter JJ, Madeleine MM, Shera K, Schwartz SM, Cushing-Haugen KL, Wipf GC, Porter P, Daling JR, McDougall JK, Galloway DA (2001) Human papillomavirus 16 and 18 L1 serology compared across anogenital cancer sites. Cancer Res 61:1934–1940

Dahlgren L, Dahlstrand HM, Lindquist D, Hogmo A, Bjornestal L, Lindholm J, Lundberg B, Dalianis T, Munck-Wikland E (2004) Human papillomavirus is more common in base of tongue than in mobile tongue cancer and is a favorable prognostic factor in base of tongue cancer patients. Int J Cancer 112:1015–1019

Dahlgren L, Mellin H, Wangsa D, Heselmeyer-Haddad K, Bjornestal L, Lindholm J, Munck-Wikland E, Auer G, Ried T, Dalianis T (2003) Comparative genomic hybridization analysis of tonsillar cancr reveals a different patter of genomic imbalances in human papillomavirus-positive and -negative tumors. Int J Cancer 107:244–249

D'Souza G, Kreimer AR, Viscidi R, Pawlita M, Fakhry C, Koch WM, Westra WH, Gillison ML (2007) Case-control study of human papillomavirus and oropharyngeal cancer. N Engl J Med 356:1944–1956

Gillison ML, Shah KV (2001) Human papillomavirus-associated head and neck squamous cell carcinoma: mounting evidence for an etiologic role for human papillomavirus in a subset of head and neck cancers. Curr Opin Oncol 13:183–188

Gravitt PE, Kovacic MB, Herrero R, Schiffman M, Bratti C, Hildesheim A, Morales J (2007) High load for most high risk human papillomavirus genotypes is associated with prevalent cervical cancer precursors but only HPV16 load predicts the development of incident disease. Int J Cancer 121:2787–2793

Hagmar B, Johansson B, Kalantari M, Petersson Z, Skyldberg B, Walaas L (1992) The incidence of HPV in a Swedish series of invasive cervical carcinoma. Med Oncol Tumor Pharmacother 9:113–117

Hammarstedt L, Dahlstrand H, Lindquist D, Onelov L, Ryott M, Luo J, Dalianis T, Ye W, Munck-Wikland E (2007) The incidence of tonsillar cancer in Sweden is increasing. Acta Otolaryngol 127:988–992

Hammarstedt L, Lindquist D, Dahlstrand H, Romanitan M, Onelöv L (Dahlgren), Joneberg J, Creson N, Lindholm J, Ye W, Dalianis T, Munck-Wikland E (2006) Human papillomavirus as a risk factor for the increase in incidence of tonsillar cancer. Int J Cancer 119:2620–2623

Hanahan D, Weinberg RA (2000) The hallmarks of cancer. Cell 100:57–70

Hesselink AT, van den Brule AJ, Brink AA, Berkhof J, van Kemenade FJ, Verheijen RH, Snijders PJ (2004) Comparison of hybrid capture 2 with in situ hybridization for the detection of high-risk human papillomavirus in liquid-based cervical samples. Cancer 102:11–18

zur Hausen H (2002) Papillomaviruses and cancer: from basic studies to clinical application. Nat Rev Cancer 2:342–350

Kim SH, Koo BS, Kang S, Park K, Kim H, Lee KR, Lee MJ, Kim JM, Choi EC, Cho NH (2007) HPV integration begins in the tonsillar crypt and leads to the alteration of p16, EGFR and c-myc during tumor formation. Int J Cancer 120:1418–1425

Kreimer AR, Alberg AJ, Daniel R, Gravitt PE, Viscidi R, Garrett ES, Shah KV, Gillison ML (2004) Oral human papillomavirus infection in adults is associated with sexual behaviour and HIV serostatus. J Infect Dis 189:686–698

Li Y, Nicols MA, Shay JW, Xiong Y (1994) Transcriptional repression of the D-type cyclin-dependent kinase inhibitor p16 by the retinoblastoma susceptibility gene product pRb. Cancer Res 54:6078–6082

Li W, Thompson CH, O'Brien CJ, McNeil EB, Scolyer RA, Cossart YE, Veness MJ, Walker DM, Morgan GJ, Rose BR (2003) Human papillomavirus positivity predicts favourable outcome for squamous carcinoma of the tonsil. Int J Cancer 106:553–558

Li W, Tran N, Lee CS, O'Brien CJ, Tse GM, Scolyer RA, Hong A, Milross C, Yu KH, Rose BR (2007) New evidence for geographic variation in the role of human papillomavirus in tonsillar carcinogenesis. Pathology 39:217–222

Lindquist D, Romanitan M, Hammarstedt L, Nasman A, Dahlstrand H, Lindholm J, Ramqvist T, Ye W, Munck-Wikland E, Dalianis T (2007) Human papillomavirus is a prognostic factor in tonsillar cancer and its oncogenic role is supported by the expression of E6 and E7. Mol Oncol 1(3):350–355

Lungu O, Wright TC Jr, Silverstein S (1992) Typing of human papillomaviruses by polymerase chain reaction amplification with L1 consensus primers and RFLP analysis. Mol Cell Probes 6:145–152

Mellin H, Dahlgren L, Munck-Wikland E, Lindholm J, Rabbani H, Kalantari M, Dalianis T (2002) Human papillomavirus type 16 is episomal and a high viral load may be correlated to better prognosis in tonsillar cancer. Int J Cancer 102:152–158

Mellin H, Friesland S, Lewensohn R, Dalianis T, Munck-Wikland E (2000) Human papillomavirus DNA in tonsillar cancer: clinical correlates, risk of relapse and survival. Int J Cancer 89:300–304

Mellin Dahlstrand H, Lindquist D, Björnestål L, Ohlsson A, Dalianis T, Munck-Wikland E, Elmberger G (2005) P16 INK4a correlates to human papillomavirus presence, response to radiotherapy and clinical outcome in tonsillar carcinoma. Anticancer Res 25:4375–4384

Mork J, Lie K, Glattre E, Hallmans G, Jellum E, Koskela P, Moller B, Pukkala E, Sciller JT, Youngman L, Lehtinen M, Dillner J (2001) Human papillomavirus infection as a risk factor for squamous-cell carcinoma of the head and neck. N Eng J Med 344:1125–1131

Paavonen J, Jenkins D, Bosch FX, Naud P, Salmeron J, Wheeler CM, Chow SN, Apter DL, Kitchener HC, Castellsague X, de Carvalho NS, Skinner SR, Harper DM, Hedrick JA, Jaisamrarn U, Limson GA, Dionne M, Quint W, Spiessens B, Peters P, Struyf F, Wieting SL, Lehtinen MO, Dubin G and HPV PATRICIA study group (2007) Efficacy of a prophylactic adjuvanted bivalent L1 virus-like-particle vaccine against infection with human papillomavirus types 16 and 18 in young women: an interim analysis of a phase III double-blind, randomised controlled trial. Lancet 369:2161–2170

Pagliusi SR, Dillner J, Pawlita M, Quint WG, Wheeler CM, Ferguson M (2006) Chapter 23: International Standard reagents for harmonization of HPV serology and DNA assays – an update. Vaccine 24(Suppl 3):S193–200

Parry D, Bates S, Mann DJ, Peters G (1995) Lack of cyclin D-Cdk complexes in Rb-negative cells correlates with high levels of p16INK4/MTS1 tumour suppressor gene product. EMBO J 14:503–511

Ragin CC, Taioli E (2007) Survival of squamous cell carcinoma of the head and neck in relation to human papillomavirus infection: review and meta-analysis. Int J Cancer 121:1813–1820

de Roda Husman AM, Walboomers JM, van den Brule AJ, Meijer CJ, Snijders PJ (1995) The use of general primers GP5 and GP6 elongated at their 3′ ends with adjacent highly conserved sequences improves human papillomavirus detection by PCR. J Gen Virol 76:1057–1062

Rose RC, Bonnez W, Reichman RC, Garcea RL (1993) Expression of human papillomavirus type 11 L1 protein in insect cells: in vivo and in vitro assembly of viruslike particles. J Virol 67:1936–1944

Smeets SJ, Braakhuis BJ, Abbas S, Snijders PJ, Ylstra B, van de Wiel MA, Meijer GA, Leemans CR, Brakenhoff RH (2006) Genome-wide DNA copy number alterations in head and neck squamous cell carcinomas with or without oncogene-expressing human papillomavirus. Oncogene 25:2558–2564

Smeets SJ, Hasselink AT, Speel EJ, Haesevoets A, Snijders PJ, Pawlita M, Meijer CJ, Braakhuis BJ, Leemans CR, Brakenhoff RH (2007) A novel algorithm for reliable detection of human papillomavirus in paraffin embedded head and neck cancer specimen. Int J Cancer 121:2465–2472

Smits HL, van Gemen B, Schukkink R, van der Velden J, Tjong-A-Hung SP, Jebbink MF, ter Schegget J (1995) Application of the NASBA nucleic acid amplification method for the detec-

tion of human papillomavirus type 16 E6–E7 transcripts. J Virol Methods 54:75–81

Sotlar K, Stubner A, Diemer D, Menton S, Menton M, Dietz K, Wallwiener D, Kandolf R, Bultmann B (2004) Detection of high-risk human papillomavirus E6 and E7 oncogene transcripts in cervical scrapes by nested RT-polymerase chain reaction. J Med Virol 74:107–116

Strome SE, Savva A, Brissett AE, Gostout BS, Lewis J, Clayton AC, McGovern R, Weaver AL, Persing D, Kasperbauer JL (2002) Squamous cell carcinoma of the tonsils: a molecular analysis of HPV associations. Clin Cancer Res 8:1093–1100

Syrjanen K, Syrjanen S, Lamberg M, Pyrhönen S, Nuutinen J (1983) Morphological and immunohistochemical evidence suggesting human papillomavirus (HPV) involvement in oral squamous cell carcinogenesis. Int J Oral Surg 12:418–424

Tieben LM, ter Schegget J, Minnaar RP, Bouwes Bavinck JN, Berkhout RJ, Vermeer BJ, Jebbink MF, Smits HL (1993) Detection of cutaneous and genital HPV types in clinical samples by PCR using consensus primers. J Virol Methods 42:265–279

Weinberger PM, Yu Z, Haffty BG, Kowalski D, Harigopal M, Brandsma J, Sasaki C, Joe J, Camp RL, Rimm DL, Psyrri A (2006) Molecular classification identifies a subset of human papillomavirus-associated oropharyngeal cancers with favourable prognosis. J Clin Oncol 24:736–747

20
Quantitative Reverse Transcription–Polymerase Chain Reaction Based Assessment of the Candidate Biomarkers for Tongue Cancer Metastasis

Xiaofeng Zhou, Tianwei Yu, and David T. Wong

INTRODUCTION

Quantitative polymerase chain reaction (QPCR), also known as real-time polymerase chain reaction or kinetic polymerase chain reaction, is a technique used to simultaneously quantify and amplify a specific part of a given DNA molecule. QPCR follows the general procedure of PCR reaction, but the DNA is quantified after each PCR amplification cycle, making the quantification "real-time". It is used to determine whether or not a specific sequence is present in a specific sample; and if present, the number of copies in the sample. When the QPCR technique is combined with the reverse transcription polymerase chain reaction (RT-PCR), known as quantitative reverse transcription–polymerase chain reaction (QRT-PCR), it enables researchers to quantify low abundance messenger RNA (mRNA) at a particular time, or in a particular cell or tissue type.

QRT-PCR is one of the most sensitive techniques for mRNA detection and quantification currently available. QRT-PCR can be used to quantify mRNA levels from much smaller samples, as compared to other commonly used techniques, such as Northern blot analysis and RNase protection assay. In fact, QRT-PCR is sensitive enough to enable quantification of RNA from a single cell. In this chapter, we first provide a description of QPCR, as well as the different QPCR chemistries and the quantification methods available. We will then provide real world examples of QRT-PCR based detection of markers for tongue cancer metastasis, which includes (1) a brief discussion on clinical significance of markers for tongue cancer metastasis, and (2) the detailed descriptions on QRT-PCR based evaluation of the expression levels (mRNA) of two genes that associated with tongue cancer metastasis.

QUANTITATIVE POLYMERASE CHAIN REACTION

Cells in all living organisms regulate their cellular functions by activating or deactivating the expression of their genes. Gene expression corresponds to the number of copies of mRNA transcribed from a particular gene. As mRNA becomes translated at the ribosome to produce functional proteins,

mRNA levels tend to roughly correlate with protein expression. Historically, the amount of a particular mRNA produced from a specific gene has been measured by techniques such as Northern blotting. In this method, purified RNA is separated by agarose gel electrophoresis, and then probed with a specific anti-sense DNA probe for the gene of interest. Although this technique is still used to measure gene expression, it requires relatively large amounts of RNA and thus cannot be performed when tissue samples are limited.

In order to assess the level of specific mRNA from single or small numbers of cells, some amplification is required. The PCR is an effective tool for amplifying DNA. The recent advancements in the development of novel chemistries and instrumentation platforms enable detection of PCR products on a real-time basis have led to widespread adoption of QRT-PCR as the method of choice for quantifying changes in gene expression. Furthermore, QRT-PCR has become the preferred method for validating results obtained from microarray analyses that evaluate gene expression changes on a genome-wide scale.

Figure 20.1 shows a representative amplification plot and defines the terms used in the quantification analysis. An amplification plot is the plot of fluorescence signal versus PCR cycle number. In the early cycles of PCR reaction, there is little change in fluorescence signal. This defines the baseline for the amplification plot. An increase in fluorescence above the baseline indicates the detection of accumulated PCR product. A fixed fluorescence threshold can be set above the baseline. The parameter C_T (threshold cycle) is defined as the fractional cycle number at which the fluorescence passes the fixed threshold.

Therefore, the higher the initial amount of the sample, the sooner accumulated product is detected in the PCR process as a significant increase in fluorescence, and the lower the C_T value. The C_T values are very reproducible in replicates because the threshold is picked to be in the exponential phase of the PCR, where there is a linear relation between log of the change in fluorescence and cycle number when the reaction components are not limiting.

QPCR Chemistries

Currently, TaqMan probes, Molecular Beacons, Self fluorescing amplicons (e.g., Scorpion primers) and SYBR Green dyes, are the four most commonly used chemistries for QPCR. All of these chemistries allow detection of PCR products via the generation of a fluorescent signal. TaqMan probes, Molecular Beacons and Scorpions depend on Förster Resonance Energy Transfer (FRET) to generate the fluorescence signal via the coupling of a fluorogenic dye molecule and a quencher moeity to the same or different oligonucleotide substrates. SYBR Green is a fluorogenic dye that exhibits little fluorescence when in solution, but emits a strong fluorescent signal upon binding to double-stranded DNA. Below are brief descriptions of each QPCR strategy.

TaqMan Probes

TaqMan probes depend on the 5′- nuclease activity of the DNA polymerase used for PCR to hydrolyze an oligonucleotide that is hybridized to the target amplicon. TaqMan probes are oligonucleotides that have a fluorescent reporter dye attached to the 5′ end and a quencher moiety coupled

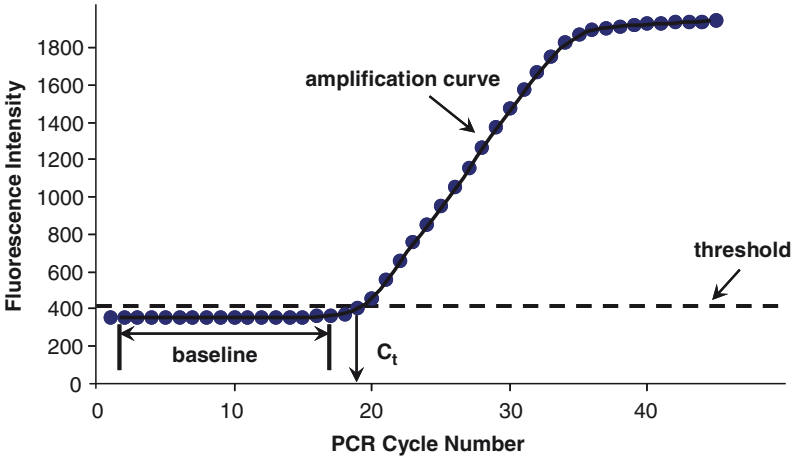

FIGURE 20.1. Quantitative polymerase chain reaction amplification plot

to the 3′ end. These probes are designed to hybridize to an internal region of a particular PCR product in a sequence-specific manner. In the unhybridized state, the proximity of the fluor and the quench molecules prevents the detection of fluorescent signal from the probe. During PCR, when the polymerase replicates a template on which a TaqMan probe is bound, the 5′-nuclease activity of the polymerase cleaves the probe. This decouples the fluorescent and quenching dyes and FRET no longer occurs. Thus, fluorescence increases in each cycle, proportional to the amount of probe cleavage.

A well-designed TaqMan probe requires very little optimization. In addition, TaqMqn probes can be used for multiplex assays by designing each probe with a spectrally unique fluor/quench pair. However, TaqMan probes can be costly to synthesize, because a separate probe is needed for each mRNA target being analyzed.

Molecular Beacons

Similar to the TaqMan probes, Molecular Beacons also utilize FRET to detect and quantitate the synthesized PCR product via a fluor coupled to the 5′ end and a quench attached to the 3′ end of an oligonucleotide substrate. Unlike TaqMan probes, Molecular Beacons are designed to remain intact during the amplification reaction, and must rebind to target in every cycle for signal measurement. Molecular Beacons form a stem-loop structure when free in solution. Thus, the close proximity of the fluor and quench molecules prevents the probe from fluorescing. When a Molecular Beacon hybridizes to a target, the fluorescent dye and quencher are separated, FRET does not occur, and the fluorescent dye emits light upon irradiation. Like TaqMan probes, molecular Beacons can be used for multiplex assays by utilizing spectrally separated fluor/quench moieties on each probe. However, as with TaqMan probes, Molecular Beacons are relatively expensive, with a separate probe required for each target.

Self Fluorescing Amplicons

In most QPCR assays, separate primers and probes are used to amplify and detect a specific DNA. An emerging technique uses a special primer that linked to the

probe so that the binding of the probe to the amplicon is now a unimolecular reaction instead of a bimolecular one. There are several variations of these probe-linked primers, including scorpion primers, sunrise primers and lux primers. These systems are believed to be as effective as probe based QPCR assays, but are less costly as a probe is not required.

For example, the Scorpion primer maintains a stem-loop configuration in the unhybridized state. The fluorophore is attached to the 5′ end and is quenched by a moiety coupled to the 3′ end. The 3′ portion of the stem also contains sequence that is complementary to the extension product of the primer. This sequence is linked to the 5′ end of a specific primer via a non-amplifiable monomer. After the Scorpion primer has been extended during the extension step in a PCR cycle, the specific probe sequence is able to bind to its complementary sequence within the extended amplicon, thus, opening up the hairpin loop. This prevents the fluorescence from being quenched and a signal is observed. Thus, the sequence-specific priming and PCR product detection is achieved using a single oligonucleotide.

SYBR Green

SYBR Green provides the simplest and most economical format of the available QPCR strategies. SYBR Green binds double-stranded DNA, and upon excitation the bound SYBR Green molecule emits light. Thus, as the PCR product accumulates, fluorescence increases. The advantages of SYBR Green based QPCR are that it is inexpensive, easy to use, and sensitive. The disadvantage is that SYBR Green will bind to any double-stranded DNA in the reaction, including primer-dimers and other nonspecific reaction products, which results in an overestimation of the target DNA concentration. For single PCR product reactions with well designed primers, SYBR Green can work very well, with spurious nonspecific background only showing up in very late cycles (Figure 20.2).

TaqMan probes, Molecular Beacons and Scorpions allow multiple DNA species to be measured in the same sample (multiplex QPCR), as fluorescent dyes with different emission spectra may be attached to the different probes. Multiplex QPCR allows internal controls to be coamplified and permits allele discrimination in single-tube, homogeneous assays. These hybridization probes provide a level of discrimination impossible to obtain with SYBR Green, because they will only hybridize to true targets in a QPCR and not to primer-dimers or other spurious products.

SYBR Green is the most economical choice for real-time PCR product detection. Because the dye binds to double-stranded DNA, there is no need to design a probe for any particular target being analyzed. This technique has been frequently utilized for validating the expression differences of many candidate genes (or biomarkers) that have been identified by microarray studies. However, detection by SYBR Green requires extensive optimization. Because the dye cannot distinguish between specific and non-specific product accumulated during PCR, follow-up assays are needed to validate results.

Quantification of Results

Two strategies are commonly employed to quantify the results obtained with QRT-PCR: the standard curve method and the

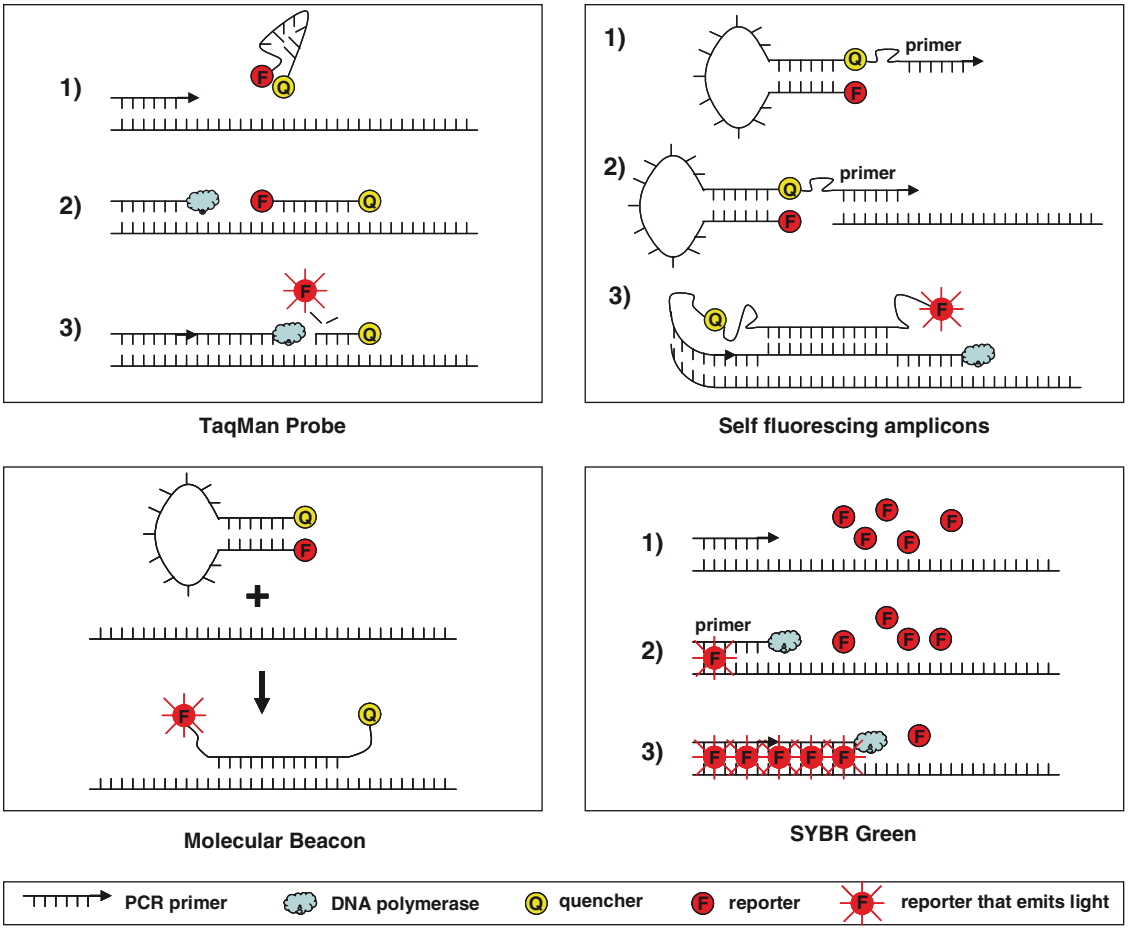

FIGURE 20.2. Quantitative polymerase chain reaction chemistries

comparative threshold method. These are discussed briefly below.

Standard Curve Method

A standard curve is first constructed from RNA of a known concentration. This curve is then used as a reference standard for extrapolating quantitative information for mRNA targets of unknown concentrations. Though RNA standards can be used, their instability can be a source of variability in the final analyses. In addition, using RNA standards would involve the time-consuming process of constructing cDNA plasmids that have to be transcribed in vitro into the RNA standards and accurately quantified. However, the use of absolutely quantified RNA standards help generate absolute copy number data.

In addition to RNA, other nucleic acid samples can be used to construct the standard curve, including purified plasmid dsDNA, in vitro generated ssDNA or any cDNA sample expressing the target gene. Spectrophotometric measurements at 260 nm can be used to assess the concentration of these DNAs, which can then be converted to a copy number value based on the molecular weight of the sample used.

cDNA plasmids are the preferred standards for standard curve quantification. However, because cDNA plasmids will not control for variations in the efficiency of the reverse transcription step, this method will only yield information on relative changes in mRNA expression. This, and variation introduced due to variable RNA inputs, can be corrected by normalization to a housekeeping gene.

Comparative C_T Method

Another quantification approach is termed the comparative C_T method. This involves comparing the C_T values of the samples of interest with a control or calibrator such as a non-treated sample or RNA from normal tissue (Livak and Schmittgen 2001). The C_T values of both the calibrator and the samples of interest are normalized to an appropriate endogenous housekeeping gene (also known as reference gene).

The comparative C_T method is also known as the $2^{-\Delta\Delta C_T}$ method, where

$$\Delta\Delta C_T = \Delta C_{T,\text{sample}} - \Delta C_{T,\text{calibrator}}$$

Here, $\Delta C_T = C_{T,\text{ gene X}} - C_{T\text{ housekeeping}}$. $\Delta C_{T,\text{sample}}$ is the C_T value for the gene of interest normalized to the endogenous housekeeping gene in the sample of interest, and $\Delta C_{T,\text{reference}}$ is the C_T value for the gene of interest in the calibrator also normalized to the endogenous housekeeping gene.

For the $\Delta\Delta C_T$ calculation to be valid, the amplification efficiencies of the target and the endogenous reference must be approximately equal and close to one, both in the sample of interest and in the calibrator. The approximate equality can be established by looking at how ΔC_T varies with template dilution. If the plot of cDNA dilution versus ΔC_T is close to zero, it implies that the efficiencies of the target and housekeeping genes are very similar. If a housekeeping gene cannot be found whose amplification efficiency is similar to the target, then the standard curve method is preferred.

In many situations, the assumption of approximately equal amplification efficiency is hard to realize, while the cost of constructing a standard curve is too high. Approaches to estimate amplification efficiency directly from the PCR kinetic curves have been developed to address the problem (Peirson et al. 2003; Wong and Medrano 2005; Schefe et al. 2006). These methods estimate the efficiency using statistical model-fitting based on the fact that there is an exponential growth phase in the qPCR kinetic curve. For further discussions, please see (Schefe et al. 2006).

ORAL TONGUE CANCER

Oral cancer is the sixth most common cancer worldwide. In the following sections, we will provide real world examples of QRT-PCR based detection of markers for tongue cancer metastasis. We will first provide a brief discussion on clinical significance of markers for tongue cancer metastasis. This will then be followed by detailed descriptions on QRT-PCR based evaluation of expression levels (mRNA) for two genes that associated with tongue cancer metastasis.

Oral Tongue Squamous Cell Carcinoma (OTSCC), A Major Subset of Oral Cancer

Oral cancer is one of the most common cancers. In the US there are >38,000 new cases of oral cancer each year. It causes over 8,000 deaths per year, killing roughly one person

per hour. Worldwide the problem is even worse, with >270,000 new cases being diagnosed each year. In some parts of the world, including South-Central Asia, home to one fifth of the world's population, oral cancer is still a major health problem. Despite the tremendous improvements in surgery, radiotherapy and chemotherapy during the last decade, the prognosis for patients with oral cancer is more or less unchanged. This is because patients continue to die from metastatic disease at regional and distant sites. Improvement in patient survival requires a better understanding of tumor metastasis so that aggressive tumors can be detected early in the disease process and targeted therapeutic interventions can be deployed. The presence of nodal metastasis in oral cancer is an important prognostic factor and crucial in making clinical decisions regarding postoperative radiation treatment and follow up.

Oral cancers are groups of diverse cancers, that develop from many different anatomic sites and are associated with different risk factors, genetic characteristics, and different clinical outcomes. In this chapter, we focused on one of the most common sites of oral cancer, oral tongue squamous cell carcinomas (OTSCC). OTSCC is significantly more aggressive than other forms of oral cancers, with a propensity for rapid local invasion and spread (Franceschi et al. 1993), and a high recurrence rate (Fakih et al. 1989a). OTSCCs also exhibit a different nodal metastasis pattern in the neck than oral cancers developed from other origins (Byers et al. 1997; Robbins et al. 2002).

Metastasis – A Major Clinical Problem of Oral Cancer

An essential characteristic of cancer is the ability to invade surrounding tissues and metastasize to regional and distant sites. Detection of local lymph node metastasis is pivotal for choosing appropriate treatment, especially for individuals diagnosed with oral cancer in the oral cavity (Pantel and Brakenhoff 2004). Most of these individuals have the primary tumor removed. Treatments of individuals clinically diagnosed with lymph node metastasis (N+ status) involve the additional surgical removal of a substantial portion of the neck, including all five local lymph node levels (radical neck dissection, RND). Upon histological examination of removed tissue, 10%–20% of clinically diagnosed N+ individuals turned out to be metastasis-free (N0 or N–) (Woolgar 1999). Clinical diagnosis of N0 status is even less accurate. Postoperative histological examination shows that approximately one-third of clinically diagnosed N0 individuals have metastasis-positive lymph nodes in the neck (Jones et al. 1993). Currently, there are several different strategies that exist for treating diagnosed N0 individuals (Pillsbury and Clark 1997). In the 'watch and wait' strategy, diagnosed N0 individuals do not undergo any neck dissection; this risks fatality by allowing overlooked metastases to spread further. Because the false-negative rate is very high, most clinics carry out a selective neck dissection (SND) for all diagnosed N0 individuals. In these cases, the three upper lymph node levels were removed (also known as supraomohyoid neck dissection) (Robbins et al. 2002). In the case of OTSCC, there is evidence indicating level IV is also at risk (Byers et al. 1997). Thus, the latest recommended SND procedure for this sub-site involves removal of lymph node levels I to IV – known as SND(I-IV) (Figure 20.3, please refer to (Robbins et al. 2002) for more details). SND is less appropriate than RND for N+ individuals falsely-diagnosed as N0 and, moreover, is completely unnecessary

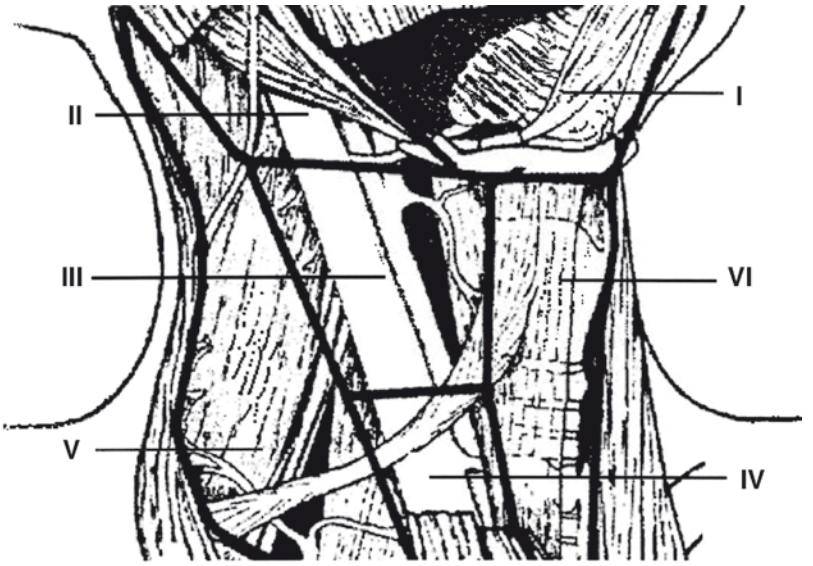

FIGURE 20.3. The anatomic six levels of the neck that delineate the location of lymph node metastasis

for individuals correctly diagnosed as N0. Although SND is less rigorous than RND, the treatment causes disfigurement, long-term discomfort and pain and can lead to additional complications such as shoulder and neck disability. Both strategies result in inappropriate treatment because of limitations in detecting lymph node metastasis reliably.

This problem is more apparent for patients with early stage OTSCCs (T1 and T2), which severely impairs the clinical decision-making. The management of the T1, T2 OTSCC has been the subject of much debate during the last 3 decades and remains a controversial issue. This is attributed partly to the inability to accurately detect the occult nodal metastasis. This inability leads to high incidence of false-negative nodal metastasis at presentation, which in turn has a negative impact on prognosis. As illustrated in Table 20.1, the incidence of false-negative diagnoses of nodal metastasis can be as high as 47% (with an average of 32.4% based on 11 studies we surveyed) for T1-T2 OTSCC. These facts point to the immediate need for new diagnostic strategies.

Currently, the detection of nodal metastasis is based on routine histopathological evaluation of the lymph nodes in the neck (TMN classification). No molecular biomarkers have been included in clinical work-up strategies for the patients. It is believed, however, that molecular "fingerprints" could exist which might define sub-groups of patients with significantly more aggressive disease. Several recent microarray based studies have suggested the existence of such molecular "fingerprints" (Schmalbach et al. 2004; O'Donnell et al. 2005; Roepman et al. 2005; Zhou et al. 2006). The following section will use these molecular "fingerprints" as examples to demonstrate the utilities of QRT-PCR based assessments of the potential biomarkers.

TABLE 20.1. Incidence of false-negative diagnosis of nodal metastasis in T1–T2 OTSCC

Authors	# patients	T stage	% false-negative
Lee and Litton (1972)[a]	94	T1–T2	23
Johnson et al. (1980)[a]	40	T1	35
Bradfield and Scruggs (1983)[a]	98	T1–T2	20
Teichgraeber and Clairmont (1984)[a]	48	T1–T2	35
Cunningham et al. (1986)[a]	23	T1–T2	35
Fakih et al. (1989b)[a]	70	T1–T2	47
Ho et al. (1992)[a]	28	T1–T2	42
Franceschi et al. (1993)[a]	211	T1–T2	31
Haddadin et al. (1999)	137	T1–T2	41
Sparano et al. (2004)	45	T1–T2	29
Lim et al. (2006)	54	T1–T2	28

[a] Based on the Haddadin et al.'s calculation methods (Haddadin et al. 1999).

THE QUANTITATIVE POLYMERASE CHAIN REACTION BASED EVALUATION OF CANDIDATE TONGUE CANCER METASTASIS MARKERS

Cancer Biomarkers

The definition for biomarker is constantly evolving consistently with the continuous advancements in biomedical research. We will define biomarker as a quantitative or qualitative measure used to classify individuals for current or future status. Examples include imaging tests, sensory tests, clinical signs and symptoms, risk factors, and genomics and proteomics measurements. These markers can be utilized in various aspects of clinical management, such as diagnosis, disease screening (early detection), prognosis, treatment selection, evaluation of therapeutic efficiency, exposure assessment and risk prediction.

Cancer biomarkers are specific markers for various cancers. They can be used for the accurate evaluation and management of these diseases in different stages. They can facilitate the clinical managements during the course of cancer including early detection, outcome prediction and detection of disease recurrence. In addition, with the clinical appearance of many new therapeutic agents, appropriate markers can be used to determine which tumors will respond to which treatment(s) in order to predict the likelihood of drug resistance.

In this section, we will focus on two biomarkers that provide predictive values for the presence of nodal metastasis in OTSCC. The presence of nodal metastasis is an important prognostic factor for OTSCC and is crucial in making clinical decisions regarding specific operation procedures and postoperative radiation treatment and follow up. Two genes, *cortactin* (*CTTN*) and *matrix metalloproteinase-9* (*MMP9*) will be used as examples in this section. These are biomarkers identified based on high-throughput genome-wide expressional profiling studies (Zhou et al. 2006). *CTTN* (GeneID: 2017), also known as *EMS1* oncogene, is a ubiquitous actin-binding protein that was originally

identified as a substrate for the protein kinase Src. It is over-expressed in a number of epithelial carcinomas, including breast cancer and head and neck cancer. Over-expression of *CTTN* in human tumors has been showed to result in increased cell migration and metastatic potential. *MMP9* (GeneID: 4318), also known as *92-kD type IV collagenase* and *gelatinase B*, belongs to the MMP family of secreted zinc metalloproteases which, in mammals, degrade the collagens of the extracellular matrix. It has been associated with tumor cell invasion and metastasis and tumor-induced angiogenesis. We will present a detailed description of the QRT-PCR based assessment of the differences in mRNA levels for these genes. We will use two groups of primary OTSCC samples with either positive or negative metastatic status.

QRT-PCR Based Assessments of CTTN and MMP9 in Tongue Cancer

In the following two sections, we will provide specific examples of using QRT-PCR to assess the mRNA levels of *CTTN* and *MMP9* in two groups of OTSCC cancer patients with either positive (n = 11) or negative status (n = 14) of lymph node metastasis. These experiments are part of a recently published study in *Neoplasia* (Zhou et al. 2006). Please refer to this article for more detail. We assume the audiences have a basic understanding of genetics and PCR technology.

Cortactin (CTTN)

In this section, we will describe the QRT-PCR based assessment of the mRNA levels of *CTTN* gene in four major steps: (1) select QRT-PCR strategy, (2) select target sequence and primer design, (3) RNA template preparation and RT reaction, and (4) QPCR. The analyses of the QPCR data will be presented in a separate section immediately follows.

1. Select QRT-PCR strategy
    a. QPCR chemistry: There are several well-developed QPCR chemistries, including TaqMan, Molecular Beacon, self-fluorescing amplicon and SYBR Green dyes based methods (as described previously). They all have their unique advantages and drawbacks. Various practical factors, such as cost, specificity, efforts required for probe design and reaction optimization, are commonly considered for selecting the optimal method for a particular QPCR test. In this section, we will use SYBR Green dye based method as an example to provide an overview of QRT-PCR based assessment of mRNA level for a specific gene (*CTTN*). We chose SYBR Green dye as it provides the simplest and most economical format for detecting and quantifying PCR products in real-time.
    b. One-step or two-step: As described earlier, to quantify the mRNA levels, the mRNA sample first needs to be reverse-transcribed to cDNA by reverse transcriptase. This step can be either integrated into the QPCR reaction (one-step QRT-PCR), or performed independently to the QPCR reaction (two-step QRT-PCR). The one-step approach provides better a streamlined experimental process, and the two-step approach provides flexibility to store the intermediate product (cDNA) for additional tests of the same gene or different genes at a different time. In this section, we will

perform the RT reaction independently (two-step), so that test for additional gene (*MMP9*) can be performed using the same cDNA sample.

c. Method of quantification: There are two common strategies for quantifying the QPCR results, the standard curve method and the comparative threshold method. The guideline for selecting the optimal method has been described in the previous section. Here, we will use the comparative threshold method for QPCR quantification of *CTTN*, where *ACTB* (*beta-actin*) will be used as reference gene.

2. Select target sequence and primer design

There are many commercial and freely distributed software packages available for the primer and probe design, with varying degree of sophistication. The choice of software package is largely dependent on the QPCR chemistry. TaqMan probes, Molecular Beacons, and Scorpion primers usually require more sophisticated software, such as Primer Express (Applied Biosystems). On the other hand, the primer set for SYBR Green dyes based QPCR can be designed using common primer design tool for regular PCR reaction. We will use the online version of the Primer3, a widely used program for designing PCR primers (http://primer3.sourceforge.net/), to design the primer set for *CTTN*. The mRNA sequence of *CTTN* can be obtained from the National Center for Biotechnology Information (NCDI) database (http://www.ncbi.nlm.nih.gov/), and will be used as the target sequence for the primer design. The primer sets are often designed against sequence in the 3′ untranslated region of the specific genes. Alternatively, since this candidate gene is identified based on the microarray expression analyses, we can also use the target sequence for the specific microarray probe (Affymetrix Probe ID: 214782_at) for the primer design. Please refer to Zhou et al. (2006) and the Affymetrix-NetAffx (http://www.affymetrix.com) for more details. It is common to design a primer set that gives a PCR product size of 75–150 base pairs in length. Other general guidelines for PCR primer design applies as well, including avoiding multiple TA at the 3′ end, avoiding potential primer-dimer, and ensuring minimum differences in annealing temperature and GC content between the primers. The following specific primer set was designed to produce a PCR product of 121 base pairs, with an optimal annealing temperature (Tm) of 60°C.

Forward: 5′- GGAACCCTCCTCCTGTCAAT-3′

Reverse: 5′- TGGGGAAGAACACACACTCA-3′

The designed PCR primers can then be evaluated based on the self-complementarity scores produced by Primer3 software, measures of its tendency to form secondary structure or primer-dimer. Alternative *in silico* search tools can also be used to provide an evaluation of the primers, such as the freely available Netprimer Software (PREMIER Biosoft International) for checking the primer dimers, hairpins, and cross dimers. This software generates a rating for each primer from 0% to 100%. In general, we found that primers with a rating above 90% generally work well. Additional wet lab tests (e.g., gel electrophoresis and melting curve analyses of the PCR products) and *in silico* tests (e.g., BLAST analyses) are also required to ensure the specificity of the QPCR reaction.

3. RNA template preparation and RT reaction
   a. RNA isolation: A variety of RNA isolation methods are available for extracting RNA from various sources. The separation of mRNA from total RNA may not be necessary if mRNA specific primer (oligo dT) will be used for the RT reaction. It is critical to ensure the quality of the RNA. The most common quality tests include: (1) To examine for RNA degradation by gel electrophoresis or microfluidics-based platform (e.g. Agilent Bioanalyzer). Degraded RNA samples will be evident in the ribosomal RNA (rRNA) bands/peaks as either smearing in the gel, or as a shoulder or shallow slope in the Agilent Bioanalyzer analysis. The optimal ratio of 28s rRNA and 18s rRNA should be ~2.0. (2) To examine for contamination / impurities of the RNA sample by spectrophotomeric analysis at OD260 and OD280 nm. This optimal OD260 and OD280 nm ratio should be between 1.8 and 2.1.
   b. Remove genomic DNA contamination: Since QRT-PCR is an amplification procedure, even trace amount of genomic DNA contamination will result in over estimation of the mRNA level of the target gene. DNase treatment of the RNA sample is highly recommended prior to reverse transcriptase (RT) reaction. The DNase will then be inactivated to avoid digesting the newly synthesized cDNA during the RT reaction. A variety of tools are available for this purpose. The DNA-free™ DNase Treatment and Removal Reagent (Ambion) is designed for easy removal of DNA contamination from RNA samples. In addition, Ambion also offers a hyperactive TURBO DNase enzyme engineered from wild-type bovine DNase. The proficiency of TURBO DNase in binding very low concentrations of DNA means that the enzyme is particularly effective in removing trace quantities of DNA contamination. A quick purification step is highly recommended prior to the RT reaction.
   c. RT reaction: The RT reaction can be performed using MuLV Reverse Transcriptase (Applied Biosystems) in the presence of RNase inhibitor. The RT reaction can be carried out using either random primer or oligo dT primer. If primer sets for both target gene(s) and reference gene are designed toward the 3′ untranslated regions, then oligo dT may provide better efficiency as the primer for the RT reaction.
4. QPCR
   a. Instrumentation: QPCR requires an instrumentation platform that consists of a thermal cycler, a computer, optics for fluorescence excitation and emission collection, and data acquisition and analysis software. These machines, available from several manufacturers, differ in sample capacity (some are 96-well or 384-well standard format; others process fewer samples or require specialized glass capillary tubes), method of excitation (some use lasers, others broad spectrum light sources with tunable filters), and overall sensitivity. There are also platform-specific differences in how the software processes data.

QPCR machines are not inexpensive, but are well within purchasing reach of core facilities or labs that have the need for high throughput quantitative analysis.

b. QPCR reaction: As with standard PCR reaction, the QPCR reaction will have normal PCR steps such as denature, annealing, and extension, with appropriate temperatures and durations. A typical PCR protocol is listed below (Table 20.2). SYBR Green dye will be used to bind double stranded PCR products. This binding will cause an increase in fluorescence intensity which is proportional to DNA concentration. Several commercial kits contain all the necessary PCR enzyme, buffers and dyes for the SYBR Green based QPCR, such as iQ SYBR Green Supermix (Bio-Rad). The QPCR reaction can be set up in a 96-well QPCR plate that is compatible to the specific instrumentation. It is common to set up three replicates for each sample, where an aliquot of RT product (cDNA) will be mixed with the SYBR Green Supermix. The cycle-to-cycle increases in fluorescence intensity will be captured in real-time by the data acquisition component of the QPCR instrument. The data analysis will be performed using the comparative threshold method (2-delta delta Ct method) described in previous section.

Table 20.2. A typical PCR protocol for the SYBR green based QPCR reaction

Cycle 1: (1X)				
	Step 1	95.0°C	3:00	
Cycle 2: (50X)				
	Step 1	95.0°C	0:30	
	Step 2	60.0°C	0:30	
	Step 3	72.0°C	0:30	Data collection
Cycle 3: (1X)				
	Step 1	95.0°C	1:00	
Cycle 4: (1X)				
	Step 1	55.0°C	1:00	
Cycle 5: (80X)				
	Step 1	55.0°C	0:10	Melt curve data collection
Increase temperature by 0.5°C after cycle 2				
Cycle 6: (1X)				
	Step 1	72.0°C	7:00	
Cycle 7: (1X)				
	Step 1	4.0°C	Hold	

The protocol is designed based on Bio-Rad iCycler iQ real-time PCR detection system using iQ SYBR Green Supermix.

Contamination is a problem often encountered with QPCR. To avoid this, all surfaces in the PCR area should be routinely cleaned using DNA decontamination solution, such as DNAzap (Ambion) to prevent cross contamination. A "No Template Control" (NTC) should be run to rule out cross contamination of reagents and surfaces. The NTC includes all of the QRT-PCR reagents except the RNA template. Typically the RNA is simply substituted with nuclease-free water. No product should be synthesized in the NTC; if a product is amplified, it indicates that one or more of the QRT-PCR reagents is contaminated with the amplicon.

a. Optional examination of the PCR product: To ensure the specificity of the reaction and avoid non-specific product, the products of the QPCR reactions are often examined further by melting curve analyses (based on the specific melting temperature for specific PCR product) or gel electrophoresis (based on the size of the specific PCR product). At this point, we have generated the raw QRT-PCR datasets for the mRNA levels of *CTTN* gene in OTSCC samples. We will also generate the raw datasets for the *MMP9*

gene in the following section. The analyses of these raw datasets (quantification) will then be performed in a separate section immediately follows.

Matrix Metallopeptidase-9 (MMP9)

MMP9 is another marker for the lymph node metastasis of OTSCC, identified by Zhou et al. (2006). For consistency, we will use SYBR Green based QPCR chemistry and two-step QRT-PCR approach to assay the *MMP9* mRNA level. The same cDNA templates generated in the previous section for evaluating *CTTN* can be used here. We will use the comparative threshold method for QPCR quantification of *MMP9*, where *ACTB* (*beta-actin*) is used as reference gene. Because we have already generated the QRT-PCR data for *ACTB* in the previous section on the same cDNA sample, the dataset can also be used as reference for the quantification of *MMP9*.

The mRNA sequence of *MMP9* is obtained from National Center for Biotechnology Information (NCDI) database (http://www.ncbi.nlm.nih.gov/). The specific primer set listed below is designed against sequence in the 3′ untranslated region of the *MMP9* sequence using Primer3 (http://primer3.sourceforge.net/), which will produce a PCR product of 97 base pairs, with an optimal annealing temperature (Tm) of 60°C.

Forward: 5′- GTGCCATGTAAATCC CCACT-3′

Reverse: 5′- CTCCACTCCTCCCTTTC CTC-3′

The template for QPCR has already been prepared in the previous section, when prepare for the QRT-PCR assay for *CTTN*. QPCR for *MMP9* will be performed as described in the previous section. A "No Template Control" (NTC) should be run to check for contamination. A melting curve analyses will be performed to ensure the specificity of the QPCR reaction.

Quantification and Statistical Evaluation of the Markers

After obtaining the C_T values for the marker and housekeeping gene in each sample of interest and the calibrator sample, estimates of the relative copy numbers can be obtained using the $\Delta\Delta C_T$ method. First, the difference of C_T values between the gene of interest and the housekeeping gene is obtained in each sample, including the calibrator sample. Then the difference between the ΔC_T's of every sample of interest and the calibrator sample is taken. Two to the power of - $\Delta\Delta C_T$ is used as an estimate of the RNA copy numbers in the samples of interest relative to the calibrator sample. In the example shown below (Table 20.3), multiple measurements (three replicates) were made from each sample, and the mean C_T was used in place of single-measurement C_T to obtain more reliable results.

In the study of biomarkers, the interest lies in obtaining contrasts between two groups of samples, e.g., the metastasis group (pN+) and the non-metastasis group (pN-). One common way of data visualization is to contrast the two groups in the same graph using boxplot. Boxplot (also known as a box-and-whisker diagram or plot or candlestick chart) is a convenient method of graphically depicting important data summary, (median, 25% quantile, and 75% quantile), as well as indicating putative outliers (Figure 20.4). Other visual inspections, such as pairwise scatter plots,

TABLE 20.3. Calculation for comparative C_T method based quantification of CTTN

Samples	Clinical info	$C_{T,CTTN}$	$C_{T,actin}$	ΔC_T	$\Delta\Delta C_T$	$2^{-\Delta\Delta C_T}$
S1	pN-	35	29.75	5.25	−0.85	1.80
S2	pN-	35.25	29.6	5.65	−0.45	1.37
S3	pN-	36.35	32.85	3.5	−2.6	6.06
S4	pN-	33.95	28.35	5.6	−0.5	1.41
S5	pN-	33.45	27.45	6	−0.1	1.07
.	.	.	.	.	.	.
.	.	.	.	.	.	.
.	.	.	.	.	.	.
R1	pN+	32.2	28.95	3.25	−2.85	7.21
R2	pN+	34.9	31.15	3.75	−2.35	5.10
R3	pN+	30.85	28.4	2.45	−3.65	12.55
R4	pN+	31.5	28.45	3.05	−3.05	8.28
R5	pN+	31.4	31.3	0.1	−6	64.00
.	.	.	.	.	.	.
.	.	.	.	.	.	.
.	.	.	.	.	.	.

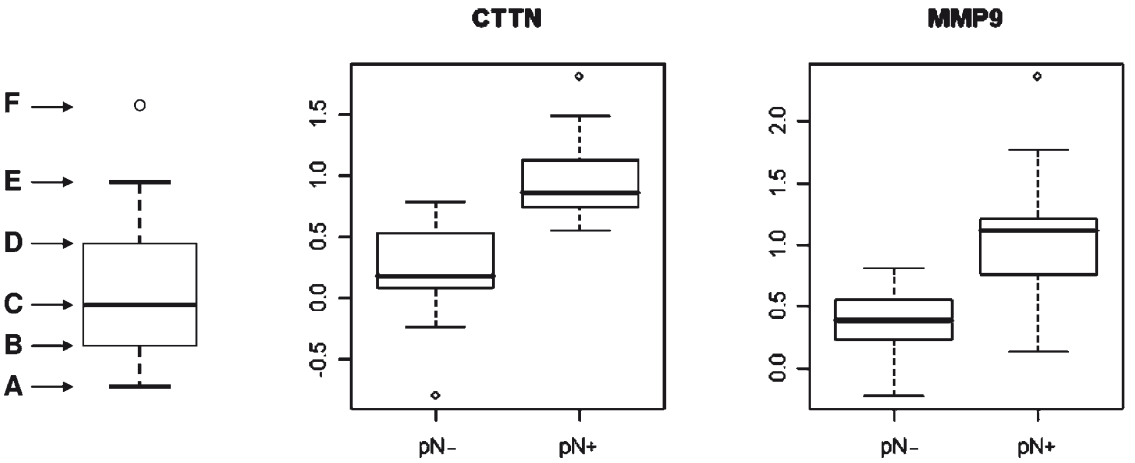

FIGURE 20.4. Boxplot for the visualization of QRT-PCR data. *Left panel*: illustration of the boxplot based data summary. The smallest non-outlier observation (**A**), lower (first) quartile (**B**), median (second quartile) (**C**), upper (third) quartile (**D**), largest non-outlier observation (**E**), and outlier (**F**) were indicated in this illustrative diagram. *Middle panel*: boxplot of log-transformed QRT-PCR data for *CTTN*. *Right panel*: boxplot of log-transformed QRT-PCR data for *MMP9*

can yield important information as to how well the markers can complement each other in the prediction of disease state.

To test the between-group significance, the Wilcoxon rank sum test is also commonly used. It tests for location shift between groups without assuming normality. In our example, the p-value is 0.0002 for *CTTN* and 0.0016 for *MMP9* (Table 20.4). To evaluate the classification power for each gene, the Receiver Operating Characteristic (ROC) curve analysis is performed with the binary outcome of pN +/− (or ECS +/−) as a dependent variable and the qRT-PCR value of a candidate gene as an independent variable.

The ROC curve shows the sensitivity on Y axis and (1- the specificity) on X axis for each possible cut-point of the fitted probabilities from the model. Area under the curve (AUC) is computed via numerical integration of the ROC curve which measures the overall diagnostic/classification power. Also, the set of sensitivity and specificity is shown using the best cut-point value suggested (that maximizes the sum of Sensitivity and Specificity).

When more than one marker is identified, it is of interest to study whether the combination of the markers yields higher prediction accuracy than each marker alone. Many statistical models can be used for the prediction. We chose to show the results from the logistic regression model for its simplicity. To find the sensitivity and specificity, leave-one-out cross-validation is used to avoid model over-fitting. The result shows that combining the two markers (*CTTN* and *MMP9*) yield better prediction than each single marker (Table 20.5).

FUTURE DEVELOPMENTS

Oncologists have long sought targeted cancer therapies focus on the specific molecular signatures (e.g., *CTTN* over expression) or clinical characteristics (e.g., lymph node metastasis) present in an individual patient's tumor. The implementation of this concept requires precise characterization of the disease as well as knowledge of patient background (e.g., genetic and environmental characteristics). For tumors with a relatively narrow range of critical genetic defects (e.g., acute promyelocytic leukemia and chronic phase chronic myeloid leukemia), the development and deployment of targeted therapies has been more easily accomplished than in more complex and heterogeneous tumor types (e.g., breast cancer, non-small-cell lung cancer, and OTSCC). The emergence of rapid, high-resolution genome analysis tools provides an opportunity to tackle these more heterogeneous malignancies (including OTSCC) at both the levels of basic research (e.g., defining pathogenetic mechanisms) and clinical treatment selection (e.g., neck dissection of the tongue cancer patients), offering unprecedented prospects for advancing knowledge of OTSCC in a translational context.

Despite its importance, there is a gap between the knowledge gained in the laboratory and its transfer into daily clinical practice. There are multiple possible

Table 20.4. Statistical values of CTTN and MMP9 with regard to metastasis status (pN+/–)

Marker	p-Value	Area under ROC	Sensitivity	Specificity	Cutoff value
CTTN	0.0002	0.94	0.91	0.80	3.98
MMP9	0.0016	0.88	0.82	0.93	5.25

Table 20.5. The Logistic Model that combining CTTN and MMP9 for predicting metastasis

Model:	Area under ROC	Sensitivity	Specificity
$\frac{p(pN+)}{p(pN-)} = e^{-14+2\times CTTN+0.56\times MMP9}$	0.987	0.91	1

explanations for this fact. Most importantly, many discovery studies have involved small sample sizes, either due to limited access to the samples, or poor quality of the samples, or the fact that studies have involved cancers from various anatomic sites. In addition, many results have not been validated through independent investigations, usually because of a lack of standardization of the analysis methods. Validation has also proven difficult because the routine use of newly identified markers is hampered by the complexity of the tests and lack of facilities in routine laboratories. A good example is microarray technology. It is an optimal tool for the discovery of the critical biomarkers with diagnostic or prognostic values. However, this technology requires advanced instrumentations and trained personnel and may not be practical to incorporate into a clinical setting. For large scale validation studies and eventual translation to the clinical setting, technology transfer to e.g., QRT-PCR would be preferable, as this technology can be handled in most clinical settings, compared to the more advanced microarray technology. One might envision that in the near future, a single tube of multiplexed tests will generate a clinically meaningful readout in hours to provide a "real-time" diagnosis.

To be clinically useful, the molecular biomarkers have to add significant diagnostic information to the established diagnostic methods, rather than merely confirm them. With the suboptimal performance of current histological based examination of lymph node metastasis, the introduction of novel biomarkers will have a critical impact on the clinical treatment of OTSCC. The accuracy of classification and diagnosis should further increase if information from several biological layers (mutations, methylation patterns, gene expression patterns, gene splice patterns, protein expression, and microRNA expression) are used in concert with clinical and histopatological information for a comprehensive classification algorithm.

Acknowledgements. This work was supported in part by Philips Morris USA Inc. and Philips Morris International. We thank Ms. Katherine Long and Ms. Minghua Chai for excellent editorial assistance.

REFERENCES

Bradfield JS, Scruggs RP (1983) Carcinoma of the mobile tongue: incidence of cervical metastases in early lesions related to method of primary treatment. Laryngoscope 93:1332–1336

Byers RM, Weber RS, Andrews T, McGill D, Kare R, Wolf P (1997) Frequency and therapeutic implications of "skip metastases" in the neck from squamous carcinoma of the oral tongue. Head Neck 19:14–19

Cunningham MJ, Johnson JT, Myers EN, Schramm VL Jr, Thearle PB (1986) Cervical lymph node metastasis after local excision of early squamous cell carcinoma of the oral cavity. Am J Surg 152:361–366

Fakih AR, Rao RS, Borges AM, Patel AR (1989a) Elective versus therapeutic neck dissection in early carcinoma of the oral tongue. Am J Surg 158:309–313

Fakih AR, Rao RS, Patel AR (1989b) Prophylactic neck dissection in squamous cell carcinoma of oral tongue: a prospective randomized study. Semin Surg Oncol 5:327–330

Franceschi D, Gupta R, Spiro RH, Shah JP (1993) Improved survival in the treatment of squamous carcinoma of the oral tongue. Am J Surg 166:360–365

Haddadin KJ, Soutar DS, Oliver RJ, Webster MH, Robertson AG, MacDonald DG (1999) Improved survival for patients with clinically T1/T2, N0 tongue tumors undergoing a prophylactic neck dissection. Head Neck 21:517–525

Ho CM, Lam KH, Wei WI, Lau SK, Lam LK (1992) Occult lymph node metastasis in small oral tongue cancers. Head Neck 14:359–363

Johnson JT, Leipzig B, Cummings CW (1980) Management of T1 carcinoma of the anterior aspect of the tongue. Arch Otolaryngol 106: 249–251

Jones AS, Phillips DE, Helliwell TR, Roland NJ (1993) Occult node metastases in head and neck squamous carcinoma. Eur Arch Otorhinolaryngol 250:446–449

Lee JG, Litton WB (1972) Occult regional metastasis: carcinoma of the oral tongue. Laryngoscope 82:1273–1281

Lim YC, Lee JS, Koo BS, Kim SH, Kim YH, Choi EC (2006) Treatment of contralateral N0 neck in early squamous cell carcinoma of the oral tongue: elective neck dissection versus observation. Laryngoscope 116:461–465

Livak KJ, Schmittgen TD (2001) Analysis of relative gene expression data using real-time quantitative PCR and the 2 (-Delta Delta C(T)) method. Methods 25:402–408

O'Donnell RK, Kupferman M, Wei SJ, Singhal S, Weber R, O'Malley B, Cheng Y, Putt M, Feldman M, Ziober B et al (2005) Gene expression signature predicts lymphatic metastasis in squamous cell carcinoma of the oral cavity. Oncogene 24:1244–1251

Pantel K, Brakenhoff RH (2004) Dissecting the metastatic cascade. Nat Rev Cancer 4:448–456

Peirson SN, Butler JN, Foster RG (2003) Experimental validation of novel and conventional approaches to quantitative real-time PCR data analysis. Nucleic Acids Res 31:e73

Pillsbury HC III, Clark M (1997) A rationale for therapy of the N0 neck. Laryngoscope 107: 1294–1315

Robbins KT, Clayman G, Levine PA, Medina J, Sessions R, Shaha A, Som P, Wolf GT (2002) Neck dissection classification update: revisions proposed by the American Head and Neck Society and the American Academy of Otolaryngology-Head and Neck Surgery. Arch Otolaryngol Head Neck Surg 128:751–758

Roepman P, Wessels LF, Kettelarij N, Kemmeren P, Miles AJ, Lijnzaad P, Tilanus MG, Koole R, Hordijk GJ, van der Vliet PC et al (2005) An expression profile for diagnosis of lymph node metastases from primary head and neck squamous cell carcinomas. Nat Genet 37:182–186

Schefe JH, Lehmann KE, Buschmann IR, Unger T, Funke-Kaiser H (2006) Quantitative real-time RT-PCR data analysis: current concepts and the novel "gene expression's CT difference" formula. J Mol Med 84:901–910

Schmalbach CE, Chepeha DB, Giordano TJ, Rubin MA, Teknos TN, Bradford CR, Wolf GT, Kuick R, Misek DE, Trask DK et al (2004) Molecular profiling and the identification of genes associated with metastatic oral cavity/pharynx squamous cell carcinoma. Arch Otolaryngol Head Neck Surg 130:295–302

Sparano A, Weinstein G, Chalian A, Yodul M, Weber R (2004) Multivariate predictors of occult neck metastasis in early oral tongue cancer. Otolaryngol Head Neck Surg 131:472–476

Teichgraeber JF, Clairmont AA (1984) The incidence of occult metastases for cancer of the oral tongue and floor of the mouth: treatment rationale. Head Neck Surg 7:15–21

Wong ML, Medrano JF (2005) Real-time PCR for mRNA quantitation. Biotechniques 39:75–85

Woolgar JA (1999) Pathology of the N0 neck. Br J Oral Maxillofac Surg 37:205–209

Zhou X, Temam S, Oh M, Pungpravat N, Huang BL, Mao L, Wong DT (2006) Global expression-based classification of lymph node metastasis and extracapsular spread of oral tongue squamous cell carcinoma. Neoplasia 8:925–932

21
Nasopharyngeal Carcinoma (Retropharyngeal Lymph Node Metastasis): Spread Pattern, Prognosis, and Staging

Li Li and Li-Zhi Liu

INTRODUCTION

Although it is rare in other parts of world, nasopharyngeal carcinoma (NPC) is endemic in certain regions, especially in Southeast Asia. The incidence is 30–80 of 100,000 people per year in Southern China (Muir et al. 1987). Nasopharyngeal carcinoma has a higher incidence of cervical lymph node metastasis compared with other head and neck cancers. There is a well-developed network of lymphatics in the nasopharynx (Sham et al. 1990). The retropharyngeal lymph node (RLN) is regarded as the most common lymph node involved in NPC (King et al. 2000a). Retropharyngeal lymph nodes (RLNs) are divided into medial and lateral groups (Rouviere, 1938). The lateral nodes lie lateral to the pharyngeal constrictors and medial to the internal carotid artery. The medial group lies along or near the midline, directly posterior to the upper pharynx. RLNs are not amenable to evaluation using manual palpation. Consequently, the diagnosis of enlarged RLNs in patients with NPC is made on the basis of imaging examinations, such as x-ray computed tomography (CT), positron emission tomography (PET), and magnetic resonance imaging (MRI).

The relationship between metastatic RLNs and primary tumor extensions and cervical nodal metastases is useful for clarification of the patterns of lymphatic drainage and nodal metastases in NPC, but has not yet been thoroughly investigated. Chua et al. (1997) observed a higher incidence of enlarged RLNs associated with oropharyngeal, paranasopharyngeal, nasal, and cervical lymph node involvement. Lam et al. (1997) found a statistical association between metastatic RLNs and Level II node involvement, but not with other groups of neck nodes. Apart from these two articles, there is little published information concerning the relationship between metastatic RLNs and tumor extensions in NPC. Also, there is no consensus on whether RLNs are the first echelon nodes. RLNs had been regarded as the first echelon nodes of the NPC (King et al. 2000a, b; Neel et al. 1985). But according to the study of Ng et al. (2004), RLNs are less frequently involved than cervical nodes. Data describing RLN spread patterns based on radiographic observations may provide critical guidance for research on prognostic significance and staging categories.

The fifth edition of the tumor (T)-node (N)-metastasis classification published by the Unio Internationale Contra Cancrum (UICC) and American Joint Committee on Cancer (AJCC) in 1997 is a universally accepted staging system (Fleming et al. 1997; Sobin and Wittekind 1997). No additional changes (except addition of the term masticator space as a synonym for infratemporal fossa) have been introduced to the current UICC/AJCC sixth edition (Greene et al. 2002). According to several recent studies, the frequency of RLN metastasis is high (Lam et al. 1997; Chong et al. 1995; Ng et al. 2004), but the prognostic value of RLN metastasis in patients with NPC is controversial (Sakata et al. 1999; Xiao et al. 2002; Chua et al. 1997), and the RLN metastasis was not recorded in the 6th edition of the AJCC staging system for NPC. Because the RLN involvement criteria are ambiguous in the published staging systems, classification of RLN varies among different centers (Lee et al. 2004).

The aim of our study was to document the patterns of RLN spread for NPC by using MRI, and to evaluate the prognostic value and staging categories of the retropharyngeal lymph node metastasis based on CT data.

MATERIALS AND METHODS

Patient Characteristics

This was a retrospective study of patients with biopsy-proved NPC without metastasis referred to the authors' hospital. As MRI scanner did not begin to be used until 2003 in the authors' hospital and we could not get enough survival date to investigate the prognostic value and staging categories of the retropharyngeal lymph node metastasis based on MRI data, we only use MRI data to document the patterns of RLN spread for NPC. The prognostic value and staging categories of the retropharyngeal lymph node metastasis were investigated based on CT data.

From July 2003 to January 2005, a total of 275 patients, who underwent MRI, were included in this study for evaluation of the patterns of RLN spread for NPC. There were 210 male patients and 65 female patients, and the median age was 45 years. Histologically, 10.2% of the patients had WHO type II disease, 88.7% had WHO type III disease, and the rest (1.1%) had WHO type I disease.

From January 1999 to December 1999, a total of 749 patients, who underwent contrast-enhanced CT, were included in this study for evaluating the prognostic value and staging categories of the retropharyngeal lymph node metastasis. There were 543 male patients and 206 female patients, with a male–female ratio of 2.6:1, and the median age was 46 years (range, 13–74 years). Histologically, 10% of the patients had WHO type II disease, 89% had WHO type III disease, and the rest (1%) had WHO type I disease.

Patients were grouped according to the UICC/AJCC 1997 staging system. RLN involvement was disregarded in determining N and T category. All patients had undergone fiber optic endoscopic biopsy of the nasopharynx. Regional disease was assessed by clinical examination combined with the CT/MRI findings, and in the case of a discrepancy between the radiographic and initial clinical findings, upgrading was allowed. Cranial nerve palsy was assessed clinically.

Imaging Protocol and Criteria for RLN Metastasis and Other Cervical Lymph Node

The CT studies were done with an Elscint Twin Flash helical scanner before treatment. Contiguous axial CT scans at 5-mm intervals were obtained in a plane parallel to the hard palate from the supracellar cistern to the C3 vertebra, followed by axial scans at 8-mm intervals to the supraclavicular fossa. CT scans were done after an i.v., injection (100 mL bolus at 2 mL/s) of contrast agents (Ultravist or Omnipaque). The images were taken using soft tissue and bone algorithms and filmed in the respective window settings.

The MRI scans were done with a 1.5-Tesla system (Signa, General Electric, CV/i) technique. The area from the suprasellar cistern to the inferior margin of the sternal end of clavicle was examined with a head and neck combined coil. T1-weighted fast spin-echo images in the axial, coronal and sagittal planes (repetition time of 500–600 ms and echo time of 10–20 ms), and T2-weighted fast spin-echo MR images in the axial plane (repetition time of 4,000–6,000 ms and echo time of 95–110 ms) were obtained before injection of contrast material. After intravenous Gd-DTPA injection at a dose of 0.1 mmol per kg of body weight, spin-echo T1-weighted axial and sagittal sequences, and spin-echo T1-weighted fat-suppressed coronal sequences were performed sequentially, with parameters similar to those used before Gd-DTPA injection. Section thickness was 5 mm with a 1 mm interslice gap for the axial plane, and 6 mm with a 1 mm interslice gap for the coronal and sagittal planes.

Two radiologists specialized in head and neck cancers separately evaluated all scans. Any disagreements were resolved by consensus. In this study, the RLN group included the medial and lateral RLNs. Diagnostic CT/MR criteria for metastatic lymphadenopathy includes (1) lateral retropharyngeal nodes with a minimal axial dimension of ≥5 mm and any node seen in the median retropharyngeal group, lymph nodes with a minimal axial diameter of ≥11 mm in the diagnostic region and 10 mm for all other cervical nodes, except the retropharyngeal group; (2) lymph nodes of any size with central necrosis or a contrast-enhancing rim; and (3) nodal grouping, the presence of three or more contiguous and confluent lymph nodes, each of which should have a minimal axial diameter of 8–10 mm (Ng et al. 2004; Van Hasselt 1999; Som 1992; Van den Brekel et al. 1990). Furthermore, the parapharyngeal space involvement was delineated according to the degree of extension by the Sham line (Sham and Choy 1991). Grade 1, grade 2, and grade 3 denoted extensions beyond the Sham line I, Sham line II, and Sham line III, respectively.

Treatment

All patients were treated by definitive intent radiation therapy. In the series of 749 patients who underwent contrast-enhanced CT, a total of 708 patients were treated with two lateral-opposing faciocervical portals to irradiate the nasopharynx and the upper neck in one volume followed by the shrinking-field technique (two lateral-opposed facial fields) to avoid excessive irradiation of the spinal cord. The remaining 41 patients with small tumors confined to the nasopharynx underwent a technique consisting of two lateral-opposed facial fields in the whole course of treatment.

An anterior cervical field was used to treat the whole neck with a laryngeal block. The accumulated radiation doses were 68–70 Gy to the primary tumor, 60–62 Gy to the involved areas of the neck, and 50 Gy to the uninvolved areas.

Booster portal was done if necessary. Different radiation energies, including megavoltage photons (6 MV or cobalt-60) and electrons, were used. In cases with nasal or ethmoidal involvement, an anterior facial electron field was added. Patients with bulky parapharyngeal disease were boosted with a ''parapharyngeal boost technique,'' as described by Tsao (1991). A boost dose of 10–14 Gy per five to seven fractions was delivered to the skull base in patients with involvement of the skull base and intracranial extension. Intracavitary after loading treatment with iridium-192 was done for local persistence 2–3 weeks after external radiotherapy (20–24 Gy per four to five fractions per 2 weeks to 1 cm above the midpoint of the iridium-192 source). Any palpable residual nodes after external radiotherapy were boosted to 70 Gy at the 90% isodose level with an electron field of 9 to 12 MeV. Whenever possible, salvage treatments were given to patients after documented relapse or when disease was persistent. In the series of 749 patients who underwent contrast-enhanced CT, a total of 160 patients with local or regional advanced disease (classified as T_3–T_4 or N_2–N_3) received neoadjuvant, concomitant, or adjuvant chemotherapy, in conjunction with a platinum-based therapeutic clinical trial.

Follow-Up and Statistical Analysis

In the series of 749 patients who underwent contrast-enhanced CT, a total of 97%, 94%, and 90% of patients had a complete follow up at 1 year, 3 years, and 5 years, respectively. The follow-up duration was calculated from the first day of radiation therapy to either the day of death or the day of last examination. The median follow up for the whole group was 62 months (range, 3–73 months). SPSS 11.0 statistical software was used to determine statistical significance. The incidences of RLN metastasis in patients with different T and N classifications and overall stages were compared and analyzed using the χ^2 test.

All events were measured from the date of commencement of radiotherapy. The actuarial rates were calculated by the Kaplan–Meier method (Kaplan and Meier 1958), and the differences were compared with the log-rank test. The following end points (time to the first defining event) were assessed: overall survival (OS), the loco-regional relapse-free survival (LRRFS), and distant metastasis-free survival (DMFS). These end points were analyzed and compared in patients with or without RLN metastasis. Multivariate analyses with the Cox proportional hazards model were used to test the independent significance by backward elimination of insignificant explanatory variables (Cox 1972). The Cox proportional hazards model was also used to test the hazard consistency and hazard discrimination. Host factors (age and sex) were included as covariates in all tests. In addition, the T classification was included as a covariable in the analysis of N classification. The hazard consistency and hazard discrimination were compared when RLN metastasis was classified as N_1 and T_{2b}. A two-tailed P value of <0.05 was considered statistically significant.

RESULTS

Incidence and Distribution of RLNs Demonstrated by MRI

In 275 patients who underwent MRI, 468 RLNs were observed in 239 (86.9%) patients. Of the 468 identifiable RLNs, 217 (46.6%) nodes were classified as negative nodes, and while 251 positive RLNs were present in 175 (63.6%) patients. The mean values of the minimal axial diameter, the maximal axial, and the longitudinal diameters of the positive nodes were 10.0 ± 4.5 mm (range 4–26 mm), 12.8 ± 5.6 mm (range 8–63 mm), and 22.8 ± 9.85 mm (range 4–63 mm), respectively. The incidence of number distribution of metastatic RLNs shows an orderly decreased from the level of C1 to C3. The distribution number of metastatic RLNs was distributed among patients as follows: 1 node, 113 (64.4%) patients; 2 nodes, 51 (29.3%) patients; 3 nodes, 8 (4.6%) patients; 4 nodes, 3 (1.7%) patients. The distribution number of ipsilateral enlarged RLNs in each side was as follows: 1 node, 201 (89.7%) sides; 2 nodes, 20 (8.9%) sides; 3 nodes, 3 (1.3%) sides.

Of 175 patients with metastatic RLNs, 122 (69.7%) patients had metastatic unilateral enlarged RLNs, 52 (29.7%) patients had metastatic bilateral enlarged RLNs, and 1 (0.6%) patient was observed with an enlarged median retropharyngeal lymph node. Of the patients with metastatic unilateral enlarged RLNs, 54 (44.3%) nodes were in on the left side, and 68 (55.7%) were on the right side. Of the 27 patients with primary tumors that did not cross the midline, 13 patients had metastatic ipsilateral enlarged RLNs, and 14 patients had metastatic RLNs on the bilateral or contralateral side enlarged RLNs.

Of the 175 patients with positive RLNs, 42 (24.0%) showed nodal necrosis. Of the 251 metastatic RLNs, 44 (17.5%) showed nodal necrosis. The minimal axial diameter of the necrotic RLNs ranged from 4 to 25 mm. Of all enlarged RLNs, only 1 (0.4%) metastatic, necrotic RLNs had a minimal axial diameter of >5 mm.

Relationship Between Metastatic RLNs and Tumor Involvement

A significantly higher incidence of metastatic RLNs was observed with involvement of the oropharynx, prestyloid space, poststyloid space, and longus colli muscle, medial pterygoid muscles, levator muscle of velum palatine, and tensor muscle of velum palatini involvement. No significant difference in the incidence of involvement of RLNs was observed when the primary tumor extended into the nasal cavity, laryngopharynx, pterygopalatine fossa, infratemporal fossa, lateral pterygoid muscle, skull base, sinus, orbit or intracranial extension. Although a higher incidence of metastatic RLNs was found with involvement of the clivus, the difference was not quite large enough to be significant.

Of 275 patients, 215 (78.25%) patients had metastatic RLNs or cervical lymph nodes. Of these 215 patients with nodal metastases, 40 (18.6%) had metastatic RLNs only, 40 (18.6%) had metastatic cervical lymph nodes only, and 135 (62.8%) had exhibited an involvement of both the enlarged RLNs and cervical lymph nodes. These 215 patients had an equal incidence (81.4% vs. 81.4%) of metastatic RLNs and cervical lymph nodes. A higher incidence of metastatic RLNs was found when cervical lymph node metastasis was present ($\chi^2 = 37.939$, $P \leq 0.001$). The incidence

of metastatic RLNs in patients with unilateral cervical lymph node metastasis was lower than in patients with bilateral cervical lymph node metastasis (73.0% vs. 84.4%), with a difference that was very close to the statistical significant (χ^2 = 2.993, P = 0.084). There was a statistically significant association between the involvement of RLNs and level II, level III, and level V nodes. However, there was no significant association between RLNs involvement and level I, level IV and supraclavicular nodes. Of 124 patients with metastatic unilateral enlarged RLNs, 54 (43.5%) had metastatic ipsilateral enlarged cervical nodes, 26 (21.0%) had metastatic bilateral enlarged cervical nodes, and only 10 (8.1%) had metastatic contralateral enlarged cervical nodes.

When RLNs involvement was disregarded in determining N and T category, the incidence of RLNs involvement in different T-, N- and M-classifications and stages was summarized. A significantly lower incidence of metastatic RLNs was found in T_1 (P = 0.002, χ^2 = 15.304), N_0 (P < 0.001, χ^2 = 43.291), and stage I (P < 0.001, χ^2 = 27.464) disease. A significant difference in the incidence of metastatic RLNs was also observed between N1, 2, and 3 disease (P = 0.030, χ^2 = 7.024). Conversely, no significant difference in the incidence of metastatic RLNs was observed between T1, 2, and 3 (P = 0.334, χ^2 = 2.129); N_2 and N_3 (P = 1.000); or Stage II, III, and IV disease (P = 0.085, χ^2 = 4.924).

Prognosis and Staging of RLN Metastasis Based on CT Data

Incidence of RLN Metastasis Demonstrated by CT

In patients, RLN metastasis includes the medial and lateral nodes; however, only the lateral RLNs were detected in the current study. The incidence of RLN metastasis in this study was 51.5% (386 of 749 patients). The mean values of the minimal axial diameter of the positive nodes were 11.53 ± 4.01 mm (range, 5–25 mm). A higher incidence of metastatic RLNs was found when cervical lymph node metastasis was present (χ^2 = 36.414, P < 0.001). The incidence of metastatic RLNs in patients with unilateral cervical lymph node metastasis was lower than in patients with bilateral cervical lymph node metastasis (52.5% vs. 67.9%, χ^2 =11.581, P = 0.001).

Based on the criteria of RLN involvement, RLNs were classified as either positive or negative. The incidences of RLN metastasis in different T and N classifications are summarized among the patients as follows: Of the 100 T_1, 318 T_2, 149 T_3 and 182 T_4 patients, 77 (77.0%), 132 (41.5%), 82 (55.0%) and 72 (39.6%) nodes were classified as negative respectively, whereas 23 (23.0%), 186 (58.5%), 67 (45.0%) and 110 (60.4%) positive RLNs were present respectively. Of the 214 N_0, 298 N_1, 156 N_2 and 81 N_3 patients, 141 (65.9%), 141 (47.3%), 48 (30.8%) and 33 (40.7%) nodes were classified as negative respectively, whereas 73 (34.1%), 157 (52.7%), 108 (69.2%) and 48 (59.3%) positive RLNs were present respectively. Of the 33 stage I, 260 stage II, 223 stage III and 233 stage IV patients, 30 (90.9%), 136 (52.3%), 103 (46.2%) and 94 (40.3%) nodes were classified as negative respectively, whereas 3 (9.1%), 124 (47.7%), 120 (53.8%) and 139 (57.9%) positive RLNs were present respectively. A higher incidence of RLN metastasis was found in the T_2 to T_4 compared with T_1 disease, N_1 to N_3 disease compared with N_0 disease, and in stage II–IV compared with stage I. These differences are statistically significant

(χ^2 = 15.869, P < 0.001; χ^2 = 36.414, P < 0.001; χ^2 = 24.900, P < 0.001, respectively). The incidence of metastatic RLNs in N_1 patients is lower than in N_2 patients (χ^2 = 11.537, P = 0.001).

Prognosis

The treatment outcome of patients with and without RLN metastasis is compared as follows: Significant differences were observed in OS (58.7% vs. 72.2%, P < 0.001) and DMFS (75.0% vs. 84.6%, P < 0.001), with better rates occurring in patients without RLN metastasis. No significant difference was observed in LRRFS (77.9% vs. 82.4%, P = 0.173). After adjusting for T and N classification, a marginal significant difference in DMFS was observed (P = 0.079). Multivariate analysis was done to adjust for various prognostic factors. The following variables were included in the Cox proportional hazards model by backward elimination of insignificant explanatory variables: age (≤50 years vs. >50 years), gender, nasal fossa, paranasopharyngeal space (grade 0/1 vs. grade 2/3) (Sham et al. 1991) oropharyngeal extension, hypopharyngeal extension, infratemporal fossa extension, RLN metastasis, base of skull erosion, pterygoprocess zone, paranasal sinus extension, cranial nerve palsy/intracranial extension, laterality of cervical lymph node, greatest diameter of cervical lymph node (≤60 vs. >60 mm), Ho's location (Ho 1978) of cervical lymph nodes, and chemotherapy.

RLN metastases were not of prognostic significance in OS but were marginally significant in DMFS. Chemotherapy was not significant for OS or DMFS. In N_0 disease, significant differences were observed in OS, DMFS, and LRRFS (P = 0.002, P = 0.02, and P = 0.01, respectively), and better rates were observed in patients without RLN metastasis. The presence of RLN metastases was a significant independent predictor for OS, LRRFS, and DMFS, as shown by multivariate analysis T_4 (P = 0.007, P = 0.023, and P = 0.008, respectively). No significant differences were observed in OS, DMFS, and LRRFS between patients with unilateral RLN (URLN) and bilateral RLN (BRLN) metastasis (P = 0.511, P = 0.190, and P = 0.132, respectively).

Hazard Consistency and Hazard Discrimination

We divided N_0 and N_1 patients into four groups: N_0 disease without RLN metastasis, N_0 disease with URLN metastasis, N_1 disease without BRLN metastasis, and $N_{0\text{-}1}$ patients with BRLN metastasis. We found no significant differences in OS and DMFS between N_1 patients without BRLN and N_0 patients with URLN (P = 0.536 and P = 0.845), N_1 patients without BRLN and $N_{0\text{-}1}$ patients with BRLN (P = 0.889 and P = 0.715), and N_0 patients with URLN and $N_{0\text{-}1}$ patients with BRLN (P = 0.708 and P = 0.924). Conversely, the difference in OS and DMFS between $N_{0\text{-}1}$ patients with BRLN and N_2 patients was very close to statistical significance (P = 0.067 and P = 0.084). Hence, N_1 patients with BRLN metastasis should not be classified as N_2.

The risk of distant metastasis and death is shown as followed by the different N subsets (N_0 disease without RLN metastasis, N_0 disease with RLN metastasis, N_1 disease, N_2 disease, and N_3 disease). The hazard ratios (HR) of death and distant failure for patients with N_0 disease and RLN metastasis were 0.596 and 0.433, respectively, which is similar to patients with N_1 disease (HR = 0.633, HR = 0.531, respectively). These results suggest that

there is no difference in HRs of OS and DMFS between patients with N_0 disease and RLN metastasis and patients with N_1 disease. The survival curve for patients with N_0 disease and RLN metastasis was approximately the same as that of patients with N_1 disease, and the log-rank test for OS and DMFS shows that the difference is insignificant ($P = 0.6096$ and $P = 0.8995$, respectively). However, the difference in OS and DMFS between patients with N_0 disease without RLN metastasis and patients with N_0 disease and RLN metastasis turned out to be significant ($P = 0.0021$ and $P = 0.0187$, respectively).

We also found that the survival curve of OS for patients with T_1 disease and RLN metastasis was approximately the same as patients with T_2 disease ($P = 0.9501$). The survival curve of DMFS for patients with T_1 disease and RLN metastasis was approximately the same as patients with T_3 disease ($P = 0.9501$).

Comparing Staging Categories of RLN Metastasis

When RLN metastasis is classified as T_{2b} and N_1, an even and orderly increase in the HRs of OS and DMFS in different N subsets is observed in the two situations. The survival curves of OS and DMFS for the N subsets were both split evenly, but there was a better segregation of different N stage diseases in terms of OS and DMFS curves when RLN metastasis was classified as N_1. When RLN metastasis was classified as N_1 and stage I patients with RLN metastasis were upstaged to stage II, the survival curves of OS and DMFS for the overall stage were also evenly distributed.

If RLN involvement is classified as T_2, a total of 23 T_1 patients with RLN involvement would be upgraded to T_2. The distribution of patients according to T classification was as follows: T_1, 77 (10.3%); T_2, 341 (45.5%); T_3, 149 (19.9%); T_4, 182 (24.3%). If RLN involvement is classified as N_1, a total of 73 N_0 patients would be upgraded to N_1. The distribution of patients according to N classification was as follows: N_0, 141 (18.8%); N_1, 371 (49.5%); N_2, 156 (20.8%); N_3, 81 (10.8%). Regardless of whether RLN metastasis is classified as T_2 or N_1, a total of three stage-I patients would be upgraded to stage II and the distribution of patients in each stage group would be as follows: stage I, 30 (4.0%); stage II, 263 (35.1%); stage III, 223 (29.8%); stage IV, 233 (31.1%).

DISCUSSION

Imaging Criteria for Metastatic RLNs

The retropharyngeal nodes are divided into medial and lateral groups (Rouviere 1938). Unlike other head and neck cancers, NPC with no distant metastasis is typically treated with nonsurgical intervention. RLNs are located deep within the neck and are very close to the primary tumor. These nodes are poorly accessible by imaging guided fine-needle aspiration biopsy. It is particularly difficult to define radiological criteria of RLNs metastasis by radiological–histopathological correlations based on a large sample. Mancuso suggested that the size limit for abnormal RLNs should be lowered to 10 mm (Mancuso et al. 1983). A maximal axial diameter ≥10 mm was used as the criteria for radiographic involvement of RLNs in early studies (Chua et al. 1997; McLaughlin et al. 1995). The measurement of minimal

axial diameter may be a more accurate predictor of tumor-positive cervical nodes (Van den Brekel et al. 1990). RLNs atrophy with age and are usually obliterated by adulthood. According to Ogura (Ogura et al. 2004), the minimal axial diameter of normal RLNs on MR images were 6.4 ± 1.4, 4.2 ± 1.1 and 3.2 ± 1.0 mm, corresponding to younger (6–19 years), intermediate (20–38 years), and older (42–74 years) age groups. The radiological criteria for cervical lymph node metastasis in other head and neck cancers, which is defined based on histopathological correlation, is not suitable for the assessment of RLN. Two MRI studies found that normal RLNs were smaller than 4 or 4.5 mm in the maximum diameter of the shortest axis. Therefore, our study used a minimal axial diameter of ≥5 mm as the size criteria for metastatic RLNs based on the recommendation of published reports (Lam et al. 1997; King et al. 2000a). It should be stressed that this size criteria was based on a normal group with noninfective and nonmalignant conditions of the head or neck. Using this size criterion, it was difficult to distinguish benign reactive adenopathy with a minimal axial diameter of ≥5 mm from malignant RLNs (Ichimura 1993). It might be necessary to redefine the size criteria of RLN involvement according to data collected from NPC patients.

Central necrosis was used as a diagnostic criterion for a metastatic node in our study. Whereas necrosis is a very reliable criterion for lymph node metastases (Van den Brekel et al. 1990; Som 1992), it is unfortunately quite rare or not visible in small lymph nodes (Don et al. 1995; Curtin et al. 1998). Only 1 (0.4%) of the metastatic RLNs was found with a minimal axial diameter <5 mm in this series, and only 20.0% of enlarged RLNs showed nodal necrosis. Our study revealed that central necrosis as a diagnostic criterion does not markedly improve the sensitivity of MRI in detecting RLN metastases.

Although the RLNs included the medial and the lateral groups, the vast majority of RLN involvement in NPC patients was among the lateral group. To our knowledge, there are only two published reports in which enlarged medial retropharyngeal node showed on MRI (Lam et al. 1997; Ng et al. 2004). One enlarged medial retropharyngeal lymph node was also found on MRI in our study. Because medial retropharyngeal nodes are usually not visible, any MRI finding of a medial retropharyngeal node is regarded as abnormal.

Incidence of RLNs Metastasis

The incidence of retropharyngeal lymph node metastasis detected on MRI in our study was 63.6%, which is similar to the other reported studies (King et al. 2000a; Lam et al. 1997; Ng et al. 2004) by MRI, and was higher than that of our study based on CT. The reason may be as follows: although computerized axial tomography (CT-scan) is also one of the methods that can give a reliable image of the nasopharyngeal cancer extensions, the retropharyngeal lymph node metastases without central necrosis or a contrast-enhancing rim were isodense and contiguous with the primary tumor, and thus may not be identified as a separate mass on the CT scan. The superior soft-tissue contrast of MRI could be of paramount importance in discriminating individual lymph nodes from direct tumor extension and adjacent normal structure

(King et al. 2000a; Lam et al. 1997), so MRI was regarded as the optimal method in diagnosing the retropharyngeal lymph node.

Spread Patterns of RLNs Metastasis

Previous studies by King et al. (2000a) and Chong et al. (1995) have detailed the locations of metastatic RLNs. The latter showed that the majority of metastatic RLNs were located superior to the C2 vertebral level. In contrast, the former found that 63% of all RLNs extended down to the level of C2, 19% to the level of the C2/3 disk and 6% to the level of C3. The difference between the two studies might have resulted from the recording method. In our study, the longitudinal center of each node was recorded. The longitudinal center of 10% of all RLNs was located at the level of the occipital bone, which was not addressed by either study. Metastatic RLNs at the oropharyngeal level might require special consideration in radiation planning. The definition of RLNs proposed by Som et al. (2000) states that RLNs must lie medial to the internal carotid arteries within 2 cm of the skull base. This definition may be not suitable for NPC, because there are so many RLNs located beyond that region. Based on our observations, the incidence of lateral RLNs metastases decreases in an orderly fashion from the C1 to C3 level, and the multiple metastatic ipsilateral RLNs were not uncommon in NPC. Are there any pathways between lateral RLNs of different levels, and does the lymphatic vessel drain descendingly to RLNs at lower levels?

A higher incidence of metastatic retropharyngeal lymph nodes was associated with primary involvement beyond the nasopharynx mucosa (T_2 to T_4 patients). Furthermore, a higher incidence of metastatic RLNs was associated with primary tumor invasions into the oropharynx, prestyloid space, poststyloid space, longus colli muscle, medial pterygoid muscles, and tensor muscle of velum palatini. These subsites are located laterally, inferiorly and posteriorly to the nasopharynx, and involvement of these sites is classified as T_2. Although RLNs metastasis was found in T_1 patients, the risk of RLN metastasis markedly increased when the primary tumor invaded beyond the confinement of the pharyngobasilar fascia (Chua et al. 1997). The lymphatic drainage of carcinoma of the head and neck was associated with the primary tumor location and adjacent subsites to which the tumor spread (Mukherji et al. 2001). Drainage regions of the retropharyngeal nodes are the nasal cavities, eustachian tubes, nasopharynx, oropharynx, hypopharynx, pharyngeal wall, and palate (Rufener and Cohen 2003). The findings of our study suggest that most of the afferent lymphatic vessels of lateral RLNs in NPC begin in the wall of the nasopharynx, oropharynx, and parapharyngeal space. Metastatic RLNs were not associated with involvement of the laryngopharynx and nasal cavity in this series. The lymphatic drainage of nasal cavity may primarily drain to the cervical lymph nodes in NPC. The incidence of laryngopharyngeal invasion was very low, so we could not evaluate the association between the laryngopharynx and RLNs. There was no apparent relationship between RLN metastasis and the laryngopharynx, pterygopalatine fossa, infratemporal fossa, lateral pterygoid muscle, skull base, sinus, orbit, or intracranial extension. The involvement of these structures is classified as T_3 or T_4.

The efferent vessels of the RLNs drain to the upper jugular chain and to the posterior triangle (Rufener and Cohen 2003). A higher incidence of metastatic RLNs was found in patients with cervical lymph node metastases (patients classified as N_1 to N_3). We also found that the incidence of metastatic RLNs in patients with unilateral cervical lymph node metastases was lower than in patients with bilateral cervical lymph node metastases. Patients with bilateral cervical lymph nodes measuring <6 cm above the supraclavicular fossa were classified as N_2. Therefore, the incidence of metastatic RLNs in N_1 patients is lower than in N_2 patients.

Prognostic Significance and Staging of RLNs Metastasis

In our study, a low incidence of metastatic RLNs was observed in patients with stage I disease. A higher incidence of metastatic RLNs was associated with primary involvement beyond the nasopharynx mucosa (T_2–T_4 patients) and cervical lymph node metastasis. The implication is that RLN involvement might affect the treatment outcome. However, the prognosis of RLN metastasis is controversial. Some studies report that higher distant metastasis rates are observed in patients with NPC with RLN metastasis (Sakata et al. 1999; Xiao et al. 2002; Mancuso et al. 1983), but those studies are based on univariate analysis. The study by Chua et al. (1997) shows no significant effect on outcome and prognosis after adjusting for T and N classifications, and suggests that there is insufficient evidence for upgrading N_0 patients with RLN lymph node metastasis to N_1, regardless of the node size. These observations are based on a relatively small number of patient, and the criteria for RLN involvement is the same as for the cervical lymph nodes. The results should, therefore, be interpreted with caution. In our study using univariate analysis, a significant difference was found in the OS and DMFS rates. RLN metastasis was not of prognostic significance in LRRFS, and a likely explanation is related to the cancer treatment. All patients in our study received lymph node irradiation, regardless of clinical lymph node status and CT finding, and the upper neck and nasopharynx were treated in one volume in 94.7% of patients. A boost treatment was also given for patients with significant disease in the paranasopharyngeal space, whether it was a direct tumor extension or RLN involvement. Thus, adequate control of RLN disease was not unexpected.

Using multivariate analysis, we found that RLN metastasis is not an independent significant prognostic factor in OS. A marginal significant difference was observed in DMFS. The effect of RLN metastasis on prognosis may have been shielded by the advanced T and N classification. RLN metastasis may contribute to DMFS. In our study, only 21.4% (160 of 749) of patients received chemoradiotherapy. The North American Intergroup study (0099) reported that chemoradiotherapy improves the 5-year OS for advanced NPC patients in 1998 (Al-Sarraf et al. 1998). However, there is controversy over whether the results were applicable to patients in endemic regions (Chua et al. 2002; Wee et al. 2005; Lee et al. 2005). In our study, chemotherapy was not an independent prognostic factor in multivariate analysis.

In contrast with the study by Chua et al. (1997), our data show a significant difference in all end points using multivariate

analysis between N_0 patients with or without RLN metastasis. These differences may be explained by a difference of RLN size criteria. A minimal axial diameter of ≥5 mm for metastatic RLNs was used as the size criteria in our study, based on the recommendation of published reports (King et al. 2000a; Lam et al. 1997). In the study by Chua et al. (1997), lymph nodes with a maximum dimension of ≥10 mm were used as the size criteria for RLN metastasis, and a decreased incidence (29.1%) of RLN metastasis was observed. The report by Chua et al. (1997) was based on a relatively small sample, with 21 metastatic RLN patients of 134 patients with clinical N_0 disease. In this study, N classification was determined solely by palpation, which may result in N_1 patients being misdiagnosed as N_0. This may reduce the prognostic difference of N_0 disease with or without RLN metastasis.

An ideal staging classification has several characteristics. First, the subgroups defined by T, N, and M should have similar survival rates (hazard consistency). Second, the survival rates should differ among the groups (hazard discrimination). Third, the distribution of patients among the groups should be balanced (Groome et al. 2001). Because RLN criteria in the published staging systems are ambiguous, RLN involvement had been classified as T_2 (Groome et al. 2001) or N_1 (Lee et al. 2004) in different studies. According to the general principle used by the AJCC staging system, RLN should be classified as N_1 if unilateral and N_2 if bilateral. However, in our series, no significant differences were observed in all end points between patients with URLN or BRLN metastasis. We also observed that there is no difference in OS and DMFS among N_0 patients with URLN, $N_{0\text{-}1}$ patients without BRLN, and $N_{0\text{-}1}$ patients with BRLN. However, the difference in OS and DMFS between N_2 patients and $N_{0\text{-}1}$ patients with BRLN turned out to be close to statistically significant. There is no evidence to upgrade N_0 and N_1 patients with BRLN metastasis to N_2.

In this study, the difference of the HRs between N_0 disease and N_0 disease with RLN metastasis is significant. The survival curve of OS and DMFS for patients with N_0 disease with RLN metastasis was approximately the same as N_1 disease. The survival curve of OS for patients with T_1 disease with RLN metastasis was approximately the same as patients with T_2 disease. However, the survival curve of DMFS for patients with T_1 disease with RLN metastasis was approximately the same as patients with T_3 disease. Thus, it seems that RLN metastasis has a tendency to affect the DMFS. Hazard discrimination was in good order when RLN metastasis was classified as N_1 or T_2, but there was a better segregation of different N stage diseases in terms of OS and DMFS curves when the RLN metastasis was classified as N_1. It is well known that RLNs are the first echelon nodes of NPC. In most cases, RLNs can be discriminated from the primary tumor on CT or magnetic resonance images. According to the principle of hazard consistency and hazard discrimination, it seems more reasonable to classify RLNs as N_1 and stage I patients with RLN involvement should be upstaged to stage II. However, when the RLN metastasis was regarded as N_1, the percentage of N_1 patients was 49.7%, which creates an uneven distribution for N classification. Furthermore, due to the current and widely accepted treatment protocol, the identification of RLN metastasis, probably, has

limited effect on treatment decision making. In our series, only 3 of 749 patients with RLNs were upstaged from stage I to stage II; thus, the actual effect on the current staging system is likely to be small. The incidence of RLN metastasis in stage I patients was 10%, and the effect of RLN involvement should not be ignored in stage I diseases.

The imaging modality also has an effect on the staging. The superior soft tissue contrast of MRI could be of paramount importance in discriminating individual lymph nodes from direct tumor extension and oropharyngeal involvement (Ng et al. 1997; Olmi et al. 1995). In contrast, CT is unable to depict the small soft tissue structure and might lead to diagnoses with a higher incidence of parapharyngeal and oropharyngeal involvement and lesser incidence of bony structures involvement than MRI (Rouviere, 1938; Ng et al. 1997; King et al. 2000b). The staging categories of RLN metastasis should be further investigated using MRI, and more explicit recommendations might be included in a future staging system. Our study comprises the largest amount of data with the longest follow-up time (median, 62 months) for investigating the prognostic value and staging categories of RLN metastasis in NPC patients. Our study provides an important reference for the further MRI study.

It should be stressed that only traditional radiotherapy techniques were used in our series. With conformal radiation therapy and intensity-modulated radiation therapy techniques, the gross tumor volume includes the nasopharyngeal primary and the retropharyngeal lymphadenopathy, so that a high dose can be delivered to RLNs. It has been shown that local control is directly related to the tumor dose (Vikram et al. 1985; Marks et al. 1982). Intensity modulated radiation therapy may improve the local control in patients with RLN involvement. The influence of intensity modulated radiation therapy on treatment outcome in patients with RLNs should be evaluated in the future.

In conclusion, a high incidence of RLN involvement is present in patients with NPC. Metastatic RLNs are associated with oropharynx, and parapharyngeal space involvement of the primary tumor. Metastatic RLNs are also associated with level II, level III, and level V cervical lymph node metastasis. Both RLNs and cervical level II nodes appeared to be the first-echelon nodes in NPC. RLN metastasis has a tendency to affect the DMFS. The RLN involvement affects OS, locoregional relapse, and distant metastasis in N_0 disease. Thus, it is our opinion that RLN metastasis should be classified as N_1, and stage I patients with RLN involvement should be upstaged to stage II.

REFERENCES

Al-Sarraf M, LeBlanc M, Giri PG, Fu KK, Cooper J, Vuong T, Forastiere AA, Adams G, Sakr WA, Schuller DE, Ensley JF (1998) Chemoradiotherapy versus radiotherapy in patients with advanced nasopharyngeal cancer: phase III randomized intergroup study 0099. J Clin Oncol 16:1310–1317

Chong VF, Fan YF, Khoo JB (1995) Retropharyngeal lymphadenopathy in nasopharyngeal carcinoma. Eur J Radiol 21:100–105

Chua DT, Sham JS, Au GK, Choy D (2002) Concomitant chemoirradiation for stage III–IV nasopharyngeal carcinoma in Chinese patients: results of a matched cohort analysis. Int J Radiat Oncol Biol Phys 53:334–343

Chua DT, Sham JS, Kwong DL, Au GK, Choy DT (1997) Retropharyngeal lymphadenopathy in patients with nasopharyngeal carcinoma:

a computed tomography-based study. Cancer 79:869–877

Cox DR (1972) Regressionmodels and life tables. J R Stat Soc Ser B 34:187–220

Curtin HD, Ishwaran H, Mancuso AA, Dalley RW, Caudry DJ, McNeil BJ (1998) Comparison of CT and MR imaging in staging of neck metastases. Radiology 207:123–130

Don DM, Anzai Y, Lufkin RB, Fu Y, Calcaterra TC (1995) Evaluation of cervical lymph node metastases in squamous cell carcinoma of the head and neck. Laryngoscope 105:669–674

Fleming ID, Cooper JS, Henson DE, Hutter RVP, Kennedy BJ, Murphy GP (1997) American Joint Committee on cancer: AJCC Cancer Staging Manual, 5th edn. Lippincott-Raven, Philadelphia

Greene FL, Page DL, Fleming ID, Fritz A, Balch CM, Haller DG, Morrow M (2002) AJCC cancer staging handbook from the AJCC cancer staging manual, 6th edn. Springer, NewYork

Groome PA, Schulze K, Boysen M, Hall SF, Mackillop WJ (2001) A comparison of published head and neck stage groupings in carcinomas of the oral cavity. Head Neck 23:613–624

Ho JHC (1978) Stage classification of nasopharyngeal carcinoma: a review. In: De-The G, EtoY (eds) Nasopharyngeal carcinoma: etiology and control. IARC Scientific publications no. 20. International Agency for Research on Cancer, Lyon, pp 99–113

Ichimura K (1993) Can Rouviere's lymph nodes in non-malignant subjects be identified with MRI? Auris Nasus Larynx 20:117–123

Kaplan EL, Meier P (1958) Nonparametric estimation from incomplete observations. J Am Stat Assoc 53:457–481

King AD, Ahuja AT, Leung SF, Lam WW, Teo P, Chan YL, Metreweli C (2000a) Neck node metastases from nasopharyngeal carcinoma: MR imaging of patterns of disease. Head Neck 22:275–281

King AD, Teo P, Lam WW, Leung SF, Metreweli C (2000b) Paranasopharyngeal space involvement in nasopharyngeal cancer: detection by CT and MRI. Clin Oncol 12:397–402

Lam WW, Chan YL, Leung SF, Metreweli C (1997) Retropharyngeal lymphadenopathy in nasopharyngeal carcinoma. Head Neck 19:176–181

Lee AW, Au JS, Teo PM, Leung TW, Chua DT, Sze WM, Zee BC, Law SC, Leung SF, Tung SY, Kwong DL, Lau WH (2004) Staging of nasopharyngeal carcinoma: suggestions for improving the current UICC/AJCC Staging System. Clin Oncol 16:269–276

Lee AW, Lau WH, Tung SY, Chua DT, Chappell R, Xu L, Siu L, Sze WM, Leung TW, Sham JS, Ngan RK, Law SC, Yau TK, Au JS, O'Sullivan B, Pang ES, O SK, Au GK, Lau JT (2005) Hong Kong Nasopharyngeal Cancer Study Group. Preliminary results of a randomized study on therapeutic gain by concurrent chemotherapy for regionally-advanced nasopharyngeal carcinoma: NPC-9901 trial by the Hong Kong Nasopharyngeal Cancer Study Group. J Clin Oncol 23:6966–6975

Mancuso AA, Harnsberger HR, Muraki AS, Stevens MH (1983) Computed tomography of cervical and retropharyngeal lymphnodes: normal anatomy, variants of normal, and applications in staging head and neck cancer. Part II. Pathology. Radiology 148:715–723

Marks JE, Bedwinek JM, Lee F, Purdy JA, Perez CA (1982) Dose–response analysis for nasopharyngeal carcinoma: An historical perspective. Cancer 50:1042–1050

McLaughlin MP, Mendenhall WM, Mancuso AA, Parsons JT, McCarty PJ, Cassisi NJ, Stringer SP, Tart RP, Mukherji SK, Million RR (1995) Retropharyngeal adenopathy as a predictor of outcome in squamous cell carcinoma of the head and neck. Head Neck 17:190–198

Muir CS, Waterhouse J, Mack T (1987) Cancer incidence in five continents, Vol. 5. IARC Scientific Publication No. 88, IARC, Lyon.

Mukherji S, Armao D, Joshi V (2001) Cervical nodal metastases in squamous cell carcinoma of the head and neck: What to expect. Head Neck 23:995–1005

Neel HB, Taylor WF, Pearson GR (1985) Prognostic determinants and a new view of staging for patients with nasopharyngeal carcinoma. Ann Otol Rhinol Laryngol 94:529–537

Ng SH, Chang JT, Chan SC, Ko SF, Wang HM, Liao CT, Chang YC, Yen TC (2004) Nodal metastases of nasopharyngeal carcinoma: patterns of disease on MRI and FDGPET. Eur J Nucl Med Mol Imaging 31:1073–1080

Ng SH, Chang TC, Ko SF, Yen PS, Wan YL, Tang LM, Tsai MH (1997) Nasopharyngeal carcinoma: MRI and CT assessment. Neuroradiology 39:741–746

Ogura I, Kaneda T, Kato M, Mori S, Motohashi J, Lee K (2004) MR study of lateral retropharyngeal lymph nodes at different ages. Oral Surg Oral Med Oral Pathol Oral Radiol Endod 98:355–358

Olmi P, Fallai C, Colagrande S, Giannardi G (1995) Staging and follow-up of nasopharyngeal carcinoma: magnetic resonance imaging versus computerized tomography. Int J Radiat Oncol Biol Phys 32:795–800

Rouviere H (1938) Antomy of human lymphatic system. Edward Brothers, Ann Arbor, MI

Rufener JB, Cohen JI (2003) Metachronous spread of parathyroid carcinoma to a retropharyngeal lymph node. Head Neck 25:968–971

Sakata K, Hareyama M, Tamakawa M, Oouchi A, Sido M, Nagakura H, Akiba H, Koito K, Himi T, Asakura K (1999) Prognostic factors of nasopharynx tumors investigated by MR imaging and the value of MR imaging in the newly published TNM staging. Int J Radiat Oncol Biol Phys 43:273–278

Sham JST, Choy D (1991) Prognostic value of parapharyngealcarcimoma: onlocalcontrolandshort-termsurvival. Head Neck 13:298–310

Sham JST, Choy D, Wei WI (1990) Nasopharyngeal carcinoma: orderly neck node spread. Int J Radiat Oncol Biol Phys 19:929–933

Sobin LH, Wittekind CH (1997) International union against cancer (UICC): TNM classification of malignant tumours, 5th edn. Wiley-Liss, NewYork

Som PM (1992) Detection of metastasis in cervical lymph nodes: CTand MR criteria and differential diagnosis. Am J Roentgenol 158:961–969

Som PM, Curtin HD, Mancuso AA (2000) Imaging-based nodal classification for evaluation of neck metastatic adenopathy. Am J Roentgenol 174: 837–844

Tsao SY (1991) Technical details for radiotherapy delivery. In: van Hasselt CA, Gibb AG (eds) Nasopharyngeal carcinoma. The Chinese University Press, Hong Kong, pp 207–208

Van den Brekel MW, Stel HV, Castelijns JA, Nauta JJ, van der Waal I, Valk J, Meyer CJ, Snow GB (1990) Cervical lymph node metastasis: assessment of radiologic criteria. Radiology 177:379–384

Van Hasselt CA (1999) Nasopharyngeal carcinoma, 2nd edn. The Chinese University Press, Hong Kong, pp 127–160

Vikram B, Mishra UB, Strong EW, Manolatos S (1985) Patterns of failure in carcinoma of the nasopharynx: I. Failure at the primary site. Int J Radiat Oncol Biol Phys 11:1455–1459

Wee J, Tan EH, Tai BC, Wong HB, Leong SS, Tan T, Chua ET, Yang E, Lee KM, Fong KW, Tan HS, Lee KS, Loong S, Sethi V, Chua EJ, Machin D (2005) Randomized trial of radiotherapy versus concurrent chemoradiotherapy followed by adjuvant chemotherapy in patients with American Joint Committee on Cancer/ International Union against cancer stage III and IV nasopharyngeal cancer of the endemic variety. J Clin Oncol 23:6730–6738

Xiao GL, Gao L, Xu GZ (2002) Prognostic influence of parapharyngeal space involvement in nasopharyngeal carcinoma. Int J Radiat Oncol Biol Phys 52:957–963

22
Retinoblastoma: Diagnosis, Treatment and Prognosis

Aubin Balmer, Francis Munier, and Leonidas Zografos

INTRODUCTION

The first detailed clinical description of retinoblastoma is attributed to the Dutch anatomist and botanist, Petrus Pavius, in an autopsy report in 1597. In 1903, with the discovery of X-rays, Hilgartner carried out the first conservative treatment, in the form of radiotherapy. Since then, enucleation and other therapeutic measures have lead to a spectacular rise in the survival rate, this extremely low at the beginning of the twentieth century, to over 90% today. Retinoblastoma holds a special place in the field of oncology, for this cancer of the retina almost exclusively concerns very young children. It can be cured, provided that diagnosis is made and treatment carried out in the early stages of disease. Retinoblastoma may be unilateral and unifocal or bilateral and multifocal, heritable or nonheritable. In heritable cases, mutation of the tumor-suppressor gene RB1 responsible for retinoblastoma also increases the risk of neuroectodermal lesions and other primary nonocular tumors. It is thus essential to identify the first manifestations of disease in order to make an early diagnosis and provide rapid treatment.

DIAGNOSIS

Epidemiology

Although a rare disease, retinoblastoma accounts for 80% of all primary ocular malignancies in children up to 15 years of age (Mahoney et al. 1990) and ~5% of malignant solid tumors in children (Shah et al. 2000). According to the literature, the incidence is 1 in 20,000. There are some geographical discrepancies, with disadvantaged countries showing a higher rate. The incidence in North America and Europe is approximately the same, with 6 to 14 cases per million children up to 4 years of age (Bunin and Orjuela 2007). Poor living conditions, maternal diet deficiency, and human papillomavirus infections have been implicated in the etiology of nonheritable retinoblastoma (Murphree 2007a). Some regional variations may be linked to genetic environmental susceptibility or specific population behavioral patterns. In vitro fertilization has been reported as an increased risk of retinoblastoma (Moll et al. 2003), but this has yet to be confirmed. There is no reported predilection concerning sex or race. The parents' age, in particular that of the father, may be a risk factor but this also remains controversial.

Genetics

Retinoblastoma is a malignant tumor of the immature sensory retina, resulting from two successive mutations that inactivate both alleles of the retinoblastoma gene RB1, a tumor suppressor gene located on the long arm of chromosome 13 (13q14). 60% of cases are nonheritable, secondary to somatic mutations and invariably resulting in unilateral, unifocal disease. The risk of a second occurrence in another healthy retinal cell is negligible. Approximately 40% of cases are heritable, carrying a germline mutation that is due either to direct familial transmission (10%) of the autosomal dominant type or to de novo prezygotic mutation (30%) in healthy parents, mostly in the paternal lineage. Inherited gene mutation is highly penetrant (90%); every retinal cell harbours a RB1 mutation or "first hit". In most cases the retinoblastoma is bilateral and plurifocal, but there are cases of low-penetrance mutation giving rise to unaffected carriers. Expression can also be variable with cases of spontaneous regression (retinoma) or unilateral unifocal hereditary retinoblastoma (10–15% of all unilateral cases). Mutation of the RB1 gene also results in increasing risks to develop cerebral tumors such as pinealoblastoma (intracranial primitive neuroectodermal tumor), or other nonocular tumors (osteosarcoma, sarcoma). This risk may be defined as the "RB1 cancer predisposition syndrome" (Murphree and Singh 2007).

Semeiology

The primary sign of retinoblastoma is leukocoria (Fig. 22.1a, b), present in 60% of the cases. Although the appearance of

FIGURE 22.1. Leukocoria, most common warning sign of retinoblastoma. (**a**) Unilateral retinoblastoma (right eye) in a 3 year-old boy. (**b**) Bilateral retinoblastoma in a 6 month-old female infant. Leukocoria (left eye) was first noticed on flash photography (reproduced with permission from Masson Ed.) (Balmer and Munier 2002)

leukocoria is a late sign, the prognosis is good, but the preservation of the eye is less certain. Leukocoria is created by the reflection of incident light from a tumoral lesion within the pupillary area when the fundus is directly illuminated. This white pupillary reflex is commonly seen on flash photography (Fig. 22.1b). Leukocoria may initially be intermittent, depending on the lighting, degree of pupil dilation, direction of gaze, angle of observation and, above all, the location and size of the tumor. Until proven otherwise, a white pupil should always be considered at best the sign of a benign lesion, at worst that of retinoblastoma.

The second major sign of retinoblastoma is strabismus, present in 20% of cases and usually secondary to a macular lesion. Identified correctly, strabismus is an invaluable early sign carrying an excellent vital prognosis and a good chance of eye preservation. In 20% of cases the first manifestation of retinoblastoma is atypical, often inflammatory. These are late signs and hold a far more reserved vital and functional prognosis.

Retinoblastoma may develop in utero and up to 4 years of age. First signs appear at a median age of 7 months in bilateral cases and 24 months in unilateral cases.

Clinical Features

The clinical features of retinoblastoma vary according to the tumor growth pattern and duration, degree of vascularization, presence of calcifications, vitreous seeding, retinal detachment, or hemorrhage. Vitreous (Fig. 22.2) and subretinal seedings are the characteristic clinical signs of advanced endo- or exophytic retinoblastoma, respectively. Arising from the developing neuroretina, tumor growth shows three variants: towards the vitreous cavity (endophytic growth) and towards the subretinal space, causing retinal detachment

Figure 22.2. Diffuse vitreous seeding from a peripheral tumor not visible here

(exophytic growth) and, more rarely, within the retinal layers with no obvious mass and no calcifications (diffuse infiltrating form).

Endophytic retinoblastoma (Fig. 22.3a–c) manifests as one or more isolated or coalesced tumors of variable size, round or oval-shaped, yellowish-white (calcifications) or pinkish (vascularized) in color, with a marked tendency to vitreous seeding. *Exophytic retinoblastoma* (Fig. 22.3d) is associated with retinal detachment, thus masking to a greater or lesser degree the underlying tumors, and secondary seeding in the subretinal space. A tumor may display both endo- and exophytic features, in which case it is considered a *mixed growth* pattern (Fig. 22.4). *Diffuse infiltrating retinoblastoma* is a progressive lesion, often of greyish plaque-like appearance, that may ultimately infiltrate the anterior segment and

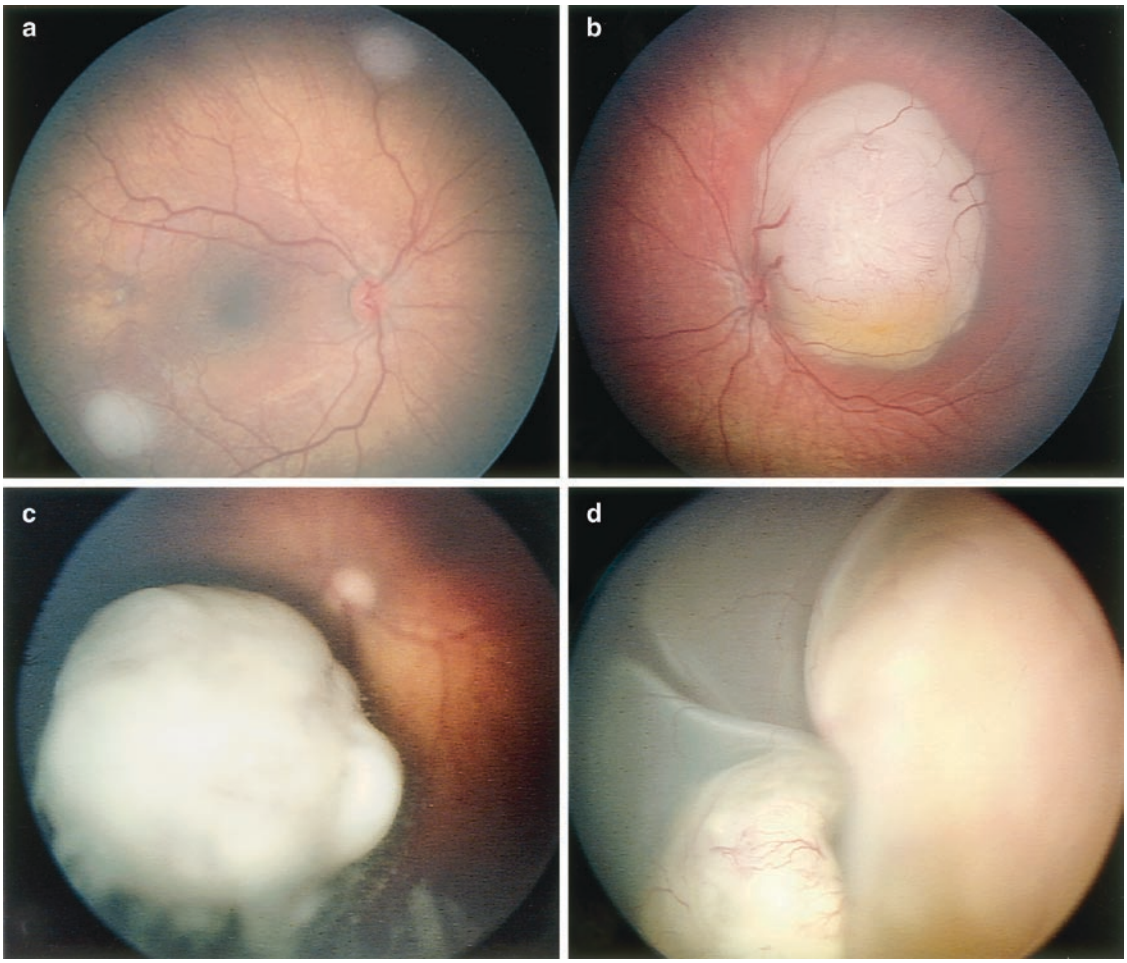

FIGURE 22.3. Various stages of retinoblastoma growth: (**a**) Two small lesions located away from the fovea and disc less than 3 mm in diameter (Group A) in an endophytic growth pattern. (**b**) Large endophytic tumor in contact with optic nerve and macula with no vitreous seeding (Group B). (**c**) Large endophytic retinoblastoma with calcifications and local vitreous inferior dissemination (Group C). (**d**) Large exophytic tumors with subretinal seeding and total retinal detachment (Group D)

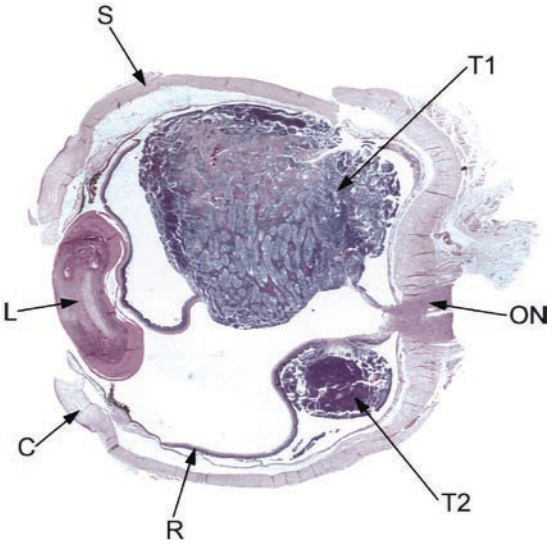

FIGURE 22.4. Macroscopic section of enucleated globe. 2 tumors (T1,T2) with partial retinal detachment (mixed growth pattern). C: cornea; L: Lens; S: Sclera; R: Retina; ON: Optic Nerve (courtesy of S. Uffer, MD)

lead to sedimentation of tumoral cells in the anterior chamber (pseudohypopyon). At this stage, the clinical appearance mimics that of severe inflammation. Retinoblastoma may present with a single or multiple tumors. It can be unilateral or bilateral, even trilateral. *Trilateral retinoblastoma* is the association of uni- or bilateral heritable retinoblastoma with an intracranial neuroblastic tumor (pinealoblastoma). It represents a form of ectopic retinoblastoma, related to the predisposition to cancer due to mutation of the RB1 gene. The association of these tumors can be explained by the phylogenic relationship between the retina and the pineal gland. The average interval between the diagnosis of retinoblastoma and that of a brain tumor is 21 months (Kivela 1999), with 90% of intracranial tumors arising within 4 years. Although more commonly associated with the pineal gland, supra- and parasellar tumors may also occur. These are primary, independent tumors and not metastases. Trilateral retinoblastoma represents the most frequent cause of mortality (50% of deaths) within 5 years of diagnosis of retinoblastoma (Kivela 1999). Histologically, these tumors may be considered primitive neuroectodermal tumors (PNET).

Mortality in trilateral retinoblastoma is very high, but survival of over 5 years has been reported (Kivela 1999). Death is usually caused by presumed metastatic dissemination along the neuroaxis and spinal cord. Cysts, forms of spontaneous regression of pinealoblastoma, may mistakenly be interpreted as cured lesions following treatment (Beck Popovic et al. 2006). The risk of developing trilateral retinoblastoma is <0.5% in unilateral retinoblastoma, 5–15% in familial retinoblastoma (Kivela 1999).

A distinctive feature of retinoblastoma is its ability, in a limited number of cases, to show spontaneous regression. The term retinoma or retinocytoma has been used in these cases, alternatively spontaneously regressed, arrested or benign retinoblastoma (Gallie et al. 1982). Retinoma, by definition a nontreated and nonprogressive lesion, presents all the clinical and histopathologic features of a successfully treated retinoblastoma: homogenous greyish more-or-less translucent or white, opaque calcified mass, with pigment migration and proliferation at the base or periphery of the lesions.

The incidence of retinoma is not exactly known, figures given in the literature vary between 2% and 10% (Singh et al. 2007). Diagnosis and follow-up of retinoma requires the same specialized care as retinoblastoma, due to the risk of malignant transformation, familial recurrence in cases of germline RB1 mutation and of developing other, nonocular tumors.

Clinical Investigation (Balmer and Munier 2002)

It is generally the role of the primary physician to determine whether suspicious first signs are indicative of retinoblastoma (Table 22.1). After taking a preliminary family history, visual function is assessed (in a young infant, a simple comparison of reaction to occlusion of each eye will generally reveal any gross unilateral visual loss) and the fundus examined with the pupils dilated. If a retinal lesion is confirmed, or if there is any doubt, the child will immediately be transferred to a specialized center for further investigation. This will include a detailed family history, physical examination (observation of any dysmorphic features, skin abnormalities, leukocoria and/or strabismus, and any external ocular or orbital abnormality), and thorough ophthalmologic examination under general anesthesia.

The ophthalmologic examination will begin with biomicroscopic evaluation of the transparency of the media (corneal or lens opacity), corneal diameter (microphthalmia or buphthalmia), ocular tension (glaucoma), rubeosis, uveitis, hypopyon, or pseudohypopyon. With clear media, tumoral cells, retinal detachment, or the summit of a large tumor may already be visible. A detailed examination of the whole retinal surface will then be carried out by indirect binocular ophthalmoscopy. Scleral indentation is required to observe the extreme periphery, including the ora serrata.

Table 22.1. Clinical investigation of a child with suspected retinoblastoma

Family history
Known retinoblastoma, ocular diseases, blindness, enucleation
Other cancers in the family
Family tree
Pregnancy, birth history, birth weight, prematurity, oxygen therapy
Age at first suspicious sign and type of sign/signs
Trauma, contact with animals
Ophthalmologic examination (completed under general anesthesia)
Physical examination: dysmorphism, skin abnormalities, leukocoria, strabismus, external ocular/orbital signs
Biomicroscopic examination: media transparency; corneal/lens opacity; rubeosis; uveitis; hypopyon; pseudohypopyon; corneal diameter; ocular tension.
Indirect ophthalmoscopy with scleral indentation: laterality; location; size; growth pattern; calcifications; vitreous, retinal and/or subretinal seeding; vascular anomalies, hemorrhage; exudates; retinal detachment (location and degree); fundus drawing and photographs
Ultrasonography
Oncopediatric examination
Dysmorphic features; skin abnormalities; neurological condition (deafness, mental retardation etc.)
Serology (differential diagnosis of ocular toxocariasis/toxoplasmosis)
Lumbar puncture and PBM (as necessary)
Radiologic examination
CT scan (calcifications, extension, intracranial tumors, astrocytoma)
MRI (extension, intracranial tumors)
Bone scintigraphy (as necessary)
Genetic analysis
High-resolution karyotyping
Molecular biology:
Haplotype analysis
Mutation screening
Family examination
Ophthalmologic examination (retinal lesions/retinoma) and genetic analysis

A detailed drawing will be made, accompanied by wide-angle retinal photographs, to report the following: laterality of the lesions; tumor dimension, size, location and growth pattern; involvement of structures such as the optic nerve, macula or ora serrata; retinal detachment (location and degree), hemorrhage or exudates; presence of calcifications; vitreous, retinal and/or subretinal seeding; inflammatory signs.

Diagnosis of retinoblastoma can be made on simple fundus ophthalmoscopy in >90% of cases. Ultrasonography is mandatory to enable indepth visualization of calcifications. If retinoblastoma is confirmed, oncopediatric and neurodiagnostic investigations will follow, including computed tomography (CT-Scan) and/or magnetic resonance imaging (MRI) to detect calcifications that might have been missed on ultrasonography, any neuroectodermal tumor (trilateral retinoblastoma), and for the diagnosis of postlaminar invasion with a normal-size optic nerve (Brisse et al. 2007). Immediate family members will be examined to detect possible retinoma in the adult members and ensure that any other children in the family are healthy. Complete genetic analysis will also be carried out, including high-resolution karyotyping, haplotype analysis with markers in the vicinity of RB1 and molecular biology (tumor or blood DNA extraction) to detect germinal mutation.

Tumor Growth

Retinoblastoma consists of very friable tissue with loosely cohesive cell clusters, these poor in stroma, developing within an enclosed space and buffered by the gelatinous vitreous body, thus providing both culture medium and path of least resistance to tumor proliferation. It is a highly malignant tumor, capable of proliferation and dissemination in any direction. Its growth potential is very high in an organ of limited capacity for vascular adaptation, hence the formation of colonies of tumor cells along the neovascular axes and massive zones of necrosis, consequence of precarious conditions of nutrition.

The initial cell divisions produce clusters of intraretinal cells that are invisible on fundus ophthalmoscopy until the tumor reaches a certain mass. As it increases in volume the whitish-grey, round or oval-shaped tumor will become clearly visible against the reddish-orange background of healthy retina. Neovascularization and calcification will appear. The tumor or tumors continue to grow until surface breakage disperses cells into the vitreous or subretinal space. This seeding creates new colonies of tumor cells that may implant anywhere on or beneath the retinal surface, forming distant tumor foci. Implantations may colonize the pars plana, ciliary body, iris, trabeculum, and the anterior chamber. At this stage of disease there may be associated inflammatory signs of the anterior uveal tract or even orbital cellulitis. The tumor may infiltrate the optic nerve and, after reaching the subarachnoid space, invade the brain via the cerebrospinal fluid. Another route of invasion outside the eye is via the choroid, sclera, and finally the orbit.

Extraocular Retinoblastoma

The term extraocular retinoblastoma covers orbital disease, regional preauricular, and cervical lymph node extension and metastatic disease (Dunkel and Chantada 2007). The most common sites of metastatic retinoblastoma include the skull, long bones, viscera (liver, kidney, pancreas), bone marrow, and the central nervous system

in the form of meningeal involvement, subarachnoidal or, less frequently, intraparenchymal. Extraocular retinoblastoma has become a rare occurrence in countries with a favorable socio-economic situation. In disadvantaged countries, however, it is often through the extension of disease that the retinoblastoma is identified, which explains the higher mortality rate in these regions of the world.

Histopathologic Risk Factors

Retinoblastoma may disseminate in three directions: *Anteriorly*, via the vitreous or subretinal space to the ciliary body and anterior chamber, where typically a pseudohypopyon is formed; *Posteriorly*, towards the optic nerve and then cerebrospinal fluid, gateway to endocranial dissemination; *Exteriorly*, towards the orbit via the choroid and sclera.

Metastatic hematogenous (choroid, ciliary body, orbit) or lymphatic (conjunctiva, eyelids) dissemination may also occur. Retinoblastoma can invade the orbit directly by traversing the sclera, or via the perforating canals for the ciliary nerves and arteries. The two major risk factors for metastatic disease are invasion of the optic nerve or orbit. The risk of metastasis due to optic nerve invasion depends on the degree of infiltration. The mortality rate due to metastatic disease is between 50% and 80% if tumor cells are present at the site of surgical section; between 13% and 69% if the invasion is posterior to the lamina cribrosa, and insignificant if anterior (Uusitalo et al. 2001). Invasion of the choroid is considered a risk factor only if the infiltration is massive. Combined simultaneous invasion of the choroid and optic nerve carries the highest risk factor.

According to Chantada et al. (2007), patients having undergone bilateral enucleation, and those with scleral invasion, are at higher risk of extraocular relapse. Orbital extension of retinoblastoma can lead to systemic dissemination via hematogenous or lymphatic pathways, by anterior invasion and along the visual pathway towards the brain. Orbital extension is considered an important risk factor, but modern aggressive management protocols have considerably improved the survival rate. Invasion of the anterior chamber does not significantly increase the mortality rate, in spite of the risk of hematogenous dissemination (Uusitalo et al. 2001). Tumor growth pattern (endo/exophytic), the degree of differentiation, mitotic index, and the presence of necrosis or calcifications do not appear to represent significant risk factors. However, the relative vascular area or angiogenic capacity of the tumor could be a good predictor of disease dissemination (Marback et al. 2003).

Second or Multiple Nonocular Tumors

Retinoblastoma is frequently associated with second (Abramson 1999), even multiple primary nonocular malignancies. All cells of the organism in inherited retinoblastoma carry the RB1 mutation and consequently a predisposition to developing a second cancer, even a third, fourth, or fifth nonocular tumor (Abramson et al. 2001). There is, however, a predilection for certain tissues. Nonocular tumors are the primary cause of mortality in these patients, before the retinoblastoma itself. According to Abramson (1999), the cumulative incidence of the tumors is around 1% per year, thus 50% after 50 years.

Radiotherapy greatly increases the risk, particularly if administered before the age of 1 year (Abramson 1999). The most common sites of second nonocular tumors are, in order of frequency: soft head tissue (24%), skull (18%), skin (15%), bones (11%,), brain (8%) other locations (25%) (Abramson et al. 2001).

Classification

Many staging systems have been proposed since the Reese–Ellsworth Classification of 1963. The latter may be outmoded, but it continues to be widely used in the literature. It is based on globe salvage prediction after external beam radiation, without taking survival into account. The new International Intraocular Retinoblastoma Classification (Murphree and Chantada 2007) (Table 22.2) is currently the system most widely used, based on the natural history of the disease as well as the probability of salvaging the eye(s) with primary chemotherapy and focal consolidation. The staging consists of 5 groups (A, B, C, D, E) (Fig. 22.3) in descending order of favorable prognosis, taking into account the size of the tumor, proximity to the macula and the optic nerve, the degree of seeding, importance of retinal detachment, and late complications.

Differential Diagnosis

There are many conditions that mimic retinoblastoma. Collectively known as "pseudoretinoblastomas", they may also present with leukocoria as a first sign. The two most frequent are Coats' disease and persistent hyperplastic primary vitreous (PHPV), followed by ocular toxocariasis, retinopathy of

Table 22.2. Grouping system for eyes in international retinoblastoma classification

Group A – very low risk	Tumors 3 mm or smaller
Small round tumor(s) located away from the fovea and disc	=/>3 mm from the fovea
	=/>1.5 mm from the optic disc
	No vitreous seeding
Group B – low risk	Tumors not in Group A
All eyes **without** tumor dissemination not in Group A	Any size, shape or location
Tumor dissemination is defined to include vitreous seeding and the presence of subretinal fluid, even if subretinal seeding is not clinically apparent	Current or RPE evidence of previous detachment of 1 quadrant or less
	No vitreous or subretinal seeding
Group C – moderate risk	Vitreous or subretinal seeding no more than 3 mm from tumor
Eyes with only **local** tumor dissemination	
Group D – high risk	Vitreous seeding large, diffuse and/or greasy
Eyes with **diffuse** tumor dissemination	Avascular masses of tumor may be present in the vitreous
endophytic or exophytic disease.	Subretinal dissemination may consist of fine seeds,large avascular plaques on the underneath of the detached retina, or extensive subretinal masses (exophytic disease)
Group E – very high risk eyes	Neovascular glaucoma
Unsalvageable eyes	Massive intraocular hemorrhage
	Blood-stained cornea
	Massive tumor necrosis associated with aseptic orbital cellulitis
	Phthisis or prephthisis
	Tumor anterior to anterior vitreous face
	Anterior segment tumor
	Tumor touching the lens
	Diffuse infiltrating retinoblastoma

prematurity, intraocular inflammatory diseases, astrocytic hamartoma (Bourneville's tuberous sclerosis), von Recklinghausen's disease, and organized vitreous hemorrhage. More rarely, medulloepithelioma or optic nerve glioma may be considered. Many other signs, such as strabismus, red eye or hypopyon may be features common to both retinoblastoma and other diseases. Long-term complications of these diseases may also mimic retinoblastoma. Late stage atypical signs, often inflammatory, frequently present major difficulties in diagnosis.

Coats' disease is characterized by telangiectasia and massive exudates. It is a congenital vascular malformation, usually unilateral, most often affecting young males in the first decade of life. The three major characteristics are: telangiectasia in the form of strings of fusiform dilatations of the retinal vessels; massive yellowish exudates sometimes giving a pseudo-tumoral appearance, and exudative retinal detachment, this sometimes total. The exudates are responsible for a luminous leukocoria, although this will take on a greyer hue in the presence of retinal detachment.

Persistent hyperplastic primary vitreous (*PHPV)* is fairly characteristic in the absence of late complications. It is a congenital malformation caused by the arrest of normal regression of the embryonic vascular tissue (hyaloid artery, vasa hyaloidea propria, tunica vasculosa lentis), regression that normally occurs after 4 months' gestation. Almost always unilateral, PHPV is often associated with microphthalmia and, in later stages, retrolental fibroplasia and characteristic traction of the ciliary processes.

Astrocytic hamartoma (Bourneville's tuberous sclerosis) is easily recognised in its typical form of elevated mulberry-shaped masses or "fish eggs", with the classical triad of mental retardation, epilepsy, and facial angiofibroma. *Von Recklinhausen's neurofibromatosis* and *Sturge-Weber's encephalotrigeminal syndrome* are easily identified by their general clinical context, as is *retinopathy of prematurity*. *Combined hamartoma* of the retina and pigment epithelium presents typical retinal and angiographic features and shows little or no progression. Finally, certain congenital ocular malformations may present with leukocoria. These include: *choroidal* or *optic nerve coloboma; falciform retinal fold; myelinated nerve fibers; "Morning Glory Syndrome"*; *ocular toxocariasis*, and *toxoplasmosis.*

TREATMENT

The primary aim of treatment of retinoblastoma is survival, then eye preservation and the best possible visual function. Every case of retinoblastoma represents a new challenge, the treatment plan tailored to the individual child and constantly reevaluated according to the response at each stage. Many factors have to be taken into consideration: stage of disease; number of tumors; tumor location, size and any seeding; threat of metastases; risk of second nonocular malignancy; visual potential; uni- or bilateral, heritable or nonheritable disease; age, general health and socioeconomic circumstances. Management thus requires a multi-disciplinary service, including ophthalmologist, anesthetist, onco-pediatrician, geneticist, radiologist, neuro-radiologist, pathologist, and ocularist. Also essential are the back-up pediatric nurses, social worker, psychologist and hospital chaplain, in addition to a well-equipped, sophisticated infrastructure. A highly malignant tumor

with rapid growth potential, the treatment plan for retinoblastoma must be decided upon with the least delay and with the full, knowledgeable consent of the parents.

Treatment Methods

At the beginning of the twentieth century, the vital prognosis for a child suffering from retinoblastoma was dismal. By the 1930s the survival rate had improved to ~30%, reaching 80% in the sixties. In reference centers today, ~95% of these children can be saved, an evolution made possible by the advent of new treatment strategies: enucleation, radiotherapy, focal treatments, and chemotherapy. Current treatment methods, singly or combined, include: enucleation; systemic chemotherapy; chemothermotherapy; thermotherapy; local chemotherapy; cryotherapy; photocoagulation; brachytherapy, and external radiotherapy.

Chemotherapy

The 1990s represented a turning point in treatment approach. The severe side effects and relative limitations of radiotherapy (radio-induced tumorigenesis) lead to a shift towards chemotherapy as first line treatment of retinoblastoma, particularly with the advent of new drugs. Neoadjuvant chemotherapy (or chemoreduction) provides significant tumor shrinkage and dries out any retinal detachment to allow subsequent, less aggressive focal treatments such as chemothermotherapy, cryocoagulation, photocoagulation, and brachytherapy (Fig. 22.5a–d). Although there have been reports of successful treatment with only chemotherapy in a few selected cases (Gombos et al. 2002), consolidation treatment is almost always necessary as permanent tumor control is rarely achieved with chemotherapy alone. New tumors may also continue to arise after primary systemic chemotherapy in patients with hereditary retinoblastoma (Wilson et al. 2007). The new strategy of first-line chemoreduction has resulted in fewer primary enucleations while avoiding the complications of external beam radiotherapy, in particular radio-induced second nonocular tumors, the risk being greater during the first year of life. Systemic chemotherapy is not, however, without non-negligible side effects such as renal and oto-toxicity, myelosuppression, leukemia (Gombos et al. 2007), and potentially dangerous long-term complications as yet unknown.

Therapeutic guidelines vary according to the reference center. Drug regimens usually include carboplatin, etopside or teniposide and vincristine, more rarely cyclophosphamide, epipodophyllotoxine, ifosfamide, doxorubicine or melphalan. Cyclosporine A is added to the protocol in some centers to reduce chemotherapy resistance. Drug combinations, dosage, number of cycles and duration vary according to the center but the protocol most widely used is that of carboplatin, etopside and vincristine administered over 6 cycles at low-dosage or 3 cycles at high-dosage, every 21 to 28 days. Other centers use only carboplatin and etopside, adapting the number of cycles to tumor response. Consolidation focal treatment is often possible after 2 or 3 cycles of chemoreduction, allowing a significant reduction in the drug dosage (Beck et al. 2000).

Chemotherapy is currently prescribed as first-line treatment in most cases of intraocular retinoblastoma, with the exclusion of small tumors away from the optic nerve and macula and directly accessible for primary focal treatment. It is also indicated in the

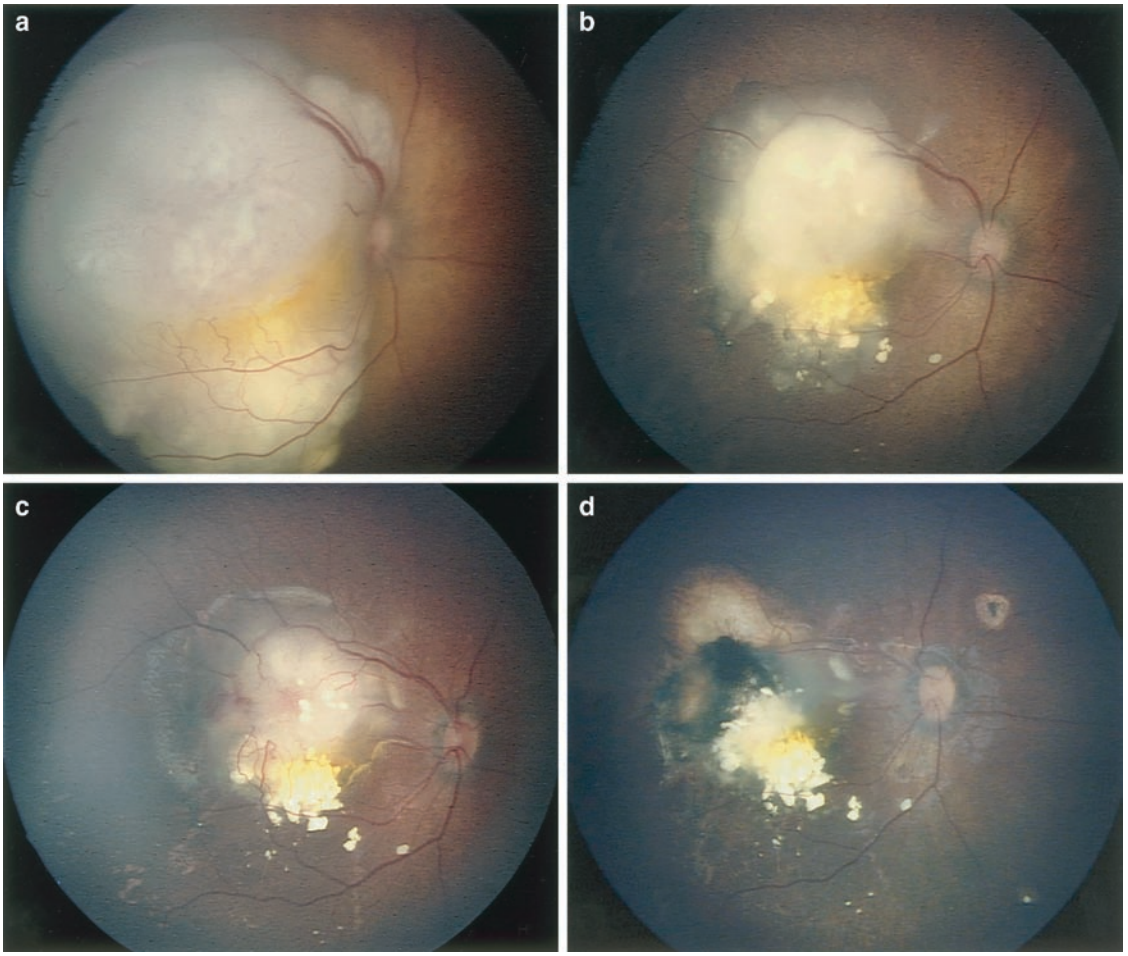

FIGURE 22.5. Voluminous retinoblastoma occupying the temporal posterior pole, treated with chemoreduction and chemothermotherapy: (**a**) Large endophytic lesion in contact with the optic nerve prior to treatment. (**b**) After 3 cycles of chemoreduction. The tumor has shrunk, calcified and withdrawn from the optic nerve. (**c**) During course of chemothermotherapy. d. Final result: the tumor is destroyed, reduced to a fibrous calcified "cottage cheese" mass and atrophied, pigmented chorioretinal scar

prevention of metastases after enucleation in the presence of histopathologic risk factors, in extraocular retinoblastoma (invasion of the optic nerve or orbit), with metastases and in trilateral retinoblastoma.

Focal Consolidation Treatment

Cryocoagulation and *photocoagulation* (532 nm argon laser, 810 nm diode laser, xenon) are simple and effective means for permanent control of small tumors, either as primary treatment or in consolidation after chemotherapy. Indications also include new tumors and local relapses.

Chemothermotherapy

Heat increases the permeability of the plasma membrane to antimitotics, thus enhancing the cytotoxic effect of these drugs. Carboplatin is administered intravenously 1–2 h prior to thermotherapy. The infrared

beam from a 810 nm diode laser, mounted on the operating microscope, is focused on the tumor via a contact lens for 5 to 30 min, depending on the size of the tumor, in order to obtain a temperature of 42° to 45° (Murphree 2007b). A follow-up session of thermotherapy is carried out after 4 to 7 days. Two or three further cycles are given as necessary, at 28-day intervals, until the tumor is destroyed (Fig. 22.5c, d).

Thermotherapy

Thermotherapy consists of increasing the temperature of the tumor to >45° (60–65°) by means of a diode laser in order to exploit the cytotoxic effects of heat (Murphree 2007b). Thermotherapy can be used alone or in conjunction with chemotherapy or even radiotherapy. Small tumors <3 mm diameter and 2 mm thick generally respond well to thermotherapy alone.

Brachytherapy

Radioactive plaques (iodine-125, ruthenium-106) (Shields et al. 2001) offer an ideal alternative in the treatment of medium-sized tumors or as second-line treatment in cases of failure or relapse. The original cobalt-60 plaque has been largely abandoned because its high-energy gamma rays cannot be shielded and irradiate in all directions. Iodine-125 is the preferred isotope today in the US (in Europe, at least in Germany and Switzerland, ruthenium is also used for retinoblastoma), its low-energy gamma rays allowing effective shielding and unidirectional irradiation. Tumors up to 15 mm diameter and 9 mm thick can be treated by this method. Ruthenium applicators can also be used (Schueler et al. 2006). These emit high-energy beta rays but poor tissue penetration limits their use to tumors up to 6 mm thick.

External Beam Radiotherapy (EBR)

When none of the focal therapies can be applied, external beam radiotherapy may be necessary. Conventional external beam radiotherapy has gradually been replaced, when available, with targeted radiotherapy adapted to the size of the tumor. This is now possible with new technology, using a multileaf photon 6 MV photon linear accelerator to produce fractionated stereotactic radiotherapy (Munier et al. 2008). The radiation dose delivered is 45–50.4 Gy in 1.8 Gy fractions, representing 25 to 28 sessions.

Tumors of only eyes in Groups B and C, with residual active tumor cells in the foveal or peri/epi-papillary region after chemoreduction, may be considered candidates for second-line stereotactic conformal radiotherapy with target volume circumscribed to the posterior pole. Group D eyes (only eyes or bilateral Group D) may require whole eye irradiation. Present indications and contraindications to modern EBR are discussed in detail by Munier et al. (2008).

Proton Therapy

Accelerated proton beam irradiation may represent the radiotherapy of the future. The finite range of dose in depth, the sharp lateral penumbra, and the ability to deliver a homogeneous dose to a target with a single field, make proton therapy the external beam radiotherapy of choice for retinoblastoma. The equipment necessary to deliver proton therapy is, however, beyond the scope of traditional medical institutions and so far remains exclusive to those having access to a cyclotron at a physics research institute.

Accelerated protons gradually lose their energy as they penetrate tissue, depositing

most of it at what is known as the Bragg peak. Modulation of the proton beam accelerator produces a succession of Bragg peaks calculated to create a uniform plateau within the tumor, normal tissues beyond the target receiving little or no radiation. Prior to proton delivery, four tantalum rings are sutured to the sclera as markers, enabling radiologic identification of the tumor site. The radiotherapy equipment comprises a beam modulator and collimator, a stereotactic couch and a custom-molded thermo-plast mask system to immobilize the patient's head.

Enucleation

Enucleation is less frequently necessary with modern therapeutic techniques, but it remains the treatment of choice for advanced disease, particularly in unilateral cases. *Primary enucleation* is indicated, or should be considered, in the following situations: neovascular glaucoma; massive intraocular hemorrhage; massive tumors taking up most of the vitreous cavity (Fig. 22.4); massive vitreous and/or subretinal seeding; rubeosis iridis; diffuse infiltrating retinoblastoma; clinical indications of high risk of extraocular dissemination (optic nerve invasion, involvement of the anterior chamber, exteriorization), phthisis or prephthisis. All these criteria are found in the Group E staging of the International Classification.

Secondary enucleation may be necessary when all other treatment modalities have failed to achieve tumor control, particularly if there is suspicion of invasion of the optic nerve, sclera or anterior segment. For the enucleation procedure, precise and controlled surgery is essential in order to prevent trauma or compression and, in particular, any perforation of the globe. The optic nerve should be sectioned as far back as possible, at least 10 mm, and the stump sent immediately for histopathologic examination in order to determine the degree of any tumoral invasion. The socket volume is reconstituted with an implant, commonly composed of biocolonizable material. New-generation hydroxyapatite or porous polyethylene (Medpor) implants are particularly recommended as they offer greater mobility to the external prosthesis later provided.

In the case of orbital retinoblastoma, exenteration is no longer carried out as it has little effect on the course of the disease. Local surgical excision combined with systemic chemotherapy and orbital radiotherapy is preferred. In extraocular retinoblastoma, combined therapy of surgery and high-dosage chemotherapy, autologous stem-cell rescue and craniospinal or focal radiotherapy may be beneficial for longer survival periods or even complete remission (Dunkel and Chantada 2007).

Future Advances

Proton therapy may become more common in the near future with the advent of, and more easily available, new-generation Gantry apparatus that enables irradiation of the whole eye or very small tumors in young patients, under general anesthesia (Munier et al. 2008).

In order to avoid the side effects of systemic chemotherapy and render the treatment more effective, targeted, locally administered chemotherapy by subconjunctival injection or by selective ophthalmic artery delivery is used in some cases (Schefler et al. 2006). Various trans-scleral delivery systems have also been developed, such as small refillable silicone reservoirs attached to the episclera to diffuse agents to the vitreous (Murphree 2007a).

New chemotherapeutic agents with higher activity and better toxicity profiles such as Topotecan, or other drugs with different mechanisms of action like small-molecule inhibitors of the MDMX-p53 interaction (Nutlin 3A) (Elison et al. 2006), glycolytic inhibitors adjuvant to chemotherapy on hypoxic cells (Boutrib et al. 2007) or anti-angiogenic proteins (Apte and Harbour 2007), are under intense research.

Molecular genetics may fundamentally change therapeutic approaches in the management of retinoblastoma: suicide gene therapy with local delivery of the herpes simplex thyrosine kinase gene followed by treatment with the prodrug ganciclovir (Hurwitz et al. 1999); gene replacement by viral vector of the retinoblastoma gene in the mutated tumoral cell by a normal RB1 gene; use of metastasis suppressor genes to block the growth of tumor cells at a distant site from the primary tumor.

Preimplantation genetic diagnosis has recently become available for couples at risk for having children with heritable disease. It is possible today, following an accurate mutation analysis procedure for retinoblastoma gene mutation sensitive at the single-cell level and using a standard in vitro fertilization procedure, to transfer only mutation-free embryos back to the mother in order to have a healthy child (Rechitsky et al. 2002).

Photodynamic therapy, based on the use of photosensitizers activated with visible nonionizing laser light and specific to malignant cells, has given some promising results with negligible toxic side effects (Laville et al. 2006).

If preliminary data supporting a role for maternal diet deficiency, and papillomavirus infections in the etiology of the nonheritable form of retinoblastoma are confirmed, then elimination of the former and a vaccine for the latter should have a dramatic impact on the disproportionate high incidence of environmental retinoblastoma (Murphree 2007a).

Ultimately, aside potential preventive measures, the best management remains that of early diagnosis. Delay in diagnosis, this sometimes months after the first manifestations of disease, continues to constitute a major factor in the prognosis for survival, globe preservation and function.

PROGNOSIS

With uni- or bilateral retinoblastoma, the survival rate in developed countries is up to 90% at 5 years, which is excellent for a malignant tumor. Rare at the time of diagnosis, metastases usually occur within the first 12 months, and 5 years with no metastases and no relapse is considered a cure. After 5 years, however, mortality increases with the risk of second non-ocular malignancies. Hereditary retinoblastoma confers an increased risk for the development of second primary tumors and for survival, especially in patients treated with radiotherapy before the age of 1 year (Abramson 1999). It would seem that early irradiation is not the cause but probably a marker for other risk factors of second primary tumors (Moll et al. 2001).

The visual prognosis depends essentially on the laterality, location, and size of the tumor(s), on the various therapeutic modalities used and their side effects. In a series of 116 bilateral cases (Migdal 1983), 21.5% were blind after bilateral enucleation, while 50% retained a visual acuity of 20/40 or better. In a study on vision after external radiation therapy in

74 cases of bilateral retinoblastoma, 58% had a visual acuity of 20/20 to 20/40, 31% had a visual acuity of 20/50 to 20/400 while 9% had <20/400 (Hall et al. 1999). In a more recent series, Berman et al. (2007) reported that newer globe-preserving treatments for retinoblastoma seem to be associated with equivalent visual outcomes, stable mortality rate and a greater number of short-term complications while avoiding the late side-effects associated with external beam radiotherapy. Overall, 43% of preserved eyes attained a visual acuity better than or equal to 20/40 and 55% achieved over 20/200.

It is evident that macular involvement represents the worst prognosis for vision (<20/200) in both unilateral and bilateral retinoblastoma. However, the prognosis is excellent (~20/20) in patients where the posterior pole is not involved, whether unilateral or bilateral. Macular involvement in an only eye allows better vision, although unpredictable, than that expected given the extent of the lesion. Visual performance in these children in activities requiring good central vision is often close to that of normal children.

The quality of life for adult survivors having undergone treatment for hereditary or non-hereditary retinoblastoma was recently compared with that of a healthy reference group in an exploratory study (van Dijk et al. 2007). It would appear that the group of adult RB survivors experience a relatively good overall, although slightly poorer, quality of life compared with the reference group. Greater problems are reported with regard to mental health (anxiety, depression, loss of control). Hereditary RB survivors differ significantly from non-hereditary RB survivors in 'general health' only. Bullying in childhood and subjective experience of impairment are the main predictors of a worse quality of life.

In conclusion, the best treatment is, and will always be, early treatment. Early treatment requires early diagnosis, which means that leukocoria, strabismus, or any unexplained sign in a young child must be considered a possible first manifestation of retinoblastoma. It must also be remembered that retinoblastoma can be hereditary and all other members of the family should be examined and referred for genetic testing and counselling. Pregnancies within a family at risk (positive family history) must be carefully monitored with antenatal ultrasonography, genetic analysis and, if in doubt, a 3 to 4-week preterm delivery.

Finally, the family, gynecologist, pediatrician or family doctor will notice the first signs of disease before any multi-disciplinary specialized team is involved. Public awareness as well as that of all medical practitioners, is thus essential in the management of this life-threatening disease.

REFERENCES

Abramson DH (1999) Second nonocular cancers in retinoblastoma: a unified hypothesis. The Franceschetti lecture. Ophthalmic Genet 3:193–204

Abramson DH, Melson MR, Dunkel IJ, Frank CM (2001) Third (fourth and fifth) nonocular tumors in survivors of retinoblastoma. Ophthalmology 10:1868–1876

Apte RS, Harbour JW (2007) Inhibiting angiogenesis in retinoblastoma. Ophthalmic Res 4: 188–190

Balmer A, Munier F (2002) In: Zografos L (ed) Tumeurs intraoculaires, Rétinoblastome: Diagnostic, Paris, pp 485–533

Beck Popovic M, Balmer A, Maeder P, Braganca T, Munier FL (2006) Benign pineal cysts in children with bilateral retinoblastoma: a new variant of trilateral retinoblastoma? Pediatr Blood Cancer 7:755–761

Beck MN, Balmer A, Dessing C, Pica A, Munier F (2000) First-line chemotherapy with local treatment can prevent external-beam irradiation and enucleation in low-stage intraocular retinoblastoma. J Clin Oncol 15:2881–2887

Berman EL, Donaldson CE, Giblin M, Martin FJ (2007) Outcomes in retinoblastoma, 1974–2005: the Children's Hospital Westmead. Clin Exp Ophthalmol 1:5–12

Boutrib H, Cebulla CM, Murray TG, Pina Y, Jockovich ME (2007) Regional hypoxia in LHBetaTAG murine retinoblastoma: implications for novel treatments. International Society of Ocular Oncology Meeting 2007, June 27–30. Siena T Hadjistilianou (ed) p 400

Brisse HJ, Guesmi M, Aerts I, Sastre-Garau X, Savignoni A, Lumbroso-Le Rouic L, Desjardins L, Doz F, Asselain B, Bours D, Neuenschwander S (2007) Relevance of CT and MRI in retinoblastoma for the diagnosis of postlaminar invasion with normal-size optic nerve: a retrospective study of 150 patients with histological comparison. Pediatr Radiol 7:649–656

Bunin GR, Orjuela M (2007) In: Singh A (ed) Clinical ophthalmic oncology, Geographic and environmental factors, pp 410–416

Chantada GL, Dunkel IJ, Antoneli CB, de Davila MT, Arias V, Beaverson K, Fandino AC, Chojniak M, Abramson DH (2007) Risk factors for extraocular relapse following enucleation after failure of chemoreduction in retinoblastoma. Pediatr Blood Cancer 3:256–260

Dunkel IJ, Chantada G (2007) In: Singh A (ed) Clinical ophthalmic oncology, Metastatic retinoblastoma, pp 484–486

Elison J, Cobrinik D, Claros N, Abramson D, Lee T (2006) Small molecule inhibition of HDM2 leads to p53-mediated cell death in retinoblastoma cells. Arch Ophthalmol 9:1269–1275

Gallie BL, Phillips RA, Ellsworth RM, Abramson DH (1982) Significance of retinoma and phthisis bulbi for retinoblastoma. Ophthalmology 12:1393–1399

Gombos DS, Kelly A, Coen PG, Kingston JE, Hungerford JL (2002) Retinoblastoma treated with primary chemotherapy alone: the significance of tumour size, location, and age. Br J Ophthalmol 1:80–83

Gombos DS, Hungerford J, Abramson DH, Kingston J, Chantada G, Dunkel IJ, Antoneli CB, Greenwald M, Haik BG, Leal CA, Medina-Sanson A, Schefler AC, Veerakul G, Wieland R, Bornfeld N, Wilson MW, Yu CB (2007) Secondary acute myelogenous leukemia in patients with retinoblastoma: is chemotherapy a factor? Ophthalmology 7:1378–1383

Hall LS, Ceisler E, Abramson DH (1999) Visual outcomes in children with bilateral retinoblastoma. J Aapos 3:138–142

Hurwitz MY, Marcus KT, Chevez-Barrios P, Louie K, Aguilar-Cordova E, Hurwitz RL (1999) Suicide gene therapy for treatment of retinoblastoma in a murine model. Hum Gene Ther 3:441–448

Kivela T (1999) Trilateral retinoblastoma: a meta-analysis of hereditary retinoblastoma associated with primary ectopic intracranial retinoblastoma. J Clin Oncol 6:1829–1837

Laville I, Pigaglio S, Blais JC, Doz F, Loock B, Maillard P, Grierson DS, Blais J (2006) Photodynamic efficiency of diethylene glycol-linked glycoconjugated porphyrins in human retinoblastoma cells. J Med Chem 8:2558–2567

Mahoney MC, Burnett WS, Majerovics A, Tanenbaum H (1990) The epidemiology of ophthalmic malignancies in New York State. Ophthalmology 9:1143–1147

Marback EF, Arias VE, Paranhos A Jr, Soares FA, Murphree AL, Erwenne CM (2003) Tumour angiogenesis as a prognostic factor for disease dissemination in retinoblastoma. Br J Ophthalmol 10:1224–1228

Migdal C (1983) Bilateral retinoblastoma: the prognosis for vision. Br J Ophthalmol 9:592–595

Moll AC, Imhof SM, Schouten-Van Meeteren AY, Kuik DJ, Hofman P, Boers M (2001) Second primary tumors in hereditary retinoblastoma: a register-based study, 1945–1997: is there an age effect on radiation-related risk? Ophthalmology 6:1109–1114

Moll AC, Imhof SM, Cruysberg JR, Schouten-van Meeteren AY, Boers M, van Leeuwen FE (2003) Incidence of retinoblastoma in children born after in vitro fertilisation. Lancet 9354:309–310

Munier FL, Verwey J, Pica A, Balmer A, Zografos L, Abouzeid H, Timmerman B, Goitein G, Moeckli R (2008) New developments in external beam radiotherapy for retinoblastoma: from lens to normal tissue sparing techniques. Clin Exp Ophthalmol 36(1):78–89

Murphree AL (2007a) In: Singh A (ed) Clinical ophthalmic oncology, Future directions, pp 501–504

Murphree AL (2007b) In: Singh A (ed) Clinical ophthalmic oncology, Local therapy, brachytherapy, and enucleation, pp 454–461

Murphree AL, Chantada G (2007) In: Singh A (ed) Clinical ophthalmic oncology, Staging and grouping of retinoblastoma, pp 422–427

Murphree AL, Singh AD (2007) In: Singh A (ed) Clinical ophthalmic oncology, Heritable retinoblastoma: the Rb1 cancer predisposition syndrome, pp 428–433

Rechitsky S, Verlinsky O, Chistokhina A, Sharapova T, Ozen S, Masciangelo C, Kuliev A, Verlinsky Y (2002) Preimplantation genetic diagnosis for cancer predisposition. Reprod Biomed Online 2:148–155

Schefler AC, Jockovich ME, Toledano S, Murray TG (2006) Historical and modern approaches to chemotherapy for retinoblastoma. Future drugs. Expert Rev Ophthalmol 1:83–95

Schueler AO, Fluhs D, Anastassiou G, Jurklies C, Neuhauser M, Schilling H, Bornfeld N, Sauerwein W (2006) Beta-ray brachytherapy with 106Ru plaques for retinoblastoma. Int J Radiat Oncol Biol Phys 4:1212–1221

Shah SH, Pervez S, Hassan SH (2000) Frequency of malignant solid tumors in children. JPMA J Pak Med Assoc 3:86–88

Shields CL, Shields JA, Cater J, Othmane I, Singh AD, Micaily B (2001) Plaque radiotherapy for retinoblastoma: Long-term tumor control and treatment complications in 208 tumors. Ophthalmology 11:2116–2121

Singh AD, Balmer A, Munier F (2007) In: Singh A (ed) Clinical ophthalmic oncology, Retinocytoma or retinoma, pp 487–490

Uusitalo MS, Van Quill KR, Scott IU, Matthay KK, Murray TG, O'Brien JM (2001) Evaluation of chemoprophylaxis in patients with unilateral retinoblastoma with high-risk features on histopathologic examination. Arch Ophthalmol 1:41–48

van Dijk J, Imhof SM, Moll AC, Ringens PJ, Cohen-Kettenis PT, Rijmen F, Huisman J (2007) Quality of life of adult retinoblastoma survivors in the Netherlands. Health Qual Life Outcomes 30

Wilson MW, Haik BG, Billups CA, Rodriguez-Galindo C (2007) Incidence of new tumor formation in patients with hereditary retinoblastoma treated with primary systemic chemotherapy: is there a preventive effect? Ophthalmology, Jul 10 [Epub ahead of print]

Part III
Thyroid Carcinoma

Diagnosis

23
Molecular Genetics of Thyroid Cancer

Deanne King, Donald Bodenner, and Brendan C. Stack Jr.

INTRODUCTION

Thyroid nodules are exceedingly common and the incidence increases steadily with age. In patients over the age of 50, feeling the neck will detect nodules in 8–10% of patients, and radiology tests such as ultrasound, magnetic resonance imaging (MRI), or computed tomography (CT) will detect nodules in over 50% of individuals over the age of 50. However, it is now clear that only 4–6% of thyroid nodules will be malignant (Belfiore et al. 1992). The incidence of thyroid cancer varies geographically, ranging from 0.5 to 10 cases per 100,000 people (American Cancer Society 2007).

The thyroid gland can be affected by a number of tumors with a variety of benign and malignant pathologies. The malignant varieties include papillary, follicular, medullary, and anaplastic thyroid carcinomas. Papillary and follicular thyroid carcinomas are often together referred to as well-differentiated thyroid cancer (WDTC). The follicular and papillary carcinomas are thought to arise from two distinct pathways. The genetics behind thyroid cancer is only beginning to be elucidated. A number of genes are thought to be involved. Molecular profiling has recently been employed to evaluate thyroid lesions. In carcinogenesis, genes associated with cancer can be classified into two categories. Oncogenes refer to the overexpression or activation of a protooncogene which otherwise has a normal cellular function. Tumor suppressor genes are typically genes involved in cell regulation or mitosis. Loss of function of the tumor suppressor results in loss of a normal gate keeping function which allows carcinogenesis to occur (Table 23.1). There is a genetic link associated with some thyroid cancers as evidenced by a familial pattern (Marchesi et al. 2000; Musholt et al. 2000). In addition, exposure to radiation, particularly as a child, leads to an increased risk of neoplastic changes (Tucker et al. 1991). These are usually papillary thyroid cancers (Samaan et al. 1987). Several mutations have been found in thyroid cancers which are thought to play a role in the carcinogenesis (Table 23.2).

PAPILLARY

Papillary thyroid carcinomas (PTC) are the most common thyroid lesions with 25,000 new cases a year in the US (Utiger 2005). Approximately 80% of WDTC is of the papillary type, with follicular

Table 23.1. Genes implicated in thyroid tumor formation

Genes		Name	Function/comments
Oncogenes	Membrane receptors	*RET*	Receptor with tyrosine kinase activity
		NTRK1	Receptor with tyrosine kinase activity
		MET	Receptor with tyrosine kinase activity
	Signal transduction proteins	*TSH-R*	Linked to heterotrimeric G proteins
	Heterotrimeric	*Gsα (gsp)*	GTP binding molecules
	G-proteins	*Giα (gip)*	GTP binding molecules
	Small G-proteins	*ras*	GTP binding molecules
Tumor suppressor genes	Cell cycle regulators	*TP53*	Arrests cell in G1, induces apoptosis
		WAF1/p21CIP1	Arrests cell in G1, dephosphorylates RB
		CDKN2/p16INK4α	Inhibits cyclin-dependent kinases
	Others	*APC*	Modulates β-catenin activity
		PTEN	Protein tyrosine phosphatase
		RB	Retinoblastoma tumor-suppressor protein.

Table 23.2. Summary of thyroid tumors and genes implicated in their pathogenesis

Gland/tumor type	Gene	Comment
Autonomous adenoma	*Gsα/gsp*	Mutations constitutively activate the cAMP cascade leading to increased hormone production and proliferation
	TSH-R	
Follicular adenoma	*Gsα*	Mutations are apparent early events in thyroid tumorigenesis
	ras	
	PTEN	Mutation or deletion in 26%
Follicular carcinoma	*ras*	Higher prevalence of mutations than in adenomas
	TP53	Implicated in the dedifferentiation process
	3p, 17p, 10q	Loss of heterozygosity (LOH) at these loci implicated in follicular tumor progression
	PTEN	Mutation or deletion in 6% of follicular cancers
Hürthle cell tumors		Phenotypically and genetically distinct from follicular tumors
Papillary thyroid cancer (PTC)	*RET/PTC*	Activated in a significant proportion of tumors with a relation to radiation exposure and possibly to clinical behavior
	TRK	Activated in some PTCs
	MET	Overexpressed
	ras	Involved early in tumor formation; more commonly in tumors with metastases
	TP53	Implicated in the dedifferentiation process
Anaplastic carcinoma	*TP53*	Overexpressed with or without mutations in some tumors
Medullary thyroid Carcinoma (MTC)	Sporadic *RET*	Codon 918 somatic mutation may have prognostic significance
	Familial *RET*	Mutations constitutively activate the receptor or alter substrate specificity and screening for germline mutations in MEN-II families important in management

cancer constituting the rest. Activation of a pathway involving RET-RAS-BRAF-MAPK is seen in the majority of papillary cancers (Duh 2005). A mutation in any one of these genes within the signaling cascade may be found in 70% of papillary cancers, but only one is necessary to lead to papillary cancer. Transgenic mice with activating mutation of either RET/PTC or BRAF lead to papillary thyroid cancer (Duh 2005). There appears to be an inherited predisposition to some PTC with 5% showing a family susceptibility (Malchoff and Malchoff 2002). In these cases, the ret proto-oncogene does not appear to be involved (Corvi et al. 2001).

RET Oncogene

The RET tyrosine kinase receptor gene (RET) is well known for its contribution to multiple endocrine neoplasia type 2 (MEN 2) (Figure 23.1). The RET oncogene has also been found to have rearrangements in up to 34% of papillary carcinomas (Fagin 2002). There are three major forms of rearrangements with many more minor variants (Puxeddu et al. 2003). The rearrangement may occur through inversion as in *ret*/PTC-1 and *ret*/PTC-3, which are paracentric inversions of chromosome 10 that fuse the tyrosine kinase domain of ret to H4 and *ele-1,* respectively. In the ret/PTC-2, the tyrosine kinase domain of *ret* is fused to the regulatory subunit RIa of cAMP-dependent protein kinase (Soravia et al. 1999). These rearrangements create a constitutively active tyrosine kinase which leads to uncontrolled growth and oncogenesis. These *ret*/PTC rearrangements are thought to be an early event in thyroid tumorigenesis and are often multifocal (Sugg et al. 1998). These RET arrangements are more common in the pediatric papillary carcinomas. Reports show 48–65% prevalence in the pediatric population (Puxeddu et al. 2003). There is an even higher incidence of 67% to 87% in tumors induced by radiation from the Chernobyl fallout (Puxeddu et al. 2003). Ionizing radiation has been shown to induce RET rearrangements in vitro and in vivo in mice. This genetic alteration is thought to be an early event in the development of papillary carcinoma as evidenced by its expression in occult microscopic foci of disease (Fagin 2002). Furthermore, overexpression of RET/PTC in transgenic mice results in tumors with a papillary phenotype. Hürthle cell cancers have been conventionally thought to be a variant of follicular carcinoma but recent studies have shown *RET/PTC1* rearrangements which may indicate a papillary origin (Chiappetta et al. 1990). The *RET* positive subset also tends to involve local lymph nodes as opposed to the distant follicular metastasis (Fagin 2002). Reverse transcriptase-polymerase chain reaction (RT-PCR) has been employed to detect

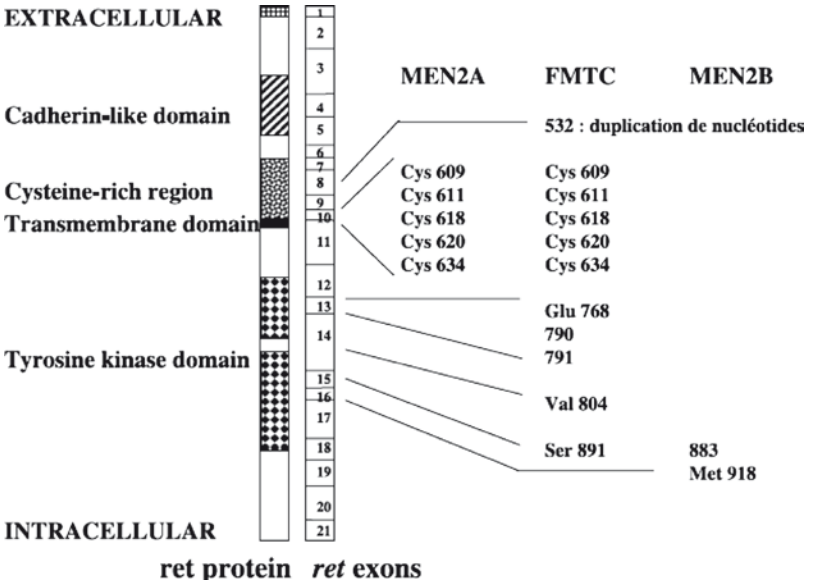

FIGURE 23.1. Map of Ret oncogene

RET rearrangements in 17 of 33 FNA samples that were deemed indeterminate or inadequate by routine cytologic analysis. There were no false-positives (Cheung et al. 2001). Studies to date, however, have not shown a clear prognostic value of the presence of RET/PTC (Puxeddu et al. 2003). The presence of a common mutation does, however, lead the way for a possible modality of both diagnosis and treatment with tyrosine kinase inhibitors (Learoyd et al. 2000).

RAS Oncogene

Ras proteins are a downstream component of the tyrosine kinase receptor/ras/mitogen-activated protein kinase pathway and consist of small GTP binding proteins that bind GDP in a resting state and GTP in an active state. There are three forms, H-ras, K-ras, and N-ras. Mutations in all three isoforms have been detected in a variety of thyroid lesions including cold nodules, toxic adenomas, PTC, FTC, and anaplastic carcinoma, and are thought to be an early step in thyroid carcinogenesis (Suarez et al. 1988). The most common mutations occur in codon 12 and 13 in the GTP binding domain and in codons 59 and 61 in the GTPase domain. These mutations constitutively activate the signal cascade leading to the stimulation of cell growth, loss of differentiation, and promotion of genetic instability. The presence of a *ras* mutation in PTC is a poor prognostic marker (Finley et al. 2004a, b, c).

BRAF

BRAF is mutated in a number of cancers including melanoma, colorectal, and ovarian cancers (Puxeddu et al. 2004). BRAF is a cytoplasmic serine-threonine protease that activates MAPK kinase when activated by *Ras* (Duh 2005). It exists in three isoforms (A-raf, B-raf, and C-raf). A transversion mutation in nucleotide 1796 mimics phosphorylation resulting in a constitutively active *B-raf* (Duh 2005). Recent studies have shown the defect is present in 29–69% of sporadic papillary thyroid cancers (Puxeddu et al. 2004), making it a more common mutation than either RET/PTC or RAS. Furthermore, its presence has been correlated with a poor prognostic outcome (Xing et al. 2004). The BRAF mutation is rarely associated with childhood cancers or radiation induced cancer (Duh 2005). The BRAF mutation is also associated with the aggressive tall cell papillary variant. BRAF is found only in papillary cancers and those anaplastic cancers derived from papillary cancers (Duh 2005).

APC

Familial adenomatous polyposis (FAP) is an autosomal dominant inherited trait that results in numerous colorectal adenomas. This polyposis is associated with mutations in the adenomatous polyposis coli (APC) tumor suppressor gene at the 5q21 locus. Gardner syndrome is a variant that is associated with upper gastrointestinal adenomas, congenital hypertrophic retinal pigment epithelial (CHRPE) lesions, desmoid tumors, osteomas, epidermoid cysts, dental abnormalities, and thyroid cancer affecting 1–2% of patients with FAP (Cetta et al. 2000). In 95% of cases, PTC is the histological type with a cribiform pattern, a variation rarely seen in non-APC associated PTC (Cetta et al. 2000). The majority of germline mutations occur in the first half of the *APC* gene. Cetta et al. (2000) analyzed PTC associated with FAP and found a majority of mutations in exon 15, most frequently at codons 1061 and 1309. However, mutations in APC are uncommon in sporadic thyroid tumors.

Although APC appears to play a role in thyroid carcinogenesis, it does not always require a loss of heterozygosity. Soravia et al. (1999) reported a high rate of *ret-PTC* activation in FAP-associated thyroid tumors. This implies a cooperative interplay of tumor suppressors and oncogenes in the development of PTC.

FOLLICULAR

Follicular lesions include conventional follicular carcinoma and Hürthle cell (oncocytic) carcinoma, as well as the benign follicular lesions and Hürthle cell adenoma. Follicular carcinomas account for 10% to 15% of all thyroid malignancies. Conventional follicular carcinoma constitutes 60–70% of follicular malignancies and typically metastizes hematogenously. Hürthle cell (oncocytic) carcinoma is less frequent and comprises approximately one quarter of these cases. It spreads hematogenously and through the lymphatics which make it unique. The only distinguishing features between benign and malignant follicular lesions are capsular or vascular invasion, only determined by postoperative pathologic examination or by detection of metastasis. Discovery of a marker present in carcinoma yet absent in benign adenomas would be extremely useful in differentiating these lesions prior to surgical excision. Studies by Nikiforova et al. (2003) have shown that there may be multiple distinct pathways in the development of follicular thyroid cancer, based on the genetic mutation detected.

RAS Oncogene

As with PTC, mutations of *ras* have been found in FTC (Horie et al. 1995). Furthermore, *ras* mutations have been found in benign follicular adenomas (Suarez et al. 1988) suggesting that *ras* mutations occur early in the pathogenesis of follicular cancers (Namba et al. 1990). *Ras* mutations may lead to the development of follicular adenoma progressing to carcinoma, but this transformation has yet to be demonstrated clinically (Nikiforova et al. 2003).

PAX8/PPARγ

The PAX8/PPARγ (paired box gene 8/peroxosome proliferators-activated receptor-gamma) rearrangement was originally found in follicular thyroid cancer. It may also be present in follicular adenomas (Duh 2005). PPARγ, a member of the nuclear hormone receptor super-family, is instrumental in the adipocyte differentiation. The PAX8-PPARγ1 product has a dominant-negative effect on wild-type PPARγ1, inhibiting its transcriptional activity (Lacroix et al. 2004). Mutations in the PAX8/PPARγ lead to follicular carcinomas that occur at a younger age and are more invasive (Nikiforova et al. 2003).

PTEN

PTEN is a protein tyrosine kinase phosphatase that is a tumor suppressor loci at 10q22–23 (Puxeddu et al. 2005). It can be detected in thyroid, brain, and prostate. Cowden's syndrome is an autosomal dominant condition associated with hamartomas, breast cancer, and thyroid cancer, and harbors germline mutation in PTEN. Thyroid carcinomas have been associated with decreased levels in PTEN (Puxeddu et al. 2005). Interestingly, PTEN mutations are more prevalent in benign follicular adenomas than follicular carcinomas (Learoyd et al. 2000).

Hürthle Cell Carcinomas

Hürthle cell carcinoma is a tumor of large acidophilic or oncocytic cells (Cooper and Schneyer 1990). These tumors represent 3% to 5% of all thyroid carcinomas and may have a slightly worse prognosis than with conventional follicular carcinomas (McDonald et al. 1996). As with a follicular lesion, the diagnosis of Hürthle cell carcinoma can only be made after surgical resection. There is some debate whether Hürthle cell carcinoma is of follicular or papillary origin. Hürthle cell tumors typically do not possess either RAS or PAX8/PPARγ mutations which are characteristic of FTC (Nikiforova et al. 2003). RET/PTC1 mutations have been found in Hurtle cell carcinomas and adenomas (Chiappetta et al. 1990). However, molecular profiling using gene array has grouped Hürthle cell carcinoma with follicular lesions, more commonly (88%) with FTCs as opposed to follicular adenomas. In all 13 cases reviewed, the Hürthle cell carcinoma clustered with follicular lesions as compared to PTC or the follicular variant PTC (Finley et al. 2004a).

MEDULLARY

Medullary thyroid carcinoma (MTC) is an uncommon form of thyroid neoplasia that accounts for 3% to 5% of all thyroid cancers. This carcinoma arises from the parafollicular C cells which are of neural crest origin and secrete calcitonin, and is sporadic in 75% of cases. In 25% of cases, MTC is inherited demonstrating an existing germline mutation in the *ret* proto-oncogene chromosome 10 (Mathew et al. 1987). Many cases of MTC are grouped in the multiple endocrine neoplasia syndromes, but may also occur as an inherited isolated disease without extra thyroidal manifestations in familial MTC (FMTC). MEN-I (Werner's syndrome) are associated with hyperparathyroidism, pancreatic tumors, and pituitary adenomas, but are the only MEN not associated with MTC. MEN-IIA (Sipple's syndrome) is the most common and is associated with MTC in 95% of cases, pheochromocytoma in 50% of cases, hyperparathyroidism in 15% cases, and occasionally Hirschprung's disease or cutaneous lichen amyloidosis. MEN-IIB (or MEN III) consists of MTC and pheochromocytomas with a Marfinoid habitus, submucosal neuromas, and intestinal ganglioneuromatosis without hyperparathyroidism. The MTC associated with MEN-IIB tend to be the most aggressive with earlier onset, often before the age of 5.

RET Oncogene

All of these syndromes are associated with mutations of the *ret* proto-oncogene. *Ret* is a tyrosine kinase receptor for neurotrophic growth factor. The RET tyrosine kinase receptor gene (RET/PTC) is well known for its contribution to multiple endocrine neoplasia type II (MEN II). Ninety-eight percent of the mutations in MEN-IIA occur as a single mutation in the extracellular region of the receptor in the cysteine encoding codons 609, 611, 618, or 620 of exon 10, or in codon 634 of exon 11 (Eng et al. 1996; Mulligan et al. 1995). Approximately 87% of MEN IIA mutations affect codon 634. In FMTC, 80% of the mutations occur in these same codons with the exception of codon 634 (Mulligan et al. 1995). Other mutations in FMTC have been described within the intracellular ret domains encoded by exons 13 (Bolino et al. 1995), 14 (Fattoruso et al. 1998), and 15 (Hofstra et al. 1997). These mutations lead to a disruption of the protein structure

yielding uncontrolled dimerization of RET. This results in constitutive activation of the ret tyrosine kinase and activation of its downstream pathways**.** In contrast, 95% of the MEN-IIB families have a mutation in codon 918 (Hofstra et al. 1994; Eng et al. 1994) or less commonly in codon 883 (Gimm et al. 1997). These mutations lie in the domain that recognizes substrate causing a change in substrate specificity. This allows phosphorylation of substrates normally preferred by other tyrosine kinases such as c-src and c-abl (Bocciardi et al. 1997). In sporadic cases of MTC, RET is often mutated, with the most common site being codon 918, and occasionally codon 883 (Learoyd et al. 2000).

This discovery of the *Ret* mutations has revolutionized the diagnostic evaluation and treatment of this disease. Prior to the identification of these mutations, screening consisted of random calcitonin measurements and pentagastrin stimulation tests for diagnosis. Medullary carcinoma of the thyroid is of a neuroendocrine origin and can secrete a variety of other polypeptide hormones including Carcinoembryonic antigen (CEA) which has been used both as a tumor marker and for nuclear medicine imaging and the somatostatin receptor enabling octreotide scanning to detect tumors.

ANAPLASTIC

Anaplastic thyroid cancer represents 2% of thyroid malignancies but accounts for half of its mortality (Utiger 2005). This is the most aggressive form of thyroid cancer with a mean survival of 3 to 7 months following diagnosis (O'Neill et al. 2005). The exact etiology of anaplastic carcinoma is uncertain but is commonly associated with existing thyroid disease. These lesions are often seen in a background of more differentiated tumors and are thought to arise from dedifferentiation of well differentiated tumors. Roughly 20% of patients have a history of PTC, FTC, or preexisting goiter, and another 30% show areas of well-differentiated carcinoma in the surgical specimen (Haugen et al. 2002). Some anaplastic carcinomas harbor the same mutations as incidentally noted precursor malignancies. For example, B-raf is found in those anaplastic cancers derived from papillary cancers. Ras mutations (see above sections) have also been found in anaplastic thyroid carcinomas. However, some feel that these tumors arise de novo. A number of genes are relatively specific to anaplastic carcinoma as described below.

P53 Mutations

P53 is a well known tumor suppressor gene. It is a transcription factor that functions as a main gate keeper during the cell cycle. In the presence of DNA damage, p53 will induce a cell cycle arrest to allow DNA repair or initiate apoptosis. P53 mutations are rarely present in well differentiated thyroid tumors (less than 10%) but are present in 40% of poorly differentiated thyroid tumors and 60–90% of anaplastic carcinoma (Haugen et al. 2002). This finding implies that the loss of p53 function may contribute to the undifferentiated and highly aggressive phenotype of these tumors (Lo et al. 1999). Reintroduction of wild-type p53 induces differentiation as evidenced by the expression of TSH and thyroglobulin proteins (Moretti et al. 1997) and increased the sensitivity of anaplastic thyroid carcinoma cell lines to adriamycin therapy (Blagosklonny et al. 1998;

Nagayama et al. 2000). In the future, p53 may serve as a potential treatment element utilizing gene therapy. This marker also shows promise as a prognostic indicator and may help determine the subset of well differentiated tumors that may have a predisposition to a poorer prognosis.

MRP-1

Multidrug resistant protein (MRP-1) is a 170 kDa glycoprotein pump that can displace a number of compounds from within a cell. Anaplastic carcinoma is the only thyroid malignancy for which chemotherapy is utilized, but MRP-1 can lead to treatment failures when expressed. It can lead to treatment failures with chemotherapy. It is expressed in anaplastic thyroid cancer (Sugawara et al. 1994). Inhibition of this protein may increase efficacy of chemotherapy in anaplastic thyroid tumors.

MOLECULAR PROFILING

Molecular profiling has recently been employed to evaluate thyroid lesions. Finley et al. (2004b) examined seven follicular variants of papillary thyroid carcinomas as compared to seven benign lesions using gene arrays. They reported 76 genes that were upregulated in carcinoma and 186 that were downregulated as compared to benign lesions. In another study that included papillary, follicular, and medullary carcinoma, they found 61 overexpressed genes and 72 underexpressed genes. Using molecular array with these genes, Finley et al. (2004c) was able to detect cancer with a sensitivity of 91.7% and specificity of 96.2%. Furthermore, they were able to segregate cancer into high risk and low risk with a sensitivity of 85.7% and specificity of 80.9%. Mazzanti et al. (2004) looked at papillary carcinoma and found 47 differentially expressed genes. They used a combination of 6 and 10 genes to perform analysis on samples with 10 of 10 cases accurately diagnosed. One study showed a minimum of five genes (caveolin-1, caveolin-2, insulin-like growth factor binding protein 6, claudin-10, and Cbp/p300-interacting transactivator) which could distinguish PTC from FTC (Aldred et al. 2004).

Thyroglobulin and thyroid peroxidase have been shown by microarray analysis to be underexpressed in both FTC and PTC (Aldred et al. 2004). A combination of three genes (cyclin D2/CCND2, protein convertase2/PCSK2, and prostate differentiation factor/PLAB) has been shown to differentiate follicular adenoma from follicular carcinoma with a sensitivity of 100%, a specificity of 95%, and accuracy of 97% (Weber et al. 2005).

FINE NEEDLE ASPIRATIONS (FNA) REPORTS

Before FNA was widely used, most nodules were surgically removed with little preoperative evaluation. However, it is now clear that only 6% of thyroid nodules will be malignant, and because about half of people over the age of 50 will have a nodule, it is impossible to surgically remove all of these nodules. FNA has emerged as one of the first diagnostic steps in the evaluation of a nodule. If cancer is found by the pathologist on a sample taken by FNA, the diagnosis is wrong <3% of the time. However, even when experienced doctors perform FNA, not enough cells will be obtained 10–20% of the time.

Additionally, 20–30% of FNA samples are read as indeterminate resulting in a diagnostic dilemma.

A number of techniques, including immunohistochemistry, functional assays, PCR and RT-PCR have been considered to augment the power of the FNA. Many studies have looked at thyroid peroxidase to measure differentiation of the cells, implying a benign lesion (Haugen et al. 2002). Reverse transcriptase polymerase chain reaction has been used to measure the level of human telomerase reverse transcriptase in FNA samples and it has been shown to correlate with malignancy (Zeiger et al. 1999). Reverse transcriptase polymerase chain reaction has been used to evaluate the expression of calcitonin in FNA samples for medullary thyroid carcinoma (Bugalho et al. 2000). Reverse transcriptase polymerase chain reaction of the RET/PTC has been performed on FNA sample but this does not appear sufficient for diagnosis of malignancy (Cheung et al. 2001). Polymerase chain reaction has been performed on FNA sample to look for mutated BRAF that was seen in half of the papillary samples and none of the follicular or benign lesions (Xing et al. 2004). The accuracy of these adjunctive tests will increase when used in conjunction with one another.

In summary, thyroid lesions are common. Determination of their malignancy (or malignant potential) still requires surgery in many cases. Fine needle aspirations allows for precise sampling of lesions of interest which has made thyroid nodule evaluation less invasive in many cases. Advances in molecular techniques and diagnosis hold promise to utilize FNA cytology material to make precision diagnosis of malignancy, thereby allowing for accurate selection of patients needing thyroidectomy.

REFERENCES

Aldred MA, Huang Y, Liyanarachchi S, Pellegata NS, Gimm O, Jhiang S, Davuluri RV, de la Chapelle A, Eng C (2004) Papillary and follicular thyroid carcinomas show distinctly different microarray expression profiles and can be distinguished by a minimum of five genes. J Clin Oncol 22:3531–3539

American Cancer Society (2007) Cancer Facts and Figures 2007. http://www.cancer.org/docroot/STT/content/STT_1x_Cancer_Facts__Figures_2007.asp

Belfiore A, La Rosa GL, La Porta GA, Giuffrida D, Milazzo G, Lupo L, Regalbuto C, Vigneri R (1992) Cancer risk in patients with cold thyroid nodules: relevance of iodine intake, sex, age, and multinodularity [see comment]. Am J Med 93:363–369

Blagosklonny MV, Giannakakou P, Wojtowicz M, Romanova LY, Ain KB, Bates SE, Fojo T (1998) Effects of p53-expressing adenovirus on the chemosensitivity and differentiation of anaplastic thyroid cancer cells. J Clin Endocrinol Metab 83:2516–2522

Bocciardi R, Mograbi B, Pasini B, Borrello MG, Pierotti MA, Bourget I, Fischer S, Romeo G, Rossi B (1997)The multiple endocrine neoplasia type 2B point mutation switches the specificity of the Ret tyrosine kinase towards cellular substrates that are susceptible to interact with Crk and Nck. Oncogene 15:2257–2265

Bolino A, Schuffenecker I, Luo Y, Seri M, Silengo M, Tocco T, Chabrier G, Houdent C, Murat A, Schlumberger M (1995) RET mutations in exons 13 and 14 of FMTC patients. Oncogene 10:2415–2419

Bugalho MJ, Mendonca E, Sobrinho LG (2000) Medullary thyroid carcinoma: an accurate preoperative diagnosis by reverse transcription-PCR. Eur J Endocrinol 143:335–338

Cetta F, Montalto G, Gori M, Curia MC, Cama A, Olschwang S (2000) Germline mutations of the APC gene in patients with familial adenomatous polyposis-associated thyroid carcinoma: results from a European cooperative study. J Clin Endocrinol Metab 85:286–292

Cheung CC, Carydis B, Ezzat S, Bedard YC, Asa SL (2001) Analysis of ret/PTC gene rearrangements refines the fine needle aspiration diagnosis

of thyroid cancer. J Clin Endocrinol Metab 86: 2187–2190

Chiappetta G, Toti P, Cetta F, Giuliano A, Pentimalli F, Amendoli I, Lazzi S, Monaco S, Cooper DS, Schneyer CR (1990) Follicular and Hürthle cell carcinoma of the thyroid. Endocrinol Metab Clin N Am 19:577–591

Cooper DS, Schneyer CR (1990) Follicular and Hürthle cell carcinoma of the thyroid. Endocrinol Metab Clin N Am 19:577–591

Corvi R, Lesueur R, Martinez-Alfaro M, Zini M, Decaussin M, Murat A, Romeo G (2001) RET rearrangements in familial papillary thyroid carcinomas. Cancer Lett 170:191–198

Duh QY (2005) What's new in general surgery: endocrine surgery. J Am Coll Surg 201:746–753

Eng C, Smith DP, Mulligan LM, Nagai MA, Healey CS, Ponder MA, Gardner E, Scheumann GF, Jackson CE, Tunnacliffe A (1994) Point mutation within the tyrosine kinase domain of the RET proto-oncogene in multiple endocrine neoplasia type 2B and related sporadic tumours. [erratum appears in Hum Mol Genet 1994 Apr; 3(4):686]. Hum Mol Genet 3:237–241

Eng C, Clayton D, Schuffenecker I, Lenoir G, Cote G, Gagel RF, van Amstel HK, Lips CJ, Nishisho I, Takai SI, Marsh DJ, Robinson BG, Frank-Raue K, Raue F, Xue F, Noll WW, Romei C, Pacini F, Fink M, Niederle B, Zedenius J, Nordenskjold M, Komminoth P, Hendy GN, Mulligan LM (1996) The relationship between specific RET proto-oncogene mutations and disease phenotype in multiple endocrine neoplasia type 2. International RET mutation consortium analysis. JAMA 276:1575–1579

Fagin JA (2002) Perspective: lessons learned from molecular genetic studies of thyroid cancer – insights into pathogenesis and tumor-specific therapeutic targets. Endocrinology 143:2025–2028

Fattoruso O, Quadro L, Libroia A, Verga U, Lupoli G, Cascone E, Colantuoni V (1998) A GTG to ATG novel point mutation at codon 804 in exon 14 of the RET proto-oncogene in two families affected by familial medullary thyroid carcinoma. Hum Mut Suppl 1:S167–S171

Finley DJ, Zhu B, Fahey TJ III (2004a) Molecular analysis of Hürthle cell neoplasms by gene profiling. Surgery 136:1160–1168

Finley DJ, Arora N, Zhu B, Gallagher L, Fahey TJ 3rd (2004b) Molecular profiling distinguishes papillary carcinoma from benign thyroid nodules. J Clin Endocrinol Metab 89:3214–3223

Finley DJ, Zhu B, Barden CB, Fahey TJ 3rd (2004c) Discrimination of benign and malignant thyroid nodules by molecular profiling. Ann Surg 240:425–437

Gimm O, Marsh DJ, Andrew SD, Frilling A, Dahia PL, Mulligan LM, Zajac JD, Robinson BG, Eng C (1997) Germline dinucleotide mutation in codon 883 of the RET proto-oncogene in multiple endocrine neoplasia type 2B without codon 918 mutation. J Clin Endocrinol Metab 82:3902–3904

Haugen BR, Woodmansee WW, McDermott MT (2002) Towards improving the utility of fine-needle aspiration biopsy for the diagnosis of thyroid tumours. Clin Endocrinol 56:281–290

Hofstra RM, Landsvater RM, Ceccherini I, Stulp RP, Stelwagen T, Luo Y, Pasini B, Hoppener JW, van Amstel HK, Romeo G (1994) A mutation in the RET proto-oncogene associated with multiple endocrine neoplasia type 2B and sporadic medullary thyroid carcinoma. [See comments]. Nature 367:375–376

Hofstra RM, Fattoruso O, Quadro L, Wu Y, Libroia A, Verga U, Colantuoni V, Buys CH (1997) A novel point mutation in the intracellular domain of the ret protooncogene in a family with medullary thyroid carcinoma. J Clin Endocrinol Metab 82:4176–4178

Horie H, Yokogashi Y, Tsuyuguchi M, Saito S (1995) Point mutations of ras and Gs alpha subunit genes in thyroid tumors. Jpn J Cancer Res 86:737–742

Lacroix L, Mian C, Barrier T, Talbot M, Caillou B, Schlumberger M, Bidart JM (2004) PAX8 and peroxisome proliferator-activated receptor gamma 1 gene expression status in benign and malignant thyroid tissues. Eur J Endocrinol 151:367–374

Learoyd DL, Messina M, Zedenius J, Robinson BG (2000) Molecular genetics of thyroid tumors and surgical decision-making. World J Surg 24:923–933

Lo CY, Lam KY, Wan KY (1999) Anaplastic carcinoma of the thyroid. Am J Surg 177:337–339

Malchoff CD, Malchoff DM (2002) The genetics of hereditary nonmedullary thyroid carcinoma. J Clin Endocr Metab 87:2455–2459

Marchesi M, Biffoni M, Cresti R, Mariotti F, Mulas M (2000) Familial papillary carcinoma of the thyroid: a report of nine first-degree relatives of four families. Eur J Surg Oncol 26:789–791

Mathew CG, Chin KS, Easton DF, Thorpe K, Carter C, Liou GI, Fong SL, Bridges CD, Haak H, Kruseman AC (1987) A linked genetic marker for multiple endocrine neoplasia type 2A on chromosome 10. Nature 328:527–528

Mazzanti C, Zeiger MA, Costouros NG, Umbricht C, Westra WH, Smith D, Somervell H, Bevilacqua G, Alexander HR, Libutti SK (2004) Using gene expression profiling to differentiate benign versus malignant thyroid tumors. Cancer Res 64:2898–2903

McDonald MP, Zhao G, Stringer JR, Medvedovic M, Moretti S, Fagin JA (1996) Hürthle cell carcinoma of the thyroid gland: prognostic factors and results of surgical treatment. Surgery 120:1000–1004, discussion 1004–1005

Moretti F, Farsetti A, Soddu S, Misiti S, Crescenzi M, Filetti S, Andreoli M, Sacchi A, Pontecorvi A (1997) p53 re-expression inhibits proliferation and restores differentiation of human thyroid anaplastic carcinoma cells. Oncogene 14:729–740

Mulligan LM, Marsh DJ, Robinson BG, Schuffenecker I, Zedenius J, Lips CJ, Gagel RF, Takai SI, Noll WW, Fink M (1995) Genotype-phenotype correlation in multiple endocrine neoplasia type 2: report of the international RET mutation consortium. J Int Med 238:343–346

Musholt TJ, Musholt PB, Petrich T, Oetting G, Knapp WH, Klempnauer J (2000) Familial papillary thyroid carcinoma: genetics, criteria for diagnosis, clinical features, and surgical treatment. World J Surg 24:1409–1417

Nagayama Y, Yokoi H, Takeda K, Hasegawa M, Nishihara E, Namba H, Yamashita S, Niwa M (2000) Adenovirus-mediated tumor suppressor p53 gene therapy for anaplastic thyroid carcinoma in vitro and in vivo. J Clin Endocrinol Metab 85:4081–4086

Namba H, Rubin SA, Fagin JA (1990) Point mutations of *ras* oncogenes are an early event in thyroid tumorigenesis. Mol Endocrinol 4:1474–1479

Nikiforova MN, Lynch RA, Biddinger PW, Alexander EK, Dorn GW 2nd, Tallini G, Kroll TG, Nikiforov YE (2003) RAS point mutations and PAX8-PPAR gamma rearrangement in thyroid tumors: evidence for distinct molecular pathways in thyroid follicular carcinoma. J Clin Endocrinol Metab 88:2318–2326

O'Neill JP, Condron C, Walsh M, Bouchier-Hayes D (2005) Anaplastic (undifferentiated) thyroid cancer: improved insight and therapeutic strategy into a highly aggressive disease. J Laryngol Otol 119:585–591

Puxeddu E, Moretti S, Giannico A, Martinelli M, Mariano C, Avenia N, Cristofani R, Farabi R, Reboldi G, Ribacchi R, Pontecorvi A, Santeusanio F (2003) Ret/PTC activation does not influence clinical and pathological features of adult papillary thyroid carcinomas. Eur J Endocrinol 148:505–513

Puxeddu E, Moretti S, Elisei R, Romei C, Pascucci R, Martinelli M, Marino C, Avenia N, Rossi ED, Fadda G, Cavaliere A, Ribacchi R, Falorni A, Pontecorvi A, Pacini F, Pinchera A, Santeusanio F (2004) BRAF(V599E) Mutation is the leading genetic event in adult sporadic papillary thyroid carcinomas. J Clin Endocrinol Metab 89:2414–2420

Puxeddu E, Zhao G, Stringer JR, Medvedovic M, Moretti S, Fagin JA (2005) Characterization of novel non-clonal intrachromosomal rearrangements between the H4 and PTEN genes (H4/PTEN) in human thyroid cell lines and papillary thyroid cancer specimens. Mut Res/Fund Mol Mech Mutagen 570:17–32

Samaan NA, Schultz DN, Ordonez NG, Hickey RC, Johnston DA (1987) A comparison of thyroid carcinoma in those who have and have not had head and neck cancer irradiation in childhood. J Clin Endocrinol Metab 64:214–223

Soravia C, Sugg SL, Berk T, Mitri A, Cheng H, Gallinger S, Cohen Z, Asa SL, Bapat BV (1999) Familial adenomatous polyposis-associated thyroid cancer: a clinical, pathological, and molecular genetics study. Am J Path 154:127–135

Suarez HG, Du Villard JA, Caillou B, Schlumberger M, Tubiana M, Parmentier C, Monier R (1988) Detection of activated *ras* oncogenes in human thyroid carcinomas. Oncogene 2:403–406

Sugawara I, Arai T, Yamashita T, Yoshida A, Masunaga A, Itoyama S (1994) Expression of multidrug resistance-associated protein (MRP) in anaplastic carcinoma of the thyroid. Cancer Lett 82:185–188

Sugg SL, Ezzat S, Rosen IB, Freeman JL, Asa SL (1998) Distinct multiple RET/PTC gene rearrangements in multifocal papillary thyroid neoplasia. J Clin Endocrinol Metab 83:4116–4122

Tucker MA, Jones PH, Boice JD Jr, Robinson LL, Stone BJ, Stovall M, Jenkin RD, Lubin JH, Baum ES, Siegel SE (1991) Therapeutic radiation at a young age is linked to secondary thyroid

cancer. The late effects study group. Cancer Res 51:2885–2888

Utiger RD (2005) The multiplicity of thyroid nodules and carcinomas. [comment]. N Eng J Med 352:2376–2378

Weber F, Shen L, Aldred MA, Morrison CD, Frilling A, Saji M, Schuppert F, Broelsch CE, Ringel MD, Eng C (2005) Genetic classification of benign and malignant thyroid follicular neoplasia based on a three-gene combination. J Clin Endocrinol Metabol 90:2512–2521

Xing M, Tufano RP, Tufano AP, Basaria S, Ewertz M, Rosenbaum E, Byrne PJ, Wang J, Sidransky D, Ladenson PW (2004) Detection of BRAF mutation on fine needle aspiration biopsy specimens: a new diagnostic tool for papillary thyroid cancer. J Clin Endocrinol Metab 89:2867–2872

Zeiger MA, Smallridge RC, Clark DP, Liang CK, Carty SE, Watson CG, Udelsman R, Saji M (1999) Human telomerase reverse transcriptase (hTERT) gene expression in FNA samples from thyroid neoplasms. Surgery 126:1195–1198

24
Thyroid Cancer: Identification of Gene Expression Markers for Diagnosis

Obi L. Griffith, Adrienne Melck, Steven J.M. Jones, and Sam M. Wiseman

INTRODUCTION

The human genome contains tens of thousands of gene loci which code for an even greater number of different protein and RNA products. The highly complex temporal and spatial expression of these genes makes possible all the biological processes of life from development and differentiation to homeostasis, aging, and programmed cell death. Therefore, it is not surprising that altered gene expression by mutation or deregulation is fundamental for the development of many human diseases including cancer. In some cases, cancers can be linked to large changes such as deletions or duplications of entire gene(s). In other cases, more subtle changes in expression levels of larger numbers of genes are involved. Until recently, cancer diagnosis was dependent on pathological methods and imaging studies that often require a tumor of significant size and suffer from poor sensitivity (Ahmed 2002). The recent development of gene expression profiling tools, promises to identify new and improved diagnostic tools at the molecular level.

Thyroid nodules are extremely common, being palpable in 4–7% of adults in North America, with new nodules detected at a yearly rate of 0.1%, and ~5% of thyroid nodules are eventually found to harbor malignancy (Gharib and Goellner 1993; Greenlee et al. 2001). Thyroid cancer is a good example of a human disease where expression profiling can help address the problem of accurate diagnoses. Currently, fine needle aspiration biopsy (FNAB) represents the most important initial test for diagnosing malignancy in individuals who present with nodular thyroid disease. The result of the FNAB cytology can be classified as: benign (70% of cases), malignant (5–10% of cases), indeterminate or suspicious (10–20% of cases), and nondiagnostic (10–15% of cases) (Goellner et al. 1987; Caraway et al. 1993; Ravetto et al. 2000). While non-diagnostic FNABs can be repeated, it is the indeterminate or suspicious group that presents a treatment dilemma for the clinician. Most individuals with indeterminate cytology will undergo thyroid surgery, and be at risk for its associated morbidities, in order to obtain a definitive pathologic diagnosis. Unfortunately, intraoperative pathologic assessment of thyroid nodules is often misleading and has been discouraged by many investigators (Baloch and LiVolsi 2002). Within the indeterminate

group are follicular neoplasms (FN) and Hürthle cell neoplasms (HN), for which FNAB has little utility, as the diagnosis of follicular or Hürthle cell thyroid cancers is based upon histological evidence of the tumor exhibiting vascular and/or capsular invasion (McHenry and Sandoval 1998). In a cohort of 370 consecutive thyroid surgeries carried out at our center we recently reported on 80 patients (22%) who underwent thyroid resection for a FNAB diagnosis of follicular neoplasm (Wiseman et al. 2006). Our data suggested that the surgeon must carry out five thyroid surgeries in order to diagnose a single cancer in the follicular neoplasm patient population and that neither preoperative patient nor tumor characteristics were of value in assisting the surgical selection process. A review found these observations to be consistent with the current literature (Wiseman et al. 2006). Thus, many patients undergo diagnostic thyroid surgery for nodular disease that which by pathologic assessment is eventually shown to be benign disease.

Given the limitations of FNAB in diagnosing thyroid malignancy, multiple investigators have carried out molecular profiling studies with hopes of developing new diagnostic tools. In addition, such studies provide valuable insight into the biology of thyroid tumors which may ultimately lead to the discovery of useful molecular prognosticators, better tailored disease management, and ultimately improved patient outcome. In this chapter, we discuss the methodology of expression profiling for the identification of diagnostic markers including the major platform technologies, data processing issues, differential expression, validation methods, clustering, classification, and the potential for cross platform integration and meta-analysis. Finally, we review some of the most promising molecular markers currently identified by expression profiling of thyroid cancer and offer suggestions for future research directions.

GENE EXPRESSION TECHNOLOGIES

A number of technologies currently exist for large-scale profiling of gene expression at the level of transcription. The most common platforms fall into two categories: spotted cDNA microarrays and oligonucleotide arrays. In addition to microarrays a number of other high-throughput methods exist such as Serial Analysis of Gene Expression (SAGE) and massively parallel signature sequencing (MPSS). Each platform is capable of quantifying the transcript levels of hundreds to tens of thousands of genes simultaneously. In the past 10 years ~20,000 papers and hundreds of reviews related to microarrays have been published covering nearly every aspect of their use from construction to data analysis and their application in cancer (Ahmed 2002). The two major microarray technologies, along with SAGE and new tag-sequencing approaches will be briefly presented here.

cDNA Microarrays

Modern cDNA microarrays are constructed by PCR amplification of cDNA or genomic clones and spotting onto a solid support by robotics. Microarrays with thousands of clones can be generated by this method. Sample detection involves

hybridizing the target cDNA labeled with fluorescent or radioactive nucleotides to the probe DNA on the array. The most common protocol involves differentially labeling control and test samples with two fluorescent dyes such as Cyanine 3 (Cy3) and Cyanine 5 (Cy5). Signals are then measured by a scanning microscope with lasers for fluorescent excitation. Finally, the relative amounts of DNA are determined by calculating the ratio of Cy3 to Cy5 or vice versa.

The initial advantage of spotted cDNA arrays was their flexibility. They allowed construction of custom arrays with any set of genes desired as long as clones and an array facility were available. Many laboratories constructed their own arrays. This allowed highly specialized arrays targeted at specific cancers or pathways. As annotation of the human genome progressed and sequence-verified clones became available, whole genome expression profiling became possible. The difficulties of clone management and array production on a genome-wide scale were also solved when commercial solutions became available. However, some of these commercial products were disadvantaged by not providing the sequence data for each clone and having poor annotation of clone sequences. Technical disadvantages arise from the presence of repetitive elements and cross-hybridization between homologous gene families. Other disadvantages include a low dynamic range of the hybridization signal which tends to compress signal intensities, making it harder to isolate minor changes in gene expression levels. Except in special cases, cDNA arrays have been largely supplanted by oligonucleotide arrays which have several important advantages.

Oligonucleotide Arrays

Oligonucleotide (oligo) arrays can be constructed by numerous methods including spotting pre-synthesized oligos, in situ oligo synthesis by photolithography, or maskless array synthesis on a glass slide. There are a large number of commercially available oligo arrays from manufacturers which include: Affymetrix, Illumina, Nimblegen, and others, each with their own advantages and disadvantages. Development of the above methods has allowed extensive miniaturization of array construction making it possible to construct arrays with hundreds of thousands of spots. For example, the current version of Affymetrix GeneChips (Human Genome U133 Plus 2.0) includes >1 million distinct oligonucleotides representing >47,000 human transcripts. Unlike two-color arrays, many oligo arrays produce an intensity signal that allows absolute quantification. Intensity is measured by laser scanning and fluorescence excitation, similar to cDNA arrays, but with only one sample and one type of dye hybridized per array. The ability to custom design large numbers of oligonucleotide sequences in parallel makes it possible to avoid repetitive sequences and create unique probes even for highly homologous gene families. For these reasons, oligonucleotide arrays have become the preferred microarray type. The use of standardized platforms such as the Affymetrix GeneChips has created new opportunities for inter-laboratory comparisons and meta-analyses whereas flexible and customizable arrays such as the Nimblegen arrays allow more frequent sequence updates, advanced designs, and rapid application to new genomes.

Serial Analysis of Gene Expression

Serial analysis of gene expression (SAGE) is a sequencing-based rather than hybridization-based approach to expression profiling. Briefly, SAGE involves the extraction of short sequences (tags) from polyadenylated RNA by conversion to cDNA followed by a series of restriction digestions. Tags are then PCR amplified, concatenated and sequenced. The resulting sequences are mapped by alignment to the transcriptome and the frequency of any particular tag sequence is taken as a quantitative measure of the source transcript's abundance. There are several data analysis issues and sources of bias in the SAGE method such as sequence biases in library construction, PCR amplification bias, production of non-canonical tags (unexpected restriction sites), sequence errors, variation in tag length, and mapping ambiguity. Also, due to the high cost of sequencing, SAGE libraries sometimes suffer from insufficient sample depth and therefore poor sensitivity for low-abundance transcripts. We have recently reviewed utilization of SAGE for transcriptome study (Pleasance and Jones 2005). SAGE can be highly reproducible if processed carefully, it is not prone to problems such as cross-hybridization, produces absolute estimates of expression, and can have detection efficiency similar to oligo arrays with sufficient sampling depth. Also, SAGE does not require *a priori* knowledge of the genes to be profiled. Thus, in addition to profiling known genes, SAGE libraries are a valuable resource for the identification of novel genes and transcripts. However, library construction and sequencing cost can be considerably greater than microarray profiling. Thus, the number replicates are generally small (often no replicates are done). This together with the sample depth issue can make statistical analysis of SAGE data challenging.

Future Tag-Sequence Methods

The recent and rapid development of 'next-generation' sequencing technologies promises to build on the advantages of tag sequencing based approaches like SAGE and address the issues of sampling depth and cost. An often cited target for these developments is the '$1000 genome', a fully sequenced human genome for the price of only $1,000. This would require a 10,000-fold reduction in cost over conventional Sanger sequencing methods (Bentley 2006). Current developments such as the Solexa system (www.solexa.com) 454 system (www.454.com) and the polony sequencing method from George Church's laboratory (Shendure et al. 2005) are still under development but do promise ~100-fold cost reductions. In these systems, single DNA molecules (usually pre-fragmented) are clonally amplified in spatially separate locations on a highly parallel array and used as templates for sequencing by synthesis. The three systems use different sequence chemistry and have different potential for scalability, but all produce vast quantities of short high-quality sequences. Thus, application of these technologies to an RNA sample has the potential to create a SAGE-like library of short sequence tags at much greater sampling depth and a fraction of the cost. Ng et al. (2006) demonstrated this potential using the 454 platform on a paired-end tag (PET) library constructed from MCF7 cells. To validate the method's quantitative ability they performed qRT-PCR on a selection of 12 PETs with a wide abundance range and showed good correlation.

Complete sequencing of the transcriptome using next generation sequencing has the potential to provide a more quantititative and sensitive enumeration of transcript abundance whilst also identifying spliced variants and polymorphisms (Bainbridge et al. 2006). In the short term this will be of greater interest for basic researchers, whereas hybridization-based methods are more likely to serve a clinical role for reasons of speed and simplicity. However, in the long term, sequencing-based methods may start to play a role in the clinic as well.

EXPERIMENTAL ISSUES

Array Design

There are many different experimental design issues to consider when selecting or designing an expression profiling experiment. Two-color microarray experiments can be carried out as a direct comparison, balanced block design, reference design, or loop design (as reviewed in Quackenbush 2005). In many cases it is advisable to conduct 'dye swaps' where the same two samples are hybridized to the array with opposite labeling. Single-color microarray experiments have only one sample per array but there still may be a large number of possible comparison combinations between arrays to consider such as different stages or disease pathologies. Some arrays are designed with positive and/or negative hybridization controls. The positive controls are typically genes thought to have relatively constant expression (i.e., 'house-keeping' genes). Negative controls might be random sequences or genes known to not be expressed (e.g., from a completely different species). These probes serve as a quality control to identify problems such as defective arrays, bad samples, or poor hybridizations. They can also provide a useful reference for normalization. Another kind of control to consider is a 'spike-in'. By adding a known quantity of a particular transcript to every sample, hybridization conditions can be assessed and a measure of bias determined. A major design issue to consider is hybridization bias. Microarrays rely on the assumption that signal intensity is directly related to the amount of hybridization which in turn is directly related to the amount of transcript complementary to the probe sequence. In reality, hybridization is a complex process with overall binding affinity affected by the length, nucleotide composition, position of labeling, and secondary structure characteristics of the probe sequence. These issues can be minimized but not eliminated by using variable length probes carefully selected from the transcript sequence to more closely match the binding affinity across the array and avoid unfavorable secondary structures. Some custom oligo arrays are able to incorporate this in their microarray designs.

Sample Preparation

Once the experimental design is finalized, high quality samples are needed. A large number of variables can affect sample preparation including the media used for growing cells, RNA preparation method, amount of source tissue, sample handling, etc. Sample quality and quantity should be tested after RNA extraction or amplification from source sample, cDNA generation (the amount of cDNA should be close to the amount of starting RNA), and label incorporation. Well established protocols and instrumentation exist for this purpose.

Replicates

Ultimately, an unknown amount of variability will exist in the expression patterns obtained from different samples. It is important to assess the level of this variability both technically and biologically. However, with modern array technologies the level of technical variation has been significantly reduced. As technical variation is reduced, biological replicates become more useful and technical replicates can be minimized. Sufficient replicates are also necessary to accurately determine the level of background intensity. Only by assessing replicate variability are meaningful levels of statistical confidence assigned to the differences or patterns observed. There is no single standard number of replicates for an experiment. A balance must be found between limiting factors such as the cost of experiments, availability of samples, and the power to detect statistically significant events. Generally, for a direct comparison between two conditions, at least three replicates are needed for reproducible differentially expressed genes (Lee et al. 2000). However, statisticians commonly do recommend considerably more than three replicate experiments. A simple rule to follow is to ensure at least five degrees of freedom (df) where df is the number of independent units minus the number of distinct treatments (Mocellin and Rossi 2007). For example, in a comparison of four tumor samples to four normal tissue samples there are six dfs (eight independent experimental units minus two experimental conditions).

DATA ANALYSIS ISSUES

The successful implementation of expression profiling analysis requires consideration of not only the various laboratory protocols employed, but also the computational issues of data collection, processing, storage, and statistical analysis. A typical microarray study can produce over a million data points (e.g., 20 samples on HGU133 Plus 2.0 array with 54,000 probe sets). The development of computational methods to deal with these massive datasets is an area of active research with a large number of databases, software packages, and algorithms now available for gene expression analysis. It is not yet clear if any standard protocols for data analysis will emerge. In some cases, the application of several different algorithms allows for the exploration of different aspects of the data. A review of some commonly used approaches for microarray data analysis has recently been reported by Mocellin and Rossi (2007).

Quality Assessment

Before proceeding to any further analysis, it is customary to perform some preliminary quality assessment of the microarray experiment. This allows the filtering out of problem arrays or spots. For example, a researcher may wish to discard arrays with a high percentage of missing values or discard probes that are missing a large proportion of samples. Image plots can be used for visual inspection to identify spatial irregularities or imperfections (e.g., fingerprints, or flaws on the array). Boxplots express the distribution of intensities and the number of outliers. Ratio-intensity plots or MA-plots can be used to assess systematic bias on intensity values (Quackenbush 2005). It is a good practice to exclude outliers before normalization as most normalization methods assume that gene expression is relatively constant across samples. This is not always true and should be evaluated.

Normalization and Background Correction

After basic image processing, normalization and background correction is generally the first step in preparing expression data for analysis. The purpose of normalization is to remove sources of technical variation by adjusting for differences in labeling and detection efficiencies and for differences in the quantity of RNA hybridized to different arrays. Background correction attempts to eliminate the effect of low-level noise inherent to the array and produce an accurate estimate of the actual transcript expression level. Many normalization methods include a background correction or summarization method. Most normalization methods can be applied either globally (to the entire dataset) or locally (to some subset of the data such as each subgrid). Three commonly used normalization strategies for two-color arrays are: (1) total intensity normalization, (2) normalization using regression techniques such as LOWESS, and (3) normalization using ratio statistics. For single-channel arrays, quantile normalization or some variation is most commonly utilized. Methods such as GCRMA start with quantile normalization but also model base-specific effects such as the stronger bonding of G/C pairs (Wu et al. 2004). A detailed review of normalization strategies for both one- and two-channel arrays is available from Ahmed (2006). To compensate for different library sizes, SAGE tag counts are commonly normalized to 10,000-tags/library as follows: Tag frequency = (tag count × 10,000)/total tags in library (Porter et al. 2001). After normalization, the data for each gene are commonly expressed as the logarithm of the normalized value (ratio, intensity or tag frequency). This makes the variation of intensities less dependent on the absolute magnitude and evens out highly skewed distributions. It has been suggested that for larger studies, the choice of normalization has relatively small effect on the final analysis outcome of larger microarray studies (compared to platform choice, RNA quality, etc.) but can have important effects for smaller studies (Verhaak et al. 2006).

Probe/Tag Mapping

A critical preliminary step to expression profiling analysis is the accurate mapping of probe, clone, or tag sequence to the correct gene locus or transcript. Mapping errors are common, can lead to misidentification in differential expression studies, and are a frequent source of discrepancy between platforms (Yauk and Berndt 2007). With genome annotations constantly being revised, it is important to periodically update the mapping information for any platform. Some commercial platforms such as Affymetrix periodically release updated annotation files. However, there are also a number of public resources such as DAVID (http://david.abcc.ncifcrf.gov/) for array probes and DiscoverySpace (http://www.bcgsc.ca/platform/bioinfo/software/ds) for SAGE tags. One difficulty is that there are several target gene identifiers that a researcher may wish to utilize (Entrez, Unigene, Refseq, Uniprot, etc.). Often, a probe sequence will be mapped by its sequence to an intermediary identifier and then cross-reference tables used to map (sometimes through several steps) to the final target identifier. This introduces increasing possibilities for error as cross-reference tables may not be current. Ideally, direct mapping by sequence from the probe to the desired target identifier should

always be used, as this will guarantee the most current mappings and best correlation with other datasets or platforms (Mecham et al. 2004).

Differential Expression Analysis

Expression profiling experiments are most commonly applied to the problem of identifying genes that are expressed differently between two distinct conditions (e.g., cancer versus normal tissue). This typically involves categorizing samples into two groups, determining some measure of change between the two categories for each gene (e.g., a mean fold-change), assigning a measure of statistical significance to each gene, and determining a cut-off value to select a final list of interesting genes.

The comparison of two conditions (e.g., cancer versus normal) is the most straightforward case. In two-condition cases, the conditions can be either independent (e.g., two different patient populations, one cancer and one normal) or dependent (e.g., a set of matched normal and cancer samples from the same patients). In more complex comparisons there may be multiple conditions. These can also be categorized as independent (e.g., four patient populations, one for each of four cancer stages) or dependent (e.g., a related set of samples taken from patients at different time points). Each of these situations requires different statistical considerations.

In cases where no replicates are available, comparisons are limited. The fold-change can be calculated between the two conditions and a fixed cut-off chosen with the most common threshold being two-fold change. In SAGE analysis, where a lack of replicates is common, the Audic-Claverie statistic is often used (Audic and Claverie 1997). This has the advantage of considering the respective library sizes and tag counts to assign a p-value to the observed tag-count difference. If replicates are available, many more options become available. A number of different statistical tests are available to assess differential expression in two-condition comparisons such as a simple t-test or a non-parametric equivalent such as a Wilcoxen rank-sum test. In cases where the samples are related to each other a paired t-test or Wilcoxon matched pairs signed-rank test could be used instead. For multi-condition comparisons more sophisticated statistics such as ANOVA may be employed. A common problem with these statistics arises when genes have small intensity differences and extremely low variance. These genes are not likely of interest but tend to have very significant p-values because of their low variance. A number of variations of the t-statistic have been proposed that use different penalizing factors to overcome this problem. Perhaps the most popular solution is the ‘significance analysis of microarrays’ (SAM) method (Tusher et al. 2001). SAM is now able to deal with all four basic situations (two- or multi-condition, independent or dependent). Using several different approaches may be a good strategy. No single approach is likely to be completely correct but if a gene passes multiple tests, observed results are more likely to be ‘real’. For a review of statistical approaches to differential expression analysis see Steinhoff and Vingron (2006).

Multiple testing is a major concern for modern genome-wide expression profiling. Typically, researchers choose a P-value cut-off of 0.05 and assume that all genes with a lower P-value will be of interest. But, supposing that the array contains 10,000 genes to test, we can expect that ~500

(5% of 10,000) of these genes would show a P-value of less than 0.05 by chance alone. Therefore, some type of multiple testing correction or test reduction (or both) should always be carried out. Test reduction can be accomplished by prefiltering the gene list based on some basic criteria, for example, genes with very low variance across conditions. Multiple testing correction involves correcting P-values so that a given false positive rate (type I error rate) is guaranteed for all tests. Methods attempt to either control the family wise error rate (FWER: probability of at least one type I error) or the false discovery rate (FDR: expected proportion of type I errors in the rejected hypotheses). A commonly used, but extremely conservative, approach is the Bonferroni correction where the P-values are simply divided by the number of tests performed. This method is so conservative that it is not uncommon to lose all significant results after its application. For this reason, less stringent procedures such as the Benjamini and Hochberg method and others have also become popular (for review see Pounds 2006).

Expression Profiling Software and Databases

There has been an explosion of algorithmic implementations, software packages, and databases for the analysis of gene expression data in the bioinformatics field. Here, we will discuss a few of the most common analysis tools based on our own experience. For expression profiling analysis from array processing to normalization, differential expression analysis, and clustering or classification we have utilized the R programming language (http://www.r-project.org) and the associated Bioconductor packages (http://www.bioconductor.org). This is a free, open-source resource with a steep learning curve, but is versatile and extremely powerful. Some useful packages are 'gcrma' for background correction and normalization of Affymetrix data, 'limma' for differential expression analysis of both one- and two-color arrays, 'samr' for SAM analysis and 'multtest' for multiple testing correction methods. For software packages with a graphical user interface, the TM4 suite (http://www.tm4.org) for cDNA microarray data and Dchip (http://www.dchip.org) for oligonucleotide array data are also available. In addition to software for analyzing expression data, a number of databases exist for the submission, storage, and dissemination of raw expression data for the research community. The Gene Expression Omnibus (http://www.ncbi.nlm.nih.gov/geo) currently holds >147,000 samples for >100 different organisms and the Stanford Microarray Database (http://genome-www5.stanford.edu) contains >10,000 public experiments for >20 organisms. Each is capable of housing multiple difference platform types. Another useful database is Oncomine (http://www.oncomine.org), a database specializing in cancer expression datasets and web-based analysis tools that contains >20,000 microarrays representing 39 different cancer types.

VALIDATION METHODS

While expression profiling technologies such as microarrays are well recognized as one of the most powerful tools for screening biological samples for expression changes, they are also known to generate a high number of false-positives. Therefore, it is a common practice to validate microarray findings with an independent assay.

There are two major levels at which validation is desired. Firstly, there is validation of the actual microarray measurement (i.e., can the changes in transcript level be confirmed?). Secondly, there is validation at the biological level (do the changes have something to do with the condition being studied?). In the first case, the original samples might undergo another comparison using a more precise quantitative assay. In the second case, validation might occur on an independent set of samples to show that the gene effect is generalizable or a functional assay designed to test the hypothesized effect of the gene expression change (e.g., a gene knockout in a model system for the disease). As microarray technologies become more reliable and less expensive (allowing more replicates) technical validation of the assay diminishes in importance leaving more resources available for biological validation. Perhaps the most common technical validation method is (semi-)quantitative real time PCR (qrt-PCR), which permits for validation at the RNA level. For an extensive review of qrtPCR and its application to cancer see Provenzano and Mocellin (2007). Other validation techniques include Northern blot analysis and in situ hybridization.

It is also becoming popular to cross-validate results by running the experiments on a second expression profiling platform. However, this raises the issues of platform concordance and comparability. Comparisons between platforms have proven problematic for a number of reasons (reviewed in Yauk and Berndt 2007). Each platform may differ in the probes represented, sample preparation methods, hybridization conditions, scanning technology and so forth. For example, our study of 5 different platforms (Affymetrix GeneChip, LongSAGE, LongSAGELite, 'Classic' MPSS and 'Signature' MPSS) demonstrated systematic and random errors resulting in different G+C content sensitivity for each (Siddiqui et al. 2006). These biases would influence whether a gene is detected, and if detected, the level of expression measured. These kinds of platform-specific biases will undoubtedly effect the accuracy of measurements and make any platform comparisons imperfect. However, as optimization and standardization methods have improved, platform correlations have transitioned from quite poor to consistently good, making cross-platform validation a viable strategy (Yauk and Berndt 2007).

Conceptually, mRNA levels are used as a surrogate for protein abundance and activity. However, it is not always the case that a change in RNA level translates to a change in protein level. Therefore, validation of changes at the protein level is commonly carried out using techniques such as Western blot analysis, ELISA, immunoblot assays, or immunohistochemistry (IHC). A final approach for validation is at the bioinformatic level. A common analysis is to evaluate a list of differentially expressed genes for over-representation of specific biological processes or pathways using the Gene Ontology or KEGG resources. The significant observations can then be assessed in the context of the current literature for the disease being studied in order to determine if expected pathways or processes are activated or deactivated. Other bioinformatic validations involve searching for concordance or significant overlap with previously published datasets or other data types (e.g., protein-protein interactions).

CLUSTERING AND CLASSIFICATION ANALYSIS

One of the most powerful uses of gene expression data in oncology is the definition of gene signatures. This involves finding similar gene expression patterns shared by a set of samples using either unsupervised or supervised approaches. Unsupervised methods such as cluster analysis, self organizing maps, and principal component analysis are used to define groups or classes among genes or samples without any a priori knowledge. This is useful for initial data exploration, and can be used to define new molecular subgroups in a cancer. In supervised methods such as support vector machines, neural networks, and random forests, relevant classes are defined before the analysis. This allows identification of the optimal set of genes for discriminating between the two classes of interest. For a review of the use of microarrays for cancer diagnosis and classification see Perez-Diez et al. (2007).

Cancer Diagnosis Using Tumor Gene Expression Signatures

Cancer classification systems currently include >200 types of human cancers (Greene et al. 2002). In addition to these, there are an even greater number of cancer subtypes and patient-specific tumor characteristics such as rate of proliferation, capacity for invasion or metastasis, and resistance to specific treatments. In order to formulate the best treatment, a clinician must determine the cancer type and tumor characteristics as accurately as possible. Molecular methods such as expression profiling arrays represent a powerful new method for precise diagnoses. Golub et al. (1999) first demonstrated this potential for diagnosis of acute leukemia. The authors used supervised analysis to identify a diagnostic panel of 50 genes differentially expressed in a test set of 27 acute lymphoblastic leukemia (ALL) cases and 11 acute myeloid leukemia (AML) cases. Using this predictor they were able to diagnose an independent set of 34 leukemias with a high degree of accuracy (29 of 34 correctly classified). Lubitz et al. (2006) recently used DNA microarray analysis to identify 25 differentially expressed genes in a comparison of 26 benign and 24 malignant thyroid carcinomas. Unsupervised hierarchical clustering was used to classify 22 FNAB specimens. The classification was 100% concordant to the final histological diagnosis compared to 76% from preoperative cytological FNAB diagnosis.

Defining New Molecular Subtypes with Gene Expression Data

In addition to discriminating between known subtypes of cancer, expression profiling provides a powerful new approach to define new cancer subtypes at the molecular level. In combination with clinical data, these new molecular subclasses can provide important information for cancer diagnosis and prognosis. Alizadeh et al. (2000) demonstrated this potential for diffuse large B-cell lymphoma (DLBCL). Using unsupervised class discovery methods, the authors were able to define two new clinically relevant subgroups of DLBCL termed ‘germinal center B-like’ and ‘activated B-like’. These two new groups have significantly different prognoses 5 years after chemotherapy treatment with 76% of germinal centre B-like DLBCL patients surviving compared to

only 16% for activated B-like DLBCL. In thyroid cancer, Giordano et al. (2005) performed expression analysis of a large cohort of 51 papillary thyroid carcinomas. They were able to define three tumor groups based on expression patterns that closely reflects tumor morphology and mutational status of *BRAF*, *RAS*, and *RET*/PTC.

Developing Biomarkers or Panels from Microarray Class Predictors

Another valuable contribution of expression profiling data for cancer diagnoses is for the selection of surrogate molecular markers. Instead of using a microarray gene-signature for diagnosis, promising genes are transferred to a low-throughput technology such as RT-PCR, ELISA, or IHC. This has the potential for a diagnostic test to be developed that is more cost effective and can rapidly be adopted into clinical practice. Also, it may be possible to test for these biomarkers in serum or other bodily fluids; thus, avoiding invasive diagnostic tests. Biomarkers can be selected from the list of predictors in the microarray classifier. However, these classifiers are often comprised of hundreds of genes which individually may have low predictive power or do not translate well into a new assay. A differentially expressed gene on a microarray will not always be validated by RT-PCR, and changes in RNA level do not always correspond to changes at the protein level. Therefore, a major challenge is to identify a gene or genes that retain good predictive power in a low-throughput assay. Using multiple classification algorithms to select genes may help to identify the most robust predictors (Fu and Fu-Liu 2004). Tissue microarrays can be used to test a large number of potential biomarkers using IHC before selecting the final candidates.

A comparison of cDNA microarrays and tissue microarrays on 55 breast tumors showed that in many cases (two thirds of the 15 breast cancer markers examined) there was no correlation between the mRNA levels and protein levels (Ginestier et al. 2002). Furthermore, in some cases, the protein levels had prognostic value but not the RNA or vice versa. Therefore, it is a good idea to test a large number of potential markers in a high or medium throughput experiment in order to choose the best candidates for the final low-throughput diagnostic assay for the clinic. A six-gene diagnostic panel (*kit*, *Hs.296031*, *Hs.24183*, *LSM7*, *SYNGR2*, and *C21or4*) was developed in this manner for thyroid cancer. The genes were first demonstrated to have classification potential in a microarray study and then confirmed by qRT-PCR as being able to differentiate between benign and malignant thyroid tumors with high sensitivity and specificity (Rosen et al. 2005).

EXPRESSION PROFILING STUDIES IN THYROID CANCER

Perhaps because of its excellent prognosis, with few individuals succumbing to disease, thyroid cancer has not received the same level of attention as some other human malignancies. However, a significant number of profiling studies have been completed. Our recent meta-analysis and meta-review (Griffith et al. 2006) summarized the current literature. This summary has been updated in Table 24.1. Of the 24 studies evaluating thyroid tumors the methods utilized were:

TABLE 24.1. Summary of gene expression profiling studies for thyroid cancer

Study	Platform	Genes/ features	Comparison		Up-/down-regulated genes
			Condition 1 (no. samples)	Condition 2 (no. samples)	
Finn et al. (2007)[a]	Applied Biosystems Human Genome Survey Array	29,098	PTC(6), FVPTC(8)	Norm(2), HN(4), FA(3), LT(1), GRT(1)	52/121
Lubitz et al. (2006)[a]	Affymetrix HG-U95Av2	12,626	HN(10), FA(16)	PTC(11), FVPTC(13)	18/7
Arnaldi et al. (2005)	Custom cDNA array	1,807	FCL(1)	Norm (1)	9/20
			FCL(1), PCL(1), UCL(1)	Norm (1)	3/6
			PCL(1)	Norm (1)	1/8
			UCL(1)	Norm (1)	1/7
Giordano et al. (2005)	Affymetrix HG-U133A	22,283	PTC(51)	Norm(4)	90/151
Jarzab et al. (2005)	Affymetrix HG-U133A	22,283	PTC(16)	Norm(16)	75/27
Lubitz et al. (2005)[a]	Affymetrix HG-U95Av2	12,626	FA(13)	WIFTC(7)	401
			MIFTC(7)	WIFTC(7)	365
			MIFTC(7)	FA(13)	223
Weber et al. (2005)	Affymetrix HG-U133A	22,283	FA(12)	FTC(12)	12/84
Aldred et al. (2004)	Affymetrix HG-U95A	12,558	FTC (9)	PTC(6), Norm(13)	0/142
			PTC (6)	FTC(9), Norm(13)	68/0
Cerutti et al. (2004)	SAGE	N/A	FA(1)	FTC(1), Norm(1)	5/0
			FTC(1)	FA(1), Norm(1)	12/0
Chevillard et al. (2004)	custom cDNA array	5,760	FTC(3)	FA(4)	12/31
			FVPTC(3)	PTC(2)	123/16
Finley et al. (2004a)	Affymetrix HG-U95A	12,558	PTC(7), FVPTC(7)	FA(14), HN(7)	48/85
Finley et al. (2004b)	Affymetrix HG-U95A	12,558	FTC(9), PTC(11), FVPTC(13)	FA(16), HN(10)	50/55
Hawthorn et al. (2004)	Affymetrix HG-U95A	12,558	GT(6)	Norm(6)	1/7
			PTC(8)	GT(6)	10/28
			PTC(8)	Norm(8)	4/4

(continued)

TABLE 24.1. (continued)

Study	Platform	Genes/ features	Comparison		Up-/down-regulated genes
			Condition 1 (no. samples)	Condition 2 (no. samples)	
Mazzanti et al. (2004)	Hs-UniGem2 human cDNA array	9,984	PTC(17), FVPTC(15)	FA(16), HN(15)	5/41
Onda et al. (2004)	Amersham custom cDNA array	27,648	ACL(11), ATC(10)	Norm(10)	31/56
Pauws et al. (2004)	SAGE	N/A	FVPTC(1)	Norm(1)	33/9
Yano et al. (2004)	Amersham custom cDNA array	3,968	PTC(7)	Norm(7)	54/0
Zou et al. (2004)	Atlas human cancer cDNA array (cancer 1.2 array)	1,176	MACL(1)	ACL(1)	43/21
Barden et al. (2003)	Affymetrix HG-U95A	12,558	FTC(9)	FA(10)	59/45
Wasenius et al. (2003)	Atlas human cancer cDNA array (cancer 1.2 array)	1,176	PTC(18)	Norm(3)	12/9
Chen et al. (2001)	Atlas human cDNA array (Clontech)	588	M (1)	FTC (1)	18/40
Eszlinger et al. (2001)	Atlas human cDNA array (Clontech)	588	AFTN(3), CTN(3)	Norm(6)	0/16
Huang et al. (2001)	Affymetrix HG-U95A	12,558	PTC (8)	Norm (8)	24/27
Takano et al. (2000)	SAGE	N/A	FTC(1)	ATC(1)	3/10
			FTC(1)	FA(1)	4/1
			Norm(1)	FA(1)	6/0
			PTC(1)	ATC(1)	2/11
			PTC(1)	FA(1)	7/0
			PTC(1)	FTC(1)	2/1
24 studies	10 platforms		39 comparisons (575 samples)		2972 genes

The 'Genes/features' column refers to the number of clones or probes spotted on the various cDNA or oligonucleotide arrays. SAGE is listed as not applicable (N/A) because the number of unique tags observed is indeterminate and depends on the library sequencing depth. The number of samples assayed for each condition in each comparison is shown in brackets in the 'condition 1/2' columns. In cases where multiple comparisons were conducted for a single study, a sample can be listed more than once. The numbers of 'up-/down-regulated' genes reported (if specified) are for condition 1 relative to condition 2 for each comparison as provided by the publication or supplementary materials.

[a]Indicates a study that was not included in our meta-analysis (Griffith et al. 2006). Abbreviations: ACL, anaplastic thyroid cancer cell line; AFTN, autonomously functioning thyroid nodules; ATC, anaplastic thyroid cancer; CTN, cold thyroid nodule; DTC, differentiated thyroid cancer; FA, follicular adenoma; FCL, follicular carcinoma cell line; FTC, follicular thyroid carcinoma; FVPTC, follicular variant papillary carcinoma; GRT, grave's thyroiditis; GT, goiter; HCC, Hürthle cell carcinoma; HN, hyperplastic nodule; LT, lymphocytic thyroiditis; M, metastatic; MACL, anaplastic thyroid cancer cell line with metastatic capacity; MIFTC, minimally invasive FTC; MTC, medullary thyroid carcinoma; Norm, normal; PCL, papillary carcinoma cell line; PTC, papillary thyroid carcinoma; TCVPTC, tall-cell variant PTC; UCL, undifferentiated carcinoma cell line; WIFTC, widely invasive FTC

3 SAGE, 6 commercial cDNA arrays, 3 custom cDNA arrays, and 12 commercial oligonucleotide arrays. The studies listed carried out 39 different comparisons using 575 patient or cell line samples and reported 2,972 differentially expressed genes.

CROSS-PLATFORM INTEGRATION AND META-ANALYSIS

To identify genes important in thyroid cancer, many studies (as detailed above) have compared the global gene expression patterns between normal and cancerous thyroid tissue or between different thyroid cancer subtypes. Such analyses usually attempt to identify differentially expressed (up- or down-regulated) genes that play an important role in disease development and progression. Unfortunately, these studies tend to identify many genes (dozens or hundreds) of which many are expected to be false-positives and only a small fraction are useful as diagnostic or prognostic markers or therapeutic targets. A logical approach for distinguishing important genes from spurious genes, given a large number of candidate gene lists, is to search for the intersection of genes identified in multiple independent studies. It is expected that biologically relevant genes will be over-represented and system-specific spurious genes will be under-represented. In these meta-analysis methods, when different platforms or studies are in agreement, there is good evidence for a biological effect. But, when there is disagreement there may not necessarily be good evidence of a non-effect. Thus, meta-analysis of expression profiling minimizes false-positives but may not necessarily minimize false-negatives.

As large numbers of cancer profiling studies have become available the identification of gene list intersections has become increasingly popular. Recent studies have looked for transcriptional profiles common for many cancer types (Rhodes et al. 2004) or focused on specific tumors such as colorectal cancer (Shih et al. 2005). One successful example of this technique was used to identify *AMACR* as a biomarker for distinguishing benign from malignant prostate samples (Rubin et al. 2002). *AMACR* was selected using four independent gene expression datasets that showed it to be over-expressed in prostate cancer. The microarray results were validated at both the RNA and protein levels using RT-PCR and immunoblot assay, respectively. Finally, the diagnostic utility of *AMACR* as a biomarker was confirmed by IHC in TMA studies. This illustrates the importance of employing multi-study confirmation and multi-method validation to facilitate biomarker discovery.

Currently, few cross-platform analyses have been carried out for the growing number of datasets available for thyroid neoplasms. Such studies, while conceptually simple, face a number of technical challenges which include: inconsistent gene identifiers, unavailable data, uncertain significance of results, poor quality of probe annotations, and poor description of samples or experimental design. If two or more experiments were carried out in the same laboratory, combining results can be very powerful. But, if carried out in different laboratories, much more caution must be exercised. We have previously attempted to overcome these challenges and presented a ‘meta-review’ of published microarray studies to identify a large number of potential biomarkers that have been consistently

reported for thyroid cancer (Griffith et al. 2006). The approach involved a 'vote-counting' strategy based on the number of studies reporting a gene as differentially expressed and further ranking based on total sample size and average fold-change. Monte Carlo simulations were used to show that the observed level of overlap between studies was highly unlikely to occur by chance alone. The method was successfully validated against a more traditional meta-analysis approach and a large number of highly significant 'multi-study' genes provided. A review of the top 12 candidates revealed well known thyroid cancer markers such as *MET*, *TFF3*, *SERPINA1*, *TIMP1*, *FN1*, and *TPO* as well as relatively novel or uncharacterized genes such as *TGFA*, *QPCT*, *CRABP1*, *FCGBP*, *EPS8*, and *PROS1*. Such 'multi-study' markers could prove a useful resource for further study by high throughput molecular analytic techniques as already discussed.

The 'meta-review' method made use of published lists of differentially expressed genes. These lists were produced using a wide variety of experimental and computational protocols. While it can be advantageous to use different technologies, as already discussed, it is less ideal to use different normalization, filtering thresholds, probe mapping techniques, etc. Improved methods may have become available since some of the studies were originally published. Also, a general advantage of meta-analysis methods is that weak but consistent effects may be detected which would likely be filtered out as uninteresting 'noise' in any individual study. To avoid these limitations, researchers performing meta-analyses need access to raw expression profiling data and high quality experimental and clinical annotations. To this end, all gene expression publications should comply with the MIAME (Minimum Information About a Microarray Experiment) standard and deposit their raw data (e.g., cel files) in a public database.

Rhodes et al. (2004) collected and analyzed data from 3,700 cancer samples representing 10 different tumor types. This dataset allowed them to identify a common transcriptional profile universally activated across most cancer types and another signature associated with more aggressive, undifferentiated cancers. Their laboratory has since released a web resource called Oncomine. The current version (Oncomine 3.0) contains 289 studies representing 20,835 samples and 39 cancer types and allows meta-analysis of differential expression for any set of studies that the user selects (Rhodes et al. 2007). This is a very powerful resource that removes many of the practical barriers (discussed above), and makes the final product (the significant genes with multi-study overlap) directly available to the researcher community. Unfortunately, the database does not follow an open model whereby users can submit their own datasets directly, access the database programmatically, or download raw data. Currently (as of June 2007), only a single thyroid cancer study has been added to this system. This is likely because many of the groups reporting thyroid cancer profiling studies have still not made their raw data available in any of the public databases. When conducting a validation of our meta-analysis using raw data for the Affymetrix platform, we found that only two of nine studies had deposited their data in public databases and only two of the remaining seven responded favorably to email requests.

MOLECULAR MARKERS FOR THYROID CANCER

Based on the results of our meta-analysis and a further literature review we will discuss some of the most promising potential biomarkers for thyroid carcinoma that have resulted from expression profiling studies.

We defined 'well-characterized' genes as those that have been validated in more than one follow-up study and at both the RNA and protein levels such as *MET*, *TFF3*, *SERPINA1*, *TIMP1*, *FN1*, and *TPO*. Several studies have implicated *MET* protein expression in thyroid cancer as both a diagnostic tool and prognostic tool. Increased *MET* expression has been associated with higher risk for metastasis, recurrence in PTC and poor prognosis in FTC (Di Renzo et al. 1992; Ramirez et al. 2000). However, in another study, decreased *MET* was shown to be an effective predictor of distant metastases among PTC cases (Belfiore et al. 1997). While no reports have evaluated *TFF3* at the protein level, numerous studies have suggested *TFF3* to be a useful biomarker at the RNA level. A two-gene panel of *SFTPB* and *TFF3* was shown to correctly diagnose PTC with a sensitivity of 88.9%, specificity of 96.7%, and accuracy of 94.9% (Hamada et al. 2005), and *TFF3/LGALS3* mRNA ratio was shown to distinguish FA from FTC with sensitivity and specificity of 80.0% and 91.5%, respectively (Takano et al. 2005). An antibody study of *SERPINA1* reported immunoreactivity in 9/10 PTCs with no staining in the adjacent normal thyroid tissues (Poblete et al. 1996). TIMP1 upregulation was confirmed by IHC with positive immunostaining in 68% of PTC cases and none of the normals (Wasenius et al. 2003). Another IHC study of TIMP1 for 86 PTC specimens showed increased immunoreactivity in the tumor regions versus nontumor regions in 92% of cases and significant correlations with unfavorable prognostic variables (Maeta et al. 2001). *FN1* has been proposed as a useful RT-PCR marker of DTC (Hesse et al. 2005), and an important modulator of thyroid cell adhesiveness and neoplastic cell growth (Liu et al. 2005). An IHC study of 85 FTCs and 21 FAs reported that coexpression of *FN1* and *GAL3* or *FN1* and *HBME1* was restricted to cancer while their concurrent absence was highly specific for benign lesions (96%) (Prasad et al. 2005). A large number of studies have investigated TPO as a marker for thyroid carcinoma. Lazar et al. (1999) found that higher thyroid cancer stage was associated with lower TPO mRNA expression. Segev et al. (2003) reviewed five IHC studies involving nearly 400 follicular lesions and found that 93% of FAs and 97% of FTCs were accurately diagnosed by TPO antibody staining. Studies using FNAB samples however have proved less promising with false positive rates as high as 32% (Segev et al. 2003). For the most part, the six genes reviewed above appear promising as thyroid cancer candidates and warrant further study.

For four genes identified in the meta-analysis (*TGFA*, *QPCT*, *CRABP1* and *FCGBP*) we could find only a single follow-up study or validation experiment confirming their potential importance in thyroid cancer. Bergstrom et al. (2000) suggest that increased expression of *TGFA* may be responsible for aberrant activation of *EGFR* and ultimately overexpression and activation of *MET* (importance discussed above). Jarzab et al. (2005) built a classifier capable of discriminating between

PTC and nonmalignant samples in 90% of cases. This classifier included *QPCT* (along with 18 other genes). *QPCT* was considered a novel gene and was validated by qPCR in the study, but has received little further study. *CRABP1* down-regulation was confirmed by RT-PCR (Hawthorn et al. 2004) and another study reported that hypermethylation of promoter CpG islands for *CRABP1* in PTC may explain the reduced expression (Huang et al. 2003). Differential expression of *FCGBP* was confirmed by restriction-mediated differential display and real-time RT-PCR (O'Donovan et al. 2002).

For two genes (*EPS8* and *PROS1*) we could find no confirmation beyond the initial microarray experiment. In our meta-analysis, five studies identified *EPS8* and four identified *PROS1* as up-regulated in comparisons of cancer to noncancer. And yet, to our knowledge, no follow-up study has confirmed either of these genes (even at the RNA level). It is unclear if genes like *EPS8* and *PROS1* have not been further validated because they were identified as false-positives but not reported as such (because negative observations are rarely reported in the literature) or simply because they have not yet been chosen for further study. These genes and the other less characterized candidates may represent novel diagnostic markers for thyroid cancer and warrant further investigation.

Comparison to a previous 'meta-review' by Segev et al. (2003) of mainly single-gene protein-level thyroid cancer studies found that four of their 12 markers identified as promising pre-operative diagnostic markers were identified as high-ranking candidates (top 30) in our meta-analysis (*TPO*, *CD44*, *KRT19,* and *LGALS3*). Two of their candidates were either not represented (*HBME-1*) or cannot be reliably assayed by the microarray platforms (*RET*/PTC rearrangements). However, six other 'promising markers' (*CDKN1B*, *TERT*, *CP*/*LTF*, *DLGAP4*, *HMGA1*, and *PAX8*) do have representation on at least some of the expression platforms and yet were not identified as differentially expressed in even a single study in our meta-analysis. These genes may have displayed some differential expression but not reached the required thresholds for inclusion in the published lists. Alternatively, they may represent cases where changes in RNA levels do not correlate well with changes in protein levels.

Since our meta-analysis, three additional studies have been published that would likely have been included (see Table 24.1). A brief look at these studies shows that the pattern of consistently reported genes has continued. Of the multi-study genes we identified as significant, 9 of the top 12 (reviewed above) and 18 of the top 39 genes were also reported in one or more of the recent studies. Two of the studies used an updated version of the Affymetrix HG-U95A platform but the third used an entirely new platform (Applied Biosystems Human Genome Survey Microarray). This demonstrates yet again that completely different expression profiling technologies do consistently identify a common set of differentially expressed genes. It should be noted that additional genes might also reach significant overlap with the inclusion of new datasets. As new datasets become available, it may be useful to update the meta-analysis.

Of all markers that have been evaluated for the diagnosis of thyroid cancer, *Galectin 3* has been the most widely studied. Galectins are involved in many of the biologic functions of the cell including:

growth, differentiation, adhesion, mRNA processing, and apoptosis (Liu and Rabinovich 2005). Multiple investigators have focused on *galectin-3*, a chimera type galectin that contains a nonlectin portion connected to a lectin domain, as a diagnostic marker for thyroid cancer because it is consistently expressed in the cytoplasm of malignant thyrocytes (Collet et al. 2005). In a recent multicenter study Bartolazzi et al. (2001) reported *galectin-3* expression in 1,009 thyroid specimens to be a sensitive and specific marker for thyroid cancer diagnosis. Other groups have improved the sensitivity and specificity of thyroid cancer diagnosis by evaluating panels of molecular markers. Some of these panel members have been identified by gene expression profiling studies and others identified as useful at either the RNA or Protein level in targeted assays. Promising panels of diagnostic markers have included: *Galectin-3*, *HBME-1*, *ERK*, *RET*, *p16*, *CK19*, *TTF-1*, *CITED-1*, and *S100A4* (Choi et al. 2005; Barroeta et al. 2006; Nakamura et al. 2006; Scognamiglio et al. 2006; Melck et al. 2007).

In conclusion, in this chapter, we have reviewed the basics of gene expression profiling and summarized their application to thyroid cancer. Such studies have identified a plethora of differentially expressed genes with a significant number being consistently identified by several different platforms and research groups. A number of these multi-study genes have since been verified as having diagnostic utility, whereas others have received relatively little attention. The multi-study genes in our meta-analysis were identified solely from reported lists of genes with each study using different significance thresholds and data processing methods. Undoubtedly, a superior approach would be to reanalyze each dataset from raw data using consistent methods. In order for this to occur, researchers must make their raw data available in the public databases and adhere to experimental annotation standards such as MIAME. This would also allow the thyroid cancer community to benefit from powerful toolkits such as the Oncomine resource which would essentially handle all the details of meta-analysis, and allow the researcher to focus on the problem of identifying clinically relevant diagnostic biomarkers.

In addition to gene transcript expression profiling, a number of other levels of gene expression should be explored to identify relevant diagnostic markers for thyroid cancer. To date, only a single study has considered genome-wide differential microRNA expression (Visone et al. 2007), and none has yet applied exon arrays or alternative splicing arrays to identify cancer-specific splicing events or splice variants. New developments to expression profiling technologies should also continue to improve the power of these methods. In particular, next-generation sequencing technologies hold the promise of affordable, highly sensitive, accurate, and absolute measurements of the complete transcriptome including information regarding microRNAs, alternative spliceforms, and the presence of mutations and polymorphisms.

Unlike other human malignancies, during the last few decades the number of new cases of thyroid cancer diagnosed annually has steadily increased. The incidence of thyroid cancer in the United States has increased from 3.6/100,000 in 1973 to 8.7/100,000 in 2002 (2.4-fold increase). This change has been attributed

to an increased detection of small papillary carcinomas (Davies and Welch 2006). During the same period the incidence of follicular carcinoma has declined, and follicular cancers currently account for <2% of newly diagnosed thyroid cancer (LiVolsi and Asa 1994). Also, the interobserver and intraobserver reproducibility in the histopathologic diagnosis of follicular thyroid cancer is low (Franc et al. 2003). These observations, along with an autopsy study which has identified a high rate of occult papillary cancers, when serial sectioning of 'normal' thyroid glands is carried out, raises the question as to which thyroid tumors will eventually become clinically important (Harach et al. 1985). Currently, papillary microcarcinoma or papillary carcinoma <1 cm in diameter is considered an incidental finding and warrants no special treatment after diagnosis (Nasir et al. 2000). Thus, 'not all thyroid cancers are created equal', and the diagnosis of thyroid cancer which is biologically significant or tumors which will progress to clinical disease, is a challenging and critically important issue that should be addressed in the future evaluation of thyroid cancer biomarkers.

Presently, a number of promising biomarkers or biomarker panels have been identified through gene expression profiling. Some of these have achieved sensitivities and specificities that make them potentially useful in the clinic. However, a simple, consistent and accurate molecular signature for the preoperative diagnosis of thyroid malignancy has remained elusive. We believe that large scale thyroid tumor expression profiling studies, evaluating many markers on lesions from large and diverse patient cohorts, are still required to identify a biomarker panel with sufficient sensitivity and specificity to accurately diagnose individuals who present with nodular thyroid disease.

REFERENCES

Ahmed FE (2002) Molecular techniques for studying gene expression in carcinogenesis. J Environ Sci Health C Environ Carcinog Ecotoxicol Rev 20: 77–116

Ahmed FE (2006) Microarray RNA transcriptional profiling: Part II. Analytical considerations and annotation. Expert Rev Mol Diagn 6:703–715

Aldred MA, Huang Y, Liyanarachchi S, Pellegata NS, Gimm O, Jhiang S, Davuluri RV, de La Chapelle A, Charis E (2004) Papillary and follicular thyroid carcinomas show distinctly different microarray expression profiles and can be distinguished by a minimum of five genes. J Clin Oncol 22:3531–3539

Alizadeh AA, Eisen MB, Davis RE, Ma C, Lossos IS, Rosenwald A, Boldrick JC, Sabet H, Tran T, Yu X, Powell JI, Yang L, Marti GE, Moore T, Hudson J Jr, Lu L, Lewis DB, Tibshirani R, Sherlock G, Chan WC, Greiner TC, Weisenburger DD, Armitage JO, Warnke R, Levy R, Wilson W, Grever MR, Byrd JC, Botstein D, Brown PO, Staudt LM (2000) Distinct types of diffuse large B-cell lymphoma identified by gene expression profiling. Nature 403:503–511

Arnaldi LAT, Borra RC, Maciel RMB, Cerutti JM (2005) Gene expression profiles reveal that *DCN, DIO1*, and *DIO2* are underexpressed in benign and malignant thyroid tumors. Thyroid 15:210–221

Audic S, Claverie JM (1997) The significance of digital gene expression profiles. Genome Res 7:986–995

Bainbridge MN, Warren RL, Hirst M, Romanuik T, Zeng T, Go A, Delaney A, Griffith M, Hickenbotham M, Magrini V, Mardis ER, Sadar MD, Siddiqui AS, Marra MA, Jones SJ (2006) Analysis of the prostate cancer cell line LNCaP transcriptome using a sequencing-by-synthesis approach. BMC Genomics 7:246

Baloch ZW, LiVolsi VA (2002) Intraoperative assessment of thyroid and parathyroid lesions. Semin Diagn Pathol 19:219–226

Barden CB, Shister KW, Zhu B, Guiter G, Greenblatt DY, Zeiger MA, Fahey TJ III (2003) Classification of follicular thyroid tumors by molecular signature: results of gene profiling. Clin Cancer Res 9:1792–1800

Barroeta JE, Baloch ZW, Lal P, Pasha TL, Zhang PJ, LiVolsi VA (2006) Diagnostic value of differential expression of CK19, Galectin-3, HBME-1, ERK, RET, and p16 in benign and malignant follicular-derived lesions of the thyroid: an immunohistochemical tissue microarray analysis. Endocr Pathol 17:225–234

Bartolazzi A, Gasbarri A, Papotti M, Bussolati G, Lucante T, Khan A, Inohara H, Marandino F, Orlandi F, Nardi F, Vecchione A, Tecce R, Larsson O (2001) Application of an immunodiagnostic method for improving preoperative diagnosis of nodular thyroid lesions. Lancet 357:1644–1650

Belfiore A, Gangemi P, Costantino A, Russo G, Santonocito GM, Ippolito O, Di Renzo MF, Comoglio P, Fiumara A, Vigneri R (1997) Negative/low expression of the Met/hepatocyte growth factor receptor identifies papillary thyroid carcinomas with high risk of distant metastases. J Clin Endocrinol Metab 82:2322–2328

Bentley DR (2006) Whole-genome re-sequencing. Curr Opin Genet Dev 16:545–552

Bergstrom JD, Westermark B, Heldin NE (2000) Epidermal growth factor receptor signaling activates met in human anaplastic thyroid carcinoma cells. Exp Cell Res 259:293–299

Caraway NP, Sneige N, Samaan NA (1993) Diagnostic pitfalls in thyroid fine-needle aspiration: a review of 394 cases. Diagn Cytopathol 9:345–350

Cerutti JM, Delcelo R, Amadei MJ, Nakabashi C, Maciel RMB, Peterson B, Shoemaker J, Riggins GJ (2004) A preoperative diagnostic test that distinguishes benign from malignant thyroid carcinoma based on gene expression. J Clin Invest 113:1234–1242

Chen KT, Lin JD, Chao TC, Hsueh C, Chang CA, Weng HF, Chan ER (2001) Identifying differentially expressed genes associated with metastasis of follicular thyroid cancer by cDNA expression array. Thyroid 11:41–46

Chevillard S, Ugolin N, Vielh P, Ory K, Levalois C, Elliott D, Clayman GL, El-Naggar AK (2004) Gene expression profiling of differentiated thyroid neoplasms. Clin Cancer Res 10:6586–6597

Choi YL, Kim MK, Suh JW, Han J, Kim JH, Yang JH, Nam SJ (2005) Immunoexpression of HBME-1, high molecular weight cytokeratin, cytokeratin 19, thyroid transcription factor-1, and E-cadherin in thyroid carcinomas. J Korean Med Sci 20:853–859

Collet JF, Hurbain I, Prengel C, Utzmann O, Scetbon F, Bernaudin JF, Fajac A (2005) Galectin-3 immunodetection in follicular thyroid neoplasms: a prospective study on fine-needle aspiration samples. Br J Cancer 93:1175–1181

Davies L, Welch HG (2006) Increasing incidence of thyroid cancer in the United States, 1973–2002. JAMA 295:2164–2167

Di Renzo MF, Olivero M, Ferro S, Prat M, Bongarzone I, Pilotti S, Belfiore A, Costantino A, Vigneri R, Pierotti MA, Comoglio P (1992) Overexpression of the c-MET/HGF receptor gene in human thyroid carcinomas. Oncogene 7:2549–2553

Eszlinger M, Krohn K, Paschke R (2001) Complementary DNA expression array analysis suggests a lower expression of signal transduction proteins and receptors in cold and hot thyroid nodules. J Clin Endocrinol Metab 86:4834–4842

Finley DJ, Arora N, Zhu B, Gallagher L, Fahey TJIII (2004a) Molecular profiling distinguishes papillary carcinoma from benign thyroid nodules. J Clin Endocrinol Metab 89:3214–3223

Finley DJ, Zhu B, Barden CB, Fahey TJ III (2004b) Discrimination of benign and malignant thyroid nodules by molecular profiling. Ann Surg 240:425–436

Finn SP, Smyth P, Cahill S, Streck C, O'Regan EM, Flavin R, Sherlock J, Howells D, Henfrey R, Cullen M, Toner M, Timon C, O'Leary JJ, Sheils OM (2007) Expression microarray analysis of papillary thyroid carcinoma and benign thyroid tissue: emphasis on the follicular variant and potential markers of malignancy. Virchows Archive 450:249–260

Franc B, de la Salmoniere P, Lange F, Hoang C, Louvel A, de Roquancourt A, Vilde F, Hejblum G, Chevret S, Chastang C (2003) Interobserver and intraobserver reproducibility in the histopathology of follicular thyroid carcinoma. Hum Pathol 34:1092–1100

Fu LM, Fu-Liu CS (2004) Multi-class cancer subtype classification based on gene expression

signatures with reliability analysis. FEBS Lett 561:186–190

Gharib H, Goellner JR (1993) Fine-needle aspiration biopsy of the thyroid: an appraisal. Ann Intern Med 118:282–289

Ginestier C, Charafe-Jauffret E, Bertucci F, Eisinger F, Geneix J, Bechlian D, Conte N, Adelaide J, Toiron Y, Nguyen C, Viens P, Mozziconacci MJ, Houlgatte R, Birnbaum D, Jacquemier J (2002) Distinct and complementary information provided by use of tissue and DNA microarrays in the study of breast tumor markers. Am J Pathol 161:1223–1233

Giordano TJ, Kuick R, Thomas DG, Misek DE, Vinco M, Sanders D, Zhu Z, Ciampi R, Roh M, Shedden K, Gauger P, Doherty G, Thompson NW, Hanash S, Koenig RJ, Nikiforov YE (2005) Molecular classification of papillary thyroid carcinoma: distinct BRAF, RAS, and RET/PTC mutation-specific gene expression profiles discovered by DNA microarray analysis. Oncogene 24:6646–6656

Goellner JR, Gharib H, Grant CS, Johnson DA (1987) Fine needle aspiration cytology of the thyroid 1980 to 1986. Acta Cytol 31:587–590

Golub TR, Slonim DK, Tamayo P, Huard C, Gaasenbeek M, Mesirov JP, Coller H, Loh ML, Downing JR, Caligiuri MA, Bloomfield CD, Lander ES (1999) Molecular classification of cancer: class discovery and class prediction by gene expression monitoring. Science 286: 531–537

Greene FL, Page DL, Fleming ID, Fritz A, Balch CM, Haller DG, Morrow M (eds) (2002) AJCC cancer staging manual. Springer, New York

Greenlee RT, Hill-Harmon MB, Murray T, Thun M (2001) Cancer statistics. CA Cancer J Clin 51:15–36

Griffith OL, Melck A, Jones SJ, Wiseman SM (2006) Meta-analysis and meta-review of thyroid cancer gene expression profiling studies identifies important diagnostic biomarkers. J Clin Oncol 24:5043–5051

Hamada A, Mankovskaya S, Saenko V, Rogounovitch T, Mine M, Namba H, Nakashima M, Demidchik Y, Demidchik E, Yamashita S (2005) Diagnostic usefulness of PCR profiling of the differentially expressed marker genes in thyroid papillary carcinomas. Cancer Lett 224:289–301

Harach HR, Franssila KO, Wasenius VM (1985) Occult papillary carcinoma of the thyroid. A "normal" finding in Finland. A systematic autopsy study. Cancer 56:531–538

Hawthorn L, Stein L, Varma R, Wiseman S, Loree T, Tan D (2004) TIMP1 and SERPIN-A overexpression and TFF3 and CRABP1 underexpression as biomarkers for papillary thyroid carcinoma. Head Neck 26:1069–1083

Hesse E, Musholt PB, Potter E, Petrich T, Wehmeier M, von Wasielewski R, Lichtinghagen R, Musholt TJ (2005) Oncofoetal fibronectin – a tumour-specific marker in detecting minimal residual disease in differentiated thyroid carcinoma. Br J Cancer 93:565–570

Huang Y, Prasad M, Lemon WJ, Hampel H, Wright FA, Kornacker K, LiVolsi V, Frankel W, Kloos RT, Eng C, Pellegata NS, de la Chapelle A (2001) Gene expression in papillary thyroid carcinoma reveals highly consistent profiles. Proc Natl Acad Sci U S A 98:15044–15049

Huang Y, de la Chapelle A, Pellegata NS (2003) Hypermethylation, but not LOH, is associated with the low expression of MT1G and CRABP1 in papillary thyroid carcinoma. Int J Cancer 104:735–744

Jarzab B, Wiench M, Fujarewicz K, Simek K, Jarzab M, Oczko-Wojciechowska M, Wloch J, Czarniecka A, Chmielik E, Lange D, Pawlaczek A, Szpak S, Gubala E, Swierniak A (2005) Gene expression profile of papillary thyroid cancer: sources of variability and diagnostic implications. Cancer Res 65:1587–1597

Lazar V, Bidart JM, Caillou B, Mahe C, Lacroix L, Filetti S, Schlumberger M (1999) Expression of the Na^+/I^- symporter gene in human thyroid tumors: a comparison study with other thyroid-specific genes. J Clin Endocrinol Metab 84:3228–3234

Lee ML, Kuo FC, Whitmore GA, Sklar J (2000) Importance of replication in microarray gene expression studies: statistical methods and evidence from repetitive cDNA hybridizations. Proc Natl Acad Sci U S A 97:9834–9839

Liu FT, Rabinovich GA (2005) Galectins as modulators of tumour progression. Nat Rev Cancer 5:29–41

Liu W, Asa SL, Ezzat S (2005) 1alpha, 25-dihydroxyvitamin D3 targets PTEN-dependent fibronectin expression to restore thyroid cancer cell adhesiveness. Mol Endocrinol 19:2349–2357

LiVolsi VA, Asa SL (1994) The demise of follicular carcinoma of the thyroid gland. Thyroid 4:233–236

Lubitz CC, Gallagher LA, Finley DJ, Zhu B, Fahey TJ III (2005) Molecular analysis of minimally invasive follicular carcinomas by gene profiling. Surgery 138:1042–1048

Lubitz CC, Ugras SK, Kazam JJ, Zhu B, Scognamiglio T, Chen YT, Fahey TJ III (2006) Microarray analysis of thyroid nodule fine-needle aspirates accurately classifies benign and malignant lesions. J Mol Diagn 8:490–498

Maeta H, Ohgi S, Terada T (2001) Protein expression of matrix metalloproteinases 2 and 9 and tissue inhibitors of metalloproteinase 1 and 2 in papillary thyroid carcinomas. Virchows Arch 438:121–128

Mazzanti C, Zeiger MA, Costourous N, Umbricht C, Westra WH, Smith D, Somervell H, Bevilacqua G, Alexander HR, Libutti SK (2004) Using gene expression profiling to differentiate benign versus malignant thyroid tumors. Cancer Res 64:2898–2903

McHenry CR, Sandoval BA (1998) Management of follicular and Hürthle cell neoplasms of the thyroid gland. Surg Oncol Clin N Am 7:893–910

Mecham BH, Klus GT, Strovel J, Augustus M, Byrne D, Bozso P, Wetmore DZ, Mariani TJ, Kohane IS, Szallasi Z (2004) Sequence-matched probes produce increased cross-platform consistency and more reproducible biological results in microarray-based gene expression measurements. Nucleic Acids Res 32:e74

Melck AL, Masoudi H, Griffith OL, Rajput A, Wilkins GE, Bugis S, Jones S, Wiseman SM (2007) Cell cycle regulators show diagnostic and prognostic utility for differentiated thyroid cancer. Ann Surg Oncol 14:3403–3411

Mocellin S, Rossi CR (2007) Principles of gene microarray data analysis. Adv Exp Med Biol 593:19–30

Nakamura N, Erickson LA, Jin L, Kajita S, Zhang H, Qian X, Rumilla K, Lloyd RV (2006) Immunohistochemical separation of follicular variant of papillary thyroid carcinoma from follicular adenoma. Endocr Pathol 17:213–223

Nasir A, Chaudhry AZ, Gillespie J, Kaiser HE (2000) Papillary microcarcinoma of the thyroid: a clinico-pathologic and prognostic review. In Vivo 14:367–376

Ng P, Tan JJ, Ooi HS, Lee YL, Chiu KP, Fullwood MJ, Srinivasan KG, Perbost C, Du L, Sung WK, Wei CL, Ruan Y (2006) Multiplex sequencing of paired-end ditags (MS-PET): a strategy for the ultra-high-throughput analysis of transcriptomes and genomes. Nucleic Acids Res 34:e84

O'Donovan N, Fischer A, Abdo EM, Simon F, Peter HJ, Gerber H, Buergi U, Marti U (2002) Differential expression of IgG Fc binding protein (FcgammaBP) in human normal thyroid tissue, thyroid adenomas and thyroid carcinomas. J Endocrinol 174:517–524

Onda M, Emi M, Yoshida A, Miyamoto S, Akaishi J, Asaka S, Mizutani K, Shimizu K, Nagahama M, Ito K, Tanaka T, Tsunoda T (2004) Comprehensive gene expression profiling of anaplastic thyroid cancers with cDNA microarray of 25 344 genes. Endocr Relat Cancer 11:843–854

Pauws E, Veenboer GJ, de Smit JW, Vijlder JJ, Morreau H, Ris-Stalpers C (2004) Genes differentially expressed in thyroid carcinoma identified by comparison of SAGE expression profiles. FASEB J 18:560–561

Perez-Diez A, Morgun A, Shulzhenko N (2007) Microarrays for cancer diagnosis and classification. Adv Exp Med Biol 593:74–85

Pleasance ED, Jones SJM (2005) Evaluation of SAGE tags for transcriptome study. In: SM Wang (ed) SAGE technologies: current technologies and applications. Norwich, UK, Horizon Bioscience

Poblete MT, Nualart F, del Pozo M, Perez JA, Figueroa CD (1996) Alpha 1-antitrypsin expression in human thyroid papillary carcinoma. Am J Surg Pathol 20:956–963

Porter DA, Krop IE, Nasser S, Sgroi D, Kaelin CM, Marks JR, Riggins G, Polyak K (2001) A SAGE (serial analysis of gene expression) view of breast tumor progression. Cancer Res 61:5697–5702

Pounds SB (2006) Estimation and control of multiple testing error rates for microarray studies. Brief Bioinform 7:25–36

Prasad ML, Pellegata NS, Huang Y, Nagaraja HN, de la Chapelle A, Kloos RT (2005) Galectin-3, fibronectin-1, CITED-1, HBME1 and cytokeratin-19 immunohistochemistry is useful for the differential diagnosis of thyroid tumors. Mod Pathol 18:48–57

Provenzano M, Mocellin S (2007) Complementary techniques: validation of gene expression data by quantitative real time PCR. Adv Exp Med Biol 593:66–73

Quackenbush J (2005) Using DNA microarrays to assay gene expression. In: Baxevanis AD, Ouellette BFF (eds) Bioinformatics: a practical guide to the analysis of genes and proteins. Wiley-Interscience, Hoboken, NJ, pp 409–444

Ramirez R, Hsu D, Patel A, Fenton C, Dinauer C, Tuttle RM, Francis GL (2000) Over-expression of hepatocyte growth factor/scatter factor (HGF/SF) and the HGF/SF receptor (cMET) are associated with a high risk of metastasis and recurrence for children and young adults with papillary thyroid carcinoma. Clin Endocrinol (Oxf) 53:635–644

Ravetto C, Colombo L, Dottorini ME (2000) Usefulness of fine-needle aspiration in the diagnosis of thyroid carcinoma: a retrospective study in 37,895 patients. Cancer 90:357–363

Rhodes DR, Yu J, Shanker K, Deshpande N, Varambally R, Ghosh D, Barrette T, Pandey A, Chinnaiyan AM (2004) Large-scale meta-analysis of cancer microarray data identifies common transcriptional profiles of neoplastic transformation and progression. Proc Natl Acad Sci U S A 101:9309–9314

Rhodes DR, Kalyana-Sundaram S, Mahavisno V, Varambally R, Yu J, Briggs BB, Barrette TR, Anstet MJ, Kincead-Beal C, Kulkarni P, Varambally S, Ghosh D, Chinnaiyan AM (2007) Oncomine 3.0: genes, pathways, and networks in a collection of 18,000 cancer gene expression profiles. Neoplasia 9:166–180

Rosen J, He M, Umbricht C, Alexander HR, Dackiw AP, Zeiger MA, Libutti SK (2005) A six-gene model for differentiating benign from malignant thyroid tumors on the basis of gene expression. Surgery 138:1050–1056

Rubin MA, Zhou M, Dhanasekaran SM, Varambally S, Barrette TR, Sanda MG, Pienta KJ, Ghosh D, Chinnaiyan AM (2002) Alpha-methylacyl coenzyme A racemase as a tissue biomarker for prostate cancer. JAMA 287:1662–1670

Scognamiglio T, Hyjek E, Kao J, Chen YT (2006) Diagnostic usefulness of HBME1, galectin-3, CK19, and CITED1 and evaluation of their expression in encapsulated lesions with questionable features of papillary thyroid carcinoma. Am J Clin Pathol 126:700–708

Segev DL, Clark DP, Zeiger MA, Umbricht C (2003) Beyond the suspicious thyroid fine needle aspirate. A Rev Acta Cytol 47:709–722

Shendure J, Porreca GJ, Reppas NB, Lin X, McCutcheon JP, Rosenbaum AM, Wang MD, Zhang K, Mitra RD, Church GM (2005) Accurate multiplex polony sequencing of an evolved bacterial genome. Science 309:1728–1732

Shih W, Chetty R, Tsao MS (2005) Expression profiling by microarrays in colorectal cancer (review). Oncol Rep 13:517–524

Siddiqui AS, Delaney AD, Schnerch A, Griffith OL, Jones SJ, Marra MA (2006) Sequence biases in large scale gene expression profiling data. Nucleic Acids Res 34:e83

Steinhoff C, Vingron M (2006) Normalization and quantification of differential expression in gene expression microarrays. Brief Bioinform 7:166–177

Takano T, Hasegawa Y, Matsuzuka F, Miyauchi A, Yoshida H, Higashiyama T, Kuma K, Amino N (2000) Gene expression profiles in thyroid carcinomas. Br J Cancer 83:1495–1502

Takano T, Miyauchi A, Yoshida H, Kuma K, Amino N (2005) Decreased relative expression level of trefoil factor 3 mRNA to galectin-3 mRNA distinguishes thyroid follicular carcinoma from adenoma. Cancer Lett 219:91–96

Tusher VG, Tibshirani R, Chu G (2001) Significance analysis of microarrays applied to the ionizing radiation response. Proc Natl Acad Sci U S A 98:5116–5121

Verhaak RG, Staal FJ, Valk PJ, Lowenberg B, Reinders MJ, de Ridder D (2006) The effect of oligonucleotide microarray data pre-processing on the analysis of patient-cohort studies. BMC Bioinformatics 7:105

Visone R, Pallante P, Vecchione A, Cirombella R, Ferracin M, Ferraro A, Volinia S, Coluzzi S, Leone V, Borbone E, Liu CG, Petrocca F, Troncone G, Calin GA, Scarpa A, Colato C, Tallini G, Santoro M, Croce CM, Fusco A (2007) Specific micro RNAs are downregulated in human thyroid anaplastic carcinomas. Oncogene 26:7590–7595

Wasenius VM, Hemmer S, Kettunen E, Knuutila S, Franssila K, Joensuu H (2003) Hepatocyte growth factor receptor, matrix metalloproteinase-11, tissue inhibitor of metalloproteinase-1,

and fibronectin are up-regulated in papillary thyroid carcinoma: a cDNA and tissue microarray study. Clin Cancer Res 9:68–75

Weber F, Shen L, Aldred MA, Morrison CD, Frilling A, Saji M, Schuppert F, Broelsch CE, Ringel MD, Eng C (2005) Genetic Classification of benign and malignant thyroid follicular neoplasia based on a three-gene combination. J Clin Endo Metab 90:2512–2521

Wiseman SM, Baliski C, Irvine R, Anderson D, Wilkins G, Filipenko D, Zhang H, Bugis S (2006) Hemithyroidectomy: The optimal initial surgical approach for individuals undergoing surgery for a cytological diagnosis of follicular neoplasm. Ann Surg Oncol 13:425–432

Wu Z, Irizarry RA, Gentleman R, Martinez-Murillo F, Spencer F (2004) A model-based background adjustment for oligonucleotide expression arrays. J Am Stat Assoc 99:909–917

Yano Y, Uematsu N, Yashiro T, Hara H, Ueno E, Miwa M, Tsujimoto G, Aiyoshi Y, Uchida K (2004) Gene expression profiling identifies platelet-derived growth factor as a diagnostic molecular marker for papillary thyroid carcinoma. Clin Cancer Res 10:2035–2043

Yauk CL, Berndt ML (2007) Review of the literature examining the correlation among DNA microarray technologies. Environ Mol Mutagen 48:380–94

Zou M, Famulski KS, Parhar RS, Baitei E, Al-Mohanna FA, Farid NR, Shi Y (2004) Microarray analysis of metastasis-associated gene expression profiling in a murine model of thyroid carcinoma pulmonary metastasis: identification of S100A4 (Mts1) gene overexpression as a poor prognostic marker for thyroid carcinoma. J Clin Endocrinol Metab 89: 6146–6154

25
Papillary Thyroid Carcinoma: Use of HBME1 and CK19 as Diagnostic Markers

M.R. Nasr and S. Mukhopadhyay

INTRODUCTION

Thyroid cancer is the most common endocrine malignancy in the United States and accounts for 1.5% of all cancers exclusive of carcinomas of the skin. Approximately 19,500 new cases of thyroid carcinoma are diagnosed each year, with most cases occurring in women. The annual death rate for thyroid cancer of all types is approximately 1,300 cases (Greenlee et al. 2001). The incidence of thyroid cancer has increased three- to fivefold between 1935 and 1975, without obvious reasons.

Papillary thyroid carcinoma (PTC) is the most common type of thyroid malignancy and constitutes ~80% of all malignant thyroid neoplasms in the United States. PTC occurs in all age groups (mean age, 40 years) and accounts for the vast majority of thyroid cancer in children. There is a predilection for females (3:1). Although the etiology of PTC is poorly understood, a strong association exists with exposure to ionizing radiation in a minority of cases (Inskip 2001). Most cases are sporadic, but as many as 6% of patients have a family history of PTC (Stoffer et al. 1986). The biologic behavior of PTC varies widely, from indolent microcarcinomas growing slowly with little or no invasion, to invasive, metastatic, and potentially fatal tumors. Overall, however, patients with PTC have an excellent long-term prognosis, with an overall survival of >90%.

Histologically, PTC has 2 major architectural patterns and a set of characteristic nuclear features. The architecture may be papillary or follicular. The papillary type is characterized by complex branching papillae containing thin fibrovascular stromal cores and lined by neoplastic cells. The follicular variant is composed entirely of follicles and lacks the classic papillary architecture. To diagnose the follicular variant, therefore, nuclear features of PTC must be present (Rosai et al. 1983). These nuclear features are nuclear clearing, overlapping, grooves and intranuclear pseudoinclusions. When these features are well developed, the diagnosis of follicular variant of PTC is not difficult. However, in the absence of classic, well-developed nuclear features, accurate differentiation of the follicular variant of PTC from cellular adenomatous nodules can be challenging. Because the identification of nuclear features of PTC is key, and because thresholds for these features differ among pathologists, there is significant interobserver variability

in the evaluations of these lesions. A study by Saxen et al. (1978) found only 58% interobserver agreement among pathologists. Another review of 87 cases of tumors with variable features of follicular variant of PTC by ten experienced thyroid pathologists revealed agreement in the diagnosis by all ten reviewers in only 39% of cases (Lloyd et al. 2004). Yet another study of 21 follicular nodules by eight pathologists showed agreement in the general categorization of benign vs. malignant in only 62% of the nodules (Hirokawa et al. 2002). Similar findings have been documented by other studies (Franc 2003).

For the reasons outlined above, there is an urgent need for immunohistochemical markers that may improve the reproducibility of a diagnosis of PTC. Several immunohistochemical markers have been studied, including CK19 (Cheung et al. 2001; Baloch et al. 1999), HBME1 (Cheung et al. 2001; Casey et al. 2003; Miettinen and Karkkainen 1996), FN1 (Fibronectin1) (Prasad et al. 2005), galectin-3 (Beesley and McLaren 2002), CITED1 (Cbp/p300 Interacting Transactivators with glutamic acid [E] and aspartic acid [D]-rich C-terminal domains, also known as melanocyte-specific gene 1) and SFTPB (Surfactant, pulmonary-associated Protein B) (Huang et al. 2001), CST6 (Cystatin E/M) and EPS8 (Epidermal growth factor receptor kinase Substrate) (Huang et al. 2001). Of these, the most useful and discriminatory markers are HBME1 and CK19 (Nasr et al. 2006).

HBME1 is a monoclonal antibody obtained using a suspension of cells from an epithelioid mesothelioma as an immunogen. The antibody is directed against the microvillous surface of mesothelial cells. Although the antibody was originally developed as a mesothelioma marker, it was subsequently applied to the diagnosis of malignant thyroid conditions (Sheibani et al. 1992). The first major report of its utility in thyroid neoplasms was by Miettinen and Karkkainen (Miettinen and Karkkainen 1996). Subsequently, several studies have confirmed the utility of HBME1 in the diagnosis of PTC (Cheung et al. 2001; Prasad et al. 2005).

PROTOCOL

Numerous studies have been published to determine the frequency of expression of HBME1 and CK19 in PTC and benign thyroid lesions. In most studies, immunohistochemistry was performed using standard methods. The major differences in methodology between different studies stem from the use of different antibody clones and dilutions. In addition, the criteria for staining pattern and cut off value for judging a reaction to be positive or negative have varied. As discussed later, these variations have resulted in significant differences in the reported sensitivity and specificity of these antibodies. Here we describe our protocol for HBME1 and CK19 detection and assessment.

MATERIALS

1. Formalin-fixed and paraffin-embedded tissue sections with a thickness of 4-μm
2. Microscope slides, positively charged
3. 100% methanol
4. 95% and 100% ethanol
5. Quench solution (mixture of 450 mL of 100% methanol and 50 mL hydrogen peroxide)
6. 10 mM Citrate buffer (pH 6.0)
7. Microwave oven (1,200 W)

8. iVIEW™ DAB Detection Kit (Ventana Medical Systems, Inc., Tucson, AZ)
9. Ventana NEXES automated system (Ventana Medical Systems, Inc., Tucson, AZ)
10. Mounting medium
11. Cover glass
12. Primary antibodies (HBME1 and CK19):
    HBME1 (Dako, clone: HBME1, 1:50 dilution)
    CK19 (Neomarkers, clone: Ks19.1, 1:50 dilution)
13. Positive controls were mesothelioma (for HBME1) and ductal carcinoma in situ of breast (for CK19)
14. The primary antibody was replaced with Tris-buffered saline to act as a negative control

METHODS

1. Deparaffinize and hydrate tissue sections through xylene and graded alcohol:
   2 × 2 min xylene
   2 × 10 min 100% ethanol
   10 Dips 100% methanol
   5 min Quench solution
   10 Dips 100% methanol
   2 × 10 Dips 95% ethanol, followed by distilled water
2. The tissue sections were then boiled in citrate buffer (pH 6.0) for 10 min to retain the antigenicity recognized by the two antibodies (HBME1 and CK19), and were cooled to 42ºC in 20 min.
3. Immunostaining was performed by a Ventana NexES automated slide stainer (Ventana Medical Systems, Inc., Tucson, AZ) using diluted antibody solution (1:50 for HBME1 and CK19) during a 32-min incubation at 37°C.
4. Antibody binding was visualized using the streptavidin-peroxidase technique (Ventana iVIEW DAB detection kit; Ventana Medical Systems, Inc.) followed by incubation with 3,3′-diaminobenzidine tetrahydrochloride.
5. The tissue sections were counterstained with hematoxylin.
6. When the staining run was complete, the tissue sections were removed from the stainer, dehydrated, and mounted with Permount.

INTERPRETATION OF STAINING

For both antibodies, we consider immunoreactivity positive only if >10% of follicular epithelial cells show staining (Prasad et al. 2005). For HBME1, staining is considered positive only if there is membrane staining along lateral and abluminal (basal) membranes of the epithelial cells. Cytoplasmic staining without membrane staining is not considered positive. Similarly, luminal membrane staining alone is considered negative. In contrast, for CK19, cytoplasmic expression *is* considered positive. It is important to define these parameters because significant differences in data may result depending on the staining pattern that is considered positive.

HBME1 IN PAPILLARY THYROID CARCINOMA AND BENIGN THYROID LESIONS

Our recently published data show that 96% PTCs are positive for HBME1 (Fig. 25.1), while the adjacent normal thyroid tissue is consistently negative (Nasr et al. 2006). HBME1 stained only 4 of 57 (7%) benign

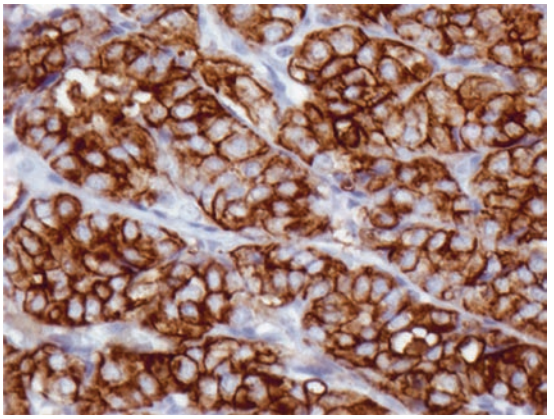

FIGURE 25.1. Follicular variant of papillary thyroid carcinoma showing cytoplasmic and membrane positivity for HBME1 immunostain (400× magnification)

lesions; all 4 were cases of Hashimoto's thyroiditis. In these cases, there was strong membrane staining for HBME1 in small foci of non-Hürthle epithelial cells. These HBME1-positive epithelial foci showed some nuclear features of PTC such as clearing, occasional grooves and slight overlapping, but these changes were not sufficiently well developed to allow a clear-cut morphologic diagnosis of PTC. Cytoplasmic HBME1 staining (without membrane staining) was commonly observed in Hürthle cells, but this staining pattern was considered negative. Overall, in our hands, HBME1 was 96% sensitive and 93% specific for PTC.

In the first major study on HBME1 (Miettinen and Karkkainen 1996), all (100%) PTCs showed strong and uniform HBME1-immunoreactivity, whereas normal thyroid, nodular goiter, and follicular adenoma did not, or showed only weak and focal staining. Although Miettinen's study showed HBME1 expression in all 145 PTC, 33% of nodular goiters also showed some positivity. Of these, however, only 5 of 90 (6%) showed staining in >10% of cells. Because we consider 10% of cells to be the cut-off for positivity, we would consider only 6% of Miettinen's benign thyroids to be false-positive for HBME1. Furthermore, Miettinen and Karkkainen (1996) considered cytoplasmic and luminal staining *without* lateral membrane staining as positive, while we consider such staining to be negative. Equivalent results were found by Mase et al. (2003), who showed HBME-1 reactivity in 35/36 (97.2%) of PTC. However, 17 of 62 (27.4%) follicular adenomas and 8 of 62 (12.9%) adenomatous goiters were also positive. de Matos et al. (2005), demonstrated HBME1 expression in 79 of 84 (94%) PTC, 10 of 18 (55.6%) follicular adenomas, 4 of 12 (33.3%) adenomatous nodules and 9 of 10 (90%) Hashimoto's thyroiditis, with no expression in normal thyroid tissue. Their results are in concordance with our data.

On the other hand, in some studies, the sensitivity of HBME1 for PTC is lower. Cheung et al. (2001) reported HBME1 positivity in 38 of 54 (70%) classic PTC and 38 of 84 (45%) follicular variant of PTC with no expression in 40 nodular hyperplasia cases and 35 follicular adenomas. Similarly, Prasad et al. (2005) demonstrated HBME1 expression in 57 of 67 (85%) PTC and only 1 of 102 (1%) non-neoplastic thyroid lesions. Recently, Scognamiglio et al. (2006) reported HBME1 expression in 43 of 49 (88%) classic PTC and 25 of 29(86%) follicular variant of PTC, while 2 of 49 (4%) follicular adenomas were positive. The lower sensitivity of these and other studies compared to ours may be explained by their use of a lower titer of the HBME1 antibody (see Table 25.1). Note that the lower sensitivity attributable to these titers

Table 25.1. HBME1 clones, sources and titers used for the diagnosis of PTC in main published papers

Reference	Antibody clone	Source	Dilution
Nasr et al. (2006)	HBME-1	DAKO, Carpinteria, CA	1:50
Cheung et al. (2001)	HBME-1	DAKO, Carpinteria, CA	1:100
Prasad et al. (2005)	HBME-1	DAKO, Carpinteria, CA	1:200
Mase et al. (2003)	HBME-1	DAKO, Carpinteria, CA	1:50
Scognamiglio et al. (2006)	HBME-1	DAKO, Carpinteria, CA	1:50
Miettinen and Karkkainen (1996)	HBME-1	DAKO, Carpinteria, CA	1:50

is accompanied by a corresponding rise in specificity. It should be remembered that HBME1 expression can be present in focal areas of Hashimoto's thyroiditis and the cells in these areas may show some nuclear features of PTC. HBME1 positivity per se should not be equated with a diagnosis of papillary carcinoma in this setting.

CK19 IN PAPILLARY THYROID CARCINOMA AND BENIGN THYROID LESIONS

In the same study as mentioned above (Nasr et al. 2006), we also reported that CK19 was positive in all 51(100 %) cases of PTC. The staining pattern was predominantly cytoplasmic with frequent enhancement along the cell membrane. Reactivity was strong and diffuse in most cases. Of the 57 benign lesions, 39 (68%) were CK19-positive, including all 10 normal thyroids, 5 of 10 adenomatous nodules, 2 of 8 Graves, 1 of 4 papillary hyperplastic nodules, 5 of 6 follicular adenomas and 16 of 19 Hashimoto's thyroiditis. Although one of four papillary hyperplastic nodules was positive, only 15% of cells stained. Staining intensity was weak and diffuse in most of these benign lesions and the staining pattern was predominantly cytoplasmic with frequent membrane enhancement. The sensitivity of CK19 for PTC was 100% but the specificity was only 32%.

A number of previous studies have examined the utility of CK19 immunoreactivity in the identification of PTC of all histological types. The verdict from these studies has not been unanimous. Some studies have reported negative CK19 staining in benign thyroid lesions and high frequencies of CK19 expression in PTC (de Matos et al. 2005; Khurana et al. 2003). CK19 was found (Cheung et al. 2001; Baloch et al. 1999; Miettinen et al. 1997) to be strongly and uniformly expressed by virtually all PTCs, including the follicular variant. Miettinen et al. (1997) observed diffuse CK19 reactivity in all PTC cases. In a recent study, Cheung et al. (2001) reported diffuse CK19 staining in 66% (91/138) of PTCs. They also observed that 17% (6/35) of follicular adenomas showed focal staining with CK19 and 3% (1/35) showed diffuse staining. Baloch et al. (1999) studied PTCs with a wide spectrum of cytokeratins, including CK19. In that study, all cases of PTC (including the follicular variant) were positive for CK19. Follicular adenoma and multinodular goiter showed no staining, normal thyroid parenchyma adjacent to the tumor nodule showed focal staining in most cases, and tissue away from the tumor nodule failed to stain. Khurana et al. (2003) found

that CK19 expression in 95% (19/20) of PTC cases. No staining was seen in non-neoplastic thyroid lesions (18 cases). Hirokawa et al. (2000, 2002) reported similar observations in touch imprints prepared from resected thyroid specimen. de Matos et al. (2005) demonstrated that 73% (61/84) of PTC cases showed diffuse strong CK19 positivity whereas 18 of 40 benign thyroid lesions revealed only focal cellular reactivity.

Others, however, have observed focal CK19 positivity in benign thyroid lesions (Casey et al. 2003; Cameron and Berean 2003). These studies have found that CK19 is also expressed in normal thyroid epithelium, Hashimoto's thyroiditis, and some benign tumors. Sahoo et al. (2001) found that CK19 immunoreactivity was also present in 100% (20/20) of follicular adenomas. Of these cases, two-thirds showed weak CK19 expression and the other one-third revealed moderate to strong CK19 reactivity. They concluded that CK19 immunoreactivity could not, by itself, be used to establish a diagnosis of PTC. Similarly, our study also noted a distressingly high rate (69%) of CK19 positivity in benign thyroid lesions. Staining intensity was weak and diffuse in most of these benign lesions (Nasr et al. 2006). The reasons for the discrepancies in the immunoreactivity for CK19 in PTC reported by different authors may be partially attributed to variations in technical methods, the antibody clone used, time of fixation, and observer bias in the interpretation of the results.

These findings indicate that the chief utility of CK19 lies in its high sensitivity for PTC. Negative staining for CK19 is strong evidence against papillary carcinoma. One situation where negative CK19 staining is especially helpful is in papillary thyroid hyperplasia, which can simulate PTC morphologically. In our study, 3 of 4 papillary hyperplastic nodules were negative for CK19 while focal staining (15%) was present in one. Therefore, the absence of CK19 expression in areas of papillary hyperplasia in any thyroid lesion should prevent misinterpretation as a papillary carcinoma.

In conclusion, HBME1 is a fairly sensitive and highly specific immunohistochemical marker of PTC. If the criterion of membrane staining is strictly utilized and the appropriate dilution used, this antibody is immensely helpful in the differential diagnosis between adenomatous nodules and the follicular variant of PTC. The major diagnostic utility of CK19 lies in its high sensitivity for PTC. Therefore, negative staining argues against the diagnosis. However, this marker is not specific for PTC, and therefore a positive result must be interpreted with caution.

REFERENCES

Baloch ZW, Abraham S, Roberts S, LiVolsi VA (1999) Differential expression of cytokeratins in follicular variant of papillary carcinoma: an immunohistochemical study and its diagnostic utility. Hum Pathol 30:1166–1171

Beesley MF, McLaren KM (2002) Cytokeratin 19 and galectin-3 immunohistochemistry in the differential diagnosis of solitary thyroid nodules. Histopathology 41:236–243

Cameron BR, Berean KW (2003) Cytokeratin subtypes in thyroid tumours: immunohistochemical study with emphasis on the follicular variant of papillary carcinoma. J Otolaryngol 32:319–322

Casey MB, Lohse CM, Lloyd RV (2003) Distinction between papillary thyroid hyperplasia and papillary thyroid carcinoma by immunohistochemical staining for cytokeratin 19, galectin-3, and HBME-1. Endocr Pathol 14:55–60

Cheung CC, Ezzat S, Freeman JL, Rosen IB, Asa SL (2001) Immunohistochemical diagnosis of papillary thyroid carcinoma. Mod Pathol 14:338–342

de Matos PS, Ferreira AP, de Oliveira Facuri F, Assumpcao LV, Metze K, Ward LS (2005) Usefulness of HBME-1, cytokeratin 19 and galectin-3 immunostaining in the diagnosis of thyroid malignancy. Histopathology 47:391–401

Franc B (2003) Observer variation of lesions of the thyroid. Am J Surg Pathol 7:1177–1179

Greenlee RT, Hill-Harmon MB, Murray T, Thun M (2001) Cancer statistics, 2001. CA Cancer J Clin 51:15–36

Hirokawa M, Inagaki A, Kobayashi H, Kanahara T, Manabe T, Sonoo H (2000) Expression of cytokeratin 19 in cytologic specimens of thyroid. Diagn Cytopathol 22:197–198

Hirokawa M, Carney JA, Goellner JR, DeLellis RA, Heffess CS, Katoh R, Tsujimoto M, Kakudo K (2002) Observer variation of encapsulated follicular lesions of the thyroid gland. Am J Surg Pathol 26:1508–1514

Huang Y, Prasad M, Lemon WJ, Hampel H, Wright FA, Kornacker K, LiVolsi V, Frankel W, Kloos RT, Eng C, Pellegata NS, de la Chapelle A (2001) Gene expression in papillary thyroid carcinoma reveals highly consistent profiles. Proc Natl Acad Sci U S A 98:15044–15049

Inskip PD (2001) Thyroid cancer after radiotherapy for childhood cancer. Med Pediatr Oncol 36:568–573

Khurana KK, Truong LD, LiVolsi VA, Baloch ZW (2003) Cytokeratin 19 immunolocalization in cell block preparation of thyroid aspirates. An adjunct to fine-needle aspiration diagnosis of papillary thyroid carcinoma. Arch Pathol Lab Med 127:579–583

Lloyd RV, Erickson LA, Casey MB, Lam KY, Lohse CM, Asa SL, Chan JK, DeLellis RA, Harach HR, Kakudo K, LiVolsi VA, Rosai J, Sebo TJ, Sobrinho-Simoes M, Wenig BM, Lae ME (2004) Observer variation in the diagnosis of follicular variant of papillary thyroid carcinoma. Am J Surg Pathol 28:1336–1340

Mase T, Funahashi H, Koshikawa T, Imai T, Nara Y, Tanaka Y, Nakao A (2003) HBME-1 immunostaining in thyroid tumors especially in follicular neoplasm. Endocr J 50:173–177

Miettinen M, Karkkainen P (1996) Differential reactivity of HBME-1 and CD15 antibodies in benign and malignant thyroid tumours. Preferential reactivity with malignant tumours. Virchows Arch 429:213–219

Miettinen M, Kovatich AJ, Karkkainen P (1997) Keratin subsets in papillary and follicular thyroid lesions. A paraffin section analysis with diagnostic implications. Virchows Arch 431:407–413

Nasr MR, Mukhopadhyay S, Zhang S, Katzenstein AL (2006) Immunohistochemical markers in diagnosis of papillary thyroid carcinoma: Utility of HBME1 combined with CK19 immunostaining. Mod Pathol 19:1631–1637

Prasad ML, Pellegata NS, Huang Y, Nagaraja HN, de la Chapelle A, Kloos RT (2005) Galectin-3, fibronectin-1, CITED-1, HBME1 and cytokeratin-19 immunohistochemistry is useful for the differential diagnosis of thyroid tumors. Mod Pathol 18:48–57

Rosai J, Zampi G, Carcangiu ML (1983) Papillary carcinoma of the thyroid. A discussion of its several morphologic expressions, with particular emphasis on the follicular variant. Am J Surg Pathol 7:809–817

Sahoo S, Hoda SA, Rosai J, DeLellis RA (2001) Cytokeratin 19 immunoreactivity in the diagnosis of papillary thyroid carcinoma: a note of caution. Am J Clin Pathol 116:696–702

Saxen E, Franssila K, Bjarnason O, Normann T, Ringertz N (1978) Observer variation in histologic classification of thyroid cancer. Acta Pathol Microbiol Scand 86:483–486

Scognamiglio T, Hyjek E, Kao J, Chen YT (2006) Diagnostic usefulness of HBME1, galectin-3, CK19, and CITED1 and evaluation of their expression in encapsulated lesions with questionable features of papillary thyroid carcinoma. Am J Clin Pathol 126:700–708

Sheibani K, Esteban JM, Bailey A, Battifora H, Weiss LM (1992) Immunopathologic and molecular studies as an aid to the diagnosis of malignant mesothelioma. Hum Pathol 23:107–116

Stoffer SS, Van Dyke DL, Bach JV, Szpunar W, Weiss L (1986) Familial papillary carcinoma of the thyroid. Am J Med Genet 25:775–782

26
Papillary Thyroid Carcinoma: Detection of Copy Gain of Platelet Derived Growth Factor B Using Array Comparative Genomic Hybridization in Combination with Laser Capture Microdissection

Stephen P. Finn, John J. O'Leary, and Orla M. Sheils

INTRODUCTION

Papillary thyroid carcinoma (PTC), the most common endocrine malignancy, is thought to be a relatively genome stable neoplasm. In contrast to follicular thyroid carcinoma (FTC), almost all PTCs are diploid (Johannessen et al. 1981). PTCs have been shown to be microsatellite stable (Soares et al. 1997) and generally show low levels of loss of heterozygosity (Kitamura et al. 2000; Gillespie et al. 2000). The literature has shown that PTC is associated with several specific molecular genetic events, the best documented of which are *ret*/PTC rearrangements (REF) and the more recently described *BRAF*^{V600E} mutation (Puxeddu et al. 2004; Kimura et al. 2003). *Ret*/PTC and *BRAF* mutations appear to largely occur in a mutually exclusive manner (Soares et al. 2003). Activating point mutations of the *RAS* oncogene are also considered to account for the development of a small subset of adult sporadic PTCs (Namba et al. 1990).

BRAF^{V600E} mutation is the most prevalent genetic event in adult sporadic PTCs and shows strong concordance with classic papillary phenotype. Mutation of one of the intermediates of the RET/PTC-RAS-BRAF pathway accounts for a genetic event, potentially involved in tumor initiation in two thirds of PTCs (Kimura et al. 2003; Soares et al. 2003).

COMPARATIVE GENOMIC HYBRIDIZATION

Kallioniemi et al. (1992) were first to describe comparative genomic hybridization (CGH). CGH is a technique that allows comprehensive analysis of multiple DNA copy number gains and losses across the entire genome in one single experiment. Genome wide analysis of DNA copy number changes by CGH has revealed a spectrum of recurrent chromosomal changes in cancer. Genes affected by these chromosomal alterations are likely to be primary mediators of cancer initiation and progression.

The rationale of CGH is based on the assumption that the ratio of the binding

of test and control DNA is proportional to the ratio of the number of sequences in the two samples. CGH incorporates the sensitivity of in-situ techniques and overcomes many of the disadvantages of conventional cytogenetic studies. However, in chromosomal or metaphase CGH the identification of genes involved in chromosomal aberrations has been difficult. The difficulties in the identification of target genes for the recurrent chromosomal aberrations identified by CGH are partly due to the limited mapping resolution of this technique, which does not allow precise localization of the genetic aberrations (Kallioniemi et al. 1994; Bentz et al. 1998). Significantly, the sensitivity of CGH can be adversely affected by contamination of tumor material with normal cells and a tumor component representing

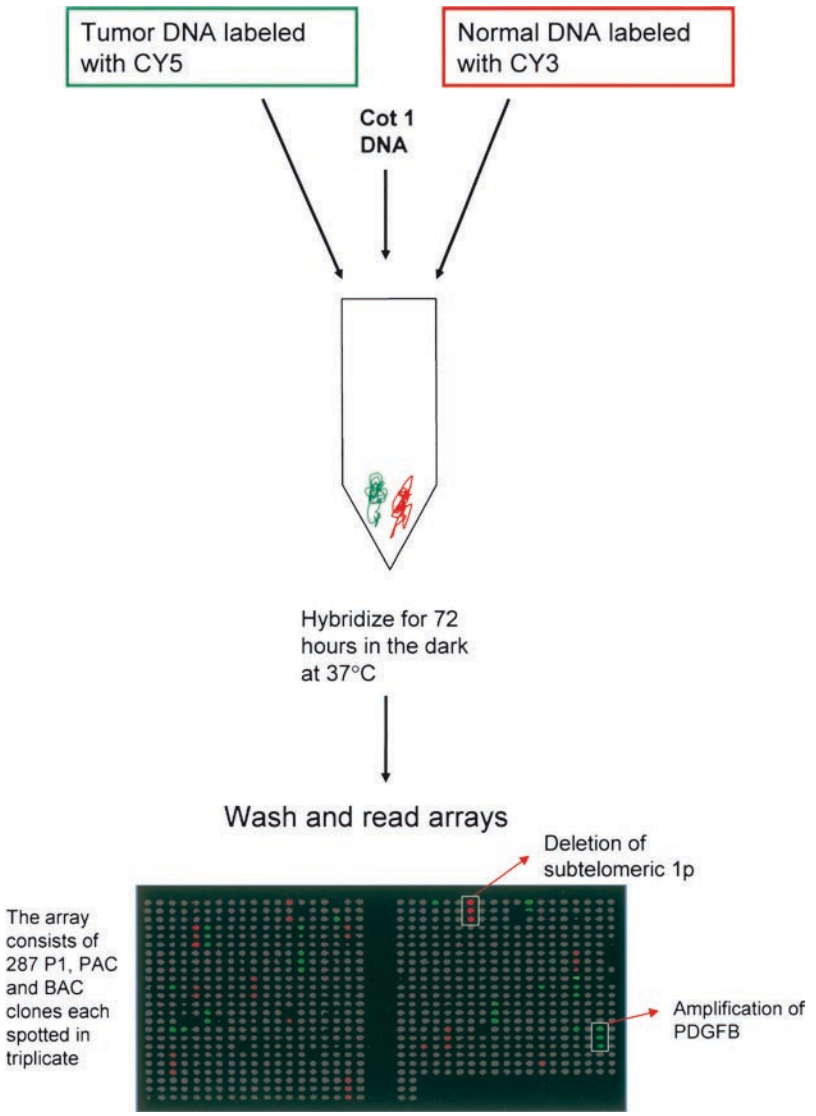

FIGURE 26.1. Outline schematic of array CGH. Equal quantities of test and reference DNA are labelled with fluorophores and co-hybridized to the microarray slide

a minimum of 70% of the DNA extracted from the tissue is highly desirable. The use of laser capture microdissection or another microdissection technique is indispensable by ensuring 100% tumor content for CGH experiments.

Arrayed DNA fragments, such as large-insert genomic clones or cDNA clones, have dramatically increased the resolution of CGH (Pinkel et al. 1998). A schematic of the array CGH concept is shown in Figure 26.1. The format of arrayed clones provides other advantages over metaphase chromosomes, including the possibility of higher throughput and the facility to directly map aberrations to the genome sequence. In addition, the technique does not require karyotyping expertise.

Vysis GenoSensor Array CGH

The Vysis Array 300 microarray (Abbott Molecular Inc., Des Plaines, Il) contains triplicates of 287-target clone DNAs (P1 and BAC clones). Therefore, there are 861 discrete spots on the array. The array contains clones that represent the more common oncogenes and tumor suppressor genes encountered in the scientific literature. In addition, the array includes clones, which mark known areas of loss of heterozygosity in cancer and loci of common microdeletions and unique subtelomeric sequences relevant to other genetic diseases. Although the array provides an average of 40 Mb coverage of each chromosome, it must be emphasized that this coverage is not homogenous along the chromosome and effectively amounts to 1% coverage of the entire genome.

We assessed DNA copy number gain and loss in PTC tumor samples and clonal cell lines using this CGH platform (Finn et al. 2007). Cells from surgically resected PTC were laser capture microdissected to ensure 100% tumor content (Figure 26.2). The BRAF status and ret/PTC status of each of the cases was assessed by TaqMan

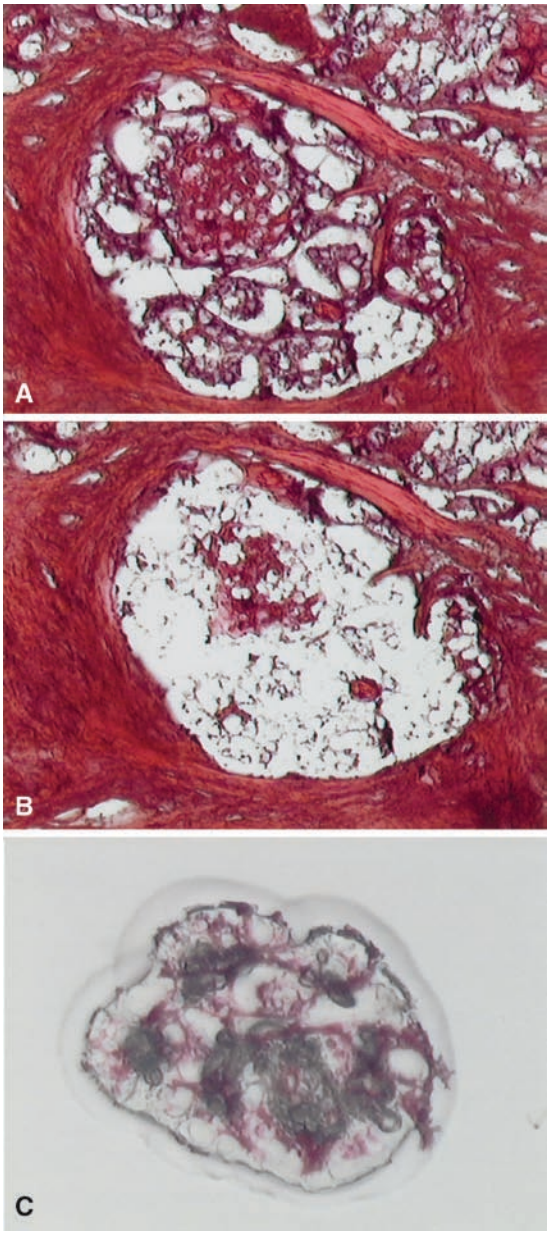

FIGURE 26.2. Laser Capture Microdissection: Panel A shows a H&E stained frozen section of follicular variant of Papillary thyroid carcinoma surrounded by dense stroma. Panel B shows the area after the carcinoma cells have been microdissected. The microdissected cells are seen adherent to the CapSure in panel C

allelic discrimination assay and TaqMan RT PCR, respectively, as described by Finn et al. (2007). These molecular abnormalities are well described in PTC and the utility of array CGH analysis is enhanced because identification of candidate oncogenes and tumor suppressor genes in PTC with none of the well described molecular triggers is likely to reveal new molecular triggers and contribute to the understanding of the molecular pathogenesis of PTC. Using this technique we identified copy gain of PDGFB in PTC occurring in a subset of PTC showing neither ret/PTC rearrangement nor BRAF V600E mutation.

METHODOLOGY

Tumors and Cell Lines

Samples of PTC were prospectively collected and snap frozen at −80°C. Prior to laser capture microdissection and DNA extraction, frozen sections were examined to confirm the presence of adequate tumor. PTC tumor cell lines were cultured and DNA extracted for CGH. Growth conditions and cell culture protocols were described by Finn et al. (2007).

Laser capture microdissection was carried out on frozen sections to preserve optimal DNA quality. After sectioning OCT embedded frozen sections, the slides were fixed in alcohol and stained rapidly with Haematoxylin and Eosin as follows.

1. Alcohol 70% – 15 dips
2. H2O – 1 dip
3. Haematoxylin – 15 dips
4. H2O – 1 dip
5. Alcohol 70% – 10 dips
6. Alcohol 95% – 15 dips
7. Eosin – 15 dips (Omit this step if using Methyl Green)
8. Alcohol 95% – 15 dips
9. Alcohol 100% (1) dips
10. Alcohol 100% (2) – 15 dips
11. Xylene (1) until clean
12. Xylene hold

LASER CAPTURE MICRODISSECTION

There are a variety of laser capture microdissection platforms. Our experience has been with the PixCell II LCM platform (Molecular Devices Corporation, Sunnyvale, CA). The system is based on the selective adherence of visually targeted cells and tissue fragments to a thermoplastic membrane activated by a low energy infrared laser pulse. The system consists of an inverted microscope, a near infrared laser diode, a laser control unit, a joystick controlled microscope stage with a vacuum chuck for immobilisation, a CCD camera, and a color monitor. The LCM microscope is connected to a computer with additional laser control and image archiving.

The thermoplastic membrane used for the transfer of selected cells has a diameter of 6 mm and is mounted on an optically clear cap (CapSure), which fits on standard 0.5 ml microcentrifuge tubes for further processing. The cap is suspended on a mechanical transport arm and positioned on the desired area of the dehydrated tissue section. Laser activation leads to focal melting of the ethylene vinyl acetate (EVA) membrane, which has its absorption maximum near the wavelength of the laser. The melted polymer expands into the section and adheres to the tissue. The adherence of tissue to the activated membrane allows removal of the cells. Sequential multiple laser pulses by the operator allows rapid isolation and counting of large numbers

of cells. The selected cells adherent to the thermoplastic membrane are harvested by simple lifting of the cap, which is then transferred to a microcentrifuge tube containing the appropriate extraction lysis buffer. Because the membrane absorbs most of the energy, the maximum temperatures reached by the tissue are only in the range of 90°C for several milliseconds.

With the PixCell II platform, the laser spot size can be adjusted to three sizes (<7.5, 15 and 30 μm). Further adjustable parameters include: pulse power, pulse width, threshold voltage and pulse duration. Laser pulse power and duration determine the size of the LCM transfer. Optimum transfers occur when, after firing the laser, the melted plastic film is similar in size to that of the target beam. The total number of pulses in each case was approximately 700. For a 30 μm spot size this yielded a tissue volume in the range of 10^{-7} to 10^{-6} μm^3. Examples of laser captured thyroid cells are seen in Figure 26.2.

DNA EXTRACTION

Extraction of DNA from alcohol fixed frozen sections and cell pellets was done using Gentra Puregene® DNA Extraction Protocols. The protocols are available from www.gentra.com.

ARRAY COMPARATIVE GENOMIC HYBRIDIZATION

As discussed above, microarray based genomic analysis is a technique intended for rapid examination of human DNA for changes in copy number of specific sequences. The assay involves labelling of sample DNA, in this case DNA from laser captured papillary thyroid carcinoma tumor cells with a fluorophore e.g., Cy3 (Perkin Elmer/NEN #NEL576) and genomic reference DNA with a second fluorophore e.g., Cy5 (Perkin Elmer/NEN #NEL577). The labelled DNA from sample and reference are mixed, in equal quantities and cohybridized to a microarray in the presence of human Cot 1 DNA. Human Cot 1 DNA is used to suppress hybridization of labelled probe to extremely common repeat sequences in the genome and represent unwanted noise in this context. A complete list of annotated clones is available from the Vysis website (www.vysis.com). Following hybridization and removal of unhybridized probe, target spots are counter-stained with a blue fluorophore included in the Array DAPI mounting solution and analyzed using the GenoSensor Reader System.

The GenoSensor Reader System is a large-field multicolour fluorescence imaging system which captures an image of the hybridized chip in three fluorescent color channels: Cy3, Cy5, and DAPI blue. The included software automatically identifies each spot and, by analysis of the set of Cy3/C5 ratios on all targets, calculates the ratio most representative of the modal DNA copy number of the sample DNA. For each target, the normalized ratio, relative to the modal DNA copy number is calculated.

This normalized ratio of a target indicates the degree of gain or loss of copy number compared with the sample's modal copy number. Detection of copy ratio changes will be highly dependent on the purity of DNA in the extracted tissue specimen. Even a very highly amplified gene will not appear as such if tumor DNA represents only a small fraction of total extracted tissue DNA. For this reason laser capture microdissection was performed to ensure truly homogenous cell populations.

Labelling Protocol

All of the materials except for the two fluorophores and the MicroSpin columns are supplied from the manufacturers in kit form. The protocols outlined below are specific to the Vysis system. Ultrapure water should be used for all reactions.

1. Tumor (Test) will be labelled with Cy3 and human reference DNA will be labelled with Cy5. In two 1.5 mL DNase free snap lock tubes labelled Test and Reference the following reagents were mixed:

4 μL of Tumor DNA (25ng/ μL) or Human Reference DNA in same concentration, 41.6 μL TE buffer, 40 μL 2.5X Random Priming Mix

2. Denature the DNA at 100°C for 10 min
3. After denaturing the sample, immediately place tubes on ice for 10 min
4. Spin down condensate inside tube
5. Place tubes back on ice and add the following reagents test and reference tubes:

GenoSensor Array 300 Nucleotide Mix 10 μL, Klenow 2 μL, Cy3 dCTP (1 mM) 2.4 μL (Test only), Cy5 dCTP (1 mM) – 2.4 μL (reference only)

6. Mix gently by vortexing and quickly spin. Incubate at 37°C, 2 h in the dark, then place tubes on ice

DNASE DIGESTION AND LABELLED PROBE PURIFICATION

Set up DNase Reactions and 1:20 DNase I Amp Grade dilution on ice. Dilute DNase Amp Grade 1:20 using DNase Dilution Buffer provided (make immediately before use and discard unused portion of the diluted DNase). Add the following to the random priming reaction.

1. DNase Reaction Buffer 17 μL (supplied by Vysis)
2. 1:20 diluted DNase Amp Grade (prepared fresh on ice) 3 μL. Then:
   a. Incubate at 15°C, 1 h in the dark.
   b. Immediately following DNase digestion, place tubes on ice.
   c. Quench reactions with 6 μL of Stop Buffer and then vortex.
   d. Prepare a MicroSpin S-200 HR column, (Amersham Biosciences Piscataway, NJ) as described in the manufacturer's protocol. Make sure that there are no visible resin particles on the outside of the column, wipe off resin deposit with a lint-free paper tissue if present.
   e. Slowly apply 126 μL of labelled probe to the column and spin the column according to the manufacturer's protocol.
   f. To the column-purified probe, add 0.1 volume of 3 M Sodium Acetate (12 μL).
   g. Add 1 μL of precipitation reagent, vortex briefly.
   h. Add 2.5 volumes of cold (–20°C) 100% Ethanol (350 μL), vortex briefly.
   i. Incubate at –20°C, 1 h.
   j. Centrifuge at 16,000 relative centrifugal force, 30 min at 4°C.
   k. Remove supernatant and then air-dry pellets (do not vacuum dry the pellet).
   l. Resuspend pellets in 4.0 μL of 10 mM Tris (pH 8.0). Gently vortex to facilitate resuspension, incubate at room temperature for 30 min prior to setting up gel, hybridization, or storage.

m. Quickly spin the tubes to collect the sample at the bottom of the tube.
n. Probe may be stored at –20°C if not used immediately for a gel analysis or hybridization reaction.

Checking the Labelled DNA

Check the labelled probe on a 2% agarose gel. If there is no DNA trailing above 200 base pairs, do not use the probe in array hybridization.

HYBRIDIZATION PROTOCOL

Preparing the Reagents

Stock solution: 20X SSC: Mix thoroughly 66 g (entire bottle) of 20X SSC in 250 mL purified H2O. Store at ambient temperature no longer than 6 months.

2X SSC/50% formamide wash: Mix thoroughly 105 mL formamide, 21 mL 20X SSC and 84 mL purified H_2O.

Label three glass Coplin jars with lids, "A", "B", "C." Pour enough formamide wash solution into each to cover the arrays but not so much as to immerse the labels on the microarray holder. Between uses, store covered at 2–8°C. Discard after washing 30 microarrays or after 2 weeks of storage.

1X SSC: Add 50 mL 20X SSC to 950 mL purified H_2O. Pour enough wash solution into each of four glass Coplin jars with lids. Label the jars "D", "E", "F", and "G". Individual washes should be discarded after use. Array DAPI Solution Store the Array DAPI solution at −20°C in the dark. Allow solution to warm to room temperature prior to pipetting.

Preparing the Hybridization Solution

Pre-warm the hybridization buffer to 37°C for 30 min, vortex and spin prior to use to ensure that the solution is uniform. It is important that the hybridization buffer is well dissolved. Due to high concentration of Cot-1 DNA in hybridization buffer, the solution may appear cloudy or opalescent. Some cloudiness in the buffer after pre-warming is acceptable as long as there are no visible clumps of precipitate. Quickly spin the tube to collect the solution at the bottom of the tube. Hold the hybridization buffer at 37°C until immediately before use.

Combine the following in a 0.5 or 1.5 mL Eppendorf microfuge tube:

1. Microarray Hybridization Buffer 25 μL. Note: Prior to addition, probes should be microcentrifuged at 12,000–16,000 relative centrifugal force (rcf) for 1 min. When pipetting probe avoid any precipitate that may be at the bottom of the tube.
2. Test DNA Probe (Cy3 dCTP) 2.5 μL.
3. Reference DNA Probe (Cy5 dCTP) 2.5 μL.
4. Vortex and quickly spin the sample.

Hybridization

1. Place the microcentrifuge tube containing the hybridization mixture into an 80°C water bath and incubate for 10 min to denature the DNA.
2. Remove from the water bath and centrifuge at 12,000–16,000 rcf for 5 s.
3. Quickly transfer the microcentrifuge tubes containing the hybridization mixture to a 37°C incubator or covered heating block, incubate in the dark for 1 h.
4. Remove the necessary number of micro arrays from their protective packaging

using the tear marks. Place the microarrays in a 37°C dry air incubator for 30 min prior to use.
5. Place a paper towel folded in half on the bottom of a sealable (air-tight) box. To the bottom of this box add 14–16 mL of 50% formamide/2XSSC wash solution to saturate the paper towel. Place the box in 37°C dry air incubator for 30 min – 1-h prior to use.

Note: Complete steps 6–8 on one array before beginning the next one. Do not allow tubes to sit at room temperature. If multiple hybridizations are to be set up at one time use a 37°C heating block to hold tubes.

6. Carefully remove the cover protecting the microarray hybridization area and discard.
7. Remove the tube containing the hybridization solution from the 37°C heating block. Mix gently and quickly spin. Draw the full amount of hybridization mixture into a Pipette tip and slowly add the hybridization mixture onto the corner of the array. Be very careful not to touch the Pipette tip on the DNA array area or introduce air bubbles (leave the microarray on the slide warmer).
8. Using forceps, carefully remove a Hybridization Coverslip from the bag. Remove lint or dust from the Hybridization Coverslip using a Kimwipe. Holding the Hybridization Coverslip at an angle, contact the hybridization solution on the microarray with the painted side of the Hybridization Coverslip touching the solution and slowly lower the Hybridization Coverslip to ensure that no air bubbles are introduced.
9. Place microarray in pre-warmed box in 37°C incubator.
10. Repeat steps 5–8 for the remaining microarrays.
11. Hybridize arrays for 60–72 h.

Washing the Microarrays

Do not wash more than 5 microarrays at one time. Optimally, washes should be done in reduced light if possible. Replace wash solutions after washing 30 microarrays, or 2 weeks of use. Prior to transferring microarrays from one bath to the next, agitate the microarray with a back and forth motion (ten times). This will help ensure proper washing.

The microarrays should not be allowed to dry at any step upon completion of the hybridization. Do not allow the microarrays to dry between washes, i.e., move chips quickly from one wash to the next without examining them. Avoid areas with high airflow when processing arrays. Do not allow chips to dry after the final rinse.

Never apply force when washing chips. Avoid twisting the arrays in the Coplin jars. Be careful when moving chips up and down in the grooves of the Coplin jars, to prevent cracking or dislodging of the chip from its holder.

If washes have been stored at 4°C, allow them to warm to room temperature. Place formamide washes (A–C) in 40°C water bath allowing them to equilibrate for 30 min. Prior to washing arrays use a thermometer to check washes are at 40°C ± 1°C. Place Coplin jars (D–G) containing 1X SSC and another jar (H) containing distilled water at room temperature.

1. Remove one microarray from the box in the incubator.

Using fine tip forceps, remove the Hybridization Coverslip by grabbing the

overhanging edge and gently lifting up. Immediately immerse the microarray in 50% 2XSSC/formamide wash solution at 40°C (Coplin jar A) and agitate briefly.

2. Repeat for remaining microarrays (up to 5), one at a time. Incubate the microarrays in Coplin jar A for 10 min.
3. After incubation, agitate each microarray in turn and transfer to Coplin jar B (formamide wash at 40°C). Incubate microarrays in Coplin jar B for 10 min.
4. After incubation, agitate microarrays and transfer, in succession as above, to Coplin jar C (formamide wash at 40°C). Incubate microarrays in Coplin jar C for 10 min.
5. Agitate as above and transfer to Coplin jar D (1X SSC at room temperature). Incubate microarrays in Coplin jar D for 5 min.
6. Agitate as above and transfer to Coplin jar E (1X SSC at room temperature). Incubate microarrays in Coplin jar E for 5 min.
7. Agitate as above and transfer to Coplin jar F (1X SSC at room temperature). Incubate microarrays in Coplin jar F for 5 min.
8. Agitate as above and transfer to Coplin jar G (1X SSC at room temperature). Incubate microarrays in Coplin jar G for 5 min.
9. After removing array from last wash, rinse in distilled H2O for 1–2 s.
10. Briskly shake chip twice to get rid of the excess water ensuring the array area itself remains wet.
11. Quickly apply coverslip-containing DAPI mounting solution to the wet chip. Chips should be stored in the dark for 45 min prior to reading on the GenoSensor instrument.

IMAGE ANALYSIS

The GenoSensor Reader Software automatically captures three images of each microarray, specific for the DAPI (counterstain), the Test DNA (green), and the reference DNA (red), respectively. The software uses the DAPI image to identify target spots and their location in the grid.

Once all spots are identified, the program analyzes each pixel within each spot for its intensity in each of the remaining color planes. An algorithm is employed to determine the local background for each of these colors, which is subtracted from the intensity of each color. The background-corrected intensities are then used to determine the ratio of Test Intensity (green) to Reference Intensity (red), which after further normalization can be used to estimate the relative abundance of a specific target sequence in the test DNA. A report page for each array is generated.

To determine the variations in the ratios of the spots in normal control DNA, comparative hybridizations using test and reference DNA from several normal samples can be performed. This approach has been used previously by other groups (Albrecht et al. 2004; Schraml et al. 2003; Hui et al. 2001). The mean ratio and mean standard of the normal array CGH can be calculated. A value of the mean ratio +/− two standard deviations can then be set as the cut-off level for normal gene copy number. In practice these values usually closely correspond to the Vysis defined values of <0.8 for deletion and >1.2 for gains.

RESULTS

Analysis Cohort

The cohort analyzed consisted of three cell lines and eight prospectively accessioned PTCs. All cases were typed for BRAF mutation status and for ret/PTC 1/3 rearrangements. Our aim was to search for potential copy gain in those tumors without evidence of BRAF mutation or ret/PTC rearrangement.

Array CGH

Array CGH revealed DNA sequence copy number changes in all three-cell lines and all eight surgical cases of PTC examined (Finn et al. 2007). Aberrations (including both gains and losses) were detected in all cases and aberrations were detected at a higher rate in the cell lines (Mean 43.8%) than in surgical tissue samples (Mean 6%). Large amplifications only occurred in cell lines. For all other cases, the maximum fluorescence ratio for a gain never exceeded 2.5. This indicates that no high-level amplifications of any of the loci occurred in tissue samples.

Recurrent Gains and Losses

Because of the great number of aberrations seen in the three cell lines in comparison with prospectively collected tissue samples and also because of the known inherent genomic instability of cell lines, the data for the tissue samples was independently analyzed for recurrent aberrations occurring exclusively in the eight tissue samples. Recurrent gains included PDGFB (22q13.1) SNRPN (15q12) and FGF4/FGF3 (11q13) and recurrent losses frequently occurred at subtelomeric loci on chromosomes 1p, 1q, 2p, 2q, 5q, 11p, 15q, 19p, and 20p.

DISCUSSION

The aim of this work was to perform an assessment of DNA copy gain and loss occurring in both Papillary Thyroid Carcinoma cell lines and prospectively collected surgical samples of PTC with knowledge of the rearranged ret/PTC and BRAF mutation status of each case to identify potentially novel aberrations. A stated aim of this study was to look for potential molecular triggers in those PTC lacking either mutant BRAF or ret/PTC activation. Gains of PDGFB (22q13), TP 73 (1p36.33) and SNRPN (15q12) were exclusively detected in tumours without these known molecular triggers.

Interestingly and contrary to previous studies, DNA copy gain and loss appears to occur in all cases of PTC when tumors are examined using a combination of laser capture microdissection and sensitive array based CGH. In the tissue specimens aberrations occurred at a low percentage of the loci examined with a mean percentage of aberrations of 6% of all loci examined (Range, 1.45–11.35%).

Taking amplified genes occurring in >36% of the cases as a threshold, the most common amplifications involved genes/loci such as FGR/SRC2 on 1p36.2-p36.1 (FGR – Gardner Rasheed Feline Sarcoma viral oncogene homolog, a protein tyrosine kinase), EGFR on 7p12.3-p12.1 (epidermal growth factor receptor, a protein tyrosine kinase), FGF4 on 11q13 (Fibroblast Growth Factor 4, a classical activator of the MAPK pathway) and PDGFB (Platelet derived growth factor B, SIS) on 22q13.1.

The literature relating to CGH data on PTC has yielded disparate results and conclusions. PTC is clearly a morphologically heterogeneous neoplasm and shows molecular heterogeneity. It may well be that

DNA copy gain and loss occurs as a secondary event to established molecular triggers such as ret/PTC activation and BRAF mutation. For this reason we attempted to assess DNA copy gain and loss in very well characterized tumours. Significantly, we attempted to overcome the effect contamination by DNA from normal cells, such as stromal and inflammatory cells by using laser capture microdissection.

Of great interest, other evidence points to a role in particular for PDGF B in the pathogenesis of PTC. A recent expression microarray study identified PDGF expression as a possible diagnostic marker of PTC (Yano et al. 2004). Over expression of the protein was confirmed by immunohistochemistry. It is possible that copy gain of this gene will lie behind the increased expression of the protein. Furthermore, PDGFB is an attractive candidate for oncogenic activation because the expressed gene has a tyrosine kinase function and is known to contribute to the mitogen activated protein kinase pathway (MAPK). Yano et al. (2004) also demonstrated over expression of FGF4 in their study.

In conclusion, the current study demonstrates that copy gain and loss occurs in more cases of PTC than heretofore seen in the literature. The combination of laser capture microdissection and array based CGH may be an optimal combination for detecting copy gain and loss in tumors. This study emphasises the central role played by the MAPK pathway in the pathogenesis of PTC. Amplification of PDGFB occurs exclusively in tumors without mutation of BRAF or expression of ret/PTC chimeras. The mechanism of overexpression of both FGF 4 receptor and PDGF, recently described in the literature, may well be copy gain at the genomic level.

REFERENCES

Albrecht B, Hausmann M, Zitzelsberger H, Stein H, Siewert JR, Hopt U, Langer R, Hofler H, Werner M, Walch A (2004) Array-based comparative genomic hybridization for the detection of DNA sequence copy number changes in Barrett's adenocarcinoma. J Pathol 203:780–788

Bentz M, Plesch A, Stilgenbauer S, Dohner H, Lichter P (1998) Minimal sizes of deletions detected by comparative genomic hybridization. Genes Chromos Cancer 21:172–175

Finn S, Smyth P, O'Regan E, Cahill S, Toner M, Timon C, Flavin R, O'Leary J, Sheils O (2007) Low-level genomic instability is a feature of papillary thyroid carcinoma: an array comparative genomic hybridization study of laser capture microdissected papillary thyroid carcinoma tumors and clonal cell lines. Arch Pathol Lab Med 131:65–73

Gillespie JW, Nasir A, Kaiser HE (2000) Loss of heterozygosity in papillary and follicular thyroid carcinoma: a mini review. In Vivo 14:139–140

Hui AB, Lo KW, Yin XL, Poon WS, Ng HK (2001) Detection of multiple gene amplifications in glioblastoma multiforme using array-based comparative genomic hybridization. Lab Invest 81:717–723

Johannessen JV, Sobrinho-Simoes M, Tangen KO, Lindmo T (1981) A flow cytometric deoxyribonucleic acid analysis of papillary thyroid carcinoma. Lab Invest 45:336–341

Kallioniemi A, Kallioniemi OP, Sudar D, Rutovitz D, Gray JW, Waldman F, Pinkel D (1992) Comparative genomic hybridization for molecular cytogenetic analysis of solid tumours. Science 258:818–821

Kallioniemi A, Kallioniemi OP, Piper J, Tanner M, Stokke T, Chen L, Smith HS, Pinkel D, Gray JW, Waldman FM (1994) Detection and mapping of amplified DNA sequences in breast cancer by comparative genomic hybridization. Proc Natl Acad Sci U S A 91:2156–2160

Kimura ET, Nikiforova MN, Zhu Z, Knauf JA, Nikiforov YE, Fagin JA (2003) High prevalence of BRAF mutations in thyroid cancer: genetic evidence for constitutive activation of the RET/PTC-RAS-BRAF signalling pathway in papillary thyroid carcinoma. Cancer Res 63:1454–1457

Kitamura Y, Shimizu K, Tanaka S, Ito K, Emi M (2000) Association of allelic loss on 1q, 4p,

7q, 9p, 9q, and 16q with postoperative death in papillary thyroid carcinoma. Clin Cancer Res 6:1819–1825

Namba H, Rubin SA, Fagin JA (1990) Point mutations of ras oncogenes are an early event in thyroid tumourigenesis. Mol Endocrinol 4:1474–1479

Pinkel D, Segraves R, Sudar D, Clark S, Poole I, Kowbel D, Collins C, Kuo WL, Chen C, Zhai Y, Dairkee SH, Ljung BM, Gray JW, Albertson DG (1998) High-resolution analysis of DNA copy number variation using comparative genomic hybridization to microarrays. Nat Genet 20: 207–211

Puxeddu E, Moretti S, Elisei R, Romei C, Pascucci R, Martinelli M, Marino C, Avenia N, Rossi ED, Fadda G, Cavaliere A, Ribacchi R, Falorni A, Pontecorvi A, Pacini F, Pinchera A, Santeusanio F (2004) BRAF (V599E) mutation is the leading genetic event in adult sporadic papillary thyroid carcinomas. J Clin Endocrinol Metab 89:2414–2420

Schraml P, Schwerdtfeger G, Burkhalter F, Raggi A, Schmidt D, Ruffalo T, King W, Wilber K, Mihatsch MJ, Moch H (2003) Combined array comparative genomic hybridization and tissue microarray analysis suggest PAK1 at 11q13.5–q14 as a critical oncogene target in ovarian carcinoma. Am J Pathol 163:985–992

Soares P, dos Santos NR, Seruca R, Lothe RA, Sobrinho-Simoes M (1997) Benign and malignant thyroid lesions show instability at microsatellite loci. Eur J Cancer 33:293–296

Soares P, Trovisco V, Rocha AS, Lima J, Castro P, Preto A, Maximo V, Botelho T, Seruca R, Sobrinho-Simoes M (2003) BRAF mutations and RET/PTC rearrangements are alternative events in the etiopathogenesis of PTC. Oncogene 22:4578–4580

Yano Y, Uematsu N, Yashiro T, Hara H, Ueno E, Miwa M, Tsujimoto G, Aiyoshi Y, Uchida K (2004) Gene expression profiling identifies platelet-derived growth factor as a diagnostic molecular marker for papillary thyroid carcinoma. Clin Cancer Res 10:2035–2043

27
PET Imaging in Thyroid Carcinoma

H.H.G. Verbeek, T.T.H. Phan, A.H. Brouwers, K.P. Koopmans, and T.P. Links

INTRODUCTION

Thyroid cancer is the most common endocrine malignancy. It is divided in several types with papillary, folliculary and Hürthle cell cancer (also called differentiated thyroid cancer) originating from the follicular epithelial cells as the most common types (>90%). Other types are medullary thyroid carcinoma (a neuroendocrine tumor originating from the calcitonin producing C-cells) (3–10%) and anaplastic carcinoma (often a dedifferentiated form of the other types) (2–10%) (Schlumberger and Pacini 2003).

There is a different treatment for each of these types of thyroid cancer. In differentiated thyroid cancer the initial therapy is total thyroidectomy with or without lymph node dissection, followed by adjuvant radioactive iodine therapy. Radioactive iodine therapy with ^{131}I can be used successfully due to the active uptake of iodine in tumor cells of thyroid origin. However, this property can be lost during dedifferentiation, which limits the use of this therapy in anaplastic carcinoma. Medullary thyroid cancer cells show no iodine uptake at all and curative options are therefore mainly limited to surgical resection of primary tumor and metastases (Sherman et al. 2005).

The prognosis for differentiated thyroid cancer is good, with an average 10-years survival between 80% and 95%. However, these tumors can dedifferentiate, which results in limited therapeutic options, leading to a much poorer prognosis with a 5-year survival of 30%. Medullary thyroid carcinoma has a 10-years survival of 20–70% (Modigliani et al. 1998) and for anaplastic thyroid carcinoma the median survival is 2–6 months (Tubiana et al. 1985; Venkatesh et al. 1990).

Imaging is especially important in determining the right therapeutic approach for patients with differentiated and medullary thyroid carcinoma. Different imaging techniques are available such as Computed Tomography, Magnetic Resonance Imaging, conventional nuclear scintigraphy and Positron Emission Tomography. While MRI and CT are imaging techniques which show morphologic structures, PET imaging depicts pathophysiological processes and is described as functional imaging. The value of PET imaging is emerging mainly in the follow-up of thyroid cancer. Several PET imaging techniques are available for different types of thyroid cancer and these techniques and their applications are discussed in this chapter.

POSITRON EMISSION TOMOGRAPHY

Positron emission tomography (PET) imaging is a technique used in nuclear medicine which is based on the use of positron emitting isotopes in specific molecules which are relevant for specific metabolic pathways. The PET technique yields a high resolution and the capability to quantify the amount of radioactivity measured in a specific region.

Positrons, emitted by an unstable atom nucleus, are the antiparticles of electrons and have the same mass, but an opposite charge. Not the positrons are detected by a PET camera, but the photons, which are formed when a positron fuses with an electron. This means that the positron binds with an electron to form a positronium which annihilates. In this annihilation process all the mass is converted into energy by which two photons are formed. These photons, always carrying an energy of 511 keV, are emitted in opposite directions under an angle of 180° and are detected by the PET camera (Bailey et al. 2003).

Radioisotopes used in PET imaging usually have a short half live, such as carbon-11(^{11}C; half-life ($T_{½}$) 20 min), nitrogen-13 (^{13}N; $T_{½}$ 10 min), oxygen-15(^{15}O; $T_{½}$ 2 min) and fluorin-18(^{18}F; $T_{½}$ 110 min). Positron emitting radionuclides are in most cases produced by bombarding the target material with highly accelerated particles (deuterons or protons) using a cyclotron and inducing a nuclear reaction. Centers which use isotopes with a very short half life, such as ^{15}O, ^{13}N and ^{11}C , need to have an on-site cyclotron. Other, longer living isotopes, can be made elsewhere and then transported to the PET imaging facility. (Mason and Mathis 2003).

A cyclotron is a type of particle accelerator which accelerates charged particles using a high-frequency, alternating voltage. A perpendicular magnetic field causes the particles to assume a circular orbit so that they re-encounter the accelerating voltage many times. When the particles are accelerated fast enough they are bombarded on to specific atoms and radionuclides are formed. These radionuclides are trapped and transported to the laboratory where they can be processed for clinical use. The resulting end-products are called (radio-) tracers. The most commonly used tracers are precursors for metabolic pathways, although many other tracertypes exist. After preparation and careful quality monitoring, tracers can be injected.

The imaging device used is the PET camera. Most PET cameras consist of a ring of special detectors which are well suited for the detection of 511 keV gamma rays. Software registers only simultaneously entering photonpairs on different detectors. This is called coincidence detection. Coincidence detection removes the need for a lead collimator such that the sensitivity of the PET imaging system is much higher than for the conventional Anger camera that is used in planar nuclear imaging or single photon emission computed tomography (SPECT). Both the specific block detector structure and the absence of a collimator contribute to a higher resolution as compared with SPECT. Another advantage of PET is that the amount of radioactivity injected in the body can be quantitatively determined. PET is a non-invasive and sensitive imaging tool for depicting of molecular and biochemical processes without changing its physical properties (Bailey et al. 2003).

In contrast to radiologic imaging which shows the morphologic structures, nuclear medicine techniques depict (patho-)physiological processes and are also described as functional imaging methods. The imaging with PET is considered to be an useful diagnostic tool for the detection of cancer, brain diseases and coronary artery diseases.

Combined PET/CT

The combination of PET and CT scanning is a new promising imaging technique. The integrated PET/CT scanner allows acquisition of CT and PET images in one session. The combination of morphologic and functional imaging leads to more precise anatomical localization of tumor lesions. The localization of tumor foci is important for initiating the appropriate treatment such as surgery. Especially in patients with a negative radioiodine scan where surgery is the only therapeutic option, the integrated PET/CT scan can be helpful in guiding therapeutic management.

^{18}FLUORINE-FLUORODEOXYGLUCOSE (^{18}F-FDG)

Mechanism

Fluorodeoxyglucose (FDG) is a glucose analogue and is used as a precursor for glucose metabolism. In both benign and malignant tissue it enters the cell by the same glucose transporters. However, the need for glucose in malignant cells is strongly increased because these cells have a considerably less efficient energy metabolism (Warburg 1930). For example, the energy production per molecule of glucose in malignant cells is decreased because anaerobic glycolysis is strongly increased instead of the much more efficient energy production from the citric acid cycle. This inefficient use of glucose is the basis for the preferential uptake of glucose or an offered glucose analogue as FDG in malignant cells.

In the cell FDG is phosphorylated by a hexokinase enzyme into FDG-6 phosphate which, in contrast to glucose-6-phospate, cannot be further metabolized. Therefore the FDG-6-phosphate does not leave the cell and becomes trapped intracellulary. The final quantity of FDG-6-phosphate is proportional to the glycolytic rate of the cell. Besides the increased glycolysis, it has been demonstrated that in malignant cells levels of transmembrane glucose transporters (e.g. the GLUT-1 transporter) and possibly some hexokinase isoenzymes are also increased, also resulting in increased FDG uptake (Brown et al. 2002).

However, in all metabolically active tissues, such as brain cells, active muscles and also activated macrophages, increased glucose metabolism leads to an increased FDG uptake. ^{18}F-FDG PET is therefore a marker for glucose metabolism in general. In most normal tissues (e.g. liver, kidney, intestine, muscle and some tumor cells) the level of phosphate activity is variable, but nevertheless FDG-6-phospate accumulation is lower than in malignant tissues. In addition, some benign tissues require more glucose (Kubota et al. 1992; Strauss 1996).

So, the uptake mechanism of FDG with irreversible trapping in malignant tissue is ideal for PET imaging and has been applied widely in oncology. However, it is important to make a correct interpretation of these PET images for also non-malignant tissue has FDG uptake.

Scan Method

Uptake of ^{18}F-FDG occurs rapidly after administration and the amount taken up increases over time. The most applicated imaging moment is 60–90 min after tracer administration. This is because of the excretion of ^{18}F-FDG via the kidneys reducing ^{18}F-FDG in the blood, which causes clearance of 'background' uptake and the decay of fluorin-18 (T½ = 110 min). Generally the patient preparation consists of an ^{18}F-FDG injection in a fasting condition and after oral prehydration. The injected dose varies between 2–8 MBq/kg.

Clinical Application

Thyroid Nodules

The value of ^{18}F-FDG PET in the distinction between malignant and benign thyroid nodules before surgery is unclear. Several studies (de Geus-Oei et al. 2006; Kresnik et al. 2003; Mitchell et al. 2005) reported that ^{18}F-FDG PET is useful in the preoperative evaluation of cytological inconclusive nodules with a high negative predictive value. de Geus-Oei et al. (2006) observed that the probability for thyroid cancer increased from 14% (pre-PET) to 32% (post-PET) in case the nodule was positive on ^{18}F-FDG PET. In this study ^{18}F-FDG PET could reduce the number of futile hemithyroidectomies by 66%.

However, recent studies by Kim et al. (2007) and Bogsrud et al. (2007) demonstrated that ^{18}F-FDG PET is not helpful in differentiating between malignant and benign nodules and therefore has only limited value in preoperative evaluation of indeterminate thyroid nodules.

So, conflicting results are reported on the usefulness of ^{18}F-FDG PET in the prediction of malignancy in thyroid nodules in case of inconclusive cytology and further research is needed. Meanwhile histopathological examination remains the gold standard.

Differentiated Thyroid Cancer (DTC): Follow-Up

More information is available about the value of ^{18}F-FDG PET in the follow-up of thyroid cancer such as the detection of recurrences or metastases, especially in patients with a negative radioiodine scan or in patients who have lost the ability to accumulate iodine. A complementary uptake of ^{18}F-FDG and radioiodine can be present, which is known as the 'flip-flop' phenomenon and was first described by Joensuu and Ahonen (1987). This phenomenon might be explained by the degree of tissue differentiation. Well differentiated thyroid tissue has the capability to take up iodine but is metabolically inactive while less differentiated thyroid cancer tissue looses its capability to trap iodine and becomes metabolically more active. This makes ^{18}F-FDG PET scanning the method of choice for the detection of ^{131}I negative metastases of differentiated thyroid carcinoma (Grunwald et al. 1996–1998; Wang et al. 1999; Schlüter et al. 2001).

Performance of ^{18}F-FDG PET during TSH stimulation improves the results in comparison to the scanning during the euthyroid state (during thyroxin treatment) as was shown by van Tol et al. (2002). In vitro studies (Filetti et al. 1987; Hosaka et al. 1992) have shown a stimulating effect of TSH on Glut 1 expression and glucose transport. This increase in glucose carriers results in a higher uptake of glucose and also ^{18}F-FDG in thyroid cancer cells, which improves the result of the PET-scan.

Stimulation with exogenous TSH (recombinant human (rh) TSH) also increases ^{18}F-FDG uptake by differentiated thyroid cancer and therefore more lesions can be detected and tumor/background contrast is enhanced (Petrich et al. 2002; Chin et al. 2004). The influence of rhTSH on the background is not well-known, but there is evidence that rhTSH increases ^{18}F-FDG uptake in the tumor lesion itself.

Several studies have been performed to asses the value of ^{18}F-FDG PET imaging in the follow up of thyroid cancer. Hooft et al. (2001) performed a meta-analysis of studies that investigated the role of ^{18}F-FDG PET in patients with thyroid cancer after negative radioiodine scintigraphy and elevated serum thyroglobulin. The diagnostic accuracy of these studies was assessed. Observed sensitivity and specificity in these studies were ranging from 70–95% and 77–100%, respectively. Furthermore, they observed that there are methodological problems in these studies such as small sample size, validity of reference tests and short follow-up. Nonetheless, ^{18}F-FDG PET is now considered a valuable diagnostic imaging tool in the follow-up of ^{131}I-negative patients for the detection of recurrences or metastases.

However, it is not known whether PET is superior to bone scintigraphy in the detection of bone metastases in thyroid cancer. Comparative studies of bone scans and ^{18}F-FDG PET are lacking. In a retrospective study 24 patients had undergone both ^{18}F-FDG PET and bone scans within 6 months because of suspected bone metastases (Phan et al. 2007b). This study shows that bone scintigraphy is still valuable in differentiated thyroid cancer as it was found that 38% of bone metastases could be missed on ^{18}F-FDG PET. Further prospective studies in a higher number of patients are required to define the exact role of bone scan and ^{18}F-FDG PET in the detection of bone metastases in patients with differentiated thyroid cancer (DTC) (see Figure 27.1).

Combined or integrated ^{18}F-FDG PET/CT in patients with negative ^{131}I scans and elevated thyroglobulin (Tg) showed that the diagnostic accuracy can be improved compared to ^{18}F-FDG PET or CT alone. The combination of these imaging techniques has also led to a change in patient management and therapy e.g. extension of surgery, by providing precise anatomical localization of the recurrent or metastatic disease (Shammas et al. 2007).

Medullary Thyroid Cancer (MTC)

The detection of recurrence or metastases in MTC is difficult and there is no single method sensitive enough to reveal all MTC recurrence or metastasis. In comparison with the calcitonin tumor marker nearly all imaging modalities (ultrasonography, CT, MRI and scintigraphy) have limited sensitivities. The clinical role of ^{18}F-FDG PET in the diagnosis and staging of recurrent and metastatic MTC seems promising (Nanni et al. 2006).

The sensitivity and specificity of ^{18}F-FDG PET ranges between 73–88% and 76–80%, respectively. In a study by de Groot et al. (2004) ^{18}F-FDG PET was performed in patients with elevated serum tumor markers after total thyroidectomy. Compared with ^{111}In-octreotide imaging (lesion based sensitivity: 41%), ^{99m} Tc(V) DMSA scintigraphy (57%) and morphological imaging (87%), ^{18}F-FDG PET (96%) was superior. However morphological imaging will always be needed since ^{18}F-FDG PET only yields functional data

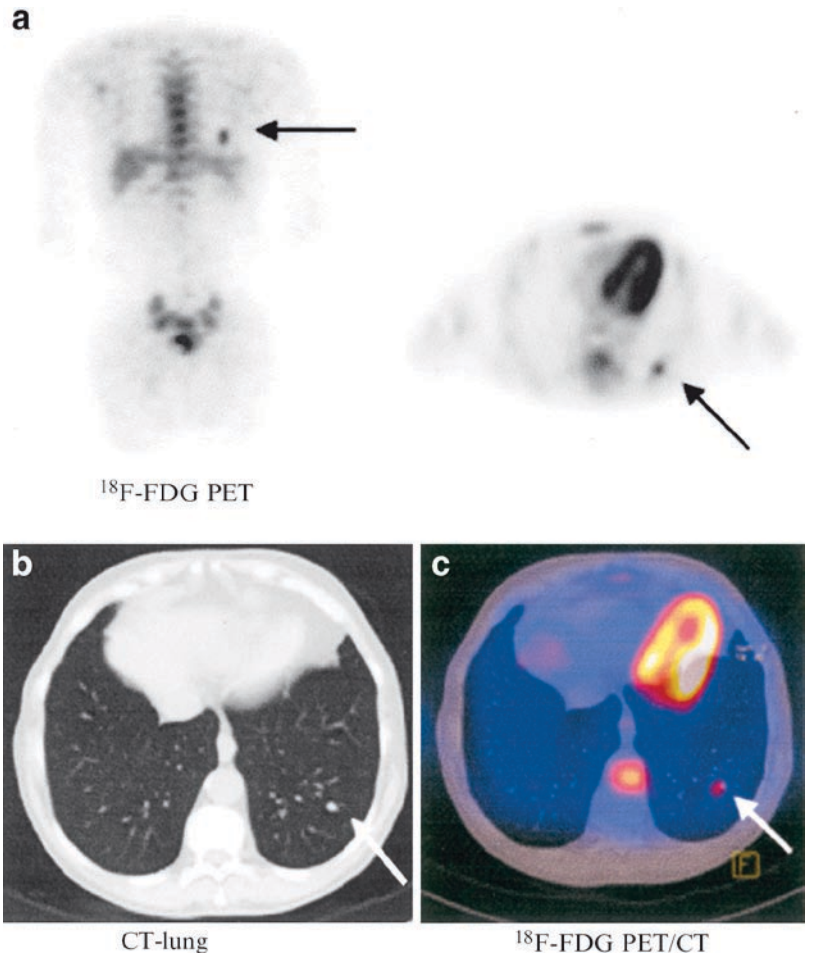

FIGURE 27.1. These are the images of an 68-year old male known with follicular thyroid cancer. This patient showed increased serum Tg level (14 ng/mL) suspected for recurrent or metastatic disease. Blind treatment with ^{131}I was given followed by a post-treatment whole body scan (WBS) after 10 days which was negative. ^{18}F-FDG PET (**a**) showed a focal lesion in the lower lobe of the left lung (*arrow*), confirmed by CT (**b**, *arrow*). Picture (**c**) showed the fusion image of ^{18}F-FDG PET and CT for the lesion in the left lung (*arrow*)

and no morphological information, which is necessary to assess resectability.

The combination of ^{18}F-FDG PET/CT can have a useful role in medullary thyroid cancer. As only surgery can cure the disease, precise anatomical localization and the extent of the recurrent or metastatic disease is mandatory. However, little data and case reports have showed an increased diagnostic accuracy and further studies are needed (Nanni et al. 2006).

^{18}FLUORINE-DIHYDROXYPHENY-LALANINE (^{18}F-DOPA)

Mechanism

The mechanism responsible for uptake of ^{18}Fluorine-dihydroxyphenylalanine (^{18}F-DOPA) in medullary thyroid carcinoma is probably the strongly upregulated transmembrane transport of amino acids through

the large amino acid transporters in medullary thyroid carcinoma cells. It is not yet clear whether the increased uptake of ^{18}F-DOPA PET is the result of the increased transporter capabilities or the increased metabolic activity of the catecholamine pathway. After transmembrane transport, ^{18}F-DOPA is intracytoplasmatically converted into dopamine by the enzyme aromatic acid decarboxylase (AADC). The formed ^{18}F-dopamine is transported into secretory vesicles through the vesicular mono aminoacid transporters (VMAT) in which it can be further metabolized to ^{18}F-noradrenalin and ^{18}F-adrenalin (Pearse 1974).

Although the ^{18}F atom influences the metabolism of ^{18}F-DOPA there is no or little effect on the transport into the intracellular environment. In the kidneys, ^{18}F-DOPA is rapidly converted into^{18}F-dopamine which is than excreted actively in urine. This conversion can be inhibited by oral administration of carbidopa prior to tracer administration (Brown et al. 1998).

Carbidopa also lowers the physiological uptake of ^{18}F-DOPA in the pancreas, but it is yet unknown which mechanism is responsible for this decrease in pancreatic uptake. The reduction in renal and urinary activity leads to a better image quality in the surroundings of the urinary system. Also, the reduced uptake in the pancreas makes the identification of lesions in the pancreatic region easier. It can be speculated that by reducing the excretion of ^{18}F-DOPA, more ^{18}F- DOPA is available for neuroendocrine tumor lesions; thereby increasing the tumor to background ratio, leading to a better discrimination of neuroendocrine lesions.

Scan Method

In most centers, patients are prepared with oral administration of carbidopa, either in a fixed dose or in a dose calibrated to bodyweight. Patients are scanned in a fasting condition for 4–6 h. In most centers a whole body study will be performed ranging from the skull to the upper femora. The average injected dose is 200 MBq, the radiation burden ~4 mSv (Brown et al. 1998). Attenuation correction is applied, either by using a CT in a PET-CT machine or by using camera-specific attenuation protocols.

Clinical Application

Medullary Thyroid Cancer

Although ^{18}F-DOPA PET is not yet widespread used, it is a promising new functional imaging procedure for imaging neuroendocrine tumors (see Figure 27.2). More and more centers gain access to this tracer either via on site production or production elsewhere. Hoegerle et al. (2001) were the first to describe the use of ^{18}F-DOPA PET in medullary thyroid cancer. In this study ^{18}F-DOPA PET was compared with ^{18}F-FDG PET, SRS and CT/MRI. A high precision of ^{18}F-DOPA PET was observed in the diagnosis of lymph node metastases (sensitivity 88%) while organ metastases were better detected with conventional imaging (sensitivity 13%). In the recently published study by Koopmans et al. (2006) diagnostic accuracy was assessed for ^{18}F-DOPA PET in patient with carcinoid tumors which are, like medullary thyroid carcinoma, neuroendocrine tumors. Compared to conventional somotostatine receptor scintigraphy (SRS) they showed improved sensitivity of ^{18}F-DOPA PET in staging and identification of carcinoid tumors.

The value of ^{18}F-DOPA PET for the detection of recurrent or residual disease in 21 patients with postsurgical elevated calcitonin or CEA was assessed by Koopmans et al. (2007). They compared ^{18}F-DOPA

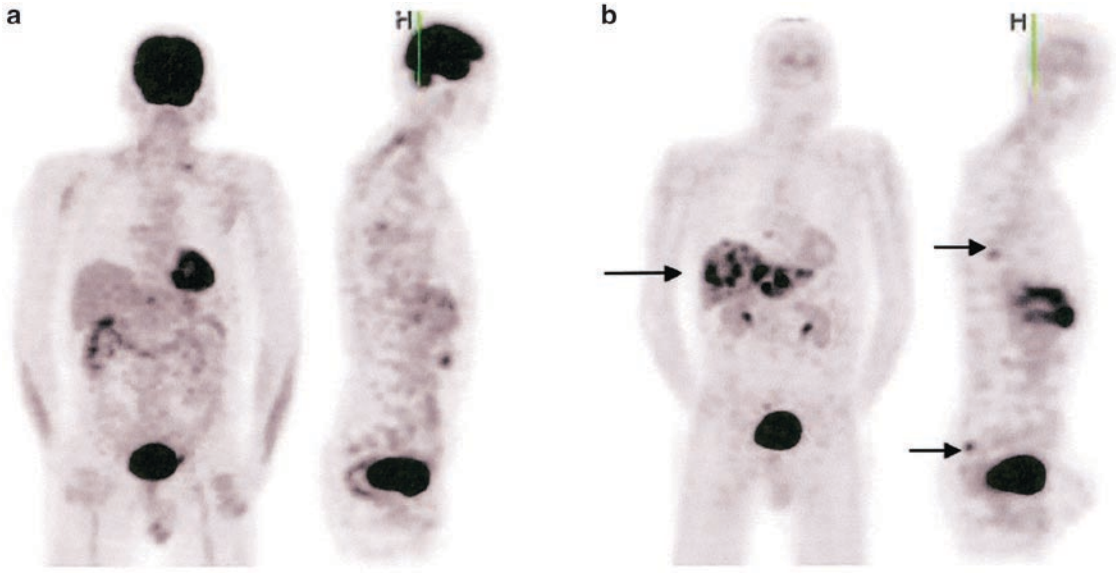

FIGURE 27.2. These are the images of a patient known with medullary thyroid cancer. In this patient ^{18}F-FDG PET (**a**) and ^{18}F-DOPA PET (**b**) were performed. The ^{18}F-DOPA PET (**b**) showed multiple lesions in the liver and several lesions in the spinal column (*arrows*) while the ^{18}F-FDG PET showed hardly any lesions

PET with ^{18}F-FDG PET, ^{99m}T(V)DMSA and CT/MRI. ^{18}F-DOPA PET was superior to conventional imaging for the detection of MTC on patient (sensitivity 87%) and regional (89%) level. On lesional level ^{18}F-DOPA PET (sensitivity 71%) was equal to morphological imaging (64%) but superior to ^{18}F-FDG PET (30%) and ^{99m}T(V) DMSA(19%).

In the recent study by Beuthien-Baumann et al. (2007) ^{18}F-DOPA-PET also seems to be more specific than ^{18}F-FDG PET for the detection of metastases of MTC. Thus, compared with ^{18}F-FDG PET and conventional imaging techniques ^{18}F-DOPA PET provides better results in the imaging of medullary thyroid cancer. However it is still unclear if this improved imaging results in different therapeutic approaches and further research is needed.

^{11}C-METHIONINE (MET) PET

Mechanism

Proteins play an important role in virtually all biological processes. Proteins are built from a set of 20 amino acids. Amino acid transport across the cell membranes into the cells occurs primarily via carrier-mediated processes. Amino acid transport is generally increased in malignant transformation (Jager et al. 2001; Isselbacher 1972; Busch et al. 1959). This increased protein metabolism in cancer cells is interesting for metabolic tumor imaging, for which radiolabeled amino acids can be applied. These amino acid tracers could help in imaging areas where ^{18}F-FDG is limited such as the interference of high (physiologic) ^{18}F-FDG uptake in the brain. Another reason is that amino acid imaging

is less influenced by inflammatory disease. The most frequent used radiolabeled amino acid is L-[methyl-^{11}C]-methionine. Normal biodistribution of radiolabeled methionine includes the pancreas, liver, spleen, kidney and salivary glands.

Scan Method

^{11}C-MET-PET scanning can be performed 10 to 20 min after intravenous injection of a fixed dose or a dose calibrated on body-weight (range 70 to 1, 100 MBq in the literature), in a fasting condition for 2–6 h. Images are corrected, either by using a CT in a PET-CT machine or by using camera-specific attenuation protocols.

Clinical Application

Differentiated Thyroid Cancer

The need for new tracers and improvement of diagnostic tools in thyroid cancer is growing. So far, no data on the application of methionine (MET) PET in thyroid cancer are available. The general feasibility of amino acid imaging in many tumor types has thus far sufficiently been shown (Jager et al. 2001).

It is imaginable that thyroid cancer could sufficiently concentrate amino acids due to its metabolically inert nature and high protein synthesis (e.g. thyroglobulin). In a feasibility study by Phan et al. (2008b), ^{11}C-MET PET has been compared with ^{18}F-FDG PET in the detection of recurrent or metastatic disease in 20 patients with negative ^{131}I scans and elevated Tg. Six of the 20 patients showed uptake on both PET scans, but the abnormalities were more ^{18}F-FDG-avid and more extensive on the ^{18}F-FDG PET in 3 patients. In 4 of the 20 patients uptake was only observed on the ^{11}C-MET PET, however, no anatomical localization could be confirmed. For now, the significance of the MET uptake in these four patients is unclear, so the clinical value of ^{11}C-MET PET in the detection of recurrent DTC disease still has to be proven in the (long-term) follow-up (Figure 27.3).

^{124}I-PET

Mechanism

Iodine-124 is a positron emitting isotope, which is suitable for positron emission tomography (PET) imaging, with a half-life of 4.2 days (Pentlow et al. 1996). This isotope has been used for dosimetric purposes or thyroid volume measurements (Eschmann et al. 2002). While the radio-isotopes ^{123}I and especially ^{131}I are used on a wide scale in diagnosis and treatment of many thyroid disorders, ^{124}I has received little attention. Chemically identical to non-radioactive iodine, this radio-isotope allows thyroid cancer imaging with the high resolution PET technique (Pentlow et al. 1996; Eschmann et al. 2002).

Scan Method

The ^{124}I -PET scan can be obtained 24 h to 6 days after administration of 74–100 MBq of ^{124}I. A whole body PET scan (from the upper thigh up until the top of the skull) can be performed in 2D or 3D mode, using standard energy window setting of 350–650 keV (or energy window setting 425–650 keV or 460–562 keV in case of the presence of high amounts of ^{131}I (Lubberink et al. 2006).

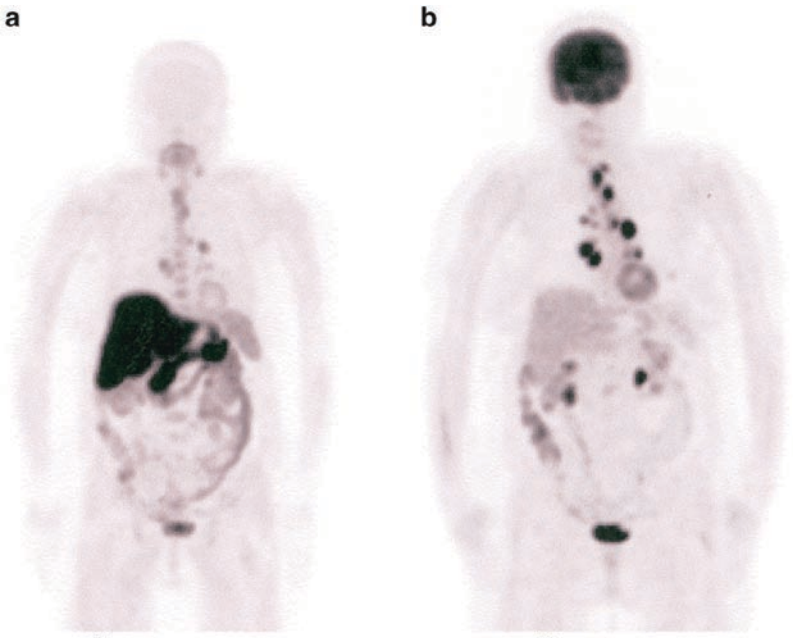

FIGURE 27.3. These are the images of a 68-year old female known with papillary thyroid cancer. This patient had unreliable Tg due to the presence of Tg antibodies (which where increasing in the course of the follow-up). The post-treatment ^{131}I whole body scan (WBS) was negative. Due to suspicion of dedifferentiated, metastatic disease ^{11}C-MET PET (**a**) and ^{18}F-FDG PET (**b**) were performed. ^{11}C-MET PET (**a**) showed lesions in the mediastinum with slightly to moderate ^{11}C-MET uptake. ^{18}F- FDG PET (**b**) also showed multiple lesions in the mediastinum, but the lesions showed clearly higher ^{18}F-FDG uptake and the abnormalities were more extensive

Clinical Application

Differentiated Thyroid Cancer

Accumulation of iodine is a highly specific characteristic for differentiated thyroid cancer (DTC) cells. In patients with increasing or recurrent detectable Tg a blind treatment (meaning after a negative diagnostic ^{131}I scan) with high dose ^{131}I followed by a post-treatment ^{131}I scan is used as a diagnostic tool. However, this strategy with (unnecessary) high radiation exposure must be taken into account in patients without ^{131}I uptake in their metastases. Besides the high radiation exposure there is a high TSH level which potentially stimulates thyroid cancer cell growth.

Based on the higher spatial resolution, ^{124}I-PET is potentially able to detect recurrent disease in DTC with a higher sensitivity than (diagnostic) ^{131}I scans. With this higher sensitivity and the possibility to combine the ^{124}I-PET scan with morphologic imaging such as CT data, an appropriate therapeutic decision in terms of surgery and/or additional high dose ^{131}I can be made. ^{124}I-PET imaging might therefore become the diagnostic tool of choice in the follow-up of DTC. In the study by Freudenberg et al. (2004) ^{124}I-PET (/CT) modalities were compared with the high dose ^{131}I-WBS in 12 patients with DTC. They showed an overall lesion detectability of 87%, 83% and 100% for

^{124}I, ^{131}I-WBS and combined ^{124}I-PET/CT respectively. So, these ^{124}I-PET (/CT) modalities are promising diagnostic tools and are a suitable alternative to the high dose ^{131}I-WBS in the follow-up of DTC patients.

In a prospective, feasibility study by Phan et al. (2008a) 20 patients with advanced DTC (T4, extranodal tumor growth, distant metastasis) underwent a low-dose diagnostic ^{131}I scan, a ^{124}I PET scan and a high-dose (posttreatment) ^{131}I scan. The ^{131}I images were compared to the ^{124}I PET images. ^{124}I-PET proved to be a superior diagnostic tool as compared to low dose diagnostic ^{131}I scans and showed comparable findings with the post-treatment ^{131}I-WBS which was in agreement with the study by Freudenberg et al. (2004) and Abdul Fatah et al. (2007). Therefore, ^{124}I-PET could be used as a diagnostic tool in the follow-up of patients with DTC for the favorable radiation exposure burden compared to the high dose diagnostic ^{131}I-WBS and the superior diagnostic accuracy compared to low dose diagnostic ^{131}I-WBS and the fusion possibility with CT which improves clinical decision making (Figure 27.4).

CONCLUSION

This chapter of PET imaging in thyroid cancer gives an overview of the different PET techniques available in thyroid cancer. PET imaging is based on two principles: the ability of unstable atom nucleus to emit positrons and the labeling of organic molecules, which are used in specific metabolic pathways.

For differentiated thyroid cancer the most frequently used PET technique is ^{18}F-FDG PET imaging, which is based on the use of a glucose analogue. Although its application in the preoperative assessment of thyroid nodules is still unclear, it is considered a useful tool in the follow up of differentiated thyroid cancer. The use of PET/CT scanning which combines functional imaging with morphological imaging is promising, providing more accurate localization of tumor sites, which is important for further treatment.

Other PET radiotracers have been developed: the clinical value of amino acid tumor imaging with ^{11}C-MET PET is unclear and still has to be proven in the follow-up of differentiated thyroid cancer. Another relative new PET imaging technique is the iodine isotope ^{124}I. Compared with the high dose diagnostic ^{131}I whole body scan, ^{124}I PET showed similar findings and can therefore be used as a diagnostic tool in the follow-up of differentiated thyroid cancer.

For the follow-up of medullary thyroid cancer ^{18}F-FDG PET is also the most employed imaging technique. However ^{18}F-DOPA PET, which is based on a precursor of dopamine, seems to be superior compared to ^{18}F-FDG PET in the follow up of medullary thyroid cancer. A potential new tracer is ^{11}C-5-HTP, which is based on a precursor of serotonin and already has been applied in neuroendocrine tumors. The value of this technique has to be further assessed in medullary thyroid cancer.

The need for new tracers and advanced PET imaging to improve the diagnostic sensitivities and accuracy in detection, staging and follow-up of thyroid cancer patients is growing. Knowledge of the pathogenesis, the molecular characteristics and the behavior of the tumor cell is crucial for developing of specific tracers and

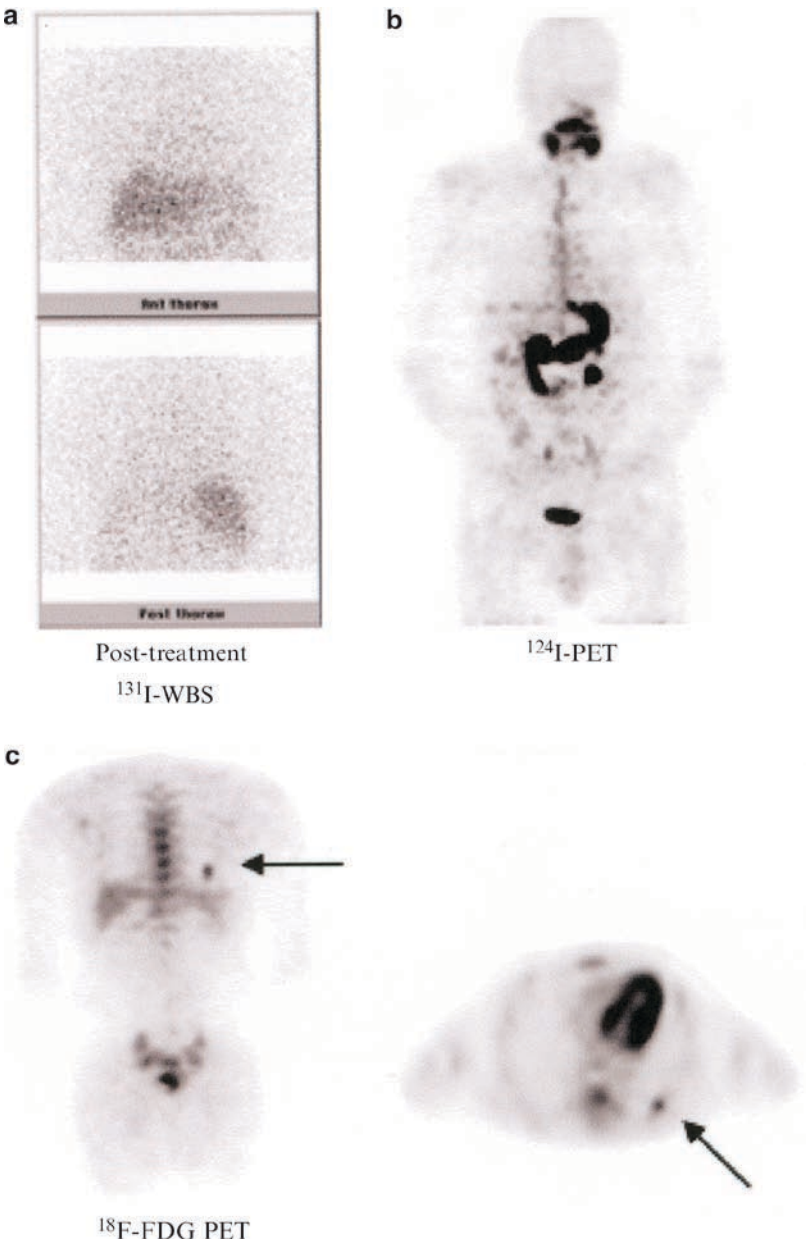

FIGURE 27.4. These are the images of a 68-year old male known with follicular thyroid cancer. This patient showed increased serum Tg level (14 ng/mL) suspected for recurrent or metastatic disease. Blind treatment with ^{131}I was given followed by a post-treatment whole body scan (WBS) after 10 days (**a**), which was negative. The ^{124}I-PET (**b**) was also negative, besides physiological uptake in the salivary glands, esophagus, gastro-intestinal tract, kidney and bladder. ^{18}F-FDG PET (**c**) showed a focal lesion in the lower lobe of the left lung (arrow), confirmed by CT. This complementary uptake of radioiodine and ^{18}F-FDG is known as the flip-flop phenomenon

techniques, e.g. radiolabeled Tg, (rh) TSH. Although new tracers are developed and applied in patients, little data is available on the changes in therapeutic management these new PET-techniques give. While PET-imaging is still in development, more

research is needed to asses the effects on therapy of these new developments. In conclusion, PET imaging is a useful diagnostic tool in thyroid cancer and new promising techniques are developed which could further improve the diagnostic accuracy and therapeutic approaches.

REFERENCES

Abdul Fatah S, Brans B, Huijberts M, Sels J, Nieuwenhuijzen Kruseman A, Teule G (2007) Impact of I-124 PET-CT in the loco-regional staging of differentiated thyroid carcinoma [abstract]. J Nucl Med 48(suppl):127

Bailey DL, Karp JS, Surti S (2003) Physics and instrumentation in PET. In: Valk PE, Bailey DL, Townsend DW, Maisey MN (eds) Positron Emission Tomopgraphy; Basic Sience and Clinical Practice, pp 41–67. Springer, London

Beuthien-Baumann B, Strumpf A, Zessin J, Bredow J, Kotzerke J (2007) Diagnostic impact of PET with (18)F-FDG, (18)F-DOPA and 3-O-methyl-6-[(18)F]fluoro-DOPA in recurrent or metastatic medullary thyroid carcinoma. Eur J Nucl Med Mol Imag. 10:1604–1609

Bogsrud TV, Karantanis D, Nathan MA, Mullan BP, Wiseman GA, Collins DA, Kasperbauer JL, Strome SE, Reading CC, Hay ID, Lowe VJ (2007) The value of quantifying 18F-FDG uptake in thyroid nodules found incidentally on whole-body PET-CT. Nucl Med Commun 28:373–381

Brown WD, Oakes TR, DeJesus OT, Taylor MD, Roberts AD, Nickles RJ, Holden JE (1998) Fluorine-18-fluoro-L-DOPA dosimetry with carbidopa pretreatment. J Nucl Med 39:1884–1891

Brown RS, Goodman TM, Zasadny KR, Greenson JK, Wahl RL (2002) Expression of hexokinase II and Glut-1 in untreated human breast cancer. Nucl Med Biol 29:443–453

Busch H, Davis JR, Honig GR, Anderson DC, Nair PV, Nyhan WL (1959) The uptake of a variety of amino acids into nuclear proteins of tumors and other tissues. Cancer Res 19:1030–1039

Chin BB, Patel P, Cohade C, Ewertz M, Wahl R, Ladenson P (2004) Recombinant human thyrotropin stimulation of fluoro-D-glucose positron emission tomography uptake in well-differentiated thyroid carcinoma. J Clin Endocrinol Metab 89:91–95

de Geus-Oei LF, Pieters GFMM, Bonenkamp JJ, Mudde AH, Bleeker-Rovers CP, Corstens FHM, Oyen WJG (2006) 18F-FDG PET reduces unnecessary hemithyroidectomies for thyroid nodules with inconclusive cytologic results. J Nucl Med 47:770–775

de Groot JW, Links TP, Jager PL, Kahraman T, Plukker JT (2004) Impact of 18F-fluoro-2-deoxy-D-glucose positron emission tomography (FDG PET) in patients with biochemical evidence of recurrent or residual medullary thyroid cancer. Ann Surg Oncol 11:786–794

Eschmann SM, Reischl G, Bilger K, Kupferschlager J, Thelen MH, Dohmen BM, Besenfelder H, Bares R (2002) Evaluation of dosimetry of radioiodine therapy in benign and malignant thyroid disorders by means of iodine-124 and PET. Eur J Nucl Med 29:760–767

Filetti S, Damante G, Foti D (1987) Thyrotropin stimulates glucose transport in cultured rat thyroid cells. Endocrinology 120:2576–2581

Freudenberg LS, Antoch G, Jentzen W, Pink R, Knust J, Gorges R, Muller SP, Bockisch A, Debatin JF, Brandau W (2004) Value of (124) I-PET/CT in staging of patients with differentiated thyroid cancer. Eur Radiol 14:2092–2098

Grunwald F, Schomburg A, Bender H, Klemm E, Menzel C, Bultmann T, Palmedo H, Ruhlmann J, Kozak B, Biersack HJ (1996). Fluorine-18 fluorodeoxyglucose positron emission tomography in the follow-up of differentiated thyroid cancer. Eur. J. Nucl. Med. 23:312–319

Grunwald F, Menzel C, Bender H, Palmedo H, Willkomm P, Ruhlmann J, Franckson T, Biersack HJ (1997) Comparison of 18FDG PET with 131iodine and 99mTc-sestamibi scintigraphy in differentiated thyroid cancer. Thyroid. 7: 327–335

Hoegerle S, Altehoefer C, Ghanem N, Brink I, Moser E, Nitzsche E (2001) 18F-DOPA positron emission tomography for tumour detection in patients with medullary thyroid carcinoma and elevated calcitonin levels. Eur J Nucl Med 28:64–71

Hooft L, Hoekstra OS, Deville W, Lips P, Teule GJ, Boers M, van Tulder MW (2001) Diagnostic accuracy of 18F-fluorodeoxyglucose positron emission tomography in the follow-up of

papillary or follicular thyroid cancer. J Clin Endocrinol Metab 86:3779–3786

Hosaka Y, Tawata M, Kurihara A, Ohtaka M, Endo T, Onaya T (1992) The regulation of two distinct glucose transporter (GLUT1 and GLUT4) gene expressions in cultured rat thyroid cells by thyrotropin. Endocrinology 131:159–165

Isselbacher KJ (1972) Sugar and amino acid transport by cells in culture – differences between normal and malignant cells. N Engl J Med 286:929–933

Jager PL, Vaalburg W, Pruim J, de Vries EGE, Langen KJL, Piers DA (2001) Radiolabeled amino acids: basic aspects and clinical applications in oncology. J Nucl Med 42:432–445

Joensuu H, Ahonen A (1987) Imaging of metastases of thyroid carcinoma with fluorine-18 fluorodeoxyglucose. J Nucl Med 28:910–914

Kim JM, Ryu JS, Kim TY, Kim WB, Kwon GY, Gong G, Moon DH, Kim SC, Hong SJ, Shong YK (2007) 18F-fluorodeoxyglucose positron emission tomography does not predict malignancy in thyroid nodules cytologically diagnosed as follicular neoplasm. J Clin Endocrinol Metab 92:1630–1634

Koopmans KP, de Vries EG, Kema IP, Elsinga PH, Neels OC, Sluiter WJ, van der Horst-Schrivers AN, Jager PL (2006) Staging of carcinoid tumours with 18F-DOPA PET: a prospective, diagnostic accuracy study. Lancet Oncol 7:728–734

Koopmans KP, de Groot JWB, Plukker JTM, de Vries EGE, Kema IP, Sluiter WJ, Jager PL, Links TP (2008) 18F-dihydroxyphenylalanine PET in patients with biochemical evidence of medullary thyroid cancer: relation to tumor differentiation. J Nucl Med. 4:524–531

Kresnik E, Gallowitsch HJ, Mikosch P, Stettner H, Igerc I, Gomez I, Kumnig G, Lind P (2003) Fluorine-18-fluorodeoxyglucose positron emission tomography in the preoperative assessment of thyroid nodules in an endemic goiter area. Surgery 133:294–299

Kubota R, Yamada S, Kubota K, Ishiwata K, Tamahashi N, Ido T (1992) Intratumoral distribution of fluorine-18-fluorodeoxyglucose in vivo: high accumulation in macrophages and granulation tissues studied by microautoradiography. J Nucl Med 33:1972–1980

Lubberink M, van Schie A, de Jong HW, van Dongen GA, Teule GJ (2006) Acquisition settings for PET of ^{124}I administered simultaneously with therapeutic amounts of ^{131}I. J Nucl Med 47:1375–1381

Mason NS, Mathis CA (2003) Radiohalogens for PET imaging. In: Valk PE, Bailey DL, Townsend DW, Maisey MN (eds) Positron emission tomopgraphy basic sience and clinical practice, Springer, London, pp 217–236

Mitchell JC, Grant F, Evenson AR, Parker JA, Hasselgren PO, Parangi S (2005) Preoperative evaluation of thyroid nodules with 18FDG PET/CT. Surgery 138:1166–1174

Modigliani E, Cohen R, Campos JM, Conte-Devolx B, Maes B, Boneu A, Schlumberger M, Bigorgne JC, Dumontier P, Leclerc L, Corcuff B, Guilhem I (1998) Prognostic factors for survival and for biochemical cure in medullary thyroid carcinoma. Results in 899 patients. The GETC study group. Groupe d'etude des tumeurs a calcitonine. Clin Endocrinol 48:265–273

Nanni C, Rubello D, Fanti S, Farsad M, Ambrosini V, Rampin L, Banti E, Carpi A, Muzzio P, Franchi R (2006) Role of 18F-FDG PET and PET/CT imaging in thyroid cancer. Biomed Pharmacother 60:409–413

Pearse AG (1974) The APUD cell concept and its implications in pathology. Pathol Ann 9:27–41

Pentlow KS, Graham MC, Lambrecht RM, Daghighian F, Bacharach SL, Bendriem B, Finn RD, Jordan K, Kalaigian H, Karp JS, Robeson WR, Larson SM (1996) Quantitative imaging of iodine-124 with PET. J Nucl Med 37:1557–1562

Petrich T, Borner AR, Otto D, Hofmann M, Knapp WH (2002) Influence of rhTSH on [(18) F]fluorodeoxyglucose uptake by differentiated thyroid carcinoma. Eur J Nucl Med Mol Imag 29:641–647

Phan HTT, Jager PL, Paans AMJ, Plukker JTM, Sturkenboom MGG, Sluiter WJ, Wolffenbuttel BHR, Dierckx RAJO, Links TP (2008a) The diagnostic value of 124I-PET in patients with differentiated thyroid cancer. Eur J Nucl Med Mol Imaging. 5:958–965

Phan HTT, Jager PL, Plukker JTM, Wolffenbuttel BHR, Dierckx RA, Links TP (2007) Detection of bone metastases in thyroid cancer patients: bone scintigraphy or 18F-FDG PET? Nucl Med Comm 28:597–602

Phan HTT, Jager PL, Plukker JTM, Wolffenbuttel BHR, Dierckx RAJO, Links TP (2008b)

Comparison of 11C-methionine PET and 18F-fluorodeoxyglucose PET in differentiated thyroid cancer. Nucl Med Commun. 8:711–716

Schlumberger M, Pacini F (2003) In: Epidemiology. Thyroid tumours. 2nd ed. Editions nucleon, Paris, pp 51–60

Schlüter B, Bohuslavizki KH, Beyer W, Plotkin M, Buchert R, Clausen M (2001) Impact of FDG PET on patients with differentiated thyroid cancer who present with elevated thyroglobulin and negative 131I scan. J Nucl Med 42:71–76

Shammas A, Degirmenci B, Mountz JM, McCook BM, Branstetter B, Bencherif B, Joyce JM, Carty SE, Kuffner HA, Avril N (2007) 18F-FDG PET/CT in patients with suspected recurrent or metastatic well-differentiated thyroid cancer. J Nucl Med 48:221–226

Sherman SI, Angelos P, Ball DW, Beenken SW, Byrd D, Clark OH, Daniels GH, Dilawari RA, Ehya H, Farrar WB, Gagel RF, Kandeel F, Kloos RT, Kopp P, Lamonica DM, Loree TR, Lydiatt WM, McCaffrey J, Olson JA Jr, Ridge JA, Robbins R, Shah JP, Sisson JC, Thompson NW (2005) National Comprehensive Cancer Network Thyroid carcinoma. J Natl Compr Canc Netw 3:404–457

Strauss LG (1996) Fluorine-18 deoxyglucose and false-positive results: a major problem in the diagnostics of oncological patients. Eur J Nucl Med 23:1409–1415

Tubiana M, Haddad E, Schlumberger M, Hill C, Rougier P, Sarrazin D (1985) External radiotherapy in thyroid cancers. Cancer 55:2062–2071

van Tol KM, Jager PL, Piers DA, Pruim J, de Vries EG, Dullaart RP, Links TP (2002) Better yield of (18)fluorodeoxyglucose-positron emission tomography in patients with metastatic differentiated thyroid carcinoma during thyrotropin stimulation. Thyroid 12:381–387

Venkatesh YS, Ordonez NG, Schultz PN, Hickey RC, Goepfert H, Samaan NA (1990) Anaplastic carcinoma of the thyroid. A clinicopathologic study of 121 cases. Cancer 66:321–330

Wang W, Macapinlac H, Larson SM, Yeh SD, Akhurst T, Finn RD, Rosai J, Robbins RJ (1999) [18F]-2-fluoro-2-deoxy-D-glucose positron emission tomography localizes residual thyroid cancer in patients with negative diagnostic (131)I whole body scans and elevated serum thyroglobulin levels. J. Clin. Endocrinol. Metab. 84:2291–2302

Warburg O (1930) The metabolism of tumours. Constable, London

Therapy

28
Metastasized Medullary Thyroid Carcinoma: Detection and Therapy Using Radiolabeled Gastrin Analogs

Martin Gotthardt, Lioe-Fee de Geus-Oei, Thomas M. Behr, and Martin Béhé

MEDULLARY THYROID CARCINOMA

Medullary thyroid carcinoma (MTC) belongs to the group of differentiated thyroid carcinomas. Though MTC had first been described in 1951 by Horn, it was 8 years later when Hazard et al (1959) proposed it as a clinical entity and it took another 8 years until Williams (1966) was able to demonstrate that it is derived from the calcitonin-producing C-cells of the thyroid. MTC accounts for ~5–10% of differentiated thyroid cancers. While sporadic MTC is responsible for 75% of cases, MTC can also be hereditary in 25% and may then either occur as an isolated form (called familial MTC (FMTC), 15%), or as part of the multiple endocrine neoplasia (MEN) syndrome type 2a (80%) or 2b (5%). In virtually all patients with hereditary MTC, a mutation of the RET protooncogene on chromosome 10 can be found. In patients with FMTC and MEN 2a, the mutation is mostly located in exon 11, but sometimes also in 10, 13, or 14. In patients with MEN 2b, the mutation is usually located in exon 16 (Machens et al. 2003).

Symptoms

In many cases, lymph node metastases are the first symptom to be found. Approximately, 50% of patients already have lymphogenic metastases when MTC is diagnosed. Other symptoms include palpable thyroid nodules that may be painful upon palpation. Invasion into adjacent tissues may occur, which results in decreased thyroid motion after swallowing. Late symptoms include pareses of the recurrent laryngeal nerve or compression of the trachea. Furthermore, diarrhea refractory to therapy may occur, which can also be the primary symptom though usually associated with advanced stages of disease.

Diagnostic Procedures

Pentagastrin Testing

As MTCs continue to produce calcitonin, it can be used as a tumor marker for detection of recurrent disease. To increase the sensitivity of calcitonin sampling, it should be measured after Pentagastrin stimulation. Pentagastrin binds to the CCK_2 (cholecystokinine 2) receptor which is overexpressed on MTC and stimulates calcitonin release.

For Pentagastrin stimulation testing, 0.5 μg of Pentagastrin per kg of body weight (kg BW) is injected intravenously after preinjection of 2 mg calcium/kg BW. Calcitonin sampling is done at time points 0, 2, 3, 5, and 10 min (other time points and dosages may be used dependent on the respective local or national guidelines). Pathological elevation of calcitonin is highly sensitive for recurrent disease. After successful surgical removal of the primary and all metastases, calcitonin should not be measurable. The value of standard calcitonin sampling and pentagastrin stimulation testing in otherwise healthy patients with thyroid nodules still needs to be elucidated. While single patients do profit from the test because MTC can be detected, a considerable number of patients will undergo surgery for C-cell hyperplasia or occult disease (Karanikas et al. 2004). Whether this may be over-treatment of clinically irrelevant disease is presently not clear and the value of calcitonin screening is a matter of debate (Hodak and Burman 2004).

Whiskey Stimulation Testing

It has been reported in the literature that oral application of whisky leads to an increase in serum calcitonin levels in patients with MTC (Dymling et al. 1976). Although this stimulation test may be very much favored by many patients, the available information suggests that calcitonin stimulation with pentagastrin is more efficient than stimulation testing with whisky (Emmertsen et al. 1980). Furthermore, whiskey stimulation testing did not only lead to variable results concerning post-whisky serum calcitonin concentrations but also to varying blood alcohol concentrations (Fletcher et al. 1984). Whether other alcoholic beverages may lead to more reliable results is still a matter of debate. Therefore, presently pentagastrin stimulation testing remains the main stay for biochemical diagnosis of MTC/recurrence of MTC. Although a lot can be said in favor of whisky, the whiskey stimulation test should not be used in the clinic.

Carcinoembrionic Antigen

Carcinoembrionic antigen (CEA) is less sensitive and less specific than calcitonin as a marker for MTC. However, in the follow-up of patients with MTC, it may be very useful as a marker of response to therapy as calcitonin levels may largely vary, and therefore are less reliable. Furthermore, if calcitonin levels are elevated in patients with metastatic MTC while CEA levels remain low, this is associated with a better prognosis than low calcitonin levels in combination with high CEA levels (Busnardo et al. 1984).

Ultrasound

Ultrasound (US) of the neck is highly sensitive for the detection of enlarged lymph nodes and cervical masses as well as thyroid nodules. However, the specificity is limited as it may be very difficult to differentiate between malignant and benign disease. This is especially true for thyroid nodules. The result of US is very much dependent on the experience of the person who performes the examination. An experienced sonographer may be capable of determining the nature of cervical abnormalities based on echogenicity, shape, location, signs of tissue invasion, etc.. In this context it is important to mention that US should always be interpreted by the persons performing the examination but not, as it is often practiced, by those who interpret images taken by another person.

Computed Tomography

Computed Tomography (CT) with contrast enhancement is able to detect cervical lymph nodes as well as local recurrence of MTC by detection of the masses and by typical contrast enhancement in tumor tissues. Furthermore, infiltration of surrounding tissues may also be visible on CT scans. The limitation is the low specificity in the assessment of lymph nodes based on size alone (above or below 1 cm in diameter). The strength of CT scanning is the detection of even small metastases in the lungs. If a follicular or papillary thyroid carcinoma is likely instead of MTC, no contrast agents should be used because postoperative radioiodine therapy may seriously be delayed by blockade of the iodine intake in thyroid and thyroid carcinoma tissue!

Magnetic Resonance Imaging

Magnetic Resonance Imaging (MRI) is better suitable than CT for the assessment of soft tissues. Though it is inferior to CT in the detection of lung metastases (due to long scanning times and resulting breathing/motion artifacts), it is very sensitive in the detection of cervical abnormalities and especially for the detection of mediastinal lesions. In comparison to CT, it is not a problem to apply MRI contrast medium in cases of possible papillary or follicular thyroid carcinoma as it does not contain iodine.

Positron Emission Tomography

Positron Emission Tomography (PET) using ^{18}F-FDG (fluorodeoxyglucose) as tracer can be used for detecting lesions in patients with metastatic or recurrent MTC. It is most sensitive in the detection of lesions in the neck and mediastinum. The sensitivity of FDG-PET seems to increase with calcitonin levels above 1,000 pg/mL (Ong et al. 2007). A potential advantage of PET is that it is not limited with respect to the field of view so that distant metastases can be detected which may not be located within the field of view of a CT or MRI scan. Furthermore, PET is more specific than anatomical imaging modalities. Another tracer that may be used for PET imaging is ^{18}F-DOPA, a dopamine receptor ligand. This tracer allows the detection of metastases of MTC with a higher sensitivity than FDG. ^{18}F-DOPA is also most efficient in detecting cervical and mediastinal metastases (Beuthien-Baumann et al. 2007).

Somatostatin Receptor Scintigraphy

For somatostatin receptor scintigraphy (SRS), the radiolabeled somatostatin analog octreotide is used for the detection of tumor tissue overexpressing the somatostatin receptor (to which the radiopeptide binds). As MTC belongs to the group of neuroendocrine tumors that do express somatostatin receptors to a high extent, SRS is feasible in patients with recurrent or metastatic MTC. However, expression of the somatostatin receptors strongly depends the level of differentiation of tissues. If MTC dedifferentiates, the somatostatin receptor expression will be lost resulting in false-negative scans (Behr et al. 1997). Therefore, SRS often is less useful in MTC patients than the sectional imaging methods described above with sensitivities below 50%.

Fine Needle Aspiration

Fine needle aspiration (FNA) is performed by puncturing a given abnormality with a

fine needle. This can be done based on palpation or guided by ultrasound. By applying a vacuum at the moment the tip of the needle is located within the abnormality, cells are sucked into the needle/syringe for cytological evaluation. The results of this procedure very much depend on the experience of the person performing the FNA and the pathologist who is interpreting the obtained cytological material. In most patients with MTC, FNA will not reveal the true diagnosis though a considerable number of patients may be operated on based on the result of the FNA (as, for example, a follicular neoplasia is diagnosed or suspicious cells are found). However, the value of FNA in diagnosing metastases or the primary in patients with MTC remains limited (Hodak and Burman 2004).

Selective Venous Sampling

Selective Venous Sampling (SVS) is an invasive method that helps to localize MTC lesions. A catheter is inserted into the body of the patient via the groin and pushed forward to the area where the lesions are expected, for example, the cervical veins. Blood samples are than drawn from different locations. This technique does not directly localize metastases, but it does allow to determine the draining vein, and therefore allows to limit the area which should be operated on. In addition to standard sampling, sampling can also be done after stimulation with pentagastrin resulting in a quick rise of calcitonin levels in the vein draining the blood from the affected region. High resolution US may help to further evaluate the respective area prior to operation.

LOCALIZING AND TREATING METASTATIC MEDULLARY THYROID CARCINOMA

As surgical therapy is the only therapeutic modality with a curative approach so far, localization of metastases of MTC is crucial. Although it is comparably easy to diagnose recurrent or metastatic MTC by pentagastrin stimulation testing, localization of tumor sites is much more complicated. Metastases may be very small and the growth rate of usually highly differentiated MTC is low. Therefore, it may take years between the biochemical diagnosis of recurrence and the actual detection of metastases. In addition, small metastases for example may be diffusely spread in the liver or lung. Imaging techniques may then not be able to easily detect these tiny lesions. Invasive techniques may be necessary in these cases to localize the disease. Liver metastases, for example, may be diagnosed by SVS (with respect to an organ or segment of an organ). However, if the metastases are not visualized, it is not possible to decide whether the patient may benefit from surgical therapy or not. Therefore, CT arteriography (CTA) or CT arterioportography may be performed. Both are invasive and time consuming but reliably localize even small lesions <5 mm in size. Furthermore, MRI with superparamagnetic ironoxide particles (SPIO) may help to localize metastases in the liver. SPIOs are taken up by the reticuloendothelial system (RES) of the liver and lead to lower signal intensity of healthy liver tissue in comparison to tissue without RES.

In the cervical area, lymph nodes of <1 cm in size may be detected by ultrasonography

(or CT/MRI) without signs of malignancy. PET may then allow differentiation between healthy and metastatic lymph nodes. Furthermore, by combination of PET and CT in dedicated PET/CT scanners, fusion images will be created combining morphological with metabolic information which will make it easier to identify sites of tumor involvement prior to surgery. The usefulness of the PET/CT hybrid technology in detecting various cancer types is discussed in detail in two recently published volumes (Hayat 2007).

Although these technologically advanced techniques offer much better possibilities to localize metastatic MTC at earlier stages than those used some years ago, their contribution to improveme the prognosis of patients remains questionable. Micrometastases may be spread all over the lung or liver preventing successful surgical intervention. Micrometastases may be present in locations missed by imaging so that after the operation the patient will still have elevated basal or pentagastrin-stimulated calcitonin levels. Aggressive systemic therapy such as chemotherapy is of limited value in metastasized MTC, but may be associated with considerable side effects. External beam irradiation may be used in an attempt to treat local inoperable disease but it remains questionable whether the therapeutic effects of external irradiation therapy will exceed potential (long-term) side effects. Early experimental approaches of radioimmunotherapy with ^{131}I or ^{90}Y-labeled anti-CEA antibodies, also in combination with radio-sensitizing chemotherapeutic agents, were of limited value. Also, the efficacy of myeloablative high-dose therapy with subsequent autologous stem cell transplantation did not compare favorably with toxicity (Behe and Behr 2002). However, in a recently published study, Chatal et al. (2006) were able to demonstrate an increased duration of survival in patients with metastatic MTC after 2-step radioimmunotherapy with a bivalent anti CEA/anti-DTPA antibody and a ^{131}I labeled hapten.

RADIOPEPTIDE SCANNING VERSUS ANATOMICAL IMAGING MODALITIES

Radiopeptide scanning is based on the principle of injection of a radiolabeled peptide which specifically targets a receptor overexpressed on a tumor. This radiopeptides is then taken up into and accumulates within the tumor cell while the unbound radiopeptide is cleared out of the body, preferably via the kidneys. In this way, high uptake into the target tissues can be achieved while the background activity is kept low. In addition to high target-to-background ratios, conventional nuclear medicine imaging as well as PET are very sensitive, allowing the detection of very small quantities of a radiopharmaceutical (in the range of micrograms). Furthermore, as an optimal radiopeptide will specifically accumulate only in the targeted tumor, it would also be possible to differentiate between local recurrence and scar tissue which is a problem of CT and MRI scanning. Higher specificity is therefore a very important potential advantage of radiopeptide scanning over anatomical imaging. Unfortunately, this is not always true: octreotide is an example

for a radiopeptide that accumulates in tumors as well as in inflammation/scar tissue because somatostatin receptors are also expressed on lymphocytes, activated leucocytes, and epitheloid cells (Gotthardt et al. 2004). A disadvantage of conventional nuclear medicine imaging is the comparably low resolution that can be achieved. In three-dimensional SPECT (single photon emission computed tomography) imaging, the spatial resolution of clinical scanners is limited to ~1 cm, which may result in a low sensitivity for small lesions. The use of higher-resolution systems leads to a decrease in physical sensitivity of the cameras requiring longer acquisition times which is not always feasible in clinical practice. For older PET scanners, the spatial resolution is also limited to 8–10 mm. New systems with time-of-flight technique and the use of other new technologies are currently improving the spatial resolution to 2–4 mm for clinical scanners. Therefore, the disadvantage of lower spatial resolution will be much less important in the future. This will help to increase sensitivity of PET for very small lesions. Furthermore, these new scanners are also capable of whole-body scans in a shorter time of <15 min which will further improve in the future.

RADIOLABELED PEPTIDES

The (over-)expression of proteins in pathological processes offers different possibilities for targeted diagnosis and therapy (Hutchinson 2007; Suzuki et al. 2007). In the case of radiopeptide imaging, this is the case for several peptide receptors expressed on different tumors (Reubi 2003). These receptors can be targeted with the respective ligand peptides which are used as Trojan Horses to deliver radioactivity for imaging and therapy or toxic substances to the cancer cells (Schally and Nagy 2004). Radiometals can be coupled via chelator to the peptides whereas other nuclides may be attached via a covalent bond (Heppeler et al. 2000).

In the chemical part of the development of radiopeptides, problems such as complex or covalent binding stability have to be overcome whereas the biological aspects are related to metabolic stability, biological properties such as receptor affinity or biodistribution, which are more complicated. Naturally occurring peptides have a low stability in blood with half-lives in the range of minutes, and therefore need to be stabilized by replacing amino acids with other natural amino acids, D-configurated amino acids or artificial amino acids. Another possibility is to change the amide bond. However, it is crucial to preserve the biological properties such as binding affinity or internalization rate. The binding affinity should be in the nanomolar or better in the subnanomolar range.

Binding of a radionuclide to a peptide highly depends on chemical properties of the radionuclides. Halogenes may be bound covalently to peptides and proteins. At least for radioactive isotopes of iodine this is a disadvantage because it is attached in the ortho position of the hydroxy group on an aromatic ring (tyrosine). This structure is known from iodinated thyroid hormones which is why it is released from cells after internalization. Furthermore, the bound iodine may be cleaved by deiodinases (the same that are responsible for de-iodination of thyroid hormones). This results in free iodine and high uptake of radioiodine in the thyroid while the target-to-background ratios become low.

Most radiometal labeled compounds stay within the cells after receptor binding and internalization and are only slowly released. This so called "residual labeling" leads to an increasing uptake in the cells over time. The reason is metabolic trapping of the radiometal-chelator complex within the target cell as there is no metabolic pathway for metabolization of these compounds. Recently, some strategies for residual radiodine labeling have also been developed.

The choice of the most suitable chelator for radiometals depends on the use of the compound. DTPA (Diethylenetriaminepentaacetic acid) can be used as monofunctional or bifunctional chelator. Monofunctional DTPA is coupled as a dianhydride to free amines (lysine or N-terminal end) to the peptide. A carbonic acid side chain is used for coupling but then lacks for the metal chelation. Therefore, the chelator stability is high for ^{111}In but not for other radiometals. This way of labeling is to prefer for proof of principle experiments of newly developed peptides because the coupling of DTPA is easy and can be performed during a Merrifield peptide synthesis. Labeling with ^{111}In can be performed at room temperature achieving high specific activities. The bifunctional DTPA chelator has a side arm for coupling to the peptide and all carbonic acids arms will remain for the metal-chelator binding. This complex is more stable and may also be suitable for ^{90}Y in addition to ^{111}In.

A very stable chelator for different radiometals is DOTA (1,4,7,10-Tetraazacyclododecane-1,4,7,10-tetraacetic acid) which is especially important for stable labeling for therapeutic applications. DOTA is coupled via a carbonic acid to a free amine of the peptide or protein. It can be labeled with ^{68}Ga, ^{90}Y, ^{111}In, ^{177}Lu etc. The disadvantage of DOTA is that it is necessary to heat up to 100°C during the labeling procedure which may destroy the peptide. Several other chelators like Deferoxamine (DFO) for ^{68}Ga or NOTA (1,4,7-triazacyclononane-1,4,7-triacetic acid) for ^{64}Cu- can be used for labeling for PET applications. A good overview of the different coupling methods is given by Anderson and Welch (1999).

The advantage of peptides as compared to other proteins with a higher molecular weight (such as antibodies and antibody fragments) is a favorable pharmacokinetic behavior with rapid uptake into the target cells, fast clearance by the kidneys, and a low background in blood, liver, and other organs. An image with a good target to background ratio can be obtained within 30 min to 24 h. Rapid clearance by the kidneys, however, also causes problems as the peptides are reabsorbed in the tubuli leading to high retention of the radiolabel in the kidney. Though this effect is of limited relevance in radiopeptide imaging, in peptide receptor radiotherapy it may cause considerable nephrotoxicity. This will be discussed in more detail later.

MINIGASTRIN FOR DETECTING METASTASIZED MEDULLARY THYROID CARCINOMA

The outstanding sensitivity of pentagastrin testing suggested that a radiolabeled peptide binding to the same receptor as pentagastrin (the cholecystokinin receptors) might be able to detect metastases of MTC. Therefore, such a compound had been developed and the results of preclinical and preliminary clinical testing indicated

that a gastrin-based scintigraphic approach may be useful as a clinical imaging modality (Behr et al. 1999). Subsequently, studies were performed that directly compared gastrin receptor scintigraphy (GRS) with somatostatin receptor scintigraphy (SRS), CT, MRI, US, and ^{18}F-FDG- PET.

Cholecystokinine 2 (CCK_2) Receptor Expression

CCK_2 receptors are overexpressed on MTC tumor cells (and also in cells of other tumors such as small-cell lung cancer, astrocytomas, neuroendocrine tumors of the gut, and others). Expression in healthy tissue is usually low (gallbladder, smooth muscles cells of the gut, pancreas, central nervous system). Only in the gastric mucosa, expression levels are high. In order to keep background activity low, a ligand specifically binding to CCK_2 receptors is favorable for imaging of MTC as additional binding to CCK_1 receptors would further increase uptake in organs physiologically expressing CCK_1 receptors. MG specifically binds to CCK_2 receptors and has therefore, apart from other favorable characteristics for imaging, been chosen as optimal compound for MTC imaging.

Labeling

A kit formulation was used for labeling. The kit was prepared by adding 250 μL of 20 μM DTPA-DGlu1-minigastrin in 0.5 M sodium acetate solution (pH 5.4) through a sterile filter into an elution flask under sterile conditions. The kit was then lyophilized and stored at −20°C until use. For reconstitution for patient studies, 250 MBq of $^{111}InCl_3$ in 500 μL 0.1 M HCl was added to the kit (Béhé et al. 2003). The radiochemical purity of the labelled minigastrin was always >95 % as evaluated by HPLC with a specific activity of 55.5 GBq/μmol.

Scanning Protocol

GRS with ^{111}In-DTPA-$DGlu_1$-minigastrin (MG) is basically performed in the same manner as SRS. Approximately, 180–250 MBq of the compound are injected intravenously. It is important to keep in mind that MG does exert the same effects as Pentagastrin, which therefore also includes the same side effects: nausea, cough, an itchy "strange feeling" in chest and abdomen, and flush-like symptoms. Therefore, injection should be done slowly via a venous catheter. Usually, the side effects resolve within a few minutes. Whole-body scans are obtained 4 and 20–24 h after injection in anterior and posterior views using a gamma-camera equipped with a parallel-hole medium energy collimator. To guarantee for a sufficient count rate, the scanning speed is set to below 10 cm/min. SPECT (single photon emission computed tomography) images should be obtained for higher sensitivity as well as in case of indeterminate findings. We suggest that 120 views should be obtained with 30s per view.

Biodistribution of Minigastrin

Physiologically, ^{111}In-DTPA-$DGlu_1$-minigastrin accumulates in organs with CCK_2 receptor expression. The stomach has the highest level of CCK_2 receptor expression and is, therefore, the organ with the most prominent MG uptake, behalf of the kidneys. Though kidneys show only a low CCK_2 receptor expression, the compound is physiologically excreted via the kidney.

A considerable part of MG is reabsorbed in the tubuli after glomerular filtration via the megalin/cubilin system (Gotthardt et al. 2007). As in tumor cells, the radiometal/chelator complex is retained in the tubuli leading to an even more pronounced uptake. Other organs with physiologic CCK_2 receptor expression are usually not visible on scans. Because MG is hydrophilic, it can not cross the blood–brain barrier and does not accumulate in the central nervous system. Only in brain tumors disturbing the blood–brain barrier, (specific) uptake can be detected (Gotthardt et al. 2003). Accumulation of activity in the guts of patients (as often detected in GRS) is most likely not caused by biliary secretion of the compound (as had been suggested) but by secretion from the gastric mucosa as in most patients, the gallbladder and liver are not visible. In addition to the organs mentioned above, in premenopausal women the breast tissue may also accumulate MG.

Clinical Studies

So far, two clinical studies evaluating GRS with MG for tumor detection in patients with MTC have been conducted. The first study focused on patients with biochemical evidence of MTC and patients with recurrent or metastatic MTC. GRS was compared to anatomical imaging modalities (CT, MRI, US) as well as bone scintigraphy and SRS. This study included 75 patients (from which 43 with known metastatic disease and 32 with occult disease) (Behe and Behr 2002). The second study included 26 patients with mostly advanced metastatic MTC (Figure 28.1) and compared GRS to PET, CT, and SRS. This second study included follow-up, histology, and comparison to all available imaging modalities for calculation of a tumor detection rate (Gotthardt et al. 2006).

Results of the first study including 75 patients:

In this study, a total of 75 patients with metastatic MTC were examined with ^{111}In–DTPA-$DGlu_1$-minigastrin. All had been staged by US, CT, MRI, SRS, and bone scanning. Of all patients, 32 suffered from occult metastatic MTC as indicated by elevated calcitonin and/or CEA levels without previous evidence for metastases in anatomical imaging modalities as listed above. In addition to scanning 4 and 24 h post injection as described above, 10 min and 1 h planar scans were also performed. Furthermore, in addition to planar whole body scans SPECT scans were obtained from thorax and abdomen at 4 and 24 h p.i. In those patients known with metastatic disease from staging, all known lesions could be identified on GRS from 1 h p.i. on. The highest tumor-to-background ratios were observed 24 h p.i. In 29 of 32 of the patients with occult MTC, tumor localizations could be detected. However, in only nine patients there is histological proof and nine were considered true positive based on follow-up. The remaining 11 patients are unconfirmed positive (they were considered inoperable and have therefore neither undergone surgery nor was a biopsy taken). In comparison to CCK-analogs used earlier, MG did not show relevant liver or spleen uptake which makes this compound ideal for detection of liver metastases (though the limited spatial resolution of SPECT has to be kept in mind here) (Behe and Behr 2002).

Results of the second study including 26 patients:

To determine the clinical performance of GRS, it was compared to SRS, CT, and

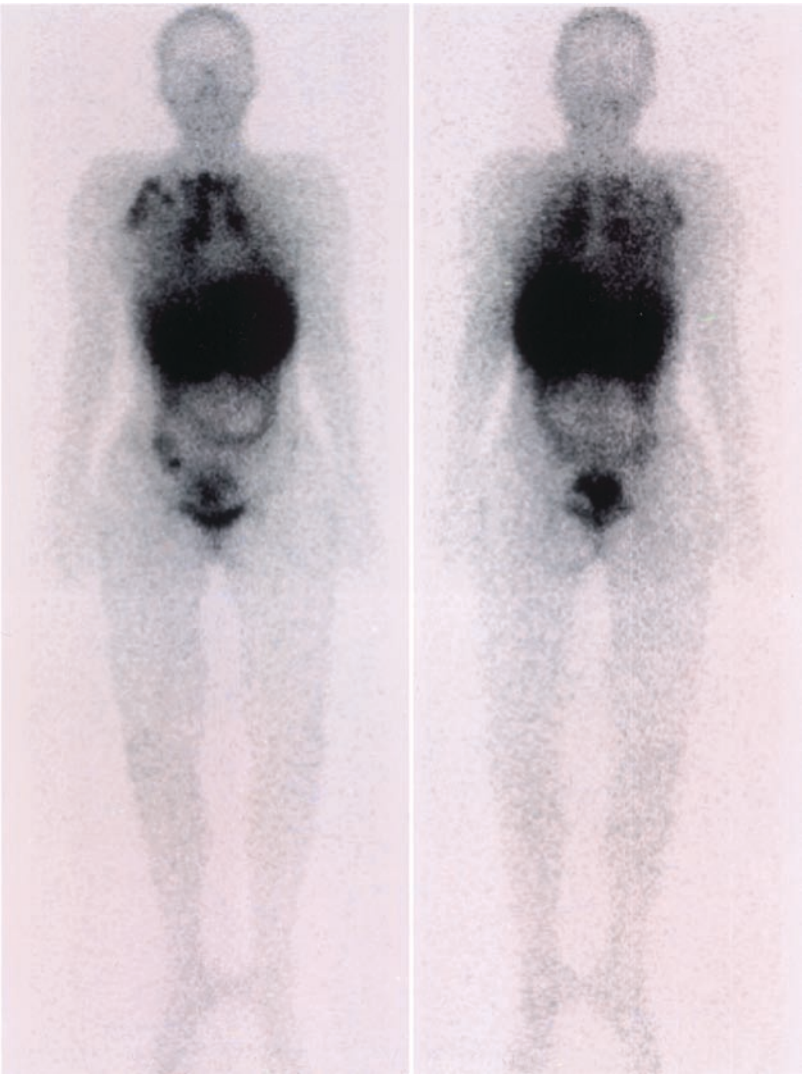

FIGURE 28.1. GRS of a 35 year old female patient with MTC metastatic to the lungs, the mediastinum, and the right axilla. High uptake in the left upper abdomen is caused by physiological gastric uptake. Kidney uptake is very high resulting in partial over-projection with liver and stomach. Anterior scan on the left, posterior scan on the right

^{18}F-FDG-PET in patients with metastasized/recurrent MTC. Consecutive patients were included who underwent imaging with GRS, SRS (19 patients), CT, and PET. GRS and SRS were compared to each other with respect to tumor detection and uptake. CT, PET, MRI, US, and follow-up were used for verification of findings. In addition, GRS, CT, and PET were directly compared to each other to determine which method performs best. If SRS and GRS were directly compared

in those 19 patients having undergone both GRS and SRS, GRS showed a tumor detection rate of 94.2% as compared to 40.7% for SRS. In all 26 patients, GRS, CT, and PET were compared. Here, GRS showed a tumor detection rate of 87.3% as compared to 76.1% for CT, and 67.2% for PET. If GRS and CT were combined, they were able to detect 96.7% of areas of tumor involvement. It needs to be noted that CT was in a disadvantage with respect to the detection of bone metastases since the images evaluated did not include the bone window. Interestingly, there was one patient included into the study who had known metastatic disease proven by CT imaging, histology, and elevated CEA levels. Calcitonin had never been elevated at all and Pentagastrin stimulation testing had always been negative. This patient did not even show any of the side effects of Pentagastrin injection. GRS was negative in this patient despite large tumor masses in the lungs and the mediastinum. It has, therefore, been postulated that this patient either did not have CCK_2 receptors or might have a receptor mutation not binding Pentagastrin or MG.

As most of the patients included into this study were patients with advanced metastatic MTC, it was concluded that further studies are needed to elucidate the role of GRS in the diagnostic evaluation of patients with occult MTC. Furthermore, though the combination of GRS and CT seems to offer a previously unknown sensitivity for the detection of MTC lesions, the therapeutic relevance of this information presently is not clear since MTC is a comparably rare disease and the therapeutic options are limited (except for surgery) (Gotthardt et al. 2006).

PEPTIDE RECEPTOR RADIOTHERAPY OF METASTASIZED MEDULLARY THYROID CARCINOMA WITH GASTRIN ANALOGS

The principle of peptide receptor radiotherapy (PRRT) is to label a given peptide with a radionuclide that has favorable properties for specific targeted therapy. These properties include a comparably short range in tissue and a linear energy transfer (i.e., the energy that is deposited in tissues) as high as possible. In addition, the half-life of the radionuclide should not be too long or too short. Presently, the radionuclides used mostly in PRRT are ^{90}Y and ^{177}Lu. Both are ß-emitters (which means that they emit electrons) with a range of several millimeters. If used for PRRT, a residualizing label is required to guarantee for long tumor retention. In the case of ^{90}Y and ^{177}Lu, DOTA is most widely used as chelator to fulfill this requirement.

Toxicity of PRRT is low in comparison to, for example, chemotherapy. Dose-limiting toxicity is usually kidney toxicity because a part of the radiopeptide which is cleared via the kidney is reabsorbed in the tubuli, and the chelator-radionuclide complex is stored within the tubule cells. Therefore, the same mechanism leading to retention of the radionuclide in the tumor cells (metabolic trapping) is also responsible for the dose limiting kidney toxicity. The range of the emitted electrons determines the maximal activity that may be applied to a patient. In the case of ^{90}Y, the maximal range in tissue is 12 mm as

opposed to only 2 mm in the case of ^{177}Lu. In PRRT, higher activities of ^{177}Lu can be a administered to the patients because the shorter range reduces the radiation exposure to the glomeruli in the kidneys. Radiation damage to the tubules can be repaired to a certain extent, whereas damage to the glomeruli leads to irreparable loss of kidney function. Application of higher activities of ^{177}Lu seems to lead to better response rates in comparison to ^{90}Y in PRRT (Kwekkeboom et al. 2007).

In the case of MG, the first therapeutic trial was done with ^{90}Y. The trial was designed as a dose-finding trial but lead to promising therapeutic results. Patients received either 30, 40, or 50 mCi/m^2. From seven patients with rapidly progressing disease, five had partial remission or stabilization. Stabilization or remissions were observed in all dose groups. However, as MG uptake into the kidney is comparably high, nephrotoxicity became a major problem with one patient developing renal failure within 1 year and one patient with severe reversible nephrotoxicity (Behe and Behr 2002). Therefore, patient treatment with ^{90}Y was discontinued in favor of another radionuclide, ^{111}In. Apart from gamma rays, ^{111}In also emits so-called Auger electrons deriving from the atomic envelop (as opposed to ß-emitters in which the electron originates from the atomic nucleus). These electrons have a very high linear energy transfer (i.e. deposition of a high energy in a comparably small volume) and a short range of several micrometers. This means that Auger electrons usually do not leave the target cells, which, in turn, leads to a reduced radiation exposition to the glomeruli in the kidney. Thus, kidney toxicity can better be avoided as the radiation damage is largely limited to the tubuli. On the other hand, high amounts of ^{111}In need to be deposited inside the target cells to achieve a good response because the so-called cross-fire effect (i.e., radiation received from neighboring cells leading to damage) lacks in the case of ^{111}In.

Therefore, a study has been conducted with ^{111}In-DTPA-DGlu$_1$-Minigastrin with therapeutic activities. Although designed as a dose escalation study in order to define the optimal dose in patient therapy, therapeutic effects have been achieved (Figure 28.2). As predicted, deterioration of kidney function was not a problem in this trial. In total, 20 patients suffering from metastasized MTC and one with a metastasized carcinoid having higher uptake of gastrin than octreotide were included into the study. The dose escalation was started at 100 mCi/m^2, increasing in 20% steps (group 2 120 mCi/m^2, group 3 144 mCi/m^2, group 4 174 mCi/m^2, group 5 209 mCi/m^2, and group 6 251 mCi/m^2). Three to four patients were included into each group. Therapy was applied in 6 cycles every 6 weeks. Hematological and nephrotoxicity were evaluated according to the WHO criteria. Staging was done before and 12 weeks after therapy, and after the third and fifth cycle. In none of the patients, nephrotoxicity has been observed. Mild hematotoxicity grade 1 has occurred in one patient of group 1, 2, 3 and 4 each. In addition, in one patient from group 1 a mild preexisting hematotoxicity grade 1 worsened. One patient from each group 1–4 died due to progressive disease. One minor response and one symptomatic response were observed, five patients had progressive disease (under therapy), all others had stabilization of their previously progressive disease (eight patients).

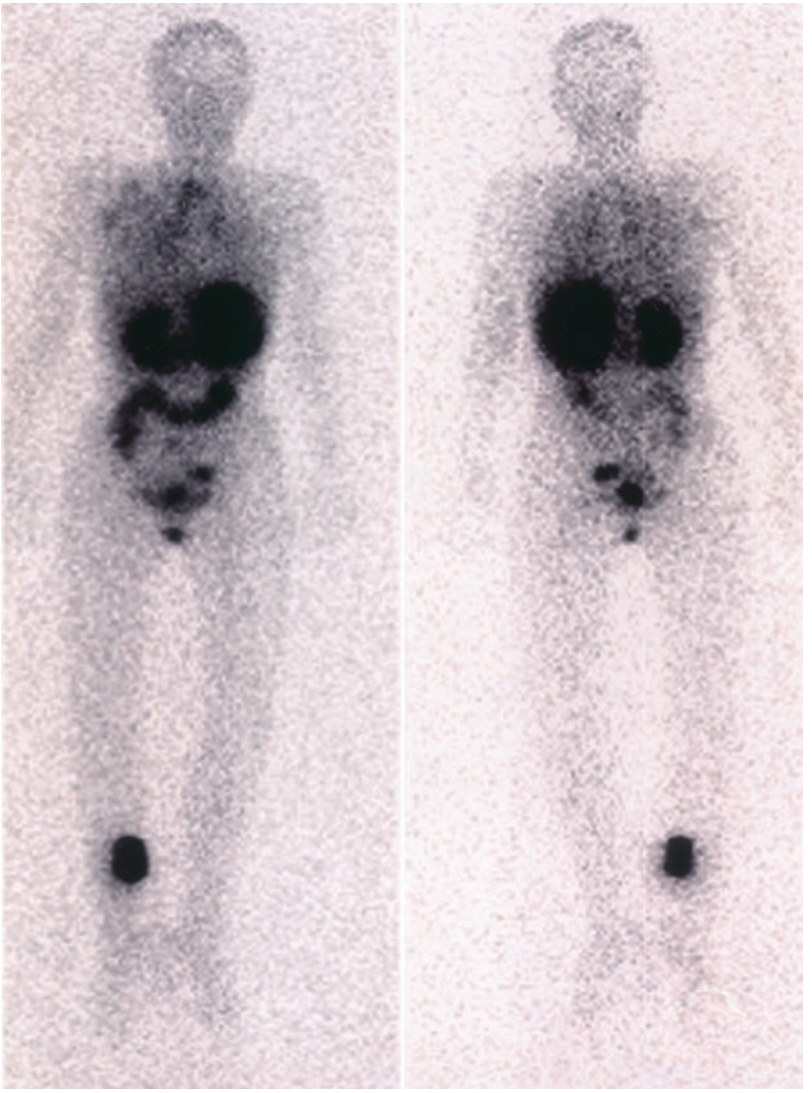

FIGURE 28.2. GRS of the same patient after 3 cycles of therapy with ^{111}In-DTPA-DGlu$_1$-Minigastrin. Note the uptake reduction in the areas of previously high uptake in the metastases in the mediastinum and the axilla. The lung uptake is also reduced. This patient experienced stabilization of her previously progressive disease. The hot spot at the right lower leg is a standard source for dosimetric purposes. Anterior scan on the left, posterior scan on the right

The data that are available for MG are promising so far as it could be demonstrated that PRRT with this compound is feasible and does show positive effects. The main problem of this kind of therapy is nephrotoxocity that can be reduced by choice of the right radionuclide. Furthermore, the side effects of this therapy are much less pronounced than for chemotherapy, which means, for example, that the quality of life does not significantly suffer from therapy. Further studies will have to be conducted to define the optimal radionuclide and therapy protocol for PRRT of MTC.

FUTURE PERSPECTIVES OF DGLU$_1$-MINIGASTRIN

In comparison to SPECT imaging, PET has a higher spatial resolution reaching 2–4 mm in the scanners of the newest generation. Furthermore, PET tracer uptake can easily be quantified. Therefore, one would expect that PET imaging has the potential to further increase sensitivity and accuracy of MTC imaging. For targeting of the somatostatin receptor on other neuroendocrine tumors, an advantage of PET over SPECT imaging has been demonstrated (Buchmann et al. 2007). PET imaging for targeting of the CCK_2 receptor could be done with DOTA-DGlu$_1$-Minigastrin labeled with the positron emitter ^{68}Ga, a generator-derived emitter. The Ge/Ga generator is ideal for local radionuclide production. For labeling with ^{68}Ga, DTPA (used for labeling with ^{111}In) is not suitable due to a low stability of the chelate. Therefore, the chelator DOTA is required. Alternative radionuclides would include ^{89}Zr and ^{64}Cu, radionuclides with longer half-lives that can easily be shipped and are therefore suitable for local labeling. They again would require another chelator (desferral or NOTA).

A major problem of PRRT with MG is kidney toxicity which can be avoided by using the auger-electron emitter ^{111}In. However, it has been demonstrated that ^{177}Lu is probably the most efficient ß-emitter for PRRT at the moment and also more efficient than ^{111}In. Its maximal range in tissue of ~2 mm makes nephrotoxicity a serious concern as MG uptake into the kidney is much higher than uptake of octreotide or its derivatives which have been extensively used in PRRT of neuroendocrine tumors. In PRRT with octreotide analogs labeled with ^{177}Lu, measures are taken to reduce kidney uptake, for example, infusion of cationic amino acids such as lysine or arginine. However, this approach is not suitable in the case of MG as these amino acids do not reduce kidney uptake of MG. Therefore, new approaches are required. Indeed, Poly-Glu has been shown to reduce kidney uptake of MG by more than 85% in rodent models (Béhé et al. 2005). However, toxicity may be an issue if Poly-Glu is used for kidney uptake reduction in humans. Therefore, alternatives such as the plasma expander Gelofusine®, have been tested in animal models. Gelofusine® has also proven its efficiency in reduction of kidney uptake for octreotide analogs in humans (Vegt et al. 2006). Still, kidney uptake reduction remains a problem as significant reduction is not easy to achieve and obviously different radiopeptides need different approaches for optimal kidney uptake reduction (Gotthardt et al. 2007). Further research needs to be conducted to significantly reduce kidney uptake of MG before ^{177}Lu can be used as radionuclide for PRRT with MG.

REFERENCES

Anderson CJ, Welch MJ (1999) Radiometal-labeled agents (non-Technetium) for diagnostic imaging. Chem Rev 99:2219–2234

Behe M, Behr TM (2002) Cholecystokinin-B (CCK-B)/gastrin receptor targeting peptides for stating and therapy of medullary thyroid cancer and other CCK-B receptor expressing malignancies. Biopolymers 66:399–418

Béhé M, Becker W, Gotthardt M, Angerstein C, Behr TM (2003) Improved kinetic stability of DTPA-D-Glu as compared with conventional monofunctional DTPA in chelating indium and yttrium: preclinical and initial clinical evaluation of radiometal labelled minigastrin derivatives. Eur J Nucl Med Mol Imag 30:1140–1146

Béhé M, Kluge W, Becker W, Gotthardt M, Behr TM (2005) Use of polyglutamic acids to reduce uptake of radiometal-labeled minigastrin in the kidneys. J Nucl Med 46:1012–1015

Behr TM, Gratz S, Markus PM, Dunn RM, Hufner M, Schauer A, Fischer M, Munz DL, Becker H, Becker W (1997) Anti-carcinoembryonic antigen antibodies versus somatostatin analogs in the detection of metastatic medullary thyroid carcinoma: are carcinoembryonic antigen and somatostatin receptor expression prognostic factors? Cancer 80:2436–2457

Behr TM, Jenner M, Béhé M, Angerstein C, Gratz S, Raue F, Becker W (1999) Radiolabeled peptides for targeting of cholecystokinin-B/gastrin receptor expressing tumours: from preclinical development to initial clinical results. J Nucl Med 40:1029–1044

Beuthien-Baumann B, Strumpf A, Zessin J, Bredow J, Kotzerke J (2007) Diagnostic impact of PET with (18)F-FDG, (18)F-DOPA and 3-O-methyl-6-[(18)F]fluoro-DOPA in recurrent or metastatic medullary thyroid carcinoma. Eur J Nucl Med Mol Imag e-pub ahead of print

Buchmann I, Henze M, Engelbrecht S, Eisenhut M, Runz A, Schafer M, Schilling T, Haufe S, Herrmann T, Haberkorn U (2007) Comparison of (68)Ga-DOTATOC PET and (111)In-DTPAOC (Octreoscan) SPECT in patients with neuroendocrine tumours. Eur J Nucl Med Mol Imag e-pub ahead of print

Busnardo B, Girelli ME, Simioni N, Nacamulli D, Busetto E (1984) Nonparallel patterns of calcitonin and carcinoembryonic antigen levels in the follow-up of medullary thyroid carcinoma. Cancer 53:278–285

Chatal JF, Campion L, Kraber-Bodéré F, Bardet S, Vuillez JP, Charbonnel B, Rohmer V, Chang CH, Sharkey RM, Goldenberg DM, Barbe TJ (2006) Survival improvement in patients with medullary thyroid carcinoma who undergo pretargeted anti-carcinoembryonic-antigen radioimmunotherapy: a collaborative study with the French endocrine tumor group. J Clin Oncol 24:1705–1711

Dymling JF, Ljungberg O, Hillyard CJ, Greenberg PB, Evans IM, MacIntyre I (1976) Whisky: a new provocative test for calcitonin secretion. Acta Endocrinol (Copenh) 82:500–509

Emmertsen KK, Nielsen HE, Mosekilde L, Hansen HH (1980) Pentagastrin, calcium and whisky stimulated serum calcitonin in medullary carcinoma of the thyroid. Acta Radiol Oncol 19:85–89

Fletcher DR, Gamvros O, Man WK, Ahmed Y, Trayner I, Adrian T (1984) Multiple endocrine neoplasia type II: the role of gastrointestinal humoral factors in calcitonin release following alcohol and pentagastrin stimulation. Aust N Z J Surg 54:271–275

Gotthardt M, Groß MW, Schipper ML, Henzel M, Béhé MP, Schurrat T, Pollum H, Pfestrof A, Schmidek A, Heinis J, Engenhart-Cabilic R, Behr TM (2003) Uptake of In-111-DTPA-D-Glu1-Minigastrin into malignant brain tumors: proof of specificity and results of the first 30 patients. Eur J Nucl Med Mol Imag 30:S237

Gotthardt M, Boermann OC, Behr TM, Béhé MP, Oyen WJG (2004) Development and clinical application of peptide-based radiopharmaceuticals. Curr Pharm Design 10:2951–2963

Gotthardt M, Behe MP, Beuter D, Battmann A, Bauhofer A, Schurrat T, Schipper M, Pollum H, Oyen WJG, Behr TM (2006) Improved tumour detection by gastrin receptor scintigraphy in patients with metastasised medullary thyroid carcinoma. Eur J Nucl Med Mol Imag 33:1273–1279

Gotthardt M, Eerd-Vismale J, Oyen WJG, de Jong M, Zhang H, Maecke HR, Behe M, Boerman O (2007) Indication for different mechanisms of kidney uptake of radio-labeled peptides. J Nucl Med 48:596–601

Hayat MA (ed) (2007) Cancer imaging, Vols. 1 and 2. Elsevier/Academic, San Diego, CA, USA

Hazard JB, Hawk WA, Crile G Jr (1959) Medullary (solid) carcinoma-a clinicopathological entity. J Clin Endocrinol 19:152–161

Heppeler A, Froidevaux S, Eberle AN, Maecke HR (2000) Receptor targeting for tumor localisation and therapy with radiopeptides. Curr Med Chem 7:971–994

Hodak SP, Burman KD (2004) The calcitonin conondrum – is it time for routine measurement of serum calcitonin in patients with thyroid nodules? J Clin Endocrinol Metab 89:511–514

Horn RC (1951) Carcinoma of the thyroid. Description of a distinctive morphological variant and report of 7 cases. Cancer 4:697–707

Hutchinson L (2007) Targeted therapies: the answer to individualized treatment? Nat Clin Pract Oncol 4:323

Karanikas G, Moamenio A, Poetzi C, Zettinig G, Kasere K, Bieglmayer C, Niederle B, Dudczak R, Pirich C (2004) Frequency and relevance of elevated serum calcitonin levels in patients with neoplastic and nonneoplastic thyroid disease and in healthy subjects. J Clin Endocrinol Metab 89:515–519

Kwekkeboom DJ, Teunissen JJ, Kam BL, Valkema R, de Herder WW, Krenning EP (2007) Treatment of patients who have endocrine gastroenteropancreatic tumors with radiolabeled somatostatin analogues. Hematol Oncol Clin North Am 21:561–573

Machens A, Niccoli-Sire P, Hoegel J, Frank-Raue K, van Vroonhoven TJ, Roeher HD, Wahl RA, Lamesch P, Raue F, Conte-Devolx B, Dralle H (2003) European Multiple Endocrine Neoplasia (EUROMEN) Study Group 2003: Early malignant progression of hereditary medullary thyroid cancer. N Engl J Med 349:1517–1525

Ong SC, Schröder H, Patel SG, Tabangay-Lim IM, Doddamane I, Gönen M, Shaha AR, Tuttle RM, Shah JP, Larson SM (2007) Diagnostic accuracy of ^{18}F-FDG PET in restaging patients with medullary thyroid carcinoma and elevated calcitonin levels. J Nucl Med 48:501–507

Reubi JC (2003) Peptide receptors as molecular targets for cancer diagnosis and therapy. Endocr Rev 24:389–427

Schally AV, Nagy A (2004) Chemotherapy targeted to cancers through tumoral hormone receptors. Trends Endocrinol Metab 15:300–310

Suzuki R, Rao P, Sasaguri S (2007) Current status and future of target-based therapeutics. Curr Cancer Drug Targets 7:273–284

Vegt E, Wetzels JF, Russel FG, Masereeuw R, Boerman OC, van Eerd JE, Corstens FH, Oyen WJG (2006) Renal uptake of radiolabeled octreotide in human subjects is efficiently inhibited by succinylated gelatin. J Nucl Med 47:432–436

Williams ED (1966) Histogenesis of medullary carcinoma of the thyroid. J Clin Pathol 19: 114–118

Prognosis

29
Medullary Thyroid Carcinoma: Prognosis based on Stage of Disease and Age

Tracy S. Wang, Julie Ann Sosa, and Sanziana A. Roman

INTRODUCTION

Medullary thyroid cancer (MTC) was first described in 1959 by Hazard et al. as a solid thyroid neoplasm without follicular histologic features, but with a high degree of lymph node metastases. It is a neuroendocrine tumor of the thyroid, derived from the parafollicular cells or C-cells; these cells are responsible for the production of calcitonin, a sensitive and specific marker for MTC. They are considered part of the amine precursor uptake and decarboxylation system, and are found mostly in the upper and middle parts of the thyroid. Calcitonin is involved in calcium regulation and bone remodeling, but its exact role in humans is not clear. MTC can be found in both sporadic and hereditary forms. The familial association of MTC has been isolated to the ret proto-oncogene.

EPIDEMIOLMOGY

Medullary thyroid cancer constitutes between 3% and 10% of all thyroid cancers, but is responsible for up to 13.4% of all deaths related to thyroid cancer (Roman et al. 2006). Sporadic MTC accounts for up to 75% of cases; three distinct familial syndromes account for the remainder of cases. Hereditary MTC is an autosomal dominant disorder associated with one of the two subtypes of multiple endocrine neoplasia (MEN) type 2 syndrome (MEN 2A and MEN 2B) or with familial MTC (FMTC).

MEN 2A is the most common syndrome, accounting for up to 80% of hereditary cases, and is primarily characterized by multifocal, bilateral MTC, pheochromocytoma, and primary hyperparathyroidism. Less commonly, patients develop lichen planus amyloidosis of the skin and/or Hirschsprung's disease. MEN 2B is characterized by MTC, pheochromocytoma, marfanoid habitus, and neuromas of the skin and gastrointestinal tract. There is 100% penetrance of MTC in patients with the MEN syndromes. Familial MTC is characterized by MTC alone.

PATHOLOGY AND PATHOGENESIS OF MEDULLARY THYROID CANCER

C-cells derive from the neural crest, and are the cell of origin for MTC. They are

scattered throughout the thyroid, but are concentrated in the superior/posterior pole of each lobe. The secretion of calcitonin and carcinoembryonic antigen (CEA) by C-cells is clinically important because both are tumor markers for MTC; when consistently elevated, plasma levels of calcitonin are indicative of C-cell pathology and are directly related to MTC cell mass.

On gross examination, MTC tumors are firm, solid tumors that appear gray-white in color and are usually well-encapsulated. Sporadic MTC are typically unilateral, while hereditary MTC are bilateral and multifocal. Histologically, MTC appears as nests of uniform oval and spindle cells, separated into nodules by thin bands of collagen. The surrounding stroma may contain areas of desmoplastic fibrosis, calcification, or contain amyloid; the presence of amyloid is a distinguishing feature of MTC and is present in up to 75–80% of tumors. Amyloid can be detected using both hematoxylin-eosin staining (pink) and polarized light (green bifrefringence). However, the most sensitive method of identifying MTC is immunohistochemical staining for calcitonin. (Figure 29.1) The precursor lesion to MTC is C-cell hyperplasia, a histologic abnormality defined as more than 6 C-cells per follicle or >50 C-cells in a single low-power field.

Mutations to the *ret* proto-oncogene have been identified as the source of oncogenesis for all of the hereditary and some sporadic cases of MTC. In 1987, *ret* had been mapped to the proximal region of the long arm of chromosome 10, and was subsequently shown to be expressed at high levels in MTC and pheochromocytomas. By 1991, the gene for MEN 2A, MEN 2B, and FMTC had been mapped to the same area, the pericentriomeric region of chromosome 10 (locus 10q11.2).

The *ret* gene encodes a transmembrane tyrosine kinase receptor, the RET protein, which is expressed in derivatives of the neural crest, including the C-cells of the thyroid and the adrenal medulla. The RET protein consists of an extracellular domain containing a ligand-binding site and a cysteine-rich region, a transmembrane

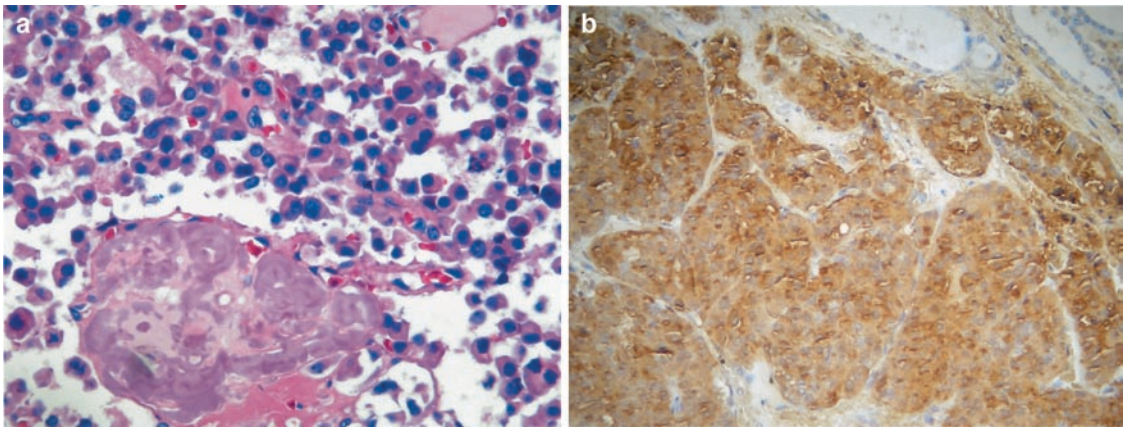

FIGURE 29.1. (**a**) Hematoxylin and eosin staining of medullary thyroid cancer showing plasmacytoid cells and amyloid; 40× magnification with1.3× enlargement. (**b**) Calcitonin staining of medullary thyroid cancer; 20× magnification with 1.3× enlargement

domain, and an intracellular domain with tyrosine kinase activity. An activating mutation on a single allele of *ret* is necessary and sufficient to cause oncogenic transformation. Mutations resulting in MEN 2A occur in the cysteine-rich region; altered disulfide bonds between cysteine residues result in ligand-independent receptor dimerization and constitutive RET activity. Mutations in codon 634 (exon 11) are present in over 80% of patients with MEN 2A, although mutations in codons 609, 610, 611, 618, and 620 are also present. In contrast, mutations resulting in MEN 2B occur in the tyrosine kinase intracellular domain and result in receptor auto-phosphorylation and activation. This mutation occurs at codon 918 (exon 16) in more than 95% of patients with MEN 2B. Familial MTC is most commonly linked to mutations of the cysteine codons of the extracellular domain, such as MEN 2A, although noncysteine mutations of the intracellular domain are also present. Somatic missense mutations in *ret* may occur in patients with sporadic MTC; the most common mutation is at codon 918.

CLINICAL PRESENTATION

The majority of cases of MTC, both sporadic and index cases of the hereditary form, present with a palpable thyroid nodule. Physical examination should include a careful assessment of the neck mass for both size and its relationship to adjacent structures, as MTC may extend posteriorly through the thyroid capsule, into the tracheal wall, the recurrent laryngeal nerve, and/or the jugular vein. Associated symptoms include dysphagia, hoarseness, dyspnea, and coughing; laryngoscopy may reveal vocal cord impairment secondary to involvement of the recurrent laryngeal nerve. Lymph node metastases occur early in MTC, and >50% of patients have cervical lymph node metastases at the time of diagnosis. Distant metastases occur in 10%–15% of patients and are most common in the mediastinum, liver, lungs, and bones. Elevated calcitonin levels are associated with flushing and/or diarrhea.

Diagnostic Testing

The diagnosis of MTC can be made by a fine needle aspiration (FNA) biopsy of the thyroid mass or cervical lymph node, with immunohistochemical staining for calcitonin, chromogranin A, or CEA. Thyroglobulin staining will be negative. The extent of disease can be defined with radiographic imaging, including cervical ultrasonography, computed tomography (CT) of the chest and abdomen, and bone scan. Nuclear imaging studies, such as ^{131}I scans, are of little use, as MTC does not concentrate iodine.

Plasma calcitonin levels correlate with the extent of disease, but are most useful when measured serially to detect changes in disease over time. Calcitonin levels are considered to be pathologic when the basal level is above the normal range, or when stimulation of calcitonin leads to an increase that is greater than two to three times the basal level. Calcitonin secretion can be stimulated by the use of either calcium or pentagastrin; the latter is not approved for use in the United States, but is commonly used in Europe.

Genetic Screening

All patients with a diagnosis of MTC should have genetic testing to evaluate for

the presence of a mutation of the *ret* proto-oncogene. The risk for hereditary MTC in a patient with a negative mutation analysis is less than one percent, effectively ruling out the presence of a familial syndrome in these patients. For patients with a familial syndrome, a positive genetic test would necessitate screening for the presence of pheochromocytoma and/or hyperparathyroidism. Most importantly, asymptomatic members of known MTC kindred should undergo genetic testing as early as possible to identify carriers of the *ret* mutation.

Genotype – Phenotype Correlations

In hereditary syndromes, the type of *ret* mutation can be correlated to the presentation and aggressiveness of MTC (Kouvaraki et al. 2005; Raue et al. 2006). Patients with MEN 2B, the majority of whom present with a mutation at codon 918, typically demonstrate the most aggressive form of MTC. The age of onset of MTC in these patients is during infancy, with metastases often present at the time of diagnosis. Mutations at codons 634 and 618 are most common in patients with MEN 2A; the course of MTC appears to be more variable.

Given the correlation between genotype and phenotype, *ret* mutations have been stratified into three groups, based on the biologic aggressiveness of MTC observed in patients with these particular mutations. Patients with level 1 mutations represent those with a high risk for the development and growth of MTC, and include codons 609, 768, 790, 791, 804, and 891. Patients with level 2 mutations (codons 618, 620, and 634) have a higher risk for the early development and growth of MTC, with invasive MTC present as early as age 5 years. Level 3 mutations (codons 833 and 918) have the highest risk for the early development and growth of MTC, and include nearly all patients with MEN 2B.

PROGNOSTIC FACTORS

Multiple clinical and population-based studies have examined the factors related to improved survival for patients with MTC. Kebebew et al. (2000) studied 104 patients with MTC or C-cell hyperplasia managed at a single institution. Patients who underwent total or subtotal thyroidectomy were less likely to have recurrent/persistent disease, and patients who had total thyroidectomy with cervical lymph node dissection required fewer subsequent reoperations for MTC. While univariate analyses demonstrated that age, gender, presenting signs and symptoms, stage of disease, distant metastases, and the extent of thyroidectomy were all significant predictors of survival, only age and stage of disease remained independent predictors of survival after multivariate analyses. Using TNM classification, 5-year survival rates were: stage I, 100%; stage II, 90%; stage III, 87%, and stage IV, 56%. (Table 29.1) Patients aged <45 years had the best overall prognosis.

In 2006, Roman et al. used the population-based Surveillance, Epidemiology, and End Results (SEER) database to study prognostic factors in 1,252 patients with MTC followed between 1973 and 2002. Twelve demographic, clinical, and pathologic prognostic variables were studied by univariate analysis. The Kaplan–Meier method and log rank test were used to identify significant prognostic factors. For the multivariate analysis, the Cox proportional hazards regression model was used

TABLE 29.1. American Joint Committee on Cancer Staging for Medullary Thyroid Cancer, Based on 6th Edition Manual, Springer, New York, 2002

Medullary carcinoma			
Stage I	T1	N0	M0
Stage II	T2	N0	M0
Stage III	T3	N0	M0
	T1	N1a	M0
	T2	N1a	M0
	T3	N1a	M0
Stage IVA	T4a	N0	M0
	T4a	N1a	M0
	T1	N1b	M0
	T2	N1b	M0
	T3	N1b	M0
	T4a	N1b	M0
Stage IVB	T4b	Any N	M0
Stage IVC	Any T	Any N	M1

TNM staging.
Primary tumor (T).
T1 – tumor ≤2 cm, limited to the thyroid.
T2 – tumor >2 cm, but ≤4 cm, limited to thyroid.
T3 – Tumor >4 cm, limited to thyroid, or minimal extrathyroidal extension (strap muscle).
T4a – Tumor any size extending beyond thyroid capsule invading major adjacent tissues (trachea, esophagus, recurrent laryngeal nerve, larynx, subcutaneous tissue).
T4b – Tumor invades prevertebral fascia or encases carotid artery or major vessels.
Regional lymph nodes (N).
Includes cervical central and lateral compartments, and upper mediastinum.
N0 – no regional lymph node metastasis.
N1 – regional lymph node metastasis
N1a – metastasis to level VI (central compartment).
N1b – metastasis to unilateral, contralateral, bilateral cervical or superior mediastinal nodes.
Metastasis (M).
M0 – no distant metastasis.
M1 – distant metastasis.

for variables identified as significant in the univariate analysis. Strength of association between each predictor variable and survival was expressed as a hazard ratio.

Multiple predictors were found to be significant for improved overall survival. These included female gender, younger age at diagnosis, localized stage of disease, well- or moderately-differentiated histologic grade, smaller tumor size (when size was treated as a continuous variable), tumor confined to within the thyroid capsule, and lack of lymph node involvement. Patients with concurrent tumors were found to have significantly worse survival than patients with MTC alone ($p < 0.0005$). Overall, patients with MTC who underwent surgery survived longer than those who had no operation ($p < 0.0001$). In general, survival correlated to extent of surgery, as the best survival was seen in patients who underwent total thyroidectomy, followed by those who underwent thyroid lobectomy ($p < 0.0001$).

Patients were then stratified by stage of disease. All patients with localized MTC underwent surgery; no significant difference in survival was observed between those who underwent lobectomy and those who underwent total/subtotal thyroidectomy. Of note, two patients did not have surgery and survived less than 1 month. In patients with regional stage disease, total thyroidectomy was associated with the best survival, followed by lobectomy. The prognosis was worst in patients who had no surgery. In patients with distant disease, while surgery was associated with improved survival ($p < 0.0001$), there was no statistically significant difference in survival based on extent of surgery (lobectomy vs total thyroidectomy). Different types of lymph node dissections were also compared; again, the extent of lymphadenectomy did not correlate to a significant survival difference. Patients who received radiation therapy had a worse prognosis than patients who had no adjuvant therapy ($p < 0.0001$). There was no association between survival and marital status, race, and diagnostic era.

Variables identified as having a significant association with survival on univariate

analysis were then studied in a Cox proportional hazards model (Table 29.2). Age at diagnosis remained a strong predictor of survival. For each additional year of age, the risk of dying increased by 5.2%, with the worst overall prognosis seen in patients over the age of 65 years. Stage of disease was also strongly associated with survival. Patients with regional stage disease had a 2.69 times greater risk of dying than patients with local disease; this increased to a 4.47 times greater risk of dying in patients with distant disease. Extent of surgery also was a significant independent predictor of survival. When controlled for all other variables, matched patients who underwent surgery did better than patients who did not; a longer overall survival also was seen in patients with more extensive surgery (i.e., total thyroidectomy) as compared to those who underwent lobectomy. After controlling for age, stage of disease and extent of surgery, adjuvant radiation therapy was determined to be an independent predictor of decreased survival ($p < 0.05$).

TABLE 29.2 Demographic, clinical and pathologic characteristics with associated hazard ratios based on multivariate analysis of overall survival in patients with medullary thyroid cancer, SEER 1973–2002

Variables	Hazard ratio (95% CI)	p value
Age (years)		
<40	1	Reference
40–65	2.35 (1.31, 4.22)	0.004
>65	6.55 (3.69, 11.63)	<0.0001
Stage		
Localized	1	Reference
Regional	2.69 (1.73, 4.18)	<0.0001
Distant	4.47 (2.58, 7.74)	<0.0001
Surgery		
None	1	Reference
Lobectomy	0.47 (0.25, 0.91)	0.04
Subtotal/total thyroidectomy without node dissection	0.29 (0.15, 0.56)	<0.0001
Subtotal/total thyroidectomy with limited node dissection	0.17 (0.08, 0.35)	<0.0001
Total thyroidectomy with radical or modified node dissection	0.25 (0.13, 0.47)	<0.0001
Radiation therapy		
None	1	Reference
Yes	1.65 (1.11, 2.45)	0.01

Source: From Roman et al. 2006.

Preoperative basal calcitonin levels have been shown to predict prospects for remission following surgery for MTC. In an institutional series of 224 consecutive patients with MTC and elevated preoperative basal calcitonin levels, Machens et al. (2005) showed through multivariate analysis that preoperative basal calcitonin levels greater than 500 pg/mL best predicted failure to achieve biochemical remission, followed by nodal metastases and reoperative status. Cumulative rates of biochemical remission fell continuously with rising basal calcitonin in node-negative patients. Node-positive patients did not achieve biochemical remission when their preoperative basal calcitonin levels were >3,000 pg/mL. Nodal metastasis emerged at basal calcitonin level of 10–40 pg/mL. Distant metastasis and extrathyroidal growth appeared in patients with node-positive MTC at calcitonin levels of 150–400 pg/mL. The authors concluded that preoperative basal calcitonin levels help to individualize extent of surgery and postoperative follow-up intervals for MTC.

TREATMENT

Surgery is the optimal modality for treatment of MTC; radiation and chemotherapy have demonstrated no benefit in long-term survival. The extent and timing of surgery are dependent on a variety of factors, including age, presence of a familial syndrome, and clinical presentation. The risk of complications, including hypoparathyroidism and injury to the recurrent laryngeal nerve, increase with remedial surgery; therefore, the goal is to perform a complete resection at the initial procedure.

Treatment of Patients with Clinically Evident MTC

The optimal surgical management for patients who present with clinical evidence of localized MTC, whether sporadic or hereditary, is total thyroidectomy, central lymph node dissection, with possible ipsilateral modified radical neck lymphadenectomy. Bilateral modified radical lymphadenectomies may be necessary if bilateral cervical lymph node metastases are suspected (Carling and Udelsman 2005; Fialkowski and Moley 2006; You et al. 2006). Central lymph node dissection involves the complete removal of lymphatic tissue in levels VI and VII; namely, from the hyoid bone superiorly to the inferior innominate vessels, inferiorly and laterally to the carotid sheaths. An ipsilateral modified radical neck lymphadenectomy includes removal of lymphatic tissue from levels II through V, while preserving the sternocleidomastoid muscles, vagus nerve, phrenic nerve, brachial plexus, spinal accessory nerve, jugular vein, and carotid artery.

Despite recent studies that have not demonstrated a significant difference in long-term survival for patients undergoing more extensive lymphadenectomy, the majority of patients with palpable MTC have been shown to have cervical lymph node metastases at the time of diagnosis. Moley and DeBenedetti (1999) found that in 73 patients with palpable MTC, >75% had associated lymph node metastases that could not be detected by the surgeon in the operating room. The incidence of lymph nodes also correlates to the size of the primary lesion and the level of serum calcitonin at the time of diagnosis. Lesions <1 cm have an 11% percent incidence of nodal disease; this increases to 60% in patients with tumors >2 cm. Contralateral nodal metastases have been reported in up to 50% of patients; some authors advocate routine bilateral modified radical neck lymphadenectomies in order to completely eradicate cervical and mediastinal disease, in the hopes of improving survival and achieving biochemical cure.

Prophylactic Surgery for Patients with *ret* Proto-Oncogene Mutations

There is 100% penetrance of MTC in patients with the hereditary syndromes of MEN 2A, MEN 2B, and FMTC. The purpose of prophylactic surgery is to preemptively remove the thyroid gland before MTC can develop and metastasize. Prophylactic thyroidectomy can be performed with minimal morbidity and mortality and thyroid hormone replacement is relatively inexpensive, with nominal burden for the patient. Studies of long-term outcome in carriers for the *ret* mutation have shown that the cure rate is close to100%, if prophylactic thyroidectomy can be performed at an early age.

A recommended timetable for intervention has been formed based on the

established relationship between genotype and phenotype/age-related malignant progression by the 2001 Consensus Conference on the diagnosis and therapy of MEN (Brandi et al. 2001). The recommendations are given within the context that disease expression can be variable, and that individual mutations may alter the course of disease from what might be expected.

The timing of thyroidectomy is guided by the three risk groups defined by the 2001 Consensus Conference. Given that the age of onset and aggressiveness of C-cell hyperplasia and MTC can vary considerably for patients in the 'high' risk group (level 1), there is no consensus for the age at which thyroidectomy should be performed, although most authors advocate thyroidectomy by age 5. Patients in the 'higher' group (level 2), have a significant age-related progression from C-cell hyperplasia to MTC, and invasive MTC has been demonstrated as early as 5 years; current guidelines recommend total thyroidectomy by age 5, possibly earlier. Patients in the 'highest' risk group (level 3) are recommended to have surgery within the first month of life.

Non-Surgical Treatment Modalities

The role of radiation and/or chemotherapy in the treatment of MTC has been limited to date. There is no indication for ^{131}I therapy, as C-cells are derived from the neural crest, and are not iodine-avid. Radiation therapy has been used for palliation in patients with bone metastases, but has been shown to decrease overall survival rates. Laboratory efforts to selectively inhibit RET have included dominant negative receptor forms, aptamers, and ligand-competing peptides. Clinical trials have focused on tyrosine kinase inhibitors (TKI). These molecules share the property of binding to the RET ATP-binding pocket and have overlapping specificities, frequently inhibiting VEGFR2 (KDR), PDGFR, and EGFR to varying degrees as well as RET (Ball 2007). Examples of such multifunctional TKI under study for MTC include ZD6474 (Zactima, AstraZeneca, Wilmington), sorafenib (Nexavar, Bayer, Leverkusen) and sunitinib (Sutent, Pfizer, New York). Wells et al. (2006, 2007) initiated Phase II clinical trials of ZD6474 in hereditary and sporadic MTC patients. Interim data on 15 patients published in abstract form showed partial tumor responses in three patients, stable disease in ten and progressive disease in two. The median duration of treatment was 136 days. Most encouraging was the significant decline in serum calcitonin measurements. Twelve of fifteen patients sustained >50% decrease in calcitonin for more than 6 weeks, with some patients having >90% biochemical response. CEA also was found to decrease. Side effects for this oral drug included diarrhea, nausea, skin rash and fatigue, often necessitating dose reductions.

SURVEILLANCE

After surgical resection, patients should be followed clinically and undergo serial measurements of plasma calcitonin levels. Studies demonstrating the development of recurrent MTC despite aggressive resection emphasize the need for vigilant biochemical follow-up in patients with MTC. Persistent or recurrent MTC is detected by elevated calcitonin levels on provocative testing; many patients with occult disease may develop hypercalcitonemia as the sole

manifestation. Remedial cervical surgery may be considered in patients with hypercalcitonemia and documented localized disease, in the absence of distant metastases.

In conclusion, conventionally, AJCC staging is used to determine prognosis of disease in patients with MTC. This staging does not take into consideration recent data showing that preoperative basal calcitonin levels may be useful in evaluating prospects for remission. Based on the population-based study by Roman et al. (2006), consideration could be given to include age as a part of the AJCC staging for MTC, as it currently is for differentiated thyroid cancer.

REFERENCES

American Joint Committee on Cancer (2002) Cancer staging manual 6th edition, Springer, New York, pp 79

Ball DW (2007) Medullary thyroid cancer: therapeutic targets and molecular markers Curr. Opin Oncol 19:18–23

Brandi ML, Gagel RF, Angeli A, Bilezikian JP, Beck-Peccoz P, Bordi C, Conte-Devolx B, Falchetti A, Gionata Gheri R, Libroia A, Lips CJM, Lombardi G, Mannelli M, Pacini F, Ponder BAJ, Raue F, Skogseid B, Tamburrano G, Thakker RV, Thomspon NW, Tomassetti P, Tonelli F, Wells SA, Marx SJ (2001) Consensus: guidelines for diagnosis and therapy of MEN type 1 and type 2. J Clin Endocrinol Metab 86:5658–5671

Carling T, Udelsman R (2005) Cancer of the endocrine system: thyroid tumors. In: Devita VT, Hellman S, Rosenberg SA (eds) Cancer: principle and practice of oncology, 7th Lippincott Williams and Wilkins, Philadelphia, p 1502

Fialkowski EA, Moley JF (2006) Current approaches to medullary thyroid carcinoma, sporadic and familial. J Surg Oncol 94:737–747

Hazard JB, Hawk WA, Crile G (1959) Medullary (solid) carcinoma of the thyroid – a clinicopathologic entity. J Clin Endocrinol Metab 19:152–161

Kebebew E, Ituarte PHG, Siperstein AE, Duh WY, Clark OH (2000) Medullary thyroid cancer: clinical characteristics, treatment, prognostic factors, and a comparison of staging systems. Cancer 88:1139–1148

Kouvaraki MA, Shapiro SE, Perrier ND, Cote GJ, Gagel RF, Hoff AO, Sherman SI, Lee JE, Evans DB (2005) RET proto-oncogene: a review and update of genotype-phenotype correlations in hereditary medullary thyroid cancer and associated endocrine tumors. Thyroid 15:531–544

Machens A, Schneier U, Holzhausen HJ, Dralle H (2005) Prospects of remission in medullary thyroid carcinoma according to basal calcitonin level. J Clin Endocrinol Metab 90:2029–2034

Moley JF, DeBenedetti MK (1999) Patterns of nodal metastases in palpable medullary thyroid carcinoma: recommendations for extent of node dissection. Ann Surg 229:880–887

Raue KF, Buhr B, Dralle H, Klar E, Senninger N, Weber T, Rondot S, Hoppner W, Raue F (2006) Long-term outcome in 46 gene carriers of hereditary medullary thyroid carcinoma after prophylactic thyroidectomy: impact of individual *RET* genotype. Eur J Endocrin 155: 229–236

Roman S, Lin R, Sosa JA (2006) Prognosis of medullary thyroid carcinoma: demographic, clinical and pathologic predictors of survival in 1252 cases. Cancer 107:2134–2142

Wells S, Lakhani V, Hou J (2006) A Phase II trial of ZD6474 in patients with hereditary metastatic medullary thyroid cancer [abstract]. J Clin Oncol 24:5553

Wells S, Gosnell J, Gagel RF, Pfister D, Sosa JA, Skinner J, Krebs A, Hou J, Schlumberger M (2007) Vandetanib in metastatic hereditary medullary thyroid cancer: follow-up results of an open-lable phase II trial. Am Soc Clin Oncol [abstract] 25:6018

You YN, Lakhani V, Wells SA, Moley JF (2006) Medullary thyroid cancer. Surg Oncol Clin N Am 15:639–660

30
Overexpression of the Components of the Plasminogen Activating System as Prognostic Factors in Human Thyroid Carcinoma

Enke Baldini, Salvatore Ulisse, and Massimino D'Armiento

PLASMINOGEN ACTIVATING SYSTEM (PAS)

The plasminogen activating system (PAS) is an ensemble of proteins involved in the extracellular conversion of the ubiquitous inactive plasminogen to the broad spectrum serine protease plasmin, which is implicated in fibrin homeostasis and in numerous physiological and pathological processes requiring the remodelling of extracellular matrix (ECM) and basement membranes (BM). The PAS consists of two serine proteases, the urokinase (uPA) and the tissue-type (tPA) plasminogen activators, the cell membrane receptor for uPA (uPAR) and two main inhibitors belonging to the serine proteinase inhibitors (serpin) superfamily, the plasminogen activator inhibitor 1 (PAI-1), and 2 (PAI-2). The uPA is first synthesized as a single-chain zymogen (pro-uPA or sc-uPA); once secreted in extracellular environs, the sc-uPA is converted to the active disulfide-linked two-chain form (tc-uPA) by a number of proteases such as plasmin, plasma kallikrein, and cathepsin B and L (Choong and Nadesapillai 2003). Plasmin is the primary activator of sc-uPA and is in turn activated by tc-uPA, thus enhancing its own production. Such phenomenon, referred as "reciprocal zymogen activation", occurs much more efficiently when the sc-uPA is associated with its receptor uPAR, a glycoprotein anchored to the plasma membrane through a glycosylphosphatidylinositol moiety (Plesner et al. 1997; Blasi and Carmeliet 2002). As a consequence, the active uPA generation is concentrated in the pericellular area, where it represents an effective and rapid source of plasmin during cell migration and invasion under physiological or pathological conditions. Moreover, in numerous cell types the expression of plasma membrane plasminogen receptors, which colocalize with uPAR, improves the local concentrations of reactants (Castellino and Ploplis 2005).

Unlike uPA, the single-chain human tPA is proteolytically active and a plasmin cleavage yields a disulfide-linked two-chain molecule which exhibits a 10–50-fold increased activity. It is generally assumed that tPA is primarily involved in fibrinolysis, but it is also abundantly expressed in the central nervous system where it is engaged in various processes, i.e., neurite outgrowth

and neuronal development (Collen 1999; Yamada et al. 2005).

The activity of PAS is counteracted by the serpin α_2-antiplasmin, the main inhibitor of plasmin, and by two specific inhibitors, PAI-1 and PAI-2, which trap the active uPA and tPA forming stably inactive equimolar complexes. Two other serpins, proteinase nexin-1 and protein C inhibitor, are also able to block plasminogen activators at physiologically relevant rates, even if they are not specifics and react more slowly (Andreasen et al. 1997; Lijnen 2004).

THE PLASMINOGEN ACTIVATING SYSTEM IN PATHOPHYSIOLOGICAL CONDITIONS

As stated earlier, PAS is implicated in fibrinolysis and in a number of physiological and pathological processes which require ECM and BM remodelling, such as wound healing, tissue regeneration and involution, immune response, angiogenesis, tumor progression, and metastasis (Danø et al. 2005). Such array of effects is due to the capability of plasmin to target several ECM and BM components, including fibronectin, laminin, vitronectin, type IV collagen, proteoglycans, and fibrin, both directly and through the activation of latent matrix metalloproteinases (MMPs) (Visse and Nagase 2003). However, the action of PAS is not limited to activation of plasminogen and the consequent degradation of ECM and BM. In fact, although lacking of an intracellular domain, the uPAR is connected with the cytoplasmic signalling machinery by means of at least three different mediators: integrins, caveolin, and G-proteins coupled receptors, which in turn activate several tyrosine- and serine-kinases, such as Src, haematopoietic cell kinase, focal adhesion kinase and mitogen-activated protein kinases (MAPK) (Blasi and Carmeliet 2002). As a consequence, uPA binding to uPAR can generate proteolytic-independent intracellular signals affecting cell motility, adhesion, differentiation, and proliferation (Blasi and Carmeliet 2002). These cellular processes may also be indirectly affected by plasmin through the activation of latent mitogenic, motogenic and/or angiogenic factors bound to ECM, such as basic fibroblast (bFGF), vascular endothelial (VEGF), hepatocyte (HGF), insulin (IGF), epidermal (EGF), and transforming (TGF- β) growth factors (Choong and Nadesapillai 2003).

Several reports have documented the ability of PAS to modulate cell migration. The latter initiates with the extension of the plasma membrane at the leading edge of the cell, associated with an intracellular reorganization and polymerization of new actin filaments, which are then stabilized by the formation of new adhesions to ECM components. Simultaneously, at the rear edge of the cells, plasma membrane releases its binding to ECM. Thus, consecutive cycles of attachment and detachment from ECM substrates take place during cell migration. The PAS affects this process by promoting ECM or adhesion receptor proteolysis at the leading edge of the cell, allowing plasma membrane extension, and causing the release from the ECM at the rear edge of the cell. Moreover, the uPA/uPAR complexes have been shown to modulate cell attachment to a variety of ECM proteins by interacting with various adhesion receptors belonging to the integrin family.

The uPAR bound to uPA can also establish direct contacts with several extracellular proteins and especially with vitronectin, leading to intracellular rearrangement of actin cytoskeleton, morphological changes and augmented adhesion to ECM (Sidenius and Blasi 2003). Interestingly, PAI-1 binds to vitronectin with high affinity and competes with uPAR for the same binding site. Following the uPA-PAI-1 interaction, PAI-1 affinity for vitronectin is greatly reduced, allowing uPAR occupancy to vitronectin, and hence promoting cell-ECM attachment (Sidenius and Blasi 2003). Furthermore, binding of uPA induces the exposition of an uPAR epitope endowed with a potent chemotactic activity, which in turn stimulates tyrosine kinase-dependent intracellular pathways required for cell migration (Blasi and Carmeliet 2002). Finally, the PAS may indirectly affect cell migration through the activation of latent motogenic growth factors such as HGF, bFGF, and TGF-β.

ROLE OF PLASMINOGEN ACTIVATING SYSTEM IN HUMAN CANCERS

Cancer progression is associated to the acquisition by malignant cells of novel functional capabilities, which include self-sufficiency in growth signals, insensitivity to anti-growth signals, evasion of apoptosis, limitless replicative potential, sustained angiogenesis, and tissue invasion and metastasis (Hanahan and Weinberg 2000). Based on the above information, it is clear that the PAS contributes directly or indirectly to the acquisition by malignant cells of some of these new biological functions. Overexpression of uPA may represent a mitogenic stimulus for the malignant cells, resulting either from abnormal uPAR-mediated cell signalling or indirectly from plasmin-mediated activation of growth factors. In addition to the proliferative action, the PAS affects all steps of neoplastic evolution, from spreading in the primary site to intra- and extravasation, neoangiogenesis, and metastasis. Destruction of extracellular structures at the advancing edge of tumor is a prerequisite for tumor growth and invasion of the surrounding tissues, and plasmin greatly contributes to this process both directly or through the activation of latent MMPs. The same products of ECM degradation may also represent new bioactive molecules, i.e., peptides derived from laminin and fibronectin cleavage, which can support cancer cell migration and dissemination. On the other hand, the PAS plays an important role in the activation of motogenic factors such as HGF, b-FGF, and TGF-β and the regulation of the consecutive cycles of malignant cell attachment and detachment from ECM substrates which take place during cell migration (Duffy 2004). Analogous events are observed for endothelial cells during tumor-associated neoangiogenesis. The expression of uPA and uPAR, undetectable in quiescent endothelial cells, is induced at the leading migratory front of new microvessels and in tumor-associated macrophages by angiogenic stimuli such as bFGF, VEGF or hypoxia. The plasmin in turn activates latent motogenic and proangiogenic factors bound to ECM; among these, the VEGF induces vascular hyperpermeability, providing an exit route for metastasizing tumor cells and allowing diffusion of fibrinogen and other plasma proteins into the extracellular space. The conversion of fibrinogen to fibrin by

plasmin leads to the formation of a transitional matrix which constitutes a structural support for endothelial cell migration (Choong and Nadesapillai 2003). A relevant contribution of PAI-1 in such processes has recently emerged (Lijnen 2004). The PAI-1 is present in resting mature vessels where it prevents both the plasmin-mediated proteolysis and the uPAR-dependent cell-ECM adhesions, but the induction of uPA and uPAR following endothelial cells activation overcomes these inhibitory actions. However, the PAI-1 is actually considered a pro-angiogenic rather than anti-angiogenic factor. Indeed, a paracrin induction of PAI-1 occurs in fibroblasts nearby the sprouting endothelium, most likely to prevent an excessive pericellular proteolysis. The PAI-1 also associates with uPA/uPAR forming a ternary complex that is internalized in endothelial cells by an LDL receptor-like molecule; thereafter, uPAR is recycled back on plasma membrane not with a random distribution, but focused on new adhesion areas at the leading edge of cell. Such uPAR relocalization seems to be a crucial event for the initial migratory phase of endothelial cells (Binder et al. 2007).

CLINICAL SIGNIFICANCE OF THE EXPRESSION OF PLASMINOGEN ACTIVATING SYSTEM COMPONENTS

In several types of human cancers, the expression of uPA, uPAR, and PAI-1 has been found to be significantly higher in malignant tissues with respect to normal matched ones. Moreover, a strong correlation between the overexpression of one or more PAS components and the poor clinical outcome for a number of human cancers has been documented (Choong and Nadesapillai 2003). Most of all, the prognostic and predictive impact of PAS has been investigated in breast cancer patients, for which the particular relevance of uPA and PAI-1 has been recently validated by a prospective randomized trial and a multicenter pooled analysis. The main clinical use is in node-negative breast cancer, where the assessment of low tissue levels of uPA and PAI-1 can avoid over-treatment by adjuvant chemotherapy in patients with non-aggressive disease.

On the other hand, high primary cancer tissue levels of uPA and PAI-1 may identify intermediate-risk patients who should receive chemotherapy because their tumor is more aggressive than classical pathological factors would suggest (Harbeck et al. 2007). Apart from breast cancer, uPA overexpression has been shown to represent a prognostic marker in several other malignancies, including lung, bladder, stomach, colorectum, cervix, ovary, kidney, and brain cancers, as well as soft tissue sarcomas (Andreasen et al. 1997). Likewise, there is now accumulated experimental and clinical data attesting a high correlation of uPAR levels with metastatic potential and advanced disease across a variety of tumors, as colon, endometrial, gastric, pancreatic, renal, and breast cancers (de Bock and Wang 2004). The uPAR appears particularly abundant at the leading edge of tumors and often polarized on the cell surface, where it seems to have a critical role in directional control on migrating or invading cells. Soluble uPAR variants (suPAR) devoid of GPI anchor, produced either by proteolytic cleavage or alternative splicing, have been identified in body fluids such as blood, urine, and ascite

(de Bock and Wang 2004). Even if their biological role still remains to be clarified, suPAR have been reported to predict BM invasion and poor prognosis in multiple myeloma patients (Rigolin et al. 2003) or disease progression after surgery and metastasis in prostate cancer (Shariat et al. 2007).

Paradoxically, high levels of PAI-1 are also associated with a poor prognosis in several tumors. This unexpected finding may be explained in view of the recent observations that PAI-1, interacting with vitronectin and uPA/uPAR complexes, has dramatic effects on the ability of cells to attach, migrate and be detached from their substratum (Czekay and Loskutoff 2004). The inhibitory action of PAI-1 is probably necessary to prevent the excessive degradation of the ECM by uPA, which could inhibit cell mobility on the matrix support. In addiction, uPAR/uPA/PAI-1 complex formation and internalization seems to be crucial for the initial migratory response of endothelial cells, and a proangiogenic role of PAI-1 has recently emerged from tumor transplantation models in PAI-$1^{-/-}$ mice (Binder et al. 2007). In contrast, different studies including various tumor types have shown contrasting correlations between tumor levels of PAI-2 and patient survival. High neoplastic tissue concentrations of PAI-2 are associated with good prognosis in patients with breast, pancreatic, and ovarian cancers, but with poor prognosis in patients with colorectal or endometrial cancers, and the meaning of these discrepancies remains to be elucidated (Osmak et al. 2001; Nordengren et al. 2002; Smith et al. 2007).

Despite the extensive investigations regarding the role of PAS in human tumors, relative little information regarding the expression of PAS components during the progression of thyroid cancers is available. The present work assembles the data on the expression profiles of PAS components in thyroid tumors that have been published to date, with a special regard to those reports which related PAS components expression to prognostic evaluation.

THE PLASMINOGEN ACTIVATING SYSTEM IN HUMAN THYROID CARCINOMAS

Neoplasms derived from the follicular thyroid cell represent the most common endocrine malignancy, accounting for ~1% of all new malignant diseases and ~0.4% of deaths related to cancer. The large majority of follicular thyroid cancers are represented by the differentiated papillary and follicular thyroid carcinomas which, following dedifferentiation, are thought to give rise to the highly aggressive and invariably fatal anaplastic thyroid carcinomas (Sherman 2003). Although derived from the same cell type, the different thyroid neoplasms show specific histological features, biological behaviour and degree of differentiation as a consequence of different genetic alterations (Kondo et al. 2006).

The first evidence of uPA implication in human thyroid tumor invasivity was provided by Packman et al. (1995), who found an increase of uPA and gelatinases activities in a follicular thyroid carcinoma cell line derived from lung metastasis (FTC-238) with respect to the less invasive clone derived from lymph node metastasis (FTC-133). Subsequently, an immunohistochemical (IHC) study described the diffuse expression of uPA, uPAR, and PAI-1

in the majority of thyroid carcinomas, while the immunoreactivity of PAI-2 was evident only in 56% of cases (Ito et al. 1996). Nevertheless, these authors did not observe any correlation between IHC findings and clinicopathological parameters. In contrast, another IHC study reported the association of high uPAR expression with poorly-differentiated and more aggressive papillary thyroid carcinomas (PTC), indicating this protein as a putative prognostic factor (Kim et al. 2002). The levels of plasminogen activators and PAI-I were also estimated in the cytosolic fraction of malignant and benign thyroid tumor tissues and various non-cancer diseases of the gland by enzyme immunoassay (Kushlinskiĭ et al. 2001). These authors demonstrated that samples from patients with thyroid cancer displayed the lowest levels of tPA and the highest levels of uPA and PAI-I, while those from patients with benign thyroid diseases showed high concentrations of tPA and relatively low levels of uPA and PAI-I. Furthermore, an interesting study evaluated the presence of uPAR in plasma membranes of normal and neoplastic human thyroid cells (Ragno et al. 1998). Normal thyrocytes were referred to express on their surface the intact form of uPAR and also a truncated form lacking the uPA-binding domain. In thyroid tumor derived cells the truncated form was highly expressed in papillary carcinoma cells, very low in follicular carcinoma cells, and not detectable in anaplastic carcinoma cells. Because the binding of uPA to uPAR requires full-size uPAR, it can be supposed that the cleavage of uPAR occurring on normal thyrocytes represents a mechanism of limitation for the invasive potential of the cell, which is maintained in the papillary carcinomas, but partially or completely lost in the more aggressive follicular and anaplastic cancers.

A relationship between uPA and thyrocytes invasivity was also indicated by Sid et al. (2006), who analysed the expression patterns of uPA, MMP-2, and low density lipoprotein receptor-related protein (LRP), a large scavenger receptor involved in the uptake and degradation of various ligands, in the FTC-133 and FTC-238 cell lines mentioned above. The authors showed that the more invasive cell line FTC-238 possessed lower LRP amount and higher uPA expression and activity than FTC-133 cells. The neutralization of LRP led to uPA accumulation and to a twofold increase of its activity in the conditioned medium of both cell lines, conferring to the cells a more invasive character. Inversely, following inhibition of uPA activity, but not MMPs activity, the invasive phenotype of FTC cells was abolished. Therefore, the authors concluded that regulation of uPA activity by LRP is likely to represent an important mechanism in controlling thyroid carcinoma cell invasion.

Recently, our group characterized the PAS components expression in human normal thyrocytes and various cell lines derived from a benign follicular adenoma and different histotypes of thyroid tumors, by means of real time RT-PCR and Western blot experiments (Ulisse et al. 2006). Our results demonstrated that malignant transformation of the human thyrocyte is associated with the augmented expression, at both mRNA and protein levels, of uPA, uPAR, and PAI-1, while tPA and PAI-2 were either unchanged or decreased in different malignant cell lines. Moreover, a zymographic assay of the conditioned media from the different cell lines demonstrated a significant increase of active

uPA secretion in all carcinoma cells with respect to normal thyrocytes. The data obtained in the cell lines were mirrored by analogous experiments on human papillary thyroid carcinoma specimens, in which the expression of the different PAS components was compared to that of normal matched tissues. In particular, the results demonstrated a significant correlation between increased uPA expression and tumor size, which represents one of the major prognostic factors in thyroid cancer (Gospodarowicz et al. 2002). Moreover, the levels of uPA and uPAR mRNAs were significantly higher in metastatic than in non-metastatic PTC.

A recent study analyzed the level of uPA and PAI-1 proteins in paired cytosolic fractions of thyroid neoplasms and normal tissues by ELISA (Horvatić Herceg et al. 2006). Both proteins concentrations were markedly different among various histological types of thyroid cancer, showing the lowest values in adenomas and the highest in anaplastic carcinomas. Furthermore, uPA and PAI-1 were found higher in anaplastic versus well-differentiated thyroid cancers, as well as in tumor with extrathyroidal invasion or distant metastasis and those exceeding 1 cm of diameter. More interestingly, the survival analysis revealed a significant impact of both uPA and PAI-1 on the progression-free survival rate, providing new indication of the potential prognostic relevance of PAS components in thyroid tumors.

In conclusion, there is an overall agreement in the literature documenting the augmented expression of uPA, uPAR, and PAI-1 in thyroid cancers. Furthermore, recent studies demonstrated a clear correlation between increased expression of PAS components and some of the major prognostic factors for thyroid cancer such as tumor size, lymph node or distant metastases. However, these findings need to be validated in larger case studies before their evaluation may be included in the assessment of the prognosis of patients affected by thyroid cancer. In Table 30.1 are summarized the data regarding the expression of the different PAS components related to prognosis in several human cancers, including thyroid carcinomas.

METHODS TO EVALUATE EXPRESSION OF PLASMINOGEN ACTIVATING SYSTEM COMPONENTS

Substrate Gel Electrophoresis (Zymograms)

Zymography is an electrophoretic technique extensively used to determine proteolytic activity in complex biological samples resolved in SDS-PAGE. The running gels

TABLE 30.1. Expression of the different PAS components related to prognosis in several types of human cancers

Cancer type	Worse prognosis	Favourable prognosis
Breast	uPA, uPAR, PAI-1	PAI-2
Colorectal cancer	uPA, uPAR, suPAR, PAI-1, PAI-2	
Gastric cancer	uPA, uPAR, PAI-1	
Esophageal cancer	uPA, PAI-1	PAI-2
Pancreatic cancer	uPA	PAI-2
Ovarian cancer	uPA, suPAR, PAI-1	PAI-2
Endometrial cancer	uPA, uPAR, PAI-1, PAI-2	
Prostate cancer	uPA, suPAR, PAI-1	
Bladder cancer	uPA, uPAR	
Gliomas	uPA	
Sarcomas	uPA, PAI-1	
Renal cell cancer	PAI-1	
Pulmonary cancer	PAI-1	
Acute myeloid leukemia	uPAR	
Thyroid cancer	uPA, uPAR, PAI-1	

are prepared by copolimeryzing the acrylamide with a substrate for the enzyme of interest. The most common zymogram to detect plasminogen activators is obtained by adding to the acrylamide plasminogen (Sigma-Aldrich) as substrate of PAs and gelatin (Euroclone) or casein (Sigma-Aldrich) as substrates of plasmin (Table 30.2). The proteins are separated in denaturing but nonreducing conditions and after refolded by means of nonionic detergent solutions (usually Triton X-100) that remove the SDS. The gels are then incubated in a suitable buffer system for the specific enzyme under study and finally stained with Coomassie blue. The presence of enzymatic activity is visualized as clear bands on the blue background, corresponding to areas where the substrate has been degraded. The following table represents the recipe for resolving (zymogram) and stacking gels.

1. A 10x running buffer is prepared as follows: 0.25 M Tris, 1.92 M glycine, 1% SDS, pH 8.3; it is stored in a glass bottle at room temperature and diluted with ddH_2O before use.
2. Biological liquid samples or conditioned culture serum-free media are collected and centrifuged for 5 min at 1,200 r.p.m. to eliminate cellular debris. If needed, they can be concentrated by centrifugal filter devices (Centricon filters with Ultracel YM regenerated cellulose membranes, Millipore). Otherwise, if cellular or tissutal protein extracts are used, the extraction should be done in the absence of serine proteases inhibitors.
3. The samples are prepared by dilution in zymography loading buffer (5x) consisting of 0.4 M Tris-HCl (pH 6.8), 5% SDS, 20% glycerol and 0.03% bromophenol blue (Kleiner and Stetler-Stevenson 1994) and loaded into the well without boiling.
4. The electrophoretic run is carried out at 20 mA constant current for 1.5–2 h until the tracking dye front reaches the bottom of resolving gel. The gel is then removed and rinsed in 50 mM Tris-HCl (pH 7.4) with 2% Triton X-100 (Euroclone) by shaking gently at room temperature for 30–60 min. After a wash in 50 mM Tris-HCl (pH 7.4), gel is incubated in a buffer containing 50 mM Tris-HCl (pH 7.4) and 0.1% Triton X-100 on a rotary shaker at 37°C for 4–6 h.
5. In order to assess the enzyme specificity, identical gels are incubated in parallel within the above buffer containing serine proteases inhibitors, i.e., 10 μM aprotinin and 1 mM PMSF; otherwise, the control gel can be prepared omitting the plasminogen.
6. The gel is stained with a solution of 0.1% Coomassie brilliant blue, 25% methanol and 7% acetic acid, and destained by repeated washes in the same mixture without dye. Both these steps are performed at room temperature on a rotary shaker for 15–60 min each.
7. Clear zones against the blue background correspond to PAs proteolytic activity.

TABLE 30.2. Resolving and stacking gels for zymography (Heussen and Dowdle 1980)

Reagents	10% Zymogram	5% Stacking gel
Acrylamide (30%)/ bisacrylamide (1%)	3.33 mL	0.833 mL
0.5 M Tris-HCl, pH 6.8	–	1.25 mL
1.5 M Tris-HCl, pH 8.8	2.5 mL	–
Gelatin or Casein 1% in ddH_2O	1 mL	–
Plasminogen 1.2 mg/ mL in PBS	0.1 mL	–
SDS 10% in ddH_2O	0.1 mL	0.05 mL
ddH_2O	2.865 mL	2.814 mL
Ammonium persulfate 100 mg/mL in ddH_2O	0.1 mL	0.05 mL
TEMED (as supplied)	0.005 mL	0.0025 mL
Final volume	10 mL	5 mL

The molecular weights of each band are evaluated in comparison with a prestained protein ladder or with a positive control, such as MDA-MB-231 cell line (American Type Culture Collection) supernatant. The intensity of bands, corresponding to the degree of digestion, can be quantified by scanning densitometry.

Invasion Assay

The invasiveness of tumor cells is one of the hallmarks of the metastatic phenotype. In order to characterize the invasive potential of malignant cells, a variety of in vitro assays have been developed, which test the capability of cells to penetrate through physiological barriers such as tissues containing basement membranes (i.e., bladder wall, amnion or lens capsule) or a matrix material reconstituted onto a filter, named matrigel (Kleinman et al. 1986). The latter is obtained with extracts prepared from the basement membrane of the Englebreth–Holm–Swarm mouse sarcoma. Under physiological conditions and in the presence of added type IV collagen and heparan sulfate proteoglycan, these extracts form gellike structures mainly composed of laminin, collagen IV, heparan sulfate proteoglycans, nidogen, and entactin, resembling the lamina dense zone of basement membranes. Matrigel represents actually the most common environment for studies of cell morphology, biochemical function, migration, or invasion. The results obtained by the Boyden chamber assay, described below, show a strong correlation between the ability of tumor cells to invade in vitro and their invasive behaviour in vivo, which validates this assay as a measure of invasive potential. Importantly, this assay represents a suitable mean to investigate the effects and the efficacy of Pas inhibitors on tumor cell migration and invasiveness.

1. Matrigel can be prepared in sterile form as previously described (Kleinman et al. 1986) or acquired from BD Biosciences (BD Biosciences, Two Oak Park, Bedford, MA 01730 USA). It is stored in aliquots at −20°C and thawed overnight at 4°C before use.
2. Matrigel is diluted up to 1–10 mg/mL with cold ddH_2O and applied on polyvinylpyrrolidone-free polycarbonate filters (Nucleopores) of 8–12 μm pore size at a quantity of 12.5–200 μg/filter, air-dried under a hood and reconstituted with serum-free cold cell culture medium.
3. The coated filters are placed into Boyden chambers (BD Biosciences).
4. The cultured cells are trypsinized and collected, washed with serum-free culture medium and resuspended in the same medium containing 0.1% bovine serum albumin, then added to the upper compartment of Boyden chambers (2–3 × 10^5 cells/each).
5. The bottom of chambers is filled with a chemoactrattant, because in the absence of any stimulus the cellular migration is very weak. Normally the conditioned medium from the murine fibroblast cell line NIH-3T3 (American Type Culture Collection) is used, obtained as follows: the cells are grown to subconfluent monolayers, washed with PBS and incubated with serum-free DMEM for 48 h. Supernatant is harvested and stored at −20°C. Alternatively, the cells under study can be preincubated in serum-free culture medium for 24 h and fetal bovine serum can be employed as chemoactrattant.

6. The assembled chambers are incubated for one to few hours at 37°C in a 5% CO_2 humidified atmosphere.
7. At the end of incubation, the noninvasive cells are scraped off from the top of filters with a cotton swab.
8. The invasive cells, migrated on the other side of filters, are fixed in cold methanol for 5 min, stained with an aqueous solution of methylene blue and eosin (DiffQuick solution, Dade Behring) and sealed on slides.
9. Quantification of invasion through the coated membranes is done by counting stained cells under a microscope, using a microgrid.

Real Time RT-PCR

Quantitative RT-PCR represents an useful technique to determine the variations of gene expression levels in cancer tissues with respect to their normal counterparts. Such analysis can be executed comparing the mRNA levels for a gene of interest between surgical samples obtained from a number of patients and healthy individuals. In the management of thyroid cancers, the total ablation of thyroid gland allows obtaining both cancer tissues and normal matched tissues from a single patient, so that mRNA variations can be determined more reliably. In the case that an alteration is found, the next attempt is to examine clinical parameters in order to identify any significant correlation between tumor progression and gene expression status.

1. Surgical samples are immediately frozen in liquid nitrogen and stored at −80°C until usage.
2. Frozen samples are homogenized in ~1 mL of a phenol-guanidine-isothiocyanate solution (i.e., TRIzol Reagent, Invitrogen) per 50–100 mg of tissue by mortar and pestle or power homogenizer. Then total RNA is extracted following the acid guanidinium thiocyanate-phenol-chloroform method (Chomczynsky and Sacchi 1987).
3. The purity and integrity of RNA preparations are checked by measuring the relative absorbance of RNA at 260 and 280 nm and by electrophoresis on 1% agarose gel with 0.5 μg/mL ethidium bromide in TAE buffer (Tris-Acetate-EDTA: 242 g Tris base, 57.1 mL Acetic acid, 100 mL 0.5 M EDTA. Add ddH_2O to 1 L and adjust pH to 8.5) at 90 V constant.
4. One ng to 5 μg of total RNA are reverse-transcribed within a reaction mix of 0.5 mM deoxyribonucleotides, 0.5 μg oligo-dT primers per μg of RNA, 2U/μL ribonuclease inhibitor, 10 mM dithiothreitol, first strand buffer and 200U M-MLV reverse transcriptase, according to the specific procedure indicated by the enzyme manufacturer.
5. The obtained cDNA is used as template for the subsequent PCR amplifications. Controls for DNA contamination are performed omitting the reverse transcriptase during reverse transcription or placing RNA directly in the PCR mixture.
6. Real-time PCR conditions are applied depending on the particular instrument adopted, but anyway it is necessary to create standard curves for each primer pair, choosing a calibrator template which expresses all the genes of interest at good levels. In particular, to analyze PAS mRNAs in human thyroid, it can be used a cDNA derived from thyrocytes, because they express all the PAS members in basal conditions (Ulisse et al. 2006).
7. To check the specificities of amplified cDNAs, they are purified with a PCR

cleanup kit (QIAquick PCR Purification Kit, QIAGEN) and analyzed by an automated DNA sequencer.

8. The calculation of data is performed with the $\Delta\Delta C_p$ method, and finally the expression levels of target genes in tumoral tissues are normalized against those found in healthy individuals or in matched normal tissues.

Immunohistochemistry

Immunohistochemistry (IHC) is one of the most diffuse approaches to visualize the distribution and localization of PAS components in normal and pathologic tissues. In addition, the intensity of immunostaining represents an approximate indication of the protein levels, which can be associated with clinicopathological parameters. A representative ABC (Avidin-Biotin Complex) method for detection of PAS members is depicted in the following protocol.

1. Cut sequential histological sections of 5 μm thickness from formalin-fixed and paraffin-embedded tissue blocks, rinse in water bath and mount onto slices.
2. Air-dry sections overnight.
3. Deparaffinize section by means of 2 passages in xilene for 5–10 min each and rehydrate in 2 changes of 100% ethanol for 5 min each, 95% and 80% ethanol for 5 min each, then rinse in ddH_2O.
4. Wet in PBS (phosphate buffered solution) for 2 × 2 min.
5. Block the endogenous peroxidase activity by incubating sections for 10 min with a peroxidase blocking solution (0.3% H_2O_2 in methanol).
6. Wet in PBS for 2 × 2 min.
7. Perform heat-induced epitope retrieval. Preheat steamer or water bath with staining dish containing sodium citrate buffer (Mix 2.94 g Tri-sodium citrate dihydrate to 1 L ddH_2O, adjust pH to 6.0 with 1N HCl and then add 0.5 mL of Tween 20. Store this solution at 4°C.) until temperature reaches 95–100°C. Immerse slides in the staining dish and incubate for 50 min. Microwave or pressure cooker can be used as the alternative heating source to replace steamer or water bath. Otherwise, an enzyme-based antigen retrieval can be adopted: incubate slides for 20 min. at 37°C with 0.05 g porcine trypsin (Sigma-Aldrich) and 0.05 g $CaCl_2$ in 50 mL 0.005 M Tris–PBS buffer (pH 7.4).
8. Wash in PBS for 2 × 2 min.
9. To block nonspecific binding of immunoglobulin, incubate sections with normal serum, species same as secondary antibody, at room temperature for 1 h. The recipe for a normal serum block solution includes the following components: 2% serum, 1% BSA, 0.1% Triton X-100, 0.05% Tween 20, 0.01 M PBS (pH 7.2). Mix and store at 4ºC.
10. Incubate sections for 1 h at room temperature or overnight at 4°C with primary antibodies diluted as follows: anti-urokinase B-chain (n. 3689, American Diagnostica), anti-PAI-2 (n. 3750, American Diagnostica) and anti-PAI-1 (n. 3785, American Diagnostica) 1:25, anti-uPAR (n. 3937, American Diagnostica) 1:100 in dilution buffer (1% BSA, 0.01 M PBS, pH 7.2).
11. In parallel experiments, carry out negative controls of the immunostaining by omission of the primary antibody. As positive control, employ sections

from tissues known to be positive for each primary antibody.
12. Rinse in PBS-Tween 20 for 3 × 2 min.
13. Incubate sections with biotinylated secondary antibody anti-mouse (Vector Laboratories) at an appropriate concentration in dilution buffer (1% BSA, 0.01 M PBS, pH 7.2) for 45 min at room temperature.
14. Rinse in PBS-Tween 20 for 3 × 2 min.
15. Incubate sections in ABC (Avidin Biotinylated Complex) solution (R.T.U. VECTASTAIN® Elite ABC Reagent, Vector Laboratories) for 30 min at room temperature.
16. Rinse in PBS-Tween 20 for 3 × 2 min.
17. Add on sections the DAB (3,3′-diaminobenzidine tetrahydrochloride) peroxidase substrate solution (0.05% DAB, 0.015% H_2O_2 in 0.01 M PBS, pH 7.2). A 1% DAB stock solution is prepared as follows: dissolve 0.1g DAB (Sigma-Aldrich) in 10 mL ddH_2O, add 3–5 drops of 10 N HCl and solution turns light brown color. Shake for 10 min to dissolve DAB completely, then aliquot and store at −20°C. To obtain the final peroxidase substrate solution, put 5 drops of 1% DAB in 5 mL of PBS (pH 7.2) and mix well, then add 5 drops of 0.3% H_2O_2 in ddH_2O and mix well.
18. Observe the development of reaction under an optical microscope until the color appears.
19. Stop the reaction in ddH_2O.
20. Counterstain slides for 30 s with hematoxylin solution (50 g aluminum potassium sulphate [Sigma-Aldrich], 1 g hematoxylin [Sigma-Aldrich], 0.2 g sodium iodate [Sigma-Aldrich], 20 mL glacial acetic acid, 1 L ddH_2O. Dissolve completely aluminum in ddH_2O, then add hematoxylin. When hematoxylin is completely dissolved, add sodium iodate and acetic acid. Bring to boil and cool, filter if necessary.)
21. Rinse in running tap water for 2–5 min.
22. Dehydrate through 70% ethanol for 1 min., 100% ethanol for 2 × 3 min. and clear in xylene for 2 × 5 min.
23. Coverslip with mounting medium.

Enzyme-Linked Immunosorbent Assay (ELISA)

To date, a number of immunosorbent assays have been designed to quantify uPAR in tumor lysates or body fluids, measuring either the collective amounts of all uPAR forms or each individual form by using specific monoclonal antibodies, or even distinguishing the ligand-occupied fraction of uPAR from the free one. An extensive description of the most advanced immunoassays techniques for this receptor have been recently provided by Høyer-Hansen and Lund (2007). A pronounced prognostic impact was first demonstrated for uPA and subsequently for PAI-1 in detergent-extracted (Triton X-100) breast cancer tissues by applying enzyme-linked immunosorbent assay techniques. This evidence has been largely confirmed by an alternative approach employing archived cytosol fractions obtained by mechanical disintegration of samples. A direct comparison of both methods with particular regard to prognosis has been executed by Jänicke et al. (1994), which recommended Triton X-100 extracts to yield optimal prognostic information.

1. Surgical samples of normal and tumor tissues are immediately frozen in liquid nitrogen and stored at −80°C until usage.
2. Frozen specimens of ~200 mg are homogenized by mortar and pestle or power

homogenizer in 0.9 mL Tris-buffered saline (TBS: 50 mM Tris base, 0.9% NaCl, pH 7.6. To prepare a 10x stock: 61 g Trizma base, 90 g NaCl, 1 L ddH_2O. Mix to dissolve and adjust pH to 7.6. Store this solution at room temperature).

3. Triton X-100 (Euroclone) is added to TBS buffer to a final concentration of 1% and the samples are incubated at 4°C for 12 h under gentle shaking.
4. Samples are centrifugated at 100,000 g for 45 min at 4°C to precipitate cellular debris, nuclei, and cell membranes. The supernatant is collected and antigens concentrations are determined by an ELISA kit (American Diagnostica). Triton X-100 1% does not interfere with the assay.

REFERENCES

Andreasen PA, Kjoller L, Christensen L, Duffy MJ (1997) The urokinase-type plasminogen activator system in cancer metastasis: a review. Int J Cancer 72:1–22

Binder BR, Mihaly J, Prager GW (2007) uPAR–uPA–PAI-1 interactions and signaling: a vascular biologist's view. Thromb Haemost 97:336–342

Blasi F, Carmeliet P (2002) uPAR: a versatile signalling orchestrator. Nat Rev Mol Cell Biol 3:932–943

Castellino FJ, Ploplis VA (2005) Structure and function of the plasminogen/plasmin system. Thromb Haemost 93:647–654

Chomczynsky P, Sacchi P (1987) Single step method of RNA isolation by guanidinium thiocyanate-phenol-chloroform extraction. Anal Biochem 162:156–159

Choong PFM, Nadesapillai APW (2003) Urokinase plasminogen activator system: a multifunctional role in tumor progression and metastasis. Clin Orthop Rel Res 415S:S46–S58

Collen D (1999) The plasminogen (fibrinolytic) system. Thromb Haemost 82:259–270

Czekay RP, Loskutoff DJ (2004) Unexpected role of plasminogen activator inhibitor 1 in cell adhesion and detachment. Exp Biol Med (Maywood) 229:1090–1096

Danø K, Behrendt N, Høyer-Hansen G, Johnsen M, Lund LR, Ploug M, Rømer J (2005) Plasminogen activation and cancer. Thromb Haemost 93: 676–681

de Bock CE, Wang Y (2004) Clinical significance of urokinase-type plasminogen activator receptor (uPAR) expression in cancer. Med Res Rev 24:13–39

Duffy MJ (2004) The urokinase plasminogen activator system: role in malignancy. Curr Pharm Designs 10:39–49

Gospodarowicz MK, Henson DE, Hutter RWP, O'Sullivan B, Sobin LH, Wittekind Ch (2002) Prognostic factors in cancer 2nd ed. UICC, Wiley-Liss, New York

Hanahan D, Weinberg RA (2000) The hallmarks of cancer. Cell 100:57–70

Harbeck N, Schmitt M, Paepke S, Allgayer H, Kates RE (2007) Tumor-associated proteolytic factors uPA and PAI-1: critical appraisal of their clinical relevance in breast cancer and their integration into decision-support algorithms. Crit Rev Clin Lab Sci 44:179–201

Horvatić Herceg G, Herceg D, Kralik M, Bence-Zigman Z, Tomić-Brzac H, Kulić A (2006) Urokinase-type plasminogen activator and its inhibitor in thyroid neoplasms: a cytosol study. Wien Klin Wochenschr 118:601–609

Høyer-Hansen G, Lund IK (2007) Urokinase receptor variants in tissue and body fluids. Adv Clin Chem 44:65–102

Ito Y, Takeda T, Kobayashi T, Wakasugi E, Tamaki Y, Umeshita K, Monden T, Shimano T, Monden M (1996) Plasminogen activation system in active even in thyroid tumors; an immunohistochemical study. Anticancer Res 16:81–89

Jänicke F, Pache L, Schmitt M, Ulm K, Thomssen C, Prechtl A, Graeff H (1994) Both the cytosols and detergent extracts of breast cancer tissues are suited to evaluate the prognostic impact of the urokinase-type plasminogen activator and its inhibitor, plasminogen activator inhibitor type 1. Cancer Res 54:2527–2530

Kim SJ, Shiba E, Taguchi T, Tsukamoto F, Miyoshi Y, Tanji Y, Takai S, Noguchi S (2002) uPA receptor expression in benign and malignant thyroid tumors. Anticancer Res 22:387–393

Kleinman HK, McGarvey ML, Hassell JR, Star VL, Cannon FB, Laurie GW, Martin GR (1986)

Basement membrane complexes with biological activity. Biochemistry 25:312–318

Kondo T, Ezzat S, Asa SL (2006) Pathogenetic mechanisms in thyroid follicular-cell neoplasia. Nat Rev Cancer 6:292–306

Kushlinskiĭ NE, Gershteĭn ES, Kazantseva IA, Kharitidi TIu, Liakina LT, Kazakov SP, Bagatyrev OP, Kalinin AP (2001) Plasminogen activators of urokinase and tissue types and their inhibitor (PAI-1) in cytosol fraction in thyroid diseases. Vestn Ross Akad Med Nauk 5:32–34

Lijnen HR (2004) Pleiotropic functions of plasminogem activator inhibitor-1. J Thromb Haemost 3:35–45

Nordengren J, Fredstorp Lidebring M, Bendahl PO, Brünner N, Fernö M, Högberg T, Stephens RW, Willén R, Casslén B (2002) High tumor tissue concentration of plasminogen activator inhibitor 2 (PAI-2) is an independent marker for shorter progression-free survival in patients with early stage endometrial cancer. Int J Cancer 97:379–385

Osmak M, Babić D, Abramić M, Milicić D, Vrhovec I, Skrk J (2001) Plasminogen activator inhibitor type 2: potential prognostic factor for endometrial carcinomas. Neoplasma 48:462–467

Packman KS, Demeure MJ, Doffek KM, Wilson SD (1995) Increased plasminogen activator and type IV collagenase activity in invasive follicular thyroid carcinoma cells. Surgery 118:1011–1016

Plesner T, Behrendt N, Ploug M (1997) Structure, function and expression on blood and bone marrow cells of the urokinase-type plasminogen activator receptor, uPAR. Stem Cells 15:398–408

Ragno P, Montuori N, Covelli B, Hoyer-Hansen G, Rossi G (1998) Differential expression of a truncated form of the urokinase-type plasminogen activator receptor in normal and tumor thyroid cells. Cancer Res 58:1315–1319

Rigolin GM, Tieghi A, Ciccone M, Bragotti LZ, Cavazzini F, Della Porta M, Castagnari B, Carroccia R, Guerra G, Cuneo A, Castoldi G (2003) Soluble urokinase-type plasminogen activator receptor (suPAR) as an independent factor predicting worse prognosis and extra-bone marrow involvement in multiple myeloma patients. Br J Haematol 120:953–959

Shariat SF, Roehrborn CG, McConnell JD, Park S, Alam N, Wheeler TM, Slawin KM (2007) Association of the circulating levels of the urokinase system of plasminogen activation with the presence of prostate cancer and invasion, progression, and metastasis. J Clin Oncol 25:349–355

Sherman SI (2003) Thyroid carcinoma. Lancet 361:501–511

Sid B, Dedieu S, Delorme N, Sartelet H, Rath GM, Bellon G, Martiny L (2006) Human thyroid carcinoma cell invasion is controlled by the low density lipoprotein receptor-related protein-mediated clearance of urokinase plasminogen activator. Int J Biochem Cell Biol 38:1729–1740

Sidenius N, Blasi F (2003) The urokinase plasminogen activator system in cancer: recent advances and implication for prognosis and therapy. Cancer Metastasis Rev 22:205–222

Smith R, Xue A, Gill A, Scarlett C, Saxby A, Clarkson A, Hugh T (2007) High expression of plasminogen activator inhibitor-2 (PAI-2) is a predictor of improved survival in patients with pancreatic adenocarcinoma. World J Surg 31:493–502

Ulisse S, Baldini E, Toller M, Marchioni E, Giacomelli L, De Antoni E, Ferretti E, Marzullo A, Graziano FM, Trimboli P, Biordi L, Curcio F, Gulino A, Ambesi-Impiombato FS, D'Armiento M (2006) Differential expression of the components of the plasminogen activating system in human thyroid tumour derived cell lines and papillary carcinomas. Eur J Cancer 42:2631–2638

Visse R, Nagase H (2003) Matrix metalloproteinases and tissue inhibitors of metalloproteinases: Structure, function, and biochemistry. Circ Res 92:827–839

Yamada K, Nagai T, Nabeshima T (2005) Drug dependence, synaptic plasticity, and tissue plasminogen activator. J Pharmacol Sci 97:157–161

Index